Summer spatial ecology of woodland caribou across northern Ontario

by

Philip D. Walker

A thesis submitted in partial fulfillment of the requirements for the degree of

Doctor of Philosophy

in

Ecology

Department of Biological Sciences
University of Alberta

Abstract

Caribou (*Rangifer tarandus*) numbers continue to decline across their circumpolar range with boreal woodland caribou (*R. t. caribou*; hereafter caribou) listed as threatened under Canada's *Species at Risk Act*. Given this conservation concern, evaluating the factors influencing reproductive success of caribou is key to developing management strategies. Survival of adult females and their calves is a function of behavioural responses that individuals make across varying spatiotemporal conditions. I evaluated calving behaviours of female caribou across three northern Ontario study regions (Pickle Lake, Nakina, and Cochrane). I first identified caribou parturition and 5-week neonatal mortality using a movement-based approach, which was validated based on footage from 22 video-collared caribou. Across regions, 76% of 107 caribou-years indicated birth events with differences in median birth date of one week later in Cochrane (23 May) than in Pickle Lake (17 May) and Nakina (16 May), which indicate possible phenological differences due to greater overwinter snow in Cochrane. Seventy percent of females that gave birth maintained their calf through the first 5-weeks postpartum, with higher risk of neonatal mortality associated with use of lowlands and greater postpartum movement rates. The ability to identify parturition and calf survival led me to propose that individual caribou may use different strategies in expressing spatial (use of same location) or habitat fidelity (use of same habitat) during calving to maximize reproduction. I identified 56 individuals with $\geq$2 predicted birth events, and compared the types of fidelity expressed (i.e., spatial, habitat, or no fidelity) to caribou age, calf survival, and habitat quality and predictability in calving ranges. Across all caribou, 36% expressed no fidelity, 29% expressed spatial fidelity, 50% expressed habitat fidelity, and 14% expressed both habitat and spatial fidelity, where older individuals were more likely to express spatial fidelity and caribou in areas of lower habitat quality increased the

probability of expressing habitat fidelity. Fidelity type did not influence calf survival, but the sample size was small.

Due to differences in body fat and pregnancy rates between Pickle Lake and Cochrane, I compared the spatiotemporal dynamics of forage resources between each area across the summer. I developed dynamic foodscapes representing forage metrics using data from field-estimates of forage quality and quantity and *in situ* captive-caribou foraging trials. Results supported my hypothesis that caribou in Cochrane were in a lower-nutritional plane than Pickle Lake, largely because accepted biomass and intake rates averaged higher in Pickle Lake than Cochrane and high-quality accepted biomass peaked ~1 month later in Cochrane indicating a possible trophic mismatch. I used the dynamic foodscapes in conjunction with spatial maps of wolf predation risk to understand if caribou of different reproductive states (barren, calf lost within 5-weeks postpartum, and calf survived at least 5-weeks postpartum) traded off their foraging opportunities under high predation risk to further understand foraging dynamics of caribou in these environments. I found that caribou selection was most closely tied to intake rates across calving to late summer irrespective of reproductive state, but caribou traded off higher intake rates for safety at areas of high predation risk. Caribou that made the least forage-predation risk trade-offs during calving lost their calf. Compared to other reproductive states, caribou whose calf survived at least 5-weeks postpartum selected for higher intake rates before making trade-offs for lower predation risk during early and late summer, which was after the energetically demanding period of peak lactation.

Results of my thesis suggest that caribou adjust their calving behaviors across a gradient of available conditions. Given caribou selection for mid-late seral (≥20 years) upland and lowland conifer forests void of linear features, and the effect it can have on expressing habitat

fidelity, management may enhance calving opportunities for caribou by protecting these forest characteristics. Given the role neonatal recruitment can have on population dynamics of caribou, management should prioritize the landscape conditions selected by parturient caribou. Early and late summer may reflect a sensitive period for caribou with a calf-at-heel because they selected for areas of higher intake rates than other reproductive states, which may expose them to higher predation risk. For caribou in northern Ontario predation risk appears to have a strong impact of resource selection and therefore management strategies that minimize risk of predation are critical to their long-term persistence.

Preface

This thesis is an original work by Philip Walker. The research project, of which this thesis is a part of, received research ethics approval from the University of Alberta Research Ethics Board, Project Name “Caribou foraging ecology”, AUP00002135, October 2017. Animal capture and handling protocols of caribou in northern Ontario during 2010–2014 were approved by the Ontario Ministry of Natural Resources and Forestry Wildlife Animal Care Committee (protocols 10-183, 11-183, 12-183, 13-183, and 14-183).

A version of Chapter 2 is published in Journal of Wildlife Management as Walker et al. 2021. To date, Chapters 3, 4, and 5 have not been submitted for publication.

Acknowledgements

The completion of this thesis would not have been possible without the support of my supervisor Dr. Evelyn Merrill, and my collaborators Dr. John Cook and Dr. Rachel Cook from National Council for Air and Stream Improvement and Dr. Art Rodgers from Ontario Ministry of Natural Resources and Forestry. All have been great mentors and fundamental in my development as a scientist. Evie was always available for discussions and to answer questions, and her feedback has been vital in my writing development. Starting this project, Evie and I came into a deep field of previous caribou research conducted in Ontario, and I appreciate the hours we spent in Evie's office figuring out our "piece of the pie." I am also grateful for Evie's generosity, ranging from opening her home for defense parties to visiting them (including Mark) at their trapping cabin in Nordegg or summer home in Dodge Cove.

John and Rachel showed me what working hard in the field really looks like. The dedication to their work is inspiring. John and Rachel were always willing to make time for me and have continued to support me throughout this thesis. They have been paramount in my ability to think critically. I look forward to continuing to work with them as we finish up publications and hopefully work on other projects in the future. Thank you, Art, for being open to collaborating with myself and Evie, and John and Rachel. Art provided great context to the management of caribou in northern Ontario and always offered productive feedback. I valued my time in Thunder Bay when I completed an internship with Art and the OMNRF.

I would also like to thank my committee member Dr. Mark Lewis, who helped me throughout my thesis. I learned a tremendous amount about modeling from him through one-on-one conversations, his Models in Ecology course, and the joint seminar series he and Evie lead on wildlife habitat selection and movement. I would also like to thank Kim Wilke-Budinski and

Shelley Scott, whose roles behind the scenes were so vital to my experience at the university. Thank you, Sydney Toni, for your help and impeccable editorial skills while reading over this thesis. I also wish to thank Dr. Stan Boutin and Dr. Philip McLoughlin for insightful comments on my thesis and during my defense.

Thank you to the Merrill, Boyce, and Boutin lab members. My time at the university would not have been the same without you. It's hard to express how invaluable our conversations were, either during lunch in the Boutin lab or at the faculty club after Wednesday Nighters. Grad school is transient, but I can confidently say I have made many life-long friends throughout this time. I specifically want to thank Michael Peers, Yasmine Majchrzak, Sean Konkolics, Kara Macaulay, Clayton Lamb, and Zac MacDonald for all the conversations and support you have shown me. Maddie Trottier, thank you for the continual love and encouragement. Many days, especially towards the end, I felt like I could not have done this without your support.

In high school, I never saw myself attending post-secondary education. I am so grateful I needed to take time off due to an injury while working construction after high school and was able to reconsider what I wanted to do with my life. Thank you, Steph Penner and Katie Leonardo, who during that time off encouraged me to take the "risk" and go get a degree in biology. I want to offer a special thank you to my family, especially my parents John and Judy Walker, who have continued to support me throughout this academic journey. I have enjoyed sharing my passion for wildlife and modeling with you two. Finally, I want to thank my grandfathers, Lang Walker and Norm Cottee, who provided me with foundational experiences in the natural world and encouraged me to marvel in it. I wish you both could see the magnitude of your impact. This thesis is dedicated to you two.

Table of Contents

List of Tables

List of Figures

Chapter 1. Introduction and Overview

Adult female survival and calf recruitment are key drivers in population dynamics of ungulates (Gaillard et al. 1998, 2000). Calf recruitment, which incorporates both parturition and neonatal mortality, generally has lower elasticity than adult female survival (Gaillard et al. 1998, Bonenfant et al. 2005), but contributes to variability in population dynamics (Gaillard et al. 2000) and can play a key role in population growth of ungulates (Raithel et al. 2007, DeCesare et al. 2012). Because the majority of calf mortality occurs in the first month postpartum (Mahoney et al. 1990, Adams et al. 1995, Linnell et al. 1995, Pinard et al. 2012, Berg et al. 2023), managing for areas used by parturient females to maximize recruitment during this period is likely important to promote ungulate persistence across local populations.

At the same time, survival of adult females and their calves is a function of behavioural responses that ungulates make in a seasonally variable landscape. Habitat selection is a key process in determining species distributions and their fitness (McLoughlin et al. 2006, Dussault et al. 2012, Losier et al. 2015, Martin et al. 2022). Maximizing nutrient intake and minimizing predation risk are critical to the lifetime fitness of an individual (Lima and Dill 1990, Cook et al. 2018, DeMars and Boutin 2018). Ungulates can increase their intake of nutritional resources by selecting habitats with higher resources, but these areas may also have high predation risk, potentially resulting in a forage-predation risk trade-off (Rachlow and Bowyer 1998, Bowyer et al. 1999, Gustine et al. 2006, Hamel and Côté 2007, Hebblewhite and Merrill 2009). Forage-predator trade-offs in habitat selection may also be state-dependent (Rachlow and Bowyer 1998, Barten et al. 2001, Leblond et al. 2016, Viejou et al. 2018). Females with a calf-at-heel have higher nutritional demands, particularly during peak lactation (~3 weeks postpartum; White and Luick 1984, Klein 1990, Parker et al. 1990), and can experience greater predation risk (Berger

1991). Ungulates are often at their lowest condition after winter and peak lactation and therefore need to accrue sufficient body reserves during the summer to increase their probability of pregnancy in fall and winter survival (Cook et al. 1996, 2004, 2021; Parker et al. 1999, 2009), which may subsequently expose them to greater predation risk.

Caribou (*Rangifer tarandus*) populations continue to decline globally (Vors and Boyce 2009, Festa-Bianchet et al. 2011), and boreal woodland caribou (*R. t. caribou*; hereafter caribou) in Canada are listed as threatened under the *Species at Risk Act* (Committee on the Status of Endangered Wildlife in Canada 2014, Government of Canada 2019). The ultimate cause of diminishing caribou numbers is attributed to a reduction and fragmentation of old-growth coniferous forest via industrial practices (Schaefer 2003, Vors et al. 2007, Festa-Bianchet et al. 2011), with the effects of these practices amplified by increased predation risk (Wittmer et al. 2005, Dickie et al. 20017, DeMars and Boutin 2018). The persistence of caribou populations is contingent on effective management of the species (Festa-Bianchet et al. 2011, Serrouya et al. 2019), which depends on identifying factors influencing caribou population dynamics (Bonenfant et al. 2005).

Evidence now supports that conditions on summer range can be nutritionally limiting for caribou (Crête and Huot 1993, Pachkowski et al. 2013, Schaefer and Mahoney 2013, Heard and Zimmerman 2021, Denryter et al. 2022*b*) and forest management can alter the extent that caribou make forage-predation risk trade-offs (Barten et al. 2001, McLoughlin et al. 2005, Gustine et al. 2006). Within Ontario, forestry cutovers have been identified as the central cause of the 50% caribou range reduction from 1880 to 1990 (Racey and Armstrong 2000, Schaefer 2003, Vors et al. 2007). The harvest of mature coniferous stands has caused a shift towards early successional (Cyr et al. 2009, Ruppert et al. 2016) and deciduous-dominated forests (Thompson et al. 2003,

Brown 2011). Greater extent of early seral and deciduous-dominated stands can support high moose (*Alces alces*) and white-tailed deer (*Odocoileus virginianus*) densities (Potvin et al. 2005, Latham et al. 2011), which sustain larger wolf (*Canis lupus*) and bear (*Ursus americanus*) populations (Schwartz and Franzmann 1991, Ballard et al. 2000), thus increasing overall risk for caribou in an area through disturbance-mediated apparent competition (Seip 1992, Wittmer et al. 2007, Serrouya et al. 2021). Forest practices that remove mature coniferous stands may also modify nutritional resources for caribou by reducing the abundance of lichen (Bock and Van Rees 2002, Bowman et al. 2010), a high-energy forage for caribou (Parker et al. 2005, Thompson et al. 2015). At the same time, greater extent of early seral and deciduous-dominated stands can provide greater availability of deciduous browse (Thompson et al. 2003, Brown 2011), a significant summer forage for caribou (Bergerud et al. 1972, Trudell and White 1981, Boertje 1984, Russell et al. 1993, Denryter et al. 2017), which has higher quality and intake rates relative to lichen (Klein 1990, Shipley and Spalinger 1992, Thompson and Barboza 2014). Therefore, forest management may have opposing effects on the availability of summer forage for caribou.

In this thesis, I evaluate caribou calving behaviour and adult female habitat selection in three study regions across northern Ontario. These regions differ in their capacity to support local populations because of varying levels of anthropogenic disturbance, forage availability, and predator densities (Fryxell et al. 2020, Walker et al. 2021). Previous habitat selection studies in Ontario supported variable caribou response to wolf predation risk and forage resources during calving and summer seasons (Avgar et al. 2015, Viejou et al. 2018), but did not focus on changes in state-dependent selection across a dynamic summer.

In Chapter 2, I focus on identifying parturition sites and 5-week neonatal mortality using a novel movement-based approach, which I validate using animal-borne video collars, across

three study regions in northern Ontario. I compare selection ratios for three cover types and linear features for 80 caribou with a calf-at-heel during a neonatal (defined by movement rates postpartum) and a post-neonatal period (up to 35 days postpartum). Finally, I evaluate neonatal mortality using a time-to-event analysis based on habitat use and movement rates postpartum.

In Chapter 3, I propose that although site fidelity related to repeated space use has previously been documented in caribou (Schaefer et al. 2000, Ferguson and Elkie 2004, Faille et al. 2010), an alternative strategy is for an individual to express habitat fidelity: use the same habitat during a specific life history event regardless of the spatial location. I evaluate this premise using parturition sites identified with methods described in Chapter 2 for 56 caribou with $\geq$2 parturition events across the three study regions. I compare the frequency at which caribou expressed 1) no fidelity, 2) spatial fidelity, 3) habitat fidelity, or 4) both spatial and habitat fidelity, and relate the type of fidelity exhibited to adult female age, calf survival, and environmental characteristics within calving areas.

In Chapters 4 and 5, I assess the potential role of foraging resources in habitat selection of caribou during calving to late summer, which is a key reproductive and nutritional period for caribou (Parker et al. 1990, Pinard et al. 2012, DeMars and Boutin 2018, Cook et al. 2021, Denryter et al. 2022*b*). In Chapter 5, I use resource selection analyses, an approach increasingly used in conservation to identify habitat elements that may be critical for threatened and endangered species (Nielsen et al. 2006, Aldridge and Boyce 2007). However, to what degree inferences can be made from habitat selection analyses depends on the biological relevance of the covariates included in the analysis (Searle et al. 2007). Therefore, in Chapter 4, I develop models based on field data for forage quantity and quality, and diet selection and intake rates from foraging trials of captive caribou (Cook et al. *in prep.*), to produce dynamic, summer

foodscapes (Searle et al. 2007) for two of the three study areas that differ in physiography, disturbance regimes, and climate. I compare the spatiotemporal dynamics of forage resources in the two areas to assess whether these differences might provide context to dissimilar performance of caribou inhabiting these areas. In Chapter 5, I then associate movement data from 91 GPS-collared caribou with known reproductive state (barren, calf died within 5-weeks postpartum, calf survived at least 5-weeks postpartum; Chapter 2) across the three study areas to compare how the reproductive groups make trade-offs across the summer in selecting areas with varying levels of forage resources and predation risk.

Finally, in Chapter 6, I summarize the main findings of my thesis and discuss their implications for caribou conservation and management.

Chapter 2

Comparison of woodland caribou calving areas determined by movement patterns across northern Ontario

Published in Journal of Wildlife Management

Introduction

Caribou populations are declining globally (Vors and Boyce 2009, Festa-Bianchet et al. 2011), and in Canada, boreal woodland caribou (*Rangifer tarandus caribou*; caribou) are listed as threatened under Canada's *Species at Risk Act* (Committee on the Status of Endangered Wildlife in Canada 2014, Government of Canada 2019) and Ontario's *Endangered Species Act* (Government of Ontario 2007). The persistence of caribou populations is contingent on effective management of the species (Festa-Bianchet et al. 2011), which depends on reliable estimates of adult female survival and calf recruitment (Bonenfant et al. 2005). Caribou exhibit low fecundity (litter size of 1; Jönsson 1997) and highly variable calf survival (0.23–0.79; Mahoney et al. 1990, Gustine et al. 2006, Pinard et al. 2012). Rates of adult female survival are typically higher than those of juveniles across their range (0.75–0.92; Mahoney and Virgl 2003, Courtois et al. 2007, Hervieux et al. 2013, Fryxell et al. 2020, Johnson et al. 2020). Some management actions that focus on improving female survival may be less effective at improving population growth than actions that target juveniles because of evolutionary canalization (Gaillard and Yoccoz 2003, Johnson et al. 2010). If adult female survival is canalized against environmental variation (Gaillard and Yoccoz 2003), substantial changes in environmental conditions by management would be necessary to observe an appreciable effect on population growth. Although juvenile recruitment in ungulates often has lower elasticity than adult survival (Gaillard et al. 1998, Bonenfant et al. 2005), it can nonetheless play a key role in population growth under favorable conditions (Raithel et al. 2007, DeCesare et al. 2012) and contribute significantly to variability in population dynamics (Gaillard et al. 2000). Therefore, assessing calf recruitment is important to understand caribou persistence in local populations.

Advancements in global positioning system (GPS) technology have facilitated the understanding of birth and calf mortality rates, two integral components of juvenile recruitment of ungulates, and what influences them. Past approaches for identifying these events included costly or time-intensive aerial and ground searches for neonates during the parturition period (Kuck et al. 1985, Ciuti et al. 2006, Whiting et al. 2012), expelled vaginal implant transmitters (VITs) from pregnant females (Carstensen et al. 2003, Barbknecht et al. 2011, Berg 2019), and radio-tagging calves to monitor survival (Mahoney and Virgl 2003, Gustine et al. 2006, Patterson et al. 2013). Recent approaches to identify parturition events of ungulates have been based on abrupt changes in movements (Ferguson and Elkie 2004, Long et al. 2009, Peterson et al. 2018, Nicholson et al. 2019) or clustering of GPS locations in space and time (Bowyer et al. 1999, Welch et al. 2000, Severud et al. 2015). In the validations of these approaches, Dzialak et al. (2011) reported a 93% correct classification accuracy of elk (*Cervus canadensis*) parturition events, and Berg (2019) reported predicted dates of elk parturition within 1.43 ± 0.85 (SD) days of the actual parturition dates. In the case of caribou, DeMars et al. (2013) developed a movement approach (i.e., the DeMars approach) to infer parturition events and neonatal mortality events up to five weeks, which coincides with most caribou neonatal mortalities events (Mahoney et al. 1990, Whitten et al. 1992, Adams et al. 1995, Stuart-Smith et al. 1997, Pinard et al. 2012). In the three studies that have used this approach (Nobert et al. 2016, Bonar et al. 2018, Cameron et al. 2018), they either did not fully meet model assumptions (e.g., applied to non-sedentary caribou) or did not assess the accuracy of predictions.

We build upon the work of Viejou et al. (2018) who reported that video-collared female caribou with calves-at-heel in the Nakina and Pickle Lake regions showed stronger selection for sites with low predation risk than those without young, especially during the post-parturition

period. Additional studies, including those in Nakina and Pickle Lake (Avgar et al. 2015, McGreer et al. 2015, Hornseth and Rempel 2016), indicate caribou select vegetation communities during calving primarily to minimize predation risk (McLoughlin et al. 2005, Wittmer et al. 2005). Low-risk areas in boreal ecosystems include lowlands (McLoughlin et al. 2005) because black bears (*Ursus americanus*) and wolves (*Canis lupus*) select against them (James et al. 2004; Latham et al. 2011; Kittle et al. 2015, 2017; DeMars and Boutin 2018) presumably because of a lack of bear-specific forages (Mosnier et al. 2008, Latham et al. 2011) or low use by moose (*Alces alces*; James et al. 2004, Street et al. 2015), which are wolves' primary prey in our study area (Fryxell et al. 2020). At the same time, caribou may select against early seral stands (<20 years old; Avgar et al. 2015, McGreer et al. 2015, Hornseth and Rempel 2016) because alternative prey like moose and white-tailed deer (*Odocoileus virginianus*) prefer these stands (Bowman et al. 2010, Street et al. 2015), which attract predators (Brodeur et al. 2008; Kittle et al. 2015, 2017) and make these areas risky. Closed-canopied stands also may reduce predation risk because low lateral cover (Thompson 1994) enhances predator detectability and evasion (Gustine et al. 2006, Carr et al. 2007, Pinard et al. 2012). Finally, if linear features, such as seismic lines and roads, provide access for wolves and black bears into prey refugia (Latham et al. 2011, DeMars and Boutin 2018) or increase movement and prey encounters (McKenzie et al. 2012; Dickie et al. 2017, 2020; Muhly et al. 2019; Newton et al. 2019), caribou may select against areas near linear features (James and Stuart-Smith 2000, Avgar et al. 2015, McGreer et al. 2015, Dickie et al. 2020).

Here we start by providing a rigorous test of the DeMars approach for 20 individual caribou with animal-borne video collars. Once validated, we applied the DeMars approach to the movements of an additional 78 individuals across three regions (Pickle Lake, Nakina, and

Cochrane) in northern Ontario, Canada. We compared pregnancy rates determined from blood assays at capture and predicted parturition and neonatal mortality rates among regions because these areas are reported to differ in their ability to support caribou (Ontario Ministry of Natural Resources and Forestry [OMNRF] 2014*a*, Fryxell et al. 2020). We compared selection and movements of female caribou with calves-at-heel during the neonatal (defined by initial low movement) and the post-neonatal period (up to 35 days postpartum) to explain potential differences observed in demographic rates among the regions. We hypothesized that caribou would select more strongly for areas of low predation risk during the neonatal period, when calves are least mobile and more vulnerable, compared to the post-natal period (Whitten et al. 1992). We predicted that if mobility of neonatal calves influenced selection for low-risk areas, overall selection by female caribou for lowlands and closed-canopied forests would be relaxed during the post-neonatal period and there would be less selection against early seral stands and areas near linear features. Changes in selection may depend on predator density and linear features, which in this study were highest at Nakina compared to Pickle Lake and Cochrane (OMNRF 2014*a*, Fryxell et al. 2020). Thus, we predicted that caribou in Nakina would maintain the strongest selection for low-risk areas and have the lowest movement rates during the post-neonatal period (Testa et al. 2000). We predicted caribou with higher movement rates would have increased neonatal mortality (Testa et al. 2000) because of greater detection or encounters with predators (Daly et al. 1990, Boinski et al. 2000). Therefore, we expected that a combination of movement rates and use of low-risk areas postpartum would best explain neonatal mortality across regions.

Study area

The Pickle Lake (90.938W, 51.568N; 23,000 km^2), Nakina (87.548W, 50.388N; 23,000 km^2), and Cochrane (80.598W, 49.908N; 23,000 km^2) areas are in the boreal region of northern Ontario (Figure 2.1). Pickle Lake and Nakina are located in the Boreal Shield of northwestern Ontario and are dominated by till soils (Thompson et al. 2015), whereas the Cochrane study region, which is situated within the Northern Clay Belt region (a transition zone between the Boreal Shield and Hudson Bay Lowlands) in northeastern Ontario, is characterized by lacustrine soils (McMullin et al. 2013). Topography was characterized as rolling hills across study regions with elevation ranging from 162 m to 461 m above sea level. Cochrane has the greatest total annual precipitation (835 mm ± 79 mm; $\bar{x}$ ± SD, 20-yr average), followed by Nakina (779 mm ± 127 mm), and Pickle Lake (728 mm ± 128 mm; Environment Canada, https://climate.weather.gc.ca/historical_data/search_historic_data_e.html, accessed 14 Jun 2019). Summer was defined as 1 May–31 October and winter as 1 November–30 April. All areas were dominated solely or by mixtures of black spruce (*Picea mariana*), jack pine (*Pinus banksiana*), balsam fir (*Abies balsamea*), trembling aspen (*Populus tremuloides*), and white birch (*Betula papyrifera*; Rowe 1972). Cochrane had the highest extent of lowlands (swamp, bog, and fen; 64%), whereas Nakina and Pickle Lake both had 28% coverage of lowlands (OMNRF 2014*a*, Fryxell et al. 2020). At the time of the study (2010), Nakina had more harvest regeneration (<40 years; 22%) than in Cochrane (13%) or Pickle Lake (0.04%; OMNRF 2014*a*, Fryxell et al. 2020). Nakina and Cochrane have been actively logged for commercial forestry since 1970 (Fryxell et al. 2020), where Pickle Lake has not been actively logged since the 1960s (Thompson et al. 2015). Pickle Lake had greater proportions of natural disturbance (proportion burned <50 years; 12%) compared to Nakina and Cochrane (both 4%; OMNRF 2014*a*, Fryxell et al. 2020).

Cochrane had the largest proportion of closed-canopied forest (>25% canopy closure; 71%) followed by Pickle Lake (64%) and Nakina (56%; OMNRF 2014*a*, Fryxell et al. 2020). Linear feature density ranged from 0.05 km/km^2 in Pickle Lake to 0.42 km/km^2 in Nakina and 0.31 km/km^2 in Cochrane (OMNRF 2014*a*, Fryxell et al. 2020). Nakina had high wolf (6.7 wolves/1,000 km^2) and moose densities (11.8 moose/100 km^2), with lower densities in Pickle Lake (4.2 wolves/1,000 km^2, 4.6 moose/100 km^2) and Cochrane (3.7 wolves/1,000 km^2, 3.8 moose/100 km^2; OMNRF 2014*a*, Fryxell et al. 2020), whereas black bear densities were similar across all 3 study regions (20–40 black bears/100 km^2; Rodgers et al. 2009, Howe et al. 2013).

Methods

Animal Data

We used three data sets from 186 adult female caribou that we captured by helicopter net-gun in 2010–2013 (Ontario Ministry of Natural Resources and Forestry Wildlife Animal Care and Use permits 10–183, 11–183, 12–183, 13-183). We fit caribou with Lotek Iridium GPS or GPS-Argos animal-borne video collars (Thompson et al. 2012), GPS-Argos radio-collars (Telonics, Mesa, AZ, USA; Lotek Wireless, Newmarket, ON, Canada), or GPS-Iridium radio-collars (Lotek Wireless). Average age at capture was 5.7 ± 2.1 years old (SD; range = 2–11) based on tooth wear (van den Berg et al. 2021). We determined pregnancy status of the 186 prime-aged caribou (2–11 years old) via blood samples using pregnancy-specific protein B (PSPB) levels (BioTracking, Moscow, ID, USA). We used location and video data from 20 caribou (22 caribou-years; Pickle Lake: n = 4, Nakina: n = 9, Cochrane: n = 9) with video collars to validate the DeMars approach for determining live parturition events and neonatal mortality rates. Video collars recorded 10-sec video clips every five mins from 0800 to 1000 and then again from 1500 to 1700 each day, resulting in eight mins of footage per day per caribou. We used location data

from an additional 78 caribou (85 caribou-years; Pickle Lake: n = 26, Nakina: n = 37, Cochrane: n = 22) to predict parturition and neonatal mortality events with the DeMars approach. Because we monitored only 9 of 98 (i.e., 78 + 20) caribou individuals for >1 year, we pooled data across years, resulting in our sample of 107 caribou-years (Pickle Lake: n = 30, Nakina: n = 46, Cochrane: n = 31). Fix rate success across all 107 caribou-years was 97% (91–100%). Of these, 80 caribou-years with a calf-at-heel contributed to the analysis of female selection postpartum, and we used 79 caribou-years to assess factors influencing neonatal mortality.

Assessment of Parturition and Neonatal Mortality Predictions

We compared predictions of parturition and neonatal mortality events from the individual-based DeMars approach made from GPS relocations of video-collared individuals to parturition and neonatal mortality events identified in the video footage. The individual-based approach differs from the population-based approach by predicting parturition and neonatal mortality events for each individual, compared to producing a population model based on individuals with known parturition and neonatal mortality events, and has higher accuracy compared to the population-based approach (DeMars et al. 2013). We identified parturition events of video-collared individuals by the presence of a calf in the footage (Figure 2.2; Thompson et al. 2012, Viejou et al. 2018). We assumed that parturition date was the time associated with the first footage of a calf and that neonatal mortality occurred on the first date when the calf was no longer present in the rest of the footage. We removed low accuracy GPS fixes (i.e., <3-dimensional fixes; Frair et al. 2010) and rarefied 1-hr fix rates to 3-hr fix rates to be similar to the 2.5-hr fix rate from all collar data sets.

DeMars et al. (2013) defined three *a priori* movement models, which are fit to an individual's sequence of step lengths (defined as the distance between regularly sampled

relocations) to distinguish reproductive status based on the scale parameter of the distribution of step lengths (Figure 2.3). When parturition does not occur (M0), the scale parameter of the movement model remains constant across the calving period (i.e., the expected distribution of step lengths is the mean step length). When a female gives birth and the calf survives to five weeks postpartum (M1), the step lengths decrease significantly from pre-parturition levels, resulting in an identifiable break point. After the break point, the step lengths of a female with a calf-at-heel increase linearly over time with a constant slope and become similar to the movement rates of pre-parturition. When the female loses its calf within the first five weeks (M2), step length increases rapidly, creating a second break point. When applied to GPS data, the best model (M0, M1, or M2) for describing the movement pattern of each individual is determined using model selection and Akaike's Information Criterion (AIC). Following DeMars et al. (2013), we specified the time it takes a female with a calf to return to pre-parturition movement rates to be 3–6 weeks postpartum, and constrained the predicted break points (parturition or neonatal mortality) to be a minimum of 2.5 days or 3.0 days (24 steps at 2.5-hr or 3-hr fix rate, respectively) away from the beginning (1 May) and the end (30 June) of the movement sequence and from each other. Therefore, parturition events could not be predicted <2.5–3.0 days after 1 May and neonatal mortality could not be predicted <2.5–3.0 days after the predicted parturition break point or <2.5–3.0 days before 30 June because there would be an inadequate number of step lengths to estimate a breakpoint. We approximated all scale parameters describing the distribution of step lengths with maximum likelihood estimators (DeMars et al. 2013). DeMars et al. (2013) rarified the step lengths by removing the top 1% of step lengths. Based on sensitivity analysis where we removed the top 1–4% of step lengths, we chose to eliminate the top 2% of step lengths for parturition timing and 4% for neonatal mortality

because the remaining data provided the most accurate model predictions when compared to results from the video collar footage (Appendix 1.1).

Calving, Neonatal Areas, and Movement Rates

We evaluated differences in the mean rates of pregnancy and parturition among regions using a pair-wise Fisher's exact test with a Bonferroni correction adjustment ($\alpha = 0.025$). We assessed differences in the timing of births by comparing cumulative frequency distributions of parturition events among study regions using Kolmogorov-Smirnov tests with Bonferroni correction ($\alpha = 0.025$).

We delineated neonatal areas for caribou that were predicted or known to give birth. For each caribou-year, we derived the neonatal area by relating the rate of net-displacement (m) from the parturition site to all subsequent relocations through time and fit a piece-wise regression (Johnson et al. 2002) to determine the first break point in the rate of increase in net displacement after parturition (Appendix 1.2). We then used all GPS relocations up to the breakpoint date to derive a 95% isopleth utilization distribution (UD) to define the neonatal area, specifying the smoothing parameter as the reference bandwidth, because it visually provided adequate representation of caribou spatial use. We then compared number of days spent within the neonatal area and size of the neonatal area among study regions using a Kruskal-Wallis test and a *post hoc* Dunn's multiple comparisons test with Bonferroni correction (Dunn 1961; $\alpha = 0.025$). We calculated mean daily postpartum movement rates (km/hr) for each caribou-year. We used linear regressions to test for differences in postpartum movement rates among study regions (interaction between day postpartum and study region with Cochrane as the reference category).

Caribou Resource Selection on Neonatal and Post-Neonatal Areas

We compared third-order selection (Johnson 1980) by caribou with calves-at-heel (n = 80) for areas of three specific land cover types and linear features within 1 km during the neonatal period (parturition to date defined by the break in the piecewise regression) and post-neonatal period (period from break in movements to date of neonatal mortality or 35 days postpartum) to random locations (10 random:1 caribou location) within calving and summer 95% UDs (1 May to 30 September). All neonatal mortality events occurred after each individual's neonatal period, and we excluded the locations of individuals after they lost their neonate from the post-neonatal selection analysis. We derived the three non-exclusive, binary land cover types by collapsing the 24 land cover types of the Ontario Far North Land Cover layer (version 1.4; OMNRF 2014*a*) and included lowlands (bog, swamp, or fen vs. upland [coniferous, sparse, mixed-wood, or deciduous]), overstory class (open vs. closed overstory canopy cover [≤25% vs. >25%]), and seral stage (early vs. mid-late seral stages [<20 vs. ≥20 years]). We used these broad land cover stand types to minimize land cover misclassification errors and because they are relevant to predation risk (McLoughlin et al. 2005, Wittmer et al. 2005, Kittle et al. 2015). We updated land cover maps annually to account for yearly disturbance created through silvicultural practices based on OMNRF depletion records (OMNRF, unpublished data), whereas we used one linear feature map (Hornseth and Rempel 2016) that included roads (primary, secondary, tertiary, winter roads), powerlines, and railways (OMNRF Road Network, Utility Line, and Railways layers) throughout.

We used a selection ratio approach rather than a general linear model to assess selection (Manly et al. 2002) because land cover types were not mutually exclusive (i.e., lowland could be an open or closed-canopied stand) and all covariates (lowlands, early seral stands, closed-

canopied, within 1 km of a linear feature) were categorical. We summarized individual selection ratios across and by study region and bootstrapped (1,000 times) ratios to acquire 95% confidence intervals. Confidence intervals not overlapping one indicated statistically significant selection. The neonatal and post-neonatal area of one individual's caribou-year was outside the extent of the Ontario Far North Land Cover layer, and therefore we used 80 caribou-years in the selection analysis.

Neonatal Mortality and Associated Factors

We derived neonatal mortality rate from the proportion of calves within a study region that died within 35 days (5 weeks) postpartum. We evaluated pair-wise mean differences in rates of mortality across this postpartum period among study regions using Fisher's exact test with a Bonferroni correction adjustment ($\alpha = 0.025$). We compared the timing (days) of mortality from parturition among regions using a Cox proportional hazard model with Cochrane set as the reference category (Cox 1972).

To test our predictions, we related the time to a mortality event (event = 1) to the proportion of GPS locations from birth to the day of neonatal mortality (or censored at 35 days; $n = 79$) within lowlands, early seral stands, closed-canopied stands, 1 km of a linear feature, and age-corrected movement rates using Cox proportional hazard models and their interactions. Because land cover types were not mutually exclusive, we did not include multiple land cover types in the same model. Because movements rates increase with calf age, we used daily age-adjusted movement rate (km/hr) calculated as the difference between the mean daily movement rate of an individual and the mean movement rate of all individuals with calves alive on that day. There was no correlation (Spearman's rank-order correlation, $|r| > 0.5$) between covariates included in competing models, but we tested top models with >2 covariates for multicollinearity

using variance inflation factors (VIF). We used Akaike's Information Criterion corrected for small sample size (AIC_c) for model selection, where the best fit model was based on $\Delta AIC_c < 2$ (Burnham and Anderson 2002). We tested the top model for proportional hazard over time, an assumption of Cox proportional hazard models, using Schoenfeld residual analysis (Cleves et al. 2008; $\alpha = 0.5$). Upon preliminary analysis, early seral stands did not pass the Schoenfeld residual test ($P = 0.01$) because of one outlier individual; therefore, we removed that individual from the analysis evaluating land cover and movement rates (Appendix 1.3), resulting in 79 caribou-years used in that analysis.

We evaluated the robustness of our top model of neonatal mortality to the potential misclassification error of the three binary land cover types within Ontario Far North Land Cover layer by conducting a sensitivity analysis, where we randomly switched the binomial classification of 5–20% of the caribou locations to assess the effect of the misclassification error on our conclusions. We re-ran the Cox proportional hazard models for the data sets with each level of induced error and, if a model resulted in $\Delta AIC_c > 2$ from the original Cox proportional hazard model with no induced error, we concluded that the model was not sufficiently robust at that level to support our conclusions. We conducted all analyses in the statistical computing program R (R version 3.5.1, www.r-project.org, accessed 8 January 2017).

Results

Of the caribou predicted to give birth, we observed one stillbirth in the video footage, which we classified as barren for subsequent analysis. Using the DeMars approach, we correctly predicted 100% ($n = 22$) of the live parturition events from the video data, and rarefication of step lengths from 1% up to 4% did not alter the outcome of predicted parturition events (Appendix 1.1). The deviation in predicted date of parturition using a 2% rarefication rate compared to the video

footage was 1.08 ± 0.28 days ($\bar{x}$ ± SE, n = 17). The mortality of live-born calves was most accurately classified when using a 4% rarefication of step lengths (Appendix 1.1) with 15 of 17 correctly classified. Two caribou were predicted to have their calves survive the full five weeks, but according to the video footage they did not; we did not observe these two calves in the later weeks of the post-neonatal period.

The pregnancy rate was 0.87 and parturition rate was 0.76 across regions (Table 2.1), with no statistically significant differences among regions (Fisher's exact test, $P > 0.16$). Dates of parturition across regions ranged from 6 May to 19 June, with the cumulative distribution of parturition dates (Figure 2.4A) indicating proportionally more calves were born later in Cochrane (median = 23 May) than in Nakina (16 May) and Pickle Lake (17 May; Kolmogorov-Smirnov, $P < 0.001$).

Caribou spent a median of ten days (range = 2.4–33.1) in a localized area of 2.4 ± 2.9 km^2 around the parturition site, which we defined as the neonatal area. Mean sizes and time spent within the neonatal area (Table 2.1) did not differ among study regions (Kruskal-Wallis, both $P = 0.9$). Caribou movement rates increased with the age of the neonate postpartum (Figure 2.5) and the rate of increase in movement with age was greater in Cochrane (i.e., reference) compared to Pickle Lake (−0.0017 ± 0.0008, β ± CI) and Nakina (−0.0023 ± 0.0008, β ± CI).

Across study regions, caribou with a calf-at-heel consistently selected for closed-canopied stands and lowlands, and mostly against linear features during the neonatal and post-neonatal periods (Table 2.2). Within study regions, caribou selection for lowlands was significant only during the post-neonatal period because of the higher variation in lowlands use among the smaller sample of individuals within regions (Appendix 1.4). Caribou generally selected against early seral stands across both periods, but high variation in individual caribou

use of early seral stands in Nakina and Pickle Lake resulted in non-significant selection during the neonatal and post-neonatal periods, respectively (Appendix 1.4). Similarly, caribou selected against areas near linear features during both periods with the exception of Cochrane during the post-neonatal period.

Thirty percent of caribou that had live births lost their calves within 5 weeks of birth (Table 2.1). The 5-week mortality rate (Fisher's exact test, $P > 0.10$) and time to mortality from birth (Figure 2.4B) did not statistically differ among study regions (Cox proportional hazard, $P > 0.11$). There was equal support ($AIC_c < 2$) for three hazard models (Table 2.3). The model with decreasing risk of neonatal mortality with increased proportional use of early seral stands had the most support, but 95% confidence intervals of the parameter estimate overlapped zero (-45.49 ± 47.49, $\beta \pm CI$). Of the other two supported models, one indicated increasing mortality risk with greater use of lowlands (3.05 ± 1.96), and the other similarly indicated increasing mortality with use of lowlands (3.40 ± 2.10) but also included the variable age-corrected movements (58.73 ± 65.78) and an interaction between use of lowlands and movements (-77.80 ± 79.34), with the latter two coefficients overlapping zero. The correlation between proportional use of early seral and lowland cover types was low ($r^2 = 0.09$), suggesting that these land use categories captured different habitat features. All three models met the assumption of proportional hazard over time based on the Schoenfeld residual analysis ($P > 0.06$) with no multicollinearity between proportional use of lowlands and age-corrected movement rates (VIF < 1.17). Sensitivity analysis indicated that the Cox proportional hazard model with early seral stands was robust (i.e., $\Delta AIC_c < 2$ from original model) up to 5% induced error, whereas models with lowlands interacted with movement rates and lowlands alone were robust up to 5% and 20% induced error, respectively (Appendix 1.5).

Discussion

The DeMars approach (DeMars et al. 2013) applied to caribou movements in Ontario provided accurate estimates of live parturition events (100%) and reasonably accurate estimates of neonatal mortality events (88%), but the extent of rarefication of step lengths influenced the accuracy of the predictions. A 2% rarefication of step lengths for parturition improved the accuracy of predicted timing of parturition by 1.5 days compared to the 1% rarefication of step lengths used in DeMars et al. (2013; Appendix 1.1). Use of a 4% rarefication of step lengths to predict neonatal mortality, instead of a 1% rarefication, improved the accuracy from 53% to 88%. By removing a greater percentage (4% vs. 1%) of step lengths, we removed larger steps that did not reflect a neonatal mortality breakpoint (i.e., the DeMars approach predicted that the neonate died, whereas the video collar footage identified the calf was alive).

A constraint pointed out by DeMars et al. (2013) in using movements to define parturition events in caribou is that it predicts live births and does reflect parturition events when calves are stillborn, non-viable (i.e., too weak to nurse), abandoned, or killed immediately postpartum because neonatal mortality cannot be predicted within 2.5–3 days of the parturition break point (depending on the fix rate interval used). This was evident in our video collar assessment where a single caribou had a stillbirth. We did not find a decrease in movement rates reflecting a parturition event, so the caribou was misclassified by the DeMars approach as barren (Appendix 1.6). In the case of the larger set of collared caribou, we also failed to detect live parturition events for 13% of the caribou that were identified as pregnant (n = 48; Appendix 1.7). This loss rate (i.e., difference between being pregnant but not predicted to give a live birth by the DeMars approach) illustrates the potential limitation of the DeMars approach to predict parturition events in general. The limited data available on loss of caribou calves indicates late *in*

utero reabsorption events are rare (Dauphiné 1976, Ringberg and Aakvaag 1982) but that perinatal mortalities can be as high as 22% (Bergerud 1971, Roffe 1993). Determining the extent of perinatal mortality by comparing pregnancy data to predicted parturition events may be necessary to assess the extent to which live births predicted by movements reflect all birth events and the combined rate of mortality.

Although our estimates of caribou pregnancy (0.90–1.00; Seip and Cichowski 1996, McLoughlin et al. 2003, Courtois et al. 2007, Mahoney and Virgil 2003) and parturition rates (0.56–0.89; Rettie and Messier 1998, Gustine et al. 2006, Nagy 2011, Pinard et al. 2012) were consistent with measures reported elsewhere, we were surprised by the low parturition rate in Pickle Lake (0.67) because of the high pregnancy rate (Table 2.1). This discrepancy could be due to greater perinatal mortality in Pickle Lake, or that by chance the subsample used to estimate rate of parturition had a lower proportion of pregnant females (81% pregnant; Appendix 1.7) versus in the full sample (92% pregnant; Table 2.1). Nevertheless, our data provide little support for differences in either pregnancy or parturition rates among regions.

The median parturition date at Cochrane was 6–7 days later than the other two regions. Later birth date is consistent with delayed ovulation in ungulates due to reduced body fat (Cameron et al. 1993, Adamczewski et al. 1997, Cook et al. 2001, Langvatn et al. 2004) and lower nutrition during or around the time of breeding (Bronson and Manning 1991, Gerhart et al. 1997, Martin et al. 2004). Crête et al. (1993) also reported caribou calving date was related to dietary quality in the previous summer, with caribou on a higher plane of nutrition giving birth earlier. Delayed births may also be related to the 1.5–2.0 times greater snow fall in November to April in Cochrane (Appendix 1.8) compared to Nakina and Pickle Lake. Barren-ground caribou give birth later following winters with deep or longer snow cover (Bergerud 1975, Skogland

1983, Cameron et al. 1993), which they attributed to maternal undernutrition during winter (Skogland 1983, Cameron et al. 1993) resulting in a longer gestation period (Bergerud 1975, Rowell and Shipka 2009).

Neonatal mortality in Cochrane was almost twice that of the other regions, although relatively low sample sizes limit the strength of this conclusion. If longer snow cover contributes to a delayed growing season in Cochrane, it also could contribute to higher neonatal mortality. Bergerud (1975) reported that the weights of calves at birth were less in years with greater snowfall, and calves with lower birth weights resulted in higher neonatal mortality (Skogland 1983, Eloranta and Niemenen 1986, Pinard et al. 2012). Furthermore, studies have documented later born calves are more susceptible to predation (Whitten et al. 1992, Adams et al. 1995, Keech et al. 2000, Johnson et al. 2019). Evidence for later births and higher early neonatal mortality in combination with lower maternal condition (i.e., late winter body fat and body mass; J. Cook, R. Cook, and G. Brown unpublished data) in Cochrane as compared to Pickle Lake, suggest further attention is needed on summer forage dynamics in this region given the importance of summer nutrition in caribou (Crête and Huot 1993, Cameron et al. 2005, Post and Forchhammer 2008, Pachkowski et al. 2013, Schaefer and Mahoney 2013) and ungulates in general (Hjeljord and Histøl 1999, Cook et al. 2013, Hurley et al. 2014, Proffitt et al. 2016, Cook et al. 2018). Whether summer nutrition under some winter climatic conditions may influence neonatal survival directly or indirectly through predation warrants further investigation.

Selection patterns by caribou were most consistent with minimizing predation by selecting against areas of high risk and using areas that predators avoid. For example, linear features enhance the travel efficiency of predators, which can increase encounters with prey (McKenzie et al. 2012; Dickie et al. 2017, 2020; Kittle et al. 2017; Newton et al. 2017). For this

reason, we expected caribou to consistently select against areas near linear features (Leclerc et al. 2012, Pinard et al. 2012, DeMars and Boutin 2018), especially with a calf-at-heel (Viejou et al. 2018), but our results were mixed. We were limited at Pickle Lake in evaluating use of linear features because they were relatively rare. Nevertheless, caribou in Nakina and Cochrane strongly selected against linear features during the neonatal period, and caribou in Cochrane relaxed their selection after they left the neonatal areas. Constant selection over time against linear features in Nakina is consistent with the highest wolf densities there (OMNRF 2014*a*, Fryxell et al. 2020), whereas in Cochrane, caribou did not as readily select against linear features after they left the neonatal area, possibly because of lower wolf densities or because their accelerated movements (Figure 2.5) made linear features more difficult to avoid.

Caribou also exhibited consistent selection against early seral stands, which has been attributed to high predation risk associated with high secondary prey, such as moose and deer, that attract predators (Seip 1992). But at Pickle Lake, use of early seral stands by caribou was highly variable in the post-neonatal period compared to caribou in Nakina and Cochrane. Pickle Lake is the least managed region and has not been actively logged since the 1960s (Thompson et al. 2015). Early seral stands (<50 yr) in this region result from fires (~100% of early seral areas) compared to timber harvest, as in the other regions (~15% and 24% of early seral stands originate from fire in Nakina and Cochrane, respectively). Relaxed selection against early seral, burned areas in Pickle Lake cannot be explained by improved lichen (e.g., *Cladonia* spp.) availability because lichens are reduced more after fire than timber harvests (Klein 1982, Schaefer and Pruitt 1991, McMullin et al. 2013). For example, in an adjacent study region, Silva et al. (2019) reported that ground lichens were essentially absent from burns 0–19 years old in dense and sparse overstory types, and it was not until 25 years after burning that lichens began to

increase in sparse-canopied forests. Also, the value of lichens to meet caribou protein requirements when lactating is very low (Bergerud 1972, Person et al. 1980, Klein 1990, Johnson et al. 2000), and energy intake may be constrained by low bite mass that reduces daily dry matter intake rates (Denryter 2017).

Deciduous shrubs dominate fire-regenerating stands, which are considered preferable moose forage (Schwartz and Franzmann 1989, MacCracken and Viereck 1990, Lord and Kielland 2015, Joly et al. 2017), and in some regions are preferable caribou forage (Bergerud 1972, Thomas et al. 1996, Denryter et al. 2017), although that was not observed by Thompson et al. (2015). High moose density also has not always been correlated with the extent of burns in boreal forests, possibly because of a lack of moose-specific browse regeneration (DeMars et al. 2019). This is consistent with lower moose densities in Pickle Lake compared to the highly managed areas in Nakina. Additionally, fire-regenerating stands do not have the extent of linear features that are associated with timber-harvested stands, which may reduce their overall predator risk; this is consistent with Johnson et al. (2020), who reported that fire had less of a negative effect on caribou recruitment compared to human disturbances. Therefore, some burns may provide caribou with habitat of reduced predation risk and sufficient nutritional resources (Denryter et al. 2017).

Instead, caribou most consistently selected for closed-canopied forest stands in both the neonatal and post-neonatal periods. Dense overstory canopies can reduce understory shrub vegetation (Thompson 1994), which provides low lateral cover and could increase visibility to detect predators (Poole et al. 2007). Previous researchers documented that woodland caribou select parturition sites with low vegetative biomass (Gustine et al. 2006) and low lateral cover (Lantin et al. 2003, Carr et al. 2007, Leclerc et al. 2012, Pinard et al. 2012) to better evade

predators (Carr et al. 2007). Why caribou would continue to select closed-canopied forest as calves gain mobility in the post-neonatal period other than to reduce predation, is unclear. Lichens are less available in closed-canopied compared to open-canopied forests (Silva et al. 2019), but as described above, they are low in protein and small bite mass may diminish their value, especially during calving. Because closed-canopied forests were defined as >25% canopy closure, they include a range of openness in the canopies of coniferous, mixed-wood, and deciduous stands where sunlight is likely to penetrate and increase the diversity of caribou-specific forage resources in the understory (e.g., shrubs, forbs, and graminoids; Bergerud 1972, Thomas et al. 1994, Thompson et al. 2015, Denryter et al. 2017). A better understanding of the variation in forage resources available for caribou across this gradient is needed, especially during the period of early calving when lactation demands are high (White and Luick 1984, Parker et al. 1990).

Caribou showed selection for lowlands across study regions for the neonatal and post-neonatal period, with selection within regions showing similar trends even if non-significant during the neonatal period. High use of lowlands has been attributed to spatial separation from alternative prey to minimize exposure to wolves (Seip 1992, James et al. 2004, Wittmer et al. 2005, Pinard et al. 2012, Latombe et al. 2014). Use of lowlands has been viewed as caribou trading off forage for safety (McLoughlin et al. 2005); however, Mallon et al. (2016) reported greater biomass and higher productivity in lowlands compared to uplands in the Nakina region and suggested caribou may not be faced with reduced forage quality or quantity as previously assumed. In particular, they reported lowland understory communities provided equal foliar nitrogen concentration, lichen, and forb biomass, and greater graminoid biomass, which studies of video-collared caribou across the regions in this study indicate are key dietary components

(Thompson et al. 2015). But much of the productivity in lowlands is related to the high abundance of evergreen and ericaceous (e.g., velvetleaf blueberry [*Vaccinium myrtilloides*]) shrubs (Zoladeski and Maycock 1990, Mallon et al. 2016), which are rarely eaten by caribou (Thompson et al. 2015, Denryter et al. 2017), and to high sphagnum moss, which outcompetes lichens where organic material accumulates (Johnson 1981, Boudreault et al. 2002, Fenton et al. 2005, Keim et al. 2017). Because low abundances of forbs and graminoids in lowlands have been reported across northwestern Ontario (Zoladeski and Maycock 1990), understanding forage variability across regions is key. Additionally, Nakina and Pickle Lake are situated within the Boreal Shield, whereas Cochrane is situated in the Northern Clay Belt region, which is characterized by lacustrine soils (ONMRF 2014*a*), therefore resulting in different understory communities available to caribou (Thompson et al. 2015).

We found the most support for 5-week mortality of caribou calves increasing with use of lowlands, even when inducing up to 20% errors in classification of lowlands. This has not been reported previously and is not consistent within the current narrative of lowlands being refugia for woodland caribou (McLoughlin et al. 2005). Consistent with that narrative, Kittle et al. (2015, 2017) reported low wolf use of lowlands by 23 packs in Pickle Lake and Nakina. Black bear selection patterns in these regions are not well documented, but James et al. (2004) and Latham et al. (2011) reported that in Alberta, Canada, black bears do not select lowlands. In contrast, DeMars and Boutin (2018) observed in northeastern British Columbia, Canada, that wolves and black bears selected lowlands when linear features were present. We did not find support for increased neonatal mortality with high proportional use of linear features by caribou (DeMars and Boutin 2018) or support for a lowland-linear feature interaction. Linear feature densities, which are primarily forestry roads in our study, are low (0.5–0.42 km/km^2) relative to

northeastern British Columbia where they are primarily seismic lines (4.04 ± 3.23 km/km^2 [SD]; DeMars and Boutin 2018). Dussault et al. (2012) also documented an interaction between linear features and mixed-deciduous stands in Quebec, Canada, where risk of calf mortality increased as mixed-deciduous stands decreased, and linear feature density increased. We did not observe a lowland (opposite of uplands, which contained mixed and deciduous stands)-linear feature interaction, but the inclusion of multiple upland land cover types likely limits our capacity to detect an effect.

Finally, we found some evidence that risk of neonatal mortality increased with increased movement rates postpartum but less so when in lowlands (i.e., lowland-movement rate interaction). Modeling and field studies have shown that increased movements lead to increased predator-prey encounters (Daly et al. 1990, McKenzie et al. 2012) and higher mortality of calves (Testa et al. 2000). If movement is motivated by evading predation risk, consistent with a predator-prey shell game (Mitchell and Lima 2002), we would have expected the highest movements in Nakina because wolf and linear feature densities were highest in this region (OMNRF 2014*a*, Fryxell et al. 2020), but we did not. Instead, we saw the highest movement rates and neonatal mortality in Cochrane, which had the greatest extent of lowlands (64% of study region). Although caribou are considered capital breeders relying on body reserves for reproduction (Taillon et al. 2013), insufficient forage during the first month of lactation can deplete body reserves (Crête and Huot 1993). As a result, we hypothesize that high variability in nutritional resources among lowland sites may compel caribou to range more widely to satisfy daily nutritional requirements (de Knegt et al. 2007), which, in turn, may increase encounters with predators. More detailed movement studies of caribou relative to body condition and available forage resources during calving with simultaneous movement of predators would be

needed to determine how movement and individual condition may contribute to neonatal mortality (Courbin et al. 2013, Latombe et al. 2014).

Table 2.1. Pregnancy rate (n = individual caribou), parturition rate (n = caribou-years), median birth date, neonatal mortality rate (first 5 weeks postpartum, n = caribou-years), median and range of days spent in the neonatal area, and mean size (km^2) and SD of neonatal area used by caribou across three study regions in northern Ontario, Canada, 2010–2013.

Study region	Pregnancy		Parturition		Median birth dates	Neonatal mortality		Days at neonatal area		Neonatal area size	
	Rate	*n*	Rate	*n*		Rate	*n*	Median	Range	x̄	SD
Cochrane	0.85	66	0.84	31	23 May[a]	0.46	26	10.4	2.4–21.0	2.1	2.3
Nakina	0.82	57	0.76	46	16 May	0.23	35	10.0	2.7–27.6	2.2	2.6
Pickle Lake	0.92	63	0.67	30	17 May	0.20	20	7.6	5.3–33.1	3.3	4.1
x̄	0.87	186	0.76	107	21 May	0.30	81	10.0	2.4–33.1	2.4	2.9

[a] Cochrane birth dates were significantly later than Nakina and Pickle Lake ($P < 0.001$).

Table 2.2. Selection ratios and 95% CIs of closed-canopied stands, early seral stands (<20 years old), lowlands, and linear features during the neonatal and post-neonatal periods of adult female caribou with calves-at-heel (caribou-years $n = 80$; we removed locations of individuals after predicted neonatal mortality events) by study region in northern Ontario, Canada, 2010–2013.

Study region	Neonatal period				Post-neonatal period			
	Closed-canopied	Early seral	Lowlands	Linear features	Closed-canopied	Early seral	Lowlands	Linear features
Cochrane	1.31	0.045	1.13	0.22	1.23	0.02	1.23	0.87
95% CI	1.18, 1.43	0.00, 0.17	0.97, 1.29	0.013, 0.48	1.12, 1.35	0.001, 0.04	1.16, 1.31	0.26, 1.77
Nakina	1.38	0.62	1.32	0.059	1.41	0.42	1.24	0.08
95% CI	1.23, 1.58	0.23, 1.05	0.99, 1.67	0.00, 0.16	1.27, 1.62	0.17, 0.78	1.05, 1.43	0.01, 0.19
Pickle Lake	1.51	0.19	1.65	0.00	1.43	2.26	1.53	0.00
95% CI	1.28, 1.85	0.00, 0.46	0.83, 2.57	0.00, 0.00	1.20, 1.71	0.65, 4.60	1.03, 2.11	0.00, 0.00
$\bar{x}$	1.39	0.34	1.34	0.12	1.36	0.82	1.32	0.40
95% CI	1.28, 1.85	0.15, 0.56	1.08, 1.63	0.025, 0.22	1.26, 1.47	0.28, 1.52	1.16, 1.51	0.12, 0.76

Table 2.3. Model coefficients, number of model parameters (*K*), Akaike's Information Criterion corrected for small sample size (AIC_c), change in AIC_c from best model (ΔAIC_c), and model weights calculated from AIC_c (w_i) for competing Cox proportional hazard models relating mortality of neonates of global positioning system collared caribou ($n = 79$) in northern Ontario, Canada, 2010–2013, to proportional use of landscape variables (early seral stands, closed-canopied stands [closed], lowlands, linear features [LF]), and age-corrected movement rates (move).

Model	Early seral	Closed	Lowland	LF	Move	*K*	AIC_c	ΔAIC_c	w_i
Early seral	−45.49					2	182.79	0.00	0.23
Lowland			3.05			2	183.30	0.51	0.18
Lowland × move[a]			3.43		58.73	4	183.86	1.07	0.14
Lowlands + LF			3.38	−1.03		3	184.79	2.00	0.09
Lowlands + move			3.22		−6.64	3	184.89	2.10	0.08
Early seral × move[b]	−81.68				2.62	4	185.03	2.24	0.08
Early seral + LF	−46.16			0.38		3	185.08	2.29	0.07
Early seral + move	−45.07				−1.44	3	185.17	2.38	0.07
Lowland × LF[c]			3.26	−54.19		4	185.40	2.61	0.06
Null						1	193.88	11.09	0.00
Closed		3.15				2	194.02	11.23	0.00
LF				0.40		2	195.92	13.13	0.00
Move					−1.10	2	196.05	13.26	0.00
LF × move[d]				0.52	4.69	4	196.66	13.87	0.00
LF + move				0.51	−2.36	3	198.25	15.46	0.00

[a] Interaction of lowlands and age-corrected movement (lowlands × move: $\beta = -78.80$)
[b] Interaction of early seral and age-corrected movement (early seral × move: $\beta = -1{,}770.26$)
[c] Interaction of lowlands and linear features (lowlands × LF: $\beta = 53.98$)
[d] Interaction of linear features and age-corrected movement (LF × move: $\beta = -133.59$)

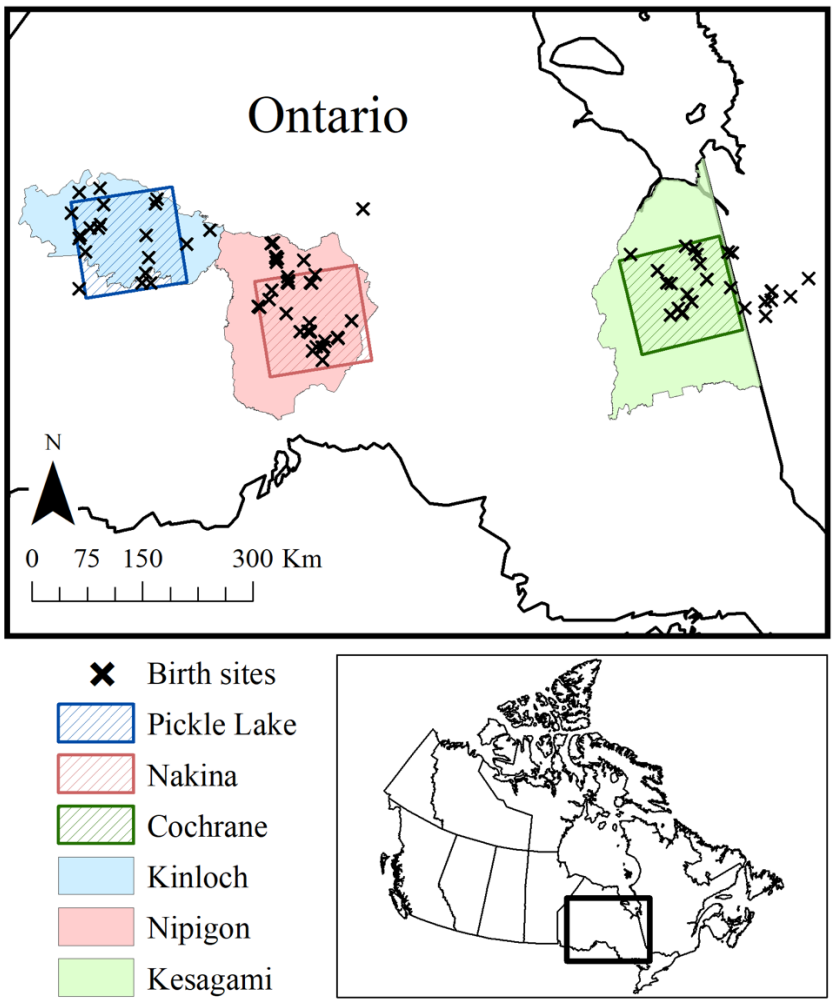

Figure 2.1. Location of the three study regions (Pickle Lake, Nakina, Cochrane) within northern Ontario, Canada, and their respective designated caribou ranges (Kinloch, Nipigon, Kesagami). The locations of caribou birth sites from 2010 to 2013 are indicated (n = 81).

Figure 2.2. Newborn caribou calf identified on 15 May 2012 from the animal-borne video collars in northern Ontario, Canada.

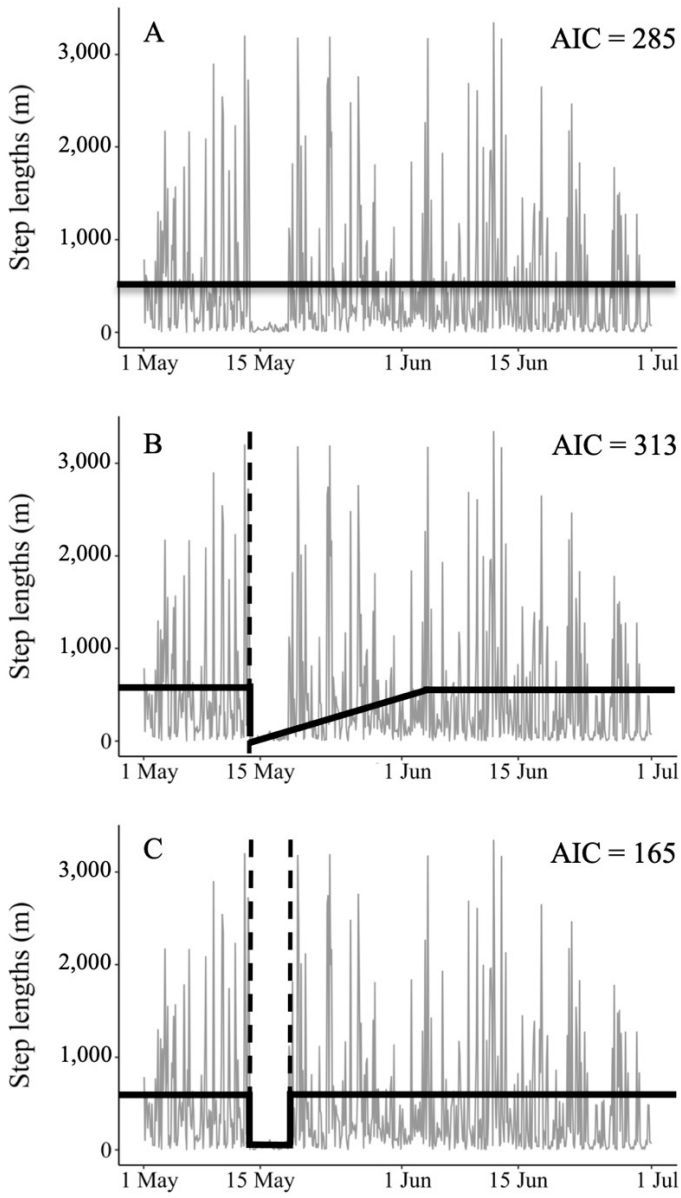

Figure 2.3. Example of three *a priori* movement models in the DeMars approach fit to movement data of the same adult female caribou between 15 May and 30 June 2013 in northern Ontario, Canada. In all three graphs, the vertical grey lines represent step lengths of a caribou that gave birth on 13 May and lost her calf on 18 May. Solid black lines represent the mean step length related to the scale parameter for each model, whereas the vertical dashed lines represent the predicted break points. Constant mean step lengths over the calving period indicate no parturition event (A; M0); a single break point followed by a linear increase in step lengths to pre-parturition movement rates indicates a female with a calf that survived (B; M1); and two break points indicate a female with a calf that died (C; M2). In this example, the model that predicted the female having a calf and losing it was the best fit, based on the lowest Akaike's Information Criterion (AIC) value.

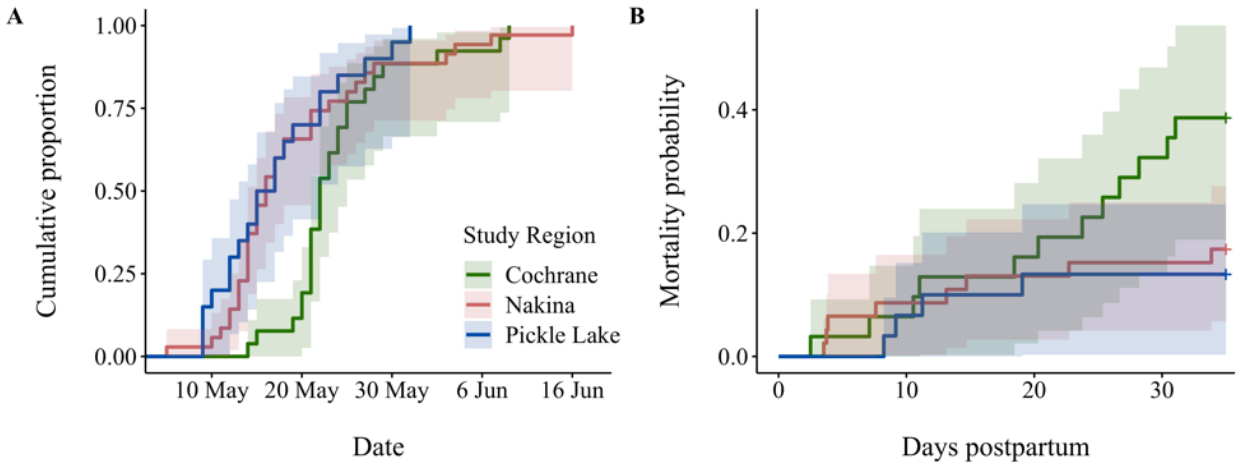

Figure 2.4. A) Cumulative proportion of parturition dates of caribou-years in Cochrane (n = 26), Nakina (n = 35), and Pickle Lake (n = 20) in northern Ontario, Canada, 2010–2013, based on combining data from video collar footage (n = 17) and predicted date (n = 64) of parturition from the DeMars approach. B) Kaplan-Meier mortality probability of neonates (n = 81) per study region, based on combining data from video collar footage (n = 17) and predicted date of neonatal mortality from the DeMars approach (n = 64). Twenty-four (30% of calves) neonatal mortality events occurred in the first 35 days postpartum.

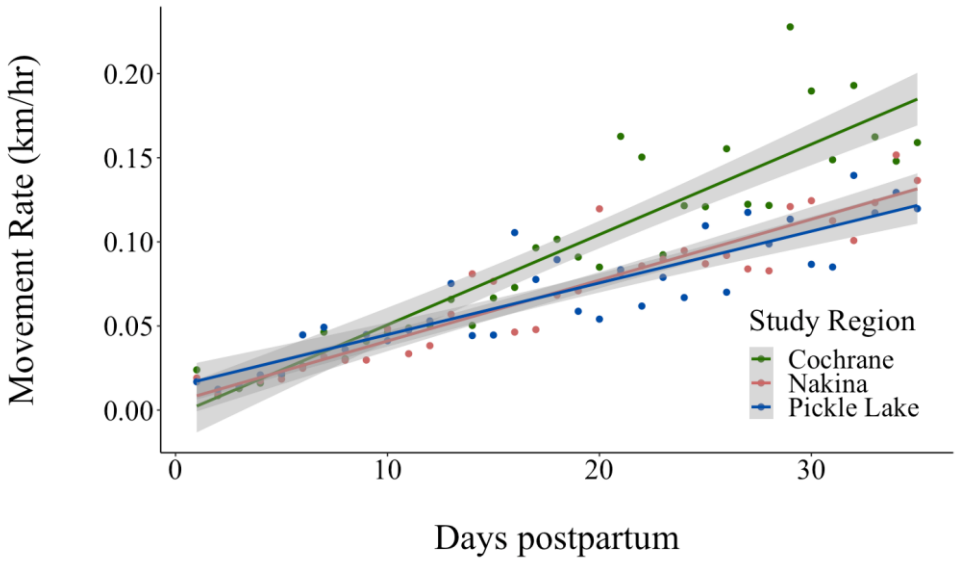

Figure 2.5. Mean individual postpartum movement rates (km/hr) of female caribou by study region in northern Ontario, Canada, 2010–2013, with fitted linear line ($r^2 > 0.80$) and 95% confidence intervals (grey shading).

Chapter 3

Woodland caribou calving fidelity: spatial location, habitat, or both?

Introduction

The lifetime fitness of decision-making animals is likely dependent on their behavioral response to trade-offs between predation risk and resource acquisition (Sih 1980, McNamara and Houston 1986). To manage these trade-offs during an annual cycle, mobile animals can choose either to move to new areas or continue to use previously used areas and express a form of site fidelity (Greenwood 1980, Switzer 1993). Where site fidelity has been expressed, previous knowledge of available resources and predation risk at the site have been shown to increase an individual's fitness (Gavin and Bollinger 1988, Welch et al. 2000, Lafontaine et al. 2017, Gehr et al. 2020). As a result, site fidelity has been reported across a range of disparate animal taxa, including fish (Bunt et al, 2021, Compaire et al. 2022), birds (Gerber et al. 2019, Willie et al. 2020), amphibians (Denoël et al. 2017, Balázs et al. 2020), reptiles (Evans et al. 2019, Baltazar-Soares et al. 2020), and mammals (Gehr et al. 2020, Morrison et al. 2021).

Site fidelity has almost exclusively been understood as a spatial evaluation in previous studies, regardless of the conditions at those locations (hereafter, referred to as spatial fidelity). For example, barren-ground caribou (*Rangifer tarandus groenlandicus*) express spatial fidelity each spring as they return to traditional calving grounds, a defining characteristic of the subspecies, which are used to delineate local populations (Gunn and Miller 1986). By returning to the same location, an individual likely benefits from the resources sufficient to support animals over time, and from some additional advantage of being familiar with them (Greenwood 1980, Switzer 1993, Wolf et al. 2009). Returning to a specific site has been attributed to an individual's decision to return and the spatial memory to relocate the area (Fagan et al. 2013, Merkle et al. 2019). However, individuals could express "habitat fidelity", i.e., faithfulness to a specific habitat during a life history event or time of year, irrespective of spatial location. Based

on foraging theory, individuals specialize on preferred resources when these are abundant because search time is low, whereas they expand their breadth of resources used when preferred resources are scarce because of the costs associated with finding them (MacArthur and Pianka 1966, Emlen 1966, Charnov 1976, Pyke 1984). As a result, we predict animals are more likely to exhibit habitat fidelity to preferred habitat, when it is abundant across the landscape, which may occur during a particular time of year (e.g., calving).

Previous studies have evaluated consistency in habitat use for a specific time period and found evidence for some similarity among individuals, but also considerable variation in habitat use among individuals (Gillingham and Parker 2008, DeMars and Boutin 2018, Merrill et al. 2020). Only rarely did these studies focus on the same individual animals across years. One exception is the focus on individual personality traits, where studies have evaluated the interannual consistency of selection for habitat characteristics by individuals in time (Leclerc et al. 2016; Spiegel et al. 2017; Hertel et al. 2019, 2020, 2021). In these few cases, the focus was on the consistency in behaviors of individuals across long periods of time, not during specific life history events. Habitat fidelity during key life history events, in particular reproduction, may improve individual fitness and does not rely on specific spatial memory of geographic locations. Where there has been a focus on consistent use of nest or birth sites, the importance of spatial location vs. habitat conditions for reproductive success has not been distinguished (Shields 1984, Hoover 2003, Vergara et al. 2006, Lafontaine et al. 2017). Understanding the relative benefits of spatial fidelity vs. habitat fidelity or their combined effects during important life history events may be key in how we approach managing critical habitat, particularly for threatened or endangered species.

Complicating an assessment of an individual's motivation for fidelity is that the advantages may also be contingent on both endogenous factors, such as age and past experiences, as well as broad-scale environmental conditions (Shields 1984, Switzer 1993, Hoover 2003). Older individuals may express spatial fidelity because of greater experience, memory, or knowledge about habitat cues, and because of the terminal investment hypothesis, which suggests animals tend to invest more in reproduction as they age (Williams 1966). In contrast, the "win-stay: lose-switch" strategy suggests that if an individual is reproductively successful (i.e., wins), then it may be beneficial to express spatial fidelity in the following year, but not if the offspring dies (i.e., loses) (Switzer 1993, Welch et al. 2000, Vergara et al. 2006, Lafontaine et al. 2017). For example, for prothonotary warblers (*Protonotaria citrea*) in Illinois, USA, Hoover (2003) showed that >80% of individuals returned to the same site when they produced two broods in the previous year, whereas <60% of individuals returned to the same site if they only produced zero or one brood. We suggest that age and reproductive success is also likely to promote habitat fidelity, but whether they influence spatial or habitat fidelity more is unknown.

Expressing fidelity may also be contingent on the spatial variability and predictability of habitat quality (Switzer 1993, Morrison et al. 2021). When spatial variability of habitat quality is low, with most areas having similar value, spatial fidelity may be common because there is no benefit to expend more energy by moving to another site (Switzer 1993). In contrast, if habitat quality is highly variable across an area, a smaller extent of the area may provide high-quality habitat (i.e., area-heterogeneity trade-off; Kadmon and Allouche 2007, Ben-Hur and Kadmon 2020) and individuals may return to that area, but only if environmental conditions are predictable (i.e., autocorrelated through time; Morrison et al. 2021). In one of the few studies that

has evaluated the impact of habitat availability on spatial fidelity, Chaverri et al. (2007) concluded tent-making bats (*Artibeus watsoni*) in Costa Rica expressed higher spatial fidelity in regions with lower roost availability; however, they did not directly assess predictability of roosts and assumed consistency of roost locations over time. Lurz et al. (1997) showed that female red squirrels (*Sciurus vulgaris*) in Cumbria, England, expressed higher spatial fidelity for home ranges in areas where food resources did not fluctuate across time. However, if high-quality sites occur randomly through time, then it may be more advantageous to randomly use the landscape and not return to previously occupied sites (Teitelbaum and Mueller 2019).

In this paper, we investigated whether boreal woodland caribou (*R. t. caribou*, hereafter caribou) express interannual spatial and/or habitat fidelity in northern Ontario, Canada, during calving, a crucial period for reproductive success (Gustine et al. 2006, Pinard et al. 2012, Walker et al. 2021). Previous studies have documented interannual spatial fidelity for caribou during the calving period, but did not assess habitat fidelity (Schaefer et al. 2000, Wittmer et al. 2006, Faille et al. 2010, Lafontaine et al. 2017). Although caribou have shown consistent selection during calving for shorelines, lowlands, and mid-late seral ($\geq$20 years) conifer stands across individuals (Carr et al. 2007, Pinard et al. 2012, Hornseth and Rempel 2016, Viejou et al. 2018, Walker et al. 2021), none of these studies focused on the interannual consistency in habitat use within individual animals to determine if they express habitat fidelity. Moreover, fidelity studies have not distinguished between habitat and spatial fidelity and the conditions under which caribou may exhibit these different forms of fidelity.

We predicted caribou would exhibit spatial fidelity when availability of high-quality habitat was limited and did not change over time (i.e., predictable), habitat fidelity when high-quality habitat was not predictable over time but was readily available, and no fidelity when

high-quality habitat was not readily available or predictable. Individuals may also show both spatial and habitat fidelity when high-quality habitats are predictable and readily available. At the same time, because fidelity itself or the type of fidelity may be influenced by caribou age and the previous year's calf survival, we also considered these factors when assessing caribou fidelity. A better understanding of whether caribou rely on specific sites or habitat conditions for reproduction is key because they are listed as threatened under Canada's *Species at Risk Act* (Government of Canada 2019) and Ontario's *Endangered Species Act* (Government of Ontario 2007).

Study Area

We evaluated calving fidelity across northern Ontario, Canada, within three study regions: Pickle Lake (90.938W, 51.568N; 23,000 km^2), Nakina (87.548W, 50.388N; 23,000 km^2), and Cochrane (80.598W, 49.908N; 23,000 km^2; Figure 3.1). All regions were within the boreal zone, which is characterized by stands of black spruce (*Picea mariana*), jack pine (*Pinus banksiana*), balsam fir (*Abies balsamea*) trembling aspen (*Populus tremuloides),* and white birch (*Betula papyrifera*) (Rowe 1972). Pickle Lake and Nakina are located within the Boreal Shield of northwestern Ontario, which is dominated by rolling topography, whereas Cochrane is in the Northern Clay Belt region of northeastern Ontario and characterized by minimal topographical variation (McMullin et al. 2013, Thompson et al. 2015). Consequently, Cochrane had the highest extent of lowland conifer forest (swamp, bog, and fen; 64%) whereas Nakina and Pickle Lake both had a lower extent at 28% (Walker et al. 2021). Disturbance regimes differed across the three study regions. At the time of the study (2010), Nakina had greater harvest regeneration (<40 years; 22%) compared to Cochrane (13%) or Pickle Lake (0.04%; OMNRF 2014*a*, Fryxell et al. 2020), whereas Pickle Lake had a higher proportion of natural disturbance (proportion burned <50

years; 12%) compared to Nakina and Cochrane (both 4%; OMNRF 2014*a*, Fryxell et al. 2020). Linear feature density was higher in Nakina (0.42 km/km^2) and Cochrane (0.31 km/km^2), compared to Pickle Lake (0.05 km/km^2; OMNRF 2014*a*, Fryxell et al. 2020). Wolf (*Canis lupus*) and moose (*Alces alces*) densities were highest in Nakina (6.7 wolves/1,000 km^2, 11.8 moose/100 km^2) with lower densities in Pickle Lake (4.2 wolves/1,000 km^2, 4.6 moose/100 km^2) and Cochrane (3.7 wolves/1,000 km^2, 3.8 moose/100 km^2; OMNRF 2014*a*, Fryxell et al. 2020), whereas black bear (*Ursus americanus*) densities were similar across all regions (20-40 black bears/100 km^2; Rodgers et al. 2009, Howe et al. 2013). Total annual precipitation was greater in Cochrane (824 mm $\pm$ 81 mm; $\bar{x} \pm$ SD, 20-yr average [1991-2010]) than Nakina (776 mm $\pm$ 130 mm) and Pickle Lake (736 mm $\pm$ 122 mm; Environment Canada, https://climate.weather.gc.ca/historical_data/search_historic_data_e.html, accessed 14 Jun 2019). January daily temperatures were highest in Cochrane (-17.82°C ± 3.69°C), followed by Nakina (-18.60°C ± 3.61°C) and Pickle Lake (-19.26°C ± 3.60°C), however July daily temperatures were similar among areas (Pickle Lake: 17.66°C ± 1.49°C; Nakina: 17.07°C ± 1.50°C; Cochrane: 17.36°C ± 1.25°C).

Methods

Caribou capture, monitoring, and ranges

We captured 166 female caribou in Pickle Lake (PL; $n = 52$), Nakina (NA; $n = 58$), and Cochrane (CO; $n = 56$) between 2010 and 2014 using a net gun and fitted them with either GPS-Argos (Telonics Inc., Mesa, AZ, USA; Lotek Wireless Inc., Newmarket, ON, Canada) or GPS-Iridium radio collars (Lotek Wireless Inc., Newmarket, ON, Canada). Animal capture and handling protocols were approved by the Ontario Ministry of Natural Resources and Forestry Wildlife Animal Care Committee (protocols 10-183, 11-183, 12-183, 13-183, and 14-183).

Caribou were aged at capture based on tooth eruption and wear (van den Berg et al. 2021). Caribou GPS fixes were obtained every 1, 2.5, 5, or 12.5 hrs for multiple years resulting in 282 caribou-years. Mean fix rate success across all 282 caribou-years was 97% (range: 90–100%).

We identified annual parturition events following DeMars et al. (2013) based on a reduction in caribou movements. DeMars et al. (2013) found a 97.5% accuracy when using a 4-hr fix rate interval to predict parturition events, whereas Walker et al. (2021) found a 100% accuracy when using 2.5- or 3-hr fix rate intervals. Because fix rate intervals of caribou in this study were more variable, we first evaluated the sensitivity of predicting parturition events with different fix rate intervals (1, 2.5, 5 or 12.5 hr) compared to parturition events identified from video footage of 20 caribou (22 caribou-years; PL: $n = 4$, NA: $n = 9$, CO: $n = 9$) with animal-borne video collars (Thompson et al. 2012, Viejou et al. 2018, Walker et al. 2021). We found accuracy levels of 91% for predicting parturition using fix rate intervals up to 12.5-hr with zero false positives (i.e., a parturition event is predicted when one did not occur; Appendix 2.1). Therefore, we applied the DeMars approach to 260 of the 282 caribou-years (PL: $n = 83$, NA: $n = 91$, CO: $n = 86$) with fix rate intervals between 1- and 12.5-hr and unknown birth status (i.e., did not have animal-borne video collars).

From the 162 caribou for which we had annual, predicted birth locations, we identified 56 individuals (133 caribou-years) with ≥ 2 known (via video collar footage) or predicted birth events and used GPS locations from these individuals to define calving-sequences. Because we assessed interannual fidelity, we derived pre-calving-neonatal ranges for each caribou-year based on the 95% utilization distribution (UD) using the reference bandwidth for smoothing (Walker et al. 2021) for the 30-day period prior to parturition (i.e., pre-calving) and a variable-day, neonatal period based on postpartum displacement (i.e., neonatal locations; Figure 3.2; see details in

Walker et al. 2021). Prior to developing 95% UDs, caribou with 1-hr fix rates were randomly resampled to 13-hr, caribou with 2.5-hr fix rates to 12.5-hr, and 5-hr fix rates to 15-hr to make sampling more comparable across caribou-years. A calving-sequence was determined from the same caribou in year *t* compared to year *t* +1 for up to three years. For example, the centroid (i.e., geometric mean) and habitat composition of the neonatal locations in year one were compared to year two, year one compared to year three, and year two compared to year three. We used 99 calving-sequences to evaluate spatial fidelity but only 98 sequences to evaluate habitat fidelity (discussed below).

Spatial and habitat fidelity

We assessed spatial and habitat fidelity in calving-sequences, and by default, we defined no fidelity to occur when we had no evidence of either spatial or habitat fidelity. We assessed the spatial fidelity of each calving-sequence by comparing the Euclidian distance (m) between the observed two neonatal centroids in year *t* and *t* +1 to an expected distribution of distances (null) based on distance between the neonatal centroid in year *t* and 1,000 random locations within the pre-calving-neonatal 95% UD in year *t* +1 (Figure 3.3). The distribution of 1,000 random distances produced the expected (i.e., null) distribution of distances reflecting where the individual could have calved in year *t*+1 given the size and shape of the pre-calving-neonatal range. We used the area of the pre-calving-neonatal area (defined above) to bound the random locations because it provides a spatial extent of where the caribou could have calved. We then calculated the proportion of random distances that were less than the distance between the two neonatal centroids and concluded a calving-sequence expressed spatial fidelity if that proportion was less than 0.05. We used a one-tailed Mann-Whitney U test to evaluate if the distances

between observed centroids of calving-sequence designated as expressing neonatal spatial fidelity were significantly less than calving-sequences that did not.

We evaluated habitat fidelity of calving-sequences by independently comparing the interannual consistency of use of four land cover types at the neonatal GPS locations in year *t* (0) and year *t* +1 (1) using logistic regression and a model selection approach based on Akaike's Information Criterion corrected for small sample size (AIC_c; Burnham and Anderson 2002). We concluded that a calving-sequence reflected habitat fidelity if the habitat model was $\Delta AIC_c < 4$ from the null model, where acceptance of the null model indicted no difference in landcover types used between years. We used an ΔAIC_c threshold of 4 to be conservative in our classification of an individual expressing habitat fidelity (Burnham and Anderson 2002). The four land cover types were lowland conifer forest (bog, swamp, or fen), upland conifer forest (coniferous and sparse), mixed-deciduous forest (mixedwood and deciduous), and early seral forest (<20 years old), which were collapsed from 24 land cover types in the Ontario Far North Land Cover layer (version 1.4; OMNRF 2014*a*). We focused on these land cover types because Walker et al. (2021) showed that caribou selected for lowland conifer forest during calving, whereas others in these study regions showed caribou selected against mixed-deciduous and early seral forests, which reflect high risk areas due to high wolf use (Avgar et al. 2015; Kittle et al. 2015, 2017; McGreer et al. 2015; Viejou et al. 2018). Land cover was updated annually to account for annual disturbance created through forest fires (Aviation, Forest Fire and Emergency Services Fire Disturbance Area layer) and silvicultural practices based on Ontario Ministry of Natural Resources and Forestry (OMNRF) depletion records (OMNRF, unpublished data). We removed one calving-sequence from the habitat fidelity analysis because the neonatal locations of the calving-sequence were outside the spatial extent of the Far North Land Cover.

Factors influencing types of fidelity

Once we assigned a type of fidelity to each calving-sequence, we classified each calving-sequence into four fidelity classes: no fidelity (neither spatial nor habitat fidelity), spatial fidelity, habitat fidelity, or both spatial and habitat fidelity. We then independently compared each fidelity type (1) to not expressing that specific fidelity type (0). These four fidelity classes were not mutually exclusive, i.e., a calving-sequence classified as expressing both spatial and habitat fidelity was also classified as expressing spatial fidelity as well as habitat fidelity. We used independent, binomial comparisons of fidelity instead of a multinomial model to distinguish among four classes simultaneously because of low within-type sample sizes. Because age and calf survival were known for only a subset of the caribou, we first used data from all caribou (55 caribou; 98 calving-sequences) to assess the association between proportional use of land cover types at neonatal locations, study region, and habitat quality and predictability (see below) within the pre-calving-neonatal 95% UD with a type of fidelity. We used a mixed-effects logistic regression with a random effect for caribou ID because there was more than 1 calving-sequence for 19% of caribou (range: 1–6 sequences per caribou). Second, for the subset of 41 caribou (70 calving-sequences) with known ages, we assessed the association between age and the probability of a caribou expressing a particular fidelity type compared to all others using the same modeling approach as above. Finally, we used a subset of 27 caribou (27 caribou-sequences) when neonatal survival at year *t* was known to assess the association between a type of fidelity and calf survival in the previous year, and did not include a random effect for caribou ID.

Study region (Pickle Lake, Nakina, and Cochrane) corresponded to the geographic area of the local population each caribou was associated with (Fryxell et al. 2020) and Cochrane was

set as the reference area. Caribou age represented year *t* adjusted over time from age at capture. Neonatal survival within 5-weeks postpartum was determined based on movement patterns of caribou with calves during the calving period (see Walker et al. 2021 for methodological details). Our metric for habitat quality was based on the values predicted from a resource selection function (RSF; Manly et al. 2002) based on a use-available design pooling data on caribou across all three regions. Used locations were the neonatal locations of the GPS-collared caribou for which we determined calving-sequences, with a median of 52 locations/caribou-year collected during the period from 7 May to 13 June. Available locations consisted of 1,000 random locations within the pre-calving-neonatal home range of each caribou, which corresponded to those used to classify spatial fidelity. RSFs were derived based on the same four land cover classes as described above (with lowland conifer forest set as the reference category) and linear feature density (km/km^2) based on roads, powerlines, and railways (Hornseth and Rempel 2016, Walker et al. 2021). We focused on these features because caribou showed strong selection responses to them during calving (Hornseth and Rempel 2016, Viejou et al. 2018, Walker et al. 2021). Covariate values were assigned at each used and available GPS location based on a 30-m resolution.

We used a mixed-effect, logistic regression to estimate the parameters of an exponential RSF and included caribou-year as a random intercept (Gillies et al. 2006). We used AIC_c and a threshold of $\Delta AIC_c < 4$ to identify a top RSF model (Burnham and Anderson 2002). The top model was used to predict RSF values across all three regions at the 30-m pixel scale. A metric of habitat quality was derived for each of the pre-calving-neonatal 95% UDs at time *t* of the calving-sequence based on the mean RSF value within the extent of the 95% UD. We used a mean value to account for differences in area of pre-calving-neonatal ranges across individuals.

Habitat predictability was calculated as the difference in mean habitat quality (P_t - P_{t+1}) between years within the spatial extent of the first year's pre-calving-neonatal 95% UD. We evaluated change in habitat quality, because these landscape covariates were informative in habitat selection of caribou during the neonatal period. High predictability reflects little change in the mean RSF values and is denoted by low values approaching zero between years; high values of predictability approaching one reflect low predictability. All analyses were conducted in the statistical computing program R (R version 4.2.1, www.R-project.org, accessed 2 July 2022).

Results

Spatial and habitat fidelity

When evaluating spatial fidelity, one calving-sequence was identified as not expressing spatial fidelity ($P = 0.14$) with 1,059 m between neonatal centroids; however, we classified this calving-sequence as expressing spatial fidelity to be consistent with the two other calving-sequences from that individual expressing spatial fidelity (Appendix 2.2). Another calving-sequence with 424 m between neonatal centroids was classified as not expressing spatial fidelity ($P = 0.07$); instead, we classified it as expressing spatial fidelity because the distance was less than half the mean distances (1,068 km) of all other calving-sequences classified as expressing spatial fidelity (Appendix 2.2). Sizes of pre-calving-neonatal ranges at year t did not differ between caribou reflecting the four fidelity classes (t-test, $P > 0.33$). The mean age of caribou with calves that survived (6.5 ± 2.1, $\pm$ SD, $n = 16$) and calves that did not survive (5.5 ± 0.6, $n = 5$) did not differ (t-test, $P = 0.11$).

Of the 99 calving-sequences across the three regions, 36% exhibited no fidelity, 29% exhibited spatial fidelity, 50% exhibited habitat fidelity, and 14% exhibited both habitat and

spatial fidelity (Table 3.1). The distances between neonatal centroids were less for calving-sequences that were classified as spatial fidelity (1,046 ± 1,245 m, $\bar{x}$ ± SD) than calving-sequences not classified as spatial fidelity (15,735 ± 16,307 m, $P < 0.001$). Caribou in Pickle Lake and Nakina exhibited less fidelity than in Cochrane ($P < 0.004$), where habitat fidelity ($P < 0.06$) was more common than in the other two regions (Table 3.2). Across regions and years, the proportion of caribou locations in neonatal ranges expressing habitat fidelity averaged 0.74 ± 0.37 in lowland conifer forest, whereas the proportion in upland conifer forest averaged 0.22 ± 0.35, early seral forest averaged 0.03 ± 0.14, and mixed-deciduous forest averaged 0.003 ± 0.01. Caribou expressing habitat fidelity showed greater proportional use of lowland conifer forest and less proportional use of upland conifer forest at neonatal locations compared to those not expressing habitat fidelity (Appendix 2.3). Greater proportional use of mixed-deciduous forests at neonatal locations was also associated with expressing no fidelity, with less proportional use associated with expressing habitat fidelity, and no effect of proportional use of early seral forests on expressing any type of fidelity (Appendix 2.3).

Habitat quality and predictability for assessing fidelity

We developed a metric of habitat quality based on an RSF using data from 55 caribou across all three study regions. The top RSF indicated that during calving caribou more strongly selected areas that were lowland conifer and upland conifer forests than early seral and mixed-deciduous forests, and areas with lower densities of linear features (Table 3.3, Appendix 2.4). There was considerable support for the top model with a model weight of 1.00 and a ΔAIC_c of 452 to the next candidate model (Table 3.3). Mean habitat quality within the pre-calving-neonatal range averaged higher in Pickle Lake (1.03 ± 0.07; ± SD) than in Nakina (0.89 ± 0.10) or Cochrane (0.81 ± 0.19, Tukey HDS test: $P \leq 0.04$). This was due to higher proportion of upland conifer

forest without linear features (within 1 km) in Pickle Lake (0.36) than in Nakina (0.16) and Cochrane (0.09).

There was very little change in habitat quality of the pre-calving-neonatal ranges between years, with 92% of the calving-sequences having no change in habitat quality, resulting in predictability values that ranged from 0.00 to 0.02 (0.0003 $\pm$ 0.002, $\bar{x} \pm$ SD). Predictability values were similarly low when measured across 100,000 random locations by study region, indicating that habitat conditions during the 5 years of the study were relatively constant and similar between Pickle Lake (0.001 $\pm$ 0.002), Nakina (0.0002 $\pm$ 0.0001) and Cochrane (0.0009 $\pm$ 0.0001). The lack of variation in predictability values resulted in models not converging such that we were unable to assess the influence of predictability on fidelity of caribou across these regions.

Factors influencing types of neonatal fidelity

We found habitat quality and age influenced whether caribou expressed spatial fidelity or habitat fidelity, but no other type of fidelity (Table 3.4). The probability of caribou expressing habitat fidelity increased as the average habitat quality (i.e., RSF value) within pre-calving-neonatal ranges declined. This trend was consistent even with smaller sample sizes within study regions, but the relationships were not significant (Appendix 2.5-2.6). We also found older individuals were more likely to express spatial fidelity, but no other type of fidelity (Table 3.4; Appendix 2.7). Conclusions based on the univariate models did not change when we included habitat quality and age in a multivariable model, and the habitat quality x age interaction was not significant (Appendix 2.8–2.9). Finally, we found no evidence that the survival of a calf in the previous year influenced probability a caribou expressing any type of fidelity, but the sample size was only 27 individuals (Table 3.4, Appendix 2.10).

Discussion

We found the majority (~60%) of caribou calving-sequences reflected spatial or habitat fidelity during the neonatal period with habitat quality associated with expressing habitat fidelity and caribou age associated with expressing spatial fidelity. The degree of spatial fidelity was similar across the three regions with almost a third of all caribou expressing spatial fidelity. This proportion is similar to the 25% of moose in Ontario, Canada (Welch et al. 2000), lower than the 64% of migratory caribou in Quebec, Canada (Brown et al. 1986), and higher than the 18% reported for pronghorn (*Antilocapra americana*) in Montana, USA (Wiseman et al. 2006). However, comparisons across studies can be difficult due to the different criteria used. A key component of detecting spatial fidelity in this study was the comparison to a null model to control for the possibility of spatial fidelity emerging randomly due to an individual's inherent movements. The comparison to a null model has not always been used in past spatial fidelity studies, adding to differences reported among studies. Instead, studies have used a subjective, *a priori* value to conclude if an individual animal expressed spatial fidelity (Brown et al. 1986, Welch et al. 2000, Wiseman et al. 2006). For example, Wiseman et al. (2006) assumed *a priori* if sequential birth sites were within 1 km of each other for individual pronghorn in Montana, USA, that expressed spatial fidelity. In contrast, Rettie and Messier (2001) compared the distances between calving sites of woodland caribou in Saskatchewan, Canada, between two years to the distribution of distances between the first-year calving site to all GPS locations used in the following year. Although this approach may control for random movements, comparison of locations of calving sites in year t to all locations used the following year likely would inflate distances in the null expectation compared to random locations within a potential calving area in year t+1, which could change conclusions. Using the latter approach, we found calving-

sequences of caribou expressing spatial fidelity were on average ~1.0 km apart, which was considerably less than individuals that did not express spatial fidelity (~15.7 km). This mean distance is closer than previously reported in sedentary woodland caribou in Quebec and Labrador (6.7 km; Schaefer et al. 2000), in woodland caribou in the central mountains of British Columbia and Alberta, Canada (8.7 km; Norbert et al. 2016), and in Svalbard reindeer (*R. t. platyrhynchus*; 1.5–3.9 km; Garfelt-Paulsen et al. 2021). In fact, three caribou observed in this study calved within 50 m of the site where they calved the previous year.

We also found the regularity in expressing spatial fidelity among individual caribou was not high, with only 2 of the 19 caribou that we monitored for greater than two years expressing spatial fidelity in all years (both individuals from Cochrane), suggesting behavioural plasticity in expressing spatial fidelity. The variation in caribou expressing spatial fidelity was not related to habitat quality, but to age. Although studies have reported that spatial fidelity in birds is related to age (Harvey et al. 1984, Beletsky and Orians 1987, Payne and Payne 1993, Pyle et al. 2001), the evidence for ungulates is limited. Morrison et al. (2021) did not find that spatial fidelity was related to age in 205 elk, 80 moose, 167 mule deer (*Odocoileus hemionus*), or 81 pronghorn. However, their conclusions were based on Euclidean distance calculated between GPS locations on each Julian day between year *t* and year *t*+1 and not for a specific life history event like calving (Schaefer et al. 2000, Lafontaine et al. 2017). Age may reflect the accumulation of experience and more familiarity with how environmental conditions influence reproductive outcomes (Fagan et al. 2013). On the other hand, an increase in spatial fidelity with age may support the terminal investment hypothesis (Williams 1966), if spatial fidelity promotes higher fitness, such as calf survival. With our small sample of only 22 caribou, we did not find evidence that caribou expressing spatial fidelity led to higher calf survival, but others have found support

in pronghorn (Wiseman et al. 2006) and mixed results in moose (Testa et al. 2000, Welch et al. 2000, McLaren and Patterson 2021). In caribou, Lafontaine et al. (2017) with a somewhat larger sample size (n = 33) in Quebec, Canada, documented that caribou were more likely to express spatial fidelity during calving if they did not lose their calf the previous year.

Compared to spatial fidelity, we found 50% of the calving-sequences of caribou expressed habitat fidelity, suggesting strong habitat preferences may also be an important strategy during the key neonatal period. We also found more frequent regularity in expressing habitat fidelity among individual caribou than spatial fidelity, with 7 of the 19 caribou monitored for greater than two years expressing habitat fidelity in all years, which included 6 individuals from Cochrane and 1 individual from Nakina. The individuals from Cochrane all predominately used lowland conifer forest across all years, whereas the individual in Nakina preferentially used upland conifer forest across all years. We predicted caribou would express habitat fidelity when availability of high-quality habitat was high, but, in fact, we observed the opposite: the probability of expressing habitat fidelity increased when the abundance of high-quality habitat declined. Shipley et al. (2009) argues that a decline in availability of high-quality resources can result in an "obligate specialist" with a very narrow realized niche. In the case of caribou, if not using high-quality calving habitat results in the loss of a calf, perhaps due to predation, then the cost of generalizing habitat use during calving may be too high, and outweigh any cost related to search. In modeling selection of calving habitat, we found caribou selected against areas of high linear feature density, early seral forest, and mixed-deciduous forest, compared to upland and lowland conifer forests during calving, which are patterns previously documented across Ontario, especially during calving (Hornseth and Rempel 2016, Viejou et al. 2018, Walker et al. 2021). Upland conifer forests may indirectly reduce predation due to spatial segregation from

alternative prey, i.e., moose, because the latter selects for mixed-deciduous forests (Bowman et al. 2010, Street et al. 2015). In contrast, selection by caribou for lowland conifer forest during calving may reflect direct avoidance of predation risk from bears and wolves that select against these areas (McLoughlin et al. 2005; Mosnier et al. 2008; Latham et al. 2011; Kittle et al. 2015, 2017). Thus, avoiding predation may be a major driver of why caribou do not generalize habitat use during calving and are instead consistent in the areas they select. However, we could not link the consistent selection for these types of areas to calf survival, but selection patterns in general have been related to fitness consequences (McLoughlin et al. 2006, Gaillard et al. 2010).

If predictability of habitat conditions influenced the expression of fidelity, we would have predicted less fidelity (neither spatial nor habitat fidelity) in Nakina because of higher disturbance (OMNRF 2014*a*, Fryxell et al. 2020). Consistent with this prediction, we observed a higher propensity to express no fidelity in Nakina than in Cochrane, but not Pickle Lake, which represented the region with the lowest disturbance. Studies in Quebec, Canada, have documented that caribou express greater spatial fidelity in regions of higher natural disturbances (i.e., forest fires; Faille et al. 2010), similar to moose in Ontario expressing greater spatial fidelity in regions with more timber harvest compared to protected areas (McLaren and Patterson 2021). However, the motivation to express spatial fidelity in these environments may be different for each species, i.e., moose select early seral forests for forage, whereas caribou may express spatial fidelity due to limited habitat availability. Our focus on habitat predictability within the pre-calving-neonatal range also may have limited our inferences. For example, based on a 30-day pre-parturition period and variable time spent at a neonatal area (Walker et al. 2021), we may not have been able to adequately assess how caribou perceive predictability of habitats given disturbance regimes. However, in these study regions, even if caribou based their expectations of predictability on

change over the full year and across several years, only 0.004–2% of any of the three study regions was cumulatively disturbed by fire and timber harvest over the 5-year period of this study. Further, even with high levels of disturbance, caribou may generally select against these areas (Hornseth and Rempel 2016, Silva et al. 2020, Walker et al. 2021). For example, Silva et al. (2020) documented that despite the relatively high extent of forest fires (~57%, <40 years) across northern Saskatchewan, Canada, a majority (71%) of caribou spent little time (<5% of GPS locations) within the spatial extent of recent forest fires throughout a year. Where disturbance events are rare, long-term studies with greater spatial or temporal sampling frame may be needed to address hypotheses of how environmental predictability influences the propensity of expressing fidelity.

Previous studies have documented the impact of fidelity, specifically spatial fidelity, on caribou populations and that the protection of calving areas should a priority for the management of caribou (Faille et al. 2010, Lafontaine et al. 2017). However, the relative importance of these management priorities will depend on their association with reproductive success, which requires obtaining sufficient data to link these behavioral tactics to fitness consequences. Merkle et al. (2022) argues that spatial fidelity may be maladaptive in regions of high anthropogenic disturbances, due to degradation of habitat quality, which results in a fitness cost associated with expressing spatial fidelity. Dussault et al. (2012) also suggested this concept in regard to caribou expressing spatial fidelity in Quebec, Canada. In the case of caribou, expressing spatial fidelity in regions recently disturbed may make calves predictable in space (Mitchell and Lima 2002) and subject them to higher predation risk (Kittle et al. 2015, 2017). If expressing spatial fidelity is maladaptive, management options may be limited to addressing predation pressure and augmenting calf survival with maternal penning (Serrouya et al. 2019). On the other hand, these

results suggest considerable behavioural plasticity in space use during calving both within and among individual caribou, which may reflect the pressure of natural selection for alternative tactics, as occurs in other behaviors such as in partial migration (Chapman et al. 2011). Given immediate conservation concerns for caribou, we advocate for broadening the management approach to provide sufficient calving habitat to promote fidelity, which includes upland and lowland conifer forests without linear features.

Table 3.1. Proportion and number (*n*) of 99 calving-sequences expressing no fidelity, spatial fidelity, habitat fidelity, or both habitat and spatial fidelity by study region in northern Ontario, Canada, based on caribou telemetry data from 2010 to 2014. Only 98 calving-sequences were used to calculate proportions expressing habitat fidelity and both spatial and habitat fidelity.

Study region	No fidelity		Spatial		Habitat		Both	
	Proportion	*n*	Proportion	*n*	Proportion	*n*	Proportion	*n*
Cochrane	0.17	7	0.38	16	0.68	28	0.22	9
Nakina	0.49	17	0.23	8	0.40	14	0.09	3
Pickle Lake	0.55	12	0.23	5	0.32	7	0.09	2
Total	0.36	36	0.29	29	0.50	49	0.14	14

Table 3.2. Beta coefficient (β) and 95% confidence intervals (CI) for two study regions in four independent, mixed-effect, logistic regressions assessing the probability of expressing a type of fidelity (1: none, spatial fidelity, habitat fidelity, or both) compared to not expressing that type of fidelity (0) based on caribou telemetry data from 2010 to 2014 in northern Ontario, Canada. A random effect was included for caribou ID and Cochrane was the reference region. Asterisk indicates confidence intervals do not overlap zero.

Fidelity type	Pickle Lake		Nakina	
	β	95% CI	β	95% CI
No fidelity	1.79*	0.62, 2.96	1.55*	0.50, 2.60
Spatial	-0.88	-2.29, 0.53	-0.81	-2.04, 0.41
Habitat	-1.80*	-3.47, -0.13	-1.46	-2.94, 0.03
Both	-0.95	-6.14, 4.24	-1.36	-6.39, 3.66

Table 3.3. Model coefficients, number of model parameters (*K*), Akaike's Information Criterion corrected for small sample size (AIC_c), change in AIC_c from best model (ΔAIC_c), and model weights calculated from AIC_c (w_i) for competing resource selection functions relating the relative probability of selection to land cover classes (LC; upland conifer forest, early seral forest, and mixed-deciduous [dec.] forest) in reference to lowland conifer forest and to linear feature density (LF; km/km^2) derived from caribou neonatal locations from 98 calving-sequennces and random locations in pre-calving-neonatal ranges across three study regions in northern Ontario, Canada, 2010–2014.

Model	Upland conifer	Early seral	Mixed-dec.	LF	*K*	AIC_c	ΔAIC_c	w_i
LC + LF	0.23	-0.56	-1.34	-0.85	5	57984.08	0.00	1.00
LC	0.23	-0.81	-1.37		4	58435.82	451.74	0.00
LF				-0.98	2	58616.85	632.77	0.00
Null					1	59299.55	1315.47	0.00

Table 3.4. Number (*n*) of calving-sequences, beta coefficients (β), and 95% confidence intervals (CI) for mean habitat quality in the pre-calving-neonatal 95% utilization distribution, caribou age (years), or calf survival (0/1) within the first 5-weeks postpartum based on four independent, mixed-effect, logistic models predicting the probability of a caribou calving-sequences expressing the type of fidelity (1: none, spatial fidelity, habitat fidelity, or both) compared to not expressing that type of fidelity (0) based on caribou telemetry data from 2010−2014 across three study regions in northern Ontario, Canada. Asterisk indicates confidence intervals do not overlap zero.

Fidelity type	Habitat quality			Age			Calf survival		
	n	β	95% CI	*n*	β	95% CI	*n*	β	95% CI
No fidelity	98	3.14	-0.21, 6.49	70	-0.50	-1.03, 0.03	27	0.12	-1.62, 1.86
Spatial	98	0.29	-3.04, 3.62	70	0.47*	0.08, 0.86	27	-0.70	-3.11, 1.73
Habitat	98	-7.66*	-13.54, -1.77	69	-0.0007	-0.50, 0.44	27	0.69	-1.08, 2.46
Both	98	-12.11	-28.59, 4.36	69	-0.02	-0.96, 0.92	27	1.21	-14.86, 17.28

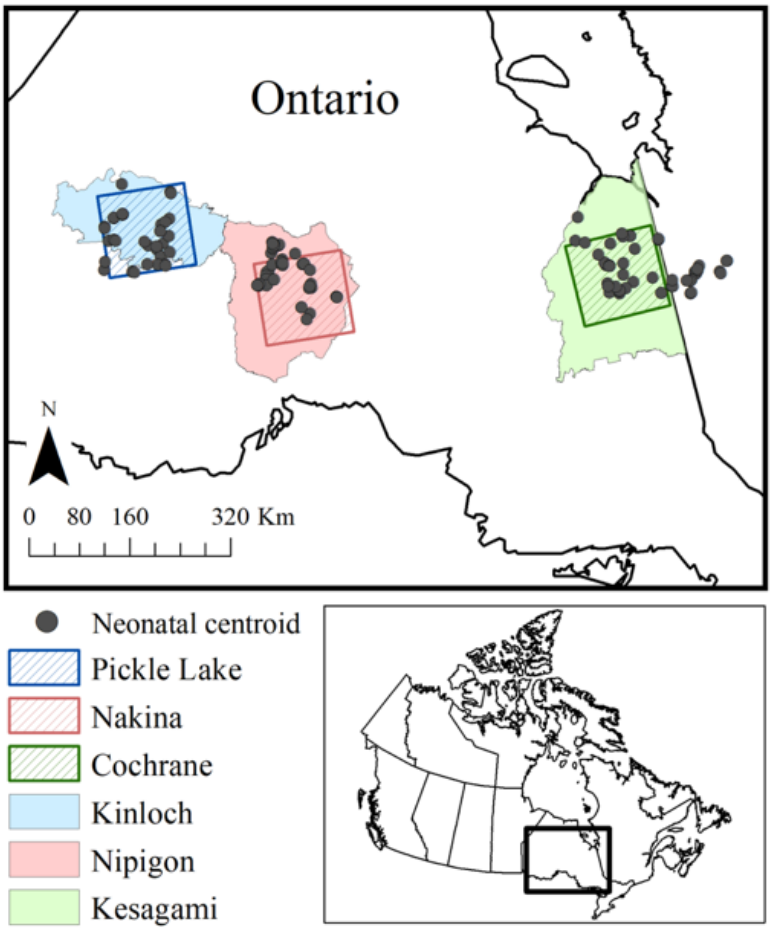

Figure 3.1. Location of neonatal centroids across the three study regions (Pickle Lake, Nakina, and Cochrane) within northern Ontario, Canada, and their respective designated local caribou populations (Kinloch, Nipigon, and Kesagami).

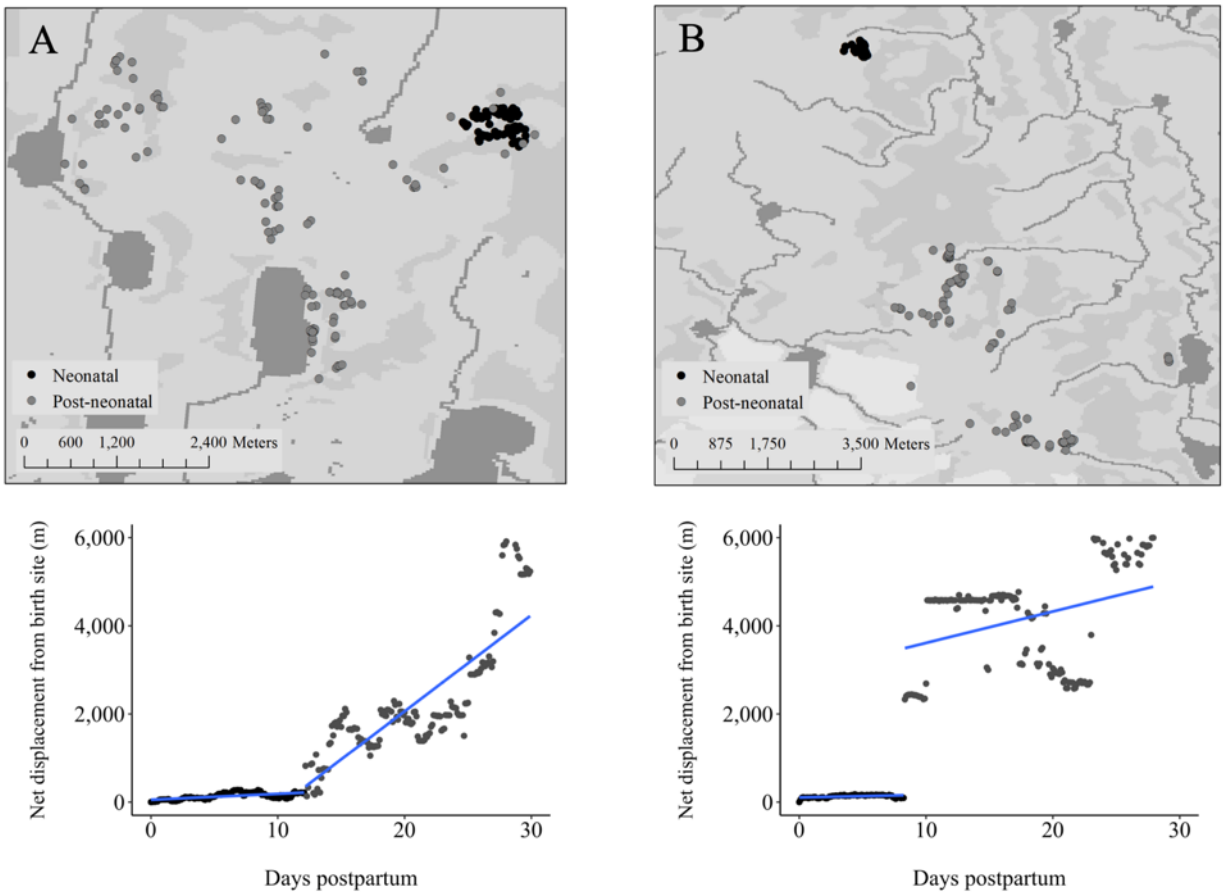

Figure 3.2. Illustration of the approach to identify habitat fidelity. We first define the neonatal locations for a calving-sequence in A) year one and B) year two by relating the rate of net displacement (m) from the parturition site to all subsequent relocations postpartum, where we fit a piece-wise regression to determine the breakpoint in the net displacement after parturition. Once the neonatal locations are determined, we identify the Far North Land Cover types used in year one and two and fit a logistic model, compared to a null model (intercept only), to identify if a calving-sequence expresses habitat fidelity or not. This approach was applied to 98 calving-sequences across northern Ontario, Canada, 2010−2014.

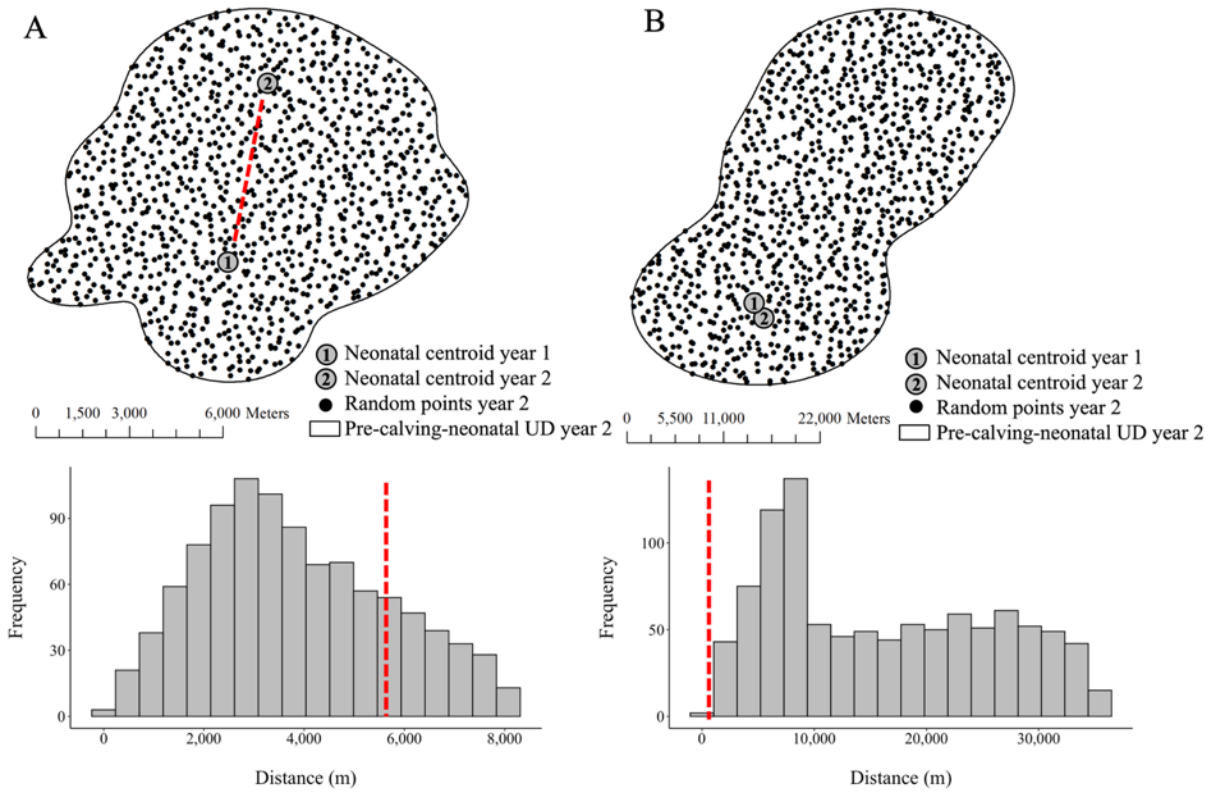

Figure 3.3. Illustration of how a calving-sequence was determined to reflect spatial fidelity, by calculating the proportion of random distances of where the individual could have calved in the following year that are less than or equal to the distance between the neonatal centroid in year one and year two. The distribution of random distances is derived by calculating the distance between the neonatal centroid in year one and the 1,000 random locations within the pre-calving-neonatal utilization distribution (UD) in year two. If the proportion of random distances that is less than or equal to the distance between neonatal centroids is A) greater than 0.05 (e.g., 0.68), then we conclude that the calving-sequence did not reflect spatial fidelity. Alternatively, if the proportion of random distances less than or equal to the distance between neonatal centroids is B) smaller than 0.05 (e.g., 0.001), then we conclude that the calving-sequence did reflect spatial fidelity. This approach was applied to 99 calving-sequence across northern Ontario, Canada, 2010−2014.

Chapter 4

Spatiotemporal dynamics of caribou forage across northern Ontario

Introduction

Nutritional resources influence large herbivores' use of their environment and influence reproductive success, survival, and growth and development of juveniles (Cook et al. 1996, 2004; Parker et al. 1999). Based on the theory of ideal free distribution (IFD), individuals are hypothesized to distribute themselves relative to available nutritional resources and adjust their density accordingly to minimize resource competition and equalize fitness across habitats (Fretwell and Lucas 1970). Therefore, areas with more extensive, resource-productive habitats would be expected to attract and support a higher abundance of individuals (Fowler 1987, Parker et al. 2009, Gaillard et al. 2010). However, most studies of large herbivores focus on how they respond to the total or average resources available (Boyce and Merrill 1991, Weisberg et al. 2002), yet variation of nutritional resources in space and time can alter the ability of an area to support a population (Hobbs and Gordon 2010). Spatial variation of high-quality nutritional resources over time may allow mobile herbivores to maximize daily intake by tracking the variation in plant development during the growing season and selecting for those areas that provide relatively superior nutrition (Illius and O'Conner 2000, Fryxell et al 2005). At the same time, variation in resources can buffer against seasonal declines in high-quality nutritional resources by prolonging the period herbivores can exploit these resources (Owen-Smith 2004). To what extent variation in nutritional resources influences population dynamics depends on the resources available and the critical nutritional thresholds. For example, animals may not directly starve, but lose condition, which can influence reproduction (Langvatn et al. 1996, Post and Stenseth 1999, Post et al. 2008). Indeed, Post and Stenseth (1999) documented that female red deer (*Cervus elaphus*) in Norway were 25% more likely to produce offspring as 2-year-olds in years with higher spatial variation of flowering plants, compared to years with low spatial

variation. Further, there is some evidence that spatial and temporal variation may influence density-dependence in opposite ways, with more animals being supported in spatially variable environments and fewer animals in temporally variable environments (Wang et al. 2006, Wang et al. 2009). Therefore, when comparing the nutritional resources among different areas, consideration must also be given not only to their availability, but to their dynamics.

In most temperate systems, forage resources for large herbivores are thought to be most limited in winter because plant senescence diminishes forage quality and snow accumulation reduces forage access, which also imposes a high energetic cost to forage (Wallmo et al. 1977, Van Soest 1982, Parker et al. 1984, Robinson and Merrill 2013). As a result, large herbivores reduce movements as well as metabolic and intake rates to cope with food reductions (Rhind et al. 2002, Dussault et al 2004, Massé and Côté 2013) and rely on body fat stores (Mautz 1978, Torbit et al. 1985, Cook et al. 2013). Entering winter with sufficient body fat stores can therefore improve an individual's probability of survival (Stephenson et al. 2020, Denryter et al. 2022*a*). Because post-winter body fat reserves are influenced by fall fat reserves (Cook et al. 2013), summer fat accumulation may also influence milk production for the current calf (White and Luick 1984, Parker et al. 1990) as well as pregnancy the following fall (Cameron et al. 1993, Cook et al. 2004). Thus, evidence points to availability of nutritional resources in summer as having strong effects on individual animal fitness (Hjeljod and Histøl 1999, Schaefer and Mahoney 2013, Hurley et al. 2014, Proffitt et al. 2016, Cook et al. 2018).

How large herbivores exploit the pronounced dynamics of forage in summer will determine the fitness consequences. As plants start to grow, fiber content and secondary metabolites of forage are relatively low resulting in higher digestibility (Bryant et al. 1983, Launchbaugh et al. 1993); as plants continue to grow, fiber accumulates and forage quality

depreciates across the growing season, which can result in decreased passage and intake rates (Van Soest 1982, Shipley and Spalinger 1992, Spalinger and Hobbs 1992, Gross et al. 1993). Therefore, maximized intake of nutritional resources may occur at intermediate levels of biomass (i.e., the forage maturation hypothesis, McNaughton 1985, Fryxell 1991, Hebblewhite et al. 2008). Large herbivores can track these forage dynamics at both broad-scale (e.g., elevational or latitudinal changes) and local-scale site conditions. For example, ungulates closely follow plant growth by "surfing" the green-wave or "jumping" to areas of new plant growth (Drent et al. 1978, Bischof et al. 2012, Merkle et al. 2016). Hebblewhite and Merrill (2009) reported elk that migrated to high elevations in Banff National Park, Canada, were exposed to 6.5% higher forage digestibility compared to resident elk, and elk that closely followed the spring green-up in Yellowstone National Park, USA, had greater fall fat body compared to residents (Middleton et al. 2018). At the same time, phenology of forage across the local scale may be asynchronous due to differences in canopy cover, aspect, and soil moisture conditions among community types, resulting in a dynamic mosaic of foraging resources (Hebblewhite et al. 2008, Luo et al. 2021). For example, Armstrong et al. (2016) demonstrated in an individual-based simulation that mobile consumers were able maintain a greater intake of energy in areas of greater spatial variation in timing of phenology than in homogenous areas. As a result, quantifying the forage dynamics of an area is central to understanding its capacity to sustain herbivore populations, and how land-use practices may alter it (Fryxell et al. 2004, Hobbs and Gordon 2010).

Several approaches have been used to quantify the dynamics of available forage resources for ungulates to link them to animal distribution or performance, or for assessing the nutritional carrying capacity of an area (Wallmo et al. 1977, Hobbs and Swift 1985, Proffitt et al. 2016, Cook et al. 2018). Proxies of forage resources, like NDVI, are commonly assumed to

reflect forage availability or quality in habitat studies, but the relationship is rarely validated (Searle et al. 2007). In fact, Johnson et al. (2018) cautioned against the use of NDVI for caribou (*Rangifer tarandus*) forage during summer in Alaska, USA, because alone it was weakly correlated (marginal $r^2 < 0.34$) with forage biomass, digestible energy, or digestible protein. Instead, field sampling has provided estimates of plant biomass usually at the peak or end of growing season within plant communities (Frair et al. 2005, Leclerc et al. 2012), which are extrapolated across a landscape using classified aerial photographs or satellite imagery, or using relationships to environmental gradient (Nelson et al. 2013, Keim et al. 2017), or both (Hebblewhite et al. 2008, Silva et al. 2019). Using estimates of standing biomass assumes forage abundance is limiting, such as in desert areas (Krausman et al. 1989, but see DeYoung et al. 2000), or that in productive areas with high plant diversity it allows selective feeding (Hebblewhite and Merrill 2009). Field estimates of standing biomass also do not explicitly reflect the forage consumed, but this can be approximated using fecal analysis, DNA barcoding, animal-borne camera collars, or *in situ* captive animals, each with their limitations (Hobbs and Spowart 1984, Hebblewhite et al. 2008, Newmaster et al. 2013, Thompson et al. 2015, Denryter et al. 2017). The explicit incorporation of the nutritional content of plants has improved the link to animal nutrition (Hobbs and Swift 1985, Hanley et al. 2012). Now referred to as "foodscapes" (Searle et al. 2007), studies have combined site data on forage biomass, nutritive values, and diet preference to estimate species-specific nutritional resources and modeled them as a function of landscape covariates (Avgar et al. 2015, Proffit et al. 2016, Cook et al. 2018, Johnson et al. 2018, Duparc et al. 2020). For example, Cook et al. (2018) used a two-stage modeling approach to predict dietary digestible energy (DDE) for elk across western Oregon and Washington, USA. They first predicted the biomass of three forage classes based on elk diet selection (determined

from captive elk foraging trials) as a function of environmental covariates, and then predicted DDE as a function of each forage class. However, the majority of these studies did not include seasonal dynamics in forage growth and quality (Avgar et al. 2015, Proffit et al. 2016, but see Johnson et al. 2018). Large herbivores live in dynamic environments where available nutritional resources change across both time and space, which are expected to impact how well these animals meet their nutritional requirements (Trudell and White 1981, Shipley and Spalinger 1992); therefore, these dynamics should be incorporated in the spatiotemporal evaluation of nutritional resources.

In this paper, we compared the dynamics of forage resources for boreal woodland caribou (*R. tarandus caribou*; hereafter caribou) in two study areas in northern Ontario, Canada, with apparent differences in their capacity to support local caribou populations (OMNR 2014, Fryxell et al. 2020). For example, from 2010 to 2014 Cochrane (CO) caribou had 7% lower pregnancy rates (CO: 85%, PL: 92%), 1.2% lower body fat levels (CO: 6.8%, PL: 8%), and 7% lower population growth rates (CO: 0.89, PL: 0.96) compared to Pickle Lake (PL; Fryxell et al. 2020, Walker et al. 2021, J. Cook, R. Cook, and G. Brown unpublished data). We hypothesized that the forage resources available to caribou during the summer were more restricted in Cochrane than in Pickle Lake due to physiography, natural and anthropogenetic disturbances, and climate. Cochrane is in the Northern Clay Belt region of northeastern Ontario with low topographic variation, predominant lacustrine soil, and extensive lowlands (Baldwin et al. 2000, Thompson 2000, McMullin et al. 2013, Walker et al. 2021), has active silviculture, and has a relatively low fire frequency (~120-year fire-cycle; Ward and Tithecott 1993, Li 2000, Thompson 2000). In contrast, Pickle Lake is a fire-prone (65-year fire-cycle) area in the Boreal Shield of northwestern Ontario, which has greater topographical variation and a diversity of associated

forested communities (Baldwin et al. 2000, Thompson 2000, Walker et al. 2021) with minimal anthropogenic disturbance over the past five decades. The two areas also differ climatically in that Cochrane is influenced by the maritime climate of Hudson and James Bay, reducing the number of growing-degree-days (Baldwin et al. 2000) with delayed phenology due to twice as much snow in winter compared to Pickle Lake (Walker et al. 2021).

As a result, we hypothesized that total standing biomass was higher in Cochrane than Pickle Lake because the extensive lowland ecosites present there may have greater overall productivity (Mallon et al. 2016); however, forage resources meeting caribou requirements would be more available in Pickle Lake because plant growth and associated forage quality may peak later in Cochrane than in Pickle Lake (Wipf et al. 2009, Legault and Cusa 2015, Kelsey et al. 2021). Moreover, this delayed plant phenology in Cochrane would subsequently cause a period of mismatch between available forage resources and caribou requirement during a critical period of reproduction when caribou are lactating and drawing down body reserves (Crête and Huot 1993). We also hypothesized that Pickle Lake would have greater spatial variation in forage resources than Cochrane because of varied topography and natural disturbances, which would facilitate efficient foraging to find and maintain intake of the highest quality forage across the summer season. We assessed these predictions by developing a dynamic foodscape for each study area and comparing the spatial and temporal patterns of caribou forage resources at the scale of a caribou summer home range.

Study area

The study was conducted in Pickle Lake (90.938W, 51.568N) within the Boreal Shield in northwestern Ontario and in Cochrane (80.598W, 49.908N, 23,000 km^2; Figure 4.1) in the Northern Clay Belt region in northeastern Ontario (McMullin et al. 2013, Thompson et al. 2015).

The Northern Clay Belt region is a postglacial lakebed characterized by fine-textured (i.e., silt and clay) luvisolic and gleysolic soils with high organic material, whereas the Boreal Shield is dominated by coarse-textured (i.e., sand) bruisolic soils that have developed on sandy glacial sediment (Baldwin et al. 2000). Forested communities within each region consisted of black and white spruce (*Picea mariana* and *P. glauca*), jack pine (*Pinus banksiana*), balsam fir (*Abies balsamea*), trembling aspen (*Populus tremuloides*), and white birch (*Betula papyrifera*) (Rowe 1972) with Cochrane having a 2-times greater extent of lowlands (bog and fen) compared to Pickle Lake (Walker et al. 2021). Cochrane had a greater total annual precipitation (824 mm $\pm$ 36 mm; $\bar{x} \pm$ SD, 20-yr average [1991-2010]) compared to Pickle Lake (736 mm $\pm$ 43 mm), whereas January daily temperatures (PL: -19.26°C ± 3.60°C; CO: -17.82°C ± 3.69°C) were slightly lower in Pickle Lake and July daily temperatures (PL: 17.66°C ± 1.49°C; CO: 17.36°C ± 1.25°C) were similar between areas (Environment Canada, https://climate.weather.gc.ca/historical_data/search_historic_data_e.html, accessed 14 June 2019).

At the time of the study (2010), Cochrane had greater extent of harvest regeneration (<40 years; 13%) compared to Pickle Lake (0.04%, OMNRF 2014*a*, Fryxell et al. 2020) because the latter had not been subject to active forest harvesting since the 1960s (Thompson et al. 2015). In contrast, Pickle Lake had a higher proportion of natural disturbance (proportion burned <50 years; 12%) compared to Cochrane (4%; OMNRF 2014*a*, Fryxell et al. 2020). Linear feature density was higher in Cochrane (0.31 km/km^2) compared to Pickle Lake (0.05 km/km^2; OMNRF 2014*a*, Fryxell et al. 2020). Wolf (*Canis lupus*) and moose (*Alces alces*) densities were higher in Pickle Lake (4.2 wolves/1,000km^2, 4.6 moose/100km^2) than Cochrane (3.7 wolves/1,000km^2, 3.8

moose/100km^2; OMNRF 2014*a*, Fryxell et al. 2020) with similar black bear (*Ursus americanus*) densities across areas (20–40 black bears/100 km^2; Rodgers et al. 2009, Howe et al. 2013).

Methods

Overview

We used several steps to develop and compare forage metrics across caribou-delineated landscapes in Cochrane and Pickle Lake, Ontario (Figure 4.2). We sampled species-specific abundances and nutritional quality at field sites in Pickle Lake during 2017–2018 and Cochrane in 2018 and used these data to develop dynamic models that predicted daily values in key forage metrics. Forage metrics included components of accepted (see below) biomass, standing biomass of accepted species that met caribou nutritional requirements in summer, and caribou intake rates derived from components of accepted biomass. We used the models to predict the forage metric values in 30-m cells across the two study areas, and then used a moving window to estimate the mean and variation of each forage metric in an area the size of a caribou summer home range. We compared seasonal changes in each of the forage metrics at daily time-steps between the two landscapes from 15 June to 15 September 2010 at the scale of the caribou home range.

Site selection and macroplot characteristics

Locations of 393 vegetation sites (hereafter, vegetation macroplots) and 79 sites where captive caribou foraging trials subsequently took place (hereafter, caribou macroplots) were randomly selected *a priori* to sampling using a geographical information system. Sites were selected within 300 m of a road and in proportion to available forest types (upland conifer, mixedwood, deciduous, bogs, and fens) and seral stages (early [<20 years] and mid-late [≥20 years]). At each location, macroplots were located within a single, homogeneous stand representing a stratum and situated ≥50 m from stand edges. We sampled vegetation biomass and recorded site

characteristics in 265 vegetation macroplots and 79 caribou macroplots in Pickle Lake from 15 June to 10 October during 2017 and 2018. In Cochrane, we sampled 128 vegetation macroplots from 5 June to 27 August during 2018. Vegetation macroplots were 0.4 ha (90 m x 45 m), but caribou macroplots were larger (≤1.7 ha) to meet requirements of captive caribou foraging trials. Based on under- and overstory characteristics, we classified each macroplot to an ecosite type following Racey et al. (1996) at Pickle Lake and Taylor et al. (2000) at Cochrane. Given the functional similarity within and between the two classifications, we cross-walked the two classification systems post-hoc (Appendix 3.1) and collapsed them into seven similar subgroups, which we refer to as ecosites (Table 4.1).

At each macroplot, we characterized tree canopy cover (%) by averaging ten canopy cover measurements along three (vegetation macroplots) or four (caribou macroplot) transects using an ocular sighting tube often referred to as a moosehorn (Bunnell & Vales 1990, Cook et al. 1995). We measured basal area (m^2/ha) at two equidistant locations along each transect using an angle gauge (Cook et al. 2016; Appendix 3.2). We measured mean stand height (m; West 2009) based on the tallest cohort of trees in the stand using a clinometer at the center of each macroplot and determined stand age from 1–2 trees within the tallest cohort of trees based on tree ring counts at 0.3 m above ground. The normalized difference moisture index (NDMI) for a macroplot was calculated from Landsat 8 as the mean value of all 30-m pixels within the spatial extent of the site, with each pixel assigned the maximum NDMI value derived between 1 June and 30 September. NDMI calculates the difference between near-infrared and mid-infrared wavelengths as a proxy of vegetation moisture (Wilson and Sader 2002) and has been used to map lichen abundance (Falldorf et al. 2014, Silva et al. 2019). We also derived change in enhanced vegetative index (ΔEVI) calculated using MODIS data at 250-m resolution where the

difference was calculated as the mean EVI value derived across 1 July–1 August (peak growing season) minus the mean value of EVI derived across 1 September–1 October (plants senesced but snowfall uncommon). EVI is an index of greenness and has been shown to be less sensitive to atmospheric aerosols compared to the normalized difference vegetation index (Huete et al. 2002). Further, we used ΔEVI because it can isolate the spectral signature for herbaceous growth, i.e., removes the effect of conifers (Villamuelas et al. 2016) and has been used as a proxy of vegetative productivity in the boreal forest (Serrouya et al. 2021). The soil at a macroplot was characterized using SoilGrid250m as percent sand, clay, or silt (at the depth of 0–5 cm) for a 250-m area across the spatial extent of the macroplot (Hengl et al. 2017).

Vegetation sampling

We sampled vegetation biomass in two 2-m^2 circular plots along three transects in vegetation macroplots or four transects in caribou macroplots (Appendix 3.2). Within each plot, all current annual growth (CAG) was clipped from 1 cm to 2 m and separated by plant species, oven dried at ≥70 °C to constant weight, and weighed to the nearest 0.1 g. For conifers and evergreen shrubs, we also separately clipped previous year's growth (PYG) based on the initial growth point of the previous year. Because of the often-high density of conifers and evergreen shrubs, which are not considered caribou forage in summer (Thompson et al. 2015, Denryter et al. 2017, Cook et al. *in prep*.), a smaller 0.50-m^2 plot was clipped within the 2-m^2 plot and estimates were multiplied by four to scale to 2-m^2.

Seasonal trends in accepted biomass

Although we provide estimates of total standing biomass, our analyses focused on biomass of species "accepted" by captive caribou via foraging trials, defined as those species that were consumed in proportion equal to or more than proportionally available (e.g., Denryter et al. 2017,

Denryter et al. 2022*b*, Cook et al. *in prep.*). We used data from Cook et al. (*in prep*.) on accepted species, where acceptance was based on a mean Ivlev's electivity index (Ivlev 1961) of ≥0 across foraging trials (n = 79). Ivlev's electivity index values range from -1 to 1 and were derived as:

Ivlev = (proportion [prop.] of diet – prop. Available) / (prop. Of diet + prop. Available) (1)

The proportion in the diet of each plant species was estimated from the proportional intake derived from direct observations of bite rates and mass pooled across 4 captive caribou per macroplot, and the proportional biomass available in the caribou macroplot. Species-specific bite masses were estimated by simulating 10–20 bites based on the direct observations of how the captive caribou cropped each species (for more detail see Denryter et al. 2017, Denryter et al. 2022*b*, Cook et al. *in prep.*). Exceptions were *Maianthemum canadensis, Melampyrum lineare, Vaccinium angustifolium,* and *V. myrtilloides*, which were classified as avoided (Ivlev's electivity index < 0) but frequently eaten by caribou (Cook et al. *in prep.*), and therefore included as accepted species in the following analyses. We tested for differences between the proportion accepted biomass of total standing biomass at macroplots between Pickle Lake and Cochrane using a beta regression with Cochrane as the reference category.

We used macroplot data collected across the summer to model the seasonal change in components of accepted biomass in the two study areas. We considered the major components of accepted biomass to include grass (*Poaceae* not *Cyperaceae* or *Juncaeceae*), forb, and deciduous shrub combined (hereafter GFS), arboreal and terrestrial lichen (hereafter lichen), horsetail (*Equisetum* spp.), and mushroom because of their value, or perceived value, for predicting caribou nutrition (Cook et al. *in prep.*). Accepted graminoid (*Cyperaceae* or *Juncaeceae* not *Poaceae*), accepted fern, and *Peltigera* spp., although classified as accepted species, were not included as major components of total accepted biomass, because they represented <2% of total

accepted biomass and were uninformative as covariates for predicting caribou nutrition by Cook et al. (*in prep.*) in their evaluation of caribou nutritional responses. In preliminary analyses, we identified biomass of accepted components in five macroplots (1% of all macroplots) to be outliers due to biomass values that far exceeded the range observed across all other macroplots (i.e., data on GFS from two macroplots, lichen from two macroplots, and mushroom from one macroplot) (Appendix 4.1) and therefore these data were excluded from further analyses. Using linear regression, we tested for differences in accepted biomass between seral stages, ecosites, or seral-specific ecosites (Early seral, Lowland-Bog, or Mid-late Lowland-Bog was the reference category) and by study area while accounting for sampling date.

Seasonal modeling was completed in several steps. First, a preliminary analysis of data pooled across all ecosites by study area indicated seasonal trends in each accepted biomass component (Appendix 4.2-4.3). As result, we evaluated linear vs. non-linear trends in each component over Julian day within seral-specific ecosites by study area using CurveExpert (CurveExpert 2.7.3, D. G. Hyams, Madison, AL. USA) based on >2 change in Akaike information criterion corrected for small sample sizes (AIC_c; Burnham and Anderson 2002). When there was no seasonal biomass trend ($\Delta AIC_c < 2$ from null) in a component of accepted biomass in one or both study areas, we tested for differences in mean accepted biomass component within an ecosite between study areas using linear regression with study area and Julian day as fixed effects. We used a mean biomass for the seral-specific ecosite for a study area if there was a difference between the study areas, or if not, we pooled the data across study areas and used the mean across the two study areas. Further, when we had data from <16 macroplots for a seral-specific ecosite across both study areas, we used a constant mean value across the two

study areas. We took this approach to ensure that when we used different values between study areas to estimate forage availability, we had support for those differences.

Second, we pooled data across study areas and seral stages for an ecosite and determined whether environmental site characteristics influenced biomass components and the nature of the relationship (i.e., linear vs. non-linear) using the same approach as above. Prior to modeling, we determined whether environmental variables were collinearly related (i.e., $|r| > 0.60$), and when they were, we identified the most informative covariate based on AIC_c, which was included in subsequent model selection. Third, we determined the top model for predicting seasonal changes in biomass components at a location for each seral-specific ecosite by including Julian day and environmental variables with candidate models informed by the previous model results, and selected the top model based on $\Delta AIC_c < 2$. We retained the most parsimonious model with a seasonal trend over models with only environmental variables when there was equal support. The maximum number of covariates included did not exceed a ratio of one covariate per ~10 macroplots. Finally, we used a within-sample approach to assess the variation explained (i.e., r^2) by the top models via linearly regressing the observed value by the model-predicted value across all macroplot for each component of accepted biomass and reported the standard error of the estimate.

Seasonal trends in high-quality acceptable biomass

Even though caribou may select certain forages, diets composed of these species may not be of sufficient quality to meet their nutritional requirements (White 1978, Mattson 1980, Hobbs and Swift 1985). As a result, we also compared study areas based on the abundance of accepted biomass (kg/ha) that would adequately meet caribou nutritional requirements. To do this, we used the Forage Resource Evaluation System for Habitat for Deer (FRESH-Deer, FRESH model

hereafter, Hanley et al. 2012; http://cervid.uaa.alaska.edu/deer/). The FRESH model uses linear programing to determine the maximum amount of standing biomass that satisfies a set nutritional level in the forage, which is referred to as suitable biomass (Hanley et al. 2012, Hull et al. 2020, Ulappa et al. 2020), but hereafter we refer to it as high-quality accepted biomass. Using only accepted biomass, we estimated three levels of suitable biomass derived for a lactating caribou with 1 calf based on constraints of: 1) only digestible energy (DE-accepted biomass), which we specified as 2.9 kcal/g (12.1 KJ/g, National Research Council 2007, Denryter et al. 2022*b*), 2) only digestible protein (DP-accepted biomass), which we specified as 8.6 g of protein/100 g of forage (National Research Council 2007, Denryter et al. 2022*b*), and 3) both digestible energy and protein (HQ-accepted biomass). We included the same accepted species that corresponded to components of accepted biomass and put no limits on the proportion of biomass a species could contribute to each estimation of high-quality accepted biomass. To account for variation in forage quality, we included within the FRESH model the standard deviation in DE and DP of each species calculated across a 2-week moving window using the predictive forage quality models discussed below. The same estimates of accepted biomass considered as outliers above were also not included in this analysis (Appendix 4.1).

Estimates of high-quality, accepted biomass derived by the FRESH model at each macroplot were based on species-specific biomass, and daily, species-specific predictions of DE and DP. Biomass of each species was estimated as described above. To estimate species-specific DE and DP over time, we derived dynamic, species-specific models of DE and DP using the values determined by Cook et al. (*in prep.*). Species-specific DE and DP were based on CAG of 1 to 53 (median = 12) samples of 55 accepted species from 15 May to 5 October in Pickle Lake in 2018 (n = 553), and 23 May to 8 October in 2018 (n = 378) in Cochrane. Sixty-nine percent of

accepted species were sampled in both study areas, which represented 92% of all forage quality samples with equal proportions of life-form groups sampled between areas (Appendix 5.6). Of the accepted species sampled in both study areas, we collected on average 13 $\pm$ 7 ($\pm$ SD; range: 3–31) samples per study area for each species throughout the summer to capture the seasonal change in DE and DP. Digestibility (%) was derived using the summative equations of Robbins et al. (1987a,b) and estimates of neutral detergent fiber (NDF), acid detergent lignin (ADL), and insoluble ash component (AIA), which had been corrected as per Cook et al. (2022). Gross energy content (kcal/g) was calculated using a bomb calorimeter, crude protein content (g protein/100 g dry matter) was based on total elemental N x 6.25, and tannin content based on tannin precipitation methods following Martin and Martin (1983). Digestible energy (DE) and protein (DP) was the product of digestibility and gross energy or crude protein content, respectively, and were adjusted for tannin concentration following Hanley et al. (1992). We modeled DE and DP across all plant samples via linear regression as a function of study area (Cochrane assigned as reference category) and Julian day, and tested rate of change between areas with an interaction between study area and Julian day.

We characterized the seasonal change in DE and DP of accepted species by modeling each species as a function of Julian day and environmental variables following a similar approach as described above for the dynamics of components of accepted biomass. When there were sufficient samples (~10 samples per covariate), we also assessed whether study area, canopy cover, and drainage class (upland vs. lowland) influenced DE or DP (main effect) or its seasonal trends (Julian day interaction). We used life-form group models for species with too few samples to produce their own seasonal model (n ~ 10). For further detail see Appendix 5. Finally, we developed seasonal models for the three metrics of high-quality accepted biomass as

a function of Julian day and environmental variables using the same methods outlined above for components of accepted biomass.

Seasonal trends in intake rates

Because relationships had been developed between standing biomass of accepted GFS, horsetail, and mushroom and per minute forage intake rate (g/min on a dry matter basis, i.e., instantaneous forage intake rate; Cook et al. *in prep.*), we also derived estimates of intake and compared seasonal changes in intake rate between study areas. Briefly, Cook et al. (*in prep.*) modeled intake rates observed during foraging trials in Pickle Lake on 4 adult captive caribou four times per day per caribou per macroplot for a total of 75 mins per caribou per day, or five hrs of foraging trials/macroplot in 79 caribou macroplots. Intake rate was calculated as the sum of the number of species-specific bites weighted by bite mass per minute. We used the regression equations for intake rates in upland (Equation 2) and lowland (Equation 3) ecosites:

$$\text{Upland intake rates (g/min)} = 0.59 + 0.69*(4.49/(1+1.39*\exp^{-0.002*GFS})) + 0.082*\text{Horsetail} + 0.103*\text{Mushroom} \quad (2)$$

$$\text{Lowland intake rates (g/min)} = 0.89 + 1.12*(4.38/(1+1.43*\exp^{-0.02*GFS})) + 0.01*\text{Horsetail} + 0.70*\text{Mushroom} \quad (3)$$

where GSF, horsetail, and mushroom are the biomass (kg/ha) of each accepted biomass component in a 30-m cell in each study area predicted based on the seasonal models described above.

Comparison of forage resources between study areas

We compared the mean and coefficient of variation (CV) in abundance of the components of accepted biomass, intake rate, and the three metrics of high-quality accepted biomass using a similar approach. We first predicted daily values within each 30-m^2 pixel in both study areas

from 15 June to 15 September using the above seasonal models based on seral-specific ecosites and environmental variables. Our predictions of forage metrics were extrapolated for ~2 weeks in Cochrane to 15 September because vegetation sampling did not occur; however, extrapolations followed the seasonal trajectory of biomass observed in Pickle Lake. We limited predicted values for each forage metric so that they did not exceed the maximum values estimated across all macroplots (Appendix 6.2). Total accepted biomass was derived as the sum of the four components of accepted biomass (GFS, lichen, horsetail, mushroom). We also capped daily predicted values of each metric of high-quality accepted biomass so that these did not exceed the predicted total accepted biomass for each cell.

We used the Ontario Far North Land Cover v1.4 (FN, OMNRF 2014*a*) to delineate the ecosite type of each 30-m^2 cell and readily cross-walked the ecosites in Table 4.1 to the FN land cover types (Appendix 7.6) with two exceptions. The FN layer distinguishes early seral (i.e., disturbed, <20 years old) from late communities, but did not indicate the land cover type for early seral. As a result, we identified ecosite for these early seral communities based on the North America Land Change Monitoring System (NALCMS) land cover layer (Latifovic et al. 2017). Further, because productive (Upland-Black Spruce-White Spruce) and unproductive (Upland–Black Spruce) upland conifer sites substantially differ in levels of caribou-specific forage (Table 4.2, Figure 4.3) but are not distinguished in either the FN or the NALCMS, we identified thresholds in maximum values of NDVI (30 m; Landsat 8, June–September 2010) at macroplots to differentiate between Upland–Black Spruce–White Spruce and Upland–Black Spruce with >75% accuracy (see further detail in Appendix 7).

Layers of tree basal area and canopy cover developed by Matasci et al. (2018); percent clay, sand, and silt from the SoilGRid250m dataset (250m; Hengl et al. 2017); and NDMI and

ΔEVI calculated from 2010 Landsat 5 imagery and 2010 MODIS imagery (250m), respectively, were used to characterize 30-m^2 pixels for predicting forage metrics in each area. We assumed no biomass in areas of silvicultural harvest (OMNRF, unpublished data) and forest fires (Aviation, Forest Fire, and Emergency Services Fire Disturbance Area layer) that occurred in 2010.

We then recalculated the value assigned to a 30-m^2 pixel values as the mean or coefficient of variation of values of all cells within a 5.21 km^2 (2.28 km x 2.28 km) window around a cell using the *focal statistics* function in ArcGIS (ArcMap 10.6, ESRI). Hereafter, we refer to these values as home range-scaled values to distinguish them from 30-m pixel-based predicted values; further, all graphed values of forage metrics are the mean or CV of home range-scaled values. The window size reflected the average home-range size derived from GPS telemetry locations from 1 June to 30 September of 29 female caribou in Pickle Lake and 25 female caribou in Cochrane (see Walker et al. 2021 for particulars of caribou captures; Appendix 8.1 provides details of the home range analysis). In graphing season trends in forage metrics, we do not present confidence intervals due to the large number of 30-m^2 pixels.

We tested for overall mean difference across the entire landscape in each study area in the daily, home-range scaled mean and CV values for each forage metric using a paired *t*-test paired by day and visually assessed the difference in the seasonal patterns of change. The spatial extent of each study area was defined as the 99% UD of GPS telemetry locations of based on 58 caribou in Pickle Lake and 60 caribou in Cochrane with 1–12.5 hr fix rate intervals from 1 June to 30 September (Figure 4.1). Unless otherwise stated, all statistical analyses were conducted in R (R version 4.2.1, www.R-project.org, accessed 2 July 2022).

Results

Spatial and temporal patterns across macroplots

We sampled a total of 472 macroplots with a median sample date of 31 July in Pickle Lake (n = 344) and 9 July in Cochrane (n = 128). Total biomass in macroplots ranged from 5 to 4,834 kg/ha across study areas with greater total biomass across seral-specific ecosites in Pickle Lake than Cochrane, except for Mid-late Upland-Black Spruce (Table 4.2, Appendix 4.3). We observed 75% greater total standing biomass in Pickle Lake (1,068 kg/ha) than Cochrane (612 kg/ha) based on mean total biomass of each seral-specific ecosite weighted by their proportional extent (Table 4.1, 4.2). The proportion of accepted biomass of total biomass across all macroplots was similar in Pickle Lake (0.39 $\pm$ 0.27; x $\pm$ SD) and Cochrane (0.36 $\pm$ 0.22; β = 0.15 $\pm$ 0.21, $\pm$ CI; Table 4.2). We observed higher proportion of accepted biomass in upland compared to lowland ecosites (Table 4.2, Appendix 4.4). In both study areas, we observed higher accepted biomass in early (<20 years) than mid-late seral ($\geq$20 years) stands, but this difference was significantly higher only in Pickle Lake (Figure 4.3, Appendix 4.5). Accepted biomass was lowest in Lowland-Bog, Lowland-Fen, and Lowland-Cedar/thicket and greatest in upland ecosites and Lowland-Marsh in Pickle Lake (Figure 4.3, Appendix 4.6). Accepted biomass did not differ among ecosites in Cochrane; however, when considering seral stage, accepted biomass was higher in Mid-late Upland-Black Spruce and Early Upland-Black Spruce-White Spruce than all other seral-specific ecosites (Figure 4.3, Appendix 4.6–4.7).

When data were pooled across ecosites, there were clear temporal patterns in accepted biomass of GFS and mushroom at both study areas, horsetail in Cochrane, but not lichen (Figure 4.4, Appendix 4.2). Accepted GFS biomass was higher across the season in all ecosites in Pickle Lake compared to Cochrane, with only Upland-Black Spruce-White Spruce and Lowland-Fen

not being significantly different (Table 4.2, Appendix 4.3). Horsetail biomass was consistently higher in Pickle Lake but differences within ecosites were not significant ($P > 0.06$). With the exception of Lowland-Bog, mushroom biomass was higher in Pickle Lake but differences within ecosites were not significant ($P > 0.09$). Finally, lichen biomass was similar in Upland-Black Spruce and Lowland-Fen across study areas ($P > 0.34$), with higher lichen biomass in Lowland-Bog in Cochrane ($P = 0.005$) and higher lichen biomass in Upland-Black Spruce-White Spruce at Pickle Lake ($P = 0.009$).

Seasonally dynamic models of accepted biomass

High variability and low sample sizes within seral-specific ecosites resulted in using a constant, seasonal mean to predict components of accepted biomass in the majority (61%) of seral-specific ecosites within one or across both study areas (Table 4.2) with about the same number of means adjusted for environmental conditions (24%) and Julian day (20%) within each study area (Table 4.3). In contrast, 6% of the models we used to predict components of accepted biomass included both Julian day and environmental covariates at Pickle Lake, whereas no models used in Cochrane had both Julian day and environmental covariates (Table 4.3). Of the models that included one or more environmental covariates, 39% included basal area, 35% included NDMI, 31% included ΔEVI, 25% included a soil metric, and 6% included canopy cover (Table 4.3). The seral-specific ecosite models used to predict accepted biomass components explained 6–52% of the observed variation in sampled biomass at macroplots, with the highest explanatory power in predicting GFS (PL: 59%, CO: 63%) followed by lichens (PL: 25%, CO: 35%), horsetails (PL: 23%, CO: 30%), and mushrooms (PL: 17%, CO: 16%; Table 4.4). For full results of model selection see Appendix 6.

Seasonally dynamic plant quality

We analyzed forage quality for 55 accepted species across the two study areas with 1 to 53 samples per species and 7 to 444 samples per life-form group. When predicting species-specific change in DE and DP over the summer, a majority of plant species were modeled as combined across study areas (DE: 63%; DP: 50%) with 13% and 35% of models including canopy cover for DE and DP models, respectively. Canopy cover had more support than other environmental variables (Appendix 5). Observed and predicted forage quality values across all forage quality samples, while accounting for sampling date and environmental conditions, were highly correlated for DE ($r = 0.83$) and DP ($r = 0.91$), with the discrepancy averaging 0.13 ± 0.13 kcal/g ($\pm$ SD) in DE and 1.53 ± 1.64 g of protein/100 g of forage in DP (Appendix 5).

DE of mushrooms averaged highest over the summer but were not significantly different from lichens, whereas they were 13–15% higher than deciduous shrubs and forbs, and 20–31% higher than grasses and horsetails (Table 4.5, Appendix 9.1). Mushrooms also were 70–85% higher in DP than forbs, grasses, and horsetails and about twice as high as deciduous shrubs. Lichen provided little to no DP across the summer (Table 4.5). DE across all samples of accepted species collected in each study area averaged 3.2% higher in Cochrane than Pickle Lake between 15 June and 15 September ($\beta = -0.09 \pm 0.04$, $\pm$ CI, $P < 0.001$; Figure 4.5A) and DP averaged 40.1% higher in Cochrane than Pickle Lake ($\beta = -2.38 \pm 0.71$, $P < 0.001$; Figure 4.5B). Trends suggest DE of accepted species averaged higher than the DE threshold requirement (2.9 kcal/g; used in the FRESH model) for 10 days longer in Cochrane than Pickle Lake, and for 36 days longer in Cochrane than Pickle Lake for the DP threshold requirement (8.6%, Figure 4.5).

Seasonally dynamic models of high-quality accepted biomass

Accepted biomass constrained by DE, DP, or both (i.e., HQ) averaged 86% ± 26%, 46% ± 41%, and 43% ± 41% of the total accepted biomass across all macroplots**,** respectively. DP had a stronger constraint on forage biomass contributing to available HQ-accepted biomass than DE based on the correlations between HQ-accepted biomass and DP-accepted biomass (r = 0.92) than DE-accepted biomass (r = 0.50) across macroplots. Biomass of each metric of high-quality was higher in Upland-Black Spruce in Pickle Lake than Cochrane when we accounted for sampling date, but similar across all other ecosites (Figure 4.6, Appendix 4.3). We used a constant, seasonal mean to predict high-quality accepted biomass in 37% of seral-specific ecosites across study areas (Table 4.6), with 33% of the means adjusted only for Julian day and 6% for environmental conditions (Table 4.7). In Pickle Lake, 18% of the high-quality accepted biomass models included both Julian day and environmental covariates, whereas no models in Cochrane included both Julian day and environmental covariates (Table 4.7). Tree basal area most frequently influenced metrics of high-quality accepted biomass (73%), followed by percent silt (20%), NDMI or ΔEVI (13%), and canopy cover (7%). High-quality models explained 50–67% of the variation in accepted biomass constrained by DE, DP, or both at macroplots across the 2 study areas (Table 4.4). For full results of model selection see Appendix 6.

Comparison of landscape-level forage resources across study areas

Although forage was predicted over comparatively similar extents in Cochrane (28,961 km^2) and Pickle Lake (25,046 km^2), there were major differences in the extents of ecosites (Table 4.1). Lowland-Bog composed 68% of the study area in Cochrane and was 2.2-times more extensive than at Pickle Lake, whereas Upland-Black Spruce composed 57% of the study area at PL and was 3-times more extensive in Pickle Lake than Cochrane (Table 4.1). The extents of Upland-

Black Spruce-White Spruce, Lowland-Fen, and Lowland-Cedar/thicket were proportionally similar between areas (Table 4.1). Upland-Black Spruce-Rocky and Lowland-Marsh were not present in the Cochrane area. Thus, uplands dominated the Pickle Lake study area, whereas lowlands dominated the Cochrane study area.

There was a non-linear change in accepted biomass over the summer that peaked in early August with consistently higher abundance in Pickle Lake than Cochrane (Figure 4.7A). Spatial variation in accepted biomass was somewhat higher in Pickle Lake, with a reciprocal seasonal trend in relation to mean accepted biomass (Figure 4.7A, B). Seasonal and spatial trends in accepted biomass mirrored those in GFS and lichens because they comprised 70% $\pm$ 31% ($\pm$ SD) and 26% $\pm$ 31% of the accepted biomass, respectively. Higher GFS biomass in Pickle Lake than Cochrane was due to the 2.6-times greater GFS biomass at Mid-late Upland-Black Spruce in Pickle Lake than Cochrane, which composed 48% of the Pickle Lake study area, and to the relatively high extent in Cochrane of Lowland-Bog (68%; Table 4.1), which had 31% less GFS biomass than in Pickle Lake (Figure 4.3). In contrast, lichens were relatively constant in space and time but averaged 83% higher across Pickle Lake than Cochrane (Figure 4.8C). This was because Early Lowland-Bog and Mid-late Upland-Black Spruce, where lichen is relatively abundant, were limited in Cochrane, whereas Mid-late Upland-Black Spruce was widespread at Pickle Lake (Figure 4.3). Higher abundance of mushrooms in Pickle Lake, especially in late summer, was likely the cumulative effect of mushrooms being about 7-times greater in Mid-late Upland-Black Spruce, which was the dominant ecosite type in Pickle Lake (Tables 4.1, 4.2). However, limited sampling in Cochrane during late summer may also contribute to dissimilar mushroom biomass between study areas. In contrast, horsetail biomass after 15 July was about

35% more abundant in Cochrane (Figure 4.8E), which was largely due to their higher abundance in Mid-late Lowland-Bogs in Cochrane during later summer (Table 4.2, Appendix 10.1).

Proportion of the available accepted biomass that met caribou DP and especially DE requirements was higher in Cochrane than in Pickle Lake except in early spring (Figure 4.9), which was consistent with the 3% and 40% higher DE and DP, respectively, across forage quality samples in Cochrane than Pickle Lake. High-quality biomass constrained by DP peaked about 29 days later (July 30) in Cochrane than in Pickle Lake (1 July), whereas when constrained by DE, biomass peaked only about 4 days later in Cochrane. Spatial variability in accepted biomass constrained by DE was somewhat lower and more pronounced seasonally in Cochrane than Pickle Lake, whereas accepted biomass constrained by DP increased over time in Pickle Lake and was less variable in Cochrane (Figure 4.7).

Based on the changing availabilities of the components of accepted biomass, potential caribou intake rates at Pickle Lake showed little seasonal trend, remaining equal or above those at Cochrane during the summer (Figure 4.10). In contrast, intakes rates in Cochrane exhibited pronounced seasonal trends that were close to those in Pickle Lake only during the peak of the growing season (23 July–14 August; Figure 4.10) when GFS biomass, the dominant driver of intake rates, was most similar between the study areas (Figure 4.8A, Appendix 10.2). As a result, intake rates averaged 15% higher in Pickle Lake than Cochrane and had on average 16% greater spatial variation in the former. In contrast, Cochrane had overall low intake rates that were less variable in space, likely due to overall lower GFS biomass and the dominant extent of Mid-late Lowland-Bogs. However, we observed a smaller magnitude of difference between Pickle Lake and Cochrane when considering intake rates versus accepted biomass across the summer, which

was due to a 9% higher predicted intake rate in lowland than upland forests (Cook et al. *in prep*.) and the 2.4-times more extensive lowlands in Cochrane than Pickle Lake.

Discussion

We quantified the spatiotemporal availability of summer caribou forage in Pickle Lake and Cochrane, Ontario, and found evidence to support our predictions that caribou in Cochrane were exposed to lower biomass of most key forage metrics with less spatial variation during a key reproductive period. Several factors may lead to reduced availability of caribou forage in Cochrane in the Northern Clay Belt region compared to Pickle Lake in the Boreal Shield. First, understory standing biomass of all species (accepted plus avoided by caribou) averaged 75% greater in Pickle Lake with biomass being higher in all seral-specific ecosites in Pickle Lake than Cochrane except Mid-late Upland-Black Spruce. The lower total standing biomass across Cochrane was not due to greater extent of ecosites with less biomass, because lowland forests, which had higher total biomass compared to uplands, were 2.4-times more extensive in Cochrane than Pickle Lake. Mallon et al. (2016) also reported higher total standing biomass in lowlands than in uplands in the Nakina area of Ontario (situated between Pickle Lake and Cochrane in Ontario), but their estimates included feather and sphagnum moss and ours did not. However, even after excluding biomass of moss (Table A5 in Mallon 2014), they observed 335% greater biomass in lowlands than uplands compared to only 46% and 21% higher standing biomass in lowlands than in uplands in Pickle Lake and Cochrane, respectively. In contrast, Mallon et al. (2016) reported no difference in total standing biomass by seral stage (early [≤30 years], mid [31–70 years], and late [≥71 years]) in Nakina, whereas we found standing biomass was higher in early seral (<20 years) than mid-late seral (≥20 years) stands in both Pickle Lake (82% higher) and Cochrane (64% higher). Methodological differences between this study (clip plots) and

Mallon et al.'s (2018) double-sampling plots may also reflect dissimilar conclusions and magnitudes of biomass reported.

At the same time, we expected similar patterns in lichen availability in Pickle Lake and Nakina because both areas are within the Boreal Shield. However, we found 7.5-times higher lichen biomass in upland than in lowland forests in Pickle Lake, whereas there was no difference in Nakina (Mallon et al. 2016). Lichen biomass ranged from 0 to 755 kg/ha (n = 12) in Nakina (Mallon 2014, Mallon et al. 2016) in contrast to 0 to 4,816 kg/ha (n = 257) in Pickle Lake, which was similar to the ~5,000 kg/ha (n = 109) reported by Silva et al. (2019) in Woodland Caribou Provincial Park, Ontario, west of Pickle Lake. A similar difference in lichen biomass was evident in lowlands with up to 475 kg/ha (n = 86) in Pickle Lake, whereas Mallon et al. (2016) reported up to 228 kg/ha (n =15). These differences were not due to the inclusion of arboreal lichen in Pickle Lake, as it comprised only 4% of total lichen biomass in uplands and lowlands; nor was it due to our exclusion of the lichens *Stereocaulon paschale*, which is not generally eaten by caribou (Denryter et al. 2017, Cook et al. *in prep.*), and *Bryoria* spp., which was classified as avoided due to low availability (Cook et al. *in prep.*), because both species comprised <0.2% of total standing biomass. Instead, the higher abundance of lichen in uplands may be because we sampled lichen across considerably more sites in Pickle Lake than did Mallon et al. (2016) at Nakina, and our area may have encompassed a broader range of ecological variability. In contrast, we observed similar lichen biomass across ecosites in Cochrane as in Pickle Lake with the exception of Lowland-Bogs, where lichen was 3.4-times greater in Cochrane than in Pickle Lake. Lichen abundance was still greater across Pickle Lake, despite the predominance of Lowland-Bogs in Cochrane (68%), because Upland-Black Spruce, which had 2.2-times greater lichen biomass than Lowland-Bogs in Cochrane, comprised 57% of Pickle Lake.

Although total standing biomass may reflect ecosystem productivity, it may not represent the forage resources available to caribou in an environment because it includes species that caribou do not consume and others that may not meet nutritional requirements (Searle et al. 2007). In contrast to total standing biomass, which was most abundant in macroplots in lowland forests, we observed higher accepted biomass in upland than in lowland forests in both Pickle Lake (73% higher) and Cochrane (56% higher). We found the greatest biomass of accepted species in northern Ontario in disturbed stands, such as from timber harvest and fire. There is a period of ~20 years after a disturbance event when the understory vegetation in uplands and lowlands comprised 50% and 64% greater accepted biomass than undisturbed forests (≥20 years), respectively. Across both study sites, the plant species eaten by caribou averaged only 36–39% of total standing biomass in macroplots, which was similar to the ~10–40% of total standing biomass in boreal forest in British Columbia, Canada, reported by Denryter et al. (2017). The lowest proportions of acceptable biomass in British Columbia were also in Lowland-Bog and Lowland-Fen (~30%) as well as wetland ecosites (~10%), whereas the proportion accepted biomass was 30–50% in alpine ecosites, due largely to a greater abundance of deciduous shrub and terrestrial lichen biomass (Denryter 2017, Denryter et al. 2017).

The comparisons above suggest that using total standing biomass to reflect forage resources for caribou during summer could be misleading. For example, Mallon et al. (2016) concluded that because of similar total standing biomass between uplands and lowlands, caribou use of lowlands may not subject them to lower forage availability, as previously proposed (McLoughlin et al. 2005). However, Mallon et al. (2016) also pointed out that a substantial proportion of total standing biomass in lowlands is evergreen shrubs, which are not readily consumed by caribou during summer (Thompson et al. 2015, Denryter et al. 2017, Cook et al. *in*

prep.). Indeed, we found conifers and evergreen shrubs contributed to 42% of total standing biomass in both uplands and lowlands, but particularly lowlands (65%) in Pickle Lake and Cochrane. Nonetheless, when we compared forage availability at the scale of the home-range in Pickle Lake to Cochrane, we found both total standing biomass (75%) and accepted biomass (65%) were lower in Pickle Lake, indicating correspondence. However, this was not true when considering ecosites. In fact, lower accepted biomass across Cochrane was driven by the low accepted biomass, but not total standing biomass in lowlands (particularly Lowland-Bog), because lowlands comprised 74% of Cochrane and only 36% of Pickle Lake.

Because ungulates are known to be selective in foraging, most studies that develop foodscapes to address questions of large herbivore distribution or nutritional carrying capacity often restrict forage estimates based on vegetation eaten by the species-of-interest (Searle et al. 2016, Hebblewhite et al. 2008, Proffitt et al. 2016, Cook et al. 2018). For example, previously in our study area, Avgar et al. (2016) weighted the vegetation sampled by Mallon et al. (2016) in Nakina by caribou diet composition, derived from animal-borne video collars (Thompson et al. 2015) in Pickle Lake and Nakina, Ontario. However, where evaluations focus on what an ungulate consumes rather than what is available in an environment, differences in methods used to quantify diets (e.g., fecal analysis, DNA barcoding, animal-borne camera collars, and *in situ* tame animals), preferences (e.g., Ivlev index, selection ratios), and subjective judgements on how plant species are combined may produce contrasting inferences. For example, in this study *Maianthemum canadensis, Melampyrum lineare, Vaccinium angustifolium,* and *V. myrtilloides* were classified as avoided species (Ivlev's electivity index < 0) because of their high availability and consistent presence among macroplots but were included in accepted biomass because they contributed to caribou diets (Cook et al. *in prep*.). All methods of determining diets have

limitations (Holechek and Vavra 1981, Holechek et al. 1982, Cook et al. 2016, Parveen et al. 2016, Garnick et al. 2018), making dietary weights a key consideration in evaluating environments and comparisons among studies potentially problematic. Avgar et al. (2016), based on observations from video collar footage in summer, combined deciduous and evergreen shrubs into a single forage class because observations indicated both life-form groups represented <1% of caribou diet during summer (Thompson et al. 2015). In contrast, results based on caribou rumen samples in Newfoundland (Bergerud 1972), and pellet samples in Alaska (Thompson and McCourt 1981, Boertje 1984) indicate no summer use of evergreen shrubs but greater use of deciduous shrubs. Similarly, tame animal diets in northeastern British Columbia (Denryter et al. 2017), and in northwestern Ontario (Cook et al. *in prep.*) concluding an avoidance of evergreen shrubs but selection of deciduous shrubs during summer. Further, local data on diet selection is not always available, and assuming similar selection from an adjacent area may be necessary. For example, in this study, we had to assume similar selection of plant species by caribou in Cochrane as Pickle Lake because captive-foraging trials were conducted only in Pickle Lake due to logistical constraints.

Studies have shown that ungulates tend to select forage species of higher quality (Hebblewhite and Merrill 2009, van Beest et al. 2010, Rowland et al. 2018), and where accepted species have been identified, they often are of higher DE and DP than avoided species (Geary et al. 2017). Nevertheless, spatiotemporal dynamics in forage quality due to phenology and environmental conditions may be key in how well caribou can maintain fat stores and meet nutritional requirements. In this study, DE of accepted species was marginally higher and DP was substantially higher in Cochrane than Pickle Lake but showed similar rates of declines across the summer. We attribute the overall higher forage quality in Cochrane to a later start in

growing season and possibly other geophysical conditions. Seasonal trends in both accepted biomass and metrics of high-quality accepted biomass clearly support later development of forage in Cochrane than in Pickle Lake, which would have resulted in higher quality at the time we sampled (Van Soest 1982). The reason for the more pronounced delay in the abundance of DP-constrained forage compared to DE-constrained forage was due to a constant, seasonal abundance of lichen that buffered the strong declines in DE compared to DP in other accepted forage. Later initiation of the growing season in Cochrane is characteristic of the maritime climate of Hudson and James Bay, resulting in greater snow during winter and a reduced number of annual growing-degree-days (Baldwin et al. 2000; Walker et al. 2021).

Despite a different timing of peak biomass, average abundance of high-quality accepted biomass at the peak of the growing season was similar in both study areas in contrast to higher accepted biomass in Pickle Lake than Cochrane. Species composition and the associated quality does not appear to provide context for similar maximum values of high-quality accepted biomass. Specifically, we observed higher or equal forb, deciduous shrub, and mushroom biomass (i.e., life-form groups with relatively high DE and DP) at Upland-Black Spruce and Lowland-Bog (dominant ecosites across each region) macroplots in Pickle Lake than Cochrane (Appendix 4.8). Alternatively, extent of drainage classes within each study area and overall soil characteristics may explain the decreased magnitude of difference between areas when considering peak HQ-accepted biomass compared to accepted biomass. We observed higher quality forage in lowland forests with on average 7.5% and 31% greater DE and DP of forbs in lowland forests than uplands across Pickle Lake and Cochrane and 3% greater DE of deciduous shrubs in lowlands than uplands in Pickle Lake between 15 June to 15 September (Appendix 5.3–5.4). These results also support Mallon et al.'s (2016) conclusion of higher quality

vegetation in lowland than upland forests in Nakina. Additionally, Cochrane is dominated by fine-texture soils (i.e., silt and clay), associated with the lacustrine soils of the Northern Clay Belt regions (Baldwin et al. 2000, McMullin et al. 2013), which have greater water retention, increased organic soil matter, and higher cation exchange capacity (Torn et al. 1997, Gurevitch et al. 2002, Hamarshid et al. 2010, Ding et al. 2014). Such soils can provide greater nitrogen and minerals for plant development (Hamarshid et al. 2010, Ding et al. 2014), consistent with higher DP across forage quality samples in Cochrane than Pickle Lake. In contrast**,** Pickle Lake is characterized by fast-draining, coarse-texture soils (i.e., sand; Baldwin et al. 2000, McMullin et al. 2013), which have reduced water and mineral availability (Torn et al. 1997, Gurevitch et al. 2002). Therefore, the 2-times greater extent of lowland forests with the general distribution of fine-textured soil in Cochrane than Pickle Lake may explain the similar peak in high-quality accepted biomass between areas.

We hypothesize that the observed differences in the timing of forage resources between Pickle Lake and Cochrane likely constrain the nutritional intake of caribou and contribute to lower population performance in Cochrane. Although peak season availability of HQ-accepted biomass was similar between study areas, the timing of peak HQ-accepted biomass may be critical for caribou. In fact, we estimated the peak in DP-accepted biomass occurred ~1 month later in Cochrane than Pickle Lake, whereas DE-accepted biomass peaked only 4 days later in the former. This is because we observed a greater proportion of the summer where DP of accepted species was below the nutritional threshold (8.9%) than DE (2.9 kcal/g; Figure 4.5), similar to Barboza et al.'s (2018) findings in Alaska, USA. In captive-caribou trials, Barboza and Parker (2006, 2008) concluded protein was more limiting to caribou reproduction, because of a 110–130% increase in nitrogen requirements compared to 40–59% increase for energy during

lactation, with evidence that most nitrogen originated from body nitrogen and not diet. However, they did not evaluate dietary energy and protein utilization based on contrasting intakes of energy. Denryter et al. (2022b) concluded that captive-caribou were unable to satisfy daily intake requirements of both protein and energy during lactation while consuming natural forage in northeastern B.C. While keeping protein constant with varying levels of energy intake, Cook et al. (2004) concluded that elk consuming high energy forage (2.9–3.0 DE/g) accrued 75% and 300% greater percent body fat with their calves 40% and 70% heavier than elk consuming medium (2.6–3.0 DE/g) and low (2.3–3.0 DE/g) energy forage across the summer, respectively. Similarly, when varying both energy and protein intake by white-tailed deer fawns, Verme and Ozoga (1980) concluded diets of higher energy resulted in greater body weights and fat reserves, whereas the level of dietary protein had minimal effects of fawn condition. Therefore, we recommend future studies vary both energy and protein intake with captive-caribou to determine the relatively effects of energy vs. protein deficiencies on the performance of caribou. Nevertheless, energy and protein requirements for lactation are highest ~3 weeks postpartum (White and Luick 1984, Parker et al. 1990) and although caribou are considered capital breeders and use body reserves to buffer the early costs of reproduction (Taillon et al. 2013), insufficient foraging resources during post-calving can be detrimental. Crête and Huot (1993) documented that caribou with inadequate forage during the first month of lactation can fully deplete their body reserves. Parturition is about a week earlier in Pickle Lake than Cochrane (17 vs. 23 May, Walker et al. 2021), but peak HQ-biomass is approximately a month later. Therefore, delayed phenology in Cochrane may reflect a relatively greater temporal mismatch in nutrient availability and caribou requirements during calving in Cochrane, contributing to the difference in body reserves, due to limited flexibility in gestation length (<10 days; Ropstad 2000).

Two factors may ameliorate the effects of later growing season on caribou in Cochrane. First, despite a lower overall abundance of HQ-accepted biomass during early summer in Cochrane, the higher spatial variation in HQ-accepted biomass early in the growing season in Cochrane may reflect patches of high-quality forage that are available but dispersed. In particular, Lowland-Fen provides greater HQ-accepted biomass early in the season, but these areas are limited in Cochrane (5%; Appendix 10.8). Dispersed forage in Cochrane is consistent with greater movement rates of caribou with calves-at-heel during calving compared to caribou in Pickle Lake (Walker et al. 2021). Further, data on growing-degree days (Appendix 11) indicate there is lower annual variation in Cochrane than Pickle Lake, likely due to its more maritime climate (Baldwin et al. 2000). Less stochastic variation among years in early-season forage growth may contribute to reduced variation in calf survival population (Post and Stenseth 1999, Post et al. 2008), which can have a stabilizing effect on this population compared to Pickle Lake (Boyce et al. 1979, Gaillard et al. 2000).

Second, delayed phenology in Cochrane may benefit caribou in late summer, particularly after the insect harassment period (Raponi et al. 2018, Villetard et al. *in prep.*) because late summer is a key period to put on body reserves for winter survival (Parker et al. 1999; Cook et al. 2004, 2021). At the same time, the high spatial variability in HQ-accepted biomass during mid- and late summer in Pickle Lake may buffer the early declines in forage quality, if caribou can efficiently "surf" local patchiness in forage conditions (Owen-Smith 2004, Owen-Smith et al. 2010). In contrast, spatial variability of HQ-accepted biomass in Cochrane during mid- and late summer is relatively low and static, which may reflect ubiquitously distributed higher forage quality, particularly DP during the peak. In Chapter 5, we attempted to explicitly link spatial variation in seasonal resources to caribou use because an area with greater spatial variation of

resources through time can support a greater number of animals and decreases the effects of density dependence (Illius and O'Connor 2000, Wang et al. 2006, Wang et al. 2009).

In conjunction with an earlier peak in HQ-accepted biomass in Pickle Lake than Cochrane, average intake rates (g/min) were greater in Pickle Lake than Cochrane, which may also beget lower population performance in Cochrane. The magnitude of difference between Pickle Lake and Cochrane was less when considering intake rates than accepted biomass, due to predicted intake rates being 9% higher in lowland than upland forests via equations developed by Cook et al. (*in prep*.) and 2.1-times more lowlands in Cochrane than Pickle Lake. However, even small differences in g/min intake rates can scale up to substantial effects per day, which are further compounded across the summer via multiplier effects (White 1983). For example, the mean difference of 0.45 g/min between Pickle Lake and Cochrane across the summer would hypothetically result in 34.5 kg less forage consumed by a caribou in Cochrane than Pickle Lake between 15 June to 15 September (assuming random use of the study area and lactating caribou foraging 13.7 hrs per day; Denryter et al. 2020), which equates to ~30% of their body weight (~110 kg; J. Cook, R. Cook, and G. Brown unpublished data).

Our study highlights the role summer nutrition can have on caribou by understanding the spatiotemporal dynamics of forage across two study areas and whether these differences may lead to difference in population performance (Gaillard et al. 2010). However, ungulates have been shown to trade-off foraging opportunities to avoid predation risk (Bowyer et al. 1999, Gustine et al. 2006, Hamel & Côté 2007, Merrill et al. 2020), which could limit their ability to exploit a nutritional environment effectively. For example, caribou in western Ontario (Pickle Lake and Nakina) consistently selected for foraging resources, but showed varying responses to predation risk, suggesting that caribou may make forage-predation risk trade-offs under some

conditions (Avgar et al. 2015). Moreover, during the summer, caribou across northern Ontario select against early seral stands (Hornseth and Rempel 2016, Walker et al. 2021), suggesting caribou may trade-off forage for less risky areas, because wolves in western Ontario preferentially used early seral forests and upland forests (Kittle et al. 2015, 2017) and we documented high accepted biomass in these ecosites. The strength of these trade-offs may depend on a caribou's reproductive state, due to nutritional requirements of lactation and greater predation risk with a calf-at-heel (White and Luick 1984, Parker et al. 1990, Berger 1991). In Chapter 5, we explore the extent of these state-dependent trade-offs in terms of caribou habitat selection.

Table 4.1. Number (*n*) of ecosite types by seral stage (early: <20 years, mid-late: ≥20 years) that were sampled in Pickle Lake (PL) during 2017–2018 and Cochrane (CO) during 2018, Ontario, Canada. Listed are the proportional extents of seral-specific ecosites (with ecosites abbreviation) across the forested region of each study area, where each study area was defined as a 99% utilization distribution of caribou GPS telemetry from 1 June to 30 September, 2010–2014.

Ecosite	Abbreviation	Description	Study area	Seral stage	*n*	Proportion study area
Upland-Black Spruce-Rocky	Upl-BS-Rocky	Unproductive rocky outcrops with fast draining soils and ericaceous shrubs and terrestrial lichens. This ecosite type was not present in CO.	PL	Early	3	<0.001
				Mid-late	20	0.03
Upland-Black Spruce	Upl-BS	Unproductive upland conifer sites predominately on shallow sandy soils with overstory dominated by jack pine and/ or black spruce and occasionally white birch with extensive ericaceous shrubs with the possibility of terrestrial lichens in the understory.	PL	Early	50	0.09
				Mid-late	136	0.48
			CO	Early	17	0.09
				Mid-late	22	0.10
Upland-Black Spruce-White Spruce	Upl-BS-WS	Productive upland conifer sites predominately on fine-textured soils with overstory consisting of black and/or white spruce, balsam fir, and trembling aspen with understory consisting of deciduous shrubs and forbs.	PL	Early	13	0.02
				Mid-late	34	0.03
			CO	Early	10	0.05
				Mid-late	28	0.02
Lowland-Bog	Lwl-Bog	Unproductive lowlands with extensive sphagnum moss and evergreen shrubs, and black spruce overstory.	PL	Early	20	0.006
				Mid-late	52	0.31
			CO	Early	7	0.007
				Mid-late	34	0.68
Lowland-Fen	Lwl-Fen	Productive lowlands with extensive sphagnum moss, forbs, and evergreen and deciduous shrubs with a mix of black spruce and larch overstory.	PL	Mid-late	7	0.04
			CO		9	0.05
Lowland-Cedar/ thicket	Lwl-Cedar/ thicket	Productive lowlands dominated with dense deciduous shrubs and white cedar overstory.	PL	Mid-late	4	0.006
			CO		1	0.005
Lowland-Marsh	Lwl-Marsh	Marsh lowland dominated by graminoids with generally no trees or shrubs. This ecosite type was not present in CO.	PL	Mid-late	1	<0.001

Table 4.2. Mean total biomass of all species, proportion accepted biomass (AB) of total biomass, biomass of accepted grass, forb, and deciduous shrub (GFS), lichen, horsetail, and mushroom by seral-stage (early [<20 years] vs. mid-late [≥20years]) specific ecosite and study area (SA) for 472 macroplots sampled in Pickle Lake (PL) and Cochrane (CO), Ontario, Canada in 2017–2018. Asterisk indicates the mean value was used to spatially predicted each component of accepted biomass across a study area.

			Total biomass			Proportion AB			GFS biomass			Lichen biomass			Horsetail biomass			Mushroom biomass		
Ecosite	Seral stage	SA	n	Mean	SD	n	Mean	SD	n	Mean	SD	n	Mean	SD	n	Mean	SD	n	Mean	SD
Upl-BS-Rocky	Early	PL	3	1507.46	371.60	3	0.70	0.27	3	314.61*	236.73	3	806.52*	874.91	3	0.00*	0.00	3	0.01*	0.01
		CO	0	---	---	0	---	---	0	---	---	0	---	---	0	---	---	0	---	---
	Mid-late	PL	20	783.93	601.63	20	0.56	0.33	20	84.79	89.05	20	460.09	529.17	20	0.00*	0.00	20	0.26*	0.88
		CO	0	---	---	0	---	---	0	---	---	0	---	---	0	---	---	0	---	---
Upl-BS	Early	PL	50	1180.72	496.47	50	0.45	0.24	50	424.47	269.38	50	89.27	225.10	50	4.47*	16.92	50	0.28	1.19
		CO	17	569.97	386.31	17	0.41	0.20	17	146.77	133.65	17	55.77	83.24	17	0.00*	0.02	17	0.001*	0.00
	Mid-late	PL	136	649.39	730.80	136	0.44	0.26	136	127.73	104.02	136	237.01	744.23	136	0.86*	5.91	136	0.63	1.74
		CO	22	627.13	1067.29	22	0.40	0.27	22	49.08*	50.21	22	410.64	1036.97	22	0.10*	0.44	22	0.01	0.01
Upl-BS-WS	Early	PL	13	1586.28	430.33	13	0.45	0.13	13	667.67*	300.76	14	12.03*	22.93	14	34.11*	56.42	14	0.27	0.51
		CO	10	1012.91	461.29	10	0.43	0.23	10	507.43	437.53	10	0.17*	0.27	10	10.24	15.09	10	0.003*	0.00
	Mid-late	PL	34	550.23	242.64	34	0.44	0.17	34	235.36	153.03	34	7.68*	15.36	34	1.58*	4.20	34	0.40	0.73
		CO	28	191.06	156.21	28	0.43	0.21	28	77.47	78.06	28	2.27	4.12	28	0.47*	1.25	28	0.16	0.56
Lwl-Bog	Early	PL	20	1642.01	432.01	20	0.21	0.12	20	258.74*	151.91	20	16.53*	44.79	20	42.46*	49.80	20	0.19	0.50
		CO	7	896.68	281.35	7	0.33	0.22	7	109.30*	127.00	7	176.21*	230.65	7	23.16*	37.43	7	0.66*	1.46
	Mid-late	PL	52	907.02	500.64	52	0.16	0.14	52	80.29	85.18	53	30.13	69.57	53	15.02*	29.46	53	0.21	0.45
		CO	32	563.09	319.06	32	0.23	0.16	34	55.26	58.52	33	72.02*	122.59	34	9.18	14.04	33	0.07*	0.29
Lwl-Marsh	Mid-late	PL	3	2173.38	407.99	3	0.53	0.15	3	1053.39*	204.99	3	58.57*	101.41	3	0.00*	0.00	3	0.00*	0.00
		CO	0	---	---	0	---	---	0	---	---	0	---	---	0	---	---	0	---	---
Lwl-Fen	Mid-late	PL & CO	15	987.37	635.20	15	0.28	0.19	16	213.32	147.33	15	11.69*	23.04	16	0.94*	1.83	16	0.10*	0.21
Lwl-Cedar/ thicket	Mid-late	PL & CO	5	963.81	590.93	5	0.47	0.32	5	538.74*	634.37	5	13.24*	28.29	5	28.42*	58.60	5	0.05*	0.07

Table 4.3. Top predictive models of grass, forbs, and deciduous shrub combined (GFS), lichen, horsetail, and mushroom biomass for each seral-specific (early: <20 years; mid-late: ≥20 years) ecosite and study area (SA) as a function of sampling date (i.e., Julian day; JD), basal area (m^2/ha; BA), canopy cover (CC%), change in enhanced vegetative index (ΔEVI), normalized difference moisture index (NDMI), or percent clay, sand, or silt, the number of macroplots (*n*) used to develop each model, and the variation explained (r^2). Subscript of *t* indicates a non-linear transformation was applied to the covariate (Appendix 6.1). Mean values used in spatial predictions are not indicated here but found in Table 4.2.

Biomass	Ecosite	Seral	SA	n	Model	r^2
GFS	Upl-BS-Rocky	Mid-late	PL	20	$0.87*BA_t + 17.19$	0.36
	Upl-BS	Early	PL	50	$1.50*BA_t + 0.1631*\Delta EVI - 788.86$	0.28
			CO	17	$0.38*JD_t + 57.58$	0.33
		Mid-late	PL	136	$1.04*JD_t + 0.63*BA_t - 80.45$	0.19
	Upl-BS-WS	Early	CO	10	$1.53*JD_t - 19.28$	0.52
		Mid-late	PL	34	$0.98*BA_t + 56.1354$	0.38
			CO	28	$0.88*JD_t + 9.30$	0.22
	Lwl-Bog	Mid-late	PL	52	$0.62*BA_t + 33.64$	0.16
			CO	34	$1.12*JD_t - 9.32$	0.41
	Lwl-Fen	Mid-late	PL & CO	16	$1.00*JD_t + 0.81$	0.51
Lichen	Upl-BS-Rocky	Mid-late	PL	20	$-14.42*CC + 1196.62$	0.30
	Upl-BS	Early	PL & CO	67	$328.97*NDMI - 4.941$	0.06
		Mid-late	PL & CO	158	$1.02*BA_t + 44.42*Sand - 3101.93*NDMI - 1345.87$	0.22
	Upl-BS-WS	Mid-late	CO	28	$-0.003*\Delta EVI + 14.62$	0.17
	Lwl-Bog	Mid-late	PL	52	$-365.38*NDMI + 166.33$	0.11
Horsetail	Upl-BS-WS	Early	CO	10	$0.01*\Delta EVI - 46.79$	0.51
	Lwl-Bog	Mid-late	CO	34	$0.83*JD_t + 2.64$	0.20
Mushroom	Upl-BS	Early	PL	50	$1.09*JD_t + 0.13*Silt - 4.02$	0.25
		Mid-late	PL	136	$0.96*JD_t + 0.06$	0.13
			CO	22	$*-0.003*Clay + 0.00001*\Delta EVI - 0.007$	0.51
	Upl- BS-WS	Early	PL	13	$0.49*JD_t - 0.04$	0.36
		Mid-late	PL	34	$0.80*JD_t - 0.0004*\Delta EVI + 1.91$	0.28
			CO	28	$0.04*Sand - 2.41$	0.17
	Lwl-Bog	Early	PL	20	$2.21*JD_t + 2.16*NDMI - 0.70$	0.49
		Mid-late	PL	52	$0.96*JD_t + 0.01$	0.14

Table 4.4. Number of macroplots (*n*), variation explained (r^2) in the top models (Tables 4.3), and standard error of the estimate (SSE) at macroplots in Pickle Lake and Cochrane, Canada in 2017–2018.

Forage metric	Pickle Lake			Cochrane		
	n	r^2	SSE	*n*	r^2	SSE
Accepted biomass	341	0.34	446.41	126	0.38	385.03
GFS	342	0.59	151.17	128	0.63	114.10
Lichen	343	0.29	436.79	127	0.35	367.96
Horsetail	344	0.23	22.04	128	0.30	11.01
Mushroom	344	0.17	1.15	127	0.16	0.43
HQ-accepted biomass	341	0.57	94.47	126	0.65	96.71
DE-accepted biomass	341	0.50	174.97	126	0.58	136.48
DP-accepted biomass	341	0.55	115.08	126	0.67	97.12

Table 4.5. Mean and standard deviation (SD) of digestible energy (kcal/g) and protein (g protein/ 100 g of forage) stratified by life-form group and number (*n*) of forage quality samples collected across Pickle Lake and Cochrane, Ontario, 2018. Superscripts indicate significant differences between life-form groups via post-hoc Tukey HSD test (Appendix 9.1).

		Digestible energy		Digestible protein	
Life-form	*n*	mean	SD	mean	SD
Deciduous shrub	444	3.01^{b}	0.28	7.58^{c}	4.18
Forb	292	2.96^{b}	0.35	9.17^{b}	5.46
Mushroom	7	3.42^{a}	0.20	15.72^{a}	3.20
Grass	15	2.60^{c}	0.32	8.75^{bc}	4.82
Horsetail	32	2.65^{c}	0.53	8.44^{bc}	4.67
Lichen	141	3.08^{ab}	0.19	-0.81^{d}	1.04

Table 4.6. Mean high-quality accepted biomass (kg/ha) subject to digestible energy (DE), digestible protein (DP) and both digestible energy and digestible protein (HQ) constraints derived using the FRESH model (Hanley et al. 2012) by seral-stage (early [<20 years] vs. mid-late [≥20years]) ecosite, and study area (SA) at 467 macroplots sampled in Pickle Lake (PL) and Cochrane (CO), Ontario, Canada in 2017–2018. Asterisk indicates the mean value was used to spatially predict the high-quality accepted biomass across the landscape across a study area.

				HQ-accepted biomass		DE-accepted biomass		DP-accepted biomass	
Ecosite	Seral stage	SA	*n*	Mean	SD	Mean	SD	Mean	SD
Upl-BS-Rocky	Early	PL	3	4.43*	7.57	795.63*	180.38	4.43*	7.57
		CO	0	---	---	---	---	---	---
	Mid-late	PL	20	25.90	37.52	325.59	362.03	29.46*	48.14
		CO	0	---	---	---	---	---	---
Upl-BS	Early	PL	50	136.40	193.43	474.21	292.96	150.03	210.91
		CO	17	56.06*	77.01	197.17	151.27	56.06*	77.01
	Mid-late	PL	136	32.23	55.13	182.06	188.62	36.22	66.53
		CO	22	41.61*	49.52	135.57	216.91	41.65*	49.49
Upl-BS-WS	Early	PL	13	304.99	337.60	506.54	303.64	310.96	339.47
		CO	10	444.29	351.41	509.20	419.61	454.00	372.98
	Mid-late	PL	34	158.63	151.35	227.42	146.61	167.69	162.91
		CO	28	69.67*	77.50	73.32	76.87	77.19	78.30
Lwl-Bog	Early	PL	20	104.66	91.30	288.30*	155.49	122.53	101.68
		CO	7	98.70*	149.03	208.77*	190.44	102.26*	148.81
	Mid-late	PL	52	75.30	96.06	116.65	111.30	76.49	95.42
		CO	32	54.50	60.64	121.52	125.69	54.92	60.50
Lwl-Marsh	Mid-late	PL	3	192.25*	282.82	391.49*	124.81	789.39*	690.72
		CO	0	---	---	---	---	---	---
Lwl-Fen	Mid-late	PL & CO	15	196.22	167.19	226.57	154.87	196.88	166.60
Lwl-Cedar/ thicket	Mid-late	PL & CO	5	160.92*	137.81	231.57*	211.44	175.61*	164.13

Table 4.7. Top predictive models of high-quality accepted biomass subject to digestible energy (DE-AB), digestible protein (DP-AB) and both digestible energy and protein (HQ-AB) constraints derived using the FRESH model (Hanley et al. 2012) for each seral-specific (early: <20 years; mid-late: ≥20 years) ecosite and study area (SA) as a function of sampling date (Julian day; JD), basal area (m^2/ha; BA), canopy cover (CC%), change in enhanced vegetative index (ΔEVI), normalized difference moisture index (NDMI), or percent silt, the number of macroplots (*n*) used to develop each model, and the variation explained (r^2). Subscript of *t* indicates a non-linear transformation was applied to the covariate (Appendix 6.1). Mean values used in spatial predictions are not indicated here but in Table 4.6.

Metric	Ecosite	Seral	SA	*n*	Model	r^2
HQ-AB	Upl-BS-Rocky	Mid-late	WO	20	$0.46*JD_t + 6.26*Silt - 197.69$	0.43
	Upl-BS	Early	WO	50	$0.88*JD_t + 28.29*Silt - 820.82$	0.45
		Mid-late	WO	136	$0.99*JD_t + 0.50*BA_t + 127.64*NDMI - 61.75$	0.30
	Upl- BS-WS	Early	WO	13	$1.40*JD_t + 90.45$	0.52
			EO	10	$1.42*JD_t + 101.69$	0.47
		Mid-late	WO	34	$0.99*JD_t\ 0.70*BA_t + - 93.42$	0.49
	Lwl-Bog	Early	WO	20	$1.13*JD_t + 15.31$	0.25
		Mid-late	WO	52	$1.02*JD_t - 2.58*BA + 50.57$	0.33
	Lwl-Bog	Mid-late	EO	34	$0.95*JD_t + 3.94$	0.29
	Lwl-Fen	Mid-late	WO & EO	15	$1.01*JD_t - 2.94$	0.81
DE-AB	Upl-BS-Rocky	Mid-late	WO	20	$-22.25*BA + 808.19$	0.34
	Upl-BS	Early	WO	50	$2.05*BA_t + 0.21*EVI - 1300.05$	0.33
			EO	17	$0.46*JD_t + 72.50$	0.35
		Mid-late	WO	136	$0.76*JD_t + 0.73*BA_t - 600.21*NDMI + 137.59$	0.25
			EO	22	$1.97*BA_t - 143.48$	0.42
	Upl- BS-WS	Early	WO	13	$3.62*JD_t - 1093.47$	0.50
			EO	10	$1.52*JD_t - 61.98$	0.52
		Mid-late	WO	34	$0.85*JD_t + 0.80*BA_t - 123.65$	0.38
			EO	28	$0.79*JD_t + 21.04$	0.23
	Lwl-Bog	Mid-late	WO	52	$-1.69*CC + 175.48$	0.15
			EO	34	$0.96*JD_t + 6.30$	0.27
	Lwl-Fen	Mid-late	WO & EO	16	$1.00*JD_t -57.64$	0.74
DP-AB	Upl-BS	Early	WO	50	$0.71*JD_t + 32.00*Silt – 923.90$	0.40
		Mid-late	WO	136	$0.63*JD_t + 0.53*BA_t - 18.81$	0.21
	Upl- BS-WS	Early	WO	13	$1.40*JD_t + 94.21$	0.51
		Early	EO	10	$1.44*JD_t + 100.08$	0.50
		Mid-late	WO	34	$2.14*JD_t + 0.86*BA_t - 100.67$	0.51
		Mid-late	EO	28	$0.89*JD_t + 8.63$	0.21
	Lwl-Bog	Early	WO	20	$-1.94*JD + 526.69$	0.24
		Mid-late	WO	52	$-1.36*JD + 1.29*BA + 281.16$	0.28
		Mid-late	EO	34	$0.95*JD_t + 3.67$	0.30
	Lwl-Fen	Mid-late	WO & EO	16	$1.01*JD_t - 1.59$	0.80

Table 4.8. Comparison of the home range-scaled, mean cell values and coefficient of variation (CV) of each forage metric across the spatial extent of Pickle Lake and Cochrane, Ontario. *P*-values reflect differences from paired t-test paired by day and mean daily difference was calculated as values from Pickle Lake to Cochrane.

Forage metric	Mean		CV	
	Mean difference	*P*-value	Mean difference	*P*-value
Accepted biomass	126.60	<0.001	0.06	<0.001
GFS	49.90	<0.001	0.22	<0.001
Lichen	77.65	---	0.00001	---
Horsetail	-1.70	<0.001	0.26	<0.001
Mushroom	0.31	<0.001	1.01	<0.001
HQ-accepted biomass	-9.19	0.04	0.14	0.005
DE-accepted biomass	10.43	<0.001	0.05	<0.001
DP-accepted biomass	-2.32	0.6	0.10	0.009

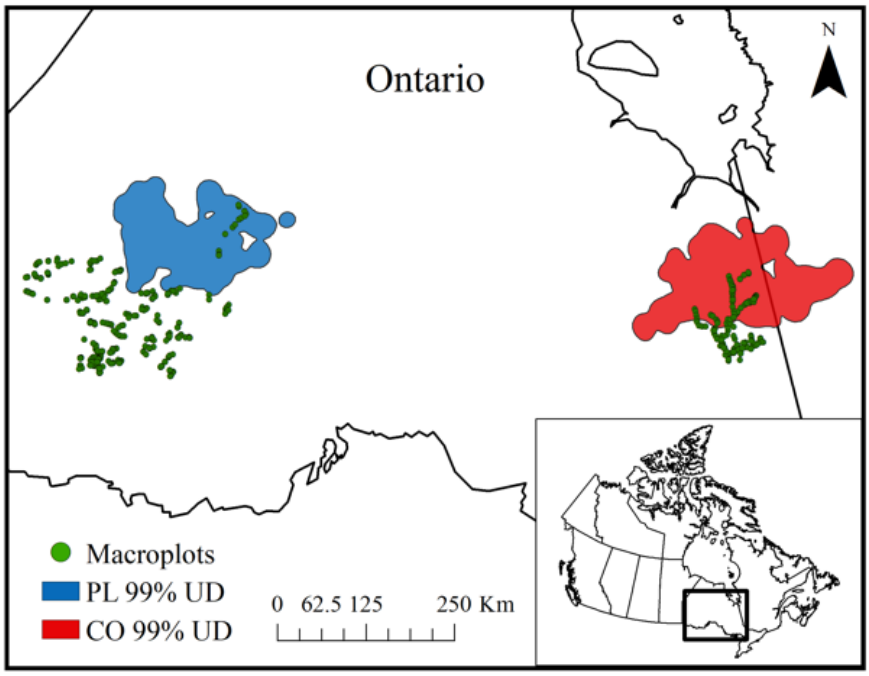

Figure 4.1. Location of vegetation macroplots sampled between 2017–2018 in Pickle Lake (PL; n = 344) and Cochrane (CO; n = 128) within northern Ontario, Canada and the study area extents defined as a 99% utilization distribution (UD) from caribou GPS telemetry within each area from 1 June to 30 September, 2010-2014.

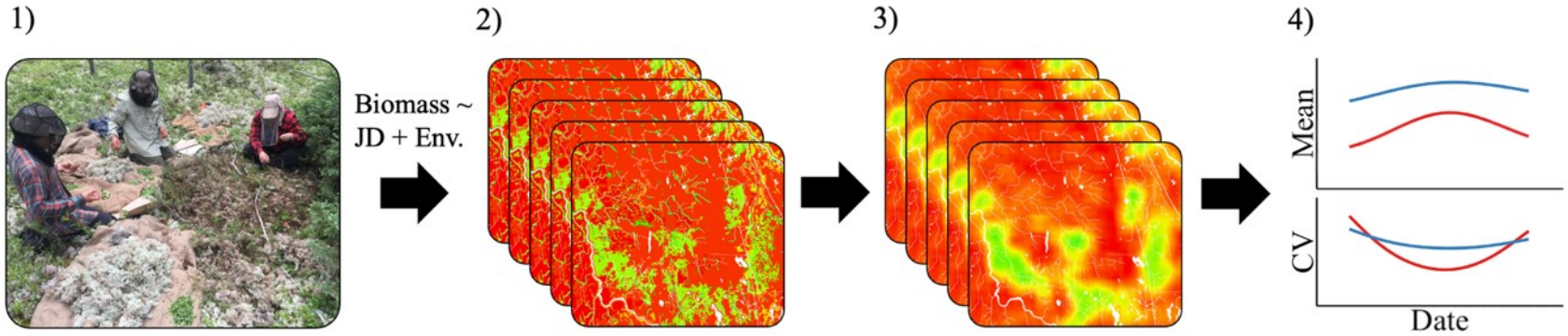

Figure 4.2. Framework used to compare caribou nutritional resources between Pickle Lake (PL) and Cochrane (CO), Ontario. Panels are 1) vegetation sampling with forage biomass and quality collected during 2017–2018 across 342 and 128 sites in PL and CO, respectively. 2) Daily maps (15 June to 15 September) of values of nutritional metrics for a study area predicted for each 30-m^2 pixels as a function of Julian day (JD) and environmental (Env.) variables. 3) Maps representing the mean value of nutritional metrics around a central pixel within a window the size of a caribou summer home range. 4) Graphs comparing the mean and coefficient of variation (CV) within each study area over time. Nutritional metrics include accepted biomass components, accepted biomass constrained by forage quality, and caribou intake rates (g/min) derived using equations developed by Cook et al. (*in prep.*).

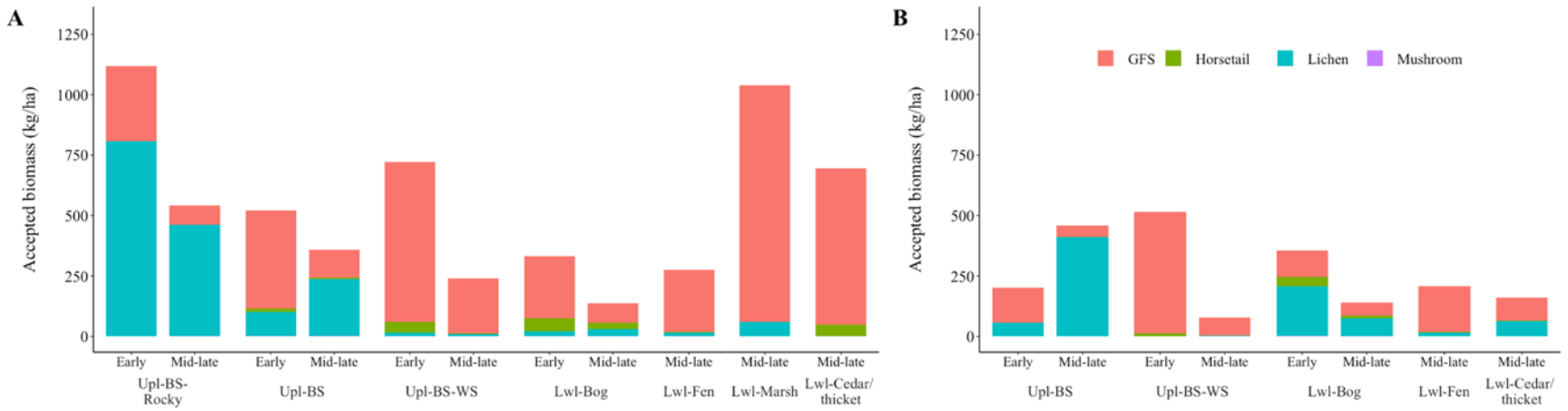

Figure 4.3. Mean accepted biomass (kg/ha) and components: grass, forb, and deciduous shrub combined (GFS), horsetail, lichen, and mushroom biomass by ecosite and seral stage (early <20 years, mid-late ≥20 years) at 341 and 126 macroplots sampled in A) Pickle Lake and B) Cochrane, Ontario, respectively, during 2017–2018. Note: not all ecosites existed in both study areas.

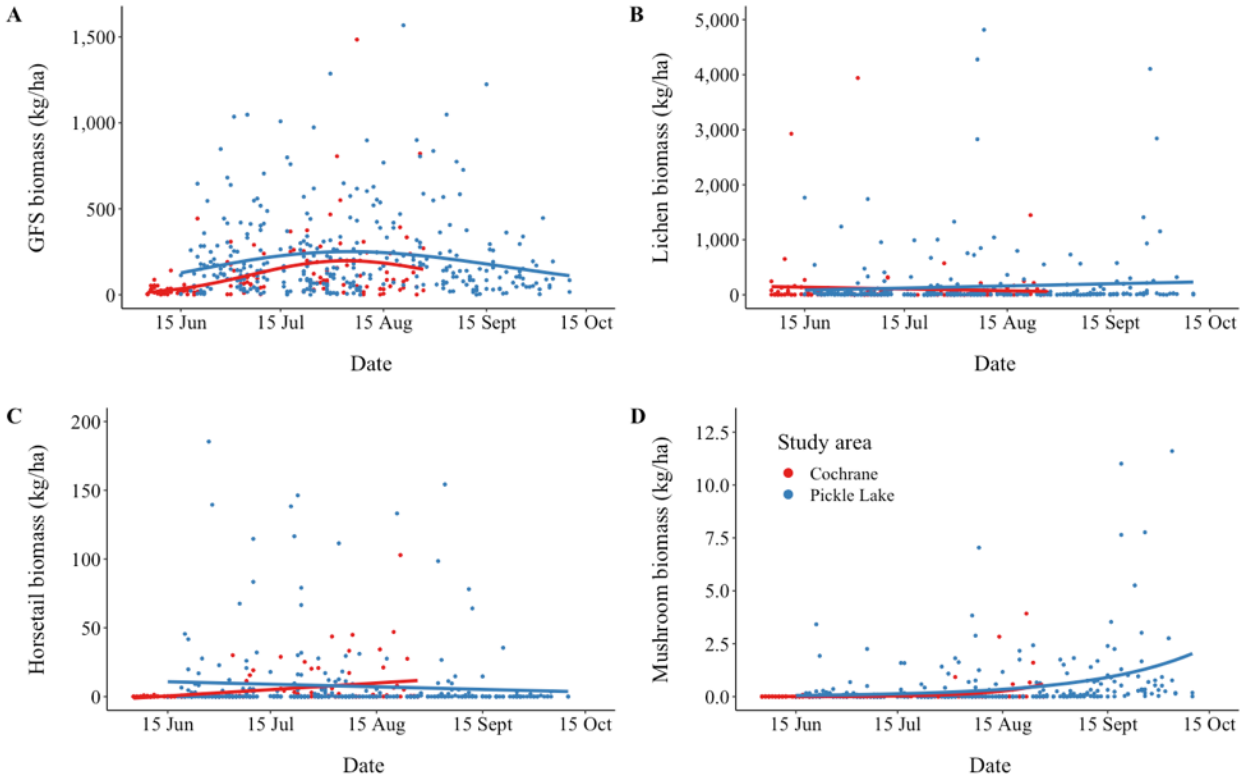

Figure 4.4. Relationships between sampling date and A) grass, forb, and deciduous shrub combined (GFS), B) lichen, C) horsetail, and D) mushroom biomass (kg/ha) at 344 macroplots in Pickle Lake (PL) and 128 macroplots in Cochrane (CO), Ontario, 2017–2018.

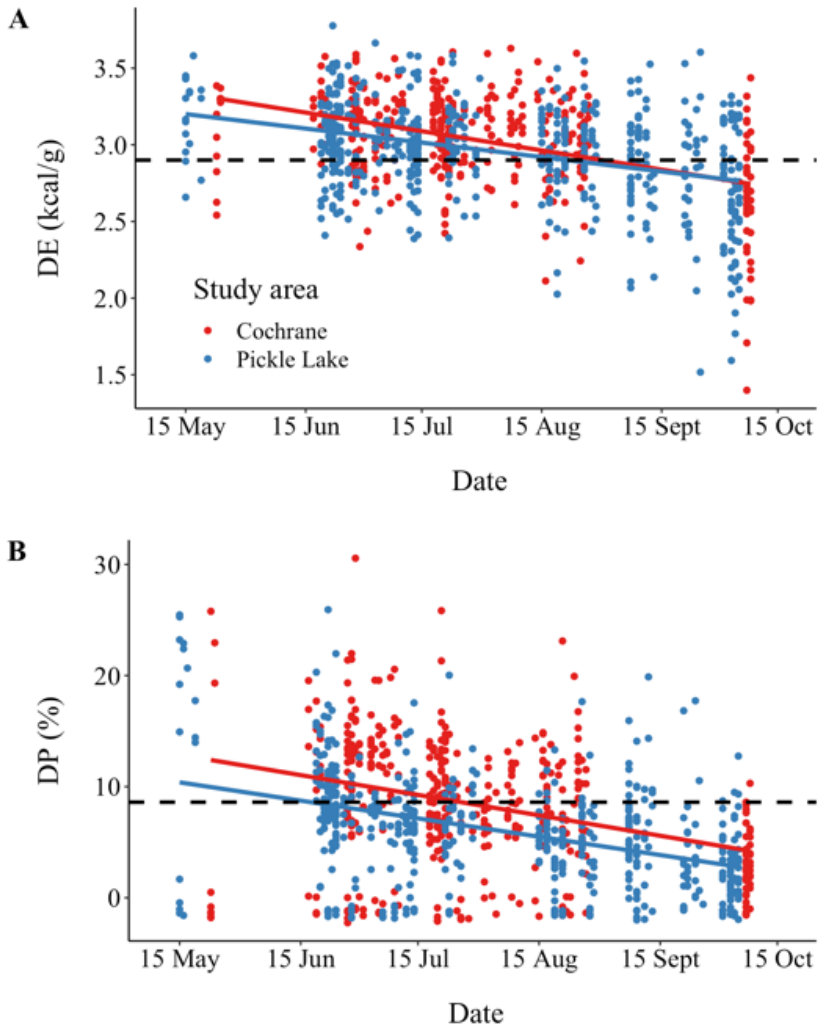

Figure 4.5. Relationship between A) digestible energy (DE; kcal/g) and B) digestible protein (DP; g of protein per 100 g of forage, %) of accepted species across 931 species-specific samples and sampling date in Pickle Lake and Cochrane, Ontario from 15 May to 8 October 2018. Dashed black line indicates the DE (2.9 kcal/g) and DP (8.6%) constraints used to estimate metrics of high-quality accepted biomass via the FRESH model (Hanley et al. 2012).

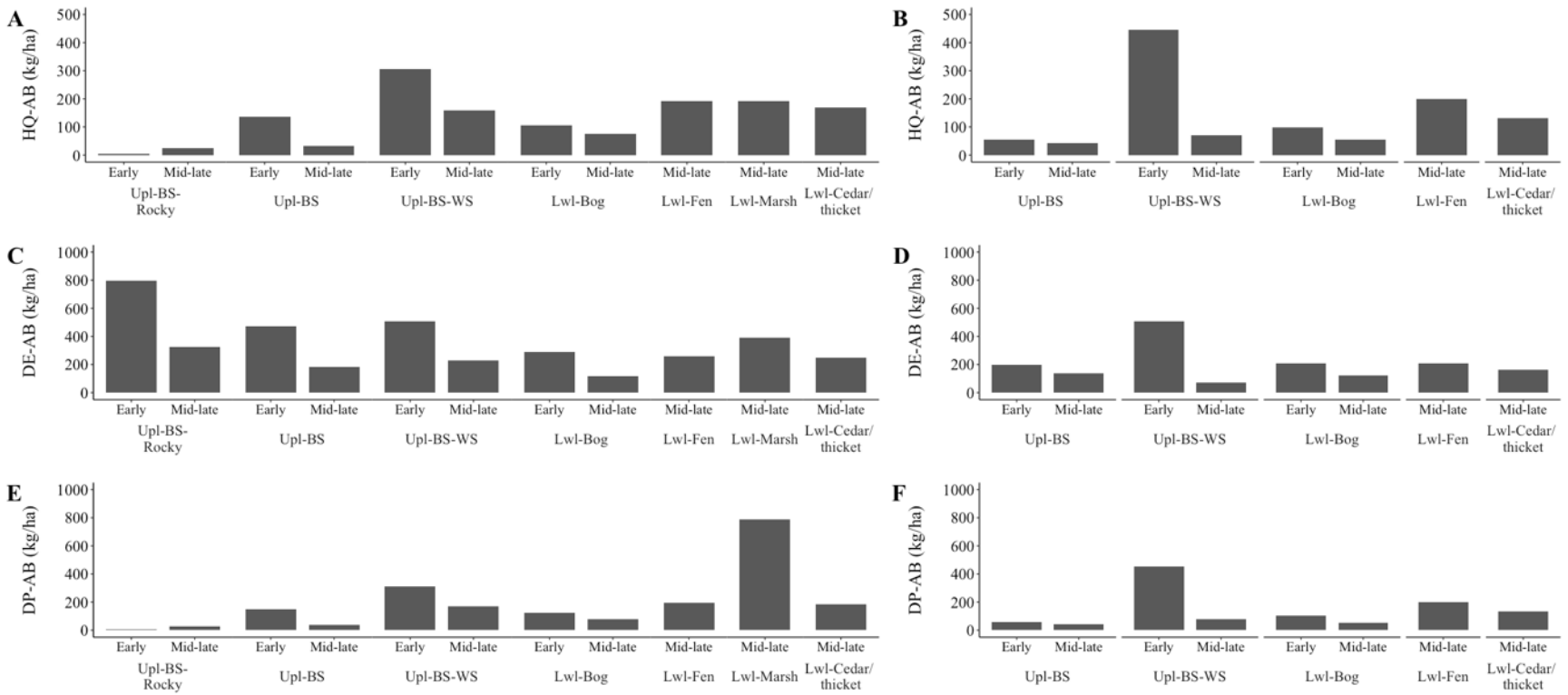

Figure 4.6. Mean high-quality (HQ) accepted biomass (AB) subject to digestible energy and protein constraints (A, B), accepted biomass subject to digestible energy constraints only (C, D) and digestible protein only (E, F) by ecosite and seral stage (early <20 years, mid-late ≥20 years) at 341 and 126 macroplots sampled in Pickle Lake (left panels) and Cochrane (right panels), Ontario, respectively, during 2017–2018. Note: not all ecosites existed in both study areas.

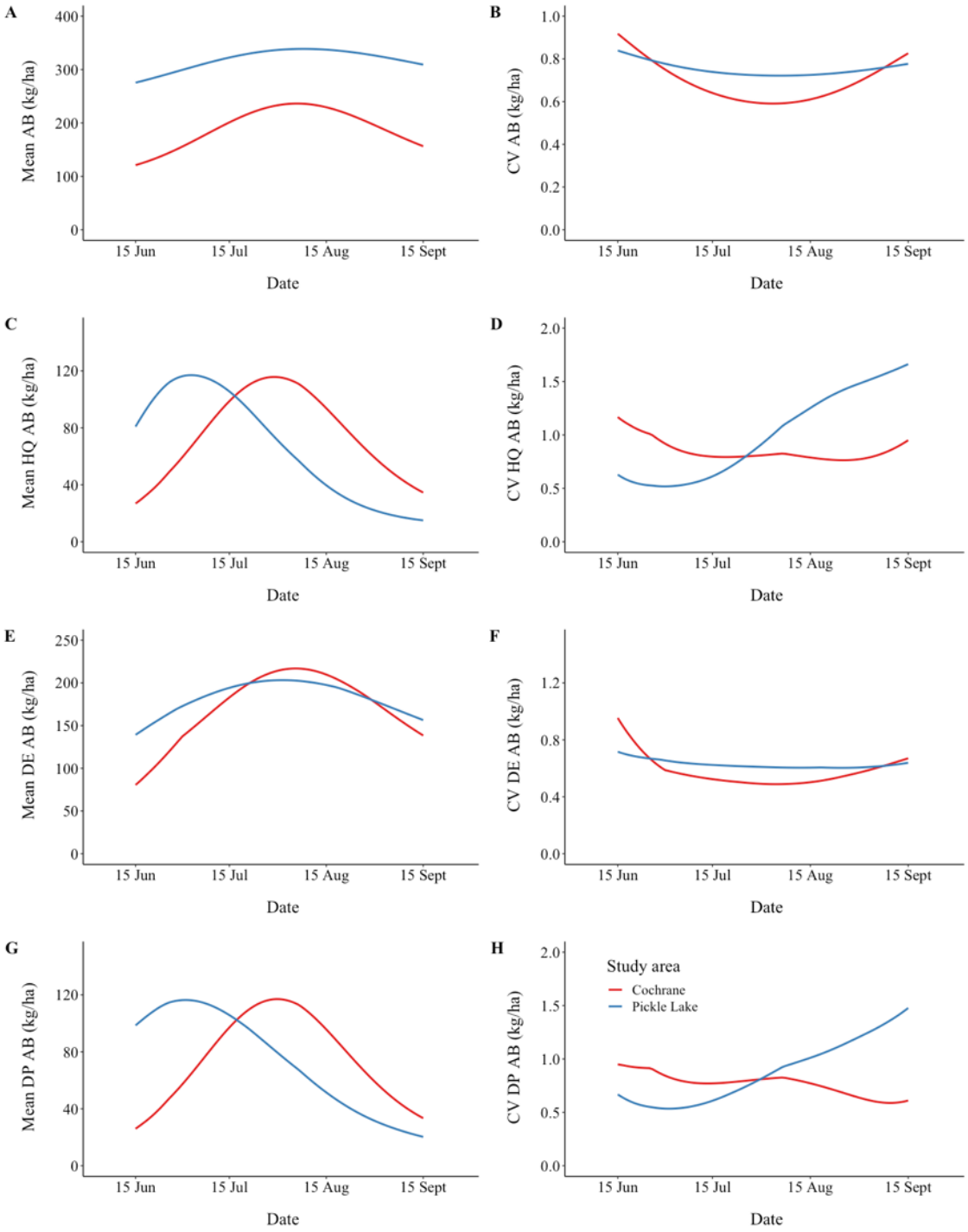

Figure 4.7. Home range-scaled, mean accepted biomass (AB, kg/ha; left panels) and coefficient of variation (CV; right panels) of total accepted biomass derived as sum of grass, forb, and deciduous shrub combined, lichen, horsetail and mushroom biomass (A, B); high-quality (HQ) accepted biomass subject to digestible energy and protein constraints (C, D), accepted biomass subject to digestible energy constraints only (E, F) and digestible protein only (G, H) calculated across the spatial extent of Pickle Lake and Cochrane, Ontario study areas in from 15 June to 15 September, 2010.

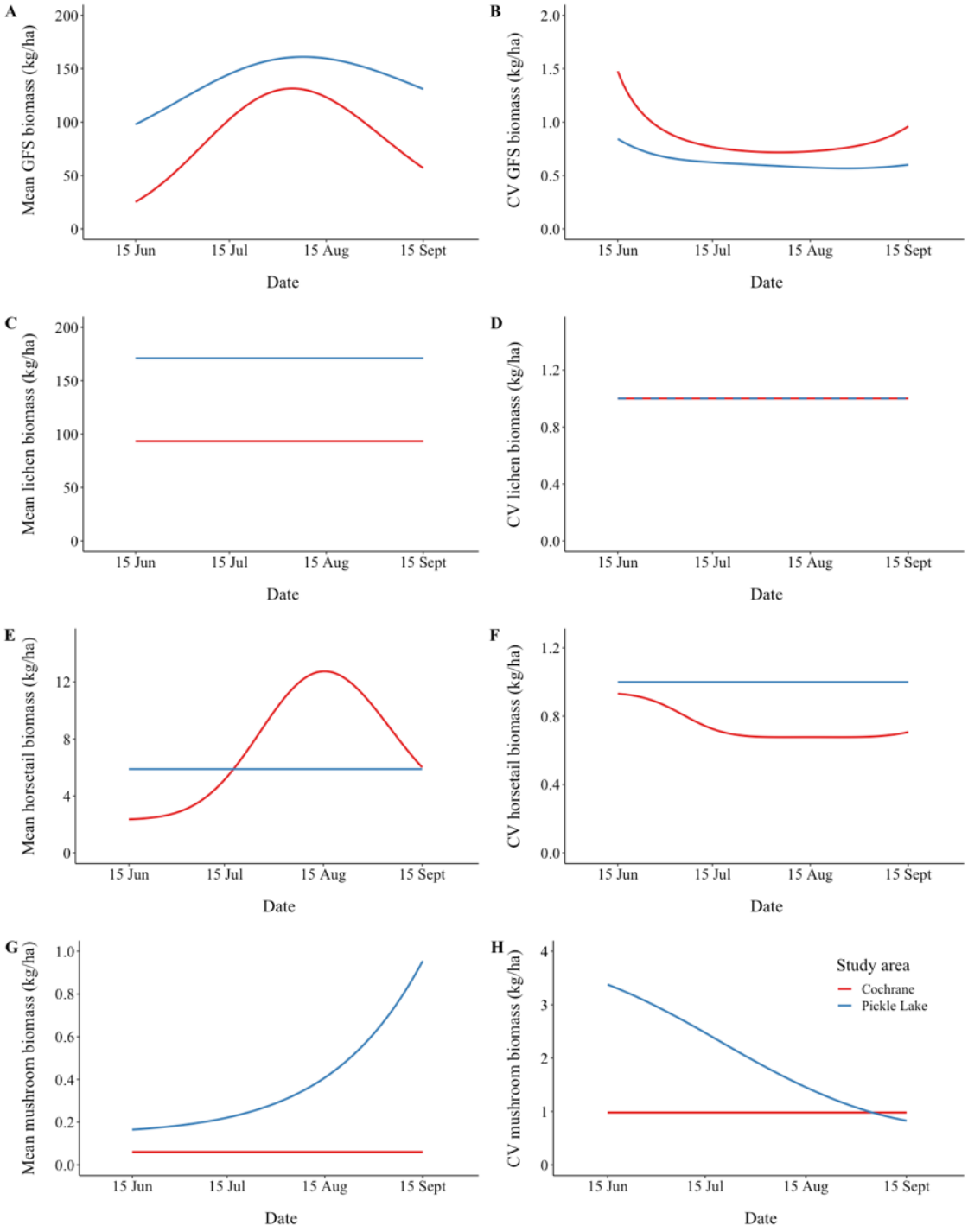

Figure 4.8. Home-range scaled, mean accepted biomass (kg/ha; left panels) and coefficient of variation (CV; right panels) of grass, forb, and deciduous shrub combined (GFS; A, B), lichen (C, D), horsetail (E, F), and mushroom (G, H) across the spatial extent of Pickle Lake and Cochrane, Ontario study areas from 15 June to 15 September, 2010.

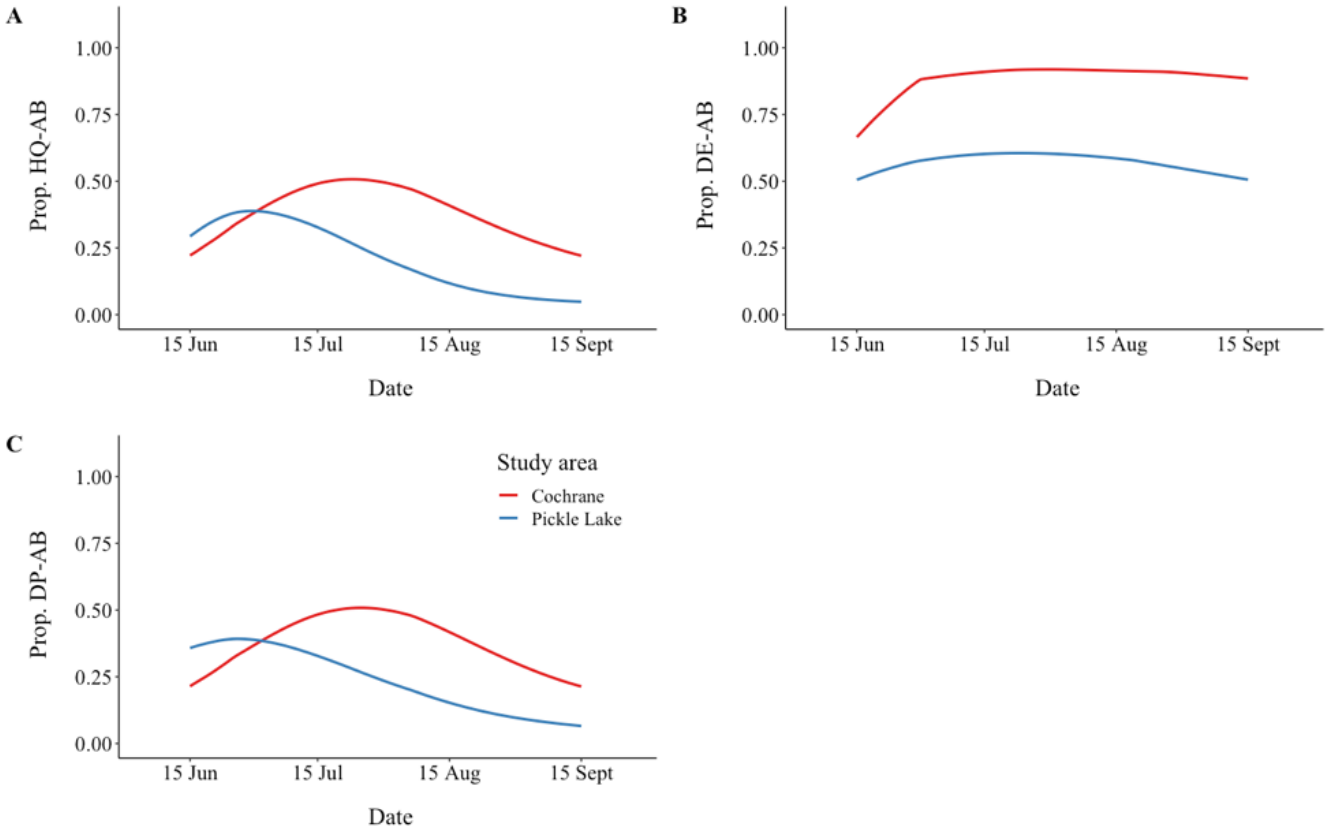

Figure 4.9. Mean proportions (prop.) of the total accepted biomass (AB, kg/ha) comprised by high-quality (HQ) accepted biomass subject to digestible energy (DE) and protein (DP) constraints (A), of accepted biomass subject to DE constraints only (B), of accepted biomass subject to DP constraints only (C) calculated across the spatial extent of Pickle Lake and Cochrane, Ontario study areas from 15 June to 15 September, 2010.

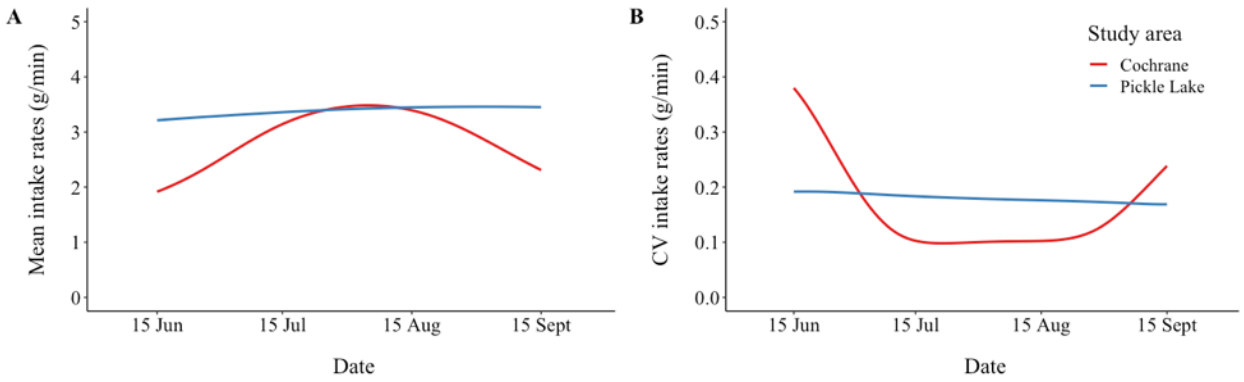

Figure 4.10. Home-range scaled, mean (A) and coefficient of variation (CV; B) of intake rates (g/min) derived from biomass (kg/ha) of grass, forb, and deciduous shrub, horsetail, and mushroom using intake equations developed my Cook et al. (*in prep.*) in Pickle Lake and Cochrane, Ontario study areas from 15 June to 15 September, 2010.

Chapter 5

Dynamic resource selection of threatened caribou is state-dependent

Introduction

Evaluating the distribution and abundance of animals is fundamental to conserving species (Andrewartha 1961). Habitat selection, where an animal chooses which kinds of areas to spend time in, is a key behavioural process influencing species' distributions and their subsequent fitness (Fretwell 1972, Boyce and McDonald 1999). The theory of ideal free distribution (IFD) predicts that individuals will use habitat patches in proportion to available resources but adjust their density to minimize competition for available resources and maximize fitness (Fretwell and Lucas 1970, Fretwell 1972). For large herbivores, acquiring forage resources is key to the life-time fitness of an individual through improved survival, growth rate, and reproductive success (Cook et al. 1996, 2004; Parker et al. 1999). Therefore, based on the IFD, "ideal free" individuals will distribute themselves relative to resources that can be efficiently exploited (Fretwell and Lucas 1970, Fretwell 1972), i.e., the habitat-matching rule (Parker 1978). However, there is limited empirical evidence of the habitat-matching rule, with animals generally underusing higher-quality sites and overusing sites of lower quality (Kennedy and Gray 1993, Kohlmann and Risenhoover 1997). Possible explanations for under-matching are that animals do not have "ideal" knowledge of patch quality and they are not "free" to enter a patch due to constraints on access via intraspecific interference (Sutherland 1983) or predation risk (McNamara and Houston 1990, Moody et al. 1996). As such, large herbivores may use areas with sub-optimal forage resources to avoid predation risk when predation risk and foraging opportunities are positively correlated in space, thus suggesting a trade-off (Rachlow and Bowyer 1998, Bowyer et al. 1999, Barten et al. 2001, Hamel & Côté, 2007).

Trade-offs that large herbivores make in habitat selection across an annual cycle can be dynamic (Dardaillon 1986, Sakuragi et al. 2003, Hornseth and Rempel 2016) because forage

resources and vulnerability to predation risk change over time (Dussault et al. 2005, Hebblewhite and Merrill 2008, Johnson et al. 2021, Chapter 4). In most temperate regions, foraging resources are of lowest quality and least available during the winter (Shipley et al. 1998) because there is little to no new growth and snow accumulation restricts access, lowering foraging efficiency (Robinson and Merrill 2012). In contrast, changes in forage quantity and quality are highly dynamic across the growing season. Fiber content of new growth is relatively low at the beginning of the growing season resulting in higher digestibility (Bryant et al. 1983, Launchbaugh et al. 1993), but accumulates across the growing season, reducing the digestibility (Van Soest 1982, Klein 1990) and thus passage rates (Spalinger and Hobbs 1992, Gross et al. 1993). The contrasting temporal trends in forage quantity and quality across the growing season indicate that large herbivores may maximize intake of nutritional resources at intermediate levels of biomass when quality is high, i.e., the forage maturation hypothesis (McNaughton 1985, Fryxell 1991, Hebblewhite et al. 2008).

In areas with predators, large herbivores are faced with spatial variability in predation risk across the growing season (Kittle et al. 2015, 2017; Leblond et al. 2016, McAuley et al. 2021) and their trade-off in space use may depend on their own nutritional requirements and the vulnerability of their young (Alonzo 2002, Viejou et al. 2018, Berg et al. 2021, Picardi et al. 2021). Individuals with offspring have high nutritional demands, particularly during peak lactation (~3 weeks postpartum; White and Luick 1984, Klein 1990, Parker et al. 1990). In predation-free environments, large herbivores would be expected to distribute themselves to maximize intake of nutritional resources (MacArthur and Pianka 1966, Emlen 1966, Charnov 1976, Pyke 1984). In contrast, in environments with predators, evidence suggests that large herbivores with young trade-off foraging opportunities to avoid predation risk differently than

barren individuals (Bowyer et al. 1999, Barten et al. 2001, Gustine et al. 2006, Hamel & Côté, 2007). For example, mountain goats (*Oreamnos americanus*) with young in Alberta, Canada, have been shown to forage closer to escape terrain than barren individuals to evade predators more easily, which exposed them to forage with lower biomass and digestibility (Hamel and Côté 2007). Similarly, in Alaska, USA, Barten et al. (2001) observed caribou (*Rangifer tarandus*) with a calf-at-heel traded off forage biomass for safety by using higher elevation sites than those used by grizzly bears and wolves, but would return to areas of lower elevation with higher forage biomass post-calving. Indeed, forage-predation risk trade-offs made by large herbivores may be particularly important for individuals with young inhabiting environments with dynamic forage resources as they balance the safety of newborn young and maintain body condition to meet long-term reproductive efforts.

Caribou, a circumpolar species inhabiting dynamic environments, continue to decline globally (Vors et al. 2007, Festa-Bianchet et al. 2011). The ultimate cause for diminishing boreal woodland caribou (*R. t. caribou*; hereafter caribou) numbers across Canada has been attributed to habitat loss and fragmentation from industrial practices (Vors et al. 2007, Festa-Bianchet et al. 2011), which is compounded by increased predation risk (Wittmer et al. 2005, Dickie et al. 2017, DeMars and Boutin 2018, Serrouya et al. 2021). Habitat loss via forest practices can modify forage availability for caribou by decreasing lichen availability (Bock and Van Rees 2002, Bowman et al. 2010) while also increasing deciduous browse (Thompson 2003, Brown 2011), a significant summer forage for caribou (Bergerud 1972, Boertje 1984, Russell et al, 1993, Denryter et al. 2017, Cook et al. *in prep*), as well as other caribou-specific forage (i.e., forbs, grasses, and horsetails; Chapter 4). Early seral stands may also represent risky areas for caribou because moose (*Alces alces*) and white-tailed deer (*Odocoileus virginianus*) prefer these stands

(Bowman et al. 2010, Street et al. 2015), which can attract predators (Brodeur et al. 2008, Kittle et al. 2015, 2017), thus suggesting a possible trade-off between summer forage availability and predation risk. However, few caribou studies have explicitly tested trade-offs between forage availability and predation risk, and how reproductive state influences these trade-offs across the summer. For example, Avgar et al. (2015) documented that caribou consistently selected for areas of higher foraging resources with variable responses to predation risk in northwestern Ontario, but they did not consider reproductive state. In contrast, Viejou et al. (2018) documented in the same region that caribou with a calf-at-heel selected more strongly against predation risk than barren individuals with similar selection by both groups of caribou for areas of high forage availability across the summer, but they did not explicitly evaluate trade-offs. In Quebec, Canada, Leblond et al. (2016) also reported that during the 2-month calving period after parturition, caribou with a calf-at-heel selected for areas of low predation risk, but at the cost of lower foraging opportunities, whereas barren individuals selected areas of higher forage and did not select against predation risk. The variable results of these studies may reflect differences in how caribou alter their forage-predation risk trade-offs throughout the summer as forage availability changes and calves become less vulnerable to predation risk across this period (Mahoney et al. 1990, Gustine et al. 2006, Pinard et al. 2012). New insights may emerge concerning how caribou of different reproductive states make these trade-offs through time by accounting for forage dynamics.

In this paper, we built on the work of Viejou et al. (2018) and addressed caribou resource selection over a broader range of individual caribou in three different reproductive states (barren, calf alive after 5-weeks postpartum, and calf died within 5-weeks postpartum) that were exposed to changing forage conditions during calving (1 May–15 June), early summer (16 June–31 July),

and late summer (1 August–15 September) across northern Ontario. We predicted that, compared to barren caribou, caribou with a calf alive after 5-weeks postpartum would trade-off areas of higher forage resources for lower predation risk during calving and early summer because of higher calf vulnerability (Mahoney et al. 1990, Gustine et al. 2006, Pinard et al. 2012). However, in late summer, we predicted both barren caribou and caribou with a calf alive after 5-weeks postpartum would show less forage-predation risk trade-offs as they select for foraging opportunities because this is a key period to accrue fat reserves and increase their probability of pregnancy and overwinter survival (Cook et al. 1996, 2004; Parker et al. 1999), but at the consequence of higher predation risk. In comparison to caribou that successfully raised a calf to at least 5-weeks postpartum, we predicted caribou that gave birth but lost their calf within the first 5-weeks postpartum would not select against predation risk, which could then lead to calf mortality, but during early and late summer their selection patterns would be most similarly to barren caribou.

To test these predictions, we first identified the forage metric(s) most related to seasonal resource selection for caribou. We predicted that during the calving season caribou would select for areas with high lichen biomass despite their low intake rates (Cook et al. *in prep.*) because they are high in digestible energy (Parker et al. 2005, Thompson et al. 2015, Chapter 4) and low abundance of vascular plants early in the growing season would be expected to support low intake rates. During early summer, we expected caribou to select for areas of high intake rate, which were associated with areas of high accepted biomass, because forage quality was generally high across the landscape (Chapter 4). In late summer, we predicted caribou would select areas with the high-quality accepted biomass because forage quality was declining overall (Chapter 4). After identifying the forage metric most associated with caribou selection in each season, we

then assessed whether caribou traded off selecting for areas of high forage as wolf predation risk increased. If caribou trade-off foraging opportunities to avoid the risk of predation, wolves may have an indirect effect on caribou nutrition by altering their selection for areas offering key foraging advantages.

Study Area

Our study was conducted across northern Ontario, Canada, within three study regions: Pickle Lake (90.938W, 51.568N, 23,000 km^2), Nakina (87.548W, 50.388N, 23,000 km^2), and Cochrane (80.598W, 49.908N, 23,000 km^2; Figure 5.1). All regions were within the boreal forest biome with Pickle Lake and Nakina situated within the Boreal Shield of northwestern Ontario and Cochrane in the Northern Clay Belt region of northeastern Ontario. All study regions were characterized by forested stands of black spruce (*Picea mariana*), jack pine (*Pinus banksiana*), balsam fir (*Abies balsamea*), trembling aspen (*Populus tremuloides),* and white birch (*Betula papyrifera*; (Rowe 1972). The extent of lowlands (swamp, bog, and fen) was greater in Cochrane (64%) compared to Nakina and Pickle Lake (both 28%; Walker et al. 2021). The level of anthropogenetic disturbance differed across the three study regions. Pickle Lake has been without silvicultural activities since the 1960s, whereas commercial forestry is active in Nakina and Cochrane (Thompson et al. 2015). Consequently, at the time of this study (2010), Nakina and Cochrane had greater harvest regeneration (<40 years; 22% and 13%, respectively) and linear feature density (0.42 and 0.31 km/km^2, respectively) compared to Pickle Lake (0.04% and 0.05 km/km^2; OMNRF 2014*a*, Fryxell et al. 2020). In contrast, Pickle Lake had a greater extent of natural disturbance (proportion burned <50 years, 12%) compared to Nakina and Cochrane (both 4%; OMNRF 2014*a*, Fryxell et al. 2020). The density of wolves (*Canis lupus*) and moose (*Alces alces*) were highest in Nakina (6.7 wolves/1,000km^2; 11.8 moose/100km^2) followed by

Pickle Lake (4.2 wolves/1,000km^2, 4.6 moose/100km^2) and Cochrane (3.7 wolves/1,000km^2, 3.8 moose/100km^2; OMNRF 2014*a*, Fryxell et al. 2020). Black bear densities were comparable across regions (20–40 black bears/100 km^2; Rodgers et al. 2009, Howe et al. 2013). Cochrane had greater total annual precipitation (824 mm $\pm$ 81 mm; $\bar{x} \pm$ SD, 20-yr average [1991-2010]) compared to Nakina (776 mm $\pm$ 130 mm) and Pickle Lake (736 mm $\pm$ 122 mm; Environment Canada, https://climate.weather.gc.ca/historical_data/search_historic_data_e.html, accessed 14 Jun 2019). January daily temperatures were lowest in Pickle Lake (-19.26°C ± 3.60°C) followed by Nakina (-18.60°C ± 3.61°C) and Cochrane (-17.82°C ± 3.69°C), whereas July daily temperatures were similar among areas (Pickle Lake: 17.66°C ± 1.49°C; Nakina: 17.07°C ± 1.50°C; Cochrane: 17.36°C ± 1.25°C).

Methods

Animal data

We used GPS telemetry data from 83 adult female caribou that were captured by helicopter net-gun in 2010−2013 (Ontario Ministry of Natural Resources and Forestry Wildlife Animal Care and Use permits 10-183, 11-183, 12-183, 13-183). Caribou were fit with either Lotek Iridium GPS or GPSArgos animal-borne video collars (Thompson et al. 2012), GPS-Argos radio collars (Telonics, Mesa, AZ, USA; Lotek Wireless, Newmarket, ON, Canada), or GPS-Iridium radio collars (Lotek Wireless). The fix rate intervals of GPS collars were 1 or 2.5 hrs, however we rarefied 1-hr fix rates to 3-hr fix rates to be similar to the 2.5-hr fix rate from all collar data sets. Because we only monitored 8% (7 of 83) of caribou individuals for >1 year, we separated location data by caribou ID and year, resulting in 91 caribou-years (Pickle Lake: $n = 28$, Nakina: $n = 38$, Cochrane: $n = 25$). Fix rate success across all 91 caribou-years was 95% ($\pm$ 4%; $\pm$SD) after removing low accuracy GPS fixes (i.e., <3-dimensional fixes; Frair et al. 2010).

All caribou-years had continuous location data from 1 May to 15 September, except two caribou-years, which did not have location data after 29 August and 7 September (<13% of sampling period). Based on results of Walker et al. (2021), reproductive state was known (via camera-collar footage; Thompson et al. 2011, Viejou et al. 2018) or predicted (via methods outlined in DeMars et al. [2013]) for all 91 caribou-years resulting in 21 barren caribou-years, 49 caribou-years with a calf-at-heel until at least 5-weeks postpartum (hereafter calf alive), and 21 caribou-years that lost their calf within the first 5-weeks postpartum (hereafter calf lost).

Landscape data

Predation risk. We used a summer predation risk model developed by Avgar et al. (2015) for Pickle Lake and Nakina, which was derived from GPS telemetry of 52 wolves across 34 packs within Nakina (37 individuals from 23 packs) and Pickle Lake (15 individuals from 11 packs) from May to October in 2010–2012. Avgar et al. (2015) followed the methods outlined in Kittle et al. (2015), which were originally used to develop a winter predation risk model. Briefly, Avgar et al. (2015) used pack-specific, 95% Brownian bridge utilization kernels weighted by pack size to estimate predation risk values from each wolf pack across study regions, which were then summated across the landscape to derive a population-level utilization distribution. The values of the population-level utilization distribution were then modeled as a function of landscape covariates (normalized difference vegetation index [NDVI], Far North Land Cover type, and distance to primary and secondary roads, waste management sites [i.e., dumps], human settlements, and rivers and large lakes [>500m in diameter]) and predicted at the scale of 30-m using a generalized least squares regression model. Predictions at the 30-m scale were then scaled to a 220 m^2 hexagonal grid by taking the average value within each hexagon, resulting in a static map of summer predation risk for Pickle Lake and Nakina in 2010–2012. For further

detail, see Avgar et al. (2015). We followed the same methods to derive comparable estimates of hexagon-level, summer predation risk in Pickle Lake and Nakina in 2013 and 2014 using spatial data for model covariates in those years.

To estimate predation risk across the Cochrane study region for 2010–2014, we used the summer predation risk model developed for Pickle Lake and Nakina and the same year-specific covariate layers for the Ontario portion of the Cochrane study area. However, because 32% of caribou-years in Cochrane inhabited regions of Quebec for the majority of the summer (Figure 5.1), we obtained equivalent geospatial layers to those used by Avgar et al. (2015) and predicted summer predation risk for the Quebec extent (see Appendix 11 for further details).

Forage availability. Forage availability was based on dynamic, spatial predictions (i.e., foodscapes) of nine forage metrics developed in Chapter 4, which spanned 15 June to 15 September (early and late summer). We extrapolated the predictions of each forage metric between 1 May and 15 June (calving) using 26 permanent phenological plots sampled across Pickle Lake between 15 May and 11 June in 2017–2018 and 13 phenological plots sampled across Cochrane between 23 May and 24 May in 2018. Phenological plots reflected the seral-specific ecosites used to develop the foodscapes in Chapter 4. In extrapolating biomass back in time to 1 May for each seral-specific ecosite (Table 4.1), we assumed biomass of each forage metric (except lichen) was zero on 1 May, and regressed study area-specific relationships between zero on 1 May and the biomass of each metric on 15 June while including estimates from the seral and ecosite-specific phenological plots. For lichen, we assumed no change in availability over this period and used the same value on 1 May as on 15 June (Chapter 4). For seral-specific ecosites for which we did not sample phenological plots (Early Upland-Black Spruce-Rocky, Mid-late Upland-Black Spruce-Rocky, Lowland-Cedar/thicket, and Lowland-

Marsh), we used estimates from all phenological plots to derive an average rate of change between zero biomass on 1 May and the biomass on 15 June. We took this approach because these ecosites were relatively uncommon or not present within a study area (Table 4.1). We tested linear vs. non-linear relationships for each extrapolation using CurveExpert (CurveExpert 2.7.3, D. G. Hyams, Madison, AL. USA) based on > 2 ΔAIC_C (Burnham and Anderson 2002) in the extrapolations between 1 May and 15 June. For further details on the extrapolation of forage metrics to the calving period, see Appendices 13 and 14.

Because we did not conduct vegetation sampling in Nakina, the calving biomass extrapolations and foodscape models developed for Pickle Lake (Chapter 4) were also applied to the Nakina region. We assumed similar vegetation composition and dynamics in Pickle Lake and Nakina because they are adjacent study areas, both situated within the Boreal Shield (Avgar et al. 2015, Kittle et al. 2015, McGreer et al. 2015, Viejou et al. 2018), and have similar annual precipitation and mean July temperature. We also assumed similar vegetative conditions in 2010–2013 based on the caribou telemetry and 2017–2018 when the vegetation sampling was conducted in each study area (only 2018 in Cochrane). Total annual precipitation in Pickle Lake during 2017 (614 mm) and 2018 (591 mm) fell within the range observed between 2010–2013 (576 mm–759 mm), whereas total annual precipitation in Cochrane was slightly lower in 2018 (680 mm) than the range observed between 2010–2013 (703 mm–1,111 mm; https://climate.weather.gc.ca/climate_data). Similarly, mean July temperature in Pickle Lake during 2017 (18.7°C) and 2018 (19.3°C) fell within the range observed between 2010–2013 (18.0°C–20.1°C), whereas mean July temperature in Cochrane was slightly higher in 2018 (20.4°C) than 2010–2013 (17.4°C–19.3°C).

State-dependent resource selection

We used integrated step selection analysis (hereafter iSSA; Avgar et al. 2016) to evaluate how the nine forage metrics and predation risk influenced resource selection of caribou based on reproductive state. iSSA includes step length and turn angles directly in the model to evaluate resource selection while accounting for movement processes (Avgar et al. 2016). We fit iSSA models for three reproductive states (barren, calf survived 5-weeks postpartum, and calf died within 5-weeks postpartum; Chapter 2) and three seasons (calving: 1 May to 15 June, early summer: 16 June to 31 July, and later summer: 1 August to 15 September), resulting in 9 iSSA. We chose these durations for seasons because the calving season encompassed all calving events of parturient individuals (except one caribou-year with a calving event on 17 June) and the period of peak lactation post calving (~3 weeks from the median birth dates; Walker et al. 2021); further, this period corresponds with our extrapolation of each forage metric via permanent phenological plots. We used 1 August to distinguish early from later summer because it represented the peak accepted biomass and intakes rates in Pickle Lake (and by extension Nakina) and Cochrane (Figure 4.7A, 4.10A). The early summer period also corresponded to peak tabanid abundance in Nakina (Raponi et al. 2018) and Cochrane (Villetard et al. *in prep*.), whereas late summer has been identified as a critical period for ungulates for accruing body fat, which can increase probability of pregnancy and overwinter survival (Cook et al. 1996, 2004; Cook et al. 2013).

GPS locations were designated as “used” and “available” locations and were sampled based on the movement patterns of individual caribou at a ratio of ten available to each used location (Fortin et al. 2005, Avgar et al. 2016) using the R package Animal Movement Tools (AMT; Singer et al. 2019). Specifically, the spatial location of each available was randomly

selected using a gamma distribution of step length (m; Euclidean distance between each subsequent used location) and a von Mises distribution of turn angles generated for each season (Avgar et al. 2016, Singer et al. 2019). Predation risk values were assigned to each used and available location at the resolution of 220-m^2 (Avgar et al. 2015, Kittle et al. 2015, McGreer et al. 2015, Viejou et al. 2018), whereas forage metrics reflected the 30-m^2 pixels of a location with each used:available set paired by Julian day to account for phenological changes in forage metrics across the growing season. Across all iSSAs, caribou-year was included as a random intercept (Gillies et al. 2006). We included as fixed effects within each iSSA the natural logarithm transformed step lengths and cosine transformed turn angles (Avgar et al. 2016, Dickie et al. 2020, Singer et al. 2019).

We took the modeling approach to first identify among the nine forage metrics which metrics or combination of metrics best explained selection, and then determined whether there was evidence caribou altered their selection for forage metrics due to predation risk (forage-predation risk trade-off) based on the interactions between the best forage metric and predation risk. For the forage metrics, we used model selection and Akaike information criterion corrected for small sample size (AIC_C) to identify the most informative forage metric ($\Delta AIC_C < 2$) among the hypothesized nine forage metrics using univariate iSSAs for each season and reproductive state (Burnham and Anderson 2002). We evaluated selection of each forage metric as a linear term, and as a linear and quadratic term to evaluate the selection of intermediate forage values. We also compared the models to a biological null model, which included step length and turn angle as covariates, to ensure the top forage metric had greater support than the null. Once we identified the top forage metric(s) for a season, that forage metric was included in subsequent

iSSAs. Because most forage metrics were highly collinear ($r = 0.58 \pm 0.24$; $\bar{x} \pm SD$), we cautiously included more than one metric within a model in our model selection.

We also used model selection and AIC_C to evaluate caribou selection of forage, predation risk, and forage x predation risk interaction between forage using six candidate models (Table 5.1) and a biological null model (step length and turn angle only), and identified the best supported iSSA based on $\Delta AIC_c < 2$. We used conditional logistic regression to estimate selection coefficient and confidence intervals of covariates within each iSSA (Singer et al. 2019). To evaluate differences in selection, we identified selection for or against each covariate (95% confidence intervals not overlapping zero) within each iSSA and contrasted the trends in selection across each reproductive state and season.

Finally, to visualize possible forage-predation risk trade-offs in selection, we graphed the predicted probability of selection under a high and a low predation risk value across a range of available intake rates for each season by reproductive state (Avgar et al. 2017). For these predictions, we assigned a mean step length and turn angle across all reproductive states within a season and used fixed-effect selection coefficients to predict the probability of selection using the exponentiated iSSA for each season and reproductive state, where we scaled the predictions between 0 and 1 (Avgar et al. 2017). We assumed equal availability and uniform distribution of intake rates across all caribou within seasons (Avgar et al. 2017). High and low predation risk values at which to graph selection were derived as the mean predation risk value of all available locations above and below the median value, respectively (Appendix 15.1).

Results

Forage Selection

In the univariate analysis of forage metrics, there was consistent and strong support ($\Delta AIC_c > 33$ and $\Delta AIC_c > 105$ for null) for a non-linear relationship between selection for an area and the expected intake rate (g/min) across all seasons and reproductive states (Appendix 15.2). Because intakes rates are predicted from grass, forbs, and deciduous shrubs (GFS), lichen, horsetail, and mushroom (Cook et al. *in prep*., Chapter 4), we compared the support for intake models and the multivariable models composed of the components predicting intake. We found the components of accepted biomass had greater support for caribou selection than a linear relationship with intake rates but not a non-linear relationship with intake (Table 5.1). This indicates weights (i.e., beta coefficients) within the intake rate models based on caribou foraging (Chapter 4; Cook et al. *in prep*.) is a more informative metric of caribou selection than the unweighted components of accepted biomass. Further, there was less support ($\Delta AIC_c > 900$) for a model including intake rate with linear or non-linear effects of lichen biomass than for a model including non-linear intake rate alone, suggesting the decline in selection at high intake rates was not due to the influence of lichen abundance (Table 5.1).

State-dependent resource selection

Predation risk and intake rate were marginally correlated at available locations during calving ($r = 0.15$), early summer ($r = 0.19$), and late summer ($r = 0.21$). Across all reproductive states and seasons, we found most support for the iSSA model with the non-linear effect of intake rate when it included predation risk and the interaction between intake rate and predation risk ($\Delta AIC_c > 9$; Appendix 15.6). Although the selection coefficients for predation risk were generally positive, the negative selection coefficient for the interaction between predation rate and intake

rates (Figure 5.2) indicated caribou selection for areas of moderate to high intake rate declined faster under high predation risk than low predation risk (Figure 5.3). Generally, the biggest trade-off in intake rates occurred during early summer compared to calving and late summer (Figure 5.3). In fact, because most areas at low predation risk were also areas that had low to moderate intake rates (<4.1 g/min), caribou that gave birth (calf alive and calf lost) selected linearly for areas with maximum available intake rates under low predation risk whereas they traded off high intakes rates under high predation (Figure 5.3). Caribou that lost their calf were less likely to make trade-offs between predation risk and forage during calving, possibly exposing them to high predation risk. In contrast, barren caribou, which have lower energetic requirements during calving (i.e., no lactation), made greater trade-offs during calving than caribou that gave birth. In both early and late summer, caribou with calf alive selected for higher intake rates before trading off for lower predation risk (~4.5 g/min) than barren and caribou with calf lost (~3 g/min; Figure 5.3).

Discussion

The life-time fitness of animals is dependent on the recruitment of offspring to local populations. We studied the seasonal resource selection patterns of caribou across northern Ontario to determine whether selection differed among individuals that successfully raised a calf to 5-weeks postpartum and those that did not. We expected that caribou with young would most strongly select for low-risk predation areas to minimize exposure to predators during the sensitive calving period, whereas as the season progressed, caribou, particularly those with calves, would select more strongly for higher forage resources to recoup the costs of lactation. In the early growing season (i.e., calving), we expected caribou, regardless of reproductive state, to select areas of high lichen biomass, because of their relatively high digestible energy content and biomass of

other available forage would be low (Chapter 4). We found some support for this hypothesis because caribou selected for areas of higher lichen biomass (i.e., model weight was higher than null model); however, we found greater support that caribou selection was related to intake rates. Because intake rates were estimated based on accepted biomass, we also compared the selection of areas based on either the individual components of accepted biomass or a combination of these components. We found the greatest support was based on intake rates, suggesting the weights of each component of accepted biomass within the intake rate models (Chapter 4; Cook et al. *in prep*.) were most closely associated with caribou selection than the components alone.

At the same time, we did not find that caribou increased their selection as intake rates increased overall, rather that caribou selected areas based on intermediate levels of available intake rates. Two reasons may explain this result. First, caribou may have selected areas offering intermediate levels of intake rates because these levels reflect intermediate level of accepted biomass; according to the forage maturation hypothesis (McNaughton 1985, Fryxell 1991, Hebblewhite et al. 2008), individuals may maximize their intake of high-quality forage at intermediate biomass. We think this is an unlikely explanation because the nutritional value of accepted biomass, compared to available biomass, is typically high (Geary et al. 2017), and we found less support for seasonal trends in caribou selection based on high-quality accepted biomass, which accounts for the concomitant seasonal decline in accepted biomass and forage quality. Second, when we considered predation risk, most areas offering the highest intake rates also had high predation risk. As a result, in low predation areas, caribou were selecting areas that maximized available intake rates during early and later summer, and because accepted biomass is higher in quality than overall forage, they may have been maximizing their nutritional intake at those areas. In contrast, caribou traded off maximizing their intake rates in areas of high

predation risk, which offered higher available intake rates than in low predation areas. Areas of highest intake rates included early seral communities and productive upland conifer forests (Upland-Black Spruce-White Spruce, which is most analogous with mixed-deciduous forests; Chapter 4), but these areas have high predation risk because they are preferentially used by wolves and black bears (Brodeur et al. 2000; Kittle et al. 2015, 2017). Reproductive state did not influence selection of intake rate and is consistent with Viejou et al.'s (2018) findings that caribou with and without a calf selected forage biomass similarly across the summer period. Viejou et al. (2018) also documented that both reproductive states selected against predation risk across the summer with a greater selection against by caribou with calf-at-heel. Although our study suggests caribou are not selecting against predation risk when we consider predation risk alone, we did observe forage-predation risk trade-offs, which indicate that caribou are selecting against predation risk, but at areas with higher intake rates.

Caribou in all reproductive states made trade-offs between intake rates and predation risk, but the extent of the trade-off varied across the seasons by reproductive states. We expected caribou with calf alive (>5-weeks postpartum) to make the greatest forage-predation risk trade-offs during calving and forgo use of risky areas with sufficient forage and rely on body reserves to meet the nutritional demand of lactation (i.e., capital breeders; Taillon et al. 2013). However, caribou with calf alive did not select against forage during the calving period and made similar trade-offs to barren caribou, which have 2-times lower nutritional requirements than lactating caribou (Chan-McLeod et al. 1994). Evidence suggests inadequate forage resources during the first month of lactation can fully deplete caribou body reserves (Crête and Huot 1993), and therefore lactating caribou may not be able to completely forgo foraging opportunities during calving. In contrast, Leblond et al. (2016) in Quebec, Canada, documented that caribou with a

calf-at-heel selected against predation risk during a 2-month calving period (21 May–21 June) whereas barren individuals expressed no selection towards predation risk. They attributed this difference in selection to lower vulnerability of predation by black bears for adult females compared to calves (Zager and Beecham 2006), which are the dominant predator of calves in their study area (Pinard et al. 2012). The influence of predation risk on trading off areas with high intake rates by barren caribou across northern Ontario may reflect a greater risk of encountering wolves, the dominant predator of caribou in Ontario (Fryxell et al. 2020). Caribou with a calf-at-heel that did not trade-off high intake rates for lower predation risk during calving also lost their calves (<5-weeks postpartum) during this period, compared to caribou with calf alive that made greater trade-offs. Leclerc et al. (2014) in Quebec, Canada, also documented caribou that did not lose their calf selected against riskier areas (i.e., high road density) more strongly than caribou that lost their calf during calving. Finally, barren caribou made the greatest forage-predation risk trade-offs during the calving period compared to caribou with young, possibly because the lower nutritional requirements (i.e., not lactating) allowed barren caribou to be more flexible in making trade-offs, i.e., they could afford to trade-off higher intake rates for lower predation risk.

The degree to which caribou select for areas of forage availability may depend on the duration spent lactating and consequentially their nutritional condition. Caribou with calf alive selected for areas with intake rates ~1.5 g/min higher than the two other reproductive states before trading off higher intake rates for lower predation risk during early and late summer. Caribou that successfully raised a calf over the duration of peak lactation, i.e., caribou with calf alive, may have exploited greater body reserves than caribou that lost their calf within the first 5-weeks postpartum, especially since 67% of neonatal mortality events occurred before three

weeks postpartum (i.e., before peak lactation; Walker et al. 2021). In northwestern Canada, caribou that lost their calf by mid-autumn had on average 3 percentage points greater body fat (11.4%) than caribou that successfully raised their calf through mid-autumn (8.4%) due to a shorter period lactating (Cook et al. 2021). Therefore, caribou with calf alive selecting for areas of higher intake rates before trading off for safety may reflect the need to recoup lost condition over the peak lactation period. Assuming selection for areas with higher intake rates allows caribou with calves-at-heel to increase their nutrient intake, even marginally higher instantaneous intake rates (g/min) can scale up to considerable effects per-day, which are then compounded across early and late summer; the multiplier effect described by White (1983).

We observed a greater degree of forage-predation risk trade-offs during early summer, particularly for caribou that gave birth, which may suggest caribou are more sensitive to predation risk during this period. A possible explanation for similar trade-offs across reproductive states could be greater insect harassment during the early summer period, which may alter their trade-offs. Field sampling of tabanids in Nakina and Cochrane indicated peak abundances during the early summer period (Nakina: ~15 June–15 July, Raponi et al. 2018; Cochrane: 23 June–27 July, Villetard et al. *in prep*.) with reduced caribou activity in Nakina corresponding to higher tabanid abundance (Raponi et al. 2018). Because tabanids are a visual predator (Raponi et al. 2018), caribou may reduce activity to avoid detection, which may decrease time spent foraging. For example, Mörschel and Klein (1997) documented a 58% decrease in foraging time of arctic caribou (*R. t. granti*) in Alaska, USA, during periods of high insect harassment compared to the pre-insect period. Weladji et al. (2003) also found that autumn calf weights of semi-domesticated reindeer in Norway were significantly lower following summers of higher insect abundance, presumably because of decreased foraging efficiency. If

insect harassment reduces foraging time, we might expect caribou to express less forage-predation risk trade-offs to maximize intake rates during these shorter foraging bouts, which we did not find evidence for. However, if insect harassment is greater at areas of high predation risk, then their combined effects may cause caribou to make a greater trade-off and select for areas with low predation risk and low insect harassment at the cost of lower intake rates. In Nakina, Raponi et al. (2018) documented higher insect abundances in younger (25–35 years) than intermediate (36–74 years) and older (≥70 years) forests. This may suggest that stands less than 25 years could have greater insect abundance, and because early seral forest (<20 years) are preferentially used by wolves in this area (Kittle et al. 2015, 2017), these areas could represent high predation risk and high insect harassment for caribou. We recommend further studies evaluate the spatiotemporal distribution of harassing insects, their impact on caribou foraging, and its effect on the forage-predation risk trade-offs made by caribou.

For caribou in the boreal forest, late summer is a period of reduced lactation (Parker et al. 1990) and insect harassment before the onset of winter, and therefore may reflect a critical time for large herbivores to accrue fat and increase their probability of pregnancy and overwinter survival (Cook et al. 1996, 2004; Parker et al. 1999). For this reason, we predicted caribou would most strongly select for areas with greater high-quality accepted biomass during this period because overall forage quality was declining, but this prediction was not supported. Instead, we found caribou selection was most closely related to non-linear intake rates, suggesting predation risk continued to influence caribou behaviour during this period. The magnitude of forage-predation risk trade-offs made by caribou during late summer was generally less than trade-offs during early summer. This suggests caribou during late summer may trade-off forage and

predation more similarly in areas of high and low predation risk and therefore endure higher predation risk at the benefit of higher intake rates.

Our metric of predation risk reflected only wolf space use (Avgar et al. 2015, Kittle et al. 2015), yet caribou may be also responding to predation risk from black bears (Mahoney et al. 1990, Pinard et al. 2012, Mahoney et al. 2016). Given similar preferential use of early seral and mixed-deciduous forests by wolves in western Ontario (Kittle et al. 2015, 2017) and black bears in the boreal forest of Quebec, Canada (Brodeur et al. 2000), our metric of predation risk may generally reflect risk of both predators to caribou. Even so, we would expect caribou to respond to black bear predation primarily during a relatively short ~1 month period postpartum (Mahoney et al. 1990, Zager and Beecham 2006, Pinard et al. 2012). Moreover, given evidence black bears do not actively search out ungulate calves and that mortality events may occur opportunistically (Bastille-Rousseau et al. 2011, Bowersock et al. 2021), caribou with young may not be able to rely on environmental cues to minimize risk of neonatal mortality by black bears during calving. In contrast, caribou may be able to rely on environmental cues to reduce predation risk by wolves across the summer. Predation risk by wolves may instead represent a relatively static probability of risk in the summer, because wolf movement rates during this period are relatively restricted as they concentrate their space use around the breeding den and rendezvous sites while raising their pups (Jędrzejekski et al. 2001, Mech and Boitani 2003, Merrill and Mech 2003). Nevertheless, more research is needed to evaluate the combined risks of black bears and wolves for caribou in northern Ontario and how these risks change across the growing season.

Predation is considered the key factor in the conservation of threatened woodland caribou across its range, including Ontario (Seip 1992, McLoughlin et al. 2005, Wittmer et al. 2005,

Fryxell et al. 2020, Serrouya et al. 2021). Direct impacts of predation on caribou can lead to reduced population growth. For example, Fryxell et al. (2020) documented ~70% of caribou mortality events were from predation and that lower population growth rates of caribou local populations across northern Ontario were strongly related to higher wolf densities. Predation on caribou can be exacerbated by landscape alterations that increase alternative prey (Potvin et al. 2005, Latham et al. 2011), resulting in a numerical response in predators (Schwartz and Franzmann 1991, Ballard et al. 2000) and therefore increased predation risk for caribou, i.e., disturbance-mediated apparent competition hypothesis (Seip 1992, Serrouya et al. 2021). A major anti-predator behavior in caribou is to spatially partition from predators by selecting habitats where predation risk is low, e.g., lowlands (Hornseth and Rempel 2016, DeMars and Boutin 2018, Walker et al. 2021). Previous studies have also shown caribou select against linear features (James and Stuart-Smith 2000, Dickie et al. 2020, Walker et al. 2021), early seral forests (Hornseth and Rempel 2016, Walker et al. 2021), and areas of high predation risk (Avgar et al. 2015, McGreer et al. 2015, Viejou et al. 2018). These shifts in caribou distribution may also have an indirect effect on caribou by altering their nutrition, particularly where high forage availability is limited via predator-sensitive foraging (McNamara and Houston 1987). We found evidence that caribou across northern Ontario selected areas based on intake rates but traded off higher intake rates for lower predation risk. Therefore, management strategies that minimize risk of predation may increase foraging opportunities for caribou and promote their long-term persistence (Serrouya et al. 2019).

Table 5.1. Candidate iSSA models used to evaluate caribou selection of forage, intermediate forage (forage as quadratic term), summer predation risk, and trade-off between forage and predation risk (i.e., interaction between forage and predation risk) by season and reproductive state across 91 caribou-years in northern Ontario, 2010–2013, with step length (SL) and turn angle (TA) as fixed-effects and caribou-year as a random effect. A model with only SL and TA was included as a biological null model.

Candidate models
SL + TA
Forage + SL + TA
Forage + Forage^2 + SL + TA
Risk + SL + TA
Forage + Risk + SL + TA
Forage + Forage^2 + Risk + SL + TA
Forage + Forage^2 + Risk + Forage*Risk + SL + TA

Table 5.2. Selection coefficients, number of model parameters (*K*), Akaike's Information Criterion corrected for small sample size (AIC_C), change in AIC_C from best model (ΔAIC_C), and model weights calculated from AIC_C (w_i) from iSSA models to evaluate selection of intake rate (intake) and components of accepted biomass (GFS, lichen [L], horsetail [horse, H], and mushroom [mush, M]), with all seasons and reproductive states combined across 91 caribou-years in northern Ontario, 2010–2013 with step length (SL) and turn angle (TA) included as fixed effects and caribou-year as a random effect. Null model included only SL and TA.

Model	Intake	Intake^2	GFS	GFS^2	Lichen	Lichen^2	Horse	Horse^2	Mush	Mush^2	*K*	AICc	ΔAICc	W_i
Intake^2	0.43	-0.06									5	459358.12	0.00	1.00
GFS^2+L^2+H^2+M^2			-1.97E-05	-4.14E-08	0.0005	-3.54E-07	0.02	-0.0004	1.95	-1.05	11	459571.96	213.83	0.00
GFS^2+H^2+M^2			1.13E-05	-1.22E-07			0.02	-0.0004	2.10	-1.14	9	459691.51	333.39	0.00
Mush^2									2.08	-1.20	5	459852.52	494.40	0.00
Intake+Lichen^2	0.11				0.0005	-3.50E-07					6	460258.70	900.58	0.00
Intake+Lichen	0.12				0.0002						5	460305.34	947.22	0.00
Mush									0.74		4	460339.78	981.66	0.00
Intake	0.12										4	460384.97	1026.85	0.00
Lichen^2					0.0007	-5.03E-07					5	460913.38	1555.26	0.00
Lichen					0.0002						4	461013.18	1655.06	0.00
GFS^2			0.001	-1.63E-06							5	461062.97	1704.85	0.00
Horse^2							0.01	-0.0003			5	461132.96	1774.84	0.00
Horse							0.004				4	461152.47	1794.35	0.00
GFS			0.0001								4	461187.38	1829.26	0.00
Null											3	461194.85	1836.73	0.00

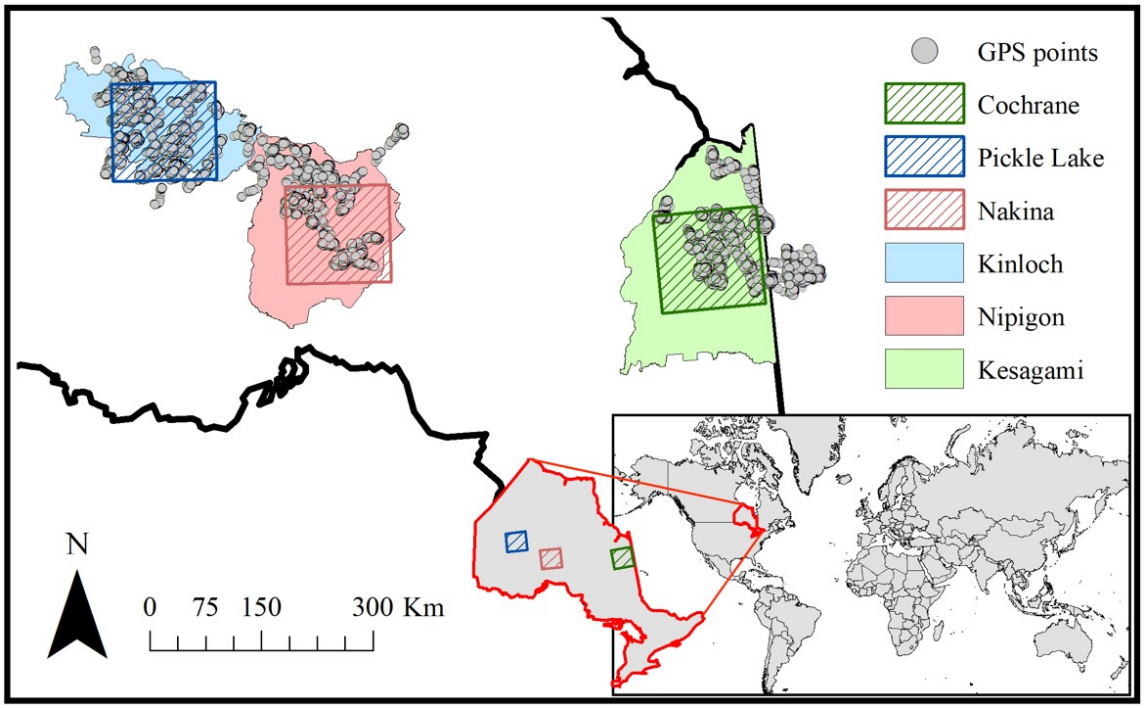

Figure 5.1. GPS points of caribou across 3 study regions (Pickle Lake, Nakina, and Cochrane) throughout northern Ontario, Canada between 1 May and 15 September, 2010–2013, and their respective designated local caribou populations (Kinloch, Nipigon, and Kesagami).

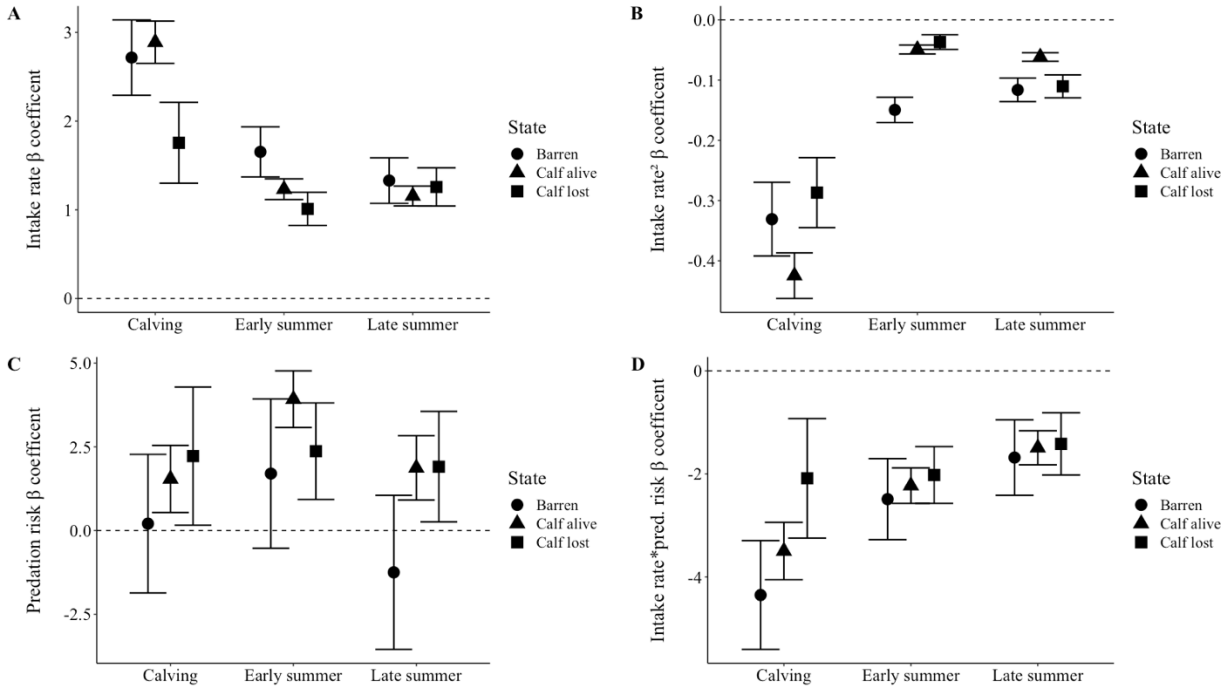

Figure 5.2. Selection (β) coefficient with upper and lower 95% confidence intervals (CIs) derived from iSSA models relating the use of intermediate intake rates, summer predation risk, and the trade-off (i.e., interaction) between intake rates and predation risk compared to available locations from 91 caribou-years across northern Ontario, 2010–2013, stratified by season and reproductive state with step length (SL) and turn angle (TA) included as fixed-effects and caribou-year included as a random effect. The 95% CIs not overlapping zero (dashed black-line) indicate selection for or against each covariate.

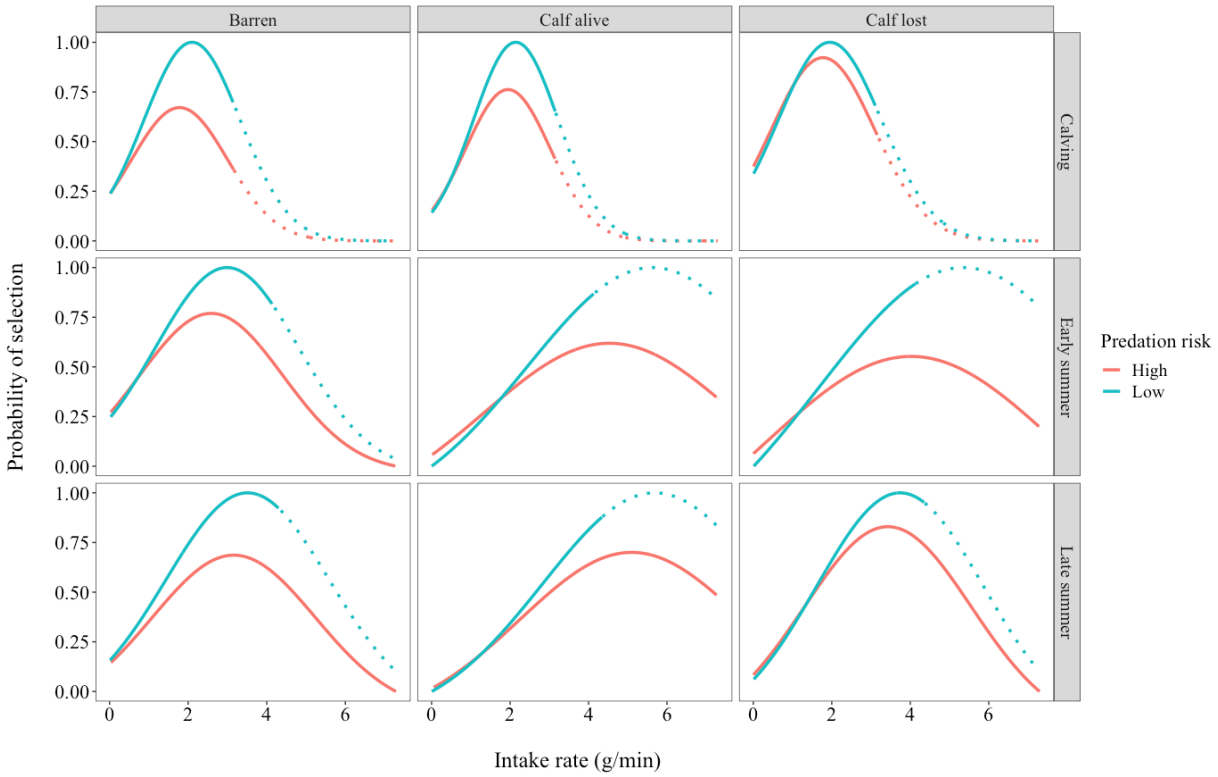

Figure 5.3. Probability of selection for intake rate across on the biological range of available values, predicted from the top exponential iSSA model for each reproductive state (barren, calf alive, and calf lost) and season (calving, early summer, and late summer) stratified by high vs. low predation risk using location data from 91 caribou-years across northern Ontario, 2010–2013. Dashed-lines indicate that these values of intake rates are likely not available to caribou at each level of predation risk, based on the maximum intake rate (after removing the top 1% of intake rates) at available locations for each level of predation risk and season (Appendix 16.6). Intake rates likely available to caribou during calving did not exceed 3.2 (g/min), regardless of predation risk level, whereas during early and later summer available intake rates did not exceed 4.1 (g/min) and 7.3 (g/min) at areas of low and high predation risk, respectively.

Chapter 6. General Discussion

Summary and significance of results

Understanding the motivation behind choices animal make in heterogeneous environments is central to informing the management of threatened and endangered species, especially behaviours that have a substantial impact on fitness. My thesis aimed to quantify and evaluate behaviours employed by boreal woodland caribou (*Rangifer tarandus caribou*; hereafter caribou) relative to forage resources and wolf predation across northern Ontario during the calving and summer period with an emphasis on comparing behaviours of different reproductive states. Calving to late summer represents a key period of dynamic forage availability for caribou as they balance predation risk with consequences for their life-time fitness (Pinard et al. 2012, DeMars and Boutin 2018, Cook et al. 2021).

In Chapter 2, I found that a movement-based model developed by DeMars et al. (2013), using caribou movement data in northern Alberta, could be applied successfully to caribou across northern Ontario. This was the first robust evaluation of the method when model assumptions were not violated (i.e., applied to non-sedentary caribou). Using this movement-based model, I was then able to quantify parturition and neonatal mortality rates for caribou across northern Ontario. I also added to the evidence that caribou select against linear features and early seral stands during calving. Although lowlands are usually viewed as areas of low predation risk for caribou, I found risk of neonatal mortality increased with higher use of lowlands and greater postpartum movement rates, which may relate to greater foraging movements that increase encounter rates with predators. This chapter provided previously unknown reproductive metrics for caribou in Ontario and identified the areas selected by caribou during the sensitive calving period and the associated fitness consequence.

As an extension of Chapter 2, in Chapter 3, I identified caribou with ≥2 parturition events to then evaluate differently motivated types of calving fidelity: spatial (i.e., geographical location) or habitat (habitat conditions) fidelity. Half of the caribou expressed habitat fidelity, whereas only a third expressed spatial fidelity. I evaluated the influence of intrinsic (age, previous calf survival) and extrinsic (environmental) factors on the potential of expressing either type of fidelity. I determined older individuals were more likely to express spatial fidelity, whereas lower availability of high-quality habitat resulted in a greater probability of expressing habitat fidelity. I did not find calf mortality in the previous year influenced the subsequent type of fidelity, but my sample size was low. My findings highlight the variability of behaviors among caribou during calving and offered a new perspective (i.e., habitat fidelity) on behaviours employed during calving, with a large proportion of caribou repeatedly using upland and lowland conifer forests.

In Chapter 4, I modeled dynamic foodscapes and compared the spatiotemporal dynamics of forage in two areas in northern Ontario where previous data indicated caribou differed in body fat levels, pregnancy rates, and lower population growth rates (Fryxell et al. 2020, Walker et al. 2021, J. Cook, R. Cook, and G. Brown unpublished data). I found accepted biomass (plants eaten by caribou) and the associated predicted rates of forage intake averaged consistently higher with greater spatial variation in Pickle Lake than Cochrane. Further, high-quality accepted biomass peaked ~1 month later in Cochrane than Pickle Lake, suggesting a possible mismatch between the period of high nutritional requirements (i.e., peak lactation) and available high-quality forage for caribou in Cochrane. The differences in forage availability found between the two study areas support that caribou in Cochrane may be more nutritionally stressed than caribou in Pickle Lake.

My results indicate that forage resources of an environment may play a role in the persistence of threatened caribou populations.

In Chapter 5, I addressed whether caribou altered their selection behavior for forage resources based on predation risk and how this compared among caribou of different reproductive states (identified in Chapter 2). I found that caribou selected for areas based on intake rates rather than other forage metrics derived in Chapter 4. Across the summer, caribou selected most strongly for areas of high intake rates where predation risk was low, but they traded off high intake rates under high predation and selected more strongly for intermediate levels of intake rates when predation risk was high. Caribou that lost their calf within the first 5-weeks postpartum made the least trade-off between forage and predation risk during the calving period, which may have exposed them to higher predation risk and resulted in calf mortality. Caribou whose calf survived at least 5-weeks postpartum selected for higher intake rates than did other reproductive states before making trade-offs for lower predation risk during early and late summer, which occurred after the energetically demanding period of peak lactation. My findings indicate that predation risk alters caribou selection of forage across the summer and is dependent on reproductive state.

Management implications

Caribou continue to decline globally (Vors and Boyce 2009, Festa-Bianchet et al. 2011) and in Canada this decline has been attributed to habitat loss and fragmentation via industrial practices (Vors et al. 2007, Festa-Bianchet et al. 2011), which increase predation risk for caribou (Wittmer et al. 2007, Dickie et al. 2017, DeMars and Boutin 2018, Serrouya et al. 2021). Therefore, the persistence of caribou populations across Canada is reliant on successful management (Festa-Bianchet et al. 2011, Serrouya et al. 2021), which depends on accurate estimates of reproductive

rates (Bonenfant et al. 2005), and information on caribou space-use that can be used to identify critical habitat. I identified informative metrics of reproduction for caribou across northern Ontario, which can be used in future efforts to model population dynamics and caribou resource selection during calving.

There has been an emphasis on identifying fidelity during calving, particularly spatial fidelity to help guide management for the persistence of caribou populations by protecting calving areas (Faille et al. 2010). For example, in Ontario, the protection of spatial locations associated with caribou calving is outlined in the provincial forest management guidelines (Racey et al. 1999, OMNRF 2014*b*); however, information on calving fidelity in Ontario has been limited. Across northern Ontario, I found more caribou expressed habitat fidelity than spatial fidelity, indicating that protecting not only specific sites but preferred calving habitat may be essential for enhancing opportunities for caribou calving. Because of the current conservation concerns for caribou, I suggest exercising management strategies that promote and maintain calving habitat, which based on this study includes both upland and lowland conifer forests void of linear features.

Evidence continues to support that conditions on summer range may be nutritionally limiting for caribou (Crête and Huot 1993, Pachkowski et al. 2013, Schaefer and Mahoney 2013, Heard and Zimmerman 2021, Denryter et al. 2022*b*). Inadequate summer forage may limit the ability for lactating female caribou to satisfy daily nutritional requirements, consequently decreasing body condition and lowering reproductive success (Cameron et al. 1993, Roffe 1993). Indeed, results from Chapter 4 appear to suggest lower availability of accepted forage and a possible trophic mismatch between availability of high-quality forage and peak nutritional requirements may correspond to caribou being in a lower nutritional plane in Cochrane than

Pickle Lake (Fryxell et al. 2020, Walker et al. 2021, J. Cook, R. Cook, and G. Brown unpublished data). I observed the highest accepted biomass in early seral (<20 years) forests, suggesting these areas offer caribou the highest forage availability. However, early seral stands are generally selected against by caribou in Ontario (Avgar et al. 2015, McGreer et al. 2015, Hornseth and Rempel 2016, Viejou et al. 2018, Walker et al. 2021), because they likely represent areas of high predation risk (Kittle et al. 2015, 2017). Therefore, simply increasing caribou forage across the landscape by creating more early seral forests via clear-cutting or prescribed burns is not a viable management strategy for the long-term persistence of caribou. Indeed, in Ontario, forestry has been identified as the ultimate cause for the 50% caribou range reduction from 1880 to 1990 (Vors et al. 2007, Racey and Armstrong 2000, Schaefer 2003). Previous forest management for caribou in Ontario has been focused on maintaining continuous tracts of winter habitat (i.e., mature [>40 years] conifer forests; Racey et al. 1999) but based on the correspondence between summer forage availability and population performance, I suggest that areas used by caribou during the summer and the associated forage should also be considered.

Given the importance of calf recruitment on population variability and growth in ungulates (Gaillard et al. 2000, Raithel et al. 2007, DeCesare et al. 2012), management of caribou should prioritize the habitat selection of caribou that successfully raise a calf. For caribou in northern Ontario, as seen across Canada, predation risk is a strong determinant of habitat selection and influences caribou selection of intake rates. In areas of high predation risk, caribou traded off selection of high intake rates for safety, whereas in areas of low predation risk caribou selected more for intake rates. Further, caribou with a calf-at-heel during late summer selected higher intake rates before making trade-offs compared to other reproductive states, which may have exposed them to higher predation risk. Therefore, management strategies that

decrease the risk of predation for caribou during summer are critical to their long-term persistence (Serrouya et al. 2019).

Literature Cited

Adamczewski, J. Z., P. F. Flood, and A. Gunn. 1997. Seasonal patterns in body composition and reproduction of female muskoxen (*Ovibos moschatus*). Journal of Zoology 241:245–269.

Adams, L. G., F. J. Singer, and B. W. Dale. 1995. Caribou calf mortality in Denali National Park, Alaska. Journal of Wildlife Management 59:584–594.

Aldridge, C. L., and M. S. Boyce. 2007. Linking occurrence and fitness to persistence: habitat-based approach for endangered greater sage-grouse. Ecological Applications 17:508–526.

Alonzo, S. H. 2002. State-dependent habitat selection games between predators and prey: the importance of behavioural interactions and expected lifetime reproductive success. Evolutionary Ecology Research 4:759–778.

Andrewartha, H. G. 1961. Introduction to the study of animal populations. University of Chicago Press, Chicago, USA.

Armstrong, J. B., G. Takimoto, D. E. Schindler, M. M. Hayes, and M. J. Kauffman. 2016. Resource waves: phenological diversity enhances foraging opportunities for mobile consumers. Ecology 97:1099–1112.

Avgar, T., J. A. Baker, G. S. Brown, J. S. Hagens, A. M. Kittle, E. E. Mallon, M. T. McGreer, A. Mosser, S. G. Newmaster, B. R. Patterson, et al. 2015. Space-use behaviour of woodland caribou based on a cognitive movement model. Journal of Animal Ecology 84:1059–1070.

Avgar, T., S. R. Lele, J. L. Keim, and M. S. Boyce. 2017. Relative selection strength: quantifying effect size in habitat- and step-selection inference. Ecology and Evolution 7:5322–5330.

Avgar, T., J. R. Potts, M. A. Lewis, and M. S. Boyce. 2016. Integrated step selection analysis: bridging the gap between resource selection and animal movement. Methods in Ecology and Evolution 7:619–630.

Balázs, G., B. Lewarne, and G. Herczeg. 2020. Extreme site fidelity of the olm (*Proteus anguinus*) revealed by a long-term capture–mark–recapture study. Journal of Zoology 311:99–105.

Baldwin, D. J., J. R. Desloges, and L. E. Band. 2000. Physical geography of Ontario. Pages 12–29 in Ecology of a managed terrestrial landscape: patterns and processes of forest landscapes in Ontario. UBC Press, Vancouver, Canada.

Ballard, W. B., P. R. Krausman, S. Boe, S. Cunningham, and H. A. Whitlaw. 2000. Short-term response of gray wolves, *Canis lupis*, to wildfire in northwestern Alaska. Canadian Field-Naturalist 114:241–247.

Baltazar-Soares, M., J. D. Klein, S. M. Correia, T. Reischig, A. Taxonera, S. M. Roque, L. Dos Passos, J. Durão, J. P. Lomba, H. Dinis, et al. 2020. Distribution of genetic diversity reveals colonization patterns and philopatry of the loggerhead sea turtles across geographic scales. Scientific Reports 10:e18001

Barbknecht, A. E., W. S. Fairbanks, J. D. Rogerson, E. J. Maichak, B. M. Scurlock, and L. L. Meadows. 2011. Elk parturition site selection at local and landscape scales. Journal of Wildlife Management 75:646–654.

Barboza, P. S., and K. L. Parker. 2006. Body protein stores and isotopic indicators of N balance in female reindeer (*Rangifer tarandus*) during winter. Physiological and Biochemical Zoology 79:628–644.

Barboza, P. S., and K. L. Parker. 2008. Allocating protein to reproduction in Arctic reindeer and caribou. Physiological and Biochemical Zoology 81:835–855.

Barboza, P. S., L. L. Van Someren, D. D. Gustine, and M. Syndonia Bret-Harte. 2018. The nitrogen window for arctic herbivores: plant phenology and protein gain of migratory caribou (*Rangifer tarandus*). Ecosphere 9:e02073.

Barten, N. L., R. T. Bowyer, and K. J. Jenkins. 2001. Habitat use by female caribou: tradeoffs associated with parturition. Journal of Wildlife Management 65:77–92.

Bastille-Rousseau, G., D. Fortin, C. Dussault, R. Courtois, and J. P. Ouellet. 2011. Foraging strategies by omnivores: are black bears actively searching for ungulate neonates or are they simply opportunistic predators? Ecography 34:588–596.

van Beest, F. M., A. Mysterud, L. E. Loe, and J. M. Milner. 2010. Forage quantity, quality and depletion as scale-dependent mechanisms driving habitat selection of a large browsing herbivore. Journal of Animal Ecology 79:910–922.

Beletsky, L. D., and G. H. Orians. 1987. Territoriality among male red-winged blackbirds. Behavioral Ecology and Sociobiology 20:21–34.

Ben-Hur, E., and R. Kadmon. 2020. An experimental test of the area-heterogeneity tradeoff. Proceedings of the National Academy of Sciences of the United States of America 117:4815–4822.

Berg, J. E. 2019. Shifts in strategy: calving and calf survival in a partially migratory elk population. Dissertation, University of Alberta, Edmonton, Canada.

Berg, J. E., D. R. Eacker, M. Hebblewhite, and E. H. Merrill. 2023. Summer elk calf survival in a partially migratory population. Journal of Wildlife Management 87:e22330.

Berg, J. E., J. Reimer, P. Smolko, H. Bohm, M. Hebblewhite, and E. H. Merrill. 2021. Mothers' movements: shifts in calving area selection by partially migratory elk. Journal of Wildlife Management 85:1476–1489.

van den Berg, M., M. J. J. E. Loonen, and C. Çakırlar. 2021. Judging a reindeer by its teeth: a user-friendly tooth wear and eruption pattern recording scheme to estimate age-at-death in reindeer (*Rangifer tarandus*). International Journal of Osteoarchaeology 31:417–428.

Berger, J. 1991. Pregnancy incentives, predation constraints and habitat shifts: experimental and field evidence for wild bighorn sheep. Animal Behaviour 41:61–77.

Bergerud, A. T. 1971. The population dynamics of Newfoundland caribou. Wildlife Monographs 25:3–53.

Bergerud, A. T. 1972. Food habits of Newfoundland caribou. Journal of Wildlife Management 36:913–923.

Bergerud, A. T. 1975. The reproductive season of Newfoundland caribou. Canadian Journal of Zoology 53:1213–1221.

Bischof, R., L. E. Loe, E. L. Meisingset, B. Zimmermann, B. van Moorter, and A. Mysterud. 2012. A migratory northern ungulate in the pursuit of spring: jumping or surfing the green wave? American Naturalist 180:407–424.

Bock, M. D., and K. C. J. Van Rees. 2002. Forest harvesting impacts on soil properties and vegetation communities in the Northwest Territories. Canadian Journal of Forest Research 32:713–724.

Boertje, R. D. 1984. Seasonal diets of the Denali caribou herd, Alaska. Arctic 37:161–165.

Boinski, S., A. Treves, and C. A. Chapman. 2000. A critical evaluation of the influence of predators on primates: effects on group travel. Pages 43–72 *in* S. A. Boinski and P. A. Garber, editors. On the move: how and why animals travel in groups. University of Chicago Press, Chicago, USA.

Bonar, M., E. Hance Ellington, K. P. Lewis, and E. Vander Wal. 2018. Implementing a novel movement-based approach to inferring parturition and neonate caribou calf survival. PLoS ONE 13:e0192204.

Bonenfant, C., J. M. Gaillard, F. Klein, and J. L. Hamann. 2005. Can we use the young: female ratio to infer ungulate population dynamics? An empirical test using red deer *Cervus elaphus* as a model. Journal of Applied Ecology 42:361–370.

Boudreault, C., Y. Bergeron, S. Gauthier, and P. Drapeau. 2002. Bryophyte and lichen communities in mature to old-growth stands in eastern boreal forests of Canada. Canadian Journal of Forest Research 32:1080–1093.

Bowersock, N. R., A. R. Litt, J. A. Merkle, K. A. Gunther, and F. T. van Manen. 2021. Responses of American black bears to spring resources. Ecosphere 12:e03773.

Bowman, J., J. C. Ray, A. J. Magoun, D. S. Johnson, and F. N. Dawson. 2010. Roads, logging, and the large-mammal community of an eastern Canadian boreal forest. Canadian Journal of Zoology 88:454–467.

Bowyer, R. T., V. Van Ballenberghe, J. G. Kie, and J. A. K. Maier. 1999. Birth-site selection by Alaskan moose: maternal strategies for coping with a risky environment. Journal of Mammalogy 80:1070–1083.

Boyce, M. S. 1979. Seasonality and patterns of natural selection for life histories. American Naturalist 114:569–583.

Boyce, M. S., and L. L. McDonald. 1999. Relating populations to habitats using resource selection functions. Trends in Ecology and Evolution 14:268–272.

Boyce, M. S., and E. H. Merrill. 1991. Effects of the 1988 fires on ungulates in Yellowstone National Park. Proceedings of the Tall Timbers Fire Ecology Conference 17:121–132.

Brodeur, V., J. P. Ouellet, R. Courtois, and D. Fortin. 2008. Habitat selection by black bears in an intensively logged boreal forest. Canadian Journal of Zoology 86:1307–1316.

Bronson, F. H., and J. M. Manning. 1991. The energetic regulation of ovulation: a realistic role for body fat. Biology of Reproduction 44:945–950.

Brown, G. S. 2011. Patterns and causes of demographic variation in a harvested moose population: evidence for the effects of climate and density-dependent drivers. Journal of Animal Ecology 80:1288–1298.

Brown, W. K., J. Huot, P. Lamothe, S. Luttich, M. Paré, G. St. Martin, and J. B. Theberge. 1986. The distribution and movement patterns of four woodland caribou herds in Quebec and Labrador. Rangifer 6:43–49.

Bryant, J. P., F. S. Chapin, D. R. Klein, and D. R. Carbon. 1983. Carbon/nutrient balance of boreal plants in relation to vertebrate herbivory. Oikos 40:357–368.

Bunnell, F. L., and D. J. Vales. 1989. Comparison of methods for estimating forest overstory cover: differences among techniques. Canadian Journal of Forest Research 20:101–107.

Bunt, C. M., B. Jacobson, T. Fernandes, L. Ridgway, and B. McMeans. 2021. Site fidelity and seasonal habitat preferences of largemouth bass (*Micropterus salmoides*) in a temperate regulated reservoir. Hydrobiologia 848:2595–2609.

Burnham, K. P., and D. J. Anderson. 2002. Model selection and multimodel infernce. Springer, New York, USA.

Cameron, M. D., K. Joly, G. A. Breed, L. S. Parrett, and K. Kielland. 2018. Movement-based methods to infer parturition events in migratory ungulates. Canadian Journal of Zoology 96:1187–1195.

Cameron, R. D., W. T. Smith, S. G. Fancy, K. L. Gerhart, and R. G. White. 1993. Calving success of female caribou in relation to body weight. Canadian Journal of Zoology 71:480–486.

Cameron, R. D., W. T. Smith, R. G. White, and B. Griffith. 2005. Central Arctic caribou and petroleum development: distributional, nutritional, and reproductive implications. Arctic 58:1–9.

Carr, N. L., A. R. Rodgers, and S. C. Walshe. 2007. Caribou nursery site habitat characteristics in two northern Ontario parks. Rangifer 27:167–179.

Carstensen, M., G. D. DelGiudice, and B. A. Sampson. 2003. Using doe behavior and vaginal-implant transmitters to capture neonate white-tailed deer in north-central Minnesota. Wildlife Society Bulletin 31:634–641.

Chan-McLeod, A. C. A., R. G. White, and D. F. Holleman. 1994. Effects of protein and energy intake, body condition, and season on nutrient partitioning and milk production in caribou and reindeer. Canadian Journal of Zoology 72:938–947.

Chapman, B. B., C. Brönmark, J. Å. Nilsson, and L. A. Hansson. 2011. The ecology and evolution of partial migration. Oikos 120:1764–1775.

Charnov, E. L. 1976. Optimal foraging, the marginal value theorem. Theoretical Population Biology 9:129–136.

Chaverri, G., O. E. Quirós, M. Gamba-Rios, and T. H. Kunz. 2007. Ecological correlates of roost fidelity in the tent-making bat *Artibeus watsoni*. Ethology 113:598–605.

Ciuti, S., P. Bongi, S. Vassale, and M. Apollonio. 2006. Influence of fawning on the spatial behaviour and habitat selection of female fallow deer (*Dama dama*) during late pregnancy and early lactation. Journal of Zoology 268:97–107.

Cleves, M., W. Gould, W. W. Gould, R. Gutierrez, and Y. Marchenko. 2008. An introduction to survival analysis using Stata. Stata Press, College Station, USA.

Compaire, J. C., J. Montes, J. M. S. Gonçalves, M. C. Soriguer, and K. Erzini. 2022. Site fidelity of fish on a rocky intertidal in the south of Portugal. Journal of Sea Research 183:102202.

Cook, J. G., R. C. Cook, R. W. Davis, M. M. Rowland, R. M. Nielson, M. J. Wisdom, J. M. Hafer, and L. L. Irwin. 2018. Development and evaluation of a landscape nutrition model for elk in western Oregon and Washington. Pages 13–30 in M. W. Rowland, et al. Modeling elk nutrition and habitat use in western Oregon and Washington. Wildlife Monographs 199:1–69.

Cook, J. G., R. C. Cook, R. W. Davis, and L. L. Irwin. 2016. Nutritional ecology of elk during summer and autumn in the Pacific Northwest. Wildlife Monographs 195:1–81.

Cook, J. G., A. P. Kelly, R. C. Cook, B. Culling, D. Culling, A. McLaren, N. C. Larter, and M. Watters. 2021. Seasonal patterns in nutritional condition of caribou (*Rangifer tarandus*) in the southern Northwest Territories and northeastern British Columbia, Canada. Canadian Journal of Zoology 99:845–858.

Cook, J. G., L. J. Quinlan, L. L. Irwin, L. D. Bryant, R. A. Riggs, and J. W. Thomas. 1996. Nutrition-growth relations of elk calves during late summer and fall. Journal of Wildlife Management 60:528–541.

Cook, J. G., R. A. Riggs, T. Delcurto, B. K. Johnson, L. L. Irwin, R. C. Cook, and L. D. Bryant. 2004. Effects of summer-autumn nutrition and parturition date on reproduction and survival of elk. Wildlife Monographs 155:1–61.

Cook, J. G., T. W. Stutzman, C. W. Bowers, K. A. Brenner, and L. L. Irwin. 1995. Spherical densiometers produce biased estimates of forest canopy cover. Wildlife Society Bulletin 23:711–717.

Cook, R. C., J. G. Cook, D. J. Vales, B. K. Johnson, S. M. McCorquodale, L. A. Shipley, R. A. Riggs, L. L. Irwin, S. L. Murphie, B. L. Murphie, K. A. et al. 2013. Regional and seasonal patterns of nutritional condition and reproduction in elk. Wildlife Monographs 184:1–45.

Cook, R. C., D. L. Murray, J. G. Cook, P. Zager, and S. L. Monfort. 2001. Nutritional influences on breeding dynamics in elk. Canadian Journal of Zoology 79:845–853.

Cook, R. C., L. A. Shipley, J. G. Cook, M. J. Camp, D. S. Monzingo, S. L. Robatcek, S. L. Berry, I. T. Hull, W. L. Myers, K. Denryter, et al. 2022. Sequential detergent fiber assay results used for nutritional ecology research: evidence of bias since 2012. Wildlife Society Bulletin 46:1–26.

Committee on the Status of Endangered Wildlife in Canada. 2014. COSEWIC assessment and status report on the caribou *Rangifer tarandus*, Newfoundland population, Atlantic-Gaspésie population and Boreal population, in Canada. Committee on the Status of Endangered Wildlife in Canada, Ottawa, Canada.

Courbin, N., D. Fortin, C. Dussault, V. Fargeot, and R. Courtois. 2013. Multi-trophic resource selection function enlightens the behavioural game between wolves and their prey. Journal of Animal Ecology 82:1062–1071.

Courtois, R., J. Ouellet, L. Breton, A. Gingras, and C. Dussault. 2007. Effects of forest disturbance on density, space use, and mortality of woodland caribou. Ecoscience 14:491–498.

Cox, D. R. 1972. Regression models and life-tables. Journal of the Royal Statistical Society: Series B (Methodological) 34:187–220.

Crête, M., and J. Huot. 1993. Regulation of a large herd of migratory caribou: summer nutrition affects calf growth and body reserves of dams. Canadian Journal of Zoology 71:2291–2296.

Crête, M., J. Huot, R. Nault, and R. Patenaude. 1993. Reproduction, growth and body composition of Rivière George caribou in captivity. Arctic 46:189–196.

Cyr, D., S. Gauthier, Y. Bergeron, and C. Carcaillet. 2009. Forest management is driving the eastern North American boreal forest outside its natural range of variability. Frontiers in Ecology and the Environment 7:519–524.

Daly, M., M. Wilson, P. R. Behrends, and L. F. Jacobs. 1990. Characteristics of kangaroo rats, *Dipodomys merriami*, associated with differential predation risk. Animal Behaviour 40:380–389.

Dardaillon, M. 1986. Seasonal variations in habitat selection and spatial distribution of wild boar (*Sus Scrofa*) in the Camargue, southern France. Behavioural Processes 13:251–268.

Dauphiné, T. C. 1976. Biology of the Kaminuriak population of barren-ground caribou. Part 4: growth, reproduction, and energy reserves. Canadian Wildlife Service Report Series 38, Ottawa, Canada.

de Knegt, H. J., G. M. Hengeveld, F. Van Langevelde, W. F. De Boer, and K. P. Kirkman. 2007. Patch density determines movement patterns and foraging efficiency of large herbivores. Behavioral Ecology 18:1065–1072.

DeCesare, N. J., M. Hebblewhite, M. Bradley, K. G. Smith, D. Hervieux, and L. Neufeld. 2012. Estimating ungulate recruitment and growth rates using age ratios. Journal of Wildlife Management 76:144–153.

DeMars, C. A., M. Auger-Méthé, U. E. Schlägel, and S. Boutin. 2013. Inferring parturition and neonate survival from movement patterns of female ungulates: a case study using woodland caribou. Ecology and Evolution 3:4149–4160.

DeMars, C. A., and S. Boutin. 2018. Nowhere to hide: effects of linear features on predator–prey dynamics in a large mammal system. Journal of Animal Ecology 87:274–284.

DeMars, C. A., R. Serrouya, M. A. Mumma, M. P. Gillingham, R. S. McNay, and S. Boutin. 2019. Moose, caribou, and fire: have we got it right yet? Canadian Journal of Zoology 97:866–879.

Denoël, M., S. Dalleur, E. Langrand, A. Besnard, and H. Cayuela. 2017. Dispersal and alternative breeding site fidelity strategies in an amphibian. Ecography 41:1543–1555.

Denryter, K. A. 2017. Foraging ecolgoy of woodland caribou in boreal and montane ecosytems of northeastern British Columbia. University of Northern British Columbia, Prince George, Canada.

Denryter, K. A., R. C. Cook, J. G. Cook, and K. L. Parker. 2017. Straight from the caribou's (*Rangifer tarandus*) mouth: detailed observations of tame caribou reveal new insights into summer–autumn diets. Canadian Journal of Zoology 95:81–94.

Denryter, K., M. M. Conner, T. R. Stephenson, D. W. German, and K. L. Monteith. 2022*a*. Survival of the fattest: how body fat and migration influence survival in highly seasonal environments. Functional Ecology 36:2569–2579.

Denryter, K., R. C. Cook, J. G. Cook, and K. L. Parker. 2022*b*. Animal-defined resources reveal nutritional inadequacies for woodland caribou during summer–autumn. Journal of Wildlife Management 86:1–32.

Denryter, K., R. C. Cook, J. G. Cook, K. L. Parker, and M. P. Gillingham. 2020. State-dependent foraging by caribou with different nutritional requirements. Journal of Mammalogy 101:544–557.

DeYoung, R. W., E. C. Hellgren, T. E. Fulbright, W. F. Robbins, I. D. Humphreys, and P. R. Krausman. 2000. Modelling nutritional carrying capacity for translocated desert bighorn sheep in western Texas. Restoration Ecology 8:57–65.

Dickie, M., S. R. McNay, G. D. Sutherland, M. Cody, and T. Avgar. 2020. Corridors or risk? Movement along, and use of, linear features varies predictably among large mammal predator and prey species. Journal of Animal Ecology 89:623–634.

Dickie, M., R. Serrouya, R. S. McNay, and S. Boutin. 2017. Faster and farther: wolf movement on linear features and implications for hunting behaviour. Journal of Applied Ecology 54:253–263.

Ding, F., Y. Huang, W. Sun, G. Jiang, and Y. Chen. 2014. Decomposition of organic carbon in fine soil particles is likely more sensitive to warming than in coarse particles: an incubation study with temperate grassland and forest soils in northern China. PLoS ONE 9:e95348.

Drent, R. H., B. S. Ebbinge, and B. Weijand. 1978. Balancing the energy budgets of Arctic breeding geese throughout the annual cycle: a progress report. Verhandlungen der Ornithologischen Gesellschaft in Bayern 23:239–264.

Dunn, O. J. 1961. Multiple comparisons among means. Journal of the American Statistical Association 56:54–64.

Duparc, A., M. Garel, P. Marchand, D. Dubray, D. Maillard, and A. Loison. 2020. Through the taste buds of a large herbivore: foodscape modeling contributes to an understanding of forage selection processes. Oikos 129:170–183.

Dussault, C., J. Ouellet, R. Courtois, J. Huot, L. Breton, and H. Jolicoeur. 2005. Linking moose habitat selection to limiting factors. Ecography 28:619–628.

Dussault, C., J. P. Oullet, R. Courtois, J. Huot, L. Breton, and J. Larochelle. 2004. Behavioural responses of moose to thermal conditions in the boreal forest. Ecoscience 11:321–328.

Dussault, C., V. Pinard, J. P. Ouellet, R. Courtois, and D. Fortin. 2012. Avoidance of roads and selection for recent cutovers by threatened caribou: fitness rewarding or maladaptive behaviour? Proceedings of the Royal Society B: Biological Sciences 279:4481–4488.

Dzialak, M. R., S. M. Harju, R. G. Osborn, J. J. Wondzell, L. D. Hayden-Wing, J. B. Winstead, and S. L. Webb. 2011. Prioritizing conservation of ungulate calving resources in multiple-use landscapes. PLoS ONE 6:e14597.

Eloranta, E., and M. Nieminen. 1986. Calving of the experimental reindeer herd in Kaamanen during 1970–85. Rangifer 6:115–121.

Emlen, J. M. 1966. The role of time and energy in food preference. American Naturalist 100:611–617.

Evans, D. R., R. R. Carthy, and S. A. Ceriani. 2019. Migration routes, foraging behavior, and site fidelity of loggerhead sea turtles (*Caretta caretta*) satellite tracked from a globally important rookery. Marine Biology 166:1–19.

Fagan, W. F., M. A. Lewis, M. Auger-Méthé, T. Avgar, S. Benhamou, G. Breed, L. Ladage, U. E. Schlägel, W. W. Tang, Y. P. Papastamatiou, et al. 2013. Spatial memory and animal movement. Ecology Letters 16:1316–1329.

Faille, G., C. Dussault, J. P. Ouellet, D. Fortin, R. Courtois, M. H. St-Laurent, and Claude Dussault. 2010. Range fidelity: the missing link between caribou decline and habitat alteration? Biological Conservation 143:2840–2850.

Falldorf, T., O. Strand, M. Panzacchi, and H. Tømmervik. 2014. Estimating lichen volume and reindeer winter pasture quality from Landsat imagery. Remote Sensing of Environment 140:573–579.

Fenton, N., N. Lecomte, S. Légaré, and Y. Bergeron. 2005. Paludification in black spruce (*Picea mariana*) forests of eastern Canada: potential factors and management implications. Forest Ecology and Management 213:151–159.

Ferguson, S. H., and P. C. Elkie. 2004. Seasonal movement patterns of woodland caribou (*Rangifer tarandus caribou*). Journal of Zoology 262:125–134.

Festa-Bianchet, M., J. C. Ray, S. Boutin, S. D. Côté, and A. Gunn. 2011. Conservation of caribou (*Rangifer tarandus*) in Canada: an uncertain future. Canadian Journal of Zoology 89:419–434.

Fortin, D., H. L. Beyer, M. S. Boyce, D. W. Smith, T. Duchesne, and J. S. Mao. 2005. Wolves influence elk movements: behavior shapes a trophic cascade in Yellowstone National Park. Ecology 86:1320–1330.

Fowler, C. W. 1987. A review of density dependence in populations of large mammals. Pages 401–441 in Current mammalogy. Springer, New York, USA.

Frair, J. L., J. Fieberg, M. Hebblewhite, F. Cagnacci, N. J. DeCesare, and L. Pedrotti. 2010. Resolving issues of imprecise and habitat-biased locations in ecological analyses using GPS telemetry data. Philosophical Transactions of the Royal Society B: Biological Sciences 365:2187–2200.

Frair, J. L., E. H. Merrill, D. R. Visscher, D. Fortin, H. L. Beyer, and J. M. Morales. 2005. Scales of movement by elk (*Cervus elaphus*) in response to heterogeneity in forage resources and predation risk. Landscape Ecology 20:273–287.

Fretwell, S. D. 1972. Populations in a seasonal environment. Princeton University Press, New Jersey, USA.

Fretwell, S. D., and H. L. Lucas Jr. 1970. On territorial behavior and other factors influencing habitat distribution in birds. 1. Theoretical development. Acta Biotheoretica 19:16–36.

Fryxell, J. M. 1991. Forage quality and aggregation by large herbivores. American Naturalist 138:478–498.

Fryxell, J. M., T. Avgar, B. Liu, J. A. Baker, A. R. Rodgers, J. Shuter, I. D. Thompson, D. E. B. Reid, A. M. Kittle, A. Mosser, et al. 2020. Anthropogenic disturbance and population viability of woodland caribou in Ontario. Journal of Wildlife Management 84:636–650.

Fryxell, J. M., J. F. Wilmshurst, and A. R. E. Sinclair. 2004. Predictive models of movement by Serengeti grazers. Ecology 85:2429–2435.

Fryxell, J. M., J. F. Wilmshurst, A. R. E. Sinclair, D. T. Haydon, R. D. Holt, and P. A. Abrams. 2005. Landscape scale, heterogeneity, and the viability of Serengeti grazers. Ecology Letters 8:328–335.

Gaillard, J. M., M. Festa-Bianchet, and N. G. Yoccoz. 1998. Population dynamics of large herbivores: variable recruitment with constant adult survival. Trends in Ecology and Evolution 13:58–63.

Gaillard, J. M., M. Festa-Bianchet, N. G. Yoccoz, A. Loison, and C. Toïgo. 2000. Temporal variation in fitness components and population dynamics of large herbivores. Annual Review of Ecology and Systematics 31:367–393.

Gaillard, J. M., M. Hebblewhite, A. Loison, M. Fuller, R. Powell, M. Basille, and B. Van Moorter. 2010. Habitat-performance relationships: finding the right metric at a given spatial scale. Philosophical Transactions of the Royal Society B: Biological Sciences 365:2255–2265.

Gaillard, J. M., and N. G. Yoccoz. 2003. Temporal variation in survival of mammals: a case of environmental canalization? Ecology 84:3294–3306.

Garfelt-Paulsen, I. M., E. M. Soininen, V. Ravolainen, L. E. Loe, B. B. Hansen, R. J. Irvine, A. Stien, E. Ropstad, V. Veiberg, E. Fuglei, et al. 2021. Don't go chasing the ghosts of the past: habitat selection and site fidelity during calving in an Arctic ungulate. Wildlife Biology 2021:1–13.

Garnick, S., P. S. Barboza, and J. W. Walker. 2018. Assessment of animal-based methods used for estimating and monitoring rangeland herbivore diet composition. Rangeland Ecology and Management 71:449–457.

Gavin, T. A., and E. K. Bollinger. 1988. Reproductive correlates of breeding-site fidelity in bobolinks (*Dolichonyx oryzivorus*). Ecology 69:96–103.

Geary, A. B., E. H. Merrill, J. G. Cook, R. C. Cook, and L. L. Irwin. 2017. Elk nutritional resources: herbicides, herbivory and forest succession at Mount St. Helens. Forest Ecology and Management 401:242–254.

Gehr, B., N. C. Bonnot, M. Heurich, F. Cagnacci, S. Ciuti, A. J. M. Hewison, J. M. Gaillard, N. Ranc, J. Premier, K. Vogt, et al. 2020. Stay home, stay safe–site familiarity reduces predation risk in a large herbivore in two contrasting study sites. Journal of Animal Ecology 89:1329–1339.

Gerber, B. D., M. B. Hooten, C. P. Peck, M. B. Rice, J. H. Gammonley, A. D. Apa, and A. J. Davis. 2019. Extreme site fidelity as an optimal strategy in an unpredictable and homogeneous environment. Functional Ecology 33:1695–1707.

Gerhart, K. L., D. E. Russell, D. Van DeWetering, R. G. White, and R. D. Cameron. 1997. Pregnancy of adult caribou (*Rangifer tarandus*): evidence for lactational infertility. Journal of Zoology 242:17–30.

Gillies, C. S., M. Hebblewhite, S. E. Nielsen, M. A. Krawchuk, C. L. Aldridge, J. L. Frair, D. J. Saher, C. E. Stevens, and C. L. Jerde. 2006. Application of random effects to the study of resource selection by animals. Journal of Animal Ecology 75:887–898.

Gillingham, M., and K. Parker. 2008. The importance of individual variation in defining habitat selection by moose in northern British Columbia. Alces 44:7–20.

Government of Canada. 2019. *Species at Risk Act*. S. C. 2002, c. 9. Government of Canada, Ottawa, Canada.

Government of Ontario. 2007. *Endangered Species Act*. S.O., 2007, Chapter 6. Government of Ontario, Toronto, Canada.

Greenwood, P. J. 1980. Mating systems, philopatry and dispersal in birds and mammals. Animal Behaviour 28:1140–1162.

Gross, J. E., N. T. Hobbs, and B. A. Wunder. 1993. Independent variables for predicting intake rate of mammalian herbivores: biomass density, plant density, or bite size. Oikos 68:75–81.

Gunn, A., and F. L. Miller. 1986. Traditional behaviour and fidelity to caribou calving grounds by barren-ground caribou. Rangifer 6:151–158.

Gustine, D. D., K. L. Parker, R. J. Lay, P. Michael, and D. C. Heard. 2006. Calf survival of woodland caribou in a multi-predator ecosystem. Wildlife Monographs 165:1–32.

Gurevitch, J., S. M. Scheiner, and G. A. Fox. 2002. The ecology of plants. Sinauer Associates, Sunderland, USA.

Hamarashid, N. H., M. A. Othman, and M.-A. H. Hussain. 2010. Effects of soil texture on chemical compositions, microbial, populations and carbon mineralization in soil. Egyptian Journal of Experimental Biology 6:59–64.

Hamel, S., and S. D. Côté. 2007. Habitat use patterns in relation to escape terrain: are alpine ungulate females trading off better foraging sites for safety? Canadian Journal of Zoology 85:933–943.

Hanley, T. A., C. T. Robbins, A. E. Hagerman, and C. McArthur. 1992. Predicting digestible protein and digestible dry matter in tannin-containing forages consumed by ruminants. Ecology 73:537–541.

Hanley, T. A., D. E. Spalinger, K. J. Mock, O. L. Weaver, and G. M. Harris. 2012. Forage resource evaluation system for habitat—deer: an interactive deer habitat model. General Technical Report PNS-GTR, U.S. Department of Agriculture Forest Service, Pacific Northwest Research Station, Portland, USA.

Harvey, P. H., M. J. Stenning, and B. Campbell. 1984. Individual variation in seasonal breeding success of pied flycatchers (*Ficedula hypoleuca*). Journal of Animal Ecology 54:391–398.

Heard, D. C., and K. L. Zimmerman. 2021. Fall supplemental feeding increases population growth rate of an endangered caribou herd. PeerJ 9:1–25.

Hebblewhite, M., and E. H. Merrill. 2009. Trade-offs between predation risk and forage differ between migrant strategies in a migratory ungulate. Ecology 90:3445–3454.

Hebblewhite, M., E. Merrill, and G. McDermid. 2008. A multi-scale test of the forage maturation hypothesis in a partially migratory ungulate population. Ecological Monographs 78:141–166.

Hengl, T., J. M. De Jesus, G. B. M. Heuvelink, M. R. Gonzalez, M. Kilibarda, A. Blagotić, W. Shangguan, M. N. Wright, X. Geng, B. Bauer-Marschallinger, et al. 2017. SoilGrids250m: global gridded soil information based on machine learning. PLoS ONE. 12:e0169748.

Hermosilla, T., M. A. Wulder, J. C. White, N. C. Coops, and G. W. Hobart. 2018. Disturbance-informed annual land cover classification maps of Canada's forested ecosystems for a 29-year Landsat time series. Canadian Journal of Remote Sensing 44:67–87.

Hertel, A. G., P. T. Niemelä, N. J. Dingemanse, and T. Mueller. 2020. A guide for studying among-individual behavioral variation from movement data in the wild. Movement Ecology 8:1–18.

Hertel, A. G., M. Leclerc, D. Warren, F. Pelletier, A. Zedrosser, and T. Mueller. 2019. Don't poke the bear: using tracking data to quantify behavioural syndromes in elusive wildlife. Animal Behaviour 147:91–104.

Hertel, A. G., R. Royauté, A. Zedrosser, and T. Mueller. 2021. Biologging reveals individual variation in behavioural predictability in the wild. Journal of Animal Ecology 90:723–737.

Hervieux, D., M. Hebblewhite, N. J. DeCesare, M. Russell, K. Smith, S. Robertson, and S. Boutin. 2013. Widespread declines in woodland caribou (*Rangifer tarandus caribou*) continue in Alberta. Canadian Journal of Zoology 91:872–882.

Hjeljord, O., and T. Histøl. 1999. Range-body mass interactions of a northern ungulate—a test of hypothesis. Oecologia 119:326–339.

Hobbs, N. T., and I. J. Gordon. 2010. How does landscape heterogeneity shape dynamics of large herbivore populations. Pages 141–164 in Dynamics of large herbivore populations in changing environments: towards appropriate models. Wiley-Blackwell, New Jersey, USA.

Hobbs, N. T., and D. M. Swift. 1985. Estimates of habitat carrying capacity incorporating explicit nutritional constraints. Journal of Wildlife Management 49:814–822.

Hobbs, N. T., and R. A. Spowart. 1984. Effects of prescribed fire on nutrition of mountain sheep and mule deer during winter and spring. Journal of Wildlife Management 48:551–560.

Holechek, J. L., B. Gross, S. M. Dado, and T. Stephenson. 1982. Effects of sample preparation, growth stage, and observer on microhistological analysis of herbivore diets. Journal of Wildlife Management 46:502–505.

Holechek, J. L., and M. Vavra. 1981. The effect of slide and frequency observation numbers on the precision of microhistological analysis. Journal of Range Management 34:337–338.

Hoover, J. P. 2003. Decision rules for site fidelity in a migratory bird, the prothonotary warbler. Ecology 84:416–430.

Hornseth, R. S., and M. L. Rempel. 2015. Seasonal resource selection of woodland caribou (*Rangifer tarandus caribou*) across a gradient of anthropogenic disturbance. Canadian Journal of Zoology 94:79–93.

Howe, E. J., M. E. Obbard, and C. J. Kyle. 2013. Combining data from 43 standardized surveys to estimate densities of female American black bears by spatially explicit capture-recapture. Population Ecology 55:595–607.

Huete, A., K. Didan, T. Miura, E. P. Rodriguez, X. Gao, and L. G. Ferreira. 2002. Overview of the radiometric and biophysical performance of the MODIS vegetation indices. Remote Sensing of Environment 83:195–213.

Hull, I. T., L. A. Shipley, S. L. Berry, C. Loggers, and T. R. Johnson. 2020. Effects of fuel reduction timber harvests on forage resources for deer in northeastern Washington. Forest Ecology and Management 458:e117757.

Hurley, M. A., M. Hebblewhite, J. M. Gaillard, S. Dray, K. A. Taylor, W. K. Smith, P. Zager, and C. Bonenfant. 2014. Functional analysis of normalized difference vegetation index curves reveals overwinter mule deer survival is driven by both spring and autumn phenology. Philosophical Transactions of the Royal Society B: Biological Sciences 369:e 20130196.

Illius, A. W., and T. G. O'Connor. 2000. Resource heterogeneity and ungulate population dynamics. Oikos 89:283–294.

Ivlev, V.S. 1961. Experimental ecology of the feeding of fishes. Yale University Press, New Haven, USA.

James, A. R. C., S. Boutin, D. M. Hebert, and A. B. Rippin. 2004. Spatial separation of caribou from moose and its relation to predation by wolves. Journal of Wildlife Management 68:799–809.

James, A. R. C., and A. K. Stuart-Smith. 2000. Distribution of caribou and wolves in relation to linear corridors. Journal of Wildlife Management 64:154–159.

Jędrzejewski, W., K. Schmidt, J. Theuerkauf, B. Jedrzejewska, and H. Okarma. 2001. Daily movements and territory use by radio-collared wolves (*Canis lupus*) in Bialowieza Primeval Forest in Poland. Canadian Journal of Zoology 79:1993–2004.

Johnson, B. K., D. H. Jackson, R. C. Cook, D. A. Clark, P. K. Coe, J. G. Cook, S. N. Rearden, S. L. Findholt, and J. H. Noyes. 2019. Roles of maternal condition and predation in survival of juvenile elk in Oregon. Wildlife Monographs 201:1–61.

Johnson, C. A., G. D. Sutherland, E. Neave, M. Leblond, P. Kirby, C. Superbie, and P. D. McLoughlin. 2020. Science to inform policy: linking population dynamics to habitat for a threatened species in Canada. Journal of Applied Ecology 57:1314–1327.

Johnson, C. J., K. L. Parker, and D. C. Heard. 2000. Feeding site selection by woodland caribou in north-central British Columbia. Rangifer 20:158–172.

Johnson, C. J., K. L. Parker, D. C. Heard, and M. P. Gillingham. 2002. A multiscale behavioral approach to understanding the movements of woodland caribou. Ecological Applications 12:1840–1860.

Johnson, D. H. 1980. The comparison of usage and availability measurements for evaluating resource preference. Ecology 61:65–71.

Johnson, E. A. 1981. Vegetation organization and dynamics of lichen woodland communities in the Northwest Territories, Canada. Ecology 62:200–215.

Johnson, H. E., T. S. Golden, L. G. Adams, D. D. Gustine, E. A. Lenart, and P. S. Barboza. 2021. Dynamic selection for forage quality and quantity in response to phenology and insects in an Arctic ungulate. Ecology and Evolution 11:11664–11688.

Johnson, H. E., D. D. Gustine, T. S. Golden, L. G. Adams, L. S. Parrett, E. A. Lenart, and P. S. Barboza. 2018. NDVI exhibits mixed success in predicting spatiotemporal variation in caribou summer forage quality and quantity. Ecosphere 9:e02461.

Johnson, H. E., L. S. Mills, T. R. Stephenson, and J. D. Wehausen. 2010. Population-specific vital rate contributions influence management of an endangered ungulate. Ecological Applications 20:1753–1765.

Joly, K., M. S. Sorum, T. Craig, and E. L. Julianus. 2017. The effects of sex, terrain, wildfire, winter severity, and maternal status on habitat selection by moose in north-central Alaska. Alces 52:101–115.

Jönsson, K. I. 1997. Capital and income breeding as alternative tactics of resource use in reproduction. Oikos 78:57–66.

Kadmon, R., and O. Allouche. 2007. Integrating the effects of area, isolation, and habitat heterogeneity on species diversity: a unification of island biogeography and niche theory. American Naturalist 170:443–454.

Keech, M. A., R. T. Bowyer, J. M. Ver Hoef, R. D. Boertje, W. Dale, and T. R. Stephenson. 2000. Life-history consequences of maternal condition in Alaskan moose. Journal of Wildlife Management 64:450–462.

Keim, J. L., P. D. DeWitt, J. J. Fitzpatrick, and N. S. Jenni. 2017. Estimating plant abundance using inflated beta distributions: applied learnings from a lichen–caribou ecosystem. Ecology and Evolution 7:486–493.

Kelsey, K. C., S. H. Pedersen, A. J. Leffler, J. O. Sexton, M. Feng, and J. M. Welker. 2021. Winter snow and spring temperature have differential effects on vegetation phenology and productivity across Arctic plant communities. Global Change Biology 27:1572–1586.

Kennedy, M., and R. D. Gray. 1993. Can ecological theory predict the distribution of foraging animals? A critical analysis of experiments on the ideal free distribution. Oikos 68:158–166.

Kittle, A. M., M. Anderson, T. Avgar, J. A. Baker, G. S. Brown, J. Hagens, E. Iwachewski, S. Moffatt, A. Mosser, B. R. Patterson et al. 2017. Landscape-level wolf space use is correlated with prey abundance, ease of mobility, and the distribution of prey habitat. Ecosphere 8:e01783.

Kittle, A. M., M. Anderson, T. Avgar, J. A. Baker, G. S. Brown, J. Hagens, E. Iwachewski, S. Moffatt, A. Mosser, B. R. Patterson et al. 2015. Wolves adapt territory size, not pack size to local habitat quality. Journal of Animal Ecology 84:1177–1186.

Klein, D. R. 1982. Fire, lichens, and caribou. Journal of Range Management 35:390–395.

Klein, D. R. 1990. Variation in quality of caribou and reindeer forage plants associated with season, plant part, and phenology. Rangifer 10:123–130.

Kohlmann, S. G., and K. L. Risenhoover. 1997. White-tailed deer in a patchy environment: a test of the ideal-free-distribution theory. Journal of Mammalogy 78:1261–1272.

Krausman, P. R., B. D. Leopold, R. F. Seegmiller, and S. G. Torres. 1989. Relationship between desert bighorn sheep and habitat in western Arizona. Wildlife Monographs 102:3–66.

Kuck, L., G. L. Hompland, and E. H. Merrill. 1985. Elk calf response to simulated mine disturbance in southeast Idaho. Journal of Wildlife Management 49:751–757.

Lafontaine, A., P. Drapeau, D. Fortin, and M. H. St-Laurent. 2017. Many places called home: the adaptive value of seasonal adjustments in range fidelity. Journal of Animal Ecology 86:624–633.

Langvatn, R., S. D. Albon, T. Burkey, and T. H. Clutton-Brock. 1996. Climate, plant phenology and variation in age of first reproduction in a temperate herbivore. Journal of Animal Ecology 65:653–670.

Langvatn, R., A. Mysterud, N. C. Stenseth, and N. G. Yoccoz. 2004. Timing and synchrony of ovulation in red deer constrained by short northern summers. American Naturalist 163:763–772.

Lantin, É., P. Drapeau, M. Paré, and Y. Bergeron. 2003. Preliminary assessment of habitat characteristics of woodland caribou calving areas in the Claybelt region of Québec and Ontario, Canada. Rangifer 23:247–254.

Latham, A. D. M., M. C. Latham, and M. S. Boyce. 2011. Habitat selection and spatial relationships of black bears (*Ursus americanus*) with woodland caribou (*Rangifer tarandus caribou*) in northeastern Alberta. Canadian Journal of Zoology 89:267–277.

Latifovic, R., D. Pouliot, and I. Olthof. 2017. Circa 2010 land cover of Canada: local optimization methodology and product development. Remote Sensing 9:1–18.

Latombe, G., D. Fortin, and L. Parrott. 2014. Spatio-temporal dynamics in the response of woodland caribou and moose to the passage of grey wolf. Journal of Animal Ecology 83:185–198.

Launchbaugh, K. L., F. D. Provenza, and E. A. Burritt. 1993. How herbivores track variable environments: response to variability of phytotoxins. Journal of Chemical Ecology 19:1047–1056.

Leblond, M., C. Dussault, J. P. Ouellet, and M. H. St-Laurent. 2016. Caribou avoiding wolves face increased predation by bears—caught between scylla and charybdis. Journal of Applied Ecology 53:1078–1087.

Leclerc, M., C. Dussault, and M. H. St-Laurent. 2012. Multiscale assessment of the impacts of roads and cutovers on calving site selection in woodland caribou. Forest Ecology and Management 286:59–65.

Leclerc, M., C. Dussault, and M. H. St-Laurent. 2014. Behavioural strategies towards human disturbances explain individual performance in woodland caribou. Oecologia 176:297–306.

Leclerc, M., E. Vander Wal, A. Zedrosser, J. E. Swenson, J. Kindberg, and F. Pelletier. 2016. Quantifying consistent individual differences in habitat selection. Oecologia 180:697–705.

Legault, G., and M. Cusa. 2015. Temperature and delayed snowmelt jointly affect the vegetative and reproductive phenologies of four sub-Arctic plants. Polar Biology 38:1701–1711.

Li, C. 2000. Fire regimes and their simulation with reference to Ontario. Pages 115–140 in Ecology of a managed terrestrial landscape: patterns and processes of forest landscapes in Ontario. UBC Press, Vancouver, Canada.

Lima, S. L., and L. M. Dill. 1990. Behavioral decisions made under the risk of predation: a review and prospectus. Canadian Journal of Zoology 68:619–640.

Linnell, J. D., R. Aanes, and R. Andersen. 1995. Who killed Bambi? The role of predation in the neonatal mortality of temperate ungulates. Wildlife Biology 1:209–223.

Long, R. A., J. G. Kie, R. T. Bowyer, and M. A. Hurley. 2009. Resource selection and movements by female mule deer *Odocoileus hemionus*: effects of reproductive stage. Wildlife Biology 15:288–298.

Lord, R., and K. Kielland. 2015. Effects of variable fire severity on forage production and foraging behavior of moose in winter. Alces 51:23–34.

Losier, C. L., S. Couturier, M. H. St-Laurent, P. Drapeau, C. Dussault, T. Rudolph, V. Brodeur, J. A. Merkle, and D. Fortin. 2015. Adjustments in habitat selection to changing availability induce fitness costs for a threatened ungulate. Journal of Applied Ecology 52:496–504.

Luo, M., F. Meng, C. Sa, Y. Duan, Y. Bao, T. Liu, and P. De Maeyer. 2021. Response of vegetation phenology to soil moisture dynamics in the Mongolian Plateau. Catena 206:e105505.

Lurz, P. W. W., P. J. Garson, and L. A. Wauters. 1997. Effects of temporal and spatial variation in habitat quality on red squirrel dispersal behaviour. Animal Behaviour 54:427–435.

MacArthur, R. H., and E. R. Pianka. 1966. On optimal use of a patchy environment. American Naturalist 100:603–609.

MacAulay, K. M., E. G. Spilker, J. E. Berg, M. Hebblewhite, and E. H. Merrill. 2022. Beyond the encounter: predicting multi-predator risk to elk (*Cervus canadensis*) in summer using predator scats. Ecology and Evolution 12:1–15.

MacCracken, J. G., and L. A. Viereck. 1990. Browse regrowth and use by moose after fire in interior Alaska. Northwest Science 64:11–18.

Mahoney, S. P., H. Abbott, L. H. Russell, and B. R. Porter. 1990. Woodland caribou calf mortality in insular newfoundland. Transactions of International Union of Game Biologists Congress 19:592–599.

Mahoney, S. P., K. P. Lewis, J. N. Weir, S. F. Morrison, J. Glenn Luther, J. A. Schaefer, D. Pouliot, and R. Latifovic. 2016. Woodland caribou calf mortality in Newfoundland: insights into the role of climate, predation and population density over three decades of study. Population Ecology 58:91–103.

Mahoney, S. P., and J. A. Virgl. 2003. Habitat selection and demography of a nonmigratory woodland caribou population in Newfoundland. Canadian Journal of Zoology 81:321–334.

Mallon, E. E. 2014. Effects of disturbance and landscape position on vegetation structure and productivity in Ontario boreal forests: implications for woodland caribou (*Rangifer tarandus caribou*) forage. University of Guelph, Guelph, Canada.

Mallon, E. E., M. R. Turetsky, I. D. Thompson, J. M. Fryxell, and P. A. Wiebe. 2016. Effects of disturbance on understory succession in upland and lowland boreal forests and implications for woodland caribou (*Rangifer tarandus caribou*). Forest Ecology and Management 364:17–26.

Manly, B. F. J., L. L. McDonald, D. L. Thomas, T. L. McDonald, and W. P. Erickson. 2002. Resource selection by animals: statistical design and analysis for field studies. Second edition. Springer, New York, USA.

Martin, G. B., J. T. B. Milton, R. H. Davidson, G. E. Banchero Hunzicker, D. R. Lindsay, and D. Blache. 2004. Natural methods for increasing reproductive efficiency in small ruminants. Animal Reproduction Science 82–83:231–245.

Martin, H. W., M. Hebblewhite, and E. H. Merrill. 2022. Large herbivores in a partially migratory population search for the ideal free home. Ecology 103:1–14.

Martin, J. S., and M. M. Martin. 1983. Tannin assays in ecological studies. Precipitation of ribulose-1, 5-bisphosphate carboxylase/oxygenase by tannic acid, quebracho, and oak foliage extracts. Journal of Chemical Ecology 9:285–294.

Massé, A., and S. D. Côté. 2013. Spatiotemporal variations in resources affect activity and movement patterns of white-tailed deer (*Odocoileus virginianus*) at high density. Canadian Journal of Zoology 91:252–263.

Matasci, G., T. Hermosilla, M. A. Wulder, J. C. White, N. C. Coops, G. W. Hobart, D. K. Bolton, P. Tompalski, and C. W. Bater. 2018. Three decades of forest structural dynamics over Canada's forested ecosystems using Landsat time-series and lidar plots. Remote Sensing of Environment 216:697–714.

Mattson, W. J. 1980. Herbivory in relation to plant nitrogen content. Annual Review of Ecology and Systematics 11:119–161.

Mautz, W. W. 1978. Sledding on a bushy hillside: the fat cycle in deer. Wildlife Society Bulletin 6:88–90.

McGreer, M. T., E. E. Mallon, L. M. Vander Vennen, P. A. Wiebe, J. A. Baker, G. S. Brown, T. Avgar, J. Hagens, A. M. Kittle, A. Mosser, et al. 2015. Selection for forage and avoidance of risk by woodland caribou (*Rangifer tarandus caribou*) at coarse and local scales. Ecosphere 6:1–11.

McKenzie, H. W., E. H. Merrill, R. J. Spiteri, and M. A. Lewis. 2012. How linear features alter predator movement and the functional response. Interface Focus 2:205–216.

McLaren, A. A. D., and B. R. Patterson. 2021. There's no place like home–site fidelity by female moose (*Alces alces*) in central Ontario, Canada. Canadian Journal of Zoology 99:557–563.

McLoughlin, P. D., M. S. Boyce, T. Coulson, and T. Clutton-Brock. 2006. Lifetime reproductive success and density-dependent, multi-variable resource selection. Proceedings of the Royal Society B: Biological Sciences 273:1449–1454.

McLoughlin, P. D., J. S. Dunford, and S. Boutin. 2005. Relating predation mortality to broad-scale habitat selection. Journal of Animal Ecology 74:701–707.

McLoughlin, P. D., E. Dzus, B. Wynes, and S. Boutin. 2003. Declines in populations of woodland caribou. Journal of Wildlife Management 67:755–761.

McMullin, R. T., I. D. Thompson, and S. G. Newmaster. 2013. Lichen conservation in heavily managed boreal forests. Conservation Biology 27:1020–1030.

McNamara, J. M., and A. I. Houston. 1986. The common currency for behavioral decisions. American Naturalist 127:358–378.

McNamara, J. M., and A. I. Houston. 1987. Starvation and predation as factors limiting population size. Ecology 68:1515–1519.

McNamara, J. M., and A. I. Houston. 1990. State-dependent ideal free distributions. Evolutionary Ecology 4:298–311.

McNaughton, S. J. 1985. Ecology of a grazing ecosystem: the Serengeti. Ecological Monographs 55:259–294.

Mech, L. D., and L. Boitani. 2007. Wolves: behavior, ecology, and conservation. University of Chicago Press, Chicago, USA.

Merkle, J. A., B. Abrahms, J. B. Armstrong, H. Sawyer, D. P. Costa, and A. D. Chalfoun. 2022. Site fidelity as a maladaptive behavior in the anthropocene. Frontiers in Ecology and the Environment 20:187–194.

Merkle, J. A., K. L. Monteith, E. O. Aikens, M. M. Hayes, K. R. Hersey, A. D. Middleton, B. A. Oates, H. Sawyer, B. M. Scurlock, and M. J. Kauffman. 2016. Large herbivores surf waves of green-up during spring. Proceedings of the Royal Society B: Biological Sciences 283:1–8.

Merkle, J. A., H. Sawyer, K. L. Monteith, S. P. H. Dwinnell, G. L. Fralick, and M. J. Kauffman. 2019. Spatial memory shapes migration and its benefits: evidence from a large herbivore. Ecology Letters 22:1797–1805.

Merrill, E., J. Killeen, J. Pettit, M. Trottier, H. Martin, J. Berg, H. Bohm, S. Eggeman, and M. Hebblewhite. 2020. Density-dependent foraging behaviors on sympatric winter ranges in a partially migratory elk population. Frontiers in Ecology and Evolution 8:1–15.

Merrill, S. B., L. D. Mech, S. B. Merrill, and L. D. Mech. 2003. The usefulness of GPS telemetry to study wolf circadian and social activity. Wildlife Society Bulletin 31:947–960.

Middleton, A. D., J. A. Merkle, D. E. McWhirter, J. G. Cook, R. C. Cook, P. J. White, and M. J. Kauffman. 2018. Green-wave surfing increases fat gain in a migratory ungulate. Oikos 127:1060–1068.

Mitchell, W. A., and S. L. Lima. 2002. Predator-prey shell games: large-scale movement and its implications for decision-making by prey. Oikos 99:249–259.

Monzingo, D. S., L. A. Shipley, R. C. Cook, and J. G. Cook. 2022. Factors influencing predictions of understory vegetation biomass from visual cover estimates. Wildlife Society Bulletin 46:e1300.

Moody, A. L., A. I. Houston, and J. M. Mcnamara. 1996. Ideal free distributions under predation risk. Behavioural Ecology and Sociobiology 38:131–143.

Morrison, T. A., J. A. Merkle, J. G. C. Hopcraft, E. O. Aikens, J. L. Beck, R. B. Boone, A. B. Courtemanch, S. P. Dwinnell, W. S. Fairbanks, B. Griffith, et al. 2021. Drivers of site fidelity in ungulates. Journal of Animal Ecology 90:955–966.

Mörschel, F. M., and D. R. Klein. 1997. Effects of weather and parasitic insects on behavior and group dynamics of caribou of the Delta Herd, Alaska. Canadian Journal of Zoology 75:1659–1670.

Mosnier, A., J.-P. Ouellet, and R. Courtois. 2008. Black bear adaptation to low productivity in the boreal forest. Écoscience 15:485–497.

Muhly, T. B., C. A. Johnson, M. Hebblewhite, E. W. Neilson, D. Fortin, J. M. Fryxell, A. D. M. Latham, M. C. Latham, P. D. McLoughlin, E. Merrill, et al. 2019. Functional response of wolves to human development across boreal North America. Ecology and Evolution 9:10801–10815.

Nagy, J. A. S. 2011. Use of space by caribou in northern Canada. Dissertation, University of Alberta, Edmonton, Canada.

National Research Council. 2007. Nutrient requirements of small ruminants: sheep, goats, cervids, and new world camelids. The National Academies Press, Washington, D.C., USA.

Nelson, P. R., C. Roland, M. J. Macander, and B. McCune. 2013. Detecting continuous lichen abundance for mapping winter caribou forage at landscape spatial scales. Remote Sensing of Environment 137:43–54.

Newmaster, S. G., I. D. Thompson, R. A. D. Steeves, A. R. Rodgers, A. J. Fazekas, J. R. Maloles, R. T. McMullin, and J. M. Fryxell. 2013. Examination of two new technologies to assess the diet of woodland caribou: video recorders attached to collars and DNA barcoding. Canadian Journal of Forest Research 43:897–900.

Newton, E. J., B. R. Patterson, M. L. Anderson, A. R. Rodgers, L. M. Vander Vennen, and J. M. Fryxell. 2017. Compensatory selection for roads over natural linear features by wolves in northern Ontario: implications for caribou conservation. PLoS ONE 12:e0186525.

Nicholson, K. L., M. J. Warren, C. Rostan, J. Månsson, T. F. Paragi, and H. Sand. 2019. Using fine-scale movement patterns to infer ungulate parturition. Ecological indicators 101:22–30.

Nielsen, S. E., G. B. Stenhouse, and M. S. Boyce. 2006. A habitat-based framework for grizzly bear conservation in Alberta. Biological Conservation 130:217–229.

Nobert, B. R., S. Milligan, G. B. Stenhouse, and L. Finnegan. 2016. Seeking sanctuary: the neonatal calving period among central mountain woodland caribou (*Rangifer tarandus caribou*). Canadian Journal of Zoology 94:837–851.

Ontario Ministry of Natural Resources and Forestry [OMNRF]. 2014*a*. State of the woodland caribou resource report. Species at Risk Branch, Thunder Bay, Canada.

Ontario Ministry of Natural Resources and Forestry [OMNRF]. 2014*b*. Forest management guide for boreal landscapes. Forest Branch, Toronto, Canada.

Owen-Smith, N. 2004. Functional heterogeneity in resources within landscapes and herbivore population dynamics. Landscape Ecology 19:761–771.

Owen-Smith, N., J. M. Fryxell, and E. H. Merrill. 2010. Foraging theory upscaled: the behavioural ecology of herbivore movement. Philosophical Transactions of the Royal Society B: Biological Sciences 365:2267–2278.

Pachkowski, M., S. D. Côté, and M. Festa-Bianchet. 2013. Spring-loaded reproduction: effects of body condition and population size on fertility in migratory caribou (*Rangifer tarandus*). Canadian Journal of Zoology 91:473–479.

Parker, G. A. 1978. Searching for mates. Pages 214–244 *in* Behavioural Ecology: an Evolutionary Approach. Blackwell Scientific Publications, New Jersey, USA.

Parker, K. L., P. S. Barboza, and M. P. Gillingham. 2009. Nutrition integrates environmental responses of ungulates. Functional Ecology 23:57–69.

Parker, K. L., P. S. Barboza, and T. R. Stephenson. 2005. Protein conservation in female caribou (*Rangifer tarandus*): effects of decreasing diet quality during winter. Journal of Mammalogy 86:610–622.

Parker, K. L., M. P. Gillingham, T. A. Hanley, and C. T. Robbins. 1999. Energy and protein balance of free-ranging black-tailed deer in a natural forest environment. Wildlife Monographs 143:3–48.

Parker, K. L., C. T. Robbins, and T. A. Hanley. 1984. Energy expenditures for locomotion by mule deer and elk. Journal of Wildlife Management 48:474–488.

Parker, K. L., R. G. White, M. P. Gillingham, and D. F. Holleman. 1990. Comparison of energy metabolism in relation to daily activity and milk consumption by caribou and muskox neonates. Canadian Journal of Zoology 68:106–114.

Parveen, I., S. Gafner, N. Techen, S. J. Murch, and I. A. Khan. 2016. DNA barcoding for the identification of botanicals in herbal medicine and dietary supplements: strengths and limitations. Planta Medica 82:1225–1235.

Patterson, B. R., J. F. Benson, K. R. Middel, K. J. Mills, A. Silver, and M. E. Obbard. 2013. Moose calf mortality in central Ontario, Canada. Journal of Wildlife Management 77:832–841.

Payne, R. B., and L. L. Payne. 1993. Breeding dispersal in indigo buntings: circumstances and consequences for breeding success and population structure. The Condor 95:1–24.

Person, S. J., R. E. Pegau, R. G. White, and J. R. Luick. 1980. In vitro and nylon-bag digestibilities of reindeer and caribou forages. Journal of Wildlife Management 44:613–622.

Peterson, M. E., C. R. Anderson, Jr, M. W. Alldredge, and P. F. Doherty, Jr. 2018. Using maternal mule deer movements to estimate timing of parturition and assist fawn captures. Wildlife Society Bulletin 42:616–621.

Picardi, S., P. Coates, J. Kolar, S. O'Neil, S. Mathews, and D. Dahlgren. 2022. Behavioural state-dependent habitat selection and implications for animal translocations. Journal of Applied Ecology 59:624–635.

Pinard, V., C. Dussault, J. P. Ouellet, D. Fortin, and R. Courtois. 2012. Calving rate, calf survival rate, and habitat selection of forest-dwelling caribou in a highly managed landscape. Journal of Wildlife Management 76:189–199.

Poole, K. G., R. Serrouya, and K. Stuart-Smith. 2007. Moose calving strategies in interior montane ecosystems. Journal of Mammalogy 88:139–150.

Potvin, F., L. Breton, and R. Courtois. 2005. Response of beaver, moose, and snowshoe hare to clear-cutting in a Quebec boreal forest: a reassessment 10 years after cut. Canadian Journal of Forest Research 35:151–160.

Post, E., and M. C. Forchhammer. 2008. Climate change reduces reproductive success of an Arctic herbivore through trophic mismatch. Philosophical Transactions of the Royal Society B: Biological Sciences 363:2369–2375.

Post, E., C. Pedersen, C. C. Wilmers, and M. C. Forchhammer. 2008. Warming, plant phenology and the spatial dimension of trophic mismatch for large herbivores. Proceedings of the Royal Society B: Biological Sciences 275:2005–2013.

Post, E., and N. C. H. R. Stenseth. 1999. Climatic variability, plant phenology, and northern ungulates. Ecology 80:1322–1339.

Proffitt, K. M., M. Hebblewhite, W. Peters, N. Hupp, and J. Shamhart. 2016. Linking landscape-scale differences in forage to ungulate nutritional ecology. Ecological Applications 26:2156–2174.

Pyke, G. H. 1984. Optimal foraging theory: a critical review. Annual Review of Ecology and Systematics 15:523–575.

Pyle, P., W. J. Sydeman, and M. Hester. 2001. Effects of age, breeding experience, mate fidelity and site fidelity on breeding performance in a declining population of Cassin's auklets. Journal of Animal Ecology 70:1088–1097.

Racey, G. D., and T. Armstrong. 2000. Woodland caribou range occupancy in northwestern Ontario: past and present. Rangifer 20:173–184.

Racey, G. D., A. G. Harris, J. K. Jeglum, R. F. Foster, and G. M. Wickware. 1996. Terrestrial and wetland ecosites of northwestern Ontario. Ontario Ministry of Natural Resources, Thunder Bay, Canada.

Racey, G. D., A. G. Harris, L. Gerrish, T. R. Armstrong, J. McNicol, and J. Baker. 1999. Forest management guidelines for the conservation of woodland caribou: a landscape approach. Ontario Ministry of Natural Resources, Thunder Bay, Canada.

Rachlow, J. L., and R. Terry Bowyer. 1998. Habitat selection by Dall's sheep (*Ovis dalli*): maternal trade-offs. Journal of Zoology 245:457–465.

Raithel, J. D., M. J. Kauffman, and D. H. Pletscher. 2007. Impact of spatial and temporal variation in calf survival on the growth of elk. Journal of Wildlife Management 71:795–803.

Raponi, M., D. V. Beresford, J. A. Schaefer, I. D. Thompson, P. A. Wiebe, A. R. Rodgers, and J. M. Fryxell. 2018. Biting flies and activity of caribou in the boreal forest. Journal of Wildlife Management 84:833–839.

Rettie, W. J., and F. Messier. 1998. Dynamics of woodland caribou populations at the southern limit of their range in Saskatchewan. Canadian Journal of Zoology 76:251–259.

Rettie, W. J., and F. Messier. 2001. Range use and movement rates of woodland caribou in Saskatchewan. Canadian Journal of Zoology 79:1933–1940.

Rhind, S. M., Z. A. Archer, and C. L. Adam. 2002. Seasonality of food intake in ruminants: recent developments in understanding. Nutrition Research Reviews 15:43–65.

Ringberg, T., and A. Aakvaag. 1982. The diagnosis of early pregnancy and missed abortion in European and Svalbard reindeer (*Rangifer tarandus tarandus* and *Rangifer tarandus platyrhyncus*). Rangifer 2:26–30.

Robbins, C. T., T. A. Hanley, A. E. Hagerman, O. Hjeljord, D. L. Baker, C. C. Schwartz, and W. W. Mautz. 1987a. Role of tannins in defending plants against ruminants: reduction in protein availability. Ecology 68:98–107.

Robbins, C. T., S. Mole, A. E. Hagerman, and T. A. . Hanley. 1987b. Role of tannins in defending plants against ruminants: reduction in dry matter digestion? Ecology 68:1606–1615.

Robinson, B. G., and E. H. Merrill. 2013. Foraging-vigilance trade-offs in a partially migratory population: comparing migrants and residents on a sympatric range. Animal Behaviour 85:849–856.

Rodgers, A. R., N. E. Berglund, J. S. Hagens, K. D. Wade, B. A. Allison, and E. P. Iwachewski. 2009. Forest-dwelling woodland caribou in Ontario candidate study areas report. Ontario Ministry of Natural Resources and Forestry, Thunder Bay, Canada.

Roffe, T. J. 1993. Perinatal mortality in caribou from the Porcupine herd, Alaska. Journal of Wildlife Diseases 29:295–303.

Ropstad, E. 2000. Reproduction in female reindeer. Animal Reproduction Science 60–61:561–570.

Rowe, J. S. 1972. Forest regions of Canada. Department of the Environment, Canadian Forestry Service, Ottawa, Canada.

Rowell, J. E., and M. P. Shipka. 2009. Variation in gestation length among captive reindeer (*Rangifer tarandus tarandus*). Theriogenology 72:190–197.

Rowland, M. M., R. M. Nielson, M. J. Wisdom, P. K. Coe, J. G. Cook, J. M. Hafer, B. K. Johnson, B. J. Naylor, R. C. Cook, M. Vavra, et al. Linking nutrition with landscape features in a regional habitat-use model for elk in western Oregon and Washington. Pages 31–49 in M. W. Rowland, et al. Modeling elk nutrition and habitat use in western Oregon and Washington. Wildlife Monographs 199:1–69.

Ruppert, J., M.J. Fortin, E. Gunn, and D. Martell. 2016. Conserving woodland caribou habitat while maintaining timber yield: a graph theory approach. Canadian Journal of Forest Research 56:914–923.

Russell, D. E., A. M. Martell, and W. A. C. Nixon. 1993. Range ecology of the Porcupine caribou herd in Canada. Rangifer 13:1–168.

Sakuragi, M., H. Igota, H. Uno, K. Kaji, M. Kaneko, R. Akamatsu, and K. Maekawa. 2003. Seasonal habitat selection of an expanding sika deer *Cervus nippon* population in eastern Hokkaido, Japan. Wildlife Biology 9:141–153.

Schaefer, J. A. 2003. Long-term range recession and the persistence of caribou in the taiga. Conservation Biology 17:1435–1439.

Schaefer, J. A., C. M. Bergman, and S. N. Luttich. 2000. Site fidelity of female caribou at multiple spatial scales. Landscape Ecology 15:731–739.

Schaefer, J. A., and S. P. Mahoney. 2013. Spatial dynamics of the rise and fall of caribou (*Rangifer tarandus*) in Newfoundland. Canadian Journal of Zoology 91:767–774.

Schaefer, J. A., and W. O. Pruitt. 1991. Fire and woodland caribou in southeastern Manitoba. Wildlife Monographs 116:3–39.

Schwartz, C. C., and A. W. Franzmann. 1989. Bears, wolves, moose, and forest succession some managment considerdations on the Kenai Peninsula, Alaska. Alces 25:1–10.

Schwartz, C. C., and A. W. Franzmann. 1991. Interrelationship of black bear to moose and forest succession in the northern coniferous forest. Wildlife Monographs 113:3–58

Searle, K. R., N. T. Hobbs, and I. J. Gordon. 2007. It's the "foodscape", not the landscape: using foraging behavior to make functional assessments of landscape condition. Israel Journal of Ecology & Evolution 53:297–316.

Serrouya, R., M. Dickie, C. Lamb, H. Van Oort, A. P. Kelly, C. Demars, P. D. McLoughlin, N. C. Larter, D. Hervieux, A. T. Ford, et al. 2021. Trophic consequences of terrestrial eutrophication for a threatened ungulate. Proceedings of the Royal Society B: Biological Sciences 288:e20202811

Serrouya, R., D. R. Seip, D. Hervieux, B. N. McLellan, R. S. McNay, R. Steenweg, D. C. Heard, M. Hebblewhite, M. Gillingham, and S. Boutin. 2019. Saving endangered species using adaptive management. Proceedings of the National Academy of Sciences of the United States of America 116:6181–6186.

Severud, W. J., G. Del Giudice, T. R. Obermoller, T. A. Enright, R. G. Wright, and J. D. Forester. 2015. Using GPS collars to determine parturition and cause-specific mortality of moose calves. Wildlife Society Bulletin 39:616–625.

Seip, D. R. 1992. Factors limiting woodland caribou populations and their interrelationships with wolves and moose in southeastern Brisitsh Columbia. Canadian Journal of Zoology 70:1494–1503.

Seip, D. R., and D. B. Cichowski. 1996. Population ecology of caribou in British Columbia. Rangifer 9:73–80.

Shields, W. M. 1984. Factors affecting nest and site fidelity in Adirondack barn swallows (*Hirundo rustica*). The Auk 101:780–789.

Shipley, L. A., S. Blomquist, and K. Danell. 1998. Diet choices made by free-ranging moose in northern Sweden in relation to plant distribution, chemistry, and morphology. Canadian Journal of Zoology 76:1722–1733.

Shipley, L. A., J. S. Forbey, and B. D. Moore. 2009. Revisiting the dietary niche: when is a mammalian herbivore a specialist. Integrative and Comparative Biology 49:274–290.

Shipley, L. A., and D. E. Spalinger. 1992. Mechanics of browsing in dense food patches: effects of plant and animal morphology on intake rate. Canadian Journal of Zoology 70:1743–1752.

Signer, J., J. Fieberg, and T. Avgar. 2019. Animal movement tools (amt): R package for managing tracking data and conducting habitat selection analyses. Ecology and Evolution 9:880–890.

Sih, A. 1980. Optimal behavior: can foragers balance two conflicting demands. Science 210:1041–1043.

Silva, J. A., S. E. Nielsen, C. T. Lamb, C. Hague, and S. Boutin. 2019. Modelling lichen abundance for woodland caribou in a fire-driven boreal landscape. Forests 10:1–23.

Silva, J. A., S. E. Nielsen, P. D. McLoughlin, A. R. Rodgers, C. Hague, and S. Boutin. 2020. Comparison of pre-fire and post-fire space use reveals varied responses by woodland caribou (*Rangifer tarandus caribou*) in the boreal shield. Canadian Journal of Zoology 98:751–760.

Skogland, T. 1983. The effects of density dependent resource limitation on size of wild reindeer. Oecologia 60:156–168.

Spalinger, D. E., and N. T. Hobbs. 1992. Mechanisms of foraging in mammalian herbivores: new models of functional response. American Naturalist 140:325–348.

Spiegel, O., S. T. Leu, C. M. Bull, and A. Sih. 2017. What's your move? Movement as a link between personality and spatial dynamics in animal populations. Ecology Letters 20:3–18.

Stephenson, T. R., D. W. German, E. Frances Cassirer, D. P. Walsh, M. E. Blum, M. Cox, K. M. Stewart, and K. L. Monteith. 2020. Linking population performance to nutritional condition in an alpine ungulate. Journal of Mammalogy 101:1244–1256.

Street, G. M., L. M. Vander Vennen, T. Avgar, A. Mosser, M. L. Anderson, A. R. Rodgers, and J. M. Fryxell. 2015. Habitat selection following recent disturbance: model transferability with implications for management and conservation of moose (*Alces alces*). Canadian Journal of Zoology 93:813–821.

Stuart-Smith, A. K., C. J. A. Bradshaw, S. Boutin, D. M. Hebert, and A. B. Rippin. 1997. Woodland caribou relative to landscape patterns in northeastern Alberta. Journal of Wildlife Management 61:622–633.

Sutherland, W. J. 1983. Aggregation and the "ideal free" distribution. Journal of Animal Ecology 52:821–828.

Switzer, P. V. 1993. Site fidelity in predictable and non predicatble populations. Evolutionary Ecology 7:533–555.

Taillon, J., P. S. Barboza, and S. D. Côté. 2013. Nitrogen allocation to offspring and milk production in a capital breeder. Ecology 94:1815–1827.

Taylor, K. C. 2000. A field guide to forest ecosystems of northeastern Ontario. Second edition. Ontario Ministry of Natural Resources, Sudbury, Canada.

Teitelbaum, C. S., and T. Mueller. 2019. Beyond migration: causes and consequences of nomadic animal movements. Trends in Ecology and Evolution 34:569–581.

Testa, J. W., E. F. Becker, and G. R. Lee. 2000. Movements of female moose in relation to birth and death of calves. Alces 36:155–162.

Thomas, D. C., E. J. Edmonds, and W. K. Brown. 1996. The diet of woodland caribou populations in west-central Alberta. Rangifer 16:337–342.

Thompson, D. C., and K. H. McCourt. 1981. Seasonal diets of the Porcupine caribou herd. American Midland Naturalist 105:70–76.

Thompson, D. P., and P. S. Barboza. 2014. Nutritional implications of increased shrub cover for caribou (*Rangifer tarandus*) in the Arctic. Canadian Journal of Zoology 92:339–351.

Thompson, I. D. 2000. Forest vegetation of Ontario: factors influencing landscape change. Pages 30–53 in Ecology of a managed terrestrial landscape: patterns and processes of forest landscapes in Ontario. UBC Press, Vancouver, Canada.

Thompson, I. D. 1994. Marten populations in uncut and logged boreal forests in Ontario. Journal of Wildlife Management 58:272–280.

Thompson, I. D., J. A. Baker, and M. Ter-Mikaelian. 2003. A review of the long-term effects of post-harvest silviculture on vertebrate wildlife, and predictive models, with an emphasis on boreal forests in Ontario, Canada. Forest Ecology and Management 177:441–469.

Thompson, I. D., M. Bakhtiari, A. R. Rodgers, J. A. Baker, J. M. Fryxell, and E. Iwachewski. 2012. Application of a high-resolution animal-borne remote video camera with global positioning for wildlife study: observations on the secret lives of woodland caribou. Wildlife Society Bulletin 36:365–370.

Thompson, I. D., P. A. Wiebe, E. Mallon, A. R. Rodgers, J. M. Fryxell, J. A. Baker, and D. Reid. 2015. Factors influencing the seasonal diet selection by woodland caribou (*Rangifer tarandus tarandus*) in boreal forests in Ontario. Canadian Journal of Zoology 93:87–98.

Torbit, S. C., L. H. Carpenter, D. M. Swift, and W. A. Alldredge. 1985. Differential loss of fat and protein by mule deer during winter. Journal of Wildlife Management 49:80–85.

Torn, M. S., S. E. Trumbore, O. A. Chadwick, P. M. Vitousek, and D. M. Hendricks. 1997. Mineral control of soil organic carbon storage and turnover content were measured by horizon down to the depth at which. Nature 389:3601–3603.

Trudell, J., and R. G. White. 1981. The effect of forage structure and availability on food intake, biting rate, bite size and daily eating time of reindeer. Journal of Animal Ecology 18:63–81.

Ulappa, A. C., L. A. Shipley, R. C. Cook, J. G. Cook, and M. E. Swanson. 2020. Silvicultural herbicides and forest succession influence understory vegetation and nutritional ecology of black-tailed deer in managed forests. Forest Ecology and Management 470–471:e118216.

Van Soest, P. J. 1982. Nutritional ecology of the ruminant. O & B Books, Corvallis, USA.

Vergara, P., J. I. Aguirre, J. A. Fargallo, and J. A. Dávila. 2006. Nest-site fidelity and breeding success in white stork *Ciconia ciconia*. Ibis 148:672–677.

Verme, L. J., and J. J. Ozoga. 1980. Influence of protein-energy intake on deer fawns in autumn. Journal of Wildlife Management 44:305–314.

Viejou, R., T. Avgar, G. S. Brown, B. R. Patterson, D. E. B. Reid, A. R. Rodgers, J. Shuter, I. D. Thompson, and J. M. Fryxell. 2018. Woodland caribou habitat selection patterns in relation to predation risk and forage abundance depend on reproductive state. Ecology and Evolution 8:5863–5872.

Villamuelas, M., N. Fernández, E. Albanell, A. Gálvez-Cerón, J. Bartolomé, G. Mentaberre, J. R. López-Olvera, X. Fernández-Aguilar, A. Colom-Cadena, J. M. López-Martín, et al. 2016. The enhanced vegetation index (EVI) as a proxy for diet quality and composition in a mountain ungulate. Ecological Indicators 61:658–666.

Vors, L. S., and M. S. Boyce. 2009. Global declines of caribou and reindeer. Global Change Biology 15:2626–2633.

Vors, L. S., J. A. Schaefer, B. A. Pond, A. R. Rodgers, and B. R. Patterson. 2007. Woodland caribou extirpation and anthropogenic landscape disturbance in Ontario. Journal of Wildlife Management 71:1249–1256.

Walker, P. D., A. R. Rodgers, J. L. Shuter, I. D. Thompson, J. M. Fryxell, J. G. Cook, R. C. Cook, and E. H. Merrill. 2021. Comparison of woodland caribou calving areas determined by movement patterns across northern Ontario. Journal of Wildlife Management 85:169–182.

Wallmo, O. C., L. H. Carpenter, W. L. Regelin, R. B. Gill, and D. L. Baker. 1977. Evaluation of deer habitat on a nutritional basis. Journal of Range Management 30:122–127.

Wang, G., N. . T. Hobbs, R. B. Boone, A. W. Illius, I. J. Gordon, J. E. Gross, and K. L. Hamlin. 2006. Spatial and temporal variability modify density dependence in populations of large herbivores. Ecology 87:95–102.

Wang, G., N. T. Hobbs, S. Twombly, R. B. Boone, A. W. Illius, I. J. Gordon, and J. E. Gross. 2009. Density dependence in northern ungulates: interactions with predation and resources. Population Ecology 51:123–132.

Ward, P. C., and A. G. Tithecott. 1993. The impact of fire management on the boreal landscape of Ontario. Ontario Ministry of Natural Resources, Sault Ste. Marie, Canada.

Weisberg, P. J., N. Thompson Hobbs, J. E. Ellis, and M. B. Coughenour. 2002. An ecosystem approach to population management of ungulates. Journal of Environmental Management 65:181–197.

Weladji, R. B., Ø. Holand, and T. Almøy. 2006. Use of climatic data to assess the effect of insect harassment on the autumn weight of reindeer (*Rangifer tarandus*) calves. Journal of Zoology 260:79–85.

Welch, I. D., A. R. Rodgers, and R. S. McKinley. 2000. Timber harvest and calving site fidelity of moose in northwestern Ontario. Alces 36:93–103.

West, P. W. 2009. Tree and forest measurement. Third edition. Springer, New York, USA.

White, R. G. 1983. Foraging patterns and their multiplier effects on productivity of northern ungulates. Oikos 40:377–384.

White, R. G., and J. R. Luick. 1984. Plasticity and constraints in the lactational strategy of reindeer and caribou. Pages 215–232 in Symposia of the Zoological Society of London. Volume 51.

White, T. C. R. 1978. The importance of a relative shortage of food in animal ecology. Oecologia 33:71–86.

Whiting, J. C., D. D. Olson, J. M. Shannon, R. T. Bowyer, R. W. Klaver, and J. T. Flinders. 2012. Timing and synchrony of births in bighorn sheep: implications for reintroduction and conservation. Wildlife Research 39:565–572.

Whitten, K. R., G. W. Garner, F. J. Mauer, and R. B. Harris. 1992. Productivity and early calf survival in the Porcupine caribou herd. Journal of Wildlife Diseases 56:201–212.

Williams, G. C. 1966. Adaptation and natural selection: a critique of some current evolutionary thought. Volume 61. Princeton University Press, New Jersey, USA.

Willie, M., D. Esler, W. S. Boyd, T. Bowman, J. Schamber, and J. Thompson. 2020. Annual winter site fidelity of Barrow's goldeneyes in the Pacific. Journal of Wildlife Management 84:161–171.

Wilson, E. H., and S. A. Sader. 2002. Detection of forest harvest type using multiple dates of Landsat TM imagery. Remote Sensing of Environment 80:385–396.

Wipf, S., V. Stoeckli, and P. Bebi. 2009. Winter climate change in alpine tundra: plant responses to changes in snow depth and snowmelt timing. Climatic Change 94:105–121.

Wiseman, P. A., M. D. Carling, and J. A. Byers. 2006. Frequency and correlates of birth-site fidelity in pronghorns (*Antilocapra americana*). Journal of Mammalogy 87:312–317.

Wittmer, H. U., B. N. McLellan, and F. W. Hovey. 2006. Factors influencing variation in site fidelity of woodland caribou (*Rangifer tarandus caribou*) in southeastern British Columbia. Canadian Journal of Zoology 84:537–545.

Wittmer, H. U., B. N. McLellan, D. R. Seip, J. A. Young, T. A. Kinley, G. S. Watts, and D. Hamilton. 2005. Population dynamics of the endangered mountain ecotype of woodland caribou (*Rangifer tarandus caribou*) in British Columbia, Canada. Canadian Journal of Zoology 83:407–418.

Wittmer, H. U., B. N. McLellan, R. Serrouya, and C. D. Apps. 2007. Changes in landscape composition influence the decline of a threatened woodland caribou population. Journal of Animal Ecology 76:568–579.

Wolf, M., J. Frair, E. Merrill, and P. Turchin. 2009. The attraction of the known: the importance of spatial familiarity in habitat selection in wapiti *Cervus elaphus*. Ecography 32:401–410.

Zager, P., and J. Beecham. 2006. The role of American black bears and brown bears as predators on ungulates in North America. Ursus 17:95–108.

Zoladeski, C. A., and P. F. Maycock. 1990. Dynamics of the boreal forest in northwestern Ontario. American Midland Naturalist 124:289–300.

Appendix 1. Supplemental materials for Chapter 2

Appendix 1.1. Accuracy of DeMars approach to predict date of birth and difference in timing of parturition events (days; $\bar{x}$ ± SE) of caribou in northern Ontario, Canada, 2010–2013, compared to video collar footage, as identified by first footage of calf, and accuracy to predict neonate mortality (of those that calved) for 22 video-collared caribou-years, when removing the top 1–-4% of step lengths.

Step-length rarefaction	Parturition event	Parturition timing	Neonatal mortality
1%	100% (22 of 22)	2.55 ± 1.71	53% (9 of 17)
2%	100% (22 of 22)	1.08 ± 0.28	59% (10 of 17)
3%	100% (22 of 22)	1.45 ± 0.30	71% (12 of 17)
4%	100% (22 of 22)	1.79 ± 0.33	88% (15 of 17)

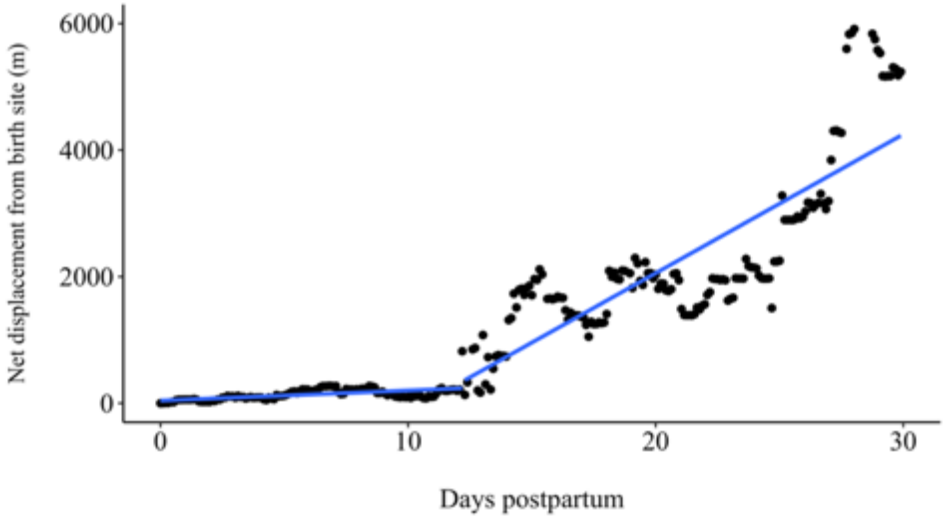

Appendix 1.2. Piece-wise regression applied to the net displacement (m) from the birth-site against days postpartum for each individual caribou (e.g., CAU268_2013) in northern Ontario, Canada, 2010–2013. Break in the piece-wise regression identifies when the caribou left their neonatal area.

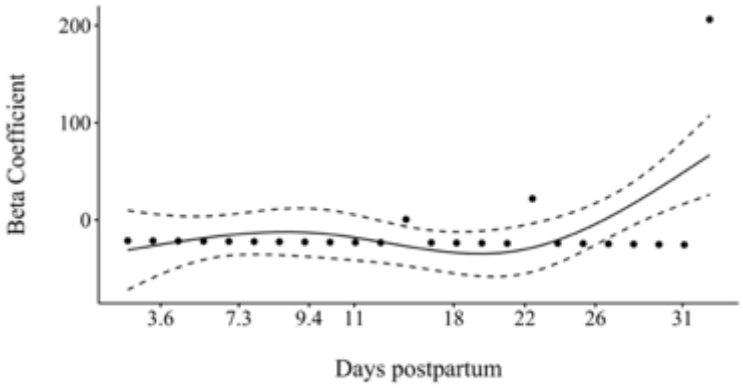

Appendix 1.3. Plot of scaled early seral stand Schoenfeld residuals (beta coefficients) against days postpartum for a Cox proportional hazards model fitting risk of caribou neonate mortality within 4 weeks postpartum as a function of proportional use of early seral stands in northern Ontario, Canada, 2010–2013. The model did not pass the Schoenfeld residual test ($P = 0.01$); therefore, we removed the outlier individual at 33.8 days from the subsequent model selection.

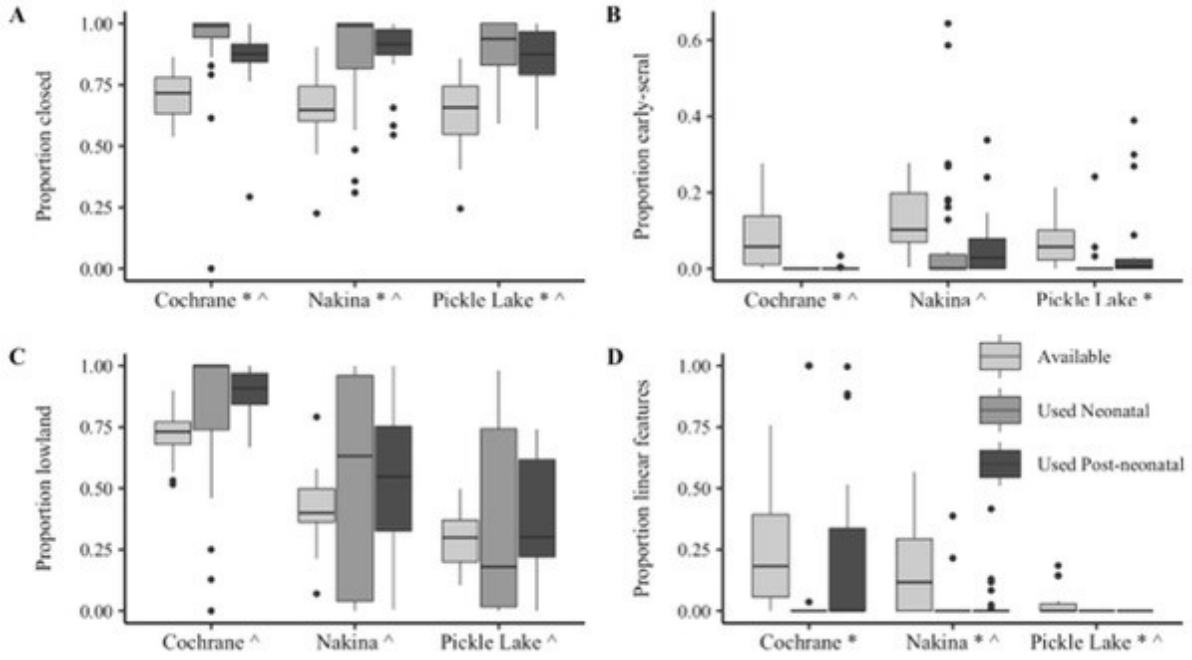

Appendix 1.4. Proportion of locations used by caribou during the neonatal and post-neonatal periods within A) closed-canopied stands, B) early seral stands (<20 years old), C) lowlands, and D) 1 km of linear features, compared to proportion of available locations (10 available/1 caribou location) randomly sampled within the calving and summer (1 May to 30 Sep) 95% utilization distribution by study region in northern Ontario, Canada, 2010–2013. Asterisk (*) and caret (^) indicate significant selection during the neonatal period and post-neonatal period (up to 35 days), respectively.

Appendix 1.5. Sensitivity analysis of Cox proportional hazard models of risk of neonatal caribou mortality within 5 weeks postpartum in northern Ontario, Canada, 2010–2013, as a function of proportional use of early seral stands and lowlands and its interaction with age-corrected movement rates (move) with errors (0–20%) induced by switching lowlands to non-lowlands and early seral to non-early seral, and vice versa. Models were robust to error if difference in Akaike's Information Criterion corrected for sample size (ΔAIC_c) was < 2 from original model with 0% induced error.

	Early seral		Lowlands		Lowlands × move	
Error	AIC_c	ΔAIC_c	AIC_c	ΔAIC_c	AIC_c	ΔAIC_c
0%	182.79	0.00	183.30	0.00	184.89	0.00
5%	183.34	0.55	183.68	0.38	185.34	0.45
10%	191.68	8.89	185.25	1.94	187.03	2.15
20%	195.57	12.78	183.60	0.30	185.12	0.22

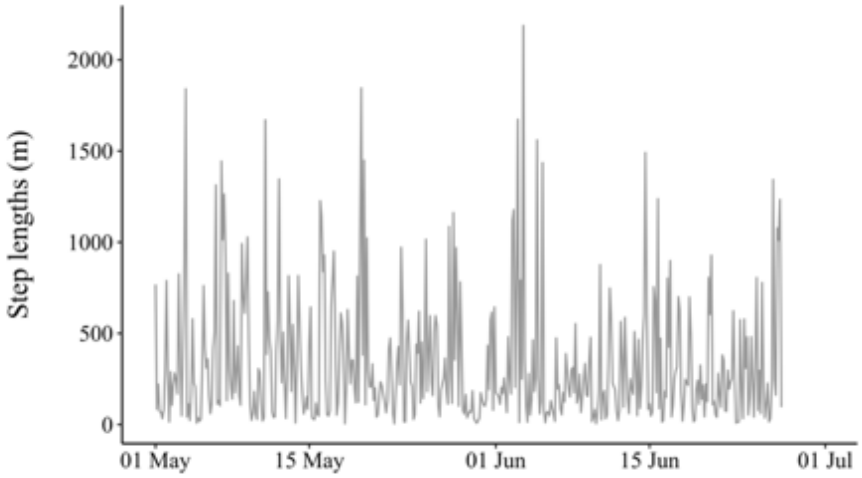

Appendix 1.6. Step lengths (m) over time for the caribou (CAU273_2011) that had a stillbirth identified in the video collar footage in northern Ontario, Canada, 2011. There was no discernible decrease in movement rates to indicate a live parturition event.

Appendix 1.7. Pregnancy rate (total individual caribou), parturition rate (total individual caribou), and loss rate (pregnant but DeMars approach predicted barren; total individual caribou) for 58 caribou with both pregnancy status and predicted parturition status across Cochrane, Nakina, and Pickle Lake in northern Ontario, Canada, 2010–2013.

Study region	Pregnancy rate	Parturition rate	Loss rate
Cochrane	0.88 (17)	0.82 (17)	0.07 (15)
Nakina	0.80 (25)	0.68 (25)	0.15 (20)
Pickle Lake	0.81 (16)	0.69 (16)	0.15 (16)
$\bar{x}$	0.83 (58)	0.72 (58)	0.13 (48)

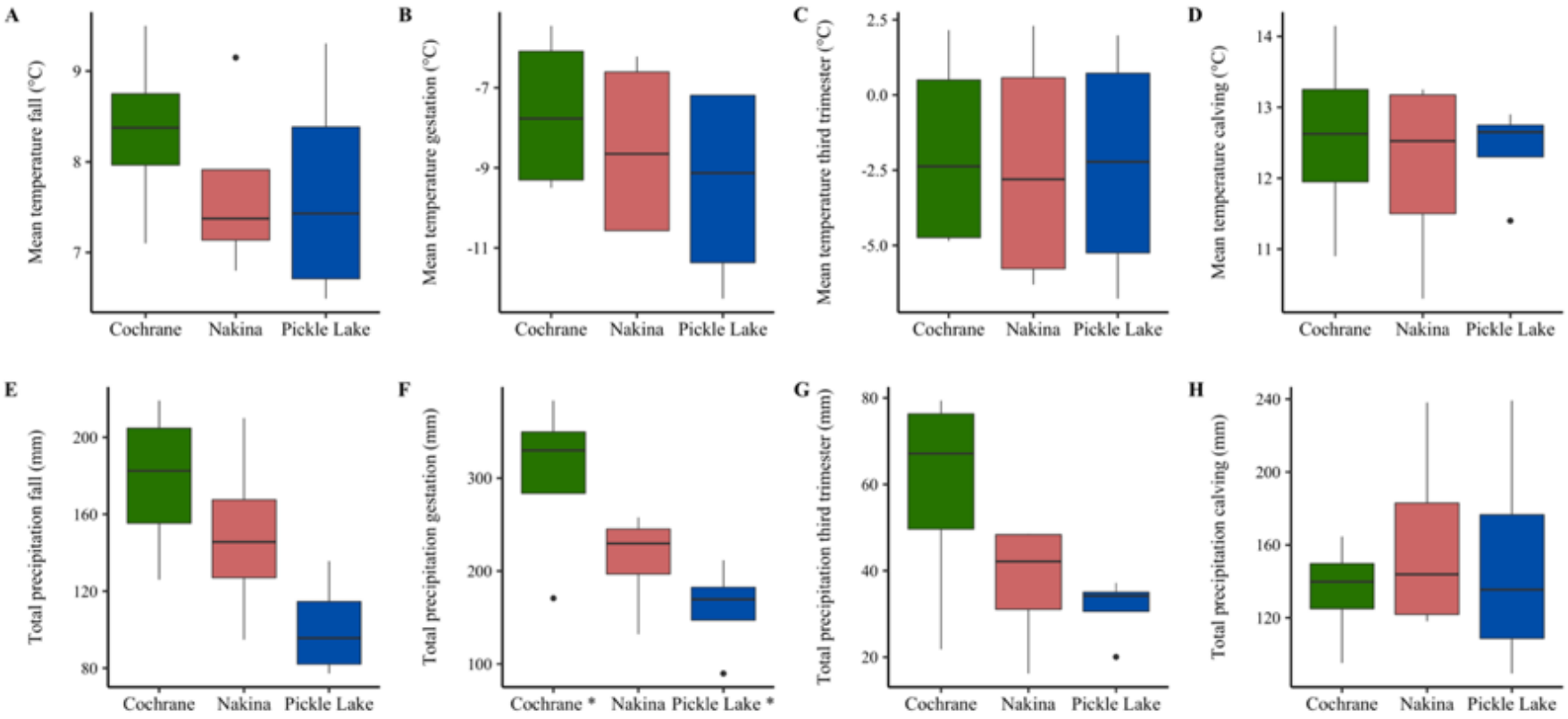

Appendix 1.8. Mean temperature (°C; A–D) and cumulative (total) precipitation (mm; E–F) across the fall (A, E; Sep and Oct), gestation (B, F; Dec to Apr), third trimester (C, G; Mar and Apr), and calving (D, H; May and Jun) seasons between 2010–2013 by study region (Cochrane, Nakina, and Pickle Lake; Environment Canada, accessed 14 Jun 2019) in northern Ontario, Canada. Asterisk (*) indicate significant difference based on a 1-way analysis of variance with a *post hoc* Tukey's range test using Bonferroni Correction ($\alpha = 0.025$)

Appendix 2. Supplemental materials for Chapter 3

Appendix 2.1. Accuracy of DeMars approach (DeMars et al. 2013) to predict parturition events of caribou in northern Ontario, Canada, 2010–2014, compared to video collar footage for 22 video collared caribou-years, when using fix rate intervals from 2.5 or 3 hrs to 12.5 or 13 hrs. One-hr fixes were rarified to 3 hrs and 13 hrs to be similar to the 2.5-hrs and 13-hrs fix rate interval, respectively, after removing the top 2% of step lengths (as per Walker et al. 2021).

Fix rate interval	Parturition event	Calf predicted	No calf predicted
2.5 or 3-hrs	100% (22 of 22)	100% (17 of 17)	100% (5 of 5)
5-hrs	100% (22 of 22)	100% (17 of 17)	100% (5 of 5)
12.5 or 13-hrs	91% (20 of 22)	88% (15 of 17)	100% (5 of 5)

Appendix 2.2. Spatial and habitat fidelity analysis for the 99 (98 for habitat fidelity) calving-sequences across northern Ontario, Canada, 2010–2014, where we identified spatial fidelity by comparing the Euclidean distance between neonatal centroids to the proportion (prop.) of random locations less than or equal to the distance between centroids, and identified habitat fidelity where a logistic regression was fit using the Far North Land Cover types (upland conifer forest, lowland conifer forest, early seral forest, and mixed-deciduous forest) used at neonatal locations compared to a null model (intercept only). Included is the caribou ID, study regions, year one and two, the use of only lowlands or conifer in both years (in which cases a logistic model was not fit), if the calving-sequence expressed habitat fidelity (based on $\Delta AIC_c > 4$ from the null model), and the dominant land cover used at neonatal locations if the calving-sequence expressed habitat fidelity (NA indicates no dominant land cover, because the calving-sequence was classified as not expressing habitat fidelity).

Caribou ID	Study Region	Year 1	Year 2	Spatial fidelity		Habitat fidelity						
				Distance	Prop.	Lowland only	Upland conifer only	Habitat fidelity	Habitat AIC_c	Null AIC_c	ΔAIC_c	Dominant land cover
CAU151	Nakina	2011	2012	10772.96	0.34	no	no	yes	94.67	94.27	0.4	lowland
CAU153	Nakina	2010	2011	2650.09	0.21	no	no	no	36.55	138.08	101.53	NA
CAU153	Nakina	2010	2012	2992.81	0.04	no	no	no	149.37	171.3	21.93	NA
CAU153	Nakina	2011	2012	643.47	0.01	no	no	no	66.23	115.43	49.2	NA
CAU252	Nakina	2012	2013	11227.35	0.17	no	no	no	48.78	70.87	22.09	NA
CAU253	Nakina	2011	2012	34814.55	0.17	no	no	yes	33.99	32.6	1.39	lowland/ conifer
CAU259	Nakina	2011	2012	11275.20	0.73	no	no	yes	61.56	59.98	1.57	conifer
CAU259	Nakina	2011	2014	3065.57	0.47	no	no	no	15.11	157.73	142.62	NA
CAU259	Nakina	2012	2014	13909.48	0.73	no	no	no	4.12	80.14	76.02	NA
CAU263	Nakina	2011	2012	6045.18	0.80	no	no	yes	120.45	123.86	3.4	lowland
CAU268	Nakina	2011	2012	7434.32	0.73	no	no	no	281.74	299.39	17.65	NA
CAU268	Nakina	2011	2013	9539.38	0.32	no	no	no	242.61	263.77	21.16	NA
CAU268	Nakina	2012	2013	2509.19	0.04	no	no	no	377.02	385.56	8.54	NA
CAU269	Nakina	2011	2012	4056.14	0.22	no	no	no	92.07	105.99	13.92	NA
CAU269	Nakina	2011	2013	24027.53	0.27	no	no	no	107.21	153.48	46.27	NA
CAU269	Nakina	2011	2014	26044.67	0.72	no	no	no	54.54	72.7	18.16	NA
CAU269	Nakina	2012	2013	7800.71	0.06	no	no	yes	69.44	70	0.56	lowland
CAU269	Nakina	2012	2014	28447.83	0.75	no	no	yes	38.8	40.64	1.84	lowland
CAU269	Nakina	2013	2014	27265.31	0.62	no	no	yes	53.62	52.7	0.93	lowland
CAU272	Nakina	2011	2012	132.68	0.003	no	no	yes	180.31	180.28	0.03	conifer

Appendix 2.2. Continued.

Caribou ID	Study Region	Year 1	Year 2	Spatial fidelity		Habitat fidelity						
				Distance	Prop.	Lowlands only	Conifer only	Habitat fidelity	Habitat AIC_c	Null AIC_c	ΔAIC_c	Dominant land cover
CAU273	Nakina	2011	2012	5632.43	0.16	no	no	no	56.78	63.62	6.84	NA
CAU273	Nakina	2011	2013	14793.36	0.63	no	no	no	119.3	187.51	68.21	NA
CAU273	Nakina	2012	2013	9181.92	0.16	no	no	yes	56.73	59.48	2.75	lowland/ conifer
CAU280	Nakina	2011	2012	2615.07	0.81	no	no	yes	228.46	230.93	2.47	lowland
CAU281	Nakina	2011	2012	423.83	0.07	no	no	no	354.7	389.65	34.95	NA
CAU283	Nakina	2011	2012	15466.34	0.72	no	no	no	257.03	331.53	74.5	NA
CAU285	Nakina	2011	2012	2707.54	0.64	no	no	no	33.63	120.14	86.52	NA
CAU296	Nakina	2011	2012	1059.41	0.14	no	no	yes	356.82	357.64	0.81	conifer
CAU296	Nakina	2011	2013	198.21	0.001	no	no	yes	237.47	234.99	2.48	conifer
CAU296	Nakina	2012	2013	947.63	0.11	no	no	yes	242.29	245.09	2.8	conifer
CAU297	Nakina	2011	2012	3504.93	0.15	no	no	no	6.17	187.53	181.36	NA
CAU297	Nakina	2011	2013	3706.00	0.09	no	no	no	72.95	163.28	90.33	NA
CAU297	Nakina	2012	2013	513.34	0.002	no	no	no	192.95	228.06	35.11	NA
CAU312	Nakina	2012	2013	1543.12	0.22	no	no	no	635.93	721.72	85.8	NA
CAU314	Nakina	2012	2013	35203.22	0.77	no	no	no	228.72	268.63	39.91	NA
CCO180	Cochrane	2010	2011	79.00	<0.001	yes	no	yes	NA	NA	NA	lowland
CCO180	Cochrane	2010	2012	2645.89	0.10	yes	no	yes	NA	NA	NA	lowland
CCO180	Cochrane	2010	2013	3093.55	0.25	yes	no	yes	NA	NA	NA	lowland
CCO180	Cochrane	2011	2012	481.57	0.01	yes	no	yes	NA	NA	NA	lowland
CCO180	Cochrane	2011	2013	2567.10	0.11	yes	no	yes	NA	NA	NA	lowland
CCO180	Cochrane	2012	2013	3014.55	0.24	yes	no	yes	NA	NA	NA	lowland
CCO209	Cochrane	2011	2012	1770.77	0.01	no	no	yes	133.91	134.49	0.58	lowland
CCO209	Cochrane	2011	2013	9929.92	0.17	no	no	yes	218.6	222.06	3.46	lowland
CCO209	Cochrane	2012	2013	9667.59	0.16	yes	no	yes	NA	NA	NA	lowland
CCO210	Cochrane	2011	2012	46363.23	0.77	no	no	no	95.42	105.86	10.44	NA
CCO212	Cochrane	2011	2012	101.91	<0.001	no	no	yes	292.5	290.95	1.56	lowland
CCO214	Cochrane	2011	2012	280.18	<0.001	no	no	yes	78.67	78.16	0.51	lowland

Appendix 2.2. Continued.

Caribou ID	Study Region	Year 1	Year 2	Spatial fidelity		Habitat fidelity						
				Distance	Prop.	Lowlands only	Conifer only	Habitat fidelity	Habitat AIC_c	Null AIC_c	ΔAIC_c	Dominant land cover
CCO214	Cochrane	2011	2013	281.84	0.001	no	no	yes	153.51	155.44	1.93	lowland
CCO214	Cochrane	2012	2013	25.74	<0.001	no	no	yes	146.66	144.74	1.93	lowland
CCO215	Cochrane	2011	2012	16269.55	0.69	no	no	no	144.71	149.98	5.27	NA
CCO219	Cochrane	2011	2012	8558.31	0.21	no	no	no	100.13	119.62	19.49	NA
CCO221	Cochrane	2011	2012	2908.50	0.13	no	no	no	193.53	203.99	10.45	NA
CCO223	Cochrane	2011	2012	4043.79	0.80	no	no	yes	359.51	361.99	2.48	lowland
CCO223	Cochrane	2011	2013	4113.91	0.52	yes	no	yes	NA	NA	NA	lowland
CCO223	Cochrane	2012	2013	156.68	0.001	no	no	yes	232.65	232.99	0.34	lowland
CCO224	Cochrane	2011	2012	15520.48	0.06	no	no	yes	84	81.85	2.15	lowland
CCO225	Cochrane	2011	2012	377.78	<0.001	no	no	no	197.42	216.02	18.6	NA
CCO225	Cochrane	2011	2013	1242.85	0.01	no	no	no	128.85	135.97	7.13	NA
CCO225	Cochrane	2012	2013	1047.58	0.001	no	no	no	69.3	95.31	26	NA
CCO226	Cochrane	2011	2012	39350.08	0.79	no	no	no	197.47	253.4	55.93	NA
CCO230	Cochrane	2011	2012	1060.92	<0.001	yes	no	yes	NA	NA	NA	lowland
CCO233	Cochrane	2011	2012	3276.48	0.08	yes	no	yes	NA	NA	NA	lowland
CCO233	Cochrane	2011	2013	19232.47	0.81	yes	no	yes	NA	NA	NA	lowland
CCO233	Cochrane	2012	2013	22364.00	0.73	yes	no	yes	NA	NA	NA	lowland
CCO234	Cochrane	2011	2012	15687.54	0.83	yes	no	yes	NA	NA	NA	lowland
CCO234	Cochrane	2011	2013	37748.85	0.66	yes	no	yes	NA	NA	NA	lowland
CCO234	Cochrane	2012	2013	42464.06	0.85	yes	no	yes	NA	NA	NA	lowland
CCO235	Cochrane	2012	2013	14084.36	0.17	no	no	no	118.84	154.56	35.72	NA
CCO235	Cochrane	2012	2014	12485.64	0.15	no	no	yes	208.01	207.34	0.66	lowland
CCO235	Cochrane	2013	2014	4573.00	0.04	no	no	no	61.51	83.84	22.33	NA
CCO236	Cochrane	2011	2013	4425.84	0.003	no	no	no	40.59	77.58	36.99	NA
CCO237	Cochrane	2011	2012	1572.52	0.001	no	no	no	4.31	28.52	24.21	NA
CCO239	Cochrane	2011	2012	21388.84	0.25	yes	no	yes	NA	NA	NA	lowland
CCO239	Cochrane	2011	2013	2306.67	0.52	no	no	no	70.45	88.36	17.91	NA

Appendix 2.2. Continued.

Caribou ID	Study Region	Year 1	Year 2	Spatial fidelity		Habitat fidelity						
				Distance	Prop.	Lowlands only	Conifer only	Habitat fidelity	Habitat AIC_c	Null AIC_c	ΔAIC_c	Dominant land cover
CCO240	Cochrane	2011	2012	343.21	0.02	NA	NA	NA	NA	NA	NA	NA
CCO305	Cochrane	2012	2013	42195.50	0.26	yes	no	yes	NA	NA	NA	lowland
CPL102	Pickle Lake	2010	2011	14212.91	0.15	no	no	no	88.49	124.24	35.74	NA
CPL103	Pickle Lake	2011	2013	31.26	<0.001	no	no	no	187.97	193.72	5.75	NA
CPL104	Pickle Lake	2010	2012	11437.95	0.40	no	no	no	48.24	124.48	76.24	NA
CPL104	Pickle Lake	2010	2013	2474.34	0.02	no	no	no	38.87	130.74	91.87	NA
CPL104	Pickle Lake	2012	2013	12054.64	0.32	no	no	yes	361.27	360.91	0.36	lowland
CPL105	Pickle Lake	2010	2011	12895.77	0.14	no	no	no	86.09	97.6	11.51	NA
CPL112	Pickle Lake	2010	2011	36378.58	0.71	no	no	no	32.71	72.29	39.58	NA
CPL112	Pickle Lake	2010	2012	36921.15	0.46	no	no	yes	38.61	42.32	3.71	lowland/ conifer
CPL112	Pickle Lake	2011	2012	726.93	0.04	no	no	no	58.26	69.31	11.04	NA
CPL113	Pickle Lake	2011	2012	15841.94	0.49	no	no	no	87.31	105.07	17.77	NA
CPL114	Pickle Lake	2010	2012	3661.34	0.09	no	yes	yes	NA	NA	NA	conifer
CPL115	Pickle Lake	2011	2012	45867.90	0.63	no	no	no	51.88	75.54	23.65	NA
CPL117	Pickle Lake	2012	2013	31802.25	0.18	no	no	no	61.03	69.5	8.48	NA
CPL121	Pickle Lake	2010	2011	25723.46	0.22	no	no	no	18.04	34.84	16.8	NA
CPL134	Pickle Lake	2010	2011	1498.08	0.08	no	no	yes	117.41	118.88	1.46	lowland
CPL134	Pickle Lake	2010	2012	769.78	0.03	no	no	no	15.72	82.91	67.18	NA
CPL134	Pickle Lake	2011	2012	1723.45	0.10	no	no	no	67.24	161.84	94.6	NA
CPL136	Pickle Lake	2010	2011	1992.83	0.07	no	no	no	85.11	165.69	80.58	NA
CPL138	Pickle Lake	2010	2011	98135.97	0.72	no	no	yes	249.71	249.33	0.39	conifer
CPL141	Pickle Lake	2012	2013	3078.52	0.06	no	no	yes	83.98	84.54	0.56	disturbed
CPL202	Pickle Lake	2011	2012	2235.27	0.54	no	no	no	4.13	131.01	126.88	NA
CPL203	Pickle Lake	2011	2012	23.81	<0.001	no	yes	yes	NA	NA	NA	conifer

Appendix 2.3. Number (*n*) of calving-sequences, beta coefficient (β) and confidence interval (CI) from independent, logistic mixed-effect models predicting the probability of caribou calving-sequences expressing a type of fidelity (1: none, spatial fidelity, habitat fidelity, or both) compared to not expressing that type of fidelity (0) as a function of proportional use of upland conifer forests, lowlands conifer forests, early seral forests, and mixed-deciduous forests at neonatal locations across three study regions in northern Ontario, Canada, based on caribou telemetry data from 2010−2014. Asterisk indicates confidence intervals do not overlap zero.

Fidelity type	*n*	Upland conifer		Lowland conifer		Early seral		Mixed-deciduous	
		β	95% CI	β	95% CI	β	95% CI	β	95% CI
No fidelity	98	1.07	-0.44, 2.58	-1.36	-2.78, 0.05	1.06	-2.70, 4.82	44.90*	9.77, 78.86
Spatial	98	1.36	-0.37, 3.08	-0.77	-2.34, 0.79	-2.67	-9.25, 3.92	-77.65	-169.92, 28.28
Habitat	98	-3.11*	-6.01, -0.20	3.12*	0.28, 5.93	-0.01	-5.49, 5.47	-43.46*	-84.79, -2.13
Both	98	-3.89	-14.24, 6.47	0.14	-5.53, 12.68	-1.24	-21.58, 19.11	-50.57	-347.77, 246.63

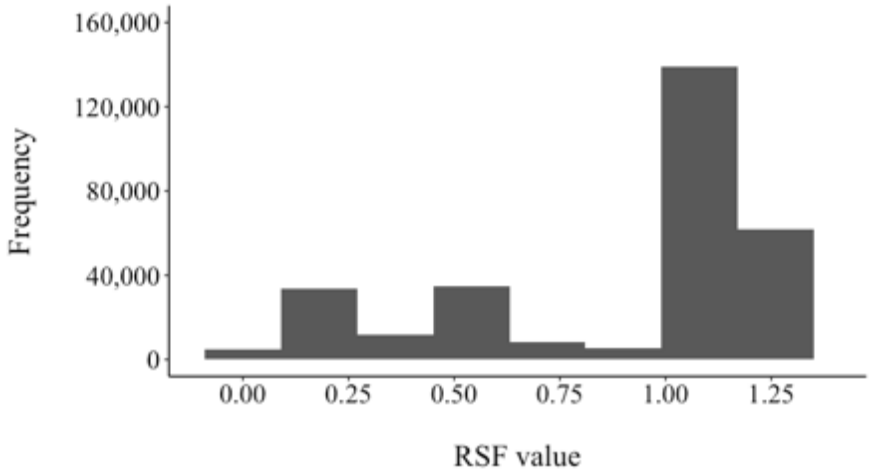

Appendix 2.4. Histogram of predicted RSF values across 100,000 random locations per study region (Pickle Lake, Nakina, and Cochrane) with values averaged at each location across five years (2010–2014).

Appendix 2.5. Number (*n*) of calving-sequences, beta coefficient (β) and confidence interval (CI) from independent, univariate logistic mixed-effect models predicting the probability of caribou calving-sequences expressing habitat fidelity (1) compared to not expressing habitat fidelity (0) as a function of habitat quality in the pre-calving-neonatal 95% utilization distribution by study regions in northern Ontario, Canada, based on caribou telemetry data from 2010−2014.

Fidelity type	Pickle Lake			Nakina			Cochrane		
	n	β	95% CI	*n*	β	95% CI	*n*	β	95% CI
Habitat	22	-8.52	-22.53, 5.48	35	-7.82	-17.51, 1.87	41	-12.63	-34.94, 9.67

Appendix 2.6. Number (*n*) of calving-sequences and mean habitat quality (i.e., predicted RSF values; with SD) within the pre-calving-neonatal home range for expressing habitat fidelity by study regions across northern Ontario, Canada, based on caribou telemetry data from 2010−2014.

Fidelity type	Pickle Lake			Nakina			Cochrane			Combined		
	n	Mean	SD	*n*	Mean	SD	*n*	Mean	SD	*n*	Mean	SD
Habitat	7	1.00	0.08	13	0.85	0.10	28	0.78	0.21	48	0.83	0.18
No habitat	15	1.04	0.06	22	0.91	0.09	13	0.89	0.11	50	0.94	0.11
Total	22	1.03	0.07	35	0.89	0.1	41	0.81	0.19	98	0.89	0.16

Appendix 2.7. Number (*n*) of calving-sequences and mean age (years; with standard deviation [SD]) for each type of fidelity expressed across northern Ontario, Canada, 2010−2014.

Fidelity type	Age		
	n	$\bar{x}$	SD
No fidelity	50	5.25	1.82
Either habitat or spatial	20	6.40	2.01
Spatial	22	7.09	2.40
No spatial	48	5.55	1.61
Habitat	36	5.78	1.59
No habitat	33	6.21	2.34
Both habitat and spatial	11	5.70	2.11
No habitat and spatial	58	6.09	2.01

Appendix 2.8. Number (*n*) of calving-sequences, beta coefficient (β) and confidence interval (CI) from independent, multivariable logistic mixed-effect models predicting the probability of caribou calving-sequences expressing a type of fidelity (1: none, spatial fidelity, habitat fidelity, or both) compared to not expressing that type of fidelity (0) as a function of habitat quality in the pre-calving-neonatal 95% utilization distribution and caribou age (years) across three study regions in northern Ontario, Canada, based on caribou telemetry data from 2010−2014. Asterisk indicates confidence intervals do not overlap zero.

Fidelity type	*n*	Habitat quality		Age	
		β	95% CI	β	95% CI
No fidelity	70	4.86	-0.44, 10.16	-0.47	-0.95, 0.02
Spatial	70	0.24	-3.47, 3.94	0.44*	0.05, 0.82
Habitat	69	-10.89	-22.99, 1.21	0.04	-0.50, 0.57
Both	69	-8.94	-22.40, 4.52	0.14	-0.84, 1.13

Appendix 2.9. Number (*n*) of calving-sequences, beta coefficient (β) and confidence interval (CI) from independent, multivariable logistic mixed-effect models predicting the probability of caribou calving-sequences expressing a type of fidelity (1: none, spatial fidelity, habitat fidelity, or both) compared to not expressing that type of fidelity (0) as a function of habitat quality (HQ) in the pre-calving-neonatal 95% utilization distribution, caribou age (years), and the interaction (HQ*Age), across three study regions in northern Ontario, Canada, based on caribou telemetry data from 2010−2014.

Fidelity type	*n*	Habitat quality		Age		HQ*Age	
		β	95% CI	β	95% CI	β	95% CI
No fidelity	70	3.54	-13.73, 20.81	-0.70	-3.70, 2.30	0.25	-2.88, 3.38
Spatial	70	3.42	-10.72, 17.57	0.94	1.25, 3.12	-0.54	-2.86, 1.77
Habitat	69	1.60	-22.12, 25.32	2.12	-2.11, 6.35	-0.24	-6.66, 2.18
Both	69	6.58	-29.74, 42.90	2.57	-3.05, 8.20	-2.84	-9.33, 3.65

Appendix 2.10. Proportion and number (*n*) of caribou calving-sequences expressing no fidelity, spatial fidelity, habitat fidelity, or both habitat and spatial fidelity based on if their calf survived (*n* = 20) or was lost (*n* = 7) in the 5-weeks postpartum across three study regions in northern Ontario, Canada, based on caribou telemetry data from 2010−2014.

Strata	No fidelity		Spatial		Habitat		Both	
	Proportion	*n*	Proportion	*n*	Proportion	*n*	Prop.	*n*
Calf survived	0.40	8	0.25	5	0.40	8	0.05	1
Calf lost	0.43	3	0.14	1	0.57	4	0.14	1

Appendix 3. Supplemental materials for Chapter 4

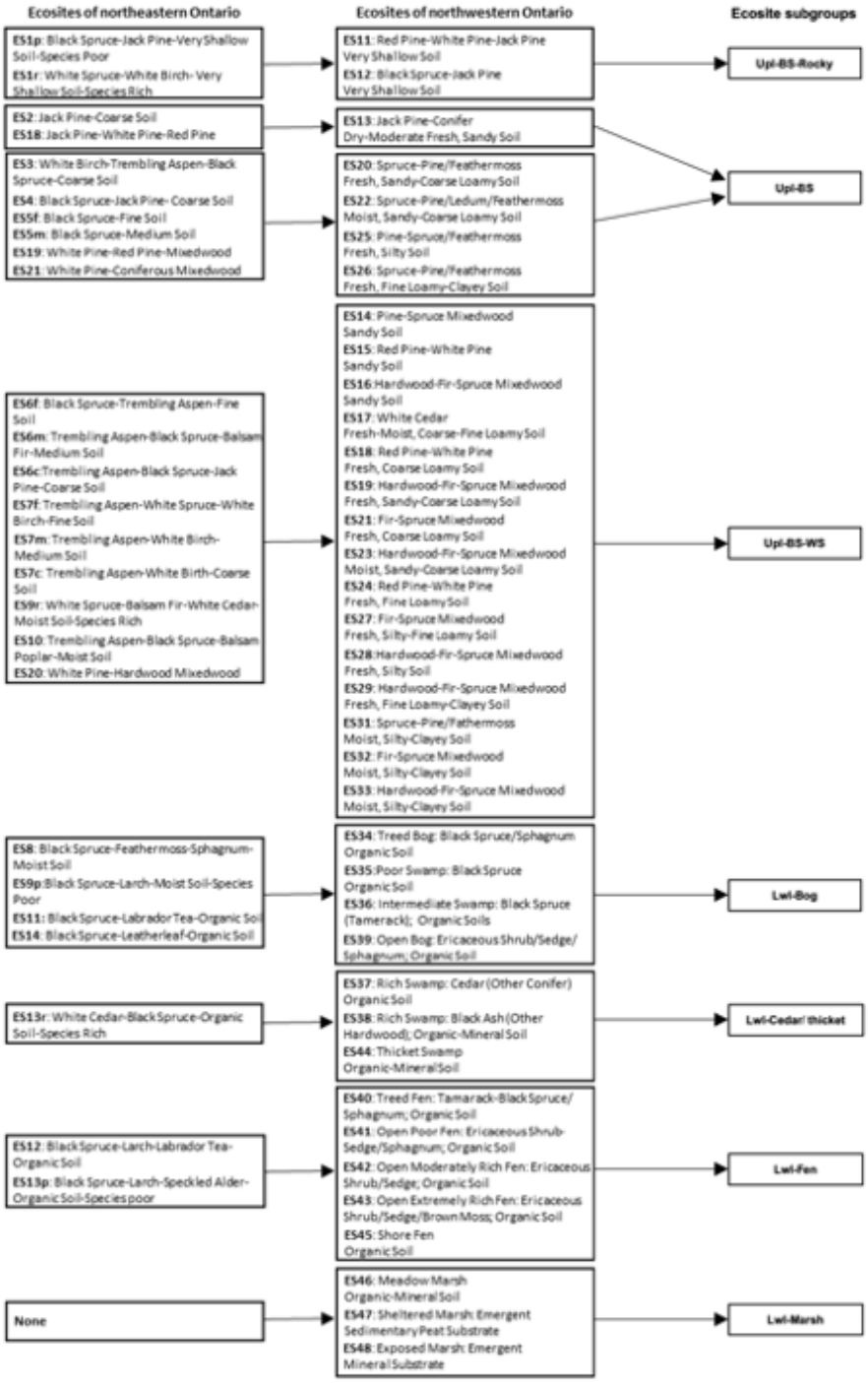

Appendix 3.1. Cross-walking diagram linking ecosites of northwestern Ontario (i.e., Pickle Lake) from Racey et al. (1996) and ecosites of northeastern Ontario (i.e., Cochrane) from Taylor et al. (2000) to ecosite subgroups based on similar understory species composition. Tree codes: BS = Black spruce, WS = White spruce.

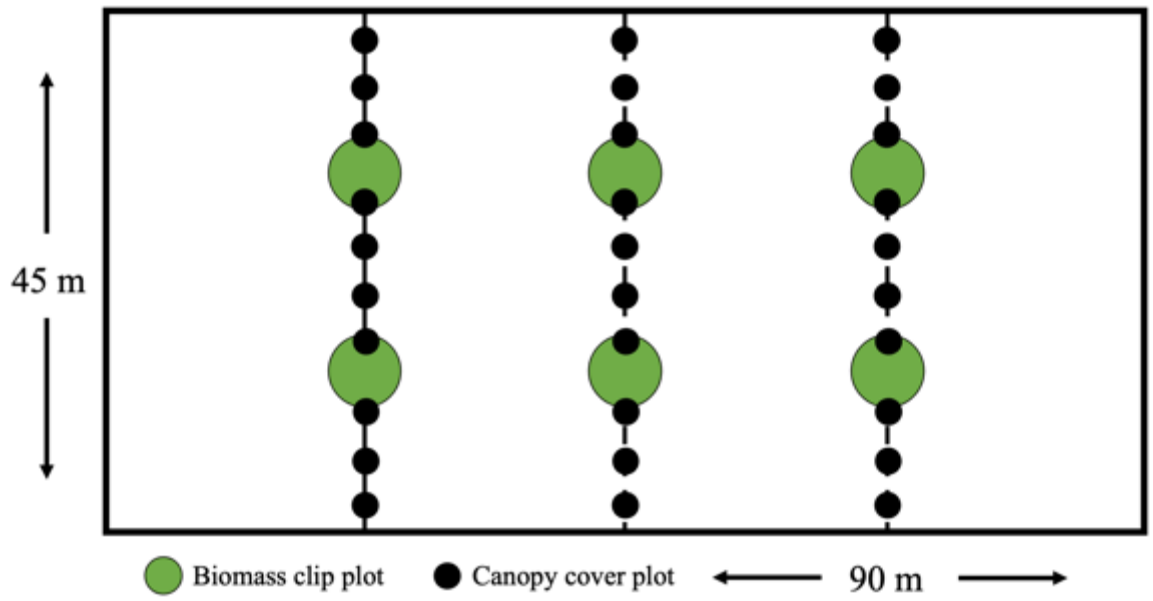

Appendix 3.2. Macroplot sampling design to estimate basal area (sampled at biomass clip plots), canopy cover, and vegetation biomass in Pickle Lake and Cochrane, Ontario, Canada, in 2017–2018.

Appendix 4. Supplemental materials for Chapter 4

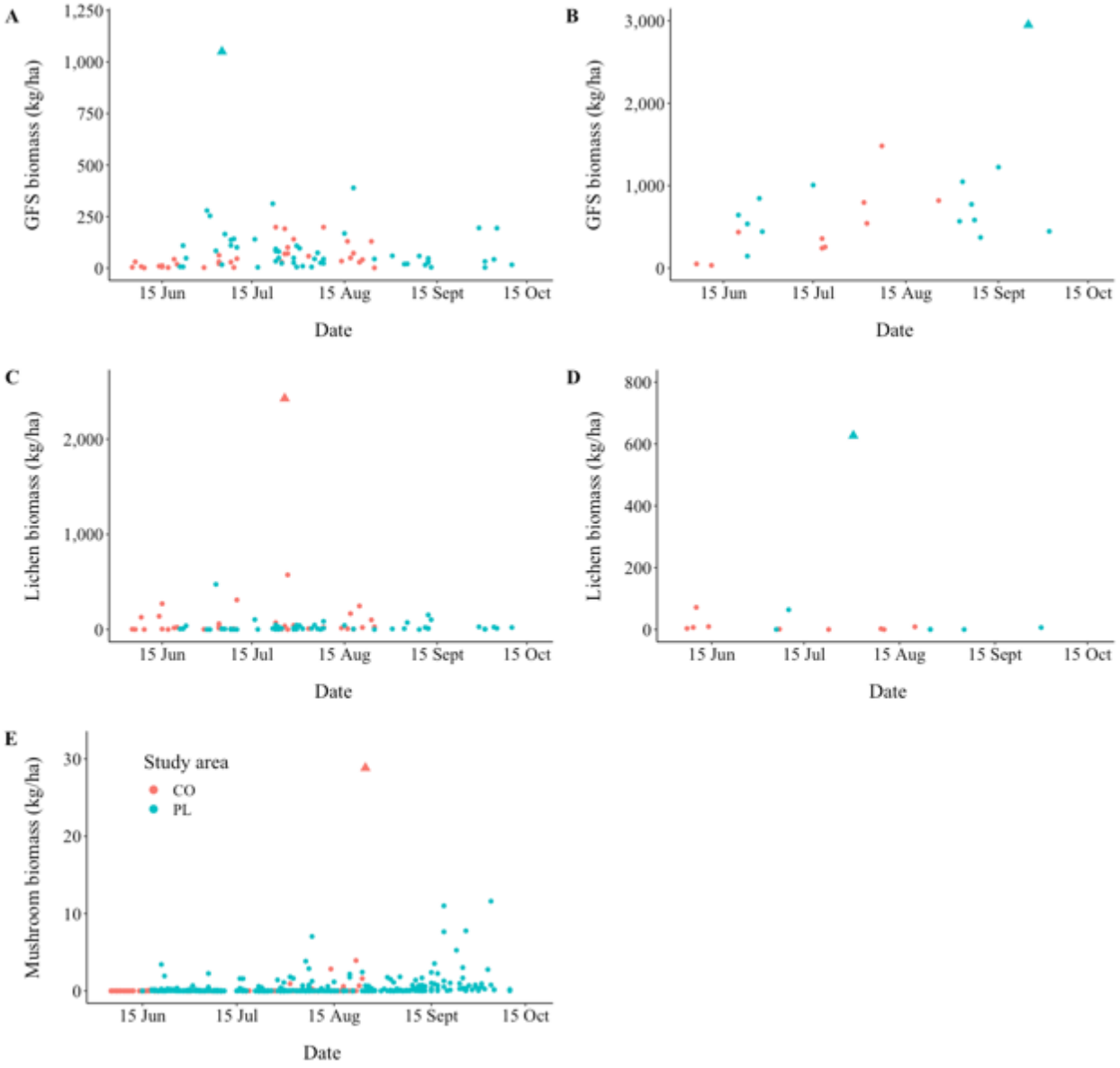

Appendix 4.1. Relationship between Julian day and grass, forb, deciduous shrub (GFS) biomass in A) Mid-late Lwl-Bog and B) Early BS-WS, lichen biomass in C) Mid-late Lwl-Bog and D) Mid-late Lwl-Fen, and E) mushrooms across ecosites and the outlier macroplots (triangles) which were removed from the modeling of biomass metric. Graphs show outlier values removed prior modeling.

Appendix 4.2. Model coefficient, number of model parameters (*K*), Akaike's Information Criterion corrected for small sample size (AIC_c), change in AIC_c from best model (ΔAIC_c), and model weights calculated from AIC_c (w_i) for competing models with Julian day (JD) for grass/forb/deciduous shrub (GFS), lichen, horsetail, and mushroom biomass (kg/ha) across all Pickle Lake (PL) and Cochrane (CO) macroplots.

Forage	SA	Model	JD	*K*	AIC_c	ΔAIC_c	W_i
GFS	PL	JD	0.89	2	4706.40	0.00	0.92
		null		1	4711.41	5.01	0.08
	CO	JD	0.99	2	1689.87	0.00	1.00
		null		1	1706.38	16.51	0.00
Lichen	PL	null		1	5261.66	0.00	0.51
		JD	1.25	2	5261.76	0.10	0.49
	CO	null		1	1918.37	0.00	0.69
		JD	-1.04	2	1919.98	1.62	0.31
Horsetail	PL	null		1	3195.85	0.00	0.52
		JD	-0.06	2	3195.97	0.12	0.48
	CO	JD	0.15	2	1014.15	0.00	1.00
		null		1	1025.49	11.33	0.00
Mushroom	PL	JD	0.99	2	1102.18	0.00	1.00
		null		1	1138.38	36.20	0.00
	CO	JD	1.05	2	154.66	0.00	1.00
		null		1	166.77	12.11	0.00

Appendix 4.3. Modeling biomass (kg/ha) of grass, forb, and deciduous shrub combined (GFS), lichen, horsetail, and mushroom (kg/ha), total biomass (accepted and avoided species combined),), HQ-accepted biomass (AB; kg/ha), DE-accepted biomass (kg/ha), and DP-accepted biomass (kg/ha) by seral stage (early [<20 years] vs. mid-late [≥20 years]) for each ecosite as a function of Julian day and study area (PL vs. CO, CO is the reference category).

Forage	Ecosite	Seral stage	*n*	Covariate	Beta	CI	*P*-value
GFS	Upl-BS	Early-late	225	JD	-0.40	0.81	0.34
				SA	114.31	70.21	0.002
		Early	67	JD	0.85	2.27	0.47
				SA	242.63	140.63	0.001
		Mid-late	158	JD	0.30	0.45	0.19
				SA	59.12	43.80	0.009
	Upl-BS-WS	Early-late	85	JD	1.92	2.14	0.08
				SA	127.82	128.22	0.05
		Early	23	JD	4.20	4.24	0.07
				SA	71.02	299.17	0.65
		Mid-late	62	JD	-0.25	1.19	0.68
				SA	160.25	66.19	<0.001
	Lwl-Bog	Early-late	113	JD	0.25	0.74	0.52
				SA	60.41	46.72	0.01
		Early	27	JD	2.56	1.89	0.01
				SA	129.26	113.80	0.04
		Mid-late	86	JD	0.01	0.55	0.97
				SA	24.76	35.24	0.17
	Lwl-Fen	Mid-late	16	JD	1.25	2.56	0.35
				SA	1.40	174.84	0.99
Lichen	Upl-BS	Early-late	225	JD	2.18	2.85	0.14
				SA	-119.45	245.97	0.34
		Early	67	JD	2.41	1.80	0.01
				SA	-15.75	111.46	0.78
		Mid-late	158	JD	1.58	3.85	0.42
				SA	-219.52	373.38	0.25
	Upl-BS-WS	Early-late	86	JD	-0.05	0.10	0.31
				SA	8.26	6.07	0.009
		Early	24	JD	-0.26	0.18	0.009
				SA	18.55	13.21	0.01
		Mid-late	62	JD	0.08	0.11	0.19
				SA	4.10	6.13	0.20

Appendix 4.3 Continued.

Forage	Ecosite	Seral stage	*n*	Covariate	Beta	CI	*P*-value
Lichen	Lwl-Bog	Early-late	113	JD	-0.15	0.65	0.66
				SA	-61.11	41.32	0.005
		Early	27	JD	-1.23	1.69	0.17
				SA	-150.46	101.64	0.008
		Mid-late	86	JD	0.05	0.67	0.88
				SA	-43.02	43.49	0.06
	Lwl-Fen	Mid-late	15	JD	-0.33	0.38	0.11
				SA	13.28	27.46	0.36
Horsetail	Upl-BS	Early-late	225	JD	-0.03	0.04	0.20
				SA	2.48	3.38	0.15
		Early	67	JD	-0.04	0.14	0.57
				SA	5.29	8.61	0.23
		Mid-late	158	JD	-0.01	0.03	0.45
				SA	1.06	2.60	0.43
	Upl-BS-WS	Early-late	86	JD	-0.16	0.19	0.09
				SA	11.20	11.41	0.06
		Early	24	JD	-0.51	0.49	0.05
				SA	36.84	35.88	0.06
		Mid-late	62	JD	-0.02	0.03	0.25
				SA	1.42	1.70	0.11
	Lwl-Bog	Early-late	114	JD	0.09	0.21	0.38
				SA	9.26	13.07	0.17
		Early	27	JD	0.22	0.69	0.54
				SA	17.65	41.39	0.41
		Mid-late	87	JD	0.11	0.18	0.23
				SA	3.45	11.27	0.55
	Lwl-Fen	Mid-late	16	JD	0.009	0.03	0.60
				SA	-0.46	2.26	0.70
Mushroom	Upl-BS	Early-late	225	JD	0.01	0.006	<0.001
				SA	0.14	0.51	0.60
		Early	67	JD	0.009	0.01	0.08
				SA	0.10	0.59	0.74
		Mid-late	158	JD	0.02	0.008	<0.001
				SA	0.18	0.73	0.62

Appendix 4.3. Continued.

Forage	Ecosite	Seral stage	*n*	Covariate	Beta	CI	*P*-value
Mushroom	Upl-BS-WS	Early-late	86	JD	0.01	0.004	0.002
				SA	0.11	0.26	0.39
		Early	24	JD	0.01	0.004	0.03
				SA	0.14	0.31	0.40
		Mid-late	62	JD	0.01	0.01	0.01
				SA	0.10	0.33	0.56
	Lwl-Bog	Early-late	113	JD	0.01	0.00	<0.001
				SA	-0.10	0.21	0.35
		Early	27	JD	0.01	0.01	0.02
				SA	-0.57	0.66	0.10
		Mid-late	86	JD	0.004	0.003	0.002
				SA	0.03	0.18	0.73
	Lwl-Fen	Mid-late	16	JD	0.00	0.00	0.91
				SA	0.21	0.22	0.09
Total	Upl-BS	Early-late	225	JD	1.27	3.11	0.42
				SA	154.45	268.74	0.26
		Early	67	JD	7.46	4.08	<0.001
				SA	458.42	252.88	<0.001
		Mid-late	158	JD	1.53	3.82	0.43
				SA	-22.18	370.85	0.91
	Upl-BS-WS	Early-late	85	JD	2.69	3.82	0.17
				SA	379.31	229.32	0.002
		Early	23	JD	3.32	5.40	0.24
				SA	501.09	380.75	0.02
		Mid-late	62	JD	0.47	1.99	0.65
				SA	351.03	110.40	<0.001
	Lwl-Bog	Early-late	111	JD	1.96	3.28	0.25
				SA	448.69	209.37	<0.001
		Early	27	JD	6.36	5.32	0.03
				SA	697.55	320.38	<0.001
		Mid-late	84	JD	2.21	3.20	0.18
				SA	290.36	208.08	0.01
	Lwl-Fen	Mid-late	15	JD	4.09	5.18	0.15
				SA	939.87	370.20	<0.001

Appendix 4.3. Continued.

Forage	Ecosite	Seral stage	*n*	Covariate	Beta	CI	*P*-value
HQ-AB	Upl-BS	Early-late	225	JD	-1.32	0.44	<0.001
				SA	49.13	38.05	0.01
		Early	67	JD	-2.65	1.50	<0.001
				SA	134.48	92.81	0.006
		Mid-late	158	JD	-0.67	0.24	<0.001
				SA	10.01	23.67	0.41
	Upl-BS-WS	Early-late	85	JD	-1.71	1.74	0.06
				SA	62.63	104.59	0.24
		Early	23	JD	-2.61	4.18	0.23
				SA	-82.35	294.35	0.59
		Mid-late	62	JD	-1.55	1.12	0.008
				SA	115.96	61.92	<0.001
	Lwl-Bog	Early-late	111	JD	-0.59	0.58	0.05
				SA	32.91	36.83	0.08
		Early	27	JD	-0.37	1.58	0.65
				SA	8.77	95.21	0.86
		Mid-late	84	JD	-0.62	0.60	0.05
				SA	35.81	39.33	0.08
	Lwl-Fen	Mid-late	15	JD	0.24	3.10	0.88
				SA	-15.06	221.74	0.90
DE-AB	Upl-BS	Early-late	225	JD	-0.83	1.04	0.12
				SA	121.22	89.53	0.009
		Early	67	JD	1.07	2.50	0.40
				SA	255.20	154.92	0.00
		Mid-late	158	JD	-0.33	0.94	0.49
				SA	56.15	91.11	0.23
	Upl-BS-WS	Early-late	85	JD	-0.10	1.97	0.92
				SA	118.46	118.50	0.05
		Early	23	JD	-0.41	4.51	0.86
				SA	6.33	317.74	0.97
		Mid-late	62	JD	-0.51	1.15	0.39
				SA	162.94	63.51	<0.001
	Lwl-Bog	Early-late	111	JD	0.25	0.93	0.60
				SA	22.05	59.46	0.47
		Early	27	JD	2.30	2.24	0.05
				SA	62.22	134.72	0.37
		Mid-late	84	JD	0.04	0.86	0.92
				SA	-5.87	55.82	0.84
	Lwl-Fen	Mid-late	15	JD	0.57	2.82	0.70

				SA	27.97	201.53	0.79

Appendix 4.3. Continued.

Forage	Ecosite	Seral stage	*n*	Covariate	Beta	CI	*P*-value
DP-AB	Upl-BS	Early-late	225	JD	-1.36	0.49	<0.001
				SA	56.83	42.42	0.009
		Early	67	JD	-2.67	1.65	0.002
				SA	148.43	102.14	0.006
		Mid-late	158	JD	-0.68	0.30	<0.001
				SA	14.43	28.71	0.33
	Upl-BS-WS	Early-late	85	JD	-1.61	1.80	0.08
				SA	61.04	108.11	0.27
		Early	23	JD	-2.41	4.34	0.29
				SA	-90.44	305.71	0.57
		Mid-late	62	JD	-1.52	1.20	0.02
				SA	116.94	66.58	0.001
	Lwl-Bog	Early-late	111	JD	-0.58	0.59	0.06
				SA	37.50	37.92	0.06
		Early	27	JD	-0.35	1.68	0.68
				SA	22.92	101.27	0.66
		Mid-late	84	JD	-0.58	0.60	0.06
				SA	35.54	39.22	0.08
	Lwl-Fen	Mid-late	15	JD	0.28	3.09	0.86
				SA	-14.71	220.90	0.90

Appendix 4.4. Modeling proportion of accepted biomass from total, standing biomass (kg/ha) by study area as a function of ecosite (Lwl-Bog is the reference category).

	Pickle Lake			Cochrane		
Ecosite	Beta	CI	*P*-value	Beta	CI	*P*-value
Upl-BS-Rocky	1.59	0.46	<0.001	---	---	---
Upl-BS	1.11	0.27	<0.001	0.72	0.41	<0.001
Upl-BS-WS	1.05	0.36	<0.001	0.74	0.41	<0.001
Lwl-Fen	0.06	0.83	0.88	0.42	0.66	0.21
Lwl-Cedar/ thicket	1.50	0.96	0.002	---	---	---
Lwl-Marsh	1.32	1.10	0.02	---	---	---

Appendix 4.5. Modeling total and accepted biomass (kg/ha) by study area (SA: PL and CO) as a function of Julian day and drainage class (upland vs. lowland, with lowland as the reference category) or seral stage (early [<20 years] vs. mid-late [≥20 years], with early seral as the reference category).

Forge metric	SA	Covariate	Beta	CI	*P*-value
Total biomass	PL	Julian day	0.94	2.29	0.42
		Drainage class	-371.08	162.80	<0.001
	CO	Julian day	4.55	3.62	0.02
		Drainage class	-97.76	198.04	0.34
	PL	Julian day	2.37	2.18	0.03
		Seral stage	-639.94	154.35	<0.001
	CO	Julian day	4.76	3.52	0.009
		Seral stage	-307.64	211.31	0.005
Accepted biomass	PL	Julian day	0.95	1.88	0.32
		Drainage class	178.85	133.56	0.009
	CO	Julian day	1.68	3.19	0.30
		Drainage class	102.45	174.38	0.25
	PL	Julian day	2.37	2.18	0.03
		Seral stage	-639.94	154.35	<0.001
	CO	Julian day	1.65	3.19	0.31
		Seral stage	-116.19	191.32	0.24

Appendix 4.6. Modeling biomass (kg/ha) of accepted species, grass, forb, and deciduous shrub combined (GFS), and lichen by study area (SA: PL and CO) as a function of Julian day and ecosite (Lwl-Bog is the reference category).

SA	Forage metric	Covariate	Beta	CI	*P*-value
PL	Accepted biomass	Julian day	0.94	1.86	0.32
		Lwl-Cedar/ thicket	500.76	539.97	0.07
		Lwl-Fen	79.41	447.20	0.73
		Lwl-Marsh	930.66	619.31	0.003
		Upl-BS	226.62	145.89	0.003
		Upl-BS-Rocky	443.65	251.79	<0.001
		Upl-BS-WS	198.00	197.12	0.05
	GFS	Julian day	-0.34	0.73	0.36
		Lwl-Cedar/ thicket	521.66	213.73	<0.001
		Lwl-Fen	111.83	164.87	0.18
		Lwl-Marsh	924.14	245.14	<0.001
		Upl-BS	77.98	57.75	0.009
		Upl-BS-Rocky	-16.18	99.67	0.75
		Upl-BS-WS	224.35	78.03	<0.001
	Lichen	Julian day	1.32	1.73	0.14
		Lwl-Cedar/ thicket	-33.04	507.02	0.90
		Lwl-Fen	-31.76	419.86	0.88
		Lwl-Marsh	29.24	581.55	0.92
		Upl-BS	169.02	136.36	0.02
		Upl-BS-Rocky	482.51	236.10	<0.001
		Upl-BS-WS	-16.71	183.45	0.86
CO	Accepted biomass	Julian day	1.92	3.22	0.24
		Lwl-Cedar/ thicket	8.20	968.70	0.99
		Lwl-Fen	50.80	354.13	0.78
		Upl-BS	193.50	217.62	0.08
		Upl-BS-WS	29.45	217.98	0.79
	GFS	Julian day	2.40	1.12	<0.001
		Lwl-Cedar/ thicket	49.90	340.32	0.77
		Lwl-Fen	146.69	123.99	0.02
		Upl-BS	46.31	75.71	0.23
		Upl-BS-WS	130.44	75.72	<0.001
	Lichen	Julian day	-0.71	2.95	0.64
		Lwl-Cedar/ thicket	-32.09	897.27	0.94
		Lwl-Fen	-83.60	327.49	0.62
		Upl-BS	160.24	200.67	0.12
		Upl-BS-WS	-89.64	200.75	0.38

Appendix 4.7. Modeling biomass (kg/ha) of accepted species, grass, forb, and deciduous shrub combined (GFS), and lichen by study area (SA: PL and CO) as a function of Julian day and seral-specific ecosite (Mid-late Lwl-Bog is the reference category).

SA	Forage metric	Covariate	Beta	CI	*P*-value
PL	Accepted biomass	Julian day	1.27	1.85	0.18
		Early-Lwl-Bog	204.53	272.17	0.14
		Mid-late-Lwl-Cedar/ thicket	555.93	535.44	0.04
		Mid-late-Lwl-Fen	132.09	445.28	0.56
		Mid-late-Lwl-Marsh	986.89	612.71	0.002
		Early-Upl-BS	408.86	205.85	<0.001
		Mid-late-Upl-BS	236.87	168.30	0.006
		Early-Upl-BS-Rocky	1007.06	612.98	0.001
		Mid-late-Upl-BS-Rocky	425.67	271.70	0.002
		Early-Upl-BS-WS	590.91	319.98	<0.001
		Mid-late-Upl-BS-WS	127.26	227.94	0.27
	GFS	Julian day	0.19	0.60	0.53
		Early-Lwl-Bog	180.43	87.70	<0.001
		Mid-late-Lwl-Cedar/ thicket	569.08	172.54	<0.001
		Mid-late-Lwl-Fen	156.47	133.94	0.02
		Mid-late-Lwl-Marsh	973.30	197.44	<0.001
		Early-Upl-BS	346.74	66.33	<0.001
		Mid-late-Upl-BS	46.99	54.23	0.09
		Early-Upl-BS-Rocky	236.20	197.52	0.02
		Mid-late-Upl-BS-Rocky	5.56	87.55	0.90
		Early-Upl-BS-WS	587.39	103.11	<0.001
		Mid-late-Upl-BS-WS	156.38	73.45	<0.001
	Lichen	Julian day	1.11	1.76	0.22
		Early-Lwl-Bog	-2.93	259.75	0.98
		Mid-late-Lwl-Cedar/ thicket	-32.66	512.16	0.90
		Mid-late-Lwl-Fen	-29.76	425.82	0.89
		Mid-late-Lwl-Marsh	28.91	586.15	0.92
		Early-Upl-BS	73.08	195.98	0.47
		Mid-late-Upl-BS	203.61	160.02	0.01
		Early-Upl-BS-Rocky	786.46	586.37	0.009
		Mid-late-Upl-BS-Rocky	435.31	259.33	0.001
		Early-Upl-BS-WS	-22.61	296.88	0.88
		Mid-late-Upl-BS-WS	-15.59	217.29	0.89

Appendix 4.7. Continued.

SA	Forage metric	Covariate	Beta	CI	*P*-value
CO	Accepted biomass	Julian day	1.59	3.15	0.33
		Early-Lwl-Bog	163.18	389.40	0.41
		Mid-late-Lwl-Cedar/ thicket	35.12	946.59	0.94
		Mid-late-Lwl-Fen	78.10	351.95	0.66
		Early-Upl-BS	81.57	281.28	0.57
		Mid-late-Upl-BS	327.90	258.24	0.01
		Early-Upl-BS-WS	378.18	337.72	0.03
		Mid-late-Upl-BS-WS	-55.59	241.17	0.65
	GFS	Julian day	2.39	0.88	<0.001
		Early-Lwl-Bog	42.44	108.81	0.45
		Mid-late-Lwl-Cedar/ thicket	57.06	265.85	0.67
		Mid-late-Lwl-Fen	153.86	98.35	0.003
		Early-Upl-BS	117.90	78.41	0.004
		Mid-late-Upl-BS	3.68	71.76	0.92
		Early-Upl-BS-WS	450.35	94.24	<0.001
		Mid-late-Upl-BS-WS	26.00	66.86	0.45
	Lichen	Julian day	-1.01	2.92	0.50
		Early-Lwl-Bog	109.40	363.56	0.56
		Mid-late-Lwl-Cedar/ thicket	-15.38	886.30	0.97
		Mid-late-Lwl-Fen	-66.55	328.73	0.69
		Early-Upl-BS	-27.08	262.48	0.84
		Mid-late-Upl-BS	334.77	240.52	0.007
		Early-Upl-BS-WS	-70.77	315.12	0.66
		Mid-late-Upl-BS-WS	-71.04	224.32	0.54

Appendix 4.8. Modeling forb, deciduous (dec.) shrub, or mushroom biomass (kg/ha) by the two dominant ecosites in each study area as a function of Julian day and study area (SA: PL and CO with CO as the reference category).

Forage metric	Ecosite	Covariate	Beta	CI	*P*-value
Forb	Lwl-Bog	SA	44.51	25.12	<0.001
		JD	-0.33	0.39	0.11
	Upl-BS	SA	39.06	17.37	<0.001
		JD	-0.29	0.20	0.006
Dec. shrub	Lwl-Bog	SA	13.67	40.04	0.51
		JD	0.53	0.63	0.10
	Upl-BS	SA	85.09	60.26	0.006
		JD	-0.17	0.70	0.62
Mushroom	Lwl-Bog	SA	-0.11	0.21	0.33
		JD	0.01	0.00	<0.001
	Upl-BS	SA	0.14	0.51	0.60
		JD	0.01	0.01	<0.001

a

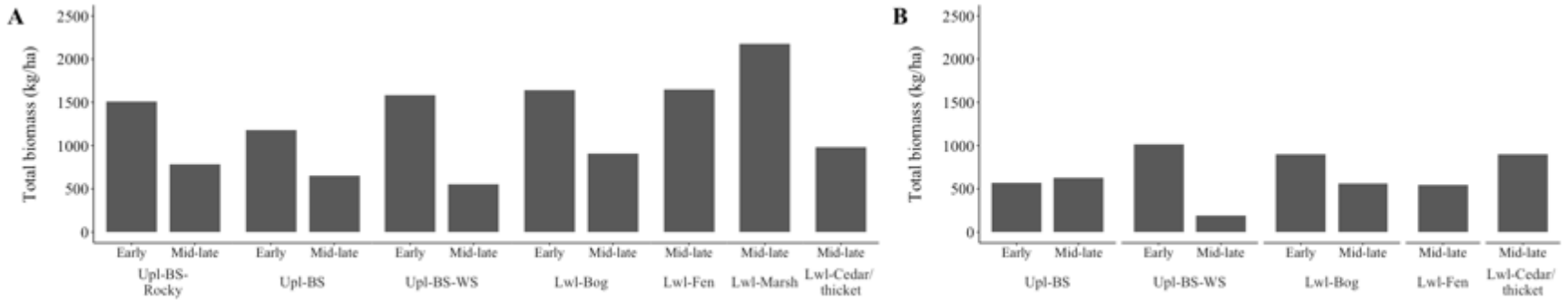

Appendix 4.8. Mean total biomass (kg/ha; accepted and avoided species combined) by ecosite and seral stage (early <20 years, mid-late ≥20 years) at 341 and 126 macroplots sampled in A) Pickle Lake and B) Cochrane, Ontario, respectively, during 2017–2018. Note: not all ecosites existed in both study areas.

Appendix 5. Supplemental materials for Chapter 4

This appendix outlines the methods and results for developing species-specific, continuous-time models to predict forage quality at all macroplots sampled in Pickle Lake and Cochrane used forage quality samples collected within each study area (Appendix 5.1-5.2).

Methods

We used values of digestible energy (DE) or digestible protein (DP) for 931 forage quality samples from 2018 in Pickle Lake (PL) and Cochrane (CO), Ontario to regress species-specific DE or DP on Julian day (Appendix 5.5, 5.6). For each species, we first compared the model fit of linear, quadratic, and exponential model forms based on Akaike Information Criterion corrected for small samples sizes (ΔAIC_c) pooling data across study regions and years. The top model was identified based on a $\Delta AIC_c < 2$. If there was equal support for competing model forms, we selected the linear model (for simplicity and parsimony). Once we determined the best model form, we assessed the relationship between DE or DP and Julian day between the study regions and proceeded to model each study region separately if study region improved model fit ($\Delta AIC_c > 2$). If we modeled a species for each study region separately, we again evaluated the model fit of linear, quadratic, and exponential model forms, to determine if the DE or DP-Julian day relationship differed when each study regions. Finally, we used model selection to assess whether inclusion of environmental covariates, specifically canopy cover (%) and drainage class (upland vs. lowland), improved the model fit ($\Delta AIC_c < 2$). Preliminary analysis indicated canopy cover as a substantially more informative ($\Delta AIC_c > 15$) forest metric compared to basal area (m^2/ha) or stand height (m; Appendix 5.155). In situations where species were collapsed to genius (to increases samples sizes, e.g., *Sorbus*), we compared the top model to a model including the genus' species as a categorical variable, where a $\Delta AIC_c < 2$ between the 2 models indicated that the inclusion of species did not improve the model fit. Again, if there was equal support for competing model forms, we selected the most parsimonious model (i.e., fewest number of parameters). We only evaluated the influence of study regions and environmental covariates when sufficient sample sizes were present (≈10 samples per covariate). Species with an insufficient number of samples to produce regression equations ($n < 7$) and previous year's growth [i.e., old] of each life-form group were assigned the mean (i.e., linear regression intercept) DE or DP value (given the minimal samples and short temporal sampling window for the later). Also, upon preliminary evaluation 1 *Smilicina trifolia* sample had a digestible energy value considerably (~30%) lower than other samples collected at a similar date and therefore was removed before developing the species-specific equation for DE and DP.

Results

Digestible Energy

Forbs. 8 of 9 forbs (except *Clintonia borealis* in PL) had a linear relationship with Julian date, with only 1 species differing between study area and 1 species being influenced by canopy cover. The DE-Julian day relationship was best modeled as a linear function for *Epilobium angustifolium, Hieracium spp.,* and *Rubus chamaemorus,* with study region, canopy cover, and drainage class not improving model fit (when applicable; Appendix 5.7-5.9). In constant, the DE-Julian day relationship for *Smilicina trifolia* was best modeled as a quadratic function, with

study region, canopy cover, and drainage class not improving model fit (Appendix 5.10). Although the DE-Julian day relationship for *Maianthemum canadensis* was best modeled as quadratic function, we decided procced to use a linear function, given the overfit of the quadratic function, with study region, canopy cover, and drainage class not improving model fit (Appendix 5.11).

We decided to model the 2 *Aster* species separately (*Aster ciliolatus* and *Aster macrophylla*), even though when we included *Aster* species as a categorical covariate in a model with Julian day it did not improve the DE-Julian day model fit (Appendix 5.12). For both *Aster ciliolatus* and *Aster macrophylla* the DE-Julian day relationship was best modeled as a linear function with study region and canopy cover did not improving model fit (Appendix 5.13-14). The model for the genius *Aster* (combining *Aster ciliolatus, Aster macrophylla*, and *Aster* spp.) was linearly related to Julian day, with study region and canopy cover not improving model fit (Appendix 5.15). Models of *Clintonia borealis* differed between study regions (Appendix 5.16) with it showing a quadratic relationship to Julian date in PL (Appendix 5.17) and a linear relationship to Julian date in PL (Appendix 5.18). The DE- Julian day relationship was best modeled as a linear function for *Viola spp.* with canopy cover, but not study region improving model fit (Appendix 5.19).

Seven species of forbs (*Apocynum androsaemifolium, Cypripedium acaule, Melampyrum lineare, Petasites palmata, Polygonum cilinode, Streptopus rosea,* and *Taraxecum spp*.) had insufficient sample sizes ($n < 5$) to produce species-specific models. As a result, we combined all forbs samples to develop a forb-specific models to produce 3 general forb equations (Appendix 5.1). Additionally, given the unrealistic seasonal dynamics of digestible energy for *Mertensia paniculata* (i.e., digestible energy increased across the growing season), we will use the general forb equation for *Mertensia paniculata.* We found a quadratic function for predicting forb DE in upland sites with each region having distinct models (Appendix 5.20-5.22), and where canopy cover was also included in the CO upland sites (Appendix 5.23). In contrast the DE-Julian day relationship for forbs in lowlands did not differ across regions but was best modeled as a quadradic function (Appendix 5.24). The 3 general equations were used when species-specific forb equations were not available.

Deciduous shrubs. All 17 deciduous shrubs (except *Vaccinium angustifolium* and *Vaccinium myrtilloides* in CO) had a linear relationship with Julian date, with 5 species differing between study region, and 4 being influenced by canopy cover. The DE-Julian day relationship was best modeled as a linear function for *Acer spicatum, Alnus crispa, Amelanchier spp.* (including *Amelanchier sanguinea* and *Amelanchier spp*), *Betula papyrifera, Betula pumilus, Corylus cornuta, Populus tremuloides,* and *Ribes glandulosum* with study region, canopy cover, and drainage class not improving model fit (when applicable; Appendix 5.25-5.32). Although the DE-Julian day relationship for *Aralia hispidula* was best modeled as a quadratic function (Appendix 5.33) we selected a linear function given that the shape of the quadratic function likely does not reflect the seasonal change in digestible energy.

Given the low number of *Sorbus spp.* samples (*Sorbus Americana* [*n*=6] *and Sorbus decora* [*n*=3]), we combined species to model the genus *Sorbus*. The DE-Julian day relationship was best modeled as a linear function for *Sorbus* (Appendix 5.34). We also included the 2 *Sorbus* species as a categorical covariate a model with Julian day, which confirmed that the DE-Julian

day relationship was similar among the 2 species (Appendix 5.35). For both *Diervilla lonicera* and *Rosa acicularia* the DE-Julian day relationship was best modeled as a linear function with canopy cover improving model fit (Appendix 5.36-37). Given the low number of *Salix spp.* samples (*Salix bebbiana, Salix discolor, Salix humilis, Salix pedicularis, Salix planifolia, Salix pyrifolia*; range: 2-9), we combined species to model the genus *Salix*. The DE-Julian day relationship was best modeled as a linear function for *Salix* with canopy cover improving model fit (Appendix 5.38). We also included the 6 *Salix* species as a categorical covariate in a model with Julian day, which confirmed that the DE-Julian day relationship was similar among all species (Appendix 5.39).

Study region improved model fit for the linear DE-Julian day relationships of *Alnus rugosa, Prunus pensylvanica,* and *Rubus pubescens* (Appendix 5.40-5.42). Within PL and CO, *Alnus rugosa, Prunus pensylvanica,* and *Rubus pubescens* were best modeled using a linear function for Julian day (Appendix 5.43-5.47), with canopy cover improving model fit for *Rubus pubescens* in CO (Appendix 5.48). We identified a similar relationship between digestible energy (DE) and Julian day for *Vaccinium angustifolium* and *Vaccinium myrtilloides,* and therefore to increase our samples sizes we combined species to model the genus *Vaccinium*. The DE-Julian day relationship was best modeled as a quadratic function for *Vaccinium*, with study region improving model fit (Appendix 5.49). Within PL, the DE-Julian day relationship was best modeled as a linear function for *Vaccinium* with canopy cover improving model fit, but not study region, or drainage class (Appendix 5.50). We also included the 2 *Vaccinium* species as a categorical variable in a model with Julian day, which confirmed that the DE-Julian day relationship was similar among the 2 species in PL (Appendix 5.51). In CO, the model including the 2 *Vaccinium* species as a categorical covariate with Julian day was the top model when compared to a model with just digestible energy as a function of Julian day (Appendix 5.52). Therefore, we modeled *Vaccinium angustifolium* and *Vaccinium myrtilloides* separately in CO, where the DE-Julian day relationship was best modeled as a quadratic function for both species, with canopy cover and drainage class not improving the model fit (Appendix 5.53-54).

One species of deciduous shrubs (*Viburnum edule)* had insufficient sample sizes ($n = 2$) to produce a species-specific model, so we combined all deciduous shrubs samples to develop a general deciduous shrub predictive equation. Three separate deciduous shrub equations were developed (Appendix 5.1). The DE-Julian day relationship was best modeled as a linear function for each study region separately (Appendix 5.55). Within PL, the DE-Julian day relationship was best modeled by drainage class, with the inclusion of canopy cover in upland sites (Appendix 5.56-58). In CO the DE-Julian day relationship was best modeled as a linear function with canopy cover, but not drainage class improving model fit (Appendix 5.59). The 3 general equations were used when species-specific deciduous shrub equations were not available (e.g., *Viburnum edule*).

Ground Lichens. All 5 ground lichens had a linear relationship with Julian date, with 3 species differing between study area, and none being influenced by environmental variables. The DE-Julian day relationship was best modeled as a linear function for both *Cladonia spp.* and *Cladonia uncialis* (Appendix 5.60-5.61). Study region improved the model fit of the linear DE-Julian day relationships for *Cladina mitis*, *Cladina rangiferina*, and *Cladina stellaris* with study region improving model fit (Appendix 5.62-5.64). Within PL and CO, *Cladina mitis*, *Cladina rangiferina*, and *Cladina stellaris* were best modeled using a linear function for Julian day

(Appendix 5.65-5.70). When combining all ground lichens, the DE-Julian day relationship was best modeled as a linear function with study region, canopy cover, and drainage class not improving model fit (Appendix 5.71).

Tree Lichens. Although the DE-Julian day relationship for *Evernia mesomorpha* was best modeled as a quadratic function (Appendix 5.72), we selected a linear function given the limited number of samples and that the shape of the quadratic function likely does not accurately reflect the seasonal change in digestible energy. The DE-Julian day relationship was best modeled as a linear function for both and *Usnea spp.* (Appendix 5.73). When combined, the DE-Julian day relationship was best modeled as a linear function for tree lichens, with study region, canopy cover, and drainage class not improving model fit (Appendix 5.74).

Horsetails. The DE-Julian day relationship was best modeled as a linear function for *Equisetum sylvaticum* (Appendix 5.75).

Grass. *Calamagrostis canadensis* was the only species of grass sampled across northern Ontario and the DE-Julian day relationship was best modeled as a linear function (Appendix 5.76).

Mushroom. The DE-Julian day relationship for mushrooms was best modeled as a linear function (Appendix 5.77).

Digestible Protein

Forbs. Nine of 9 forbs (except Aster spp. in CO, and *Clintonia borealis* and *Maianthemum canadensis* in PL) had a linear relationship with Julian date, with 3 species differing between study regions, and 5 species being influenced by canopy cover. The DP -Julian day relationship was best modeled as a linear function for *Hieracium spp.* and *Mertensia paniculata* (Appendix 5.78-5.79). Canopy cover, but not study region or drainage class (which applicable), improving the DP- Julian day linear relationship for *Epilobium angustifolium, Smilicina trifolia,* and *Viola spp.* (Appendix 5.80-5.82). Models of *Rubus chamaemorus* differed between study regions (Appendix 5.83) with both regions showing a linear relationship to Julian day (Appendix 5.84-5.85).

We decided to model the 2 *Aster* species together (*Aster ciliolatus* and *Aster macrophylla*), because when *Aster* species was included as a categorical covariate in a model with Julian day it did not improve the DE-Julian day model fit (Appendix 5.86). Models of *Aster spp.* differed between study regions (Appendix 5.87) with it showing a linear relationship to Julian day in PL with canopy cover improving model fit (Appendix 5.88), whereas in CO the DP-Julian day relationship was best modeled as an exponential function and canopy cover did not improve model fit (Appendix 5.89). Models of *Clintonia borealis* and *Maianthemum canadensis* differed between study regions (Appendix 5.90-5.91). For both species, in PL an exponential relationship to Julian date with canopy cover improved the relationship (Appendix 5.92-5.93) with a linear relationship to Julian date in CO (Appendix 5.94-5.95).

Seven species of forbs (*Apocynum androsaemifolium, Cypripedium acaule, Melampyrum lineare, Petasites palmata, Polygonum cilinode, Streptopus rosea,* and *Taraxecum spp*.) had insufficient sample sizes ($n < 5$) to produce species-specific models. As a result, we combined all

forbs samples to develop a forb-specific models to produce 4 general forb equations (Appendix 5.2). Models of all forbs combined differed between study regions (Appendix 5.96). In PL the DP-Julian day relationship for all forbs combined was best modeled as an exponential function in uplands and a linear function in lowlands with canopy cover improving the relationship in uplands (Appendix 5.97-99). In contrast, the DP-Julian day relationship for all forbs combined in PL was best modeled as an exponential function with canopy cover in uplands, and a linear function in lowlands (Appendix 5.100-102).

Deciduous shrubs. Fourteen of 17 deciduous shrubs (except *Diervilla lonicera* and *Prunus pensylvanica* in PL) had a linear relationship with Julian date, with 6 species differing between study region, and 8 being influenced by canopy cover. The DP-Julian day relationship was best modeled as a linear function for *Alnus crispa, Amelanchier spp.* (*Amelanchier sanguinea* and *Amelanchier spp. combined*), *Betula papyrifera, Corylus cornuta, Populus tremuloides,* and *Sorbus spp.* with study region, canopy cover, and drainage class not improving model fit (when applicable; Appendix 5.103-5.108). Additionally, when we included *Sorbus* species (*Sorbus Americana* and *Sorbus decora*) as a categorical covariate in the model with Julian day, it confirmed a similar DP-Julian day relationship between the 2 species (Appendix 5.109).

The DP-Julian day relationship was best modeled as an exponential function for *Acer spicatum, Betula pumilus*, *Ribes glandulosum* with study region and canopy cover not improving model fit (when applicable; Appendix 5.110-112). Although study region improved the exponential relationship between DP-Julian day for *Aralia hispidula,* given the low number of samples in CO (n=5), we decided to not model the species by study region (Appendix 5.113). The DP-Julian day relationship was best modeled as a linear function for the *Rosa acicularia* and *Alnus rugosa* with canopy cover improving the model fit (Appendix 5.114-115). Although drainage class improved the model fit for *Alnus rugosa,* our upland samples were not evenly distributed across the growing season (i.e., all samples were collected in the first half of the field season and therefore we did not model *Alnus rugosa* by drainage class.

Study region improved model fit for the DP-Julian day relationship of *Diervilla lonicera, Prunus pensylvanica, Rubus pubescens, Salix spp., Vaccinium angustifolium,* and *Vaccinium myrtilloides* (Appendix 5.116-121). *Vaccinium angustifolium* and *Vaccinium myrtilloides* were modeled separately, because including species improved the DP-Julian day relationship (Appendix 5.122). *Diervilla lonicera* and *Prunus pensylvanica* were best modeled using an exponential function in PL and linear function in CO, with canopy cover improving model fit in both regions for *Diervilla lonicera* and only in PL for *Prunus pensylvanica* (Appendix 5.123-126). *Salix spp.* was best modeled using a linear function in both PL and CO (Appendix 5.127-128). We also included the 6 *Salix* species as a categorical covariate in a model with Julian day, which confirmed that the DE-Julian day relationship was similar among all species (Appendix 5.129). In both study regions, *Rubus pubescens* was best modeled using a linear function for Julian day with canopy cover improving model fit in CO (Appendix 5.130-131). *Vaccinium angustifolium* and *Vaccinium myrtilloides* were best modeled using a linear function in both study regions with canopy cover improving model fit for all models (Appendix 5.132-135).

One species of deciduous shrubs (*Viburnum edule)* had insufficient sample sizes ($n = 2$) to produce a species-specific model, so we combined all deciduous shrubs samples to develop a general deciduous shrub predictive equation. Two separate deciduous shrub equations were

developed (Appendix 5.2). The DP-Julian day relationship was best modeled as an exponential function in PL and a linear function in CO with canopy cover improving the model fit in both study regions (Appendix 5.136-138). The 2 general equations will be used when species-specific deciduous shrub equations are unavailable (e.g., *Viburnum edule*).

Ground Lichens. The DP-Julian day relationship was best modeled as a linear function for *Cladonia spp, Cladonia uncialis, Cladina mitis*, *Cladina rangiferina*, and *Cladina stellaris* with study region, canopy cover, and drainage class not improving model fit (when applicable; Appendix 5.139-143). When combining all ground lichens, the DP-Julian day relationship was best modeled as a linear function with study region, canopy cover, and drainage class not improving model fit (Appendix 5.144).

Tree Lichens. Since including species collected (*Evernia mesomorpha* and *Usnea spp.*) did not improve the DP-Julian day relationship for all for tree lichens combined, we decided to proceed with modeling tree lichens combined (Appendix 5.145). Study region improved model fit for the DP-Julian day linear relationship of tree lichens with canopy cover and drainage class not improving model fit (when applicable; Appendix 5.146-148).

Horsetail. Study region improved model fit for the exponential DP-Julian day relationship of *Equisetum sylvaticum,* with canopy cover further improving the model fit in PL (Appendix 5.149-151).

Grass. *Calamagrostis canadensis* was the only species of grass sampled across northern Ontario and the DP-Julian day relationship was best modeled as a linear function (Appendix 5.152).

Mushroom. The DP-Julian day relationship for mushrooms was best modeled as a linear function (Appendix 5.153).

Finally, when we compared lab-derived measured vs predicted values, based on the models above, of DE and DP of a species at a specific macroplot on the day of collection, we found high correlation of 0.83 for DE and 0.91 for DP across all samples, with the average, absolute discrepancy in the observed and predicted values being 0.13 $\pm$ 0.13 kcal/g ($\pm$ SD) in DE and 1.53 $\pm$ 1.64 g of protein/ 100 g of forage in DP (Appendix 5.154).

Appendix 5.1. Number (*n*) of samples used to model life form group or species-specific digestible energy as a linear function of Julian day (JD), and when it improved model fit (based on model selection; Appendix 5.7–5.77) stratified by study region (SR), and/or including Julian day as a quadratic term (JD^2) or canopy cover (CC) interacted with Julian day (JD*CC) or Julian day as quadratic term (JD^2*CC) as covariates, and the model's intercept (B_0; or mean value for species with an insufficient number of samples), covariate coefficient estimates, and r^2 value.

Life form group/ species	n	SR	B_0	JD	JD^2	CC	JD*CC	JD^2*CC	r^2
Upland Forbs	128	PL	2.24	0.01	-0.00004	NA	NA	NA	0.33
Upland Forbs	106	CO	2.56	0.01	-0.00004	-0.006	NA	8.00E-08	0.43
Lowland Forbs	58	Both	-0.02	0.04	-0.0001	NA	NA	NA	0.57
Aster spp.	49	Both	3.59	-0.003	NA	NA	NA	NA	0.28
Aster ciliolatus	17	Both	3.33	-0.002	NA	NA	NA	NA	0.07
Aster macrophylla	31	Both	3.7	-0.003	NA	NA	NA	NA	0.54
Clintonia borealis	25	PL	0.57	0.03	-0.00007	NA	NA	NA	0.72
Clintonia borealis	19	CO	-0.004	0.001	NA	NA	NA	NA	0.53
Epilobium angustifolium	27	Both	4.61	-0.009	NA	NA	NA	NA	0.52
Hieracium spp.	9	Both	4.47	-0.007	NA	NA	NA	NA	0.79
Maianthemum canadensis	53	Both	4.94	-0.008	NA	-0.01	0.00003	NA	0.61
Rubus chamaemorus	22	Both	3.92	-0.004	NA	NA	NA	NA	0.60
Smilicina trifolia	30	Both	-2.52	0.06	0.0002	NA	NA	NA	0.78
Viola spp.	26	Both	4.37	-0.006	NA	-0.01	0.00003	NA	0.51
Upland Deciduous	232	PL	3.75	-0.003	NA	-0.006	0.00002	NA	0.18
Lowland Deciduous	40	PL	3.94	-0.004	NA	NA	NA	NA	0.24
Deciduous	171	CO	4.01	-0.004	NA	-0.003	-0.00005	NA	0.37
Acer spicatum	26	Both	3.36	-0.002	NA	NA	NA	NA	0.30
Alnus crispa	15	Both	3.06	-0.001	NA	NA	NA	NA	0.05
Alnus rugosa	11	PL	4.84	-0.007	NA	NA	NA	NA	0.80
Alnus rugosa	16	CO	4.23	-0.005	NA	NA	NA	NA	0.42
Amelanchier spp.	15	Both	2.87	-0.0002	NA	NA	NA	NA	0.0008
Aralia hispidula	17	Both	4.08	-0.005	NA	NA	NA	NA	0.19
Betula papyrifera	29	Both	3.74	-0.003	NA	NA	NA	NA	0.22
Betula pumilus	15	Both	4.12	-0.006	NA	NA	NA	NA	0.64
Corylus cornuta	8	Both	3.25	-0.003	NA	NA	NA	NA	0.43
Diervilla lonicera	41	Both	3.87	-0.002	NA	-0.002	-0.000004	NA	0.63
Populus tremuloides	16	Both	3.95	-0.004	NA	NA	NA	NA	0.40
Prunus pensylvanica	19	PL	3.94	-0.004	NA	NA	NA	NA	0.47
Prunus pensylvanica	9	CO	4.09	-0.004	NA	NA	NA	NA	0.74
Ribes glandulosum	12	Both	4.25	-0.006	NA	NA	NA	NA	0.86
Rosa acicularia	21	Both	2.66	0.002	NA	0.02	-0.00008	NA	0.47
Rubus pubescens	14	PL	2.74	-0.0004	NA	NA	NA	NA	0.01
Rubus pubescens	23	CO	3.66	-0.003	NA	-0.0008	-0.00001	NA	0.70

Appendix 5.1. Continued.

Life form group/ species	n	SR	B_0	JD	JD^2	CC	JD*CC	JD^2*CC	r^2
Salix spp.	23	Both	3.49	-0.002	NA	NA	NA	NA	0.08
Sorbus spp.	9	Both	3.32	-0.001	NA	NA	NA	NA	0.16
Vaccinium spp.	54	PL	2.98	0.00002	NA	0.01	-0.00006	NA	0.48
Vaccinium angustifolium	27	CO	1.7	0.02	-0.00005	NA	NA	NA	0.82
Vaccinium myrtilloides	21	CO	0.39	0.03	-0.00007	NA	NA	NA	0.53
Ground lichens	112	Both	2.83	0.001	NA	NA	NA	NA	0.06
Cladina mitis	19	PL	2.72	0.001	NA	NA	NA	NA	0.41
Cladina mitis	8	CO	2.52	0.001	NA	NA	NA	NA	0.38
Cladina rangiferina	19	PL	2.86	0.001	NA	NA	NA	NA	0.24
Cladina rangiferina	22	CO	2.49	0.002	NA	NA	NA	NA	0.13
Cladina stellaris	14	PL	2.73	0.002	NA	NA	NA	NA	0.42
Cladina stellaris	8	CO	3.22	0.0001	NA	NA	NA	NA	0
Cladonia spp.	13	Both	3.86	-0.003	NA	NA	NA	NA	0.55
Cladonia uncialis	10	Both	3.18	-0.001	NA	NA	NA	NA	0.06
Tree lichens	28	Both	3.14	0.0001	NA	NA	NA	NA	0
Evernia mesomorpha	12	Both	2.65	0.002	NA	NA	NA	NA	0.11
Usnea spp	16	Both	3.4	-0.001	NA	NA	NA	NA	0.12
Equisetum sylvaticum	33	Both	-2.59	0.06	-0.0002	NA	NA	NA	0.83
Calamagrostis canadensis	15	Both	3.92	-0.006	NA	NA	NA	NA	0.46
Mushroom	7	Both	1.93	0.006	NA	NA	NA	NA	0.19

Appendix 5.2. Number (*n*) of samples used to model life form group or species-specific digestible energy as a function of Julian day (JD), and when it improved model fit (based on model selection; Appendix 5.78–5.153) stratified by study region (SR), or canopy cover (CC) interacted with Julian day (JD*CC) as covariates, and the model's structure (STR; linear or exponential [exp.]) and intercept (B_0; or mean value for species with an insufficient number of samples), covariate coefficient estimates, and r^2 value or pseudo r^2 for non-linear exponential models.

Life form group/ species	n	SR	STR	B_0	JD	CC	JD*CC	r^2
Upland Forbs	127	PL	Exp.	104.67	-0.01	0.03	0.10	0.48
Lowland Forbs	38	PL	Linear	28.18	-0.08	NA	NA	0.30
Upland Forbs	105	CO	Exp.	233.6	-0.02	0.06	-0.38	0.61
Lowland Forbs	19	CO	Linear	37.37	-0.11	NA	NA	0.17
Aster spp.	30	PL	Linear	18.69	-0.06	0.08	-0.0002	0.66
Aster spp.	19	CO	Exp.	121.32	-0.01	NA	NA	0.82
Clintonia borealis	25	PL	Exp.	33.92	-0.008	-0.01	0.2	0.79
Clintonia borealis	19	CO	Linear	29.89	-0.09	NA	NA	0.69
Epilobium angustifolium	27	Both	Linear	33.57	-0.13	0.30	-0.001	0.71
Hieracium spp.	9	Both	Linear	21.75	-0.07	NA	NA	0.77
Maianthemum canadensis	31	PL	Exp.	3718.72	-0.04	0.04	-12.90	0.91
Maianthemum canadensis	22	CO	Linear	26.89	-0.09	NA	NA	0.48
Mertensia paniculata	9	Both	Linear	23.39	-0.05	NA	NA	0.07
Rubus chamaemorus	15	PL	Linear	27.96	-0.10	NA	NA	0.76
Rubus chamaemorus	7	CO	Linear	39.69	-0.14	NA	NA	0.76
Smilicina trifolia	30	Both	Linear	30.36	-0.08	0.1	0.0003	0.71
Viola spp.	26	Both	Linear	17.06	-0.04	0.18	-0.0006	0.60
Deciduous	232	PL	Exp.	139.27	-0.02	0.03	0.15	0.59
Deciduous	171	CO	Linear	22.33	-0.07	0.08	-0.0002	0.52
Acer spicatum	26	Both	Exp.	161.09	-0.01	NA	NA	0.70
Alnus crispa	15	Both	Linear	17.97	-0.04	NA	NA	0.58
Alnus rugosa	27	Both	Linear	16.66	-0.03	0.03	0.00005	0.55
Amelanchier spp.	15	Both	Linear	19.90	-0.06	NA	NA	0.48
Aralia hispidula	17	Both	Exp.	98.31	-0.01	NA	NA	0.58
Betula papyrifera	29	Both	Linear	18.77	-0.05	NA	NA	0.22
Betula pumilus	15	Both	Exp.	4.12	-0.006	NA	NA	0.64
Corylus cornuta	8	Both	Linear	26.83	-0.08	NA	NA	0.54
Diervilla lonicera	24	PL	Exp.	53.47	-0.01	0.004	0.89	0.93
Diervilla lonicera	17	CO	Linear	24.86	-0.08	0.06	-0.00008	0.95
Populus tremuloides	16	Both	Linear	26.61	-0.08	NA	NA	0.67

Appendix 5.2. Continued.

Life form group/ species	n	SR	STR	B_0	JD	CC	JD*CC	r^2
Prunus pensylvanica	19	PL	Exp.	327.72	-0.02	0.06	-0.84	0.86
Prunus pensylvanica	9	CO	Linear	29.49	-0.09	NA	NA	0.79
Ribes glandulosum	12	Both	Exp.	472.44	-0.02	NA	NA	0.96
Rosa acicularia	21	Both	Linear	10.24	-0.03	0.14	-0.0004	0.62
Rubus pubescens	14	PL	Linear	16.77	-0.05	NA	NA	0.29
Rubus pubescens	23	CO	Linear	17.73	-0.06	0.13	-0.0003	0.64
Salix spp.	15	PL	Linear	19.99	-0.06	NA	NA	0.50
Salix spp.	8	CO	Linear	14.06	-0.01	NA	NA	0.01
Sorbus spp.	9	Both	Linear	19.19	-0.06	NA	NA	0.64
Vaccinium angustifolium	25	PL	Linear	9.41	-0.03	0.09	-0.0003	0.81
Vaccinium angustifolium	27	CO	Linear	15.94	-0.05	0.13	-0.0004	0.87
Vaccinium myrtilloides	29	PL	Linear	14.20	-0.05	0.11	-0.0003	0.86
Vaccinium myrtilloides	21	CO	Linear	16.52	-0.05	0.29	-0.0009	0.81
Ground lichens	112	Both	Linear	-1.21	-0.00007	NA	NA	0.00003
Cladina mitis	27	Both	Linear	-1.31	-0.0003	NA	NA	0.001
Cladina rangiferina	41	Both	Linear	-1.48	0.0008	NA	NA	0.01
Cladina stellaris	22	Both	Linear	-0.93	-0.002	NA	NA	0.05
Cladonia spp.	13	Both	Linear	1.10	-0.007	NA	NA	0.37
Cladonia uncialis	10	Both	Linear	-2.43	0.004	NA	NA	0.25
Tree lichens	19	PL	Linear	1.74	-0.002	NA	NA	0.008
Tree lichens	9	CO	Linear	0.08	-0.0003	NA	NA	0.0004
Equisetum sylvaticum	17	PL	Exp.	87.42	-0.01	0.03	0.68	0.93
Equisetum sylvaticum	16	CO	Exp.	182.53	-0.01	NA	NA	0.76
Calamagrostis canadensis	15	Both	Linear	30.63	-0.1	NA	NA	0.56
Mushroom	7	Both	Linear	16.39	-0.003	NA	NA	0.0001

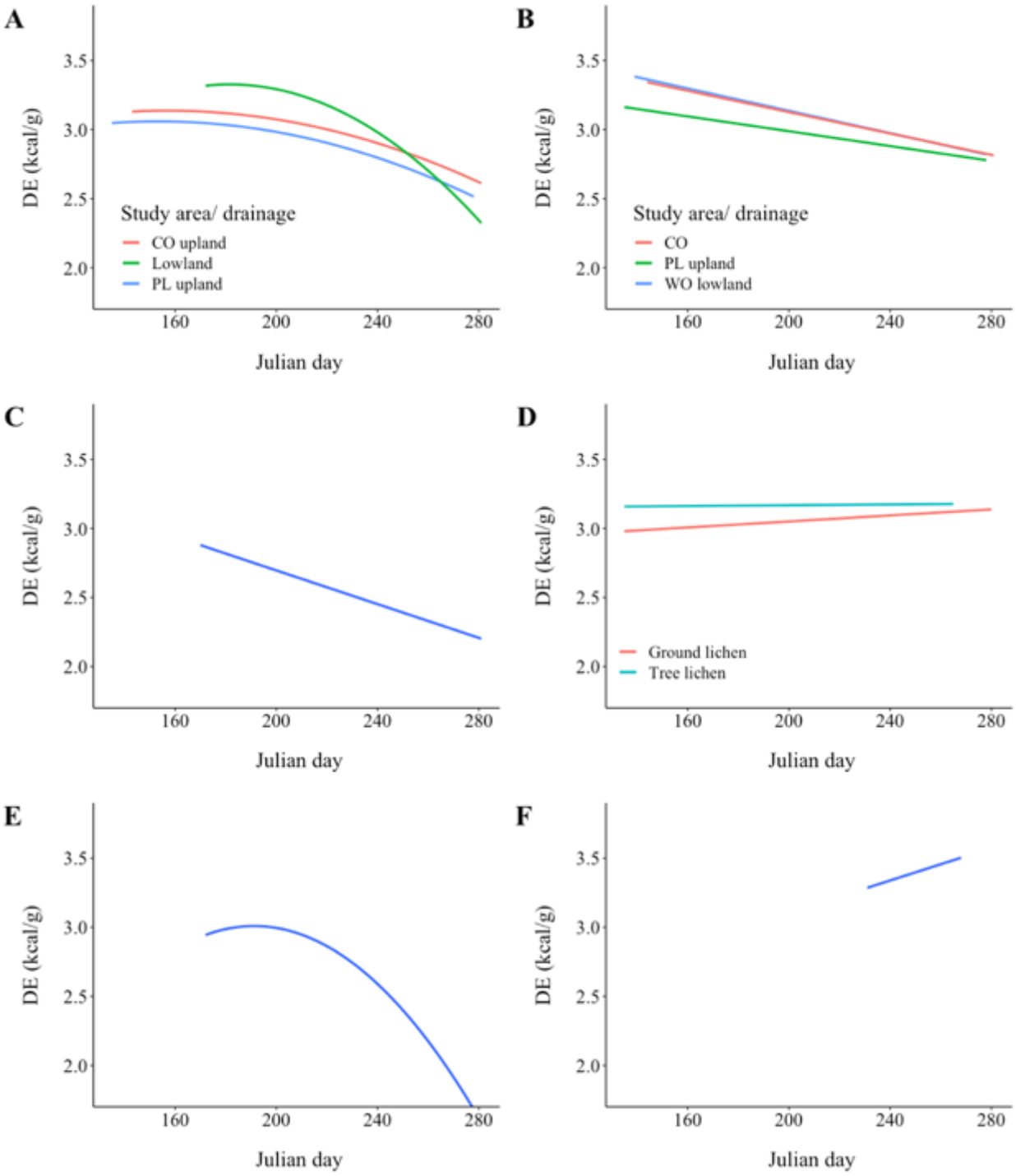

Appendix 5.3. Relationship between digestible energy (kcal/g) of A) forbs, B) deciduous shrubs, C) grasses, D) ground and tree lichens, E) horsetails, and F) mushrooms and Julian day.

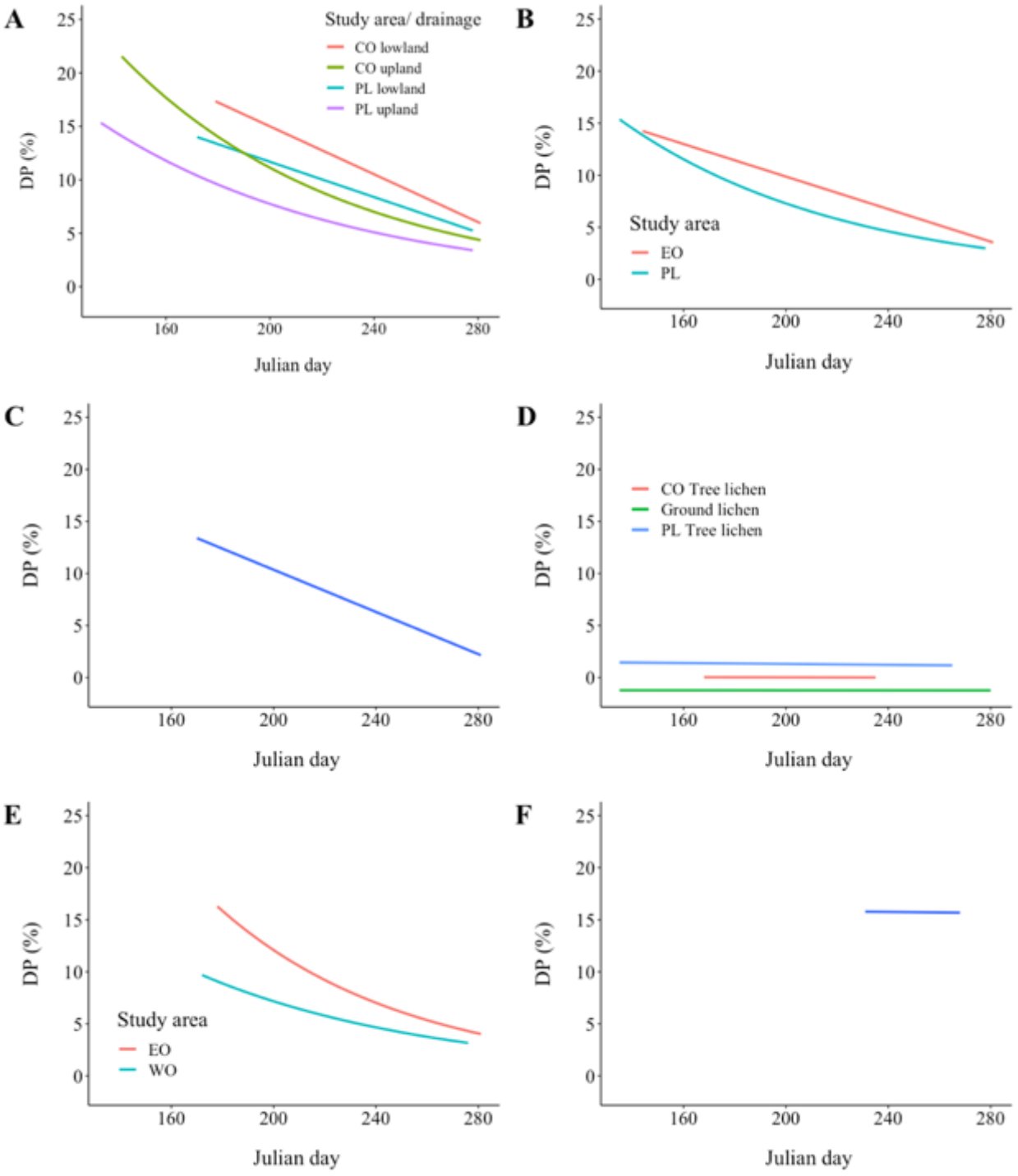

Appendix 5.4. Relationship between digestible protein (%) of A) forbs, B) deciduous shrubs, C) ground lichens, D) tree lichens, E) rock lichens, F) ferns, G) graminoids, H) grasses, and I) mushrooms and Julian day.

Appendix 5.5. Number of species-specific (and life-form group) forage quality samples collected in Pickle Lake (PL) and Cochrane (CO), Ontario, 2018.

Species	PL	CO	Total
Acer spicatum	16	10	26
Alnus crispa	15	0	15
Alnus rugosa	11	16	27
Amelanchier sanguinea	8	0	8
Amelanchier spp.	3	4	7
Apocynum androsaemifolium	3	0	3
Aralia hispidula	12	5	17
Aster ciliolatus	12	5	17
Aster macrophylla	18	13	31
Aster spp.	0	1	1
Betula papyrifera	22	7	29
Betula pumilus	11	4	15
Calamagrostis canadensis	6	9	15
Cladina mitis	19	8	27
Cladina rangiferina	19	22	41
Cladina stellaris	14	8	22
Cladonia spp.	5	8	13
Cladonia uncialis	10	0	10
Clintonia borealis	25	19	44
Corylus cornuta	5	3	8
Cypripedium acaule	1	0	1
Diervilla lonicera	24	17	41
Epilobium angustifolium	15	12	27
Equisetum sylvaticum	16	16	32
Evernia mesomorpha	7	5	12
Hieracium spp.	6	3	9
Maianthemum canadensis,	31	22	53
Melampyrum lineare	1	0	1
Mertensia paniculata	0	9	9
Mushrooms	7	0	7

Appendix 5.5. Continued.

Species	PL	CO	Total
Petasites palmata	3	0	3
Polygonum cilinode	3	0	3
Populus tremuloides	12	4	16
Prunus pensylvanica	19	9	28
Ribes glandulosum	8	4	12
Rosa acicularia	14	7	21
Rubus chamaemorus	15	7	22
Rubus pubescens	14	23	37
Salix bebbiana	4	1	5
Salix discolor	3	0	3
Salix humilis	6	3	9
Salix pedicularis	0	2	2
Salix planifolia	2	0	2
Salix pyrifolia	0	3	3
Smilicina trifolia	20	11	31
Solidago hispida	0	3	3
Sorbus americana	6	0	6
Sorbus decora	3	0	3
Streptopus rosea	4	0	4
Taraxecum spp.	0	4	4
Usnea spp	12	4	16
Vaccinium angustifolium	25	27	52
Vaccinium myrtilloides	29	21	50
Viburnum edule	0	2	2
Viola spp.	9	17	26
Total	553	378	931

Appendix 5.6 . Number and proportion of forage quality samples by life-form groups collected in Pickle Lake (PL) and Cochrane (CO), Ontario, 2018.

	Pickle Lake		Cochrane	
Life-form	*n*	Proportion	*n*	Proportion
Deciduous	272	0.49	171	0.45
Forb	166	0.30	126	0.33
Mushroom	7	0.01	0	0.00
Grass	6	0.01	9	0.02
Horsetail	16	0.03	17	0.04
Ground lichen	67	0.12	46	0.12
Tree Lichen	19	0.03	9	0.02
Total	554	1.00	378	1.00

Appendix 5.7. Model coefficient, number of model parameters (*K*), Akaike's Information Criterion corrected for small sample size (AIC_c), change in AIC_c from best model (ΔAIC_c), and model weights calculated from AIC_c (w_i) for competing models with Julian day (JD) as a linear, quadratic, and exponential term, competing models with Julian day (JD), study region (SR), and their interaction (JD*SR), competing models with Julian day (JD), canopy cover (CC), and their interaction (JD*CC), and competing models with Julian day (JD), drainage class (DC), and their interaction (JD*DC) for digestible energy of *Epilobium angustifolium*.

Model	JD	JD^2	SR	JD*SR	CC	JD*CC	DC	JD*DC	*K*	AIC_c	ΔAIC_c	w_i
Linear	-0.009								2	14.62	0.00	0.46
Exponential	-0.003								2	15.40	0.78	0.31
Quadratic	0.02	-5.39E-05							3	15.95	1.33	0.23
Study region	-0.01		+	+					4	13.55	0.00	0.63
Linear	-0.009								2	14.62	1.08	0.37
Linear	-0.009								2	14.62	0.00	0.83
Canopy cover	-0.01				-0.02	9.12E-05			4	17.77	3.15	0.17
Linear	-0.009								2	14.62	0.00	0.95
Drainage class	-0.008						+	+	4	20.33	5.71	0.05

Appendix 5.8. Model coefficient, number of model parameters (*K*), Akaike's Information Criterion corrected for small sample size (AIC_c), change in AIC_c from best model (ΔAIC_c), and model weights calculated from AIC_c (w_i) for competing models with Julian day (JD) as a linear, quadratic, and exponential term for digestible energy of *Hieracium spp*.

Model	JD	JD^2	*K*	AIC_c	ΔAIC_c	w_i
Quadratic	0.02	-0.0001	3	1.24	0.00	0.58
Linear	-0.007		2	2.75	1.51	0.27
Exponential	-0.002		2	3.96	2.72	0.15

Appendix 5.9. Model coefficient, number of model parameters (*K*), Akaike's Information Criterion corrected for small sample size (AIC_c), change in AIC_c from best model (ΔAIC_c), and model weights calculated from AIC_c (w_i) for competing models with Julian day (JD) as a linear, quadratic, and exponential term, competing models with Julian day (JD), study region (SR), and their interaction (JD*SR), and competing models with Julian day (JD), canopy cover (CC), and their interaction (JD*CC) for digestible energy of *Rubus chamaemorus*.

Model	JD	JD^2	SR	JD*SR	CC	JD*CC	*K*	AIC_c	ΔAIC_c	w_i
Linear	-0.004						2	-27.40	0.00	0.44
Exponential	-0.001						2	-27.15	0.24	0.39
Quadratic	0.007	-2.59E-05					3	-25.50	1.89	0.17
Linear	-0.004						2	-27.40	0.00	0.84
Study region	-0.01		+	+			4	-24.08	3.31	0.16
Linear	-0.004						2	-27.40	0.00	0.87
Canopy cover	-0.003				0.01	-6.17E-05	4	-23.68	3.72	0.13

Appendix 5.10. Model coefficient, number of model parameters (*K*), Akaike's Information Criterion corrected for small sample size (AIC_c), change in AIC_c from best model (ΔAIC_c), and model weights calculated from AIC_c (w_i) for competing models with Julian day (JD) as a linear, quadratic, and exponential term, competing models with Julian day (JD), study region (SR), and their interaction (JD*SR, JD^2*SR), competing models with Julian day (JD), canopy cover (CC), and their interaction (JD*CC, JD^2*CC), and competing models with Julian day (JD), drainage class (DC), and their interaction (JD*DC, JD^2*DC) for digestible energy of *Smilicina trifolia* with the 1 outlier sample removed.

Model	JD	JD^2	SR	JD*SR	JD^2*SR	CC	JD*CC	JD^2*CC	*K*	AIC_c	ΔAIC_c	w_i
Quadratic	0.08	-0.0002							3	-7.56	0.00	1.00
Linear	-0.01								2	12.56	20.12	0.00
Exp.	-0.004								2	16.01	23.57	0.00
Quadratic	0.08	-0.0002							3	-7.56	0.00	0.90
SR 1	0.08	-0.0002	+	+					5	-1.53	6.03	0.04
SR 2	0.08	-0.0002	+		+				5	-1.53	6.03	0.04
SR 3	0.08	-0.0002	+	+	+				6	1.91	9.47	0.01
Quadratic	0.08	-0.0002							3	0.00	0.90	0.00
CC 1	0.08	-0.0002				0.0004	-1.28E-05		5	5.95	0.05	5.95
CC 2	0.08	-0.0002				-0.001		-2.38E-08	5	5.95	0.05	5.95
CC 3	0.09	-0.0002				0.09	-0.0009	1.95E-06	6	9.23	0.01	9.23

Appendix 5.11. Model coefficient, number of model parameters (*K*), Akaike's Information Criterion corrected for small sample size (AIC_c), change in AIC_c from best model (ΔAIC_c), and model weights calculated from AIC_c (w_i) for competing models with Julian day (JD) as a linear, quadratic, and exponential term, competing models with Julian day (JD), study region (SR), and their interaction (JD*SR), competing models with Julian day (JD), canopy cover (CC), and their interaction (JD*CC), and competing models with Julian day (JD), drainage class (DC), and their interaction (JD*DC) for digestible energy of *Maianthemum canadensis*.

Model	JD	JD^2	SR	JD*SR	CC	JD*CC	DC	JD*DC	*K*	AIC_c	ΔAIC_c	w_i
Quadratic	0.04	-0.0001							3	12.47	0.00	1.00
Linear	-0.01								2	24.39	11.93	0.00
Exponential	-0.002								2	25.06	13.59	0.00
Linear	-0.006								2	24.39	0.00	0.80
Study region	-0.005		+	+					4	27.15	2.75	0.20
Canopy cover	-0.008				-0.01	2.67E-05			4	4.72	0.00	1.00
Linear	-0.006								2	24.39	19.67	0.00
Linear	-0.006								2	24.39	0.00	0.62
Drainage class	-0.006						+	+	4	25.41	1.02	0.38

Appendix 5.12. Model coefficient, number of model parameters (*K*), Akaike's Information Criterion corrected for small sample size (AIC_c), change in AIC_c from best model (ΔAIC_c), and model weights calculated from AIC_c (w_i) for competing models with Julian day (JD), species collected (SC), and their interaction (JD*SC) for digestible energy of *Aster spp*.

Model	JD	SC	JD*SC	*K*	AIC_c	ΔAIC_c	w_i
Linear	-0.003			2	-32.80	0.00	0.93
Species collected	-0.002	+	+	4	-27.56	5.24	0.07

Appendix 5.13. Model coefficient, number of model parameters (*K*), Akaike's Information Criterion corrected for small sample size (AIC_c), change in AIC_c from best model (ΔAIC_c), and model weights calculated from AIC_c (w_i) for competing models with Julian day (JD) as a linear, quadratic, and exponential term, competing models with Julian day (JD), study region (SR), and their interaction (JD*SR), and competing models with Julian day (JD), canopy cover (CC), and their interaction (JD*CC) for digestible energy of *Aster ciliolatus*.

Model	JD	JD^2	SR	JD*SR	CC	JD*CC	*K*	AIC_c	ΔAIC_c	w_i
Linear	-0.002						2	5.75	0.00	0.45
Exponential	-0.0005						2	5.76	0.01	0.45
Quadratic	0.009	-2.47E-05					3	8.87	3.12	0.10
Linear	-0.002						2	5.75	0.00	0.97
Study region	-0.004		+	+			4	12.63	5.88	0.03
Linear	-0.002						2	5.75	0.00	0.95
Canopy cover	0.0002				0.009	-4.59E-05	4	11.48	5.73	0.05

Appendix 5.14. Model coefficient, number of model parameters (*K*), Akaike's Information Criterion corrected for small sample size (AIC_c), change in AIC_c from best model (ΔAIC_c), and model weights calculated from AIC_c (w_i) for competing models with Julian day (JD) as a linear, quadratic, and exponential term, competing models with Julian day (JD), study region (SR), and their interaction (JD*SR), and competing models with Julian day (JD), canopy cover (CC), and their interaction (JD*CC) for digestible energy of *Aster macrophylla*.

Model	JD	JD^2	SR	JD*SR	CC	JD*CC	*K*	AIC_c	ΔAIC_c	w_i
Exponential	-0.001						2	-44.30	0.00	0.44
Linear	-0.003						2	-44.25	0.05	0.43
Quadratic	-0.006	5.90E-06					3	-41.71	2.59	0.12
Study region	-0.004		+	+			4	-44.48	0.00	0.53
Linear	-0.003						2	-44.25	0.23	0.47
Canopy cover	-0.004				-0.006	2.54E-05	4	-45.21	0.00	0.73
Linear	-0.003						2	-44.25	1.97	0.27

Appendix 5.15. Model coefficient, number of model parameters (*K*), Akaike's Information Criterion corrected for small sample size (AIC_c), change in AIC_c from best model (ΔAIC_c), and model weights calculated from AIC_c (w_i) for competing models with Julian day (JD) as a linear, quadratic, and exponential term, competing models with Julian day (JD), study region (SR), and their interaction (JD*SR), and competing models with Julian day (JD), canopy cover (CC), and their interaction (JD*CC) for digestible energy of *Aster spp*.

Model	JD	JD^2	SR	JD*SR	CC	JD*CC	*K*	AIC_c	ΔAIC_c	w_i
Linear	-0.003						2	-32.80	0.00	0.43
Exponential	-0.0009						2	-32.69	0.10	0.41
Quadratic	0.002	-1.10 E-05					3	-30.89	1.90	0.17
Study region	-0.004		+	+			4	-33.15	0.00	0.54
Linear	-0.003						2	-32.8	0.35	0.46
Linear	-0.003						2	-32.8	0.00	0.77
Canopy cover	-0.003				-0.001	-1.43E-07	4	-30.43	2.37	0.23

Appendix 5.16. Model coefficient, number of model parameters (*K*), Akaike's Information Criterion corrected for small sample size (AIC_c), change in AIC_c from best model (ΔAIC_c), and model weights calculated from AIC_c (w_i) for competing models with Julian day (JD) as a linear, quadratic, and exponential term, and competing models with Julian day (JD), study region (SR), and their interaction (JD*SR) for digestible energy of *Clintonia borealis*.

Model	JD	JD^2	SR	JD*SR	*K*	AIC_c	ΔAIC_c	w_i
Quadratic	0.014	-4.29E-05			3	-13.20	0.00	0.41
Linear	-0.006				2	-12.88	0.32	0.35
Exponential	-0.002				2	-12.16	1.04	0.24
Study region	-0.004		+	+	4	-25.45	0.00	1
Linear	-0.006				2	-12.88	12.57	0

Appendix 5.17. Model coefficient, number of model parameters (*K*), Akaike's Information Criterion corrected for small sample size (AIC_c), change in AIC_c from best model (ΔAIC_c), and model weights calculated from AIC_c (w_i) for competing models with Julian day (JD) as a linear, quadratic, and exponential term for digestible energy of *Clintonia borealis* in Pickle Lake.

Model	JD	JD^2	*K*	AIC_c	ΔAIC_c	w_i
Quadratic	0.03	-7.43E-05	3	-13.78	0.00	0.75
Linear	-0.006		2	-10.58	3.20	0.15
Exponential	-0.002		2	-9.61	4.17	0.09

Appendix 5.18. Model coefficient, number of model parameters (*K*), Akaike's Information Criterion corrected for small sample size (AIC_c), change in AIC_c from best model (ΔAIC_c), and model weights calculated from AIC_c (w_i) for competing models with Julian day (JD) as a linear, quadratic, and exponential term, and competing models with Julian day (JD), canopy cover (CC), and their interaction (JD*CC) for digestible energy of *Clintonia borealis* in Cochrane.

Model	JD	JD^2	CC	JD*CC	*K*	AIC_c	ΔAIC_c	w_i
Linear	-0.004				2	-12.31	0.00	0.46
Exponential	-0.001				3	-12.27	0.04	0.45
Quadratic	-0.003	-3.31E-06			3	-9.07	3.24	0.09
Canopy cover	-0.01		-0.02	9.30E-05	4	-13.04	0.00	0.59
Linear	-0.004				2	-12.31	0.73	0.41

Appendix 5.19. Model coefficient, number of model parameters (*K*), Akaike's Information Criterion corrected for small sample size (AIC_c), change in AIC_c from best model (ΔAIC_c), and model weights calculated from AIC_c (w_i) for competing models with Julian day (JD) as a linear, quadratic, and exponential term, competing models with Julian day (JD), study region (SR), and their interaction (JD*SR), and competing models with Julian day (JD), canopy cover (CC), and their interaction (JD*CC) for digestible energy of *Viola spp.*

Model	JD	JD^2	SR	JD*SR	CC	JD*CC	*K*	AIC_c	ΔAIC_c	w_i
Linear	-0.003						2	-1.81	0.00	0.45
Exponential	-0.001						2	-1.72	0.09	0.43
Quadratic	0.004	-1.60E-05					3	0.67	2.48	0.13
Linear	-0.003						2	-1.81	0.00	0.95
Study region	-0.003		+	+			4	4.01	5.82	0.05
Canopy cover	-0.006				-0.01	3.21E-05	4	-5.65	0.00	0.87
Linear	-0.003						2	-1.81	3.85	0.13

Appendix 5.20. Model coefficient, number of model parameters (*K*), Akaike's Information Criterion corrected for small sample size (AIC_c), change in AIC_c from best model (ΔAIC_c), and model weights calculated from AIC_c (w_i) for competing models with Julian day (JD) as a linear, quadratic, and exponential term, competing models with Julian day (JD), study region (SR), and their interaction (JD*SR, JD^2*SR), competing models with Julian day (JD), canopy cover (CC), and their interaction (JD*CC, JD^2*CC), and competing models with Julian day (JD), drainage class (DC), and their interaction (JD*DC, JD^2*DC) for digestible energy of all forbs combined.

Model	JD	JD^2	SR	JD*SR	JD^2*SR	CC	JD*CC	JD^2*CC	DC	JD*DC	JD^2*DC	*K*	AIC_c	ΔAIC_c	w_i
Quadratic	0.02	-4.90E-05										3	80.65	0.00	1.00
Linear	-0.005											2	95.44	14.78	0.00
Exp.	-0.002											2	98.84	18.18	0.00
SR 1	0.02	-4.58E-05	+		+							5	78.79	0.00	0.37
SR 2	0.02	-4.69E-05	+	+								5	78.81	0.02	0.36
Quadratic	0.02	-4.90E-05										3	80.65	1.86	0.14
SR 3	0.02	-4.51E-05	+	+	+							6	80.89	2.10	0.13
CC 3	0.03	-7.45E-05				0.02	-0.0002	5.60E-07				6	57.52	0.00	0.39
CC 2	0.02	-5.18E-05				-0.005		7.33E-08				5	57.70	0.18	0.36
CC 1	0.01	-4.83E-05				-0.009	3.13E-05					5	58.42	0.90	0.25
Quadratic	0.02	-4.90E-05										3	80.65	23.13	0.00
DC 3	0.04	-0.0001							+	+	+	6	55.92	0.00	0.42
DC 2	0.01	-5.15E-05							+		+	5	56.34	0.41	0.34
DC 1	0.01	-4.42E-05							+	+		5	57.12	1.19	0.23
Quadratic	0.02	-4.90E-05										3	80.65	24.73	0.00

Appendix 5.21. Model coefficient, number of model parameters (*K*), Akaike's Information Criterion corrected for small sample size (AIC_c), change in AIC_c from best model (ΔAIC_c), and model weights calculated from AIC_c (w_i) for competing models with Julian day (JD) as a linear, quadratic, and exponential term, and competing models with Julian day (JD), study region (SR), and their interaction (JD*SR, JD^2*SR) for digestible energy of all forbs in uplands.

Model	JD	JD^2	SR	JD*SR	JD^2*SR	*K*	AIC_c	ΔAIC_c	w_i
Quadratic	0.01	-3.70E-05				3	37.27	0.00	0.97
Linear	-0.005					2	44.85	7.58	0.02
Exponential	-0.002					2	46.82	9.56	0.01
SR 3	0.02		+		+	5	33.09	0.00	0.41
SR 2	0.008		+	+		5	33.09	0.00	0.40
SR 1	0.007		+	+	+	6	35.22	2.13	0.14
Quadratic	0.01					3	37.27	4.17	0.05

Appendix 5.22. Model coefficient, number of model parameters (*K*), Akaike's Information Criterion corrected for small sample size (AIC_c), change in AIC_c from best model (ΔAIC_c), and model weights calculated from AIC_c (w_i) for competing models with Julian day (JD) as a linear, quadratic, and exponential term, and competing models with Julian day (JD), canopy cover (CC), and their interaction (JD*CC, JD^2*CC) for digestible energy of all forbs in uplands within Pickle Lake.

Model	JD	JD^2	CC	JD*CC	JD^2*CC	*K*	AIC_c	ΔAIC_c	w_i
Quadratic	0.01	-3.50E-05				3	29.08	0.00	0.66
Linear	-0.005					2	31.37	2.30	0.21
Exponential	-0.002					2	32.28	3.21	0.13
CC 1	0.01	-3.27E-05	-0.002		1.93E-09	5	27.51	0.00	0.36
CC 2	0.01	-3.26E-05	-0.002	3.34E-07		5	27.52	0.00	0.36
Quadratic	0.01	-3.50E-05				3	29.08	1.56	0.16
CC1	0.01	-4.34E-05	0.008	-9.14E-05	2.10E-07	6	29.62	2.10	0.12

Appendix 5.23. Model coefficient, number of model parameters (*K*), Akaike's Information Criterion corrected for small sample size (AIC_c), change in AIC_c from best model (ΔAIC_c), and model weights calculated from AIC_c (w_i) for competing models with Julian day (JD) as a linear, quadratic, and exponential term, and competing models with Julian day (JD), canopy cover (CC), and their interaction (JD*CC, JD^2*CC) for digestible energy of all forbs in uplands within Cochrane.

Model	JD	JD^2	CC	JD*CC	JD^2*CC	*K*	AIC_c	ΔAIC_c	w_i
Quadratic	0.01	-3.42E-05				3	7.53	0.00	0.62
Linear	-0.005					2	9.53	2.00	0.23
Exponential	-0.002					2	10.40	2.87	0.15
CC 1	0.01	-4.04E-05	-0.006		8.60E-08	5	-6.02	0.00	0.44
CC 2	0.01	-3.60E-05	-0.01	3.76E-05		5	-5.60	0.42	0.36
Quadratic	0.02	-5.54E-05	0.01	-0.0001	3.93E-07	6	-4.40	1.62	0.20
CC1	0.01	-3.42E-05				3	7.53	13.55	0.00

Appendix 5.24. Model coefficient, number of model parameters (*K*), Akaike's Information Criterion corrected for small sample size (AIC_c), change in AIC_c from best model (AIC_c (w_i) for competing models with Julian day (JD) as a linear, quadratic, and exponential term, and competing models with Julian day (JD), study region (SR), and their interactions (JD*SR, JD^2*SR), competing models with Julian day (JD), canopy cover (CC), and their interactions (JD*CC, JD^2*CC), for digestible energy of all forbs in lowlands.

Model	JD	JD^2	SR	JD*SR	JD^2*SR	CC	JD*CC	JD^2*CC	*K*	AIC_c	ΔAIC_c	w_i
Quadratic	0.04	-0.0001							3	21.01	0.00	0.93
Linear	-0.009								2	26.72	5.71	0.05
Exp.	-0.003								2	28.54	7.53	0.02
Quadratic	0.04	-0.0001							3	21.01	0.00	0.80
SR 2	0.04	-0.0001	+		+				5	25.48	4.47	0.09
SR 1	0.04	-0.0001	+	+					5	25.51	4.50	0.08
SR 3	0.05	-0.0001	+	+	+				6	27.94	6.92	0.03
Quadratic	0.04	-0.0001							3	21.01	0.00	0.82
CC 1	0.04	-9.88E-05				0.0005	1.50E-06		5	25.70	4.69	0.08
CC 2	0.04	-9.89E-05				0.0008		1.43E-09	5	25.70	4.69	0.08
CC 3	0.03	-8.69E-05				-0.04	0.0004	-8.47E-07	6	28.20	7.18	0.02

Appendix 5.25. Model coefficient, number of model parameters (*K*), Akaike's Information Criterion corrected for small sample size (AIC_c), change in AIC_c from best model (ΔAIC_c), and model weights calculated from AIC_c (w_i) for competing models with Julian day (JD) as a linear, quadratic, and exponential term, competing models with Julian day (JD), study region (SR), and their interaction (JD*SR), and competing models with Julian day (JD), canopy cover (CC), and their interaction (JD*CC) for digestible energy of *Acer spicatum*.

Model	JD	JD^2	SR	JD*SR	CC	JD*CC	*K*	AIC_c	ΔAIC_c	w_i
Exponential	-0.0009						2	-15.31	0.00	0.45
Linear	-0.002						2	-15.29	0.02	0.44
Quadratic	-0.004	3.93E-06					3	-12.47	2.84	0.11
Linear	-0.002						2	-15.29	0.00	0.92
Study region	-0.003		+	+			4	-10.52	4.77	0.08
Linear	-0.002						2	-15.29	0.00	0.75
Canopy cover	-0.002				-0.0006	-6.19E-06	4	-13.14	2.15	0.25

Appendix 5.26. Model coefficient, number of model parameters (*K*), Akaike's Information Criterion corrected for small sample size (AIC_c), change in AIC_c from best model (ΔAIC_c), and model weights calculated from AIC_c (w_i) for competing models with Julian day (JD) as a linear, quadratic, and exponential term for digestible energy of *Alnus crispa*.

Model	JD	JD^2	*K*	AIC_c	ΔAIC_c	w_i
Linear	-0.001		2	-5.84	0.00	0.45
Exponential	-0.0004		2	-5.83	0.01	0.45
Quadratic	0.02	-3.83E-05	3	-2.91	2.93	0.10

Appendix 5.27. Model coefficient, number of model parameters (*K*), Akaike's Information Criterion corrected for small sample size (AIC_c), change in AIC_c from best model (ΔAIC_c), and model weights calculated from AIC_c (w_i) for competing models with Julian day (JD) as a linear, quadratic, and exponential term for digestible energy of *Amelanchier spp.* (including *Amelanchier sanguinea* and *Amelanchier spp.*).

Model	JD	JD^2	*K*	AIC_c	ΔAIC_c	w_i
Linear	-0.0002		2	-0.32	0.00	0.43
Exponential	-5.96E-05		2	-0.32	0.00	0.43
Quadratic	0.04	-8.10E-05	3	1.77	2.09	0.15

Appendix 5.28. Model coefficient, number of model parameters (*K*), Akaike's Information Criterion corrected for small sample size (AIC_c), change in AIC_c from best model (ΔAIC_c), and model weights calculated from AIC_c (w_i) for competing models with Julian day (JD) as a linear, quadratic, and exponential term, competing models with Julian day (JD), study region (SR), and their interaction (JD*SR), competing models with Julian day (JD), canopy cover (CC), and their interaction (JD*CC), and competing models with Julian day (JD), drainage class (DC), and their interaction (JD*DC) for digestible energy of *Betula papyrifera*.

Model	JD	JD^2	SR	JD*SR	CC	JD*CC	DC	JD*DC	*K*	AIC_c	ΔAIC_c	w_i
Linear	-0.003								2	-3.07	0.00	0.44
Exponential	-0.001								2	-3.05	0.02	0.44
Quadratic	-0.001	-4.52E-06							3	-0.39	2.68	0.12
Linear	-0.003								2	-3.07	0.00	0.85
Study region	0.0004		+	+					4	0.35	3.42	0.15
Linear	-0.003								2	-3.07	0.00	0.83
Canopy cover	-0.003				-0.01	1.23E-05			4	0.17	3.23	0.17
Linear	-0.003								2	-3.07	0.00	0.86
Drainage class	-0.0007						+	+	4	0.64	3.71	0.14

Appendix 5.29. Model coefficient, number of model parameters (*K*), Akaike's Information Criterion corrected for small sample size (AIC_c), change in AIC_c from best model (ΔAIC_c), and model weights calculated from AIC_c (w_i) for competing models with Julian day (JD) as a linear, quadratic, and exponential term, competing models with Julian day (JD) for digestible energy of *Betula pumilus.*

Model	JD	JD^2	SR	JD*SR	CC	JD*CC	*K*	AIC_c	ΔAIC_c	w_i
Linear	-0.006						2	-6.08	0.00	0.49
Exponential	-0.002						2	-5.64	0.45	0.39
Quadratic	0.004	-2.31E-05					3	-3.23	2.85	0.12

Appendix 5.30. Model coefficient, number of model parameters (*K*), Akaike's Information Criterion corrected for small sample size (AIC_c), change in AIC_c from best model (ΔAIC_c), and model weights calculated from AIC_c (w_i) for competing models with Julian day (JD) as a linear, quadratic, and exponential term for digestible energy of *Corylus cornuta*.

Model	JD	JD^2	*K*	AIC_c	ΔAIC_c	w_i
Linear	-0.003		2	1.40	0.00	0.50
Exponential	-0.001		2	1.43	0.03	0.49
Quadratic	0.006	-2.05E-05	3	10.58	9.18	0.01

Appendix 5.31. Model coefficient, number of model parameters (*K*), Akaike's Information Criterion corrected for small sample size (AIC_c), change in AIC_c from best model (ΔAIC_c), and model weights calculated from AIC_c (w_i) for competing models with Julian day (JD) as a linear, quadratic, and exponential term, competing models with Julian day (JD), study region (SR), and their interaction (JD*SR), competing models with Julian day (JD), canopy cover (CC), and their interaction (JD*CC), and competing models with Julian day (JD), drainage class (DC), and their interaction (JD*DC) for digestible energy of *Populus tremuloides*.

Model	JD	JD^2	SR	JD*SR	CC	JD*CC	DC	JD*DC	*K*	AIC_c	ΔAIC_c	w_i
Exponential	-0.001								2	-5.51	0.00	0.46
Linear	-0.004								2	-5.49	0.02	0.46
Quadratic	-0.008	9.11E-06							3	-1.90	3.61	0.08
Linear	-0.004								2	-5.49	0.00	0.83
Study region	-0.01		+	+					4	-2.32	3.17	0.17
Linear	-0.004								2	-5.49	0.00	0.93
Canopy cover	-0.006				-0.02	6.80E-05			4	-0.32	5.17	0.07
Linear	-0.004								2	-5.49	0.00	0.96
Drainage class	-0.005						+	+	4	0.99	6.48	0.04

Appendix 5.32. Model coefficient, number of model parameters (*K*), Akaike's Information Criterion corrected for small sample size (AIC_c), change in AIC_c from best model (ΔAIC_c), and model weights calculated from AIC_c (w_i) for competing models with Julian day (JD) as a linear, quadratic, and exponential term for digestible energy of *Ribes glandulosum*.

Model	JD	JD^2	*K*	AIC_c	ΔAIC_c	w_i
Exponential	-0.002			-5.70	0.00	0.49
Linear	-0.006		2	-5.57	0.13	0.46
Quadratic	-0.009	6.47E-06	3	-0.99	4.71	0.05

Appendix 5.33. Model coefficient, number of model parameters (*K*), Akaike's Information Criterion corrected for small sample size (AIC_c), change in AIC_c from best model (ΔAIC_c), and model weights calculated from AIC_c (w_i) for competing models with Julian day (JD) as a linear, quadratic, and exponential term, competing models with Julian day (JD), study region (SR), and their interaction (JD*SR), competing models with Julian day (JD), canopy cover (CC), and their interaction (JD*CC), and competing models with Julian day (JD), drainage class (DC), and their interaction (JD*DC) for digestible energy of *Aralia hispidula*.

Model	JD	JD^2	SR	JD*SR	CC	JD*CC	DC	JD*DC	*K*	AIC_c	ΔAIC_c	w_i
Quadratic	-0.10	0.0002							3	20.43	0.00	0.73
Exponential	-0.002								2	23.69	3.26	0.14
Linear	-0.005								2	23.90	3.48	0.13
Linear	-0.005								2	23.9	0.00	0.89
Study region	-0.004		+	+					4	28.02	4.12	0.11
Linear	-0.005								2	23.9	0.00	0.98
Canopy cover	-0.005				0.01	5.80E-05			4	31.43	7.53	0.02
Drainage class	0.03						+	+	4	23.17	0.00	0.59
Linear	-0.005								2	23.9	0.74	0.41

Appendix 5.34. Model coefficient, number of model parameters (*K*), Akaike's Information Criterion corrected for small sample size (AIC_c), change in AIC_c from best model (ΔAIC_c), and model weights calculated from AIC_c (w_i) for competing models with Julian day (JD) as a linear, quadratic, and exponential term for digestible energy of *Sorbus*.

Model	JD	JD^2	*K*	AIC_c	ΔAIC_c	w_i
Linear	-0.001		2	0.14	0.00	0.37
Exponential	-0.0005		2	0.18	0.03	0.37
Quadratic	0.04	-9.54E-05	3	0.87	0.73	0.26

Appendix 5.35. Model coefficient, number of model parameters (*K*), Akaike's Information Criterion corrected for small sample size (AIC_c), change in AIC_c from best model (ΔAIC_c), and model weights calculated from AIC_c (w_i) for competing models with Julian day (JD), species collected (SC), and their interaction (JD*SC) for digestible energy of *Sorbus*.

Model	JD	SC	JD*SC	*K*	AIC_c	ΔAIC_c	w_i
Linear	-0.001			2	0.14	0.00	0.98
Species collected	-0.002	+	+	4	8.23	8.09	0.02

Appendix 5.36. Model coefficient, number of model parameters (*K*), Akaike's Information Criterion corrected for small sample size (AIC_c), change in AIC_c from best model (ΔAIC_c), and model weights calculated from AIC_c (w_i) for competing models with Julian day (JD) as a linear, quadratic, and exponential term, competing models with Julian day (JD), study region (SR), and their interaction (JD*SR), and competing models with Julian day (JD), canopy cover (CC), and their interaction (JD*CC) for digestible energy of *Diervilla lonicera*.

Model	JD	JD^2	SR	JD*SR	CC	JD*CC	*K*	AIC_c	ΔAIC_c	w_i
Linear	-0.002						2	-28.79	0.00	0.42
Exponential	-0.0005						2	-28.74	0.05	0.41
Quadratic	0.004	-1.34E-05					3	-26.96	1.82	0.17
Linear	-0.002						2	-28.79	0.00	0.87
Study region	-0.002		+	+			4	-24.90	3.88	0.13
Canopy cover	-0.003				-0.002	-4.40E-06	4	-57.80	0.00	1.00
Linear	-0.003						2	-28.79	29.01	0.00

Appendix 5.37. Model coefficient, number of model parameters (*K*), Akaike's Information Criterion corrected for small sample size (AIC_c), change in AIC_c from best model (ΔAIC_c), and model weights calculated from AIC_c (w_i) for competing models with Julian day (JD) as a linear, quadratic, and exponential term, competing models with Julian day (JD), study region (SR), and their interaction (JD*SR), competing models with Julian day (JD), canopy cover (CC), and their interaction (JD*CC), and competing models with Julian day (JD), drainage class (DC), and their interaction (JD*DC) for digestible energy of *Rosa acicularia.*

Model	JD	JD^2	SR	JD*SR	CC	JD*CC	DC	JD*DC	*K*	AIC_c	ΔAIC_c	w_i
Linear	-0.002								2	-13.81	0.00	0.39
Exponential	-0.0006								2	-13.77	0.04	0.38
Quadratic	0.03	-6.12E-05							3	-12.79	1.02	0.23
Linear	-0.002								2	-13.81	0.00	0.68
Study region	0.004		+	+					4	-12.28	1.54	0.32
Canopy cover	0.002				0.02	-8.16E-05			4	-17.56	0.00	0.87
Linear	-0.002								2	-13.81	3.74	0.13
Linear	-0.002								2	-13.81	0.00	0.82
Drainage class	-0.004						+	+	4	-10.76	3.05	0.18

Appendix 5.38. Model coefficient, number of model parameters (*K*), Akaike's Information Criterion corrected for small sample size (AIC_c), change in AIC_c from best model (ΔAIC_c), and model weights calculated from AIC_c (w_i) for competing models with Julian day (JD) as a linear, quadratic, and exponential term, competing models with Julian day (JD), study region (SR), and their interaction (JD*SR), competing models with Julian day (JD), canopy cover (CC), and their interaction (JD*CC), and competing models with Julian day (JD), drainage class (DC), and their interaction (JD*DC) for digestible energy of *Salix.*

Model	JD	JD^2	SR	JD*SR	CC	JD*CC	DC	JD*DC	*K*	AIC_c	ΔAIC_c	w_i
Linear	-0.002								2	4.47	0.00	0.45
Exponential	-0.0007								2	4.48	0.01	0.45
Quadratic	0.005	-1.63E-05							3	7.31	2.84	0.11
Study region	-0.002		+	+					4	3.02	0.00	0.67
Linear	-0.002								2	4.47	1.45	0.33
Linear	-0.002								2	4.47	0.00	0.93
Canopy cover	-0.004				-0.008	4.43E-05			4	9.50	5.03	0.07
Linear	-0.002								2	4.47	0.00	0.91
Drainage class	-0.005						+	+	4	9.08	4.61	0.09

Appendix 5.39. Model coefficient, number of model parameters (*K*), Akaike's Information Criterion corrected for small sample size (AIC_c), change in AIC_c from best model (ΔAIC_c), and model weights calculated from AIC_c (w_i) for competing models with Julian day (JD), species collected (SC), and their interaction (JD*SC) for digestible energy of *Salix*.

Model	JD	SC	JD*SC	*K*	AIC_c	ΔAIC_c	w_i
Linear	-0.002			2	4.47	0.00	1.00
Species collected	-0.003	+	+	12	42.01	37.54	0.00

Appendix 5.40. Model coefficient, number of model parameters (*K*), Akaike's Information Criterion corrected for small sample size (AIC_c), change in AIC_c from best model (ΔAIC_c), and model weights calculated from AIC_c (w_i) for competing models with Julian day (JD) as a linear, quadratic, and exponential term, and competing models with Julian day (JD), study region (SR), and their interaction (JD*SR) for digestible energy of *Alnus rugosa*.

Model	JD	JD^2	SR	JD*SR	*K*	AIC_c	ΔAIC_c	w_i
Linear	-0.006				2	-5.28	0.00	0.45
Exponential	-0.002				2	-5.07	0.22	0.41
Quadratic	0.005	-2.39E-05			3	-2.98	2.30	0.14
Study region	-0.005		+	+	4	-11.7	0.00	0.96
Linear	-0.006				2	-5.28	6.42	0.04

Appendix 5.41. Model coefficient, number of model parameters (*K*), Akaike's Information Criterion corrected for small sample size (AIC_c), change in AIC_c from best model (ΔAIC_c), and model weights calculated from AIC_c (w_i) for competing models with Julian day (JD) as a linear, quadratic, and exponential term, and competing models with Julian day (JD), study region (SR), and their interaction (JD*SR) for digestible energy of *Prunus pensylvanica.*

Model	JD	JD^2	SR	JD*SR	*K*	AIC_c	ΔAIC_c	w_i
Quadratic	0.01	-3.63E-05			3	-14.94	0.00	0.41
Linear	-0.004				2	-14.44	0.50	0.32
Exponential	-0.001				2	-14.03	0.91	0.26
Study region	-0.004		+	+	4	-19.80	0.00	0.94
Linear	-0.004				2	-14.44	5.36	0.06

Appendix 5.42. Model coefficient, number of model parameters (*K*), Akaike's Information Criterion corrected for small sample size (AIC_c), change in AIC_c from best model (ΔAIC_c), and model weights calculated from AIC_c (w_i) for competing models with Julian day (JD) as a linear, quadratic, and exponential term, and competing models with Julian day (JD), study region (SR), and their interaction (JD*SR) for digestible energy of *Rubus pubescens.*

Model	JD	JD^2	SR	JD*SR	*K*	AIC_c	ΔAIC_c	w_i
Linear	-0.003				2	-8.99	0.00	0.41
Exponential	-0.001				2	-8.88	0.10	0.39
Quadratic	0.01	-2.92E-05			3	-7.51	1.48	0.20
Study region	-0.004		+	+	4	-15.17	0.00	0.96
Linear	-0.003				2	-8.99	6.18	0.04

Appendix 5.43. Model coefficient, number of model parameters (*K*), Akaike's Information Criterion corrected for small sample size (AIC_c), change in AIC_c from best model (ΔAIC_c), and model weights calculated from AIC_c (w_i) for competing models with Julian day (JD) as a linear, quadratic, and exponential term for digestible energy of *Alnus rugosa* in Pickle Lake.

Model	JD	JD^2	*K*	AIC_c	ΔAIC_c	w_i
Linear	-0.007		2	-3.61	0.00	0.52
Exponential	-0.002		2	-3.03	0.58	0.39
Quadratic	0.01	-4.54E-05	3	-0.21	3.40	0.09

Appendix 5.44. Model coefficient, number of model parameters (*K*), Akaike's Information Criterion corrected for small sample size (AIC_c), change in AIC_c from best model (ΔAIC_c), and model weights calculated from AIC_c (w_i) for competing models with Julian day (JD) as a linear, quadratic, and exponential term for digestible energy of *Alnus rugosa* in Cochrane.

Model	JD	JD^2	*K*	AIC_c	ΔAIC_c	w_i
Linear	-0.005		2	-4.10	0.00	0.46
Exponential	-0.002		2	-3.90	0.20	0.42
Quadratic	0.01	-3.85E-05	3	-1.30	2.80	0.11

Appendix 5.45. Model coefficient, number of model parameters (*K*), Akaike's Information Criterion corrected for small sample size (AIC_c), change in AIC_c from best model (ΔAIC_c), and model weights calculated from AIC_c (w_i) for competing models with Julian day (JD) as a linear, quadratic, and exponential term, competing models with Julian day (JD), canopy cover (CC), and their interaction (JD*CC), and competing models with Julian day (JD), drainage class (DC), and their interaction (JD*DC) for digestible energy of *Prunus pensylvanica* in Pickle Lake.

Model	JD	JD^2	CC	JD*CC	DC	JD*DC	*K*	AIC_c	ΔAIC_c	w_i
Linear	-0.004						2	-8.52	0.00	0.44
Exponential	-0.001						2	-8.28	0.24	0.39
Quadratic	0.008	-2.76E-05					3	-6.71	1.82	0.18
Linear	-0.004						2	-8.52	0.00	0.85
Canopy cover	-0.006		-0.01	5.53E-05			4	-5.05	3.48	0.15
Linear	-0.003						2	-8.52	0.00	0.78
Drainage class	-0.003				+	+	4	-5.96	2.56	0.22

Appendix 5.46. Model coefficient, number of model parameters (*K*), Akaike's Information Criterion corrected for small sample size (AIC_c), change in AIC_c from best model (ΔAIC_c), and model weights calculated from AIC_c (w_i) for competing models with Julian day (JD) as a linear, quadratic, and exponential term for digestible energy of *Prunus pensylvanica* in Cochrane.

Model	JD	JD^2	*K*	AIC_c	ΔAIC_c	w_i
Linear	-0.004		2	-13.13	0.00	0.45
Exponential	-0.001		2	-12.75	0.38	0.37
Quadratic	0.02	-4.29E-05	3	-11.23	1.90	0.17

Appendix 5.47. Model coefficient, number of model parameters (*K*), Akaike's Information Criterion corrected for small sample size (AIC_c), change in AIC_c from best model (ΔAIC_c), and model weights calculated from AIC_c (w_i) for competing models with Julian day (JD) as a linear, quadratic, and exponential term, and competing models with Julian day (JD), canopy cover (CC), and their interaction (JD*CC) for digestible energy of *Rubus pubescens* in Pickle Lake.

Model	JD	JD^2	CC	JD*CC	*K*	AIC_c	ΔAIC_c	w_i
Exponential	-0.0001				2	-5.29	0.00	0.47
Linear	-0.0004				2	-5.29	0.00	0.47
Quadratic	-0.007	1.52E-05			3	-1.41	3.89	0.07
Linear	-0.0004				2	-5.29	0.00	0.94
Canopy cover	-0.003		-0.01	5.10E-05	4	0.13	5.43	0.06

Appendix 5.48. Model coefficient, number of model parameters (*K*), Akaike's Information Criterion corrected for small sample size (AIC_c), change in AIC_c from best model (ΔAIC_c), and model weights calculated from AIC_c (w_i) for competing models with Julian day (JD) as a linear, quadratic, and exponential term, competing models with Julian day (JD), canopy cover (CC), and their interaction (JD*CC), and competing models with Julian day (JD), drainage class (DC), and their interaction (JD*DC) for digestible energy of *Rubus pubescens* in Cochrane.

Model	JD	JD^2	CC	JD*CC	DC	JD*DC	*K*	AIC_c	ΔAIC_c	w_i
Linear	-0.004						2	-6.72	0.00	0.45
Exponential	-0.002						2	-6.58	0.14	0.42
Quadratic	-0.003	-3.31E-06					3	-4.20	2.52	0.13
Canopy cover	-0.003		-0.0008	-1.28E-05			4	-16.85	0.00	0.99
Linear	-0.004						2	-6.72	10.12	0.01
Linear	-0.004						2	-6.72	0.00	0.90
Drainage class	0.0007				+	+	4	-2.24	4.49	0.10

Appendix 5.49. Model coefficient, number of model parameters (*K*), Akaike's Information Criterion corrected for small sample size (AIC_c), change in AIC_c from best model (ΔAIC_c), and model weights calculated from AIC_c (w_i) for competing models with Julian day (JD) as a linear, quadratic, and exponential term, and competing models with Julian day (JD), study region (SR), and their interaction (JD*SR, JD^2*SR) for digestible energy of *Vaccinium.*

Model	JD	JD^2	SR	JD*SR	JD^2*SR	*K*	AIC_c	ΔAIC_c	w_i
Quadratic	0.01	-3.87E-05				3	-34.14	0.00	0.66
Linear	-0.003					2	-31.60	2.54	0.19
Exponential	-0.001					2	-31.15	2.98	0.15
SR 3	0.02		+	+	+	6	-72.57	0.00	0.79
SR 2	0.008		+		+	5	-68.87	3.70	0.12
SR 1	0.007		+	+		5	-68.16	4.41	0.09
Quadratic	0.01					3	-34.14	38.43	0.00

Appendix 5.50. Model coefficient, number of model parameters (*K*), Akaike's Information Criterion corrected for small sample size (AIC_c), change in AIC_c from best model (ΔAIC_c), and model weights calculated from AIC_c (w_i) for competing models with Julian day (JD) as a linear, quadratic, and exponential term, competing models with Julian day (JD), canopy cover (CC), and their interaction (JD*CC), and competing models with Julian day (JD), drainage class (DC), and their interaction (JD*DC) for digestible energy of *Vaccinium* in Pickle Lake.

Model	JD	JD^2	CC	JD*CC	DC	JD*DC	*K*	AIC_c	ΔAIC_c	w_i
Exponential	-0.0009						2	-23.92	0.00	0.43
Linear	-0.002						2	-23.87	0.05	0.42
Quadratic	-0.008	1.28E-05					3	-21.83	2.09	0.15
Canopy cover	1.62E-06		0.01	-5.97E-05			4	-41.41	0.00	1.00
Linear	-0.002						2	-23.87	17.54	0.00
Drainage class	-0.002				+	+	4	-25.31	0.00	0.67
Linear	-0.002						2	-23.87	1.44	0.33

Appendix 5.51. Model coefficient, number of model parameters (*K*), Akaike's Information Criterion corrected for small sample size (AIC_c), change in AIC_c from best model (ΔAIC_c), and model weights calculated from AIC_c (w_i) for competing models with Julian day (JD), species collected (SC), and their interaction (JD*SC) for digestible energy of *Vaccinium* in Pickle Lake.

Model	JD	SC	JD*SC	*K*	AIC_c	ΔAIC_c	w_i
Linear	-0.002			2	-23.87	0.00	0.68
Species collected	-0.002	+	+	4	-22.41	1.46	0.32

Appendix 5.52. Model coefficient, number of model parameters (*K*), Akaike's Information Criterion corrected for small sample size (AIC_c), change in AIC_c from best model (ΔAIC_c), and model weights calculated from AIC_c (w_i) for competing models with Julian day (JD), species collected (SC), and their interaction (JD*SC) for digestible energy of *Vaccinium* in Cochrane.

Model	JD	SC	JD*SC	*K*	AIC_c	ΔAIC_c	w_i
Species collected	-0.006			4	-53.14	0.00	0.99
Linear	-0.004	+	+	2	-44.43	8.72	0.01

Appendix 5.53. Model coefficient, number of model parameters (*K*), Akaike's Information Criterion corrected for small sample size (AIC_c), change in AIC_c from best model (ΔAIC_c), and model weights calculated from AIC_c (w_i) for competing models with Julian day (JD) as a linear, quadratic, and exponential term, competing models with Julian day (JD), canopy cover (CC), and their interaction (JD*CC, JD^2*CC), and competing models with Julian day (JD), drainage class (DC), and their interaction (JD*DC, JD^2*DC) for digestible energy of *Vaccinium angustifolium* in Cochrane.

Model	JD	JD^2	CC	JD*CC	JD^2*CC	DC	JD*DC	JD^2*DC	*K*	AIC_c	ΔAIC_c	w_i
Quadratic	0.02	-5.03E-05							3	-37.32	0.00	0.87
Linear	-0.006								2	-32.76	4.55	0.09
Exp.	-0.002								2	-31.42	5.89	0.05
Quadratic	0.02	-5.03E-05							3	-37.32	0.00	0.81
CC 2	0.02	-5.47E-05	-0.001		-2.68E-09				5	-32.85	4.46	0.09
CC 1	0.02	-5.47E-05	-0.001	-4.98E-07					5	-32.85	4.47	0.09
CC 3	0.02	-4.67E-05	-0.02	0.0001	-3.00E-07				6	-29.32	8.00	0.01
Quadratic	0.02	-5.03E-05							3	-37.32	0.00	0.84
DC 1	0.02	-5.15E-05				+	+		5	-32.45	4.87	0.07
DC 2	0.02	-5.09E-05				+		+	5	-32.41	4.90	0.07
DC 3	0.03	-7.15E-05				+	+	+	6	-29.43	7.88	0.02

Appendix 5.54. Model coefficient, number of model parameters (*K*), Akaike's Information Criterion corrected for small sample size (AIC_c), change in AIC_c from best model (ΔAIC_c), and model weights calculated from AIC_c (w_i) for competing models with Julian day (JD) as a linear, quadratic, and exponential term, competing models with Julian day (JD), canopy cover (CC), and their interaction (JD*CC, JD^2*CC), and competing models with Julian day (JD), drainage class (DC), and their interaction (JD*DC, JD^2*DC) for digestible energy of *Vaccinium myrtilloides* in Cochrane.

Model	JD	JD^2	CC	JD*CC	JD^2*CC	DC	JD*DC	JD^2*DC	*K*	AIC_c	ΔAIC_c	w_i
Quadratic	0.03	-6.65E-05							3	-22.59	0.00	0.85
Linear	-0.003								2	-17.80	4.79	0.08
Exp.	-0.0008								2	-17.58	5.01	0.07
Quadratic	0.03	-6.65E-05							3	-22.59	0.00	0.93
CC 2	0.03	-6.75E-05	0.004	-1.76E-05					5	-15.77	6.82	0.03
CC 1	0.03	-6.62E-05	0.002		-2.96E-08				5	-15.66	6.93	0.03
CC 3	0.05	-0.0001	0.08	-0.0007	1.54E-06				6	-13.90	8.69	0.01
Quadratic	0.03	-6.65E-05							3	-37.32	0.00	0.84
DC 2	0.03	-5.68E-05				+		+	5	-32.45	4.87	0.07
DC 1	0.03	-6.21E-05				+	+		5	-32.41	4.90	0.07
DC 3	-0.80	1.83E-03				+	+	+	6	-29.43	7.88	0.02

Appendix 5.55. Model coefficient, number of model parameters (*K*), Akaike's Information Criterion corrected for small sample size (AIC_c), change in AIC_c from best model (ΔAIC_c), and model weights calculated from AIC_c (w_i) for competing models with Julian day (JD) as a linear, quadratic, and exponential term, and competing models with Julian day (JD), study region (SR), and their interaction (JD*SR) for digestible energy of all deciduous shrubs combined.

Model	JD	JD^2	SR	JD*SR	*K*	AIC_c	ΔAIC_c	w_i
Quadratic	0.003	-1.45E-05			3	67.34	0.00	0.41
Linear	-0.003				2	67.72	0.38	0.34
Exponential	-0.001				2	68.31	0.97	0.25
Study region	-0.004		+	+	4	52.21	0.00	1.00
Linear	-0.003				2	67.72	15.51	0.00

Appendix 5.56. Model coefficient, number of model parameters (*K*), Akaike's Information Criterion corrected for small sample size (AIC_c), change in AIC_c from best model (ΔAIC_c), and model weights calculated from AIC_c (w_i) for competing models with Julian day (JD) as a linear, quadratic, and exponential term, competing models with Julian day (JD), study region (SR), and their interaction (JD*SR), and competing models with Julian day (JD), canopy cover (CC), and their interaction (JD*CC) for digestible energy of all deciduous shrubs in Pickle Lake.

Model	JD	JD^2	CC	JD*CC	DC	JD*DC	*K*	AIC_c	ΔAIC_c	w_i
Exponential	-0.001						2	62.77	0.00	0.43
Linear	-0.003						2	62.84	0.07	0.41
Quadratic	-0.004	3.78E-06					3	64.80	2.03	0.16
Canopy cover	-0.004		-0.007	2.21E-05			4	48.98	0.00	1.00
Linear	-0.003						2	62.84	13.86	0.00
Drainage class	-0.004				+	+	4	59.03	0.00	0.87
Linear	-0.003						2	62.84	3.80	0.13

Appendix 5.57. Model coefficient, number of model parameters (*K*), Akaike's Information Criterion corrected for small sample size (AIC_c), change in AIC_c from best model (ΔAIC_c), and model weights calculated from AIC_c (w_i) for competing models with Julian day (JD) as a linear, quadratic, and exponential term, and competing models with Julian day (JD), canopy cover (CC), and their interaction (JD*CC) for digestible energy of all deciduous shrubs in uplands within Pickle Lake.

Model	JD	JD^2	CC	JD*CC	*K*	AIC_c	ΔAIC_c	w_i
Exponential	-0.0009				2	46.34	0.00	0.43
Linear	-0.003				2	46.45	0.11	0.40
Quadratic	-0.01	7.31E-06			3	48.19	1.85	0.17
Canopy cover	-0.003		-0.006	2.04E-05	4	38.59	0.00	0.98
Linear	-0.003				2	46.45	7.87	0.02

Appendix 5.58. Model coefficient, number of model parameters (*K*), Akaike's Information Criterion corrected for small sample size (AIC_c), change in AIC_c from best model (ΔAIC_c), and model weights calculated from AIC_c (w_i) for competing models with Julian day (JD) as a linear, quadratic, and exponential term, and competing models with Julian day (JD), canopy cover (CC), and their interaction (JD*CC) for digestible energy of all deciduous shrubs in lowlands within Pickle Lake.

Model	JD	JD^2	CC	JD*CC	*K*	AIC_c	ΔAIC_c	w_i
Linear	-0.004				2	15.10	0.00	0.44
Exponential	-0.001				2	15.15	0.05	0.43
Quadratic	-0.0006	-7.72E-06			3	17.52	2.42	0.13
Linear	-0.004				2	15.10	0.00	0.91
Canopy cover	-0.004		-0.002	-4.70E-06	4	19.63	4.53	0.09

Appendix 5.59. Model coefficient, number of model parameters (*K*), Akaike's Information Criterion corrected for small sample size (AIC_c), change in AIC_c from best model (ΔAIC_c), and model weights calculated from AIC_c (w_i) for competing models with Julian day (JD) as a linear, quadratic, and exponential term, competing models with Julian day (JD), study region (SR), and their interaction (JD*SR), and competing models with Julian day (JD), canopy cover (CC), and their interaction (JD*CC) for digestible energy of all deciduous shrubs in Cochrane.

Model	JD	JD^2	CC	JD*CC	DC	JD*DC	*K*	AIC_c	ΔAIC_c	w_i
Quadratic	0.01	-2.83E-05					3	-15.42	0.00	0.55
Linear	-0.004						2	-13.95	1.47	0.26
Exponential	-0.001						2	-13.33	2.09	0.19
Canopy cover	-0.004		-0.003	-4.67E-07			4	-44.59	0.00	1.00
Linear	-0.004						2	-13.95	30.63	0.00
Linear	-0.004						2	-13.95	0.00	0.84
Drainage class	-0.005				+	+	4	-10.70	3.25	0.16

Appendix 5.60. Model coefficient, number of model parameters (*K*), Akaike's Information Criterion corrected for small sample size (AIC_c), change in AIC_c from best model (ΔAIC_c), and model weights calculated from AIC_c (w_i) for competing models with Julian day (JD) as a linear, quadratic, and exponential term for digestible energy of *Cladonia spp.*

Model	JD	JD^2	*K*	AIC_c	ΔAIC_c	w_i
Linear	-0.003		2	-13.01	0.00	0.48
Exponential	-0.0008		2	-12.98	0.03	0.47
Quadratic	-0.001	-3.68E-06	3	-8.71	4.29	0.06

Appendix 5.61. Model coefficient, number of model parameters (*K*), Akaike's Information Criterion corrected for small sample size (AIC_c), change in AIC_c from best model (ΔAIC_c), and model weights calculated from AIC_c (w_i) for competing models with Julian day (JD) as a linear, quadratic, and exponential term for digestible energy of *Cladonia uncialis.*

Model	JD	JD^2	*K*	AIC_c	ΔAIC_c	w_i
Exponential	-0.0002		2	-10.51	0.00	0.48
Linear	-0.0007		2	-10.50	0.00	0.48
Quadratic	-0.01	2.88E-05	3	-5.47	5.03	0.04

Appendix 5.62. Model coefficient, number of model parameters (*K*), Akaike's Information Criterion corrected for small sample size (AIC_c), change in AIC_c from best model (ΔAIC_c), and model weights calculated from AIC_c (w_i) for competing models with Julian day (JD) as a linear, quadratic, and exponential term, and competing models with Julian day (JD), study region (SR), and their interaction (JD*SR) for digestible energy of *Cladina mitis.*

Model	JD	JD^2	SR	JD*SR	*K*	AIC_c	ΔAIC_c	w_i
Exponential	0.0005				2	-34.17	0.00	0.45
Linear	0.002				2	-34.16	0.01	0.44
Quadratic	0.0006	2.38E-06			3	-31.42	2.75	0.11
Study region	0.001		+	+	4	-50.80	0.00	1.00
Linear	0.002				2	-34.16	16.64	0.00

Appendix 5.63. Model coefficient, number of model parameters (*K*), Akaike's Information Criterion corrected for small sample size (AIC_c), change in AIC_c from best model (ΔAIC_c), and model weights calculated from AIC_c (w_i) for competing models with Julian day (JD) as a linear, quadratic, and exponential term, and competing models with Julian day (JD), study region (SR), and their interaction (JD*SR) for digestible energy of *Cladina rangiferina.*

Model	JD	JD^2	SR	JD*SR	*K*	AIC_c	ΔAIC_c	w_i
Linear	0.002				2	-11.12	0.00	0.44
Exponential	0.0006				2	-11.10	0.02	0.43
Quadratic	0.004	-4.41E-06			3	-8.73	2.39	0.13
Study region	0.002		+	+	4	-11.56	0.00	0.56
Linear	0.002				2	-11.12	0.44	0.44

Appendix 5.64. Model coefficient, number of model parameters (*K*), Akaike's Information Criterion corrected for small sample size (AIC_c), change in AIC_c from best model (ΔAIC_c), and model weights calculated from AIC_c (w_i) for competing models with Julian day (JD) as a linear, quadratic, and exponential term, and competing models with Julian day (JD), study region (SR), and their interaction (JD*SR) for digestible energy of *Cladina stellaris.*

Model	JD	JD^2	SR	JD*SR	*K*	AIC_c	ΔAIC_c	w_i
Linear	0.001				2	-29.23	0.00	0.45
Exponential	0.0003				2	-29.22	0.01	0.45
Quadratic	0.002	-2.91E-06			3	-26.25	2.98	0.10
Study region	5.29E-05		+	+	4	-35.16	0.00	0.95
Linear	0.001				2	-29.23	5.94	0.05

Appendix 5.65. Model coefficient, number of model parameters (*K*), Akaike's Information Criterion corrected for small sample size (AIC_c), change in AIC_c from best model (ΔAIC_c), and model weights calculated from AIC_c (w_i) for competing models with Julian day (JD) as a linear, quadratic, and exponential term, and competing models with Julian day (JD), canopy cover (CC), and their interaction (JD*CC) for digestible energy of *Cladina mitis* in Pickle Lake.

Model	JD	JD^2	CC	JD*CC	*K*	AIC_c	ΔAIC_c	w_i
Exponential	0.0005				2	-36.97	0.00	0.44
Linear	0.001				2	-36.90	0.07	0.42
Quadratic	-0.002	9.13E-06			3	-34.63	2.34	0.14
Linear	0.001				2	-36.90	0.00	0.63
Canopy cover	1.17E-05		-0.008	2.84E-05	4	-35.87	1.03	0.37

Appendix 5.66. Model coefficient, number of model parameters (*K*), Akaike's Information Criterion corrected for small sample size (AIC_c), change in AIC_c from best model (ΔAIC_c), and model weights calculated from AIC_c (w_i) for competing models with Julian day (JD) as a linear, quadratic, and exponential term for digestible energy of *Cladina mitis* in Cochrane.

Model	JD	JD^2	*K*	AIC_c	ΔAIC_c	w_i
Linear	0.001		2	-7.16	0.00	0.48
Exponential	0.0005		2	-7.05	0.11	0.46
Quadratic	0.01	-2.66E-05	3	-2.93	4.23	0.06

Appendix 5.67. Model coefficient, number of model parameters (*K*), Akaike's Information Criterion corrected for small sample size (AIC_c), change in AIC_c from best model (ΔAIC_c), and model weights calculated from AIC_c (w_i) for competing models with Julian day (JD) as a linear, quadratic, and exponential term, and competing models with Julian day (JD), canopy cover (CC), and their interaction (JD*CC) for digestible energy of *Cladina rangiferina* in Pickle Lake.

Model	JD	JD^2	CC	JD*CC	*K*	AIC_c	ΔAIC_c	w_i
Exponential	0.0004				2	-29.95	0.00	0.45
Linear	0.001				2	-29.92	0.03	0.44
Quadratic	-0.002	8.03E-06			3	-27.19	2.76	0.11
Linear	0.001				2	-29.92	0.00	0.86
Canopy cover	0.003		0.009	-3.70E-05	4	-26.35	3.57	0.14

Appendix 5.68. Model coefficient, number of model parameters (*K*), Akaike's Information Criterion corrected for small sample size (AIC_c), change in AIC_c from best model (ΔAIC_c), and model weights calculated from AIC_c (w_i) for competing models with Julian day (JD) as a linear, quadratic, and exponential term, competing models with Julian day (JD), canopy cover (CC), and their interaction (JD*CC), and competing models with Julian day (JD), drainage class (DC), and their interaction (JD*DC) for digestible energy of *Cladina rangiferina* in Cochrane.

Model	JD	JD^2	CC	JD*CC	DC	JD*DC	*K*	AIC_c	ΔAIC_c	w_i
Linear	0.002						2	5.89	0.00	0.44
Exponential	0.0008						2	5.94	0.05	0.43
Quadratic	0.01	-1.98E-05					3	8.36	2.47	0.13
Linear	0.002						2	5.89	0.00	0.95
Canopy cover	0.003		0.007	-3.04E-05			4	11.92	6.03	0.05
Linear	0.002						2	5.89	0.00	0.92
Drainage class	0.001				+	+	4	10.90	5.01	0.08

Appendix 5.69. Model coefficient, number of model parameters (*K*), Akaike's Information Criterion corrected for small sample size (AIC_c), change in AIC_c from best model (ΔAIC_c), and model weights calculated from AIC_c (w_i) for competing models with Julian day (JD) as a linear, quadratic, and exponential term, and competing models with Julian day (JD), canopy cover (CC), and their interaction (JD*CC) for digestible energy of *Cladina stellaris* in Pickle Lake.

Model	JD	JD^2	CC	JD*CC	*K*	AIC_c	ΔAIC_c	w_i
Linear	0.002				2	-19.18	0.00	0.47
Exponential	0.0006				2	-19.15	0.03	0.46
Quadratic	0.004	-5.50E-06			3	-15.28	3.90	0.07
Canopy cover	0.001		-0.009	2.51E-05	4	-29.99	0.00	1.00
Linear	0.002				2	-19.18	10.81	0.00

Appendix 5.70. Model coefficient, number of model parameters (*K*), Akaike's Information Criterion corrected for small sample size (AIC_c), change in AIC_c from best model (ΔAIC_c), and model weights calculated from AIC_c (w_i) for competing models with Julian day (JD) as a linear, quadratic, and exponential term for digestible energy of *Cladina stellaris* in Cochrane.

Model	JD	JD^2	*K*	AIC_c	ΔAIC_c	w_i
Linear	5.29E-05		2	-11.40	0.00	0.50
Exponential	1.64E-05		2	-11.40	0.00	0.50
Quadratic	0.0006	-1.28E-06	3	-2.07	9.33	0.00

Appendix 5.71. Model coefficient, number of model parameters (*K*), Akaike's Information Criterion corrected for small sample size (AIC_c), change in AIC_c from best model (ΔAIC_c), and model weights calculated from AIC_c (w_i) for competing models with Julian day (JD) as a linear, quadratic, and exponential term, competing models with Julian day (JD), study region (SR), and their interaction (JD*SR), competing models with Julian day (JD), canopy cover (CC), and their interaction (JD*CC), and competing models with Julian day (JD), drainage class (DC), and their interaction (JD*DC) for digestible energy of all ground lichens combined.

Model	JD	JD^2	SR	JD*SR	CC	JD*CC	DC	JD*DC	*K*	AIC_c	ΔAIC_c	w_i
Linear	0.001								2	-56.26	0.00	0.42
Exponential	0.0004								2	-56.24	0.02	0.41
Quadratic	0.004	-5.96E-06							3	-54.45	1.81	0.17
Linear	-0.001								2	-56.26	0.00	0.88
Study region	-0.001		+	+					4	-52.21	4.05	0.12
Linear	0.001								2	-56.26	0.00	0.88
Canopy cover	0.001				-0.0007	1.74E-06			4	-52.21	4.05	0.12
Linear	0.001								2	-56.26	0.00	0.89
Drainage class	0.001						+	+	4	-51.99	4.27	0.11

Appendix 5.72. Model coefficient, number of model parameters (*K*), Akaike's Information Criterion corrected for small sample size (AIC_c), change in AIC_c from best model (ΔAIC_c), and model weights calculated from AIC_c (w_i) for competing models with Julian day (JD) as a linear, quadratic, and exponential term for digestible energy of *Evernia mesomorpha*.

Model	JD	JD^2	*K*	AIC_c	ΔAIC_c	w_i
Quadratic	0.08	-0.0002	3	-10.87	0.00	0.97
Linear	0.002		2	-2.24	8.63	0.01
Exponential	0.0007		2	-2.16	8.71	0.01

Appendix 5.73. Model coefficient, number of model parameters (*K*), Akaike's Information Criterion corrected for small sample size (AIC_c), change in AIC_c from best model (ΔAIC_c), and model weights calculated from AIC_c (w_i) for competing models with Julian day (JD) as a linear, quadratic, and exponential term, competing models with Julian day (JD), study region (SR), and their interaction (JD*SR), competing models with Julian day (JD), canopy cover (CC), and their interaction (JD*CC), and competing models with Julian day (JD), drainage class (DC), and their interaction (JD*DC) for digestible energy of *Usnea spp.*

Model	JD	JD^2	SR	JD*SR	CC	JD*CC	DC	JD*DC	*K*	AIC_c	ΔAIC_c	w_i
Exponential	-0.0003								2	-18.71	0.00	0.46
Linear	-0.001								2	-18.71	0.00	0.46
Quadratic	-0.003	4.58E-06							3	-15.12	3.59	0.08
Linear	-0.001								2	-18.70	0.00	0.98
Study region	-0.001		+	+					4	-10.72	7.99	0.02
Linear	-0.001								2	-18.70	0.00	0.97
Canopy cover	-0.0005				0.0006	-9.27E-06			4	-11.64	7.06	0.03
Linear	-0.001								2	-18.70	0.00	0.95
Drainage class	-0.001						+	+	4	-12.68	6.02	0.05

Appendix 5.74. Model coefficient, number of model parameters (*K*), Akaike's Information Criterion corrected for small sample size (AIC_c), change in AIC_c from best model (ΔAIC_c), and model weights calculated from AIC_c (w_i) for competing models with Julian day (JD) as a linear, quadratic, and exponential term, competing models with Julian day (JD), study region (SR), and their interaction (JD*SR), competing models with Julian day (JD), canopy cover (CC), and their interaction (JD*CC), and competing models with Julian day (JD), drainage class (DC), and their interaction (JD*DC) for digestible energy of all tree lichens combined.

Model	JD	JD^2	SR	JD*SR	CC	JD*CC	DC	JD*DC	*K*	AIC_c	ΔAIC_c	w_i
Exponential	0.0001								2	-24.18	0.00	0.44
Linear	4.54E-05								2	-24.17	0.00	0.44
Quadratic	0.003	-6.60E-06							3	-21.53	2.65	0.12
Linear	0.0001								2	-24.18	0.00	0.61
Study region	0.0009		+	+					4	-23.31	0.86	0.39
Linear	0.0001								2	-24.18	0.00	0.82
Canopy cover	0.004				0.01	-6.32E-05			4	-21.13	3.04	0.18
Linear	0.0001								2	-24.18	0.00	0.87
Drainage class	0.002						+	+	4	-20.43	3.74	0.13

Appendix 5.75. Model coefficient, number of model parameters (*K*), Akaike's Information Criterion corrected for small sample size (AIC_c), change in AIC_c from best model (ΔAIC_c), and model weights calculated from AIC_c (w_i) for competing models with Julian day (JD) as a linear, quadratic, and exponential term, competing models with Julian day (JD), study region (SR), and their interaction (JD*SR, JD^2*SR), competing models with Julian day (JD), canopy cover (CC), and their interaction (JD*CC, JD^2*CC), and competing models with Julian day (JD), drainage class (DC), and their interaction (JD*DC, JD^2*DC) for digestible energy of *Equisetum sylvaticum.*

Model	JD	JD^2	SR	JD*SR	JD^2*SR	CC	JD*CC	JD^2*CC	DC	JD*DC	JD^2*DC	*K*	AIC_c	ΔAIC_c	w_i
Quadratic	0.06	-0.0002										3	-0.20	0.00	1.00
Linear	-0.01											2	24.85	25.05	0.00
Exp.	-0.004											2	29.51	29.71	0.00
Quadratic	0.06	-0.0002										3	-0.20	0.00	0.83
SR 2	0.07	-0.0002	+			+						5	4.55	4.75	0.08
SR 1	0.07	-0.0002	+		+							5	4.60	4.79	0.08
SR 3	0.06	-0.0002	+		+	+						6	7.75	7.95	0.02
CC 2	0.06	-0.0002				-0.01		1.53E-07				5	-0.57	0.00	0.29
CC 3	0.08	-0.0002				0.07	-0.0007	1.73E-06				6	-0.28	0.29	0.25
Quadratic	0.06	-0.0002										3	-0.20	0.38	0.24
CC 1	0.06	-0.0002				-0.02	6.65E-05					5	-0.02	0.56	0.22
DC 3	0.06	-0.0002										3	-0.20	0.00	0.50
DC 2	0.11	-0.0003							+	+	+	6	0.29	0.49	0.39
DC 1	0.06	-0.0002							+		+	5	3.90	4.10	0.06
Quadratic	0.06	-0.0002							+	+		5	4.37	4.56	0.05

Appendix 5.76. Model coefficient, number of model parameters (*K*), Akaike's Information Criterion corrected for small sample size (AIC_c), change in AIC_c from best model (ΔAIC_c), and model weights calculated from AIC_c (w_i) for competing models with Julian day (JD) as a linear, quadratic, and exponential term for digestible energy of *Calamagrostis canadensis*.

Model	JD	JD^2	*K*	AIC_c	ΔAIC_c	w_i
Linear	-0.006		2	6.30	0.00	0.46
Exponential	-0.002		2	6.66	0.36	0.39
Quadratic	0.02	-6.28E-05	3	8.54	2.24	0.15

Appendix 5.77. Model coefficient, number of model parameters (*K*), Akaike's Information Criterion corrected for small sample size (AIC_c), change in AIC_c from best model (ΔAIC_c), and model weights calculated from AIC_c (w_i) for competing models with Julian day (JD) as a linear, quadratic, and exponential term for digestible energy of mushrooms.

Model	JD	JD^2	*K*	AIC_c	ΔAIC_c	w_i
Linear	0.006		2	8.61	0.00	0.50
Exponential	0.002		2	8.64	0.03	0.50
Quadratic	0.33	-0.0007	3	20.35	11.75	0.00

Appendix 5.78. Model coefficient, number of model parameters (*K*), Akaike's Information Criterion corrected for small sample size (AIC_c), change in AIC_c from best model (ΔAIC_c), and model weights calculated from AIC_c (w_i) for competing models with Julian day (JD) as a linear, quadratic, and exponential term for digestible protein of *Hieracium spp*.

Model	JD	JD^2	*K*	AIC_c	ΔAIC_c	w_i
Exponential	-0.01		2	44.97	0.00	0.66
Linear	-0.07		2	46.38	1.41	0.33
Quadratic	-0.19	0.0003	3	52.68	7.72	0.01

Appendix 5.79. Model coefficient, number of model parameters (*K*), Akaike's Information Criterion corrected for small sample size (AIC_c), change in AIC_c from best model (ΔAIC_c), and model weights calculated from AIC_c (w_i) for competing models with Julian day (JD) as a linear, quadratic, and exponential term for digestible protein of *Mertensia paniculata* in Cochrane.

Model	JD	JD^2	*K*	AIC_c	ΔAIC_c	w_i
Exponential	-0.005		2	57.62	0.00	0.40
Linear	-0.05		2	57.74	0.11	0.37
Quadratic	-3.69	0.009	3	58.72	1.10	0.23

Appendix 5.80. Model coefficient, number of model parameters (*K*), Akaike's Information Criterion corrected for small sample size (AIC_c), change in AIC_c from best model (ΔAIC_c), and model weights calculated from AIC_c (w_i) for competing models with Julian day (JD) as a linear, quadratic, and exponential term, competing models with Julian day (JD), study region (SR), and their interaction (JD*SR), competing models with Julian day (JD), canopy cover (CC), and their interaction (JD*CC), and competing models with Julian day (JD), drainage class (DC), and their interaction (JD*DC) for digestible protein of *Epilobium angustifolium*.

Model	JD	JD^2	SR	JD*SR	CC	JD*CC	DC	JD*DC	*K*	AIC_c	ΔAIC_c	w_i
Linear	-0.14								2	159.09	0.00	0.43
Exponential	-0.02								2	159.25	0.16	0.40
Quadratic	-0.41	0.0006							3	161.00	1.91	0.17
Linear	-0.14								2	159.09	0.00	0.81
Study region	-0.15		+	+					3	161.95	2.85	0.19
Canopy cover	-0.13				0.30	-0.001			4	156.46	0.00	0.79
Linear	-0.14								2	159.09	2.63	0.21
Linear	-0.14								2	159.09	0.00	0.73
Drainage class	-0.12						+	+	4	161.05	1.96	0.27

Appendix 5.81. Model coefficient, number of model parameters (*K*), Akaike's Information Criterion corrected for small sample size (AIC_c), change in AIC_c from best model (ΔAIC_c), and model weights calculated from AIC_c (w_i) for competing models with Julian day (JD) as a linear, quadratic, and exponential term, competing models with Julian day (JD), study region (SR), and their interaction (JD*SR), competing models with Julian day (JD), canopy cover (CC), and their interaction (JD*CC) for digestible protein of *Smilicina trifolia*.

Model	JD	JD^2	SR	JD*SR	CC	JD*CC	*K*	AIC_c	ΔAIC_c	w_i
Exponential	-0.006						2	181.70	0.00	0.44
Linear	-0.09						2	181.70	0.00	0.44
Quadratic	-0.15	0.0001					3	184.35	2.66	0.12
Linear	-0.09						2	179.96	0.00	0.70
Study region	-0.09		+	+			3	181.70	1.74	0.30
Canopy cover	-0.08				0.10	0.0003	4	164.75	0.00	1.00
Linear	-0.09						2	181.70	16.95	0.00

Appendix 5.82. Model coefficient, number of model parameters (*K*), Akaike's Information Criterion corrected for small sample size (AIC_c), change in AIC_c from best model (ΔAIC_c), and model weights calculated from AIC_c (w_i) for competing models with Julian day (JD) as a linear, quadratic, and exponential term, competing models with Julian day (JD), study region (SR), and their interaction (JD*SR), and competing models with Julian day (JD), canopy cover (CC), and their interaction (JD*CC) for digestible protein of *Viola spp.*

Model	JD	JD^2	SR	JD*SR	CC	JD*CC	*K*	AIC_c	ΔAIC_c	w_i
Linear	-0.01						2	151.95	0.00	0.55
Exponential	-0.09						2	153.01	1.06	0.32
Quadratic	-0.31	0.0005					3	154.95	3.00	0.12
Linear	-0.09						2	153.01	0.00	0.83
Study region	-0.10		+	+			4	156.22	3.21	0.17
Canopy cover	-0.04				0.18	-0.0006	4	149.34	0.00	0.86
Linear	-0.09						2	153.01	3.67	0.14

Appendix 5.83. Model coefficient, number of model parameters (*K*), Akaike's Information Criterion corrected for small sample size (AIC_c), change in AIC_c from best model (ΔAIC_c), and model weights calculated from AIC_c (w_i) for competing models with Julian day (JD) as a linear, quadratic, and exponential term, competing models with Julian day (JD), study region (SR), and their interaction (JD*SR) for digestible protein of *Rubus chamaemorus*.

Model	JD	JD^2	SR	JD*SR	*K*	AIC_c	ΔAIC_c	w_i
Linear	-0.11				2	110.35	0.00	0.65
Exponential	-0.01				2	112.65	2.30	0.21
Quadratic	-0.06	-0.0001			3	113.34	2.99	0.15
Study region	-0.14		+	+	4	105.98	0.00	0.90
Linear	-0.11				2	110.35	4.37	0.10

Appendix 5.84. Model coefficient, number of model parameters (*K*), Akaike's Information Criterion corrected for small sample size (AIC_c), change in AIC_c from best model (ΔAIC_c), and model weights calculated from AIC_c (w_i) for competing models with Julian day (JD) as a linear, quadratic, and exponential term for digestible protein of *Rubus chamaemorus* in Pickle Lake.

Model	JD	JD^2	*K*	AIC_c	ΔAIC_c	w_i
Exponential	-0.02		2	71.93	0.00	0.53
Linear	-0.10		2	72.68	0.75	0.36
Quadratic	-0.38	0.0006	3	75.10	3.17	0.11

Appendix 5.85. Model coefficient, number of model parameters (*K*), Akaike's Information Criterion corrected for small sample size (AIC_c), change in AIC_c from best model (ΔAIC_c), and model weights calculated from AIC_c (w_i) for competing models with Julian day (JD) as a linear, quadratic, and exponential term for digestible protein of *Rubus chamaemorus* in Cochrane.

Model	JD	JD^2	*K*	AIC_c	ΔAIC_c	w_i
Exponential	-0.14		2	41.39	0.00	0.52
Linear	-0.01		2	41.59	0.20	0.47
Quadratic	0.12	-0.0006	3	55.35	13.96	0.00

Appendix 5.86. Model coefficient, number of model parameters (*K*), Akaike's Information Criterion corrected for small sample size (AIC_c), change in AIC_c from best model (ΔAIC_c), and model weights calculated from AIC_c (w_i) for competing models with Julian day (JD), species collected (SC), and their interaction (JD*SC) for digestible protein of *Aster spp*.

Model	JD	SC	JD*SC	*K*	AIC_c	ΔAIC_c	w_i
Linear	-0.003			2	240.44	0.00	0.91
Species collected	-0.002	+	+	4	244.97	4.53	0.09

Appendix 5.87. Model coefficient, number of model parameters (*K*), Akaike's Information Criterion corrected for small sample size (AIC_c), change in AIC_c from best model (ΔAIC_c), and model weights calculated from AIC_c (w_i) for competing models with Julian day (JD) as a linear, quadratic, and exponential term, competing models with Julian day (JD), study region (SR), and their interaction (JD*SR) for digestible protein of *Aster spp*.

Model	JD	JD^2	SR	JD*SR	*K*	AIC_c	ΔAIC_c	w_i
Linear	-0.08				2	240.44	0.00	0.49
Exponential	-0.008				2	241.09	0.64	0.36
Quadratic	-0.11	6.66E-05			3	242.78	2.34	0.15
Study region	-0.11		+	+	4	231.48	0.00	0.99
Linear	-0.08				2	240.44	8.96	0.01

Appendix 5.88. Model coefficient, number of model parameters (*K*), Akaike's Information Criterion corrected for small sample size (AIC_c), change in AIC_c from best model (ΔAIC_c), and model weights calculated from AIC_c (w_i) for competing models with Julian day (JD) as a linear, quadratic, and exponential term, and competing models with Julian day (JD), canopy cover (CC), and their interaction (JD*CC) for digestible protein of *Aster spp.* in Pickle Lake.

Model	JD	JD^2	CC	JD*CC	*K*	AIC_c	ΔAIC_c	w_i
Exponential	-0.007				2	143.87	0.00	0.44
Linear	-0.06				2	143.88	0.02	0.44
Quadratic	-0.08	5.15E-05			3	146.53	2.67	0.12
Canopy cover	-0.06		0.08	-0.0002	4	135.68	0.00	0.98
Linear	-0.06				2	143.88	8.20	0.02

Appendix 5.89. Model coefficient, number of model parameters (*K*), Akaike's Information Criterion corrected for small sample size (AIC_c), change in AIC_c from best model (ΔAIC_c), and model weights calculated from AIC_c (w_i) for competing models with Julian day (JD) as a linear, quadratic, and exponential term, and competing models with Julian day (JD), canopy cover (CC), and their interaction (JD*CC) for digestible protein of *Aster spp.* in Cochrane.

Model	JD	JD^2	CC	JD*CC	*K*	AIC_c	ΔAIC_c	w_i
Exponential	-0.01				2	87.46	0.00	0.72
Quadratic	-0.49	0.0009			3	90.75	3.29	0.14
Linear	-0.11				2	90.79	3.33	0.14
Canopy cover	-0.06		0.05	-0.59	4	87.32	0.00	0.52
Exponential	-0.01				2	87.46	0.14	0.48

Appendix 5.90. Model coefficient, number of model parameters (*K*), Akaike's Information Criterion corrected for small sample size (AIC_c), change in AIC_c from best model (ΔAIC_c), and model weights calculated from AIC_c (w_i) for competing models with Julian day (JD) as a linear, quadratic, and exponential term, and competing models with Julian day (JD), study region (SR), and their interaction (JD*SR) for digestible protein of *Clintonia borealis*.

Model	JD	JD^2	SR	JD*SR	*K*	AIC_c	ΔAIC_c	w_i
Exponential	-0.07				2	204.51	0.00	0.47
Linear	-0.01				2	204.96	0.45	0.38
Quadratic	-0.12	9.91E-05			3	206.84	2.32	0.15
Study region	-0.09		+	+	4	187.08	0.00	1.00
Linear	-0.07				2	204.51	17.43	0.00

Appendix 5.91. Model coefficient, number of model parameters (*K*), Akaike's Information Criterion corrected for small sample size (AIC_c), change in AIC_c from best model (ΔAIC_c), and model weights calculated from AIC_c (w_i) for competing models with Julian day (JD) as a linear, quadratic, and exponential term, and competing models with Julian day (JD), study region (SR), and their interaction (JD*SR) for digestible protein of *Maianthemum canadensis*.

Model	JD	JD^2	SR	JD*SR	*K*	AIC_c	ΔAIC_c	w_i
Exponential	-0.02				2	268.35	0.00	0.93
Quadratic	-0.40	0.0007			2	273.88	5.53	0.06
Linear	-0.08				3	277.18	8.83	0.01
Study region	-0.02		+	+	4	255.49	0.00	1.00
Exponential	-0.02				2	268.35	12.86	0.00

Appendix 5.92. Model coefficient, number of model parameters (*K*), Akaike's Information Criterion corrected for small sample size (AIC_c), change in AIC_c from best model (ΔAIC_c), and model weights calculated from AIC_c (w_i) for competing models with Julian day (JD) as a linear, quadratic, and exponential term for digestible protein of *Clintonia borealis* in Pickle Lake.

Model	JD	JD^2	CC	JD*CC	*K*	AIC_c	ΔAIC_c	w_i
Exponential	-0.01				2	95.48	0.00	0.64
Linear	-0.06				2	97.75	2.26	0.21
Quadratic	-0.24	0.0004			3	98.36	2.87	0.15
Canopy cover	-0.01		-0.01	0.20	4	93.83	0.00	0.70
Exponential	-0.06				2	95.48	1.65	0.30

Appendix 5.93. Model coefficient, number of model parameters (*K*), Akaike's Information Criterion corrected for small sample size (AIC_c), change in AIC_c from best model (ΔAIC_c), and model weights calculated from AIC_c (w_i) for competing models with Julian day (JD) as a linear, quadratic, and exponential term for digestible protein of *Maianthemum canadensis* in Pickle Lake.

Model	JD	JD^2	CC	JD*CC	*K*	AIC_c	ΔAIC_c	w_i
Exponential	-0.02				2	134.23	0.00	0.99
Quadratic	-0.72	0.001			3	143.81	9.58	0.01
Linear	-0.08				2	163.06	28.83	0.00
Canopy cover	-0.04		0.04	-12.90	4	117.44	0.00	1.00
Exponential	-0.02				2	134.23	16.79	0.00

Appendix 5.94. Model coefficient, number of model parameters (*K*), Akaike's Information Criterion corrected for small sample size (AIC_c), change in AIC_c from best model (ΔAIC_c), and model weights calculated from AIC_c (w_i) for competing models with Julian day (JD) as a linear, quadratic, and exponential term, and competing models with Julian day (JD), canopy cover (CC), and their interaction (JD*CC) for digestible protein of *Clintonia borealis* in Cochrane.

Model	JD	JD^2	CC	JD*CC	*K*	AIC_c	ΔAIC_c	w_i
Linear	-0.09				2	89.80	0.00	0.51
Exponential	-0.01				2	90.35	0.54	0.39
Quadratic	-0.14	9.81E-05			3	93.01	3.20	0.10
Linear	-0.01				2	89.80	0.00	0.74
Canopy cover	-0.004		0.07	-0.0002	4	91.92	2.12	0.26

Appendix 5.95. Model coefficient, number of model parameters (*K*), Akaike's Information Criterion corrected for small sample size (AIC_c), change in AIC_c from best model (ΔAIC_c), and model weights calculated from AIC_c (w_i) for competing models with Julian day (JD) as a linear, quadratic, and exponential term, and competing models with Julian day (JD), canopy cover (CC), and their interaction (JD*CC) for digestible protein of *Maianthemum canadensis* in Cochrane.

Model	JD	JD^2	CC	JD*CC	*K*	AIC_c	ΔAIC_c	w_i
Linear	-0.09				2	112.24	0.00	0.51
Exponential	-0.01				2	112.86	0.62	0.38
Quadratic	-0.10	2.42E-05			3	115.25	3.02	0.11
Linear	-0.09				2	112.24	0.00	0.78
Canopy cover	-0.09		0.03	-1.03E-05	4	114.82	2.58	0.22

Appendix 5.96. Model coefficient, number of model parameters (*K*), Akaike's Information Criterion corrected for small sample size (AIC_c), change in AIC_c from best model (ΔAIC_c), and model weights calculated from AIC_c (w_i) for competing models with Julian day (JD) as a linear, quadratic, and exponential term, competing models with Julian day (JD), study region (SR), and their interaction (JD*SR) for digestible protein of all forbs combined.

Model	JD	JD^2	SR	JD*SR	*K*	AIC_c	ΔAIC_c	w_i
Exponential	-0.01				2	1693.63	0.00	0.77
Quadratic	-0.26	0.0004			3	1696.77	3.13	0.16
Linear	-0.08				2	1698.63	4.99	0.06
Study region	-0.01		+	+	4	1659.39	0.00	1.00
Exponential	-0.01				2	1693.63	34.24	0.00

Appendix 5.97. Model coefficient, number of model parameters (*K*), Akaike's Information Criterion corrected for small sample size (AIC_c), change in AIC_c from best model (ΔAIC_c), and model weights calculated from AIC_c (w_i) for competing models with Julian day (JD) as a linear, quadratic, and exponential term, competing models with Julian day (JD), canopy cover (CC), and their interaction (JD*CC), and competing models with Julian day (JD), drainage class (DC), and their interaction (JD*DC) for digestible protein of all forbs combined in Pickle Lake.

Model	JD	JD^2	CC	JD*CC	DC	JD*DC	*K*	AIC_c	ΔAIC_c	w_i
Exponential	-0.01						2	930.21	0.00	0.63
Quadratic	-0.37	0.0007					3	931.43	1.22	0.34
Linear	-0.07						2	936.81	6.60	0.02
Exponential	-0.01						2	930.21	0.00	0.66
Canopy cover	-0.01		0.02	-0.08			4	931.54	1.33	0.34
Drainage class	-0.01				+	+	4	912.24	0.00	1.00
Exponential	-0.01						2	930.21	17.97	0.00

Appendix 5.98. Model coefficient, number of model parameters (*K*), Akaike's Information Criterion corrected for small sample size (AIC_c), change in AIC_c from best model (ΔAIC_c), and model weights calculated from AIC_c (w_i) for competing models with Julian day (JD) as a linear, quadratic, and exponential term, and competing models with Julian day (JD), canopy cover (CC), and their interaction (JD*CC) for digestible protein of all forbs combined in uplands of Pickle Lake.

Model	JD	JD^2	CC	JD*CC	*K*	AIC_c	ΔAIC_c	w_i
Exponential	-0.01				2	669.60	0.00	0.80
Quadratic	-0.31	0.0006			3	672.65	3.05	0.17
Linear	-0.07				2	676.64	7.04	0.02
Canopy cover	-0.01		0.03	0.10	4	655.03	0.00	1.00
Exponential	-0.01				2	669.60	14.57	0.00

Appendix 5.99. Model coefficient, number of model parameters (*K*), Akaike's Information Criterion corrected for small sample size (AIC_c), change in AIC_c from best model (ΔAIC_c), and model weights calculated from AIC_c (w_i) for competing models with Julian day (JD) as a linear, quadratic, and exponential term, and competing models with Julian day (JD), canopy cover (CC), and their interaction (JD*CC) for digestible protein of all forbs combined in lowlands of Pickle Lake.

Model	JD	JD^2	CC	JD*CC	*K*	AIC_c	ΔAIC_c	w_i
Exponential	-0.01				2	234.97	0.00	0.44
Quadratic	-0.77	0.002			3	235.34	0.37	0.36
Linear	-0.08				2	236.50	1.53	0.20
Canopy cover	-0.06		0.58	-0.002	4	235.87	0.00	0.58
Linear	-0.08				2	236.50	0.63	0.42

Appendix 5.100. Model coefficient, number of model parameters (*K*), Akaike's Information Criterion corrected for small sample size (AIC_c), change in AIC_c from best model (ΔAIC_c), and model weights calculated from AIC_c (w_i) for competing models with Julian day (JD) as a linear, quadratic, and exponential term, competing models with Julian day (JD), canopy cover (CC), and their interaction (JD*CC), and competing models with Julian day (JD), drainage class (DC), and their interaction (JD*DC) for digestible protein of all forbs combined in Cochrane.

Model	JD	JD^2	CC	JD*CC	DC	JD*DC	*K*	AIC_c	ΔAIC_c	w_i
Exponential	-0.01						2	730.48	0.00	0.75
Quadratic	-0.34	0.0005					3	733.75	3.27	0.15
Linear	-0.10						2	734.40	3.92	0.11
Canopy cover	-0.01		0.04	-0.12			4	719.59	0.00	1.00
Exponential	-0.01						2	730.48	10.89	0.00
Drainage class	-0.01				+	+	4	723.27	0.00	0.97
Exponential	-0.01						2	730.48	7.21	0.03

Appendix 5.101. Model coefficient, number of model parameters (*K*), Akaike's Information Criterion corrected for small sample size (AIC_c), change in AIC_c from best model (ΔAIC_c), and model weights calculated from AIC_c (w_i) for competing models with Julian day (JD) as a linear, quadratic, and exponential term, and competing models with Julian day (JD), canopy cover (CC), and their interaction (JD*CC) for digestible protein of all forbs combined in uplands of Cochrane.

Model	JD	JD^2	CC	JD*CC	*K*	AIC_c	ΔAIC_c	w_i
Exponential	-0.01				2	578.28	0.00	0.82
Linear	-0.34	0.0005			3	582.12	3.84	0.12
Quadratic	-0.10				2	583.51	5.23	0.06
Canopy cover	-0.02		0.06	-0.38	4	554.55	0.00	1.00
Exponential	-0.01				2	578.28	23.74	0.00

Appendix 5.102. Model coefficient, number of model parameters (*K*), Akaike's Information Criterion corrected for small sample size (AIC_c), change in AIC_c from best model (ΔAIC_c), and model weights calculated from AIC_c (w_i) for competing models with Julian day (JD) as a linear, quadratic, and exponential term, and competing models with Julian day (JD), canopy cover (CC), and their interaction (JD*CC) for digestible protein of all forbs combined in lowlands of Cochrane.

Model	JD	JD^2	CC	JD*CC	*K*	AIC_c	ΔAIC_c	w_i
Exponential	-0.01				2	137.10	0.00	0.50
Linear	-0.11				3	138.05	0.95	0.31
Quadratic	-1.17	0.002			2	139.01	1.91	0.19
Canopy cover	-0.08		0.12	0.0001	4	137.96	0.00	0.51
Linear	-0.11				2	138.05	0.09	0.49

Appendix 5.103. Model coefficient, number of model parameters (*K*), Akaike's Information Criterion corrected for small sample size (AIC_c), change in AIC_c from best model (ΔAIC_c), and model weights calculated from AIC_c (w_i) for competing models with Julian day (JD) as a linear, quadratic, and exponential term for digestible protein of *Alnus crispa*.

Model	JD	JD^2	*K*	AIC_c	ΔAIC_c	w_i
Exponential	-0.004		2	55.06	0.00	0.50
Linear	-0.04		2	55.87	0.80	0.33
Quadratic	-0.25	0.0005	3	57.26	2.20	0.17

Appendix 5.104. Model coefficient, number of model parameters (*K*), Akaike's Information Criterion corrected for small sample size (AIC_c), change in AIC_c from best model (ΔAIC_c), and model weights calculated from AIC_c (w_i) for competing models with Julian day (JD) as a linear, quadratic, and exponential term for digestible protein of *Amelanchier spp.*

Model	JD	JD^2	*K*	AIC_c	ΔAIC_c	w_i
Linear	-0.06		2	66.28	0.00	0.52
Exponential	-0.01		2	66.99	0.71	0.36
Quadratic	0.20	-0.0006	3	69.15	2.87	0.12

Appendix 5.105. Model coefficient, number of model parameters (*K*), Akaike's Information Criterion corrected for small sample size (AIC_c), change in AIC_c from best model (ΔAIC_c), and model weights calculated from AIC_c (w_i) for competing models with Julian day (JD) as a linear, quadratic, and exponential term, competing models with Julian day (JD), study region (SR), and their interaction (JD*SR), competing models with Julian day (JD), canopy cover (CC), and their interaction (JD*CC), and competing models with Julian day (JD), drainage class (DC), and their interaction (JD*DC) for digestible protein of *Betula papyrifera*.

Model	JD	JD^2	SR	JD*SR	CC	JD*CC	DC	JD*DC	*K*	AIC_c	ΔAIC_c	w_i
Exponential	-0.006								2	152.36	0.00	0.47
Linear	-0.05								2	153.46	1.10	0.27
Quadratic	-0.32	0.0006							3	153.56	1.19	0.26
Study region	0.06		+	+					4	152.24	0.00	0.65
Linear	-0.05								2	153.46	1.22	0.35
Linear	-0.05								2	153.46	0.00	0.92
Canopy cover	-0.05				-0.03	0.0002			4	158.41	4.95	0.08
Linear	-0.05								2	153.46	0.00	0.62
Drainage class	0.01						+	+	4	154.45	0.99	0.38

Appendix 5.106. Model coefficient, number of model parameters (*K*), Akaike's Information Criterion corrected for small sample size (AIC_c), change in AIC_c from best model (ΔAIC_c), and model weights calculated from AIC_c (w_i) for competing models with Julian day (JD) as a linear, quadratic, and exponential term for digestible protein of *Corylus cornuta*.

Model	JD	JD^2	*K*	AIC_c	ΔAIC_c	w_i
Linear	-0.08		2	48.88	0.00	0.61
Exponential	-0.01		2	49.92	1.04	0.36
Quadratic	0.67	-0.002	3	55.08	6.20	0.03

Appendix 5.107. Model coefficient, number of model parameters (*K*), Akaike's Information Criterion corrected for small sample size (AIC_c), change in AIC_c from best model (ΔAIC_c), and model weights calculated from AIC_c (w_i) for competing models with Julian day (JD) as a linear, quadratic, and exponential term, competing models with Julian day (JD), study region (SR), and their interaction (JD*SR), competing models with Julian day (JD), canopy cover (CC), and their interaction (JD*CC), and competing models with Julian day (JD), drainage class (DC), and their interaction (JD*DC) for digestible protein of *Populus tremuloides*.

Model	JD	JD^2	SR	JD*SR	CC	JD*CC	DC	JD*DC	*K*	AIC_c	ΔAIC_c	w_i
Exponential	-0.01								2	72.69	0.00	0.49
Linear	-0.08								2	72.98	0.28	0.43
Quadratic	-0.21	0.0003							3	76.29	3.60	0.08
Linear	-0.08								2	72.98	0.00	0.94
Study region	-0.17		+	+					4	78.43	5.45	0.06
Linear	-0.08								2	72.98	0.00	0.90
Canopy cover	-0.11				-0.21	0.001			4	77.39	4.41	0.10
Linear	-0.08								2	72.98	0.00	0.97
Drainage class	-0.07						+	+	4	79.98	7.01	0.03

Appendix 5.108. Model coefficient, number of model parameters (*K*), Akaike's Information Criterion corrected for small sample size (AIC_c), change in AIC_c from best model (ΔAIC_c), and model weights calculated from AIC_c (w_i) for competing models with Julian day (JD) as a linear, quadratic, and exponential term for digestible protein of *Sorbus spp*.

Model	JD	JD^2	*K*	AIC_c	ΔAIC_c	w_i
Linear	-0.06		2	46.97	0.00	0.59
Exponential	-0.01		2	48.66	1.69	0.25
Quadratic	0.45	-0.001	3	49.65	2.68	0.15

Appendix 5.109. Model coefficient, number of model parameters (*K*), Akaike's Information Criterion corrected for small sample size (AIC_c), change in AIC_c from best model (ΔAIC_c), and model weights calculated from AIC_c (w_i) for competing models with Julian day (JD), species collected (SC), and their interaction (JD*SC) for digestible protein of *Sorbus spp*.

Model	JD	SC	JD*SC	*K*	AIC_c	ΔAIC_c	w_i
Linear	-0.06			2	46.97	0.00	0.98
Species collected	-0.08	+	+	4	54.63	7.66	0.02

Appendix 5.110. Model coefficient, number of model parameters (*K*), Akaike's Information Criterion corrected for small sample size (AIC_c), change in AIC_c from best model (ΔAIC_c), and model weights calculated from AIC_c (w_i) for competing models with Julian day (JD) as a linear, quadratic, and exponential term, competing models with Julian day (JD), study region (SR), and their interaction (JD*SR), and competing models with Julian day (JD), canopy cover (CC), and their interaction (JD*CC) for digestible protein of *Acer spicatum*.

Model	JD	JD^2	SR	JD*SR	CC	JD*CC	*K*	AIC_c	ΔAIC_c	w_i
Exponential	-0.01						2	133.62	0.00	0.77
Linear	-0.11						2	136.82	3.20	0.16
Quadratic	-0.33	0.0005					3	138.20	4.58	0.08
Exponential	-0.01						2	133.62	0.00	0.80
Study region	-0.02		+	+			4	136.40	2.78	0.20
Exponential	-0.01						2	133.62	0.00	0.67
Canopy cover	-0.01				-0.004	0.85	4	135.02	1.40	0.33

Appendix 5.111. Model coefficient, number of model parameters (*K*), Akaike's Information Criterion corrected for small sample size (AIC_c), change in AIC_c from best model (ΔAIC_c), and model weights calculated from AIC_c (w_i) for competing models with Julian day (JD) as a linear, quadratic, and exponential term for digestible protein of *Betula pumilus.*

Model	JD	JD^2	*K*	AIC_c	ΔAIC_c	w_i
Exponential	-0.01		2	75.97	0.00	0.75
Linear	-0.08		2	79.11	3.14	0.16
Quadratic	-0.36	0.0006	3	80.20	4.23	0.09

Appendix 5.112. Model coefficient, number of model parameters (*K*), Akaike's Information Criterion corrected for small sample size (AIC_c), change in AIC_c from best model (ΔAIC_c), and model weights calculated from AIC_c (w_i) for competing models with Julian day (JD) as a linear, quadratic, and exponential term for digestible protein of *Ribes glandulosum*.

Model	JD	JD^2		*K*	AIC_c	ΔAIC_c	w_i
Exponential	-0.02			2	53.51	0.00	0.95
Quadratic	-0.76		0.002	3	59.48	5.96	0.05
Linear	-0.12			2	73.96	20.44	0.00

Appendix 5.113. Model coefficient, number of model parameters (*K*), Akaike's Information Criterion corrected for small sample size (AIC_c), change in AIC_c from best model (ΔAIC_c), and model weights calculated from AIC_c (w_i) for competing models with Julian day (JD) as a linear, quadratic, and exponential term, competing models with Julian day (JD), study region (SR), and their interaction (JD*SR), competing models with Julian day (JD), canopy cover (CC), and their interaction (JD*CC), and competing models with Julian day (JD), drainage class (DC), and their interaction (JD*DC) for digestible protein of *Aralia hispidula*.

Model	JD	JD^2	SR	JD*SR	CC	JD*CC	DC	JD*DC	*K*	AIC_c	ΔAIC_c	w_i
Exponential	-0.01								2	81.57	0.00	0.57
Quadratic	-0.52	0.001							3	83.17	1.61	0.25
Linear	-0.06								2	83.90	2.34	0.18
Study region	-0.009		+		+				4	75.88	0.00	0.94
Exponential	-0.01								2	81.57	5.69	0.06
Exponential	-0.01								2	81.57	0.00	0.87
Canopy cover	-0.01				0.01	5.80E-05			4	85.40	3.83	0.13
Drainage class	-0.02								2	81.57	0.00	0.93
Exponential	-0.01						+	+	4	86.71	5.14	0.07

Appendix 5.114. Model coefficient, number of model parameters (*K*), Akaike's Information Criterion corrected for small sample size (AIC_c), change in AIC_c from best model (ΔAIC_c), and model weights calculated from AIC_c (w_i) for competing models with Julian day (JD) as a linear, quadratic, and exponential term, competing models with Julian day (JD), study region (SR), and their interaction (JD*SR), competing models with Julian day (JD), canopy cover (CC), and their interaction (JD*CC), and competing models with Julian day (JD), drainage class (DC), and their interaction (JD*DC) for digestible protein of *Rosa acicularia.*

Model	JD	JD^2	SR	JD*SR	CC	JD*CC	DC	JD*DC	*K*	AIC_c	ΔAIC_c	w_i
Linear	-0.06								2	101.98	0.00	0.46
Exponential	-0.01								2	102.05	0.07	0.44
Quadratic	-0.11	0.0001							3	105.04	3.06	0.10
Linear	-0.06								2	101.98	0.00	0.88
Study region	-0.13		+	+					4	105.95	3.97	0.12
Canopy cover	-0.03				0.14	-0.0005			4	97.45	0.00	0.91
Linear	-0.06								2	101.98	4.53	0.09
Linear	-0.06								2	101.98	0.00	0.95
Drainage class	-0.12						+	+	4	107.75	5.77	0.05

Appendix 5.115. Model coefficient, number of model parameters (*K*), Akaike's Information Criterion corrected for small sample size (AIC_c), change in AIC_c from best model (ΔAIC_c), and model weights calculated from AIC_c (w_i) for competing models with Julian day (JD) as a linear, quadratic, and exponential term, competing models with Julian day (JD), study region (SR), and their interaction (JD*SR), competing models with Julian day (JD), canopy cover (CC), and their interaction (JD*CC), and competing models with Julian day (JD), drainage class (DC), and their interaction (JD*DC) for digestible protein of *Alnus rugosa*.

Model	JD	JD^2	SR	JD*SR	CC	JD*CC	DC	JD*DC	*K*	AIC_c	ΔAIC_c	w_i
Linear	-0.03								2	120.36	0.00	0.43
Exponential	-0.003								2	120.70	0.34	0.36
Quadratic	0.15	-0.0004							3	121.76	1.40	0.21
Linear	-0.01								2	120.36	0.00	0.78
Study region	-0.02		+	+					4	122.92	2.55	0.22
Canopy cover	-0.03				0.03	4.61E-05			4	111.88	0.00	0.99
Linear	-0.03								2	120.36	8.48	0.01
Drainage class	-0.03						+	+	4	110.25	0.00	0.99
Linear	-0.03								2	120.36	10.11	0.01

Appendix 5.116. Model coefficient, number of model parameters (*K*), Akaike's Information Criterion corrected for small sample size (AIC_c), change in AIC_c from best model (ΔAIC_c), and model weights calculated from AIC_c (w_i) for competing models with Julian day (JD) as a linear, quadratic, and exponential term, competing models with Julian day (JD), study region (SR), and their interaction (JD*SR) for digestible protein of *Diervilla lonicera*.

Model	JD	JD^2	SR	JD*SR	*K*	AIC_c	ΔAIC_c	w_i
Exponential	-0.01				2	208.22	0.00	0.77
Quadratic	-0.31	0.0005			3	212.03	3.82	0.11
Linear	-0.09				2	212.07	3.85	0.11
Study region	-0.01		+	+	4	200.16	0.00	0.98
Exponential	-0.01				2	208.22	8.06	0.02

Appendix 5.117. Model coefficient, number of model parameters (*K*), Akaike's Information Criterion corrected for small sample size (AIC_c), change in AIC_c from best model (ΔAIC_c), and model weights calculated from AIC_c (w_i) for competing models with Julian day (JD) as a linear, quadratic, and exponential term, and competing models with Julian day (JD), study region (SR), and their interaction (JD*SR) for digestible protein of *Prunus pensylvanica.*

Model	JD	JD^2	SR	JD*SR	*K*	AIC_c	ΔAIC_c	w_i
Exponential	-0.01				2	143.80	0.00	0.67
Linear	-0.09				2	145.90	2.10	0.23
Quadratic	-0.25	0.0004			3	147.64	3.84	0.10
Study region	-0.01		+	+	4	134.74	0.00	0.99
Exponential	-0.01				2	143.80	9.05	0.01

Appendix 5.118. Model coefficient, number of model parameters (*K*), Akaike's Information Criterion corrected for small sample size (AIC_c), change in AIC_c from best model (ΔAIC_c), and model weights calculated from AIC_c (w_i) for competing models with Julian day (JD) as a linear, quadratic, and exponential term, and competing models with Julian day (JD), study region (SR), and their interaction (JD*SR) for digestible protein of *Rubus pubescens.*

Model	JD	JD^2	SR	JD*SR	*K*	AIC_c	ΔAIC_c	w_i
Linear	-0.07				2	211.03	0.00	0.47
Exponential	-0.009				2	211.34	0.30	0.40
Quadratic	-0.09	4.61E-05			3	213.55	2.52	0.13
Study region	-0.08		+	+	4	205.40	0.00	0.94
Linear	-0.07				2	211.03	5.64	0.06

Appendix 5.119. Model coefficient, number of model parameters (*K*), Akaike's Information Criterion corrected for small sample size (AIC_c), change in AIC_c from best model (ΔAIC_c), and model weights calculated from AIC_c (w_i) for competing models with Julian day (JD) as a linear, quadratic, and exponential term, competing models with Julian day (JD), study region (SR), and their interaction (JD*SR) for digestible protein of *Salix spp.*

Model	JD	JD^2	SR	JD*SR	*K*	AIC_c	ΔAIC_c	w_i
Linear	-0.06				2	129.43	0.00	0.45
Exponential	-0.007				2	130.06	0.63	0.33
Quadratic	0.40	-0.001			3	130.76	1.33	0.23
Study region	-0.01		+	+	4	115.52	0.00	1.00
Linear	-0.06				2	129.43	13.91	0.00

Appendix 5.120. Model coefficient, number of model parameters (*K*), Akaike's Information Criterion corrected for small sample size (AIC_c), change in AIC_c from best model (ΔAIC_c), and model weights calculated from AIC_c (w_i) for competing models with Julian day (JD) as a linear, quadratic, and exponential term, and competing models with Julian day (JD), study region (SR), and their interaction (JD*SR) for digestible protein of *Vaccinium angustifolium.*

Model	JD	JD^2	SR	JD*SR	*K*	AIC_c	ΔAIC_c	w_i
Linear	-0.05				2	204.94	0.00	0.64
Quadratic	0.02	-0.0002			3	206.72	1.78	0.26
Exponential	-0.01				2	208.73	3.79	0.10
Study region	-0.06		+	+	4	190.52	0.00	1.00
Linear	-0.05				2	204.94	14.42	0.00

Appendix 5.121. Model coefficient, number of model parameters (*K*), Akaike's Information Criterion corrected for small sample size (AIC_c), change in AIC_c from best model (ΔAIC_c), and model weights calculated from AIC_c (w_i) for competing models with Julian day (JD) as a linear, quadratic, and exponential term, and competing models with Julian day (JD), study region (SR), and their interaction (JD*SR) for digestible protein of *Vaccinium myrtilloides.*

Model	JD	JD^2	SR	JD*SR	*K*	AIC_c	ΔAIC_c	w_i
Linear	-0.07				2	237.06	0.00	0.61
Quadratic	-0.002	-0.0001			3	239.21	2.14	0.21
Exponential	-0.01				2	239.42	2.35	0.19
Study region	-0.08		+	+	4	230.36	0.00	0.97
Linear	-0.07				2	237.06	6.70	0.03

Appendix 5.122. Model coefficient, number of model parameters (*K*), Akaike's Information Criterion corrected for small sample size (AIC_c), change in AIC_c from best model (ΔAIC_c), and model weights calculated from AIC_c (w_i) for competing models with Julian day (JD) as a linear, quadratic, and exponential term, and competing models with Julian day (JD), species collected (SC), and their interaction (JD*SC) for digestible protein of *Vaccinium spp*.

Model	JD	JD^2	SC	JD*SC	*K*	AIC_c	ΔAIC_c	w_i
Exponential	-0.05				2	217.26	0.00	0.49
Linear	-0.01				2	217.86	0.60	0.36
Quadratic	-0.07	5.20E-05			3	219.54	2.28	0.16
Species collected			+	+	4	447.49	0.00	0.99
Linear					2	456.98	9.48	0.01

Appendix 5.123. Model coefficient, number of model parameters (*K*), Akaike's Information Criterion corrected for small sample size (AIC_c), change in AIC_c from best model (ΔAIC_c), and model weights calculated from AIC_c (w_i) for competing models with Julian day (JD) as a linear, quadratic, and exponential term, and competing models with Julian day (JD), canopy cover (CC), and their interaction (JD*CC) for digestible protein of *Diervilla lonicera* in Pickle Lake.

Model	JD	JD^2	CC	JD*CC	*K*	AIC_c	ΔAIC_c	w_i
Exponential	-0.01				2	130.55	0.00	0.50
Linear	-0.11				2	131.23	0.68	0.35
Quadratic	-1.02	0.002			3	132.89	2.34	0.15
Canopy cover	-0.01		0.004	0.89	4	90.17	0.00	1.00
Exponential	-0.01				2	117.99	27.82	0.00

Appendix 5.124. Model coefficient, number of model parameters (*K*), Akaike's Information Criterion corrected for small sample size (AIC_c), change in AIC_c from best model (ΔAIC_c), and model weights calculated from AIC_c (w_i) for competing models with Julian day (JD) as a linear, quadratic, and exponential term, and competing models with Julian day (JD), canopy cover (CC), and their interaction (JD*CC) for digestible protein of *Diervilla lonicera* in Cochrane.

Model	JD	JD^2	CC	JD*CC	*K*	AIC_c	ΔAIC_c	w_i
Linear	-0.09				2	80.78	0.00	0.56
Exponential	-0.01				2	81.81	1.03	0.34
Quadratic	-0.10	2.69E-05			3	84.26	3.48	0.10
Canopy cover	-0.08		0.06	-7.15E-05	4	55.91	0.00	1.00
Linear	-0.09				2	80.78	24.87	0.00

Appendix 5.125. Model coefficient, number of model parameters (*K*), Akaike's Information Criterion corrected for small sample size (AIC_c), change in AIC_c from best model (ΔAIC_c), and model weights calculated from AIC_c (w_i) for competing models with Julian day (JD) as a linear, quadratic, and exponential term, competing models with Julian day (JD), canopy cover (CC), and their interaction (JD*CC), and competing models with Julian day (JD), drainage class (DC), and their interaction (JD*DC) for digestible protein of *Prunus pensylvanica* in Pickle Lake.

Model	JD	JD^2	CC	JD*CC	DC	JD*DC	*K*	AIC_c	ΔAIC_c	w_i
Exponential	-0.01						2	90.91	0.00	0.92
Quadratic	-0.49	0.0009					3	96.22	5.31	0.06
Linear	-0.09						2	99.49	8.58	0.01
Canopy cover	-0.02		0.06	-0.84			4	87.45	0.00	0.85
Exponential	-0.01						2	90.91	3.46	0.15
Exponential	-0.01						2	89.30	0.00	0.69
Drainage class	-0.03				+	+	4	90.91	1.61	0.31

Appendix 5.126. Model coefficient, number of model parameters (*K*), Akaike's Information Criterion corrected for small sample size (AIC_c), change in AIC_c from best model (ΔAIC_c), and model weights calculated from AIC_c (w_i) for competing models with Julian day (JD) as a linear, quadratic, and exponential term for digestible protein of *Prunus pensylvanica* in Cochrane.

Model	JD	JD^2	*K*	AIC_c	ΔAIC_c	w_i
Quadratic	0.37	-0.001	2	40.67	0.00	0.53
Linear	-0.09		2	41.26	0.59	0.39
Exponential	-0.007		3	44.47	3.80	0.08

Appendix 5.127. Model coefficient, number of model parameters (*K*), Akaike's Information Criterion corrected for small sample size (AIC_c), change in AIC_c from best model (ΔAIC_c), and model weights calculated from AIC_c (w_i) for competing models with Julian day (JD) as a linear, quadratic, and exponential term for digestible protein of *Salix spp.* in Pickle Lake.

Model	JD	JD^2	*K*	AIC_c	ΔAIC_c	w_i
Linear	-0.06		2	46.97	0.00	0.59
Exponential	-0.009		2	48.66	1.69	0.25
Quadratic	0.02	-0.0002	3	49.65	2.68	0.15

Appendix 5.128. Model coefficient, number of model parameters (*K*), Akaike's Information Criterion corrected for small sample size (AIC_c), change in AIC_c from best model (ΔAIC_c), and model weights calculated from AIC_c (w_i) for competing models with Julian day (JD) as a linear, quadratic, and exponential term for digestible protein of *Salix spp.* in Cochrane.

Model	JD	JD^2	*K*	AIC_c	ΔAIC_c	w_i
Exponential	-0.001		2	49.54	0.00	0.49
Linear	-0.01		2	49.55	0.01	0.49
Quadratic	-0.64	0.002	3	55.52	5.98	0.02

Appendix 5.129. Model coefficient, number of model parameters (*K*), Akaike's Information Criterion corrected for small sample size (AIC_c), change in AIC_c from best model (ΔAIC_c), and model weights calculated from AIC_c (w_i) for competing models with Julian day (JD), species collected (SC), and their interaction (JD*SC) for digestible protein of *Salix spp*.

Model	JD	SC	JD*SC	*K*	AIC_c	ΔAIC_c	w_i
Linear	-0.06			2	129.43	0.00	1.00
Species collected	-0.08	+	+	4	159.93	30.50	0.00

Appendix 5.130. Model coefficient, number of model parameters (*K*), Akaike's Information Criterion corrected for small sample size (AIC_c), change in AIC_c from best model (ΔAIC_c), and model weights calculated from AIC_c (w_i) for competing models with Julian day (JD) as a linear, quadratic, and exponential term, and competing models with Julian day (JD), canopy cover (CC), and their interaction (JD*CC) for digestible protein of *Rubus pubescens* in Pickle Lake.

Model	JD	JD^2	*K*	AIC_c	ΔAIC_c	w_i
Exponential	-0.01		2	78.47	0.00	0.51
Linear	-0.05		2	78.90	0.43	0.41
Quadratic	-0.30	0.0006	3	82.39	3.92	0.07

Appendix 5.131. Model coefficient, number of model parameters (*K*), Akaike's Information Criterion corrected for small sample size (AIC_c), change in AIC_c from best model (ΔAIC_c), and model weights calculated from AIC_c (w_i) for competing models with Julian day (JD) as a linear, quadratic, and exponential term, competing models with Julian day (JD), canopy cover (CC), and their interaction (JD*CC), and competing models with Julian day (JD), drainage class (DC), and their interaction (JD*DC) for digestible protein of *Rubus pubescens* in Cochrane.

Model	JD	JD^2	CC	JD*CC	DC	JD*DC	*K*	AIC_c	ΔAIC_c	w_i
Exponential	-0.009						2	129.81	0.00	0.45
Linear	-0.08						2	129.86	0.04	0.44
Quadratic	-0.16	0.0002					3	132.74	2.93	0.10
Canopy cover	-0.06		0.13	-0.0003			4	121.86	0.00	0.98
Linear	-0.08						2	129.86	7.99	0.02
Linear	-0.08						2	129.86	0.00	0.83
Drainage class	0.04				+	+	4	132.97	3.12	0.17

Appendix 5.132. Model coefficient, number of model parameters (*K*), Akaike's Information Criterion corrected for small sample size (AIC_c), change in AIC_c from best model (ΔAIC_c), and model weights calculated from AIC_c (w_i) for competing models with Julian day (JD) as a linear, quadratic, and exponential term, competing models with Julian day (JD), canopy cover (CC), and their interaction (JD*CC), and competing models with Julian day (JD), drainage class (DC), and their interaction (JD*DC) for digestible protein of *Vaccinium angustifolium* in Pickle Lake.

Model	JD	JD^2	CC	JD*CC	DC	JD*DC	*K*	AIC_c	ΔAIC_c	w_i
Exponential	-0.04						2	91.81	0.00	0.51
Linear	-0.01						2	92.48	0.68	0.36
Quadratic	-0.02	-4.45E-05					3	94.63	2.83	0.12
Canopy cover	-0.03		0.09	-0.0003			4	77.14	0.00	1.00
Linear	-0.04						2	91.81	14.66	0.00
Linear	-0.04						2	91.81	0.00	0.95
Drainage class	-0.05				+	+	4	97.51	5.71	0.05

Appendix 5.133. Model coefficient, number of model parameters (*K*), Akaike's Information Criterion corrected for small sample size (AIC_c), change in AIC_c from best model (ΔAIC_c), and model weights calculated from AIC_c (w_i) for competing models with Julian day (JD) as a linear, quadratic, and exponential term, competing models with Julian day (JD), canopy cover (CC), and their interaction (JD*CC), and competing models with Julian day (JD), drainage class (DC), and their interaction (JD*DC) for digestible protein of *Vaccinium angustifolium* in Cochrane.

Model	JD	JD^2	CC	JD*CC	DC	JD*DC	*K*	AIC_c	ΔAIC_c	w_i
Linear	-0.06						2	101.51	0.00	0.70
Quadratic	0.01	-0.0002					3	103.87	2.36	0.22
Exponential	-0.01						2	105.77	4.26	0.08
Canopy cover	-0.05		0.13	-0.0004			4	87.88	0.00	1.00
Linear	-0.06						2	101.51	13.63	0.00
Linear	-0.06						2	101.51	0.00	0.55
Drainage class	-0.08				+	+	4	101.95	0.44	0.45

Appendix 5.134. Model coefficient, number of model parameters (*K*), Akaike's Information Criterion corrected for small sample size (AIC_c), change in AIC_c from best model (ΔAIC_c), and model weights calculated from AIC_c (w_i) for competing models with Julian day (JD) as a linear, quadratic, and exponential term, competing models with Julian day (JD), canopy cover (CC), and their interaction (JD*CC), and competing models with Julian day (JD), drainage class (DC), and their interaction (JD*DC) for digestible protein of *Vaccinium myrtilloides* in Pickle Lake.

Model	JD	JD^2	CC	JD*CC	DC	JD*DC	*K*	AIC_c	ΔAIC_c	w_i
Linear	-0.06						2	118.13	0.00	0.57
Exponential	-0.01						2	119.54	1.40	0.28
Quadratic	-0.05	-1.86E-05					3	120.84	2.70	0.15
Canopy cover	-0.05		0.11	-0.0003			4	82.04	0.00	1.00
Linear	-0.06						2	118.13	36.09	0.00
Linear	-0.06						2	118.13	0.00	0.86
Drainage class	-0.05				+	+	4	121.83	3.69	0.14

Appendix 5.135. Model coefficient, number of model parameters (*K*), Akaike's Information Criterion corrected for small sample size (AIC_c), change in AIC_c from best model (ΔAIC_c), and model weights calculated from AIC_c (w_i) for competing models with Julian day (JD) as a linear, quadratic, and exponential term, competing models with Julian day (JD), canopy cover (CC), and their interaction (JD*CC), and competing models with Julian day (JD), drainage class (DC), and their interaction (JD*DC) for digestible protein of *Vaccinium myrtilloides* in Cochrane.

Model	JD	JD^2	CC	JD*CC	DC	JD*DC	*K*	AIC_c	ΔAIC_c	w_i
Exponential	-0.01						2	108.83	0.00	0.47
Linear	-0.08						2	109.02	0.18	0.43
Quadratic	-0.17	0.0002					3	111.97	3.14	0.10
Canopy cover	-0.05		0.13	-0.0004			4	95.71	0.00	1.00
Linear	-0.08						2	109.02	13.30	0.00
Linear	-0.08						2	109.02	0.00	0.96
Drainage class	-0.03				+	+	4	115.34	6.33	0.04

Appendix 5.136. Model coefficient, number of model parameters (*K*), Akaike's Information Criterion corrected for small sample size (AIC_c), change in AIC_c from best model (ΔAIC_c), and model weights calculated from AIC_c (w_i) for competing models with Julian day (JD) as a linear, quadratic, and exponential term, and competing models with Julian day (JD), study region (SR), and their interaction (JD*SR) for digestible protein of all deciduous shrubs combined.

Model	JD	JD^2	SR	JD*SR	*K*	AIC_c	ΔAIC_c	w_i
Exponential	-0.01				2	2292.42	0.00	0.99
Quadratic	-0.20	0.0003			3	2301.97	9.54	0.01
Linear	-0.07				2	2306.32	13.90	0.00
Study region	-0.01		+	+	4	2249.75	0.00	1.00
Exponential	-0.01				2	2292.42	42.68	0.00

Appendix 5.137. Model coefficient, number of model parameters (*K*), Akaike's Information Criterion corrected for small sample size (AIC_c), change in AIC_c from best model (ΔAIC_c), and model weights calculated from AIC_c (w_i) for competing models with Julian day (JD) as a linear, quadratic, and exponential term, competing models with Julian day (JD), study region (SR), and their interaction (JD*SR), and competing models with Julian day (JD), canopy cover (CC), and their interaction (JD*CC) for digestible protein of all deciduous shrubs in Pickle Lake.

Model	JD	JD^2	CC	JD*CC	DC	JD*DC	*K*	AIC_c	ΔAIC_c	w_i
Exponential	-0.01						2	1345.48	0.00	0.98
Quadratic	-0.38	0.0007					3	1352.88	7.40	0.02
Linear	-0.07						2	1380.04	34.56	0.00
Canopy cover	-0.02		0.03	0.15			4	1296.11	0.00	1.00
Exponential	-0.01						2	1345.48	49.37	0.00
Drainage class	-0.02				+	+	4	1343.74	0.00	0.70
Exponential	-0.01						2	1345.48	1.74	0.30

Appendix 5.138. Model coefficient, number of model parameters (*K*), Akaike's Information Criterion corrected for small sample size (AIC_c), change in AIC_c from best model (ΔAIC_c), and model weights calculated from AIC_c (w_i) for competing models with Julian day (JD) as a linear, quadratic, and exponential term, competing models with Julian day (JD), study region (SR), and their interaction (JD*SR), and competing models with Julian day (JD), canopy cover (CC), and their interaction (JD*CC) for digestible protein of all deciduous shrubs in Cochrane.

Model	JD	JD^2	CC	JD*CC	DC	JD*DC	*K*	AIC_c	ΔAIC_c	w_i
Exponential	-0.08						2	893.76	0.00	0.64
Quadratic	-0.03	-0.0001					3	895.62	1.86	0.25
Linear	-0.009						2	897.33	3.57	0.11
Canopy cover	-0.07		0.08	-0.0002			4	850.89	0.00	1.00
Linear	-0.08						2	893.76	42.87	0.00
Drainage class	-0.08						2	893.76	0.00	0.88
Linear	-0.08				+	+	4	897.78	4.02	0.12

Appendix 5.139. Model coefficient, number of model parameters (*K*), Akaike's Information Criterion corrected for small sample size (AIC_c), change in AIC_c from best model (ΔAIC_c), and model weights calculated from AIC_c (w_i) for competing models with Julian day (JD) as a linear, quadratic, and exponential term for digestible protein of *Cladonia spp.*

Model	JD	JD^2	*K*	AIC_c	ΔAIC_c	w_i
Linear	-0.01		2	18.85	0.00	0.80
Quadratic	-0.04	7.41E-05	3	21.69	2.84	0.19
Exponential	-0.10		2	30.15	11.30	0.00

Appendix 5.140. Model coefficient, number of model parameters (*K*), Akaike's Information Criterion corrected for small sample size (AIC_c), change in AIC_c from best model (ΔAIC_c), and model weights calculated from AIC_c (w_i) for competing models with Julian day (JD) as a linear, quadratic, and exponential term for digestible protein of *Cladonia uncialis,*

Model	JD	JD^2	*K*	AIC_c	ΔAIC_c	w_i
Exponential	-0.003		2	10.05	0.00	0.50
Linear	0.004		2	10.16	0.11	0.47
Quadratic	0.03	-6.94E-05	3	15.45	5.40	0.03

Appendix 5.141. Model coefficient, number of model parameters (*K*), Akaike's Information Criterion corrected for small sample size (AIC_c), change in AIC_c from best model (ΔAIC_c), and model weights calculated from AIC_c (w_i) for competing models with Julian day (JD) as a linear, quadratic, and exponential term, competing models with Julian day (JD), study region (SR), and their interaction (JD*SR), competing models with Julian day (JD), canopy cover (CC), and their interaction (JD*CC), and competing models with Julian day (JD), drainage class (DC), and their interaction (JD*DC) for digestible protein of *Cladina mitis*.

Model	JD	JD^2	SR	JD*SR	CC	JD*CC	DC	JD*DC	*K*	AIC_c	ΔAIC_c	w_i
Quadratic	-0.03	6.61E-05							3	29.98	0.00	0.38
Linear	-0.0003								2	30.35	0.37	0.31
Exponential	0.0002								2	30.35	0.37	0.31
Study region	-0.002		+	+					4	29.36	0.00	0.62
Linear	-0.0003								2	30.35	0.99	0.38
Linear	-0.0003								2	30.35	0.00	0.80
Canopy cover	-0.001				0.002	1.12E-05			4	33.09	2.74	0.20
Linear	-0.0003								2	30.35	0.00	0.54
Drainage class	-0.002						+	+	4	30.65	0.30	0.46

Appendix 5.142. Model coefficient, number of model parameters (*K*), Akaike's Information Criterion corrected for small sample size (AIC_c), change in AIC_c from best model (ΔAIC_c), and model weights calculated from AIC_c (w_i) for competing models with Julian day (JD) as a linear, quadratic, and exponential term, competing models with Julian day (JD), study region (SR), and their interaction (JD*SR), competing models with Julian day (JD), canopy cover (CC), and their interaction (JD*CC), and competing models with Julian day (JD), drainage class (DC), and their interaction (JD*DC) for digestible protein of *Cladina rangiferina*.

Model	JD	JD^2	SR	JD*SR	CC	JD*CC	DC	JD*DC	*K*	AIC_c	ΔAIC_c	w_i
Exponential	-0.0007								2	42.83	0.00	0.37
Linear	0.0008								2	42.86	0.02	0.36
Quadratic	0.02	-4.31E-05							3	43.42	0.58	0.27
Linear	0.0008								2	42.86	0.00	0.83
Study region	0.0002		+	+					4	45.97	3.12	0.17
Linear	0.0008								2	42.86	0.00	0.53
Canopy cover	0.001				0.008	-1.47E-05			4	43.11	0.25	0.47
Linear	0.0008								2	42.86	0.00	0.90
Drainage class	-0.001						+	+	4	47.22	4.36	0.10

Appendix 5.143. Model coefficient, number of model parameters (*K*), Akaike's Information Criterion corrected for small sample size (AIC_c), change in AIC_c from best model (ΔAIC_c), and model weights calculated from AIC_c (w_i) for competing models with Julian day (JD) as a linear, quadratic, and exponential term, competing models with Julian day (JD), study region (SR), and their interaction (JD*SR), and competing models with Julian day (JD), canopy cover (CC), and their interaction (JD*CC) for digestible protein of *Cladina stellaris*.

Model	JD	JD^2	SR	JD*SR	CC	JD*CC	*K*	AIC_c	ΔAIC_c	w_i
Linear	-0.002						2	14.72	0.00	0.37
Exponential	0.001						2	14.80	0.08	0.36
Quadratic	-0.03	5.81E-05					3	15.37	0.66	0.27
Linear	-0.002						2	14.72	0.00	0.91
Study region	0.001		+	+			4	19.25	4.54	0.09
Linear	-0.002						2	14.72	0.00	0.86
Canopy cover	-0.001				0.01	-3.94E-05	4	18.41	3.70	0.14

Appendix 5.144. Model coefficient, number of model parameters (*K*), Akaike's Information Criterion corrected for small sample size (AIC_c), change in AIC_c from best model (ΔAIC_c), and model weights calculated from AIC_c (w_i) for competing models with Julian day (JD) as a linear, quadratic, and exponential term, competing models with Julian day (JD), study region (SR), and their interaction (JD*SR), competing models with Julian day (JD), canopy cover (CC), and their interaction (JD*CC), and competing models with Julian day (JD), drainage class (DC), and their interaction (JD*DC) for digestible protein of all ground lichens combined.

Model	JD	JD^2	SR	JD*SR	CC	JD*CC	DC	JD*DC	*K*	AIC_c	ΔAIC_c	w_i
Linear	-6.74E-05								2	164.15	0.00	0.39
Exponential	5.29E-05								2	164.15	0.00	0.39
Quadratic	-0.01	2.78E-05							3	165.25	1.10	0.22
Linear	-6.74E-05								2	164.15	0.00	0.88
Study region	-0.0008		+	+					4	168.09	3.94	0.12
Linear	-6.74E-05								2	164.15	0.00	0.88
Canopy cover	-0.0009				-0.003	1.83E-05			4	168.18	4.03	0.12
Linear	-6.74E-05								2	164.15	0.00	0.77
Drainage class	-0.002						+	+	4	166.59	2.44	0.23

Appendix 5.145. Model coefficient, number of model parameters (*K*), Akaike's Information Criterion corrected for small sample size (AIC_c), change in AIC_c from best model (ΔAIC_c), and model weights calculated from AIC_c (w_i) for competing models with Julian day (JD), species collected (SC; *Evernia mesomorpha* and *Usnea spp*.), and their interaction (JD*SC) for digestible protein of all tree lichens combined.

Model	JD	SC	JD*SC	*K*	AIC_c	ΔAIC_c	w_i
Linear	-0.06			2	125.38	0.00	1.00
Species collected	-0.07	+	+	4	160.62	35.24	0.00

Appendix 5.146. Model coefficient, number of model parameters (*K*), Akaike's Information Criterion corrected for small sample size (AIC_c), change in AIC_c from best model (ΔAIC_c), and model weights calculated from AIC_c (w_i) for competing models with Julian day (JD) as a linear, quadratic, and exponential term, and competing models with Julian day (JD), study region (SR), and their interaction (JD*SR) for digestible protein of all tree lichens combined.

Model	JD	JD^2	SR	JD*SR	*K*	AIC_c	ΔAIC_c	w_i
Linear	-0.002				2	55.57	0.00	0.46
Exponential	0.003				2	55.57	0.00	0.45
Quadratic	0.006	-2.02E-05			3	58.81	3.24	0.09
Study region	-0.0003		+	+	4	74.22	0.00	0.98
Linear	0.002				2	82.58	8.36	0.02

Appendix 5.147. Model coefficient, number of model parameters (*K*), Akaike's Information Criterion corrected for small sample size (AIC_c), change in AIC_c from best model (ΔAIC_c), and model weights calculated from AIC_c (w_i) for competing models with Julian day (JD) as a linear, quadratic, and exponential term, competing models with Julian day (JD), study region (SR), and their interaction (JD*SR), and competing models with Julian day (JD), canopy cover (CC), and their interaction (JD*CC) for digestible protein of all tree lichens combined in Pickle Lake.

Model	JD	JD^2	CC	JD*CC	DC	JD*DC	*K*	AIC_c	ΔAIC_c	w_i
Linear	-0.002						2	55.57	0.00	0.46
Exponential	-0.002						2	55.57	0.00	0.45
Quadratic	0.01	-2.02E-05					3	58.81	3.24	0.09
Linear	-0.002		-0.004	2.86E-05			2	55.57	0.00	0.97
Canopy cover	-0.004						4	62.56	6.99	0.03
Linear	-0.002						2	55.57	0.00	0.97
Drainage class	-0.002				+	+	4	62.30	6.73	0.03

Appendix 5.148. Model coefficient, number of model parameters (*K*), Akaike's Information Criterion corrected for small sample size (AIC_c), change in AIC_c from best model (ΔAIC_c), and model weights calculated from AIC_c (w_i) for competing models with Julian day (JD) as a linear, quadratic, and exponential term for digestible protein of all tree lichens combined in Cochrane.

Model	JD	JD^2	*K*	AIC_c	ΔAIC_c	w_i
Exponential	-0.10		2	14.90	0.00	0.51
Linear	-0.0003		2	15.08	0.18	0.47
Quadratic	-0.06	0.0002	3	21.88	6.99	0.02

Appendix 5.149. Model coefficient, number of model parameters (*K*), Akaike's Information Criterion corrected for small sample size (AIC_c), change in AIC_c from best model (ΔAIC_c), and model weights calculated from AIC_c (w_i) for competing models with Julian day (JD) as a linear, quadratic, and exponential term, and competing models with Julian day (JD), study region (SR), and their interaction (JD*SR) for digestible protein of *Equisetum sylvaticum.*

Model	JD	JD^2	SR	JD*SR	*K*	AIC_c	ΔAIC_c	w_i
Exponential	-0.09				2	176.85	0.00	0.54
Linear	-0.01				2	178.02	1.17	0.30
Quadratic	-0.16	0.0001			3	179.29	2.44	0.16
Study region	-0.11		+	+	4	161.71	0.00	1.00
Exponential	-0.09				2	176.85	15.14	0.00

Appendix 5.150. Model coefficient, number of model parameters (*K*), Akaike's Information Criterion corrected for small sample size (AIC_c), change in AIC_c from best model (ΔAIC_c), and model weights calculated from AIC_c (w_i) for competing models with Julian day (JD) as a linear, quadratic, and exponential term, competing models with Julian day (JD), study region (SR), and their interaction (JD*SR), and competing models with Julian day (JD), canopy cover (CC), and their interaction (JD*CC) for digestible protein of *Equisetum sylvaticum* in Pickle Lake.

Model	JD	JD^2	CC	JD*CC	DC	JD*DC	*K*	AIC_c	ΔAIC_c	w_i
Exponential	-0.01						2	78.84	0.00	0.68
Linear	-0.07						2	81.01	2.17	0.23
Quadratic	-0.25	0.0004					3	82.72	3.89	0.10
Canopy cover	-0.01		0.03	0.68			4	61.57	0.00	1.00
Exponential	-0.01						2	78.84	17.27	0.00
Exponential	-0.01						2	78.84	0.00	0.93
Drainage class	-0.02				+	+	4	84.07	5.23	0.07

Appendix 5.151. Model coefficient, number of model parameters (*K*), Akaike's Information Criterion corrected for small sample size (AIC_c), change in AIC_c from best model (ΔAIC_c), and model weights calculated from AIC_c (w_i) for competing models with Julian day (JD) as a linear, quadratic, and exponential term, competing models with Julian day (JD), study region (SR), and their interaction (JD*SR), and competing models with Julian day (JD), canopy cover (CC), and their interaction (JD*CC) for digestible protein of *Equisetum sylvaticum* in Cochrane.

Model	JD	JD^2	CC	JD*CC	DC	JD*DC	*K*	AIC_c	ΔAIC_c	w_i
Exponential	-0.01						2	79.81	0.00	0.73
Quadratic	-0.69	0.001					3	82.86	3.05	0.16
Linear	-0.11						2	83.60	3.79	0.11
Exponential	-0.01						2	79.81	0.00	0.75
Canopy cover	-0.02		0.02	0.24			4	82.01	2.20	0.25
Exponential	-0.01						2	79.81	0.00	0.91
Drainage class	-0.02				+	+	4	84.42	4.60	0.09

Appendix 5.152. Model coefficient, number of model parameters (*K*), Akaike's Information Criterion corrected for small sample size (AIC_c), change in AIC_c from best model (ΔAIC_c), and model weights calculated from AIC_c (w_i) for competing models with Julian day (JD) as a linear, quadratic, and exponential term for digestible protein of *Calamagrostis canadensis.*

Model	JD	JD^2	*K*	AIC_c	ΔAIC_c	w_i
Linear	-0.10		2	84.40	0.00	0.61
Exponential	-0.01		2	86.48	2.09	0.21
Quadratic	0.25	-0.0008	3	86.83	2.43	0.18

Appendix 5.153. Model coefficient, number of model parameters (*K*), Akaike's Information Criterion corrected for small sample size (AIC_c), change in AIC_c from best model (ΔAIC_c), and model weights calculated from AIC_c (w_i) for competing models with Julian day (JD) as a linear, quadratic, and exponential term for digestible protein of mushrooms.

Model	JD	JD^2	*K*	AIC_c	ΔAIC_c	w_i
Linear	-0.003		2	49.09	0.00	0.50
Exponential	-0.0002		2	49.09	0.00	0.50
Quadratic	5.67	-0.01	3	61.05	11.96	0.00

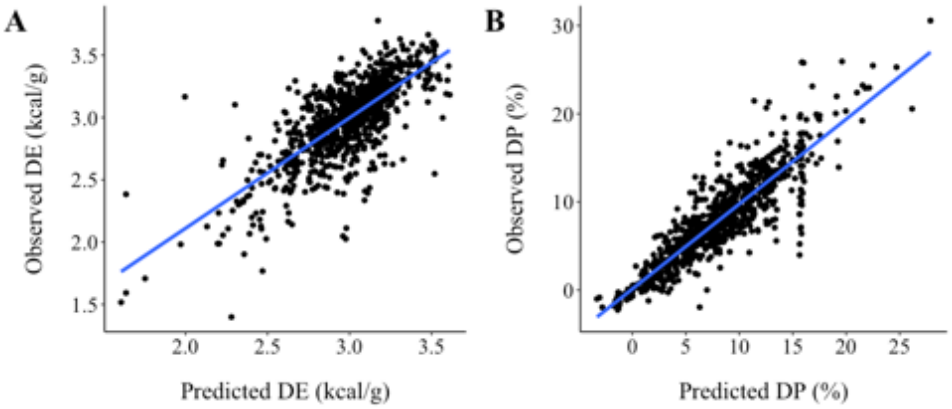

Appendix 5.154. Relationship between lab-derived and model-predicted A) digestible energy (kcal/g) and B) digestible protein (%) across 931 species-specific, forage quality samples.

Appendix 5.155. Model coefficient, number of model parameters (*K*), Akaike's Information Criterion corrected for small sample size (AIC_c), change in AIC_c from best model (ΔAIC_c), and model weights calculated from AIC_c (w_i) for competing models with basal area (BA; m^2/ha), canopy cover (CC; %), and stand height (SH; m) for digestible energy (DE) and protein (DP) across all forage quality samples.

Metric	Model	BA	CC	SH	*K*	AIC_c	ΔAIC_c	w_i
DE	CC		-0.002		2	475.50	0.00	1.00
	SH			-0.002	2	491.15	15.66	0.00
	BA	-0.003			2	496.96	21.46	0.00
	Null				1	507.47	31.97	0.00
DP	CC		0.04		2	5646.53	0.00	1.00
	SH			0.05	2	5666.51	19.98	0.00
	BA	0.06			2	5680.84	34.31	0.00
	Null				1	5697.72	51.19	0.00

Appendix 6. Supplemental materials for Chapter 4

Appendix 6.1. Non-linear transformations applied to Julian day and basal area across grass, forbs, deciduous shrubs (GFS), lichen, horsetail, and mushroom, high-quality accepted biomass (both DE and DP constraints), DE accepted biomass (only DE constraint), and DP accepted biomass (only DP constraint) by seral-specific ecosite or a combination of ecosites in Pickle Lake (PL) and Cochrane, Ontario (CO).

Biomass metric	Covariate	Ecosite	Seral	SA	Transformation	Equation	a	b	c
GFS	Julian day	BS-upland	Mid-late	PL	Hoerl	a*b^x*x^c	1.28884E-51	0.88322	27.73960
		Not upland early	Early-late	PL	Hoerl	a*b^x*x^c	1.93749E-46	0.89146	25.18290
		Upland	Early	CO	Hoerl	a*b^x*x^c	1.51652E-87	0.81468	46.59300
		Not upland early	Early-late	CO	Hoerl	a*b^x*x^c	2.03221E-96	0.78772	51.47770
		Lwl-Bog	Mid-late	CO	Hoerl	a*b^x*x^c	2.03455E-121	0.73939	64.68140
		Lowland	Early-late	CO	Hoerl	a*b^x*x^c	4.33641E-85	0.81841	45.11520
		Lwl-Fen	Mid-late	PL & CO	Hoerl	a*b^x*x^c	4.10597E-88	0.79335	47.81600
	Basal area	BS-upland	Early-late	PL & CO	Logistic Power	a/(1+(x/b)^c)	413.83500	11.08420	1.30946
		BS-WS-upland	Early-late	PL & CO	Logistic Power	a/(1+(x/b)^c)	672.30600	8.98543	1.36679
		BS-upland-Rocky	Early-late	PL	Exponential	a*exp(b*x)	340.89000	-0.08089	
		Lwl-Bog	Early-late	PL & CO	Logistic Power	a/(1+(x/b)^c)	219.26000	4.44245	0.860362
Lichen	Basal area	BS-upland	Early-late	PL & CO	Hoerl	a*b^x*x^c	11.24490	0.78715	2.69769
Horsetail	Julian day	Lwl-Bog	Mid-late	CO	Hoerl	a*b^x*x^c	3.30300E-239	0.57782	124.71200
		Lwl-Fen	Mid-late	PL and CO	Hoerl	a*b^x*x^c	1.53225E-87	0.79452	47.51000
Mushroom	Basal area	BS-upland	Early-late	PL & CO	Hoerl	a*b^x*x^c	3.31007E-09	0.52786	10.76360
	Julian day	Upland	Early-late	PL	Power	a*x^b	6.64772E-22	8.80103	
		BS-upland	Mid-late	PL	Power	a*x^b	1.46698E-22	9.09398	
		Lowland	Early-late	PL	Power	a*x^b	5.73546E-15	5.73923	
		Lwl-Bog	Mid-late	PL	Power	a*x^b	4.12149E-15	5.79928	
		Upland	Early-late	CO	Power	a*x^b	3.55042E-17	6.62655	
		Lowland	Early-late	CO	Power	a*x^b	2.39056E-40	16.68280	

Appendix 6.1. Continued.

Biomass metric	Covariate	Ecosite	Seral	SA	Transformation	Equation	a	b	c
HQ-AB	Basal area	BS-upland	Early-late	PL & CO	Geometric	a*x^(b*x)	121.14520	-0.01898	
		BS-WS-upland	Early-late	PL & CO	Geometric	a*x^(b*x)	374.51317	-0.01740	
	Julian day	BS-upland	Early	PL	Vapour pressure	exp(a + b/x + c*log(x))	940.53840	-27253.58284	-150.87096
		BS-upland	Mid-late	PL	Vapour pressure	exp(a + b/x + c*log(x))	415.80904	-12123.07164	-66.28053
		BS-WS-upland	Mid-late	PL	Vapour pressure	exp(a + b/x + c*log(x))	307.08048	-8980.26660	-48.45924
		Upland	Early	PL	Vapour pressure	exp(a + b/x + c*log(x))	431.33825	-11770.03351	-69.35395
		Not upland early	Early-late	PL	Vapour pressure	exp(a + b/x + c*log(x))	419.20323	-12384.68413	-66.54286
		Upland	Early	CO	Vapour pressure	exp(a + b/x + c*log(x))	638.26780	-21497.91859	-99.10144
		Not upland early	Early-late	CO	Vapour pressure	exp(a + b/x + c*log(x))	302.93719	-9934.59645	-46.91706
		Lowlands	Early-late	CO	Vapour pressure	exp(a + b/x + c*log(x))	222.57127	-7611.49573	-33.92744
		Lwl-Bog	Mid-late	CO	Vapour pressure	exp(a + b/x + c*log(x))	522.69385	-17064.74319	-81.69890
		Lwl-Fen	Mid-late	PL & CO	Vapour pressure	exp(a + b/x + c*log(x))	526.13993	-16588.73905	-82.49942
DE-AB	Basal area	BS-upland & BS-WS-upland	Early-late	PL & CO	Geometric	a*x^(b*x)	467.24962	-0.01443	
		Lwl-Bog	Early-late	PL & CO	Logistic Power	a/(1+(x/b)^c)	257.87529	10.93694	0.79404
	Julian day	Upland & Lowland	Mid-late	PL	Vapour pressure	exp(a + b/x + c*log(x))	92.71240	-2810.81856	-13.82677
		Upl-BS	Mid-late	PL	Vapour pressure	exp(a + b/x + c*log(x))	155.08561	-5016.54841	-23.51861
		Upl-BS-WS	Mid-late	PL	Vapour pressure	exp(a + b/x + c*log(x))	185.97666	-5710.98469	-28.64340
		Upland	Early	PL	Vapour pressure	exp(a + b/x + c*log(x))	94.47639	-2832.40355	-13.96561
		Upland	Early	CO	Vapour pressure	exp(a + b/x + c*log(x))	179.53920	-6204.98799	-26.88575
		Upl-BS-WS	Late	CO	Vapour pressure	exp(a + b/x + c*log(x))	763.60114	-24568.15747	-120.00675
		Lwl-Bog	Mid-late	CO	Vapour pressure	exp(a + b/x + c*log(x))	285.44014	-9538.37260	-43.90712
		Lwl-Fen	Mid-late	PL & CO	Vapour pressure	exp(a + b/x + c*log(x))	369.98460	-11708.48671	-57.64109

Appendix 6.1. Continued.

Biomass metric	Covariate	Ecosite	Seral	SA	Transformation	Equation	a	b	c
DP-AB	Basal area	BS-upland	Early-late	PL & CO	Geometric	a*x^(b*x)	128.87164	-0.01727	
		BS-WS-upland	Early-late	PL & CO	Geometric	a*x^(b*x)	382.28664	-0.01613	
		Lwl-Bog	Early-late	PL & CO	Linear	a + b*x	106.53283	-1.99032	
	Julian day	Upland	Early	PL	Vapour pressure	exp(a + b/x + c*log(x))	443.19739	-12268.99027	-71.09775
		Upland	Mid-late	PL	Vapour pressure	exp(a + b/x + c*log(x))	442.17918	-13128.30679	-70.19421
		Upland	Early	CO	Vapour pressure	exp(a + b/x + c*log(x))	827.45316	-27966.37675	-128.71235
		Not upland Early	Early-late	CO	Vapour pressure	exp(a + b/x + c*log(x))	318.39326	-10460.32040	-49.33036
		Lwl-Bog	Mid-late	CO	Vapour pressure	exp(a + b/x + c*log(x))	504.08722	-16481.35648	-78.73869
		Lwl-Fen	Mid-late	PL & CO	Vapour pressure	exp(a + b/x + c*log(x))	524.38232	-16532.94131	-82.22050

Appendix 6.2. Minimum and maximum values used to restrict our spatial predictions of each component of accepted biomass (kg/ha), accepted biomass constrained based on DE, DP, or both (HQ; kg/ha), and intake rates (g/min).

Metric	Minimum	Maximum
GFS	0.00	1567.78
Lichen	0.00	4816.38
Horsetail	0.00	185.42
Mushroom	0.00	11.60
HQ-AB	0.00	1233.21
DE-AB	0.00	1415.07
DP-AB	0.00	1317.59
Intake rates	0.00	9.56

Appendix 6.3. Model coefficient, number of model parameters (K), Akaike's Information Criterion corrected for small sample size (AIC_c), change in AIC_c from best model (ΔAIC_c), and model weights calculated from AIC_c (w_i) for competing models with Julian day (JD) for grass, forb, and deciduous shrub biomass (kg/ha) in Pickle Lake (PL) and Cochrane (CO) by seral-specific ecosites.

SA	Ecosite	Model	Julian day	K	AIC_c	ΔAIC_c	w_i
PL	Mid-late-Upl-BS-Rocky	null		1	240.00	0.00	0.79
		JD	-0.15	2	242.71	2.71	0.21
	Early-Upl-BS	null		1	704.75	0.00	0.76
		JD	0.08	2	707.02	2.26	0.24
	Mid-late-Upl-BS	JD	1.04	2	1640.66	0.00	1.00
		null		1	1652.37	11.71	0.00
	Early-Upl-BS-WS	null		1	189.42	0.00	0.81
		JD	1.61	2	192.27	2.86	0.19
	Mid-late-Upl-BS-WS	null		1	441.94	0.00	0.75
		JD	0.44	2	444.11	2.16	0.25
	Early-Lwl-Bog	JD	1.71	2	260.77	0.00	0.57
		null		1	261.37	0.60	0.43
	Mid-late-Lwl-Bog	null		1	613.06	0.00	0.75
		JD	-0.02	2	615.31	2.25	0.25
CO	Early-Upl-BS	JD	0.38	2	214.80	0.00	0.86
		null		1	218.51	3.71	0.14
	Mid-late-Upl-BS	JD	0.43	2	237.33	0.00	0.63
		null		1	238.36	1.02	0.37
	Early-Upl-BS-WS	JD	1.53	2	151.65	0.00	0.82
		null		1	154.66	3.01	0.18
	Mid-late-Upl-BS-WS	JD	0.88	2	322.35	0.00	0.91
		null		1	326.94	4.59	0.09

Appendix 6.3. Continued.

SA	Ecosite	Model	Julian day	*K*	AIC_c	ΔAIC_c	w_i
CO	Early-Lwl-Bog	null		1	93.60	0.00	0.81
		JD	1.39	2	96.52	2.91	0.19
	Mid-late-Lwl-Bog	JD	1.12	2	361.23	0.00	1.00
		null		1	376.58	15.35	0.00
PL & CO	Mid-late-Lwl-Fen	JD	1.00	2	200.78	0.00	0.98
		null		1	209.06	8.29	0.02

Appendix 6.4. Model coefficient, number of model parameters (*K*), Akaike's Information Criterion corrected for small sample size (AIC_c), change in AIC_c from best model (ΔAIC_c), and model weights calculated from AIC_c (w_i) for competing models with basal area (BA; m^2/ha), canopy cover (CC; %), and stand height (SH; m) for grass, forb, and deciduous shrub biomass (kg/ha) in Pickle Lake (PL) and Cochrane (CO) by seral-specific ecosites.

SA	Ecosite	Model	BA	CC	SH	*K*	AIC_c	ΔAIC_c	w_i
PL	Mid-late-Upl-BS-Rocky	BA	0.87			2	233.83	0.00	0.84
		SH			-12.76	2	238.51	4.68	0.08
		CC		-1.94		2	238.62	4.79	0.08
	Early-Upl-BS	BA	1.06			2	701.21	0.00	0.62
		CC		-3.63		2	703.43	2.21	0.20
		SH			-26.21	2	703.68	2.47	0.18
	Mid-late-Upl-BS	BA	0.63			2	1641.52	0.00	1.00
		CC		-0.34		2	1654.05	12.53	0.00
		SH			-1.16	2	1654.17	12.65	0.00
	Early-Upl-BS-WS	CC		-5.14		2	191.56	0.00	0.38
		BA	1.07			2	191.75	0.18	0.35
		SH			22.53	2	192.30	0.74	0.27
	Mid-late-Upl-BS-WS	BA	0.98			2	428.53	0.00	1.00
		CC		-3.00		2	441.66	13.13	0.00
		SH			-5.97	2	442.95	14.42	0.00
	Early-Lwl-Bog	BA	0.86			2	263.22	0.00	0.41
		CC		-13.08		2	263.80	0.58	0.31
		SH			-8.70	2	263.95	0.73	0.28
	Mid-late-Lwl-Bog	CC		-1.51		2	603.35	0.00	0.73
		BA	0.62			2	606.06	2.70	0.19
		SH			-6.34	2	607.87	4.52	0.08
CO	Early-Upl-BS	CC		-2.41		2	218.31	0.00	0.45
		BA	0.70			2	218.56	0.24	0.40
		SH			-14.53	2	220.42	2.10	0.16
	Mid-late-Upl-BS	SH			4.48	2	238.98	0.00	0.40
		CC		-1.08		2	239.28	0.30	0.35
		BA	0.29			2	239.96	0.98	0.25

Appendix 6.4. Continued.

SA	Ecosite	Model	BA	CC	SH	K	AIC_c	ΔAIC_c	w_i
CO	Early-Upl-BS-WS	CC		-5.29		2	158.43	0.00	0.37
		BA	0.79			2	158.70	0.27	0.33
		SH			-28.13	2	158.86	0.44	0.30
	Mid-late-Upl-BS-WS	SH			8.48	2	321.80	0.00	0.95
		BA	0.18			2	328.92	7.13	0.03
		CC		-0.62		2	329.28	7.48	0.02
	Early-Lwl-Bog	CC		3.37		2	99.33	0.00	0.43
		SH			26.59	2	99.96	0.63	0.31
		BA	0.59			2	100.37	1.04	0.26
	Mid-late-Lwl-Bog	BA	0.43			2	373.94	0	0.62
		CC		-0.61		2	376.01	2.07	0.22
		SH			-3.97	2	376.62	2.68	0.16
PL & CO	Mid-late-Lwl-Fen	BA	-7.2			2	210.13	0	0.56
		CC		-1.14		2	211.88	1.76	0.23
		SH			-0.62	2	212.13	2.01	0.21

Appendix 6.5. Model coefficient, number of model parameters (K), Akaike's Information Criterion corrected for small sample size (AIC_c), change in AIC_c from best model (ΔAIC_c), and model weights calculated from AIC_c (w_i) for competing models with percent of clay, sand, and silt for grass, forb, and deciduous shrub biomass (kg/ha) in Pickle Lake (PL) and Cochrane (CO) by seral-specific ecosites.

SA	Ecosite	Model	Clay	Sand	Silt	K	AIC_c	ΔAIC_c	w_i
PL	Mid-late-Upl-BS-Rocky	Silt			11.35	2	240.54	0.00	0.48
		Clay	-14.32			2	241.20	0.67	0.34
		Sand		-3.82		2	242.52	1.99	0.18
	Early-Upl-BS	Clay	-12.69			2	706.56	0.00	0.36
		Silt			9.34	2	706.61	0.05	0.35
		Sand		-3.45		2	706.95	0.39	0.29
	Mid-late-Upl-BS	Sand		1.75		2	1654.01	0.00	0.35
		Clay	-2.72			2	1654.03	0.02	0.35
		Silt			1.03	2	1654.39	0.38	0.29
	Early-Upl-BS-WS	Clay	-34.13			2	191.77	0.00	0.39
		Silt			38.09	2	191.83	0.06	0.38
		Sand		3.94		2	192.86	1.09	0.23
	Mid-late-Upl-BS-WS	Clay	14.79			2	442.47	0.00	0.39
		Sand		-6.66		2	442.65	0.18	0.36
		Silt			7.73	2	443.42	0.95	0.25
	Early-Lwl-Bog	Clay	-4.48			2	264.08	0.00	0.34
		Silt			2.54	2	264.12	0.04	0.33
		Sand		1.41		2	264.15	0.06	0.33

Appendix 6.5. Continued.

SA	Ecosite	Model	Clay	Sand	Silt	*K*	AIC_c	ΔAIC_c	w_i
PL	Mid-late-Lwl-Bog	Sand		3.21		2	614.48	0.00	0.39
		Clay	-3.30			2	614.89	0.41	0.32
		Silt			-2.32	2	615.05	0.56	0.29
	Early-Upl-BS	Clay	-23.12			2	218.65	0.00	0.48
		Sand		9.57		2	219.37	0.72	0.34
		Silt			-8.49	2	220.65	2.00	0.18
	Mid-late-Upl-BS	Clay	-7.41			2	238.82	0.00	0.59
		Sand		1.12		2	240.77	1.95	0.22
		Silt			-0.03	2	241.06	2.24	0.19
CO	Early-Upl-BS-WS	Silt			45.23	2	157.17	0.00	0.48
		Clay	52.14			2	158.06	0.88	0.31
		Sand		4.94		2	158.89	1.72	0.21
	Mid-late-Upl-BS-WS	Silt			5.78	2	328.25	0.00	0.35
		Clay	4.83			2	328.34	0.09	0.33
		Sand		-2.90		2	328.40	0.16	0.32
	Early-Lwl-Bog	Silt			16.42	2	99.65	0.00	0.44
		Sand		-2.35		2	100.52	0.87	0.28
		Clay	-4.28			2	100.54	0.89	0.28
	Mid-late-Lwl-Bog	Sand		-2.74		2	377.71	0.00	0.47
		Clay	2.12			2	378.74	1.04	0.28
		Silt			1.22	2	378.93	1.22	0.25
PL & CO	Mid-late-Lwl-Fen	Clay	-19.60			2	211.03	0.00	0.43
		Sand		9.62		2	211.57	0.54	0.33
		Silt			2.61	2	212.12	1.09	0.25

Appendix 6.6. Model coefficient, number of model parameters (*K*), Akaike's Information Criterion corrected for small sample size (AIC_c), change in AIC_c from best model (ΔAIC_c), and model weights calculated from AIC_c (w_i) for competing models with basal area (BA; m^2/ha), percent silt, normalized difference moisture index (NDMI), and change in enhanced vegetation index (ΔEVI) for grass, forb, and deciduous shrub biomass (kg/ha) at Mid-late-Upl-BS-Rocky macroplots in Pickle Lake.

Model	BA	Silt	NDMI	ΔEVI	*K*	AIC_c	ΔAIC_c	w_i
m1	0.87				2	233.83	0.00	0.47
m7	0.80			0.03	3	236.15	2.32	0.15
m6	1.08		179.87		3	236.41	2.58	0.13
m5	0.80	4.21			3	236.59	2.77	0.12
m9		15.56		0.08	3	239.07	5.24	0.03
null					1	240.00	6.18	0.02
m3			-314.63		2	240.15	6.33	0.02
m2		11.35			2	240.54	6.71	0.02
m4				0.06	2	240.57	6.74	0.02
m10			-317.83	0.06	3	240.69	6.86	0.02
m8		7.77	-236.52		3	242.33	8.50	0.01

Appendix 6.7. Model coefficient, number of model parameters (*K*), Akaike's Information Criterion corrected for small sample size (AIC_c), change in AIC_c from best model (ΔAIC_c), and model weights calculated from AIC_c (w_i) for competing models with Julian day (JD), basal area (BA; m^2/ha), percent sand, normalized difference moisture index (NDMI), and change in enhanced vegetation index (ΔEVI) for grass, forb, and deciduous shrub biomass (kg/ha) at Mid-late-Upl-BS and Mid-late-Lwl-Bog macroplots in Pickle Lake.

Ecosite	Model	JD	BA	Sand	NDMI	ΔEVI	*K*	AIC_c	ΔAIC_c	w_i
Mid-late-Upl-BS	m7	0.95	0.56		-214.90		4	1626.42	0.00	0.38
	m12	0.96	0.55	2.49	-223.70		5	1627.47	1.05	0.23
	m2	1.04	0.63				3	1628.37	1.95	0.14
	m15	0.96	0.55	2.48	-223.01	-0.0004	6	1629.69	3.27	0.07
	m6	1.05	0.63	2.10			4	1629.73	3.31	0.07
	m8	1.04	0.64			-0.01	4	1630.07	3.64	0.06
	m13	1.05	0.63	1.93		-0.008	5	1631.59	5.17	0.03
	m4	0.92			-292.19		3	1635.55	9.13	0.00
	m9	0.93		2.78	-301.03		4	1636.39	9.97	0.00
	m11	0.92			-294.57	0.001	4	1637.70	11.28	0.00
	m14	0.93		2.88	-308.29	0.004	5	1638.51	12.09	0.00
	m1	1.04					2	1640.66	14.24	0.00
	m3	1.05		2.29			3	1641.93	15.51	0.00
	m5	1.04				-0.008	3	1642.48	16.06	0.00
	m10	1.05		2.16		-0.007	4	1643.90	17.47	0.00
	null						1	1652.37	25.95	0.00
Mid-late-Lwl-Bog	m1		0.62				2	606.06	0.00	0.48
	m5		0.60	1.87			3	608.08	2.02	0.17
	m7		0.61			-0.01	3	608.22	2.17	0.16
	m6		0.62		-28.95		3	608.38	2.32	0.15
	null						1	613.06	7.00	0.01
	m2			3.21			2	614.48	8.43	0.01
	m4					-0.01	2	615.01	8.95	0.01
	m3				-39.71		2	615.27	9.21	0.00
	m9			3.57		-0.02	3	616.34	10.29	0.00
	m8			3.18	-31.19		3	616.81	10.75	0.00
	m10				-31.13	-0.01	3	617.33	11.27	0.00

Appendix 6.8. Model coefficient, number of model parameters (*K*), Akaike's Information Criterion corrected for small sample size (AIC_c), change in AIC_c from best model (ΔAIC_c), and model weights calculated from AIC_c (w_i) for competing models with basal area (BA; m^2/ha), percent clay, normalized difference moisture index (NDMI), and change in enhanced vegetation index (ΔEVI) for grass, forb, and deciduous shrub biomass (kg/ha) at Early-Upl-BS, Mid-late-Upl-BS-WS, Early-Upl-BS-WS, and Early-Lwl-Bog at macroplots in Pickle Lake.

Ecosite	Model	BA	Clay	NDMI	ΔEVI	*K*	AIC_c	ΔAIC_c	w_i
Early-Upl-BS	m7	1.50			0.16	3	693.31	0.00	0.49
	m12	1.54	-18.79		0.17	4	694.40	1.09	0.28
	m14	1.93	-19.03	389.07	0.14	5	695.61	2.31	0.15
	m6	1.95		749.08		3	698.50	5.20	0.04
	m11	1.99	-17.49	759.44		4	699.90	6.60	0.02
	m1	1.06				2	701.21	7.91	0.01
	m5	1.09	-16.26			3	702.74	9.44	0.00
	m4				0.11	2	702.89	9.58	0.00
	m10			-385.81	0.15	3	703.48	10.18	0.00
	m9		-13.39		0.11	3	704.70	11.40	0.00
	null					1	704.75	11.45	0.00
	m13		-14.55	-396.89	0.15	4	705.28	11.98	0.00
	m2		-12.69			2	706.56	13.26	0.00
	m3			-24.53		2	707.01	13.70	0.00
	m8		-12.76	-30.13		3	708.92	15.61	0.00
Mid-late-Upl-BS-WS	m5	0.97	13.88			3	428.44	0.00	0.28
	m1	0.98				2	428.53	0.09	0.27
	m11	0.90	14.37	556.36		4	429.53	1.09	0.16
	m6	0.91		521.17		3	429.76	1.32	0.14
	m7	0.98			0.001	3	431.10	2.66	0.07
	m12	0.97	13.85		0.001	4	431.20	2.76	0.07
	m3			989.82		2	440.98	12.54	0.00
	m8		15.58	1020.69		3	441.24	12.80	0.00
	null					1	441.94	13.50	0.00
	m2		14.79			2	442.47	14.03	0.00
	m10			1080.64	-0.01	3	443.45	15.01	0.00
	m13		15.50	1100.12	-0.01	4	443.91	15.47	0.00
	m4				0.02	2	444.04	15.60	0.00
	m9		15.07		0.02	3	444.64	16.20	0.00

Appendix 6.8. Continued.

Ecosite	Model	BA	Clay	NDMI	ΔEVI	*K*	AIC_c	ΔAIC_c	w_i
Early-Upl-BS-WS	null					1	189.40	0.00	0.50
	m4				0.11	2	191.50	2.04	0.20
	m1	1.10				2	191.80	2.33	0.10
	m2		-34.10			2	191.80	2.36	0.10
	m3			-476.39		2	192.60	3.17	0.10
Early-Lwl-Bog	null					1	261.37	0.00	0.30
	m3			-395.08		2	262.20	0.83	0.20
	m1	0.86				2	263.22	1.85	0.12
	m4				-0.01	2	264.06	2.69	0.08
	m2		-4.48			2	264.08	2.72	0.08
	m8		-17.44	-533.94		3	264.27	2.90	0.07
	m10			-494.56	0.03	3	265.06	3.69	0.05
	m6	0.11		-371.21		3	265.35	3.98	0.04
	m5	1.03	-10.09			3	266.00	4.63	0.03
	m7	1.03			0.01	3	266.31	4.94	0.03
	m9		-5.69		-0.02	3	267.10	5.73	0.02

Appendix 6.9. Model coefficient, number of model parameters (*K*), Akaike's Information Criterion corrected for small sample size (AIC_c), change in AIC_c from best model (ΔAIC_c), and model weights calculated from AIC_c (w_i) for competing models with Julian day (JD), basal area (BA; m^2/ha), percent clay, normalized difference moisture index (NDMI), and change in enhanced vegetation index (ΔEVI) for grass, forb, and deciduous shrub biomass (kg/ha) at Early and Mid-late Upl-BS macroplots in Cochrane.

Ecosite	Model	JD	BA	Clay	NDMI	ΔEVI	*K*	AIC_c	ΔAIC_c	w_i
Early-Upl-BS	m4	0.38			-285.55		3	214.71	0.00	0.27
	m1	0.38					2	214.80	0.10	0.26
	m2	0.35	0.59				3	215.25	0.54	0.20
	m3	0.34		-17.68			3	215.93	1.23	0.15
	m5	0.45				-0.06	3	216.97	2.27	0.09
	null						1	218.51	3.80	0.04
Mid-late-Upl-BS	null						1	238.36	0.00	0.25
	m2			-7.41			2	238.82	0.46	0.20
	m1		0.29				2	239.96	1.60	0.11
	m4					0.01	2	240.66	2.30	0.08
	m3				-56.83		2	240.72	2.36	0.08
	m9			-8.50		0.02	3	240.78	2.42	0.08
	m5		0.17	-6.36			3	241.47	3.11	0.05
	m8			-7.11	-32.40		3	241.72	3.37	0.05
	m10				-143.97	0.03	3	242.22	3.86	0.04
	m6		0.31		-66.95		3	242.49	4.13	0.03
	m7		0.28			0.01	3	242.65	4.29	0.03

Appendix 6.10. Model coefficient, number of model parameters (*K*), Akaike's Information Criterion corrected for small sample size (AIC_c), change in AIC_c from best model (ΔAIC_c), and model weights calculated from AIC_c (w_i) for competing models with Julian day (JD), basal area (BA; m^2/ha), percent silt, normalized difference moisture index (NDMI), and change in enhanced vegetation index (ΔEVI) for grass, forb, and deciduous shrub biomass (kg/ha) at Early Upl-BS-WS, Mid-late Upl-BS-WS and Early-Lwl-Bog macroplots in Cochrane.

Ecosite	Model	JD	BA	Silt	NDMI	ΔEVI	*K*	AIC_c	ΔAIC_c	w_i
Early-Upl-BS-WS	m1	1.53					2	151.65	0.00	0.69
	null						1	154.66	3.01	0.15
	m5					0.23	2	156.28	4.63	0.07
	m3			45.23			2	157.17	5.52	0.04
	m4				-846.85		2	158.45	6.80	0.02
	m2		0.79				2	158.70	7.05	0.02
Mid-late-Upl-BS-WS	m6	1.05	0.39	8.52			4	322.14	0.00	0.13
	m4	0.85			-460.92		3	322.16	0.01	0.13
	m1	0.88					2	322.35	0.21	0.12
	m3	0.93		7.35			3	322.53	0.39	0.11
	m11	0.85			-558.25	0.03	4	322.58	0.44	0.10
	m9	0.90		6.84	-432.94		4	322.70	0.56	0.10
	m2	0.97	0.33				3	322.88	0.73	0.09
	m7	0.94	0.31		-444.87		4	322.91	0.77	0.09
	m5	0.88				0.02	3	323.94	1.80	0.05
	m10	0.93		6.86		0.02	4	324.65	2.51	0.04
	m8	0.97	0.31			0.02	4	324.83	2.69	0.03
	null						1	326.94	4.80	0.01
Early-Lwl-Bog	null						1	93.60	0.00	0.87
	m2			16.42			2	99.65	6.04	0.04
	m1		0.59				2	100.37	6.76	0.03
	m4					0.03	2	100.50	6.90	0.03
	m3				104.62		2	100.57	6.97	0.03

Appendix 6.11. Model coefficient, number of model parameters (*K*), Akaike's Information Criterion corrected for small sample size (AIC_c), change in AIC_c from best model (ΔAIC_c), and model weights calculated from AIC_c (w_i) for competing models with Julian day (JD), basal area (BA; m^2/ha), percent sand, normalized difference moisture index (NDMI), and change in enhanced vegetation index (ΔEVI) for grass, forb, and deciduous shrub biomass (kg/ha) at Mid-late-Lwl-Bog macroplots in Cochrane.

Model	JD	BA	Sand	NDMI	ΔEVI	*K*	AIC_c	ΔAIC_c	w_i
m1	1.12					2	361.23	0.00	0.27
m2	1.02	0.22				3	361.88	0.64	0.20
m3	1.10		-1.45			3	363.23	1.99	0.10
m4	1.11			40.50		3	363.68	2.44	0.08
m5	1.13				0.00	3	363.79	2.56	0.08
m6	0.99	0.23	-1.54			4	363.93	2.70	0.07
m7	0.98	0.26		90.39		4	363.97	2.74	0.07
m8	1.00	0.24			-0.01	4	364.50	3.27	0.05
m9	1.09		-1.36	20.32		4	365.96	4.72	0.03
m10	1.09		-1.58		0.00	4	365.96	4.73	0.03
m11	1.12			39.44	0.00	4	366.43	5.20	0.02
null						1	376.58	15.35	0.00

Appendix 6.12. Model coefficient, number of model parameters (*K*), Akaike's Information Criterion corrected for small sample size (AIC_c), change in AIC_c from best model (ΔAIC_c), and model weights calculated from AIC_c (w_i) for competing models with Julian day (JD), basal area (BA; m^2/ha), percent sand, normalized difference moisture index (NDMI), and change in enhanced vegetation index (ΔEVI) for grass, forb, and deciduous shrub biomass (kg/ha) at Mid-late-Lwl-Fen macroplots in Pickle Lake and Cochrane.

Model	JD	BA	Clay	NDMI	ΔEVI	*K*	AIC_c	ΔAIC_c	w_i
m1	1.00					2	200.78	0.00	0.96
null						1	209.06	8.29	0.02
m2		-7.21				2	210.13	9.35	0.01
m3			-19.60			2	211.03	10.26	0.01
m5					-0.06	2	211.44	10.66	0.00
m4				365.62		2	211.86	11.09	0.00

Appendix 6.13. Model coefficient, number of model parameters (*K*), Akaike's Information Criterion corrected for small sample size (AIC_c), change in AIC_c from best model (ΔAIC_c), and model weights calculated from AIC_c (w_i) for competing models with Julian day (JD) for lichen biomass (kg/ha) in Pickle Lake (PL) and Cochrane (CO) across all seral-specific ecosites.

SA	Model	JD	*K*	AIC_c	ΔAIC_c	w_i
	null		1	5261.66	0.00	0.51
PL	JD	1.25	2	5261.76	0.10	0.49
	null		1	1918.37	0.00	0.69
CO	JD	-1.04	2	1919.98	1.62	0.31

Appendix 6.14. Model coefficient, number of model parameters (*K*), Akaike's Information Criterion corrected for small sample size (AIC_c), change in AIC_c from best model (ΔAIC_c), and model weights calculated from AIC_c (w_i) for competing models with basal area (BA; m^2/ha), canopy cover (CC; %), and stand height (SH; m) for lichen biomass (kg/ha) in Pickle Lake (PL) and Cochrane (CO) by seral-specific ecosites.

SA	Ecosite	Model	BA	CC	SH	*K*	AIC_c	ΔAIC_c	w_i
PL	Mid-late-Upl-BS-Rocky	CC		-14.42		2	307.08	0.00	0.76
		BA	-25.10			2	309.60	2.52	0.21
		SH			-21.45	2	313.77	6.69	0.03
	Early-Upl-BS-WS	BA	-1.01			2	134.32	0.00	0.36
		SH			-1.52	2	134.34	0.02	0.35
		CC		-0.07		2	134.76	0.44	0.29
	Mid-late-Upl-BS-WS	SH			0.77	2	285.65	0.00	0.62
		BA	0.06			2	288.00	2.35	0.19
		CC		-0.007		2	288.03	2.38	0.19
	Early-Lwl-Bog	SH			1.87	2	215.20	0.00	0.34
		BA	-0.82			2	215.29	0.09	0.33
		CC		0.22		2	215.31	0.11	0.33
	Mid-late-Lwl-Bog	CC		-0.25		2	605.13	0.00	0.38
		BA	0.28			2	605.44	0.31	0.32
		SH			0.05	2	605.57	0.45	0.30
CO	Early-Upl-BS-WS	SH			0.04	2	10.67	0.00	0.39
		BA	0.01			2	11.10	0.43	0.31
		CC		-0.0006		2	11.14	0.47	0.30
	Mid-late-Upl-BS-WS	BA	-0.03			2	164.56	0.00	0.35
		CC		0.02		2	164.65	0.09	0.33
		SH			-0.01	2	164.69	0.13	0.32
	Early-Lwl-Bog	BA	81.64			2	106.87	0.00	0.42
		SH			82.76	2	106.88	0.00	0.42
		CC		1.84		2	108.85	1.98	0.16
	Mid-late-Lwl-Bog	CC		-1.49		2	412.92	0.00	0.41
		BA	-2.92			2	413.20	0.28	0.35
		SH			-9.36	2	413.96	1.04	0.24
PL & CO	Early-Upl-BS	SH			15.79	2	901.90	0.00	0.60
		CC		1.01		2	903.95	2.05	0.21
		BA	0.08			2	904.20	2.29	0.19
	Mid-late-Upl-BS	BA	1.34			2	2548.41	0.00	0.63
		CC		-12.79		2	2549.88	1.47	0.30
		SH			-44.79	2	2552.89	4.49	0.07
	Mid-late-Lwl-Fen	CC		-0.95		2	213.70	0.00	0.34
		SH			2.74	2	213.77	0.07	0.33
		BA	-1.07			2	213.82	0.12	0.32

Appendix 6.15. Model coefficient, number of model parameters (*K*), Akaike's Information Criterion corrected for small sample size (AIC_c), change in AIC_c from best model (ΔAIC_c), and model weights calculated from AIC_c (w_i) for competing models with percent of clay, sand, and silt for lichen biomass (kg/ha) in Pickle Lake (PL) and Cochrane (CO) by seral-specific ecosites.

SA	Ecosite	Model	Clay	Sand	Silt	*K*	AIC_c	ΔAIC_c	w_i
PL	Mid-late-Upl-BS-Rocky	Sand		30.51		2	313.58	0.00	0.36
		Clay	-43.14			2	313.69	0.10	0.34
		Silt			-19.94	2	313.90	0.31	0.30
	Early-Upl-BS-WS	Silt			1.92	2	134.34	0.00	0.37
		Sand		-1.09		2	134.48	0.14	0.34
		Clay	-0.06			2	134.80	0.47	0.29
	Mid-late-Upl-BS-WS	Sand		-0.53		2	286.96	0.00	0.35
		Silt			0.78	2	287.07	0.11	0.33
		Clay	1.05			2	287.10	0.14	0.32
	Early-Lwl-Bog	Sand		2.49		2	214.78	0.00	0.37
		Clay	-2.25			2	215.08	0.30	0.32
		Silt			-1.37	2	215.17	0.39	0.31
	Mid-late-Lwl-Bog	Silt			1.70	2	605.34	0.00	0.35
		Clay	-1.86			2	605.37	0.03	0.34
		Sand		-0.23		2	605.57	0.23	0.31
CO	Early-Upl-BS-WS	Sand		-0.03		2	4.54	0.00	0.87
		Silt			0.03	2	9.39	4.85	0.08
		Clay	0.03			2	10.11	5.57	0.05
	Mid-late-Upl-BS-WS	Sand		-0.12		2	164.03	0.00	0.40
		Silt			0.09	2	164.60	0.57	0.30
		Clay	-0.06			2	164.63	0.61	0.30
	Early-Lwl-Bog	Silt			-52.51	2	105.43	0.00	0.45
		Sand		24.04		2	105.69	0.26	0.40
		Clay	-32.59			2	107.72	2.29	0.14
	Mid-late-Lwl-Bog	Sand		4.07		2	416.21	0.00	0.37
		Silt			-7.50	2	416.25	0.04	0.36
		Clay	-0.62			2	416.84	0.63	0.27
PL & CO	Early-Upl-BS	Clay	9.10			2	903.59	0.00	0.45
		Sand		-2.05		2	904.50	0.91	0.28
		Silt			-2.13	2	904.58	0.99	0.27
	Mid-late-Upl-BS	Sand		39.93		2	2554.36	0.00	0.68
		Silt			-46.96	2	2557.14	2.77	0.17
		Clay	-55.92			2	2557.37	3.01	0.15
	Mid-late-Lwl-Fen	Clay	39.51			2	209.37	0.00	0.46
		Sand		-26.88		2	209.40	0.03	0.46
		Silt			20.18	2	212.92	3.54	0.08

Appendix 6.16. Model coefficient, number of model parameters (*K*), Akaike's Information Criterion corrected for small sample size (AIC_c), change in AIC_c from best model (ΔAIC_c), and model weights calculated from AIC_c (w_i) for competing models with canopy cover (CC; %) percent sand, normalized difference moisture index (NDMI), and change in enhanced vegetation index (ΔEVI) for lichen biomass (kg/ha) at Mid-late-Upl-BS-Rocky macroplots in Pickle Lake.

Model	CC	Sand	NDMI	ΔEVI	*K*	AIC_c	ΔAIC_c	w_i
m1	-14.42				2	307.08	0.00	0.28
m5	-16.85	64.41			3	307.11	0.04	0.28
m7	-12.94			0.28	3	308.11	1.03	0.17
m6	-22.56		2037.31		3	308.69	1.61	0.13
m4				0.38	2	311.10	4.02	0.04
null					1	311.29	4.21	0.03
m10			-1603.44	0.39	3	312.03	4.95	0.02
m3			-1581.73		2	312.23	5.15	0.02
m2		30.51			2	313.58	6.50	0.01
m8		57.04	-2118.61		3	313.64	6.56	0.01
m9		21.75		0.37	3	313.97	6.89	0.01

Appendix 6.17. Model coefficient, number of model parameters (*K*), Akaike's Information Criterion corrected for small sample size (AIC_c), change in AIC_c from best model (ΔAIC_c), and model weights calculated from AIC_c (w_i) for competing models with basal area (BA; m^2/ha), percent silt, normalized difference moisture index (NDMI), and change in enhanced vegetation index (ΔEVI) for lichen biomass (kg/ha) at Mid-late-Upl-BS-WS, Early-Upl-BS-WS, and Mid-late-Lwl-Bog macroplots in Pickle Lake.

Ecosite	Model	BA	Silt	NDMI	ΔEVI	*K*	AIC_c	ΔAIC_c	w_i
Mid-late-Upl-BS-WS	null					1	285.62	0.00	0.28
	m2		-0.53			2	286.96	1.35	0.14
	m3			-41.58		2	287.46	1.85	0.11
	m4				-0.002	2	287.81	2.19	0.09
	m1	0.06				2	288.00	2.39	0.09
	m8		-0.57	-46.50		3	288.81	3.20	0.06
	m9		-0.57		-0.002	3	289.19	3.57	0.05
	m5	0.07	-0.54			3	289.50	3.88	0.04
	m10			-37.73	-0.0006	3	290.02	4.41	0.03
	m6	-0.04		-44.26		3	290.03	4.41	0.03
	m7	0.02			-0.002	3	290.39	4.77	0.03
	m14		-0.58	-39.95	-0.001	4	291.52	5.91	0.01
	m12	-0.04	-0.57	-48.92		4	291.56	5.95	0.01
	m13	0.03	-0.57		-0.002	4	291.94	6.32	0.01
	m11	-0.05		-40.37	-0.0006	4	292.77	7.15	0.01

Appendix 6.17. Continued.

Ecosite	Model	BA	Silt	NDMI	ΔEVI	*K*	AIC_c	ΔAIC_c	w_i
Early-Upl-BS-WS-	null					1	131.49	0.00	0.42
	m3			-96.68		2	132.39	0.89	0.27
	m4				-0.01	2	134.26	2.77	0.11
	m1	-1.01				2	134.32	2.82	0.10
	m2		1.92			2	134.34	2.84	0.10
Mid-late-Lwl-Bog	m3			-365.38		2	599.40	0.00	0.31
	m6	0.68		-391.50		3	600.92	1.51	0.15
	m10			-367.85	-0.01	3	601.08	1.68	0.14
	m8		1.28	-362.61		3	601.60	2.20	0.10
	m11	0.63		-391.67	-0.01	4	602.82	3.41	0.06
	m12	0.84	2.38	-392.49		4	602.88	3.47	0.06
	m14		2.14	-363.72	-0.02	4	603.13	3.72	0.05
	null					1	603.32	3.92	0.04
	m15	0.83	3.21	-393.06	-0.02	5	604.53	5.13	0.02
	m4				-0.01	2	605.06	5.65	0.02
	m2		1.70			2	605.34	5.93	0.02
	m1	0.28				2	605.44	6.04	0.02
	m9		2.55		-0.02	3	606.90	7.50	0.01
	m7	0.23			-0.01	3	607.31	7.91	0.01
	m5	0.44	2.29			3	607.39	7.99	0.01
	m13	0.42	3.11		-0.02	4	609.07	9.67	0.00

Appendix 6.18. Model coefficient, number of model parameters (*K*), Akaike's Information Criterion corrected for small sample size (AIC_c), change in AIC_c from best model (ΔAIC_c), and model weights calculated from AIC_c (w_i) for competing models with basal area (BA; m^2/ha), percent silt, normalized difference moisture index (NDMI), and change in enhanced vegetation index (ΔEVI) for lichen biomass (kg/ha) at Early-Lwl-Bog macroplots in Pickle Lake.

Model	BA	Sand	NDMI	ΔEVI	*K*	AIC_c	ΔAIC_c	w_i
null					1	212.52	0.00	0.28
m3			122.01		2	213.14	0.63	0.21
m6	-8.75		194.58		3	214.65	2.14	0.10
m4				0.009	2	214.77	2.25	0.09
m2		2.49			2	214.78	2.27	0.09
sm1	-0.82				2	215.29	2.78	0.07
m8		1.06	113.92		3	216.21	3.70	0.04
m10			126.00	-0.001	3	216.30	3.79	0.04
m9		2.33		0.009	3	217.46	4.95	0.02
m7	-3.99			0.01	3	217.59	5.07	0.02
m5	-2.12	2.81			3	217.83	5.31	0.02

Appendix 6.19. Model coefficient, number of model parameters (*K*), Akaike's Information Criterion corrected for small sample size (AIC_c), change in AIC_c from best model (ΔAIC_c), and model weights calculated from AIC_c (w_i) for competing models with basal area (BA; m^2/ha), percent sand, normalized difference moisture index (NDMI), and change in enhanced vegetation index (ΔEVI) for lichen biomass (kg/ha) at Early and Mid-late-Upl-BS-WS macroplots in Cochrane.

Ecosite	Model	BA	Sand	NDMI	ΔEVI	*K*	AIC_c	ΔAIC_c	w_i
Early-Upl-BS-WS	m2		-0.03			2	4.54	0.00	0.70
	null					1	6.88	2.33	0.22
	m3			0.32		2	10.98	6.44	0.03
	m1	0.01				2	11.10	6.56	0.03
	m4				0.00001	2	11.14	6.60	0.03
Mid-late-Upl-BS-WS	m4				-0.003	2	159.33	0.00	0.34
	m9		-0.16		-0.003	3	160.72	1.40	0.17
	m7	-0.05			-0.003	3	161.71	2.39	0.10
	m10			1.78	-0.003	3	162.05	2.73	0.09
	null					1	162.18	2.85	0.08
	m13	-0.06	-0.17		-0.003	4	163.15	3.83	0.05
	m14		-0.16	3.85	-0.003	4	163.64	4.32	0.04
	m2		-0.12			2	164.03	4.70	0.03
	m3			-6.76		2	164.53	5.20	0.03
	m1	-0.03				2	164.56	5.23	0.02
	m11	-0.05		1.91	-0.003	4	164.69	5.36	0.02
	m5	-0.04	-0.13			3	166.55	7.23	0.01
	m8		-0.12	-5.63		3	166.65	7.32	0.01
	m6	-0.03		-6.78		3	167.13	7.80	0.01
	m12	-0.04	-0.12	-5.59		4	169.42	10.10	0.00

Appendix 6.20. Model coefficient, number of model parameters (*K*), Akaike's Information Criterion corrected for small sample size (AIC_c), change in AIC_c from best model (ΔAIC_c), and model weights calculated from AIC_c (w_i) for competing models with basal area (BA; m^2/ha), percent silt, normalized difference moisture index (NDMI), and change in enhanced vegetation index (ΔEVI) for lichen biomass (kg/ha) at Early and Mid-late-Lwl-Bog macroplots in Cochrane.

Ecosite	Model	BA	Silt	NDMI	ΔEVI	*K*	AIC_c	ΔAIC_c	w_i
Early-Lwl-Bog	null					1	101.96	0.00	0.75
	m2		-52.51			2	105.43	3.47	0.13
	m1	81.64				2	106.87	4.92	0.06
	m3			484.71		2	108.73	6.77	0.03
	m4				0.04	2	108.87	6.91	0.02

Appendix 6.20. Continued.

Ecosite	Model	BA	Silt	NDMI	ΔEVI	*K*	AIC_c	ΔAIC_c	w_i
Mid-late-Lwl-Bog	m1	-2.92				2	413.20	0.00	0.24
	null					1	414.42	1.21	0.13
	m5	-3.07	5.01			3	414.73	1.52	0.11
	m3			-413.49		2	414.85	1.65	0.10
	m6	-2.43		-223.66		3	415.27	2.07	0.08
	m7	-2.92			0.0004	3	415.80	2.60	0.06
	m2		4.07			2	416.21	3.01	0.05
	m4				0.02	2	416.67	3.47	0.04
	m10			-425.26	0.02	3	417.16	3.96	0.03
	m8		2.28	-376.96		3	417.26	4.06	0.03
	m13	-2.95	5.74		0.02	4	417.35	4.15	0.03
	m12	-2.77	4.31	-128.60		4	417.36	4.16	0.03
	m11	-2.36		-232.34	0.01	4	418.05	4.84	0.02
	m9		5.57		0.03	3	418.22	5.02	0.02
	m14		3.74	-370.88	0.03	4	419.49	6.29	0.01

Appendix 6.21. Model coefficient, number of model parameters (*K*), Akaike's Information Criterion corrected for small sample size (AIC_c), change in AIC_c from best model (ΔAIC_c), and model weights calculated from AIC_c (w_i) for competing models with basal area (BA; m^2/ha), percent clay, normalized difference moisture index (NDMI), and change in enhanced vegetation index (ΔEVI) for lichen biomass (kg/ha) at Early-Upl-BS and Mid-late-Lwl-Fen macroplots in Pickle Lake and Cochrane.

Ecosite	Model	BA	Clay	NDMI	ΔEVI	*K*	AIC_c	ΔAIC_c	w_i
Early-Upl-BS	m3			328.97		2	900.38	0.00	0.23
	m10			418.99	-0.04	3	901.56	1.18	0.13
	m6	-0.15		460.60		3	901.75	1.38	0.12
	m8		6.80	312.17		3	902.01	1.64	0.10
	null					1	902.47	2.09	0.08
	m11	-0.16		567.40	-0.05	4	902.85	2.47	0.07
	m14		6.71	401.72	-0.04	4	903.28	2.90	0.05
	m2		9.10			2	903.59	3.21	0.05
	m12	-0.13	5.57	431.15		4	903.68	3.30	0.04
	m1	0.08				2	904.20	3.82	0.03
	m4				-0.001	2	904.65	4.28	0.03
	m15	-0.15	5.35	537.75	-0.04	5	904.87	4.50	0.02
	m5	0.09	9.34			3	905.32	4.94	0.02
	m9		9.07		-0.001	3	905.85	5.47	0.01
	m7	0.09			-0.001	3	906.45	6.08	0.01
	m13	0.09	9.43		-0.01	4	907.63	7.26	0.01

Appendix 6.21. Continued.

Ecosite	Model	BA	Clay	NDMI	ΔEVI	*K*	AIC_c	ΔAIC_c	w_i
Mid-late-Lwl-Fen	m2		39.51			2	209.37	0.00	0.51
	null					1	210.78	1.40	0.25
	m4				-0.10	2	212.32	2.94	0.12
	m3			-553.57		2	213.28	3.91	0.07
	m1	-1.07				2	213.82	4.44	0.05

Appendix 6.22. Model coefficient, number of model parameters (*K*), Akaike's Information Criterion corrected for small sample size (AIC_c), change in AIC_c from best model (ΔAIC_c), and model weights calculated from AIC_c (w_i) for competing models with basal area (BA; m^2/ha), percent sand, normalized difference moisture index (NDMI), and change in enhanced vegetation index (ΔEVI) for lichen biomass (kg/ha) at Mid-late-Upl-BS macroplots in Pickle Lake and Cochrane.

Model	BA	Sand	NDMI	ΔEVI	*K*	AIC_c	ΔAIC_c	w_i
m12	1.02	44.42	-3101.93		4	2526.30	0.00	0.70
m15	1.01	45.55	-3192.47	0.05	5	2528.28	1.98	0.26
m8		47.84	-3454.33		3	2533.14	6.84	0.02
m14		49.53	-3587.96	0.07	4	2534.86	8.57	0.01
m6	1.11		-2806.82		3	2535.10	8.81	0.01
m11	1.12		-2760.03	-0.03	4	2537.18	10.88	0.00
m3			-3170.27		2	2543.07	16.77	0.00
m5	1.28	36.64			3	2543.73	17.44	0.00
m13	1.28	34.71		-0.10	4	2545.06	18.77	0.00
m10			-3161.46	-0.005	3	2545.17	18.88	0.00
m1	1.34				2	2548.41	22.11	0.00
m7	1.34			-0.14	3	2548.91	22.62	0.00
m2		39.93			2	2554.36	28.07	0.00
m9		38.20		-0.09	3	2555.86	29.57	0.00
null					1	2559.73	33.43	0.00
m4				-0.13	2	2560.45	34.16	0.00

Appendix 6.23. Model coefficient, number of model parameters (*K*), Akaike's Information Criterion corrected for small sample size (AIC_c), change in AIC_c from best model (ΔAIC_c), and model weights calculated from AIC_c (w_i) for competing models with Julian day (JD) for horsetail biomass (kg/ha) in Pickle Lake (PL) and Cochrane (CO) by seral-specific ecosites.

SA	Ecosite	Model	Julian day	*K*	AIC_c	ΔAIC_c	w_i
PL	Early-Upl-BS	null		1	428.00	0.00	0.72
		JD	-0.05	2	429.93	1.93	0.28
	Mid-late-Upl-BS	null		1	872.07	0.00	0.68
		JD	-0.01	2	873.55	1.48	0.32
	Early-Upl-BS-WS	JD	-0.72	2	155.69	0.00	0.62
		null		1	156.70	1.02	0.38
	Mid-late-Upl-BS-WS	null		1	197.53	0.00	0.56
		JD	-0.04	2	198.01	0.49	0.44
	Early-Lwl-Bog	null		1	216.76	0.00	0.80
		JD	-0.02	2	219.55	2.79	0.20
	Mid-late-Lwl-Bog	null		1	512.23	0.00	0.74
		JD	0.05	2	514.35	2.12	0.26
CO	Early-Upl-BS	null		1	-80.58	0.00	0.74
		JD	-0.0002	2	-78.45	2.14	0.26
	Mid-late-Upl-BS	null		1	30.23	0.00	0.72
		JD	0.003	2	32.08	1.84	0.28
	Early-Upl-BS-WS	null		1	87.32	0.00	0.83
		JD	0.19	2	90.47	3.15	0.17
	Mid-late-Upl-BS-WS	null		1	95.29	0.00	0.73
		JD	0.007	2	97.25	1.96	0.27
	Early-Lwl-Bog	null		1	76.50	0.00	0.87
		JD	0.71	2	80.32	3.82	0.13
	Mid-late-Lwl-Bog	JD	0.83	2	274.32	0.00	0.93
		null		1	279.53	5.21	0.07
PL & CO	Mid-late-Lwl-Fen	null		1	68.61	0.00	0.81
		JD	0.005	2	71.51	2.90	0.19

Appendix 6.24. Model coefficient, number of model parameters (*K*), Akaike's Information Criterion corrected for small sample size (AIC_c), change in AIC_c from best model (ΔAIC_c), and model weights calculated from AIC_c (w_i) for competing models with basal area (BA; m^2/ha), canopy cover (CC; %), and stand height (SH; m) for horsetail biomass (kg/ha) in Pickle Lake (PL) and Cochrane (CO) by seral-specific ecosites.

SA	Ecosite	Model	BA	CC	SH	*K*	AIC_c	ΔAIC_c	w_i
PL	Early-Upl-BS	SH			-0.70	2	429.68	0.00	0.40
		CC		-0.02		2	430.23	0.56	0.30
		BA	-0.002			2	430.26	0.59	0.30
	Mid-late-Upl-BS	SH			-0.16	2	872.43	0.00	0.45
		CC		-0.03		2	873.36	0.93	0.29
		BA	-0.04			2	873.54	1.11	0.26
	Early-Upl-BS-WS	SH			-9.26	2	156.90	0.00	0.56
		BA	-4.02			2	158.71	1.81	0.23
		CC		-0.89		2	158.88	1.98	0.21
	Mid-late-Upl-BS-WS	BA	-0.19			2	195.57	0.00	0.73
		SH			-0.18	2	198.29	2.71	0.19
		CC		-0.02		2	199.79	4.22	0.09
	Early-Lwl-Bog	SH			-7.09	2	218.20	0.00	0.45
		BA	-4.26			2	219.14	0.94	0.28
		CC		-3.86		2	219.26	1.06	0.27
	Mid-late-Lwl-Bog	SH			2.14	2	507.24	0.00	0.91
		BA	0.45			2	512.59	5.35	0.06
		CC		0.09		2	514.13	6.89	0.03
CO	Early-Upl-BS	BA	-0.0009			2	-78.09	0.00	0.36
		CC		-0.0001		2	-77.97	0.12	0.34
		SH			-0.0007	2	-77.71	0.38	0.30
	Mid-late-Upl-BS	SH			0.02	2	32.53	0.00	0.37
		BA	0.006			2	32.71	0.18	0.33
		CC		0.00		2	32.92	0.39	0.30
	Early-Upl-BS-WS	CC		-0.19		2	91.01	0.00	0.39
		SH			-1.11	2	91.50	0.48	0.31
		BA	0.41			2	91.58	0.56	0.30
	Mid-late-Upl-BS-WS	SH			0.09	2	94.52	0.00	0.61
		CC		0.03		2	96.15	1.63	0.27
		BA	0.01			2	97.74	3.22	0.12
	Early-Lwl-Bog	SH			10.12	2	82.40	0.00	0.37
		BA	-9.52			2	82.50	0.11	0.35
		CC		-0.62		2	83.03	0.64	0.27
	Mid-late-Lwl-Bog	CC		-0.03		2	281.78	0.00	0.35
		SH			0.18	2	281.86	0.08	0.33
		BA	-0.02			2	281.94	0.15	0.32
PL & CO	Mid-late-Lwl-Fen	SH			0.47	2	45.90	0.00	0.68
		CC		-0.02		2	48.75	2.85	0.16
		BA	-0.03			2	48.93	3.03	0.15

Appendix 6.25. Model coefficient, number of model parameters (*K*), Akaike's Information Criterion corrected for small sample size (AIC_c), change in AIC_c from best model (ΔAIC_c), and model weights calculated from AIC_c (w_i) for competing models with percent of clay, sand, and silt for horsetail biomass (kg/ha) in Pickle Lake (PL) and Cochrane (CO) by seral-specific ecosites.

SA	Ecosite	Model	Clay	Sand	Silt	*K*	AIC_c	ΔAIC_c	w_i
PL	Early-Upl-BS	Silt			1.41	2	427.89	0.00	0.46
		Sand		-1.17		2	428.37	0.48	0.36
		Clay	-0.75			2	429.86	1.97	0.17
	Mid-late-Upl-BS	Silt			0.33	2	871.74	0.00	0.58
		Clay	-0.17			2	873.61	1.86	0.23
		Sand		-0.08		2	873.88	2.13	0.20
	Early-Upl-BS-WS	Sand		-2.06		2	159.82	0.00	0.35
		Clay	1.88			2	159.92	0.10	0.33
		Silt			1.70	2	159.95	0.13	0.32
	Mid-late-Upl-BS-WS	Silt			-0.19	2	199.16	0.00	0.39
		Clay	0.20			2	199.50	0.34	0.33
		Sand		0.04		2	199.87	0.71	0.28
	Early-Lwl-Bog	Silt			2.16	2	219.27	0.00	0.36
		Sand		-0.90		2	219.50	0.22	0.32
		Clay	-0.83			2	219.53	0.25	0.32
	Mid-late-Lwl-Bog	Silt			2.11	2	512.43	0.00	0.49
		Clay	-1.92			2	513.24	0.81	0.32
		Sand		-0.45		2	514.33	1.90	0.19
CO	Early-Upl-BS	Clay	0.002			2	-78.67	0.00	0.46
		Sand		-0.0003		2	-77.65	1.02	0.27
		Silt			-0.0003	2	-77.63	1.04	0.27
	Mid-late-Upl-BS	Clay	-0.06			2	31.34	0.00	0.50
		Sand		0.01		2	32.56	1.21	0.27
		Silt			-0.002	2	32.92	1.58	0.23
	Early-Upl-BS-WS	Clay	-3.04			2	88.82	0.00	0.48
		Sand		1.05		2	89.22	0.39	0.39
		Silt			-0.43	2	91.49	2.66	0.13
	Mid-late-Upl-BS-WS	Clay	0.12			2	95.26	0.00	0.51
		Sand		-0.06		2	96.25	1.00	0.31
		Silt			0.06	2	97.38	2.12	0.18
	Early-Lwl-Bog	Silt			8.07	2	80.43	0.00	0.66
		Sand		-1.88		2	82.87	2.43	0.20
		Clay	0.50			2	83.49	3.06	0.14
	Mid-late-Lwl-Bog	Sand		-0.63		2	280.76	0.00	0.47
		Silt			-0.30	2	281.87	1.11	0.27
		Clay	0.10			2	281.94	1.17	0.26
PL & CO	Mid-late-Lwl-Fen	Clay	-0.54			2	45.86	0.00	0.64
		Sand		0.22		2	48.29	2.42	0.19
		Silt			0.23	2	48.54	2.68	0.17

Appendix 6.26. Model coefficient, number of model parameters (*K*), Akaike's Information Criterion corrected for small sample size (AIC_c), change in AIC_c from best model (ΔAIC_c), and model weights calculated from AIC_c (w_i) for competing models with basal area (BA; m^2/ha), percent silt, normalized difference moisture index (NDMI), and change in enhanced vegetation index (ΔEVI) for horsetail biomass (kg/ha) at Early-Upl-BS, Mid-late-Upl-BS, Mid-late-Upl-BS-WS, Early-Lwl-Bog, and Mid-late-Lwl-Bog macroplots in Pickle Lake.

Ecosite	Model	BA	Silt	NDMI	ΔEVI	*K*	AIC_c	ΔAIC_c	w_i
Early-Upl-BS	m2		1.41			2	427.89	0.00	0.20
	null					1	428.00	0.11	0.19
	m9		1.71		-0.004	3	428.98	1.09	0.11
	m4				-0.002	2	429.88	1.99	0.07
	m5	-0.09	1.43			3	430.22	2.33	0.06
	m3			2.03		2	430.25	2.36	0.06
	m8		1.41	1.20		3	430.25	2.36	0.06
	m1	-0.002				2	430.26	2.37	0.06
	m14		1.81	14.35	-0.005	4	430.86	2.97	0.04
	m13	0.09	1.71		-0.004	4	431.42	3.53	0.03
	m10			9.61	-0.003	3	431.99	4.10	0.03
	m7	0.12			-0.002	3	432.20	4.31	0.02
	m6	-0.08		3.73		3	432.60	4.71	0.02
	m12	-0.21	1.44	5.70		4	432.63	4.74	0.02
	m15	-0.26	1.85	20.06	-0.006	5	433.30	5.41	0.01
	m11	-0.08		11.44	-0.003	4	434.45	6.56	0.01
Mid-late-Upl-BS	m2		0.33			2	871.74	0.00	0.19
	null					1	872.07	0.32	0.16
	m5	-0.04	0.33			3	873.20	1.46	0.09
	m8		0.32	-4.32		3	873.42	1.67	0.08
	m1	-0.04				2	873.54	1.79	0.08
	m3			-4.95		2	873.58	1.83	0.08
	m9		0.33		-0.00002	3	873.87	2.12	0.07
	m4				0.0002	2	874.11	2.37	0.06
	m12	-0.03	0.32	-3.41		4	875.09	3.34	0.04
	m6	-0.03		-4.10		3	875.27	3.53	0.03
	m13	-0.04	0.33		-0.00005	4	875.36	3.61	0.03
	m10			-5.56	0.0004	3	875.54	3.79	0.03
	m14		0.31	-4.56	0.0001	4	875.55	3.81	0.03
	m7	-0.04			0.0002	3	875.63	3.88	0.03
	m15	-0.03	0.32	-3.54	0.00007	5	877.27	5.53	0.01
	m11	-0.03		-4.66	0.0003	4	877.31	5.57	0.01

Appendix 6.26. Continued.

Ecosite	Model	BA	Silt	NDMI	ΔEVI	*K*	AIC$_c$	ΔAIC$_c$	w_i
Mid-late-Upl-BS-WS	m1	-0.19				2	195.57	0.00	0.30
	m5	-0.19	-0.19			3	197.30	1.73	0.13
	null					1	197.53	1.95	0.11
	m7	-0.20			-0.0005	3	197.92	2.35	0.09
	m6	-0.19		-0.16		3	198.15	2.58	0.08
	m2		-0.19			2	199.16	3.59	0.05
	m3			11.23		2	199.39	3.81	0.05
	m4				-0.00001	2	199.94	4.36	0.03
	m13	-0.19	-0.18		-0.0003	4	199.96	4.39	0.03
	m12	-0.18	-0.19	1.77		4	200.05	4.48	0.03
	m11	-0.19		3.64	-0.0006	4	200.64	5.07	0.02
	m8		-0.22	13.06		3	200.98	5.41	0.02
	m9		-0.20		0.0002	3	201.72	6.15	0.01
	m10			14.47	-0.0005	3	201.80	6.23	0.01
	m14		-0.21	15.28	-0.0003	4	203.66	8.09	0.01
Early-Lwl-Bog	m4				-0.03	2	214.88	0.00	0.39
	null					1	216.76	1.88	0.15
	m9		2.77		-0.03	3	217.46	2.59	0.11
	m10			64.73	-0.03	3	217.63	2.75	0.10
	m7	3.33			-0.03	3	217.80	2.93	0.09
	m3			-61.50		2	219.13	4.25	0.05
	m1	-4.26				2	219.14	4.26	0.05
	m2		2.16			2	219.27	4.40	0.04
	m8		2.23	-62.88		3	221.99	7.11	0.01
	m5	-3.86	1.84			3	222.10	7.22	0.01
	m6	-2.65		-39.53		3	222.18	7.31	0.01
Mid-late-Lwl-Bog	m5	0.65	2.99			3	510.98	0.00	0.18
	null					1	512.23	1.25	0.10
	m13	0.66	2.58		0.008	4	512.23	1.25	0.10
	m2		2.11			2	512.43	1.45	0.09
	m1	0.45				2	512.59	1.61	0.08
	m7	0.50			0.01	3	512.64	1.66	0.08
	m4				0.01	2	512.68	1.70	0.08
	m12	0.70	3.00	-46.87		4	512.85	1.87	0.07
	m9		1.70		0.008	3	513.75	2.77	0.04
	m15	0.71	2.59	-46.59	0.008	5	514.20	3.22	0.04
	m3			-26.60		2	514.31	3.33	0.03
	m6	0.50		-45.62		3	514.43	3.45	0.03
	m11	0.55		-45.47	0.01	4	514.56	3.58	0.03
	m8		2.08	-22.09		3	514.65	3.67	0.03
	m10			-24.81	0.01	3	514.87	3.89	0.03
	m14		1.68	-21.58	0.008	4	516.08	5.10	0.01

Appendix 6.27. Model coefficient, number of model parameters (*K*), Akaike's Information Criterion corrected for small sample size (AIC_c), change in AIC_c from best model (ΔAIC_c), and model weights calculated from AIC_c (w_i) for competing models with basal area (BA; m^2/ha), percent sand, normalized difference moisture index (NDMI), and change in enhanced vegetation index (ΔEVI) for horsetail biomass (kg/ha) at Early-Upl-BS-WS macroplots in Pickle Lake.

Model	BA	Sand	NDMI	ΔEVI	*K*	AIC_c	ΔAIC_c	w_i
m3			-329.61		2	154.93	0.00	0.57
null					1	156.70	1.77	0.24
m1	-4.02				2	158.71	3.78	0.09
m4				0.01	2	159.53	4.60	0.06
m2		-2.06			2	159.82	4.89	0.05

Appendix 6.28. Model coefficient, number of model parameters (*K*), Akaike's Information Criterion corrected for small sample size (AIC_c), change in AIC_c from best model (ΔAIC_c), and model weights calculated from AIC_c (w_i) for competing models with basal area (BA; m^2/ha), percent silt, normalized difference moisture index (NDMI), and change in enhanced vegetation index (ΔEVI) for horsetail biomass (kg/ha) at Early-Upl-BS, Mid-late-Upl-BS, Early-Upl-BS-WS, and Mid-late-Upl-BS-WS macroplots in Cochrane.

Ecosite	Model	BA	Clay	NDMI	ΔEVI	*K*	AIC_c	ΔAIC_c	w_i
Early-Upl-BS	m6	-0.004		0.10		3	-81.39	0.00	0.32
	null					1	-80.58	0.80	0.21
	m3			0.03		2	-78.81	2.58	0.09
	m10			0.06	-0.00002	3	-78.68	2.71	0.08
	m2		0.002			2	-78.67	2.72	0.08
	m4				-0.00001	2	-78.63	2.75	0.08
	m1	-0.001				2	-78.09	3.30	0.06
	m9		0.002		-0.00001	3	-76.53	4.85	0.03
	m8		0.002	0.02		3	-75.83	5.55	0.02
	m5	-0.001	0.002			3	-75.55	5.84	0.02
	m7	-0.0005			-0.00001	3	-75.27	6.11	0.01
Mid-late-Upl-BS	null					1	30.23	0.00	0.30
	m2		-0.06			2	31.34	1.11	0.17
	m4				0.0002	2	32.26	2.03	0.11
	m1	0.006				2	32.71	2.48	0.09
	m3			0.01		2	32.93	2.70	0.08
	m9		-0.07		0.0002	3	33.00	2.76	0.08
	m5	0.01	-0.07			3	33.43	3.20	0.06
	m8		-0.06	0.21		3	34.30	4.07	0.04
	m10			-0.63	0.0002	3	34.93	4.69	0.03
	m7	0.006			0.0002	3	35.04	4.81	0.03
	m6	0.006		0.07		3	35.72	5.49	0.02

Appendix 6.28. Continued.

Ecosite	Model	BA	Clay	NDMI	ΔEVI	*K*	AIC_c	ΔAIC_c	w_i
Early-Upl-BS-WS	m4				0.01	2	84.44	0.00	0.71
	null					1	87.32	2.88	0.17
	m2		-3.04			2	88.82	4.38	0.08
	m1	0.41				2	91.58	7.14	0.02
	m3			2.99		2	91.60	7.16	0.02
Mid-late-Upl-BS-WS	m2		0.12			2	95.26	0.00	0.24
	null					1	95.29	0.03	0.23
	m4				0.0003	2	97.20	1.94	0.09
	m9		0.11		0.0002	3	97.68	2.42	0.07
	m1	0.007				2	97.74	2.48	0.07
	m3			-1.14		2	97.75	2.50	0.07
	m5	0.003	0.11			3	97.98	2.72	0.06
	m8		0.11	-0.54		3	97.98	2.73	0.06
	m10			-2.16	0.0003	3	99.75	4.50	0.02
	m7	0.008			0.0003	3	99.83	4.57	0.02
	m6	0.007		-1.14		3	100.42	5.17	0.02
	m14		0.11	-1.29	0.0002	4	100.60	5.34	0.02
	m13	0.004	0.11		0.0002	4	100.64	5.38	0.02
	m12	0.003	0.11	-0.54		4	100.96	5.70	0.01
	m11	0.009		-2.18	0.0003	4	102.63	7.37	0.01

Appendix 6.29. Model coefficient, number of model parameters (*K*), Akaike's Information Criterion corrected for small sample size (AIC_c), change in AIC_c from best model (ΔAIC_c), and model weights calculated from AIC_c (w_i) for competing models with basal area (BA; m^2/ha), percent silt, normalized difference moisture index (NDMI), and change in enhanced vegetation index (ΔEVI) for horsetail biomass (kg/ha) at Early-Lwl-Bog macroplots in Cochrane.

Model	BA	Silt	NDMI	ΔEVI	*K*	AIC_c	ΔAIC_c	w_i
null					1	76.50	0.00	0.80
m2		8.07			2	80.43	3.93	0.11
m1	-9.52				2	82.50	6.00	0.04
m4				-0.01	2	83.29	6.79	0.03
m3			-42.30		2	83.44	6.93	0.02

Appendix 6.30. Model coefficient, number of model parameters (*K*), Akaike's Information Criterion corrected for small sample size (AIC_c), change in AIC_c from best model (ΔAIC_c), and model weights calculated from AIC_c (w_i) for competing models with Julian day (JD), basal area (BA; m^2/ha), percent sand, normalized difference moisture index (NDMI), and change in enhanced vegetation index (ΔEVI) for horsetail biomass (kg/ha) at Mid-late-Lwl-Bog macroplots in Cochrane.

Model	JD	BA	Sand	NDMI	ΔEVI	*K*	AIC_c	ΔAIC_c	w_i
m1	0.83					2	274.32	0.00	0.37
m2	0.80	-0.50				3	275.97	1.65	0.16
m3	0.83		13.32			3	276.71	2.39	0.11
m4	0.82			-0.0005		3	276.88	2.56	0.10
m5	0.86	-0.52			0.13	4	278.13	3.81	0.05
m9	0.75	-0.63		-0.002		4	278.41	4.09	0.05
m8	0.80	-0.48	5.85			4	278.70	4.38	0.04
m6	0.88		5.49		0.10	4	279.13	4.81	0.03
m7	0.89			0.0003	0.12	4	279.15	4.83	0.03
m10	0.82		13.69	-0.0007		4	279.44	5.12	0.03
null						1	279.53	5.21	0.03

Appendix 6.31. Model coefficient, number of model parameters (*K*), Akaike's Information Criterion corrected for small sample size (AIC_c), change in AIC_c from best model (ΔAIC_c), and model weights calculated from AIC_c (w_i) for competing models with Julian day (JD) for mushroom biomass (kg/ha) in Pickle Lake (PL) and Cochrane (CO) by seral-specific ecosites.

SA	Ecosite	Model	Julian day	*K*	AIC_c	ΔAIC_c	w_i
PL	Mid-late-Upl-BS-Rocky	null		1	55.32	0.00	0.80
		JD	-0.08	2	58.08	2.76	0.20
	Early-Upl-BS	JD	1.16	2	155.76	0.00	0.97
		null		1	162.50	6.74	0.03
	Mid-late-Upl-BS	JD	0.96	2	523.61	0.00	1.00
		null		1	540.29	16.68	0.00
	Early-Upl-BS-WS	JD	0.49	2	22.10	0.00	0.81
		null		1	25.04	2.95	0.19
	Mid-late-Upl-BS-WS	JD	0.90	2	75.36	0.00	0.85
		null		1	78.91	3.55	0.15
	Early-Lwl-Bog	JD	2.24	2	30.08	0.00	0.77
		null		1	32.52	2.44	0.23
	Mid-late-Lwl-Bog	JD	0.96	2	64.41	0.00	0.94
		null		1	70.02	5.61	0.06

Appendix 6.31. Continued.

SA	Ecosite	Model	Julian day	K	AIC_c	ΔAIC_c	w_i
CO	Early-Upl-BS	null		1	-148.20	0.00	0.70
		JD	-0.01	2	-146.48	1.72	0.30
	Mid-late-Upl-BS	null		1	-127.95	0.00	0.68
		JD	0.05	2	-126.48	1.47	0.32
	Early-Upl-BS-WS	null		1	-75.94	0.00	0.79
		JD	-0.03	2	-73.25	2.69	0.21
	Mid-late-Upl-BS-WS	JD	3.26	2	49.58	0.00	0.57
		null		1	50.13	0.55	0.43
	Early-Lwl-Bog	null		1	31.10	0.00	0.74
		JD	2.77	2	33.16	2.06	0.26
	Mid-late-Lwl-Bog	null		1	15.92	0.00	0.70
		JD	-2.52E+75	2	17.62	1.71	0.30
PL & CO	Mid-late-Lwl-Fen	null		1	-1.05	0.00	0.68
		JD	0.002	2	0.48	1.54	0.32

Appendix 6.32. Model coefficient, number of model parameters (K), Akaike's Information Criterion corrected for small sample size (AIC_c), change in AIC_c from best model (ΔAIC_c), and model weights calculated from AIC_c (w_i) for competing models with basal area (BA; m^2/ha), canopy cover (CC; %), and stand height (SH; m) for mushroom biomass (kg/ha) in Pickle Lake (PL) and Cochrane (CO) by seral-specific ecosites.

SA	Ecosite	Model	BA	CC	SH	K	AIC_c	ΔAIC_c	w_i
PL	Mid-late-Upl-BS-Rocky	m3	0.01			2	57.69	0.00	0.38
		m4			-0.02	2	58.01	0.33	0.32
		m2		0.002		2	58.09	0.40	0.31
	Early-Upl-BS	m3	1.15			2	160.85	0.00	0.50
		m2		0.01		2	161.89	1.04	0.30
		m4			0.09	2	162.72	1.87	0.20
	Mid-late-Upl-BS	m3	0.79			2	537.93	0.00	0.79
		m4			-0.02	2	541.96	4.02	0.11
		m2		0.005		2	542.09	4.16	0.10
	Early-Upl-BS-WS	m3	0.11			2	9.68	0.00	1.00
		m4			0.06	2	26.67	17.00	0.00
		m2		0.002		2	28.25	18.58	0.00
	Mid-late-Upl-BS-WS	m3	0.01			2	80.55	0.00	0.42
		m4			0.005	2	81.28	0.73	0.29
		m2		0.0006		2	81.32	0.77	0.29
	Early-Lwl-Bog	m2		0.28		2	6.92	0.00	1.00
		m4			0.11	2	31.95	25.03	0.00
		m3	0.09			2	33.46	26.53	0.00
	Mid-late-Lwl-Bog	m4			0.02	2	70.14	0.00	0.38
		m3	0.007			2	70.19	0.05	0.37
		m2		0.003		2	70.91	0.77	0.26

Appendix 6.32. Continued.

SA	Ecosite	Model	BA	CC	SH	*K*	AIC_c	ΔAIC_c	w_i
CO	Early-Upl-BS	m2		0.00003		2	-146.55	0.00	0.48
		m3	-0.001			2	-145.33	1.22	0.26
		m4			0.0001	2	-145.26	1.29	0.25
	Mid-late-Upl-BS	m4			0.001	2	-126.01	0.00	0.42
		m3	-0.002			2	-125.34	0.67	0.30
		m2		2.38E-07		2	-125.25	0.76	0.29
	Early-Upl-BS-WS	m3	0.001			2	-73.30	0.00	0.49
		m4			0.001	2	-72.12	1.17	0.27
		m2		0.00003		2	-71.78	1.52	0.23
	Mid-late-Upl-BS-WS	m3	0.002			2	52.61	0.00	0.34
		m4			-0.004	2	52.63	0.02	0.33
		m2		0.001		2	52.65	0.03	0.33
	Early-Lwl-Bog	m4			0.44	2	36.70	0.00	0.49
		m3	-0.20			2	37.84	1.14	0.27
		m2		-0.002		2	38.10	1.40	0.24
	Mid-late-Lwl-Bog	m4			0.02	2	14.92	0.00	0.60
		m3	0.004			2	16.92	2.00	0.22
		m2		0.002		2	17.32	2.40	0.18
PL & CO	Mid-late-Lwl-Fen	m3	-0.01			2	-2.46	0.00	0.45
		m4			-0.02	2	-2.28	0.17	0.42
		m2		-0.004		2	0.01	2.46	0.13

Appendix 6.33. Model coefficient, number of model parameters (*K*), Akaike's Information Criterion corrected for small sample size (AIC_c), change in AIC_c from best model (ΔAIC_c), and model weights calculated from AIC_c (w_i) for competing models with percent of clay, sand, and silt for mushroom biomass (kg/ha) in Pickle Lake (PL) and Cochrane (CO) by seral-specific ecosites.

SA	Ecosite	Model	Clay	Sand	Silt	*K*	AIC_c	ΔAIC_c	w_i
PL	Mid-late-Upl-BS-Rocky	Silt			-0.10	2	56.25	0.00	0.47
		Sand		0.07		2	57.20	0.95	0.29
		Clay	0.08			2	57.60	1.34	0.24
	Early-Upl-BS	Silt			0.15	2	159.19	0.00	0.79
		Sand		-0.08		2	162.86	3.66	0.13
		Clay	-0.08			2	163.76	4.57	0.08
	Mid-late-Upl-BS	Sand		0.03		2	541.83	0.00	0.38
		Silt			-0.03	2	542.19	0.36	0.32
		Clay	0.01			2	542.36	0.53	0.30
	Early-Upl-BS-WS	Silt			0.07	2	27.04	0.00	0.47
		Sand		-0.02		2	28.09	1.05	0.28
		Clay	-0.01			2	28.29	1.25	0.25

Appendix 6.33. Continued.

SA	Ecosite	Model	Clay	Sand	Silt	K	AIC_c	ΔAIC_c	w_i
PL	Mid-late-Upl-BS-WS	Silt			0.02	2	80.99	0.00	0.35
		Sand		-0.01		2	81.08	0.09	0.33
		Clay	0.02			2	81.18	0.19	0.32
	Early-Lwl-Bog	Clay	-0.09			2	32.46	0.00	0.60
		Sand		0.04		2	34.40	1.94	0.23
		Silt			0.02	2	35.04	2.58	0.17
	Mid-late-Lwl-Bog	Sand		-0.02		2	70.34	0.00	0.47
		Silt			0.02	2	71.40	1.06	0.28
		Clay	0.02			2	71.62	1.28	0.25
CO	Early-Upl-BS	Sand		-0.0003		2	-149.57	0.00	0.46
		Clay	0.0005			2	-148.77	0.80	0.31
		Silt			0.0003	2	-148.13	1.44	0.23
	Mid-late-Upl-BS	Clay	-0.003			2	-131.26	0.00	0.86
		Sand		0.0006		2	-126.90	4.37	0.10
		Silt			-0.0001	2	-125.30	5.97	0.04
	Early-Upl-BS-WS	Clay	0.0006			2	-72.69	0.00	0.43
		Silt			0.0002	2	-71.98	0.72	0.30
		Sand		0.00004		2	-71.70	1.00	0.26
	Mid-late-Upl-BS-WS	Sand		0.04		2	47.43	0.00	0.47
		Silt			-0.08	2	48.32	0.89	0.30
		Clay	-0.06			2	48.82	1.39	0.23
	Early-Lwl-Bog	Silt			0.19	2	37.19	0.00	0.42
		Clay	-0.10			2	37.85	0.66	0.31
		Sand		-0.003		2	38.10	0.91	0.27
	Mid-late-Lwl-Bog	Sand		0.005		2	18.16	0.00	0.34
		Clay	-0.006			2	18.26	0.10	0.33
		Silt			-0.007	2	18.26	0.10	0.33
PL & CO	Mid-late-Lwl-Fen	Silt			-0.005	2	1.99	0.00	0.34
		Sand		0.001		2	2.02	0.03	0.33
		Clay	0.002			2	2.02	0.03	0.33

Appendix 6.34. Model coefficient, number of model parameters (*K*), Akaike's Information Criterion corrected for small sample size (AIC_c), change in AIC_c from best model (ΔAIC_c), and model weights calculated from AIC_c (w_i) for competing models with Julian day (JD), basal area (BA; m^2/ha), percent silt, normalized difference moisture index (NDMI), and change in enhanced vegetation index (ΔEVI) for mushroom biomass (kg/ha) at Mid-late-Upl-BS-Rocky, Early-Upl-BS, Early-Upl-BS-WS, and Mid-late-Upl-BS-WS macroplots in Pickle Lake.

Ecosite	Model	JD	BA	Silt	NDMI	ΔEVI	*K*	AIC_c	ΔAIC_c	w_i
Mid-late-Upl-BS-Rocky	null						1	55.32	0.00	0.26
	m4				0.0006		2	55.89	0.57	0.20
	m2		-0.10				2	56.25	0.93	0.16
	m7				0.0007	0.03	3	57.15	1.83	0.10
	m9		-0.08		0.0005		3	57.96	2.64	0.07
	m3			-0.19			2	58.11	2.79	0.06
	m8		-0.12	-1.43			3	58.92	3.60	0.04
	m10			-0.22	0.0006		3	59.04	3.72	0.04
	m5		-0.10			0.003	3	59.40	4.08	0.03
	m6			-2.09		0.03	3	60.25	4.93	0.02
Early-Upl-BS	m6	1.06	0.96	0.13			4	151.66	0.00	0.29
	m3	1.09		0.13			3	152.75	1.09	0.17
	m14	1.02	1.09	0.14		-0.0002	5	153.48	1.82	0.11
	m13	1.09	1.12	0.12	-0.64		5	153.93	2.27	0.09
	m2	1.12	1.06				3	154.17	2.51	0.08
	m9	1.06		0.13	0.45		4	155.02	3.36	0.05
	m10	1.08		0.14		-0.00006	4	155.14	3.48	0.05
	m1	1.16					2	155.76	4.10	0.04
	m15	1.04	1.13	0.14	-0.21	-0.0002	6	156.17	4.51	0.03
	m7	1.15	1.24		-0.71		4	156.29	4.63	0.03
	m8	1.11	1.09			-0.00004	4	156.61	4.95	0.02
	m4	1.13			0.50		3	157.91	6.25	0.01
	m5	1.17				0.00009	3	157.97	6.31	0.01
	m12	1.16	1.23		-0.77	0.00002	5	158.87	7.21	0.01
	m11	1.14			0.38	0.00005	4	160.35	8.69	0.00
	null						1	162.50	10.84	0.00
Early-Upl-BS-WS	m2		0.11				2	9.68	0.00	1.00
	m1	0.49					2	22.10	12.42	0.00
	null						1	25.04	15.37	0.00
	m3			0.07			2	27.04	17.37	0.00
	m4				0.66		2	28.15	18.47	0.00
	m5					0.00002	2	28.34	18.67	0.00

Appendix 6.34. Continued.

Ecosite	Model	JD	BA	Silt	NDMI	ΔEVI	*K*	AIC_c	ΔAIC_c	w_i
Mid-late-Upl-BS-WS	m5	0.80				-0.0004	3	72.96	0.00	0.34
	m10	0.79		0.03		-0.0004	4	74.65	1.69	0.15
	m1	0.90					2	75.36	2.40	0.10
	m11	0.80			-1.35	-0.0003	4	75.44	2.48	0.10
	m8	0.80	0.0007			-0.0004	4	75.72	2.76	0.09
	m4	0.86			-3.48		3	75.83	2.87	0.08
	m3	0.89		0.02			3	77.62	4.66	0.03
	m2	0.87	0.007				3	77.73	4.77	0.03
	m9	0.85		0.03	-3.71		4	77.99	5.03	0.03
	m7	0.87	-0.001		-3.55		4	78.59	5.63	0.02
	null						1	78.91	5.95	0.02
	m6	0.86	0.007	0.02			4	80.17	7.21	0.01

Appendix 6.35. Model coefficient, number of model parameters (*K*), Akaike's Information Criterion corrected for small sample size (AIC_c), change in AIC_c from best model (ΔAIC_c), and model weights calculated from AIC_c (w_i) for competing models with Julian day (JD), basal area (BA; m^2/ha), percent sand, normalized difference moisture index (NDMI), and change in enhanced vegetation index (ΔEVI) for musrhoom biomass (kg/ha) at Mid-late-Upl-BS and Mid-late-Lwl-Bog macroplots in Pickle Lake.

Ecosite	Model	JD	BA	Sand	NDMI	ΔEVI	*K*	AIC_c	ΔAIC_c	w_i
Mid-late-Upl-BS	m2	0.91	0.60				3	522.91	0.00	0.18
	m1	0.96					2	523.61	0.70	0.12
	m6	0.94	0.56	0.04			4	523.99	1.08	0.10
	m8	0.89	0.60			-0.0002	4	524.29	1.38	0.09
	m3	0.98		0.05			3	524.29	1.39	0.09
	m7	0.92	0.57		-0.83		4	524.85	1.94	0.07
	m5	0.93				-0.0002	3	525.01	2.10	0.06
	m4	0.97			-1.31		3	525.20	2.29	0.06
	m14	0.91	0.57	0.04		-0.0002	5	525.63	2.72	0.05
	m9	0.99		0.05	-1.50		4	525.74	2.83	0.04
	m13	0.95	0.52	0.04	-1.04		5	525.84	2.94	0.04
	m10	0.96		0.05		-0.0002	4	525.97	3.06	0.04
	m12	0.89	0.58		-0.47	-0.0002	5	526.42	3.51	0.03
	m11	0.94			-1.00	-0.0002	4	526.87	3.96	0.02
	m15	0.92	0.54	0.04	-0.74	-0.0002	6	527.70	4.79	0.02
	null						1	540.29	17.38	0.00

Appendix 6.35. Continued.

Ecosite	Model	JD	BA	Sand	NDMI	ΔEVI	*K*	AIC_c	ΔAIC_c	w_i
Mid-late-Lwl-Bog	m2	1.02	0.009				3	63.35	0.00	0.19
	m7	0.98	0.007		1.09		4	64.35	1.00	0.12
	m1	0.96					2	64.41	1.06	0.11
	m4	0.93			1.38		3	64.44	1.09	0.11
	m6	0.93	0.009	-0.02			4	65.01	1.66	0.08
	m8	1.00	0.008			-0.00003	4	65.70	2.35	0.06
	m13	0.90	0.008	-0.02	1.09		5	66.09	2.74	0.05
	m3	0.90		-0.01			3	66.36	3.01	0.04
	m9	0.86		-0.01	1.40		4	66.41	3.06	0.04
	m5	0.94				-0.00006	3	66.50	3.15	0.04
	m11	0.90			1.38	-0.00006	4	66.64	3.29	0.04
	m12	0.97	0.007		1.09	-0.00004	5	66.80	3.45	0.03
	m14	0.91	0.009	-0.02		-0.00004	5	67.43	4.08	0.03
	m10	0.86		-0.01		-0.00006	4	68.49	5.14	0.01
	m16	0.87	0.008	-0.02	1.10	-0.00004	6	68.60	5.25	0.01
	m15	0.82		-0.01	1.40	-0.00006	5	68.65	5.30	0.01
	null						1	70.02	6.67	0.01

Appendix 6.36. Model coefficient, number of model parameters (*K*), Akaike's Information Criterion corrected for small sample size (AIC_c), change in AIC_c from best model (ΔAIC_c), and model weights calculated from AIC_c (w_i) for competing models with Julian day (JD), basal area (BA; m^2/ha), percent clay, normalized difference moisture index (NDMI), and change in enhanced vegetation index (ΔEVI) for mushroom biomass (kg/ha) at Early-Lwl-Bog macroplots in Pickle Lake.

Model	JD	BA	Clay	NDMI	ΔEVI	*K*	AIC_c	ΔAIC_c	w_i
m4	2.20			2.16		3	24.96	0.00	0.78
m3	2.16		-0.08			3	29.95	4.99	0.06
m1	2.24					2	30.08	5.12	0.06
m2	2.32	0.10				3	30.36	5.39	0.05
m5	2.20				0.0001	3	32.20	7.24	0.02
null						1	32.52	7.55	0.02

Appendix 6.37. Model coefficient, number of model parameters (*K*), Akaike's Information Criterion corrected for small sample size (AIC_c), change in AIC_c from best model (ΔAIC_c), and model weights calculated from AIC_c (w_i) for competing models with Julian day (JD), basal area (BA; m^2/ha), percent clay or silt, normalized difference moisture index (NDMI), and change in enhanced vegetation index (ΔEVI) for mushroom biomass (kg/ha) at Mid-late-Upl-BS, Early-Upl-BS-WS, and Early-Lwl-Bog macroplots in Cochrane.

Ecosite	Model	BA	Clay	Silt	NDMI	ΔEVI	*K*	AIC_c	ΔAIC_c	w_i
Mid-late-Upl-BS	m9		-0.003			0.00001	3	-137.99	0.00	0.92
	m2		-0.003				2	-131.26	6.73	0.03
	m8		-0.003		0.02		3	-129.57	8.42	0.01
	m4					0.00001	2	-129.15	8.84	0.01
	m5	-0.006	-0.003				3	-128.99	9.00	0.01
	null						1	-127.95	10.04	0.01
	m10				-0.02	0.00001	3	-126.71	11.28	0.00
	m7	-0.002				0.00001	3	-126.21	11.79	0.00
	m3				0.01		2	-125.57	12.42	0.00
	m1	-0.002					2	-125.34	12.65	0.00
	m6	-0.003			0.02		3	-122.73	15.26	0.00
Early-Upl-BS-WS	m3				0.02		2	-76.74	0.00	0.49
	null						1	-75.94	0.80	0.32
	m1	0.0008					2	-73.30	3.44	0.09
	m2		0.0006				2	-72.69	4.05	0.06
	m4					-2.20E-07	2	-71.67	5.07	0.04
Early-Lwl-Bog	null						1	31.10	0.00	0.87
	m2			0.19			2	37.19	6.08	0.04
	m1	-0.20					2	37.84	6.73	0.03
	m3				3.16		2	37.86	6.76	0.03
	m4					0.00009	2	38.10	6.99	0.03

Appendix 6.38. Model coefficient, number of model parameters (*K*), Akaike's Information Criterion corrected for small sample size (AIC_c), change in AIC_c from best model (ΔAIC_c), and model weights calculated from AIC_c (w_i) for competing models with Julian day (JD), basal area (BA; m^2/ha), percent sand, normalized difference moisture index (NDMI), and change in enhanced vegetation index (ΔEVI) for mushroom biomass (kg/ha) at Early-Upl-BS, Mid-late-Upl-BS-WS, and Mid-late-Lwl-Bog macroplots in Cochrane.

Ecosite	Model	BA	Sand	NDMI	ΔEVI	*K*	AIC_c	ΔAIC_c	w_i
Early-Upl-BS	m2		-0.0003			2	-149.57	0.00	0.21
	m3			0.008		2	-149.43	0.14	0.20
	m6	-0.006		0.01		3	-148.58	0.99	0.13
	m8		-0.0002	0.005		3	-148.25	1.32	0.11
	m10			0.01	-0.000002	3	-148.24	1.33	0.11
	null					1	-148.20	1.37	0.11
	m5	-0.002	-0.0003			3	-146.61	2.97	0.05
	m9		-0.0003		-7.64E-07	3	-146.52	3.05	0.05
	m1	-0.001				2	-145.33	4.24	0.03
	m4				-3.49E-07	2	-145.28	4.29	0.02
	m7	-0.001			-3.29E-07	3	-141.91	7.66	0.00
Mid-late-Upl-BS-WS	m2		0.04			2	47.43	0.00	0.39
	m5	0.005	0.05			3	49.94	2.51	0.11
	m8		0.04	0.80		3	50.01	2.58	0.11
	null					1	50.13	2.70	0.10
	m9		0.04		0.00003	3	50.14	2.71	0.10
	m3			1.22		2	52.35	4.92	0.03
	m1	0.002				2	52.61	5.18	0.03
	m4				-0.000009	2	52.65	5.22	0.03
	m12	0.005	0.04	0.80		4	52.78	5.35	0.03
	m13	0.005	0.05		0.00003	4	52.88	5.45	0.03
	m14		0.04	0.76	0.00001	4	52.99	5.56	0.02
	m6	0.002		1.23		3	55.05	7.62	0.01
	m10			1.32	-0.00003	3	55.05	7.62	0.01
	m7	0.002			-0.000007	3	55.35	7.92	0.01
	m11	0.002		1.32	-0.00003	4	58.01	10.58	0.00

Appendix 6.38. Continued.

Ecosite	Model	BA	Sand	NDMI	ΔEVI	*K*	AIC_c	ΔAIC_c	w_i
Mid-late-Lwl-Bog	null					1	15.92	0.00	0.27
	m1	0.004				2	16.92	1.00	0.17
	m4				-0.00007	2	17.77	1.86	0.11
	m2		0.005			2	18.16	2.24	0.09
	m3			0.09		2	18.33	2.41	0.08
	m7	0.004			-0.00004	3	19.29	3.37	0.05
	m6	0.005		-0.29		3	19.37	3.46	0.05
	m5	0.004	0.004			3	19.40	3.48	0.05
	m10			0.13	-0.00007	3	20.34	4.42	0.03
	m9		0.002		-0.00006	3	20.35	4.43	0.03
	m8		0.006	0.19		3	20.70	4.78	0.03
	m11	0.004		-0.22	-0.00004	4	22.00	6.08	0.01
	m13	0.004	0.002		-0.00004	4	22.05	6.13	0.01
	m12	0.005	0.003	-0.23		4	22.12	6.20	0.01
	m14		0.003	0.17	-0.00006	4	23.08	7.16	0.01

Appendix 6.39. Model coefficient, number of model parameters (*K*), Akaike's Information Criterion corrected for small sample size (AIC_c), change in AIC_c from best model (ΔAIC_c), and model weights calculated from AIC_c (w_i) for competing models with Julian day (JD), basal area (BA; m^2/ha), percent silt, normalized difference moisture index (NDMI), and change in enhanced vegetation index (ΔEVI) for mushroom biomass (kg/ha) at Mid-late-Lwl-Fen macroplots in Pickle Lake and Cochrane.

Model	BA	Silt	NDMI	ΔEVI	*K*	AIC_c	ΔAIC_c	w_i
m1	-0.01				2	-2.46	0.00	0.53
null					1	-1.05	1.40	0.26
m3			-0.90		2	1.16	3.62	0.09
m4				0.00007	2	1.59	4.05	0.07
m2		-0.005			2	1.99	4.44	0.06

Appendix 6.40. Model coefficient, number of model parameters (*K*), Akaike's Information Criterion corrected for small sample size (AIC_c), change in AIC_c from best model (ΔAIC_c), and model weights calculated from AIC_c (w_i) for competing models with Julian day (JD) for HQ-accepted biomass (kg/ha) in Pickle Lake (PL) and Cochrane (CO) by seral-specific ecosites.

SA	Ecosite	Model	Julian day	*K*	AIC_c	ΔAIC_c	w_i
PL	Mid-late-Upl-BS-Rocky	JD	0.45	2	202.43	0.00	0.82
		null		1	205.43	3.00	0.18
	Early-Upl-BS	JD	0.96	2	655.12	0.00	1.00
		null		1	671.63	16.51	0.00
	Mid-late-Upl-BS	JD	0.98	2	1443.62	0.00	1.00
		null		1	1479.69	36.07	0.00
	Early-Upl-BS-WS	JD	1.40	2	186.27	0.00	0.96
		null		1	192.42	6.15	0.04
	Mid-late-Upl-BS-WS	JD	1.03	2	428.18	0.00	1.00
		null		1	441.19	13.01	0.00
	Early-Lwl-Bog	JD	1.13	2	238.11	0.00	0.81
		null		1	241.00	2.89	0.19
	Mid-late-Lwl-Bog	JD	0.95	2	614.53	0.00	1.00
		null		1	625.56	11.03	0.00
CO	Early-Upl-BS	null		1	199.76	0.00	0.76
		JD	0.10	2	202.02	2.25	0.24
	Mid-late-Upl-BS	JD	0.43	2	237.38	0.00	0.55
		null		1	237.75	0.37	0.45
	Early-Upl-BS-WS	JD	1.41	2	148.17	0.00	0.74
		null		1	150.28	2.11	0.26
	Mid-late-Upl-BS-WS	JD	0.76	2	324.93	0.00	0.69
		null		1	326.54	1.61	0.31
	Early-Lwl-Bog	null		1	95.84	0.00	0.92
		JD	1.33	2	100.60	4.75	0.08
	Mid-late-Lwl-Bog	JD	0.95	2	348.30	0.00	0.99
		null		1	356.93	8.63	0.01
PL & CO	Mid-late-Lwl-Fen	JD	1.01	2	178.63	0.00	1.00
		null		1	200.11	21.48	0.00

Appendix 6.41. Model coefficient, number of model parameters (*K*), Akaike's Information Criterion corrected for small sample size (AIC_c), change in AIC_c from best model (ΔAIC_c), and model weights calculated from AIC_c (w_i) for competing models with basal area (BA; m^2/ha), canopy cover (CC; %), and stand height (SH; m) for HQ-accepted biomass (kg/ha) in Pickle Lake (PL) and Cochrane (CO) by seral-specific ecosites.

SA	Ecosite	Model	BA	CC	SH	*K*	AIC_c	ΔAIC_c	w_i
PL	Mid-late-Upl-BS-Rocky	SH			-4.66	2	205.09	0.00	0.66
		BA	-0.73			2	207.54	2.45	0.19
		CC		0.19		2	208.01	2.92	0.15
	Early-Upl-BS	BA	0.60			2	673.69	0.00	0.35
		SH			2.26	2	673.85	0.16	0.33
		CC		0.16		2	673.89	0.20	0.32
	Mid-late-Upl-BS	BA	0.36			2	1479.04	0.00	0.56
		CC		0.33		2	1480.42	1.38	0.28
		SH			0.59	2	1481.51	2.47	0.16
	Early-Upl-BS-WS	CC		-5.01		2	194.90	0.00	0.41
		BA	3.49			2	195.37	0.47	0.33
		SH			-6.32	2	195.85	0.95	0.26
	Mid-late-Upl-BS-WS	BA	0.78			2	437.88	0.00	0.79
		CC		-2.55		2	441.64	3.76	0.12
		SH			-5.54	2	442.37	4.49	0.08
	Early-Lwl-Bog	SH			20.05	2	240.41	0.00	0.71
		CC		7.82		2	243.44	3.03	0.16
		BA	-2.08			2	243.77	3.36	0.13
	Mid-late-Lwl-Bog	CC		-1.44		2	619.60	0.00	0.85
		BA	-2.11			2	623.97	4.37	0.10
		SH			-4.53	2	624.95	5.35	0.06
CO	Early-Upl-BS	BA	0.68			2	202.35	0.00	0.37
		CC		-0.37		2	202.55	0.19	0.33
		SH			-1.21	2	202.73	0.38	0.30
	Mid-late-Upl-BS	SH			5.67	2	236.91	0.00	0.70
		BA	-0.54			2	239.59	2.69	0.18
		CC		0.08		2	240.44	3.53	0.12
	Early-Upl-BS-WS	CC		-4.01		2	154.10	0.00	0.37
		BA	2.28			2	154.30	0.20	0.33
		SH			-17.84	2	154.51	0.41	0.30
	Mid-late-Upl-BS-WS	SH			7.58	2	323.01	0.00	0.90
		BA	0.17			2	328.54	5.53	0.06
		CC		-0.44		2	328.96	5.95	0.05
	Early-Lwl-Bog	BA	-39.56			2	101.75	0.00	0.40
		SH			33.11	2	102.12	0.37	0.33
		CC		-1.80		2	102.60	0.85	0.26

Appendix 6.41. Continued.

SA	Ecosite	Model	BA	CC	SH	*K*	AIC_c	ΔAIC_c	w_i
CO	Mid-late-Lwl-Bog	BA	-0.70			2	358.58	0.00	0.38
		CC		-0.30		2	358.79	0.20	0.35
		SH			-0.73	2	359.31	0.72	0.27
PL & CO	Mid-late-Lwl-Fen	SH			7.68	2	202.71	0.00	0.38
		BA	-3.13			2	203.01	0.30	0.33
		CC		-0.21		2	203.28	0.57	0.29

Appendix 6.42. Model coefficient, number of model parameters (*K*), Akaike's Information Criterion corrected for small sample size (AIC_c), change in AIC_c from best model (ΔAIC_c), and model weights calculated from AIC_c (w_i) for competing models with percent of clay, sand, and silt for HQ-accepted biomass (kg/ha) in Pickle Lake (PL) and Cochrane (CO) by seral-specific ecosites.

SA	Ecosite	Model	Clay	Sand	Silt	*K*	AIC_c	ΔAIC_c	w_i
PL	Mid-late-Upl-BS-Rocky	Silt			6.07	2	204.45	0.00	0.56
		Clay	-7.80			2	205.49	1.04	0.33
		Sand		-1.93		2	207.83	3.38	0.10
	Early-Upl-BS	Silt			33.22	2	662.91	0.00	0.75
		Sand		-27.79		2	665.16	2.25	0.24
		Clay	-3.73			2	673.82	10.91	0.00
	Mid-late-Upl-BS	Clay	2.88			2	1480.03	0.00	0.54
		Sand		0.19		2	1481.77	1.73	0.23
		Silt			-0.18	2	1481.78	1.74	0.23
	Early-Upl-BS-WS	Silt			45.40	2	194.70	0.00	0.45
		Sand		-12.36		2	195.70	1.00	0.28
		Clay	-14.39			2	195.74	1.04	0.27
	Mid-late-Upl-BS-WS	Sand		-0.19		2	443.61	0.00	0.33
		Clay	-0.28			2	443.61	0.00	0.33
		Silt			-0.13	2	443.61	0.00	0.33
	Early-Lwl-Bog	Clay	-6.15			2	243.38	0.00	0.37
		Sand		2.33		2	243.69	0.31	0.32
		Silt			0.08	2	243.80	0.42	0.30
	Mid-late-Lwl-Bog	Sand		5.08		2	626.16	0.00	0.44
		Clay	-5.30			2	626.95	0.79	0.30
		Silt			-3.98	2	627.19	1.04	0.26
CO	Early-Upl-BS	Clay	-11.13			2	200.82	0.00	0.44
		Sand		4.39		2	201.44	0.62	0.32
		Silt			-4.66	2	201.99	1.17	0.24
	Mid-late-Upl-BS	Silt			2.67	2	239.33	0.00	0.43
		Sand		-1.48		2	239.93	0.60	0.32
		Clay	-0.34			2	240.45	1.12	0.25

Appendix 6.42. Continued.

SA	Ecosite	Model	Clay	Sand	Silt	*K*	AIC_c	ΔAIC_c	w_i
CO	Early-Upl-BS-WS	Silt			39.47	2	152.43	0.00	0.54
		Clay	38.56			2	153.81	1.38	0.27
		Sand		4.75		2	154.48	2.05	0.19
	Mid-late-Upl-BS-WS	Clay	5.63			2	327.50	0.00	0.37
		Sand		-3.17		2	327.76	0.26	0.32
		Silt			5.77	2	327.83	0.32	0.31
	Early-Lwl-Bog	Silt			27.02	2	100.82	0.00	0.56
		Sand		-4.80		2	102.59	1.77	0.23
		Clay	-3.87			2	102.81	1.99	0.21
	Mid-late-Lwl-Bog	Sand		-4.49		2	356.08	0.00	0.41
		Clay	7.71			2	356.21	0.13	0.39
		Silt			6.41	2	357.56	1.48	0.20
PL & CO	Mid-late-Lwl-Fen	Clay	-25.17			2	202.26	0.00	0.40
		Sand		14.67		2	202.53	0.27	0.35
		Silt			-1.94	2	203.28	1.03	0.24

Appendix 6.43. Model coefficient, number of model parameters (*K*), Akaike's Information Criterion corrected for small sample size (AIC_c), change in AIC_c from best model (ΔAIC_c), and model weights calculated from AIC_c (w_i) for competing models with Julian day (JD), basal area (BA; m^2/ha), percent silt, normalized difference moisture index (NDMI), and change in enhanced vegetation index (ΔEVI) for HQ-accepted biomass (kg/ha) at Mid-late-Upl-BS-Rocky, Early-Upl-BS, Early-Upl-BS-WS, and Mid-late-Upl-BS-WS macroplots in Pickle Lake.

Ecosite	Model	JD	BA	Silt	NDMI	ΔEVI	*K*	AIC_c	ΔAIC_c	w_i
Mid-late-Upl-BS-Rocky	m3	0.46		6.26			3	199.99	0.00	0.41
	m2	0.62	-1.82				3	200.25	0.26	0.36
	m1	0.45					2	202.43	2.45	0.12
	m4	0.60			-111.93		3	203.93	3.95	0.06
	m5	0.46				0.01	3	204.93	4.94	0.03
	null						1	205.43	5.44	0.03

Appendix 6.43. Continued.

Ecosite	Model	JD	BA	Silt	NDMI	ΔEVI	*K*	AIC_c	ΔAIC_c	w_i
Early-Upl-BS	m3	0.88		28.29			3	646.03	0.00	0.25
	m13	0.81	2.29	29.66	362.57		5	646.51	0.48	0.20
	m10	0.87		25.67		0.03	4	647.19	1.16	0.14
	m9	0.86		28.11	149.99		4	647.35	1.32	0.13
	m6	0.87	0.67	28.82			4	648.03	2.00	0.09
	m14	0.86	1.08	25.79		0.04	5	648.62	2.59	0.07
	m16	0.81	2.24	28.17	310.39	0.02	6	648.88	2.85	0.06
	m15	0.87		26.34	92.13	0.02	5	649.46	3.43	0.05
	m5	0.94				0.06	3	653.86	7.83	0.01
	m1	0.96					2	655.12	9.09	0.00
	m8	0.93	1.03			0.07	4	655.44	9.41	0.00
	m11	0.94			17.67	0.06	4	656.32	10.29	0.00
	m4	0.94			160.79		3	656.43	10.40	0.00
	m7	0.91	1.77		325.79		4	657.29	11.26	0.00
	m12	0.91	1.71		179.76	0.06	5	657.34	11.31	0.00
	m2	0.96	0.33				3	657.40	11.37	0.00
	null						1	671.63	25.60	0.00
Early-Upl-BS-WS	m1	1.40					2	186.27	0.00	0.92
	null						1	192.42	6.15	0.04
	m3			45.40			2	194.70	8.42	0.01
	m2		3.49				2	195.37	9.10	0.01
	m4				-404.96		2	195.72	9.44	0.01
	m5					-0.04	2	195.73	9.46	0.01
Mid-late-Upl-BS-WS	m2	0.99	0.70				3	423.47	0.00	0.46
	m6	1.02	0.70	5.03			4	425.47	2.00	0.17
	m7	0.99	0.65		214.20		4	425.97	2.50	0.13
	m8	0.99	0.71			-0.009	4	426.15	2.67	0.12
	m1	1.03					2	428.18	4.71	0.04
	m4	1.03			558.77		3	429.07	5.60	0.03
	m3	1.06		4.60			3	430.24	6.77	0.02
	m5	1.03				0.006	3	430.72	7.25	0.01
	m9	1.05		3.63	528.06		4	431.50	8.03	0.01
	m11	1.05			665.11	-0.02	4	431.61	8.14	0.01
	m10	1.06		4.52		0.002	4	433.00	9.53	0.00
	null						1	441.19	17.72	0.00

Appendix 6.44. Model coefficient, number of model parameters (*K*), Akaike's Information Criterion corrected for small sample size (AIC_c), change in AIC_c from best model (ΔAIC_c), and model weights calculated from AIC_c (w_i) for competing models with Julian day (JD), basal area (BA; m^2/ha), percent clay, normalized difference moisture index (NDMI), and change in enhanced vegetation index (ΔEVI) for HQ-accepted biomass (kg/ha) at Mid-late-Upl-BS and Early-Lwl-Bog macroplots in Pickle Lake.

Ecosite	Model	JD	BA	Clay	NDMI	ΔEVI	*K*	AIC_c	ΔAIC_c	w_i
Mid-late-Upl-BS	m7	0.99	0.50		127.64		4	1437.29	0.00	0.27
	m13	0.98	0.50	2.72	138.63		5	1437.29	0.00	0.27
	m12	0.98	0.49		117.67	0.006	5	1438.86	1.57	0.12
	m16	0.97	0.49	2.66	129.25	0.005	6	1438.99	1.70	0.12
	m2	0.99	0.41				3	1441.05	3.76	0.04
	m8	0.98	0.40			0.009	4	1441.46	4.17	0.03
	m6	0.98	0.40	2.03			4	1442.03	4.74	0.03
	m4	0.98			97.42		3	1442.28	5.00	0.02
	m9	0.96		2.73	108.47		4	1442.35	5.07	0.02
	m14	0.97	0.39	2.00		0.009	5	1442.48	5.20	0.02
	m11	0.97			85.80	0.007	4	1443.53	6.24	0.01
	m1	0.98					2	1443.62	6.34	0.01
	m15	0.95		2.66	97.32	0.007	5	1443.74	6.45	0.01
	m5	0.97				0.01	3	1443.94	6.66	0.01
	m3	0.97		2.16			3	1444.45	7.16	0.01
	m10	0.96		2.14		0.01	4	1444.82	7.53	0.01
	null						1	1479.69	42.41	0.00
Early-Lwl-Bog	m5	1.15				0.04	3	237.27	0.00	0.40
	m1	1.13					2	238.11	0.84	0.26
	m4	1.16			204.09		3	239.35	2.09	0.14
	m3	1.17		-8.04			3	240.33	3.06	0.09
	null						1	241.00	3.74	0.06
	m2	1.13	-2.54				3	241.22	3.95	0.06

Appendix 6.45. Model coefficient, number of model parameters (*K*), Akaike's Information Criterion corrected for small sample size (AIC_c), change in AIC_c from best model (ΔAIC_c), and model weights calculated from AIC_c (w_i) for competing models with Julian day (JD), basal area (BA; m^2/ha), percent sand, normalized difference moisture index (NDMI), and change in enhanced vegetation index (ΔEVI) for HQ-accepted biomass (kg/ha) at Mid-late-Lwl-Bog macroplots in Pickle Lake.

Model	JD	BA	Sand	NDMI	ΔEVI	*K*	AIC_c	ΔAIC_c	w_i
m2	1.02	-2.58				3	609.32	0.00	0.39
m6	0.98	-2.62	2.10			4	611.39	2.07	0.14
m8	1.02	-2.58			-0.01	4	611.52	2.21	0.13
m7	1.03	-2.65		76.96		4	611.58	2.26	0.13
m14	0.98	-2.62	2.41		-0.01	5	613.59	4.27	0.05
m13	0.99	-2.69	2.17	82.47		5	613.73	4.41	0.04
m12	1.03	-2.66		85.22	-0.01	5	613.85	4.54	0.04
m1	0.95					2	614.53	5.21	0.03
m16	0.99	-2.71	2.52	93.39	-0.02	6	615.99	6.67	0.01
m5	0.95				-0.01	3	616.67	7.35	0.01
m3	0.92		1.47			3	616.71	7.40	0.01
m4	0.95			-13.17		3	616.87	7.56	0.01
m10	0.92		1.76		-0.01	4	618.89	9.58	0.00
m11	0.95			-6.00	-0.01	4	619.12	9.81	0.00
m9	0.92		1.46	-10.42		4	619.16	9.85	0.00
m15	0.92		1.76	-1.52	-0.01	5	621.46	12.14	0.00
null						1	625.56	16.24	0.00

Appendix 6.45. Model coefficient, number of model parameters (*K*), Akaike's Information Criterion corrected for small sample size (AIC_c), change in AIC_c from best model (ΔAIC_c), and model weights calculated from AIC_c (w_i) for competing models with Julian day (JD), basal area (BA; m^2/ha), percent clay, normalized difference moisture index (NDMI), and change in enhanced vegetation index (ΔEVI) for HQ-accepted biomass (kg/ha) at Early-Upl-BS and Mid-late-Upl-BS-WS macroplots in Cochrane.

Ecosite	Model	BA	Clay	NDMI	ΔEVI	*K*	AIC_c	ΔAIC_c	w_i
Early-Upl-BS	null					1	199.76	0.00	0.33
	m2		-11.13			2	200.82	1.05	0.19
	m4				0.03	2	202.16	2.40	0.10
	m1	0.68				2	202.35	2.59	0.09
	m3			-50.86		2	202.54	2.78	0.08
	m9		-11.82		0.03	3	203.39	3.62	0.05
	m5	0.85	-11.85			3	203.60	3.84	0.05
	m8		-11.20	2.67		3	204.30	4.54	0.03
	m7	1.05			0.04	3	204.75	4.99	0.03
	m10			-113.07	0.04	3	204.78	5.02	0.03
	m6	0.65		-5.02		3	205.84	6.08	0.02

Appendix 6.45. Continued.

Ecosite	Model	BA	Clay	NDMI	ΔEVI	*K*	AIC_c	ΔAIC_c	w_i
Mid-late-Upl-BS-WS	null					1	326.54	0.00	0.19
	m3			-460.17		2	326.77	0.24	0.17
	m2		5.63			2	327.50	0.97	0.12
	m8		5.13	-433.17		3	328.12	1.59	0.09
	m10			-532.13	0.02	3	328.46	1.93	0.07
	m1	-0.97				2	328.69	2.15	0.07
	m4				0.01	2	328.69	2.15	0.07
	m6	-0.98		-460.87		3	329.10	2.57	0.05
	m5	-1.17	5.96			3	329.67	3.14	0.04
	m9		5.32		0.009	3	330.06	3.52	0.03
	m14		4.47	-495.57	0.02	4	330.40	3.87	0.03
	m12	-1.16	5.46	-432.28		4	330.51	3.97	0.03
	m7	-0.90			0.01	3	331.10	4.57	0.02
	m11	-0.86		-529.72	0.02	4	331.12	4.59	0.02
	m13	-1.12	5.68		0.008	4	332.53	5.99	0.01

Appendix 6.46. Model coefficient, number of model parameters (*K*), Akaike's Information Criterion corrected for small sample size (AIC_c), change in AIC_c from best model (ΔAIC_c), and model weights calculated from AIC_c (w_i) for competing models with Julian day (JD), basal area (BA; m^2/ha), percent clay, normalized difference moisture index (NDMI), and change in enhanced vegetation index (ΔEVI) for HQ-accepted biomass (kg/ha) at Mid-late-Lwl-Bog macroplots in Cochrane.

Model	JD	BA	Sand	NDMI	ΔEVI	*K*	AIC_c	ΔAIC_c	w_i
m1	0.95					2	348.30	0.00	0.27
m3	0.88		-3.27			3	348.57	0.26	0.24
m5	0.96				0.008	3	350.64	2.34	0.09
m2	0.93	-0.24				3	350.80	2.50	0.08
m4	0.94			26.83		3	350.88	2.58	0.08
m6	0.87	-0.16	-3.23			4	351.33	3.03	0.06
m9	0.88		-3.37	-23.67		4	351.36	3.05	0.06
m10	0.88		-3.30		-0.001	4	351.39	3.09	0.06
m8	0.95	-0.15			0.007	4	353.42	5.12	0.02
m11	0.95			21.61	0.008	4	353.44	5.13	0.02
m7	0.90	-0.38		58.47		4	353.45	5.15	0.02
null						1	356.93	8.63	0.00

Appendix 6.47. Model coefficient, number of model parameters (*K*), Akaike's Information Criterion corrected for small sample size (AIC_c), change in AIC_c from best model (ΔAIC_c), and model weights calculated from AIC_c (w_i) for competing models with Julian day (JD), basal area (BA; m^2/ha), percent clay, normalized difference moisture index (NDMI), and change in enhanced vegetation index (ΔEVI) for HQ-accepted biomass (kg/ha) at Mid-late-Lwl-Fen macroplots in Pickle Lake and Cochrane.

Model	JD	BA	Clay	NDMI	ΔEVI	*K*	AIC_c	ΔAIC_c	w_i
m1	1.01					2	178.63	0.00	1.00
null						1	200.11	21.48	0.00
m5					-0.12	2	201.41	22.77	0.00
m3			-25.17			2	202.26	23.62	0.00
m4				493.38		2	202.91	24.28	0.00
m2		-3.13				2	203.01	24.38	0.00

Appendix 6.48. Model coefficient, number of model parameters (*K*), Akaike's Information Criterion corrected for small sample size (AIC_c), change in AIC_c from best model (ΔAIC_c), and model weights calculated from AIC_c (w_i) for competing models with Julian day (JD) for DE-accepted biomass (kg/ha) in Pickle Lake (PL) and Cochrane (CO) by seral-specific ecosites.

SA	Ecosite	Model	Julian day	*K*	AIC_c	ΔAIC_c	w_i
PL	Mid-late-Upl-BS-Rocky	null		1	296.11	0.00	0.73
		JD	-2.02	2	298.09	1.98	0.27
	Early-Upl-BS	null		1	713.14	0.00	0.66
		JD	0.70	2	714.45	1.31	0.34
	Mid-late-Upl-BS	JD	0.98	2	1810.94	0.00	0.84
		null		1	1814.25	3.31	0.16
	Early-Upl-BS-WS	JD	3.62	2	184.18	0.00	0.94
		null		1	189.66	5.48	0.06
	Mid-late-Upl-BS-WS	JD	1.06	2	436.33	0.00	0.79
		null		1	439.03	2.70	0.21
	Early-Lwl-Bog	null		1	262.30	0.00	0.76
		JD	0.95	2	264.60	2.30	0.24
	Mid-late-Lwl-Bog	JD	0.72	2	640.74	0.00	0.52
		null		1	640.88	0.13	0.48
CO	Early-Upl-BS	JD	0.46	2	218.41	0.00	0.90
		null		1	222.72	4.30	0.10
	Mid-late-Upl-BS	null		1	302.74	0.00	0.78
		JD	0.72	2	305.24	2.50	0.22
	Early-Upl-BS-WS	JD	1.52	2	150.69	0.00	0.83
		null		1	153.83	3.14	0.17
	Mid-late-Upl-BS-WS	JD	0.79	2	321.40	0.00	0.91
		null		1	326.08	4.68	0.09
	Early-Lwl-Bog	JD	5.11	2	97.30	0.00	0.73
		null		1	99.30	2.00	0.27
	Mid-late-Lwl-Bog	JD	0.96	2	395.80	0.00	0.98
		null		1	403.57	7.77	0.02

Appendix 6.48. Continued.

SA	Ecosite	Model	Julian day	*K*	AIC_c	ΔAIC_c	w_i
PL & CO	Mid-late-Lwl-Fen	JD	1.00	2	180.83	0.00	1.00
		null		1	197.81	16.98	0.00

Appendix 6.49. Model coefficient, number of model parameters (*K*), Akaike's Information Criterion corrected for small sample size (AIC_c), change in AIC_c from best model (ΔAIC_c), and model weights calculated from AIC_c (w_i) for competing models with basal area (BA; m^2/ha), canopy cover (CC; %), and stand height (SH; m) for DE-accepted biomass (kg/ha) in Pickle Lake (PL) and Cochrane (CO) by seral-specific ecosites.

SA	Ecosite	Model	BA	CC	SH	*K*	AIC_c	ΔAIC_c	w_i
PL	Mid-late-Upl-BS-Rocky	CC		-10.77		2	290.22	0.00	0.55
		BA	-22.25			2	290.69	0.46	0.43
		SH			-35.05	2	297.06	6.83	0.02
	Early-Upl-BS	BA	1.36			2	710.53	0.00	0.72
		SH			-21.37	2	713.56	3.04	0.16
		CC		-2.40		2	714.11	3.58	0.12
	Mid-late-Upl-BS	BA	0.85			2	1793.79	0.00	1.00
		CC		-3.07		2	1805.62	11.83	0.00
		SH			-10.36	2	1808.89	15.10	0.00
	Early-Upl-BS-WS	CC		-6.48		2	191.01	0.00	0.43
		BA	5.47			2	191.34	0.33	0.36
		SH			-25.51	2	192.40	1.39	0.21
	Mid-late-Upl-BS-WS	BA	0.87			2	429.52	0.00	0.99
		CC		-2.59		2	439.26	9.75	0.01
		SH			-4.01	2	440.76	11.24	0.00
	Early-Lwl-Bog	BA	1.73			2	262.84	0.00	0.46
		CC		-28.98		2	263.35	0.51	0.36
		SH			-12.50	2	264.67	1.83	0.18
	Mid-late-Lwl-Bog	CC		-1.69		2	634.64	0.00	0.91
		BA	0.43			2	640.62	5.98	0.05
		SH			-4.73	2	640.82	6.18	0.04
CO	Early-Upl-BS	CC		-1.90		2	224.24	0.00	0.42
		BA	0.73			2	224.56	0.32	0.36
		SH			6.88	2	225.52	1.28	0.22
	Mid-late-Upl-BS	BA	1.97			2	293.55	0.00	0.87
		CC		-9.26		2	297.38	3.83	0.13
		SH			-4.32	2	305.34	11.79	0.00
	Early-Upl-BS-WS	CC		-5.48		2	157.50	0.00	0.37
		BA	3.18			2	157.70	0.20	0.34
		SH			-30.90	2	158.00	0.50	0.29

Appendix 6.49. Continued.

SA	Ecosite	Model	BA	CC	SH	K	AIC_c	ΔAIC_c	w_i
CO	Mid-late-Upl-BS-WS	SH			7.74	2	322.16	0.00	0.91
		BA	0.16			2	327.87	5.72	0.05
		CC		-0.29		2	328.56	6.40	0.04
	Early-Lwl-Bog	CC		6.77		2	103.79	0.00	0.45
		SH			72.23	2	103.90	0.12	0.42
		BA	0.51			2	106.23	2.45	0.13
	Mid-late-Lwl-Bog	CC		-1.68		2	401.41	0.00	0.50
		BA	0.77			2	402.16	0.75	0.35
		SH			-8.61	2	403.79	2.38	0.15
PL & CO	Mid-late-Lwl-Fen	BA	-6.86			2	199.35	0.00	0.50
		CC		-1.61		2	200.53	1.18	0.28
		SH			1.31	2	200.97	1.62	0.22

Appendix 6.50. Model coefficient, number of model parameters (K), Akaike's Information Criterion corrected for small sample size (AIC_c), change in AIC_c from best model (ΔAIC_c), and model weights calculated from AIC_c (w_i) for competing models with percent of clay, sand, and silt for DE-accepted biomass (kg/ha) in Pickle Lake (PL) and Cochrane (CO) by seral-specific ecosites.

SA	Ecosite	Model	Clay	Sand	Silt	K	AIC_c	ΔAIC_c	w_i
PL	Mid-late-Upl-BS-Rocky	Silt			24.94	2	298.27	0.00	0.38
		Clay	-29.00			2	298.52	0.25	0.33
		Sand		-9.17		2	298.81	0.54	0.29
	Early-Upl-BS	Sand		-5.92		2	715.25	0.00	0.35
		Silt			3.45	2	715.36	0.11	0.33
		Clay	1.86			2	715.40	0.15	0.32
	Mid-late-Upl-BS	Silt			-9.61	2	1814.32	0.00	0.45
		Sand		6.08		2	1814.68	0.36	0.38
		Clay	1.96			2	1816.27	1.95	0.17
	Early-Upl-BS-WS	Clay	-32.59			2	192.14	0.00	0.39
		Sand		23.16		2	192.29	0.15	0.36
		Silt			-9.00	2	193.08	0.93	0.25
	Mid-late-Upl-BS-WS	Sand		-5.33		2	440.26	0.00	0.37
		Silt			7.19	2	440.56	0.30	0.32
		Clay	9.62			2	440.58	0.33	0.31
	Early-Lwl-Bog	Sand		7.87		2	264.66	0.00	0.36
		Clay	-9.70			2	264.74	0.08	0.35
		Silt			-1.59	2	265.08	0.42	0.29
	Mid-late-Lwl-Bog	Clay	-5.44			2	642.46	0.00	0.40
		Sand		2.02		2	642.94	0.49	0.31
		Silt			1.27	2	643.09	0.63	0.29

Appendix 6.50. Continued.

SA	Ecosite	Model	Clay	Sand	Silt	*K*	AIC_c	ΔAIC_c	w_i
CO	Early-Upl-BS	Sand		12.41		2	222.86	0.00	0.45
		Silt			-14.42	2	223.74	0.89	0.29
		Clay	-20.51			2	224.01	1.16	0.25
	Mid-late-Upl-BS	Clay	-42.32			2	301.37	0.00	0.51
		Sand		15.46		2	302.30	0.93	0.32
		Silt			-14.93	2	303.58	2.21	0.17
	Early-Upl-BS-WS	Silt			44.35	2	156.25	0.00	0.50
		Clay	46.42			2	157.35	1.10	0.29
		Sand		6.02		2	158.02	1.77	0.21
	Mid-late-Upl-BS-WS	Clay	5.71			2	326.97	0.00	0.38
		Sand		-3.29		2	327.19	0.21	0.34
		Silt			5.42	2	327.50	0.53	0.29
	Early-Lwl-Bog	Silt			27.45	2	105.07	0.00	0.43
		Clay	16.27			2	105.85	0.78	0.29
		Sand		-6.92		2	105.95	0.88	0.28
	Mid-late-Lwl-Bog	Silt			-4.45	2	405.82	0.00	0.35
		Clay	2.99			2	405.91	0.09	0.33
		Sand		-0.89		2	405.99	0.17	0.32
PL & CO	Mid-late-Lwl-Fen	Clay	-24.06			2	199.89	0.00	0.42
		Sand		12.12		2	200.39	0.50	0.33
		Silt			1.69	2	200.99	1.10	0.25

Appendix 6.51. Model coefficient, number of model parameters (*K*), Akaike's Information Criterion corrected for small sample size (AIC_c), change in AIC_c from best model (ΔAIC_c), and model weights calculated from AIC_c (w_i) for competing models with Julian day (JD), basal area (BA; m^2/ha), percent sand, normalized difference moisture index (NDMI), and change in enhanced vegetation index (ΔEVI) for DE-accepted biomass (kg/ha) at Early-Upl-BS, Mid-late-Upl-BS-WS, and Early-Lwl-Bog macroplots in Pickle Lake.

Ecosite	Model	JD	BA	Sand	NDMI	ΔEVI	*K*	AIC_c	ΔAIC_c	w_i
Early-Upl-BS	m7		2.05			0.21	3	697.64	0.00	0.47
	m11		2.46		352.85	0.19	4	698.98	1.34	0.24
	m13		2.09	10.38		0.22	4	699.45	1.81	0.19
	m15		2.47	9.13	329.31	0.20	5	701.05	3.40	0.09
	m6		2.52		828.86		3	706.98	9.34	0.00
	m4					0.15	2	707.86	10.22	0.00
	m10				-361.34	0.19	3	708.82	11.18	0.00
	m12		2.51	-4.49	824.28		4	709.34	11.70	0.00
	m9			5.72		0.16	3	710.07	12.43	0.00
	m1		1.36				2	710.53	12.88	0.00
	m14			8.15	-384.90	0.20	4	710.97	13.33	0.00
	m5		1.36	-5.86			3	712.72	15.08	0.00
	null						1	713.14	15.50	0.00
	m2			-5.92			2	715.25	17.60	0.00
	m3				111.23		2	715.26	17.61	0.00
	m8			-5.74	107.83		3	717.47	19.83	0.00
Mid-late-Upl-BS-WS	m2	0.85	0.80				3	427.54	0.00	0.44
	m7	0.92	0.71		508.45		4	428.99	1.45	0.21
	m6	0.80	0.80	-3.93			4	429.28	1.74	0.18
	m8	0.84	0.82			-0.02	4	430.04	2.50	0.13
	m4	1.15			995.87		3	434.57	7.03	0.01
	m1	1.06					2	436.33	8.79	0.01
	m11	1.16			1219.40	-0.03	4	436.48	8.94	0.01
	m9	1.10		-3.07	964.40		4	436.83	9.29	0.00
	m3	1.00		-3.94			3	438.18	10.64	0.00
	m5	1.06				0.006	3	438.87	11.33	0.00
	null						1	439.03	11.49	0.00
	m10	1.00		-3.89		0.003	4	440.93	13.39	0.00
Early-Lwl-Bog	m1		-36.35				2	261.75	0.00	0.24
	null						1	262.30	0.55	0.18
	m5		-43.04	14.50			3	263.23	1.48	0.12
	m3				-379.91		2	263.37	1.62	0.11
	m4					-0.05	2	263.65	1.91	0.09
	m2			7.87			2	264.66	2.91	0.06
	m7		-32.18			-0.02	3	264.77	3.02	0.05
	m6		-31.52		-118.41		3	264.79	3.04	0.05
	m8			13.97	-486.63		3	265.15	3.40	0.04
	m10				-269.82	-0.03	3	266.19	4.44	0.03
	m9			8.85		-0.06	3	266.23	4.48	0.03

Appendix 6.52. Model coefficient, number of model parameters (*K*), Akaike's Information Criterion corrected for small sample size (AIC_c), change in AIC_c from best model (ΔAIC_c), and model weights calculated from AIC_c (w_i) for competing models with Julian day (JD), basal area (BA; m^2/ha), percent silt or clay, normalized difference moisture index (NDMI), and change in enhanced vegetation index (ΔEVI) for DE-accepted biomass (kg/ha) at Mid-late-Upl-BS-Rocky, Mid-late-Upl-BS, and Early-Upl-BS-WS macroplots in Pickle Lake.

Ecosite	Model	JD	BA	Silt	Clay	NDMI	ΔEVI	*K*	AIC_c	ΔAIC_c	w_i
Mid-late-Upl-BS-Rocky	m1		-22.25					2	290.69	0.00	0.85
	null							1	296.11	5.42	0.06
	m4						0.21	2	296.98	6.29	0.04
	m3					-1052.99		2	297.15	6.46	0.03
	m2			24.94				2	298.27	7.58	0.02
Mid-late-Upl-BS	m16	0.67	0.69	-11.19		-707.32	0.04	6	1781.24	0.00	0.32
	m13	0.74	0.71	-9.47		-624.58		5	1781.53	0.29	0.28
	m7	0.76	0.73			-600.21		4	1781.92	0.68	0.23
	m12	0.71	0.71			-661.50	0.03	5	1782.55	1.31	0.17
	m2	0.96	0.84					3	1789.72	8.48	0.00
	m6	0.95	0.83	-7.86				4	1790.21	8.97	0.00
	m8	0.95	0.84				0.01	4	1791.74	10.50	0.00
	m14	0.93	0.83	-8.42			0.02	5	1792.07	10.83	0.00
	m15	0.60		-13.14		-897.92	0.05	5	1795.79	14.54	0.00
	m9	0.69		-11.08		-802.77		4	1797.01	15.77	0.00
	m11	0.65				-851.67	0.04	4	1797.92	16.68	0.00
	m4	0.72				-779.07		3	1797.96	16.72	0.00
	m1	0.98						2	1810.94	29.70	0.00
	m3	0.96		-9.29				3	1811.11	29.87	0.00
	m10	0.94		-9.96			0.02	4	1812.84	31.59	0.00
	m5	0.96					0.01	3	1812.88	31.64	0.00
	null							1	1814.25	33.01	0.00
Early-Upl-BS-WS	m1	3.62						2	184.18	0.00	0.88
	null							1	189.66	5.48	0.06
	m2		5.47					2	191.34	7.16	0.02
	m4					-890.57		2	192.07	7.89	0.02
	m3				-32.59			2	192.14	7.96	0.02
	m5						-0.04	2	192.99	8.81	0.01

Appendix 6.53. Model coefficient, number of model parameters (*K*), Akaike's Information Criterion corrected for small sample size (AIC_c), change in AIC_c from best model (ΔAIC_c), and model weights calculated from AIC_c (w_i) for competing models with Julian day (JD), canopy cover (CC; %), percent clay, normalized difference moisture index (NDMI), and change in enhanced vegetation index (ΔEVI) for DE-accepted biomass (kg/ha) at Mid-late-Lwl-Bog macroplots in Pickle Lake.

Model	CC	Clay	NDMI	ΔEVI	*K*	AIC_c	ΔAIC_c	w_i
m1	-1.69				2	634.64	0.00	0.34
m6	-1.49		-247.16		3	635.92	1.28	0.18
m5	-1.66	-3.57			3	636.65	2.01	0.12
m7	-1.67			-0.01	3	636.90	2.26	0.11
m12	-1.46	-3.51	-245.71		4	638.04	3.40	0.06
m11	-1.48		-244.13	-0.008	4	638.31	3.67	0.05
m13	-1.61	-4.62		-0.02	4	638.84	4.20	0.04
m3			-445.42		2	639.76	5.12	0.03
m15	-1.43	-4.44	-239.57	-0.02	5	640.39	5.75	0.02
null					1	640.88	6.24	0.01
m8		-4.93	-437.49		3	641.51	6.87	0.01
m10			-435.99	-0.02	3	641.89	7.25	0.01
m2		-5.44			2	642.46	7.82	0.01
m4				-0.02	2	642.77	8.13	0.01
m14		-6.44	-419.47	-0.03	4	643.42	8.78	0.00
m9		-7.29		-0.03	3	644.00	9.36	0.00

Appendix 6.54. Model coefficient, number of model parameters (*K*), Akaike's Information Criterion corrected for small sample size (AIC_c), change in AIC_c from best model (ΔAIC_c), and model weights calculated from AIC_c (w_i) for competing models with Julian day (JD), basal area (BA; m^2/ha), percent sand or clay, normalized difference moisture index (NDMI), and change in enhanced vegetation index (ΔEVI) for DE-accepted biomass (kg/ha) at Early-Upl-BS, Mid-late-Upl-BS, and Mid-late-Upl-BS-WS macroplots in Cochrane.

Ecosite	Model	JD	BA	Sand	Clay	NDMI	ΔEVI	*K*	AIC_c	ΔAIC_c	w_i
Early-Upl-BS	m3	0.46		12.55				3	217.19	0.00	0.48
	m1	0.46						2	218.41	1.22	0.26
	m5	0.55					-0.09	3	219.99	2.80	0.12
	m2	0.44	0.53					3	220.98	3.79	0.07
	m4	0.46				-63.95		3	221.77	4.58	0.05
	null							1	222.72	5.53	0.03

Appendix 6.54. Continued.

Ecosite	Model	JD	BA	Sand	Clay	NDMI	ΔEVI	*K*	AIC$_c$	ΔAIC$_c$	w_i
Mid-late-Upl-BS	m1		1.97					2	293.55	0.00	0.43
	m5		1.75		-22.77			3	294.86	1.31	0.22
	m6		2.05			-413.77		3	294.90	1.35	0.22
	m7		1.96				0.03	3	296.38	2.83	0.10
	m2				-42.32			2	301.37	7.81	0.01
	null							1	302.74	9.19	0.00
	m9				-46.78		0.09	3	303.36	9.81	0.00
	m8				-41.19	-122.70		3	304.29	10.74	0.00
	m3					-264.21		2	305.05	11.50	0.00
	m4						0.04	2	305.22	11.67	0.00
	m10					-590.52	0.12	3	306.93	13.38	0.00
Mid-late-Upl-BS-WS	m4	0.78				-469.37		3	320.97	0.00	0.22
	m1	0.79						2	321.40	0.43	0.18
	m7	0.82	-1.78			-469.72		4	322.11	1.14	0.12
	m2	0.83	-1.77					3	322.50	1.53	0.10
	m9	0.74			3.76	-450.29		4	322.97	2.00	0.08
	m3	0.75			4.27			3	323.00	2.02	0.08
	m11	0.75				-515.91	0.01	4	323.39	2.42	0.07
	m6	0.79	-1.91		4.72			4	324.01	3.03	0.05
	m5	0.78					0.01	3	324.06	3.09	0.05
	m8	0.82	-1.75				0.00	4	325.46	4.49	0.02
	m10	0.74			4.19		0.00	4	325.97	4.99	0.02
	null							1	326.08	5.11	0.02

Appendix 6.55. Model coefficient, number of model parameters (*K*), Akaike's Information Criterion corrected for small sample size (AIC$_c$), change in AIC$_c$ from best model (ΔAIC$_c$), and model weights calculated from AIC$_c$ (w_i) for competing models with Julian day (JD), basal area (BA; m^2/ha), percent silt, normalized difference moisture index (NDMI), and change in enhanced vegetation index (ΔEVI) for DE-accepted biomass (kg/ha) at Early-Upl-BS-WS, Early-Lwl-Bog, and Mid-late-Lwl-Bog macroplots in Cochrane.

Ecosite	Model	JD	BA	Silt	NDMI	ΔEVI	*K*	AIC$_c$	ΔAIC$_c$	w_i
Early-Upl-BS-WS	m1	1.52					2	150.69	0.00	0.70
	null						1	153.83	3.14	0.14
	m5					0.23	2	155.22	4.53	0.07
	m3			44.35			2	156.25	5.56	0.04
	m4				-878.83		2	157.53	6.84	0.02
	m2		3.18				2	157.70	7.02	0.02
Early-Lwl-Bog	m1	5.08					2	97.41	0.00	0.69
	null						1	99.28	1.87	0.27
	m3			27.45			2	105.07	7.66	0.01
	m5					0.12	2	105.20	7.79	0.01
	m4				197.25		2	106.22	8.81	0.01
	m2		0.51				2	106.23	8.82	0.01

Appendix 6.55. Continued.

Ecosite	Model	JD	BA	Silt	NDMI	ΔEVI	*K*	AIC_c	ΔAIC_c	w_i
Mid-late-Lwl-Bog	m1	0.96					2	395.80	0.00	0.25
	m2	0.86	0.51				3	396.30	0.50	0.20
	m4	0.99			-246.21		3	397.53	1.73	0.11
	m3	0.98		-7.54			3	397.65	1.84	0.10
	m6	0.89	0.50	-7.20			4	398.37	2.56	0.07
	m5	0.96				0.0005	3	398.43	2.62	0.07
	m8	0.82	0.58			-0.02	4	398.81	3.00	0.06
	m7	0.89	0.45		-139.21		4	398.86	3.05	0.05
	m9	1.01		-6.54	-218.45		4	399.77	3.96	0.03
	m10	1.01		-9.79		0.02	4	400.23	4.42	0.03
	m11	1.00			-248.46	0.003	4	400.35	4.55	0.03
	null						1	403.57	7.77	0.01

Appendix 6.56. Model coefficient, number of model parameters (*K*), Akaike's Information Criterion corrected for small sample size (AIC_c), change in AIC_c from best model (ΔAIC_c), and model weights calculated from AIC_c (w_i) for competing models with Julian day (JD), basal area (BA; m^2/ha), percent clay, normalized difference moisture index (NDMI), and change in enhanced vegetation index (ΔEVI) for DE-accepted biomass (kg/ha) at Mid-late-Lwl-Fen macroplots in Pickle Lake and Cochrane.

Model	JD	BA	Clay	NDMI	ΔEVI	*K*	AIC_c	ΔAIC_c	w_i
m1	1.00					2	180.83	0.00	1.00
null						1	197.81	16.98	0.00
m2		-6.86				2	199.35	18.52	0.00
m5					-0.09	2	199.84	19.01	0.00
m3			-24.06			2	199.89	19.06	0.00
m4				343.64		2	200.78	19.95	0.00

Appendix 6.57. Model coefficient, number of model parameters (*K*), Akaike's Information Criterion corrected for small sample size (AIC_c), change in AIC_c from best model (ΔAIC_c), and model weights calculated from AIC_c (w_i) for competing models with Julian day (JD) for DP-accepted biomass (kg/ha) in Pickle Lake (PL) and Cochrane (CO) by seral-specific ecosites.

SA	Ecosite	Model	Julian day	*K*	AIC_c	ΔAIC_c	w_i
PL	Mid-late-Upl-BS-Rocky	m1	0.57	2	213.81	0.00	0.69
		null		1	215.40	1.60	0.31
	Early-Upl-BS	m1	0.82	2	668.12	0.00	1.00
		null		1	680.28	12.16	0.00
	Mid-late-Upl-BS	m1	0.62	2	1506.76	0.00	1.00
		null		1	1530.81	24.04	0.00
	Early-Upl-BS-WS	m1	1.40	2	186.69	0.00	0.95
		null		1	192.56	5.87	0.05

Appendix 6.57. Continued.

SA	Ecosite	Model	Julian day	*K*	AIC_c	ΔAIC_c	w_i
PL	Mid-late-Upl-BS-WS	m1	2.21	2	433.91	0.00	1.00
		null		1	446.20	12.29	0.00
	Early-Lwl-Bog	m1	-1.94	2	242.69	0.00	0.79
		null		1	245.31	2.62	0.21
	Mid-late-Lwl-Bog	m1	-1.25	2	617.36	0.00	0.98
		null		1	624.87	7.52	0.02
CO	Early-Upl-BS	null		1	199.76	0.00	0.78
		m1	0.08	2	202.24	2.48	0.22
	Mid-late-Upl-BS	m1	0.40	2	237.41	0.00	0.54
		null		1	237.72	0.31	0.46
	Early-Upl-BS-WS	m1	1.44	2	148.78	0.00	0.79
		null		1	151.47	2.69	0.21
	Mid-late-Upl-BS-WS	m1	0.89	2	322.98	0.00	0.89
		null		1	327.12	4.13	0.11
	Early-Lwl-Bog	null		1	95.82	0.00	0.94
		m1	1.36	2	101.49	5.67	0.06
	Mid-late-Lwl-Bog	m1	0.95	2	347.97	0.00	0.99
		null		1	356.78	8.81	0.01
PL & CO	Mid-late-Lwl-Fen	m1	2.89	2	107.77	0.00	1.00
		null		1	121.46	13.69	0.00

Appendix 6.58. Model coefficient, number of model parameters (*K*), Akaike's Information Criterion corrected for small sample size (AIC_c), change in AIC_c from best model (ΔAIC_c), and model weights calculated from AIC_c (w_i) for competing models with basal area (BA; m^2/ha), canopy cover (CC; %), and stand height (SH; m) for DP-accepted biomass (kg/ha) in Pickle Lake (PL) and Cochrane (CO) by seral-specific ecosites.

SA	Ecosite	Model	BA	CC	SH	*K*	AIC_c	ΔAIC_c	w_i
PL	Mid-late-Upl-BS-Rocky	SH			-6.39	2	214.57	0.00	0.71
		CC		0.42		2	217.58	3.00	0.16
		BA	-0.62			2	217.90	3.33	0.13
	Early-Upl-BS	CC		0.61		2	682.38	0.00	0.35
		SH			3.36	2	682.46	0.08	0.33
		BA	0.10			2	682.54	0.16	0.32
	Mid-late-Upl-BS	BA	0.47			2	1529.05	0.00	0.74
		SH			0.97	2	1532.39	3.34	0.14
		CC		0.11		2	1532.79	3.74	0.11
	Early-Upl-BS-WS	CC		-5.05		2	195.04	0.00	0.42
		BA	3.57			2	195.55	0.51	0.32
		SH			-1.26	2	196.03	0.99	0.26
	Mid-late-Upl-BS-WS	BA	0.91			2	441.70	0.00	0.83
		CC		-3.27		2	445.78	4.08	0.11
		SH			-7.21	2	446.79	5.09	0.07

Appendix 6.58. Continued.

SA	Ecosite	Model	BA	CC	SH	*K*	AIC_c	ΔAIC_c	w_i
PL	Early-Lwl-Bog	SH			13.27	2	246.97	0.00	0.45
		BA	3.84			2	247.78	0.81	0.30
		CC		1.66		2	248.09	1.12	0.26
	Mid-late-Lwl-Bog	CC		-1.47		2	618.32	0.00	0.86
		BA	1.10			2	622.94	4.62	0.09
		SH			-4.67	2	624.03	5.72	0.05
CO	Early-Upl-BS	BA	0.69			2	202.36	0.00	0.37
		CC		-0.37		2	202.55	0.19	0.33
		SH			-1.21	2	202.73	0.37	0.30
	Mid-late-Upl-BS	SH			5.69	2	236.86	0.00	0.70
		BA	-0.49			2	239.59	2.73	0.18
		CC		0.08		2	240.41	3.56	0.12
	Early-Upl-BS-WS	CC		-4.06		2	155.34	0.00	0.37
		BA	2.35			2	155.53	0.19	0.33
		SH			-15.99	2	155.72	0.38	0.30
	Mid-late-Upl-BS-WS	SH			8.48	2	322.03	0.00	0.95
		BA	0.14			2	329.28	7.24	0.03
		CC		-0.72		2	329.39	7.36	0.02
	Early-Lwl-Bog	BA	21.12			2	101.57	0.00	0.43
		SH			28.50	2	102.29	0.72	0.30
		CC		-1.92		2	102.54	0.97	0.27
	Mid-late-Lwl-Bog	BA	0.35			2	358.42	0.00	0.38
		CC		-0.30		2	358.61	0.19	0.35
		SH			-0.75	2	359.15	0.73	0.27
PL & CO	Mid-late-Lwl-Fen	SH			7.63	2	202.61	0.00	0.38
		BA	-3.19			2	202.89	0.28	0.33
		CC		-0.19		2	203.18	0.57	0.29

Appendix 6.59. Model coefficient, number of model parameters (*K*), Akaike's Information Criterion corrected for small sample size (AIC_c), change in AIC_c from best model (ΔAIC_c), and model weights calculated from AIC_c (w_i) for competing models with percent of clay, sand, and silt for DP-accepted biomass (kg/ha) in Pickle Lake (PL) and Cochrane (CO) by seral-specific ecosites.

SA	Ecosite	Model	Clay	Sand	Silt	*K*	AIC_c	ΔAIC_c	w_i
PL	Mid-late-Upl-BS-Rocky	Silt			8.40	2	213.72	0.00	0.59
		Clay	-10.90			2	214.90	1.18	0.33
		Sand		-2.88		2	217.65	3.93	0.08
	Early-Upl-BS	Silt			37.72	2	670.51	0.00	0.70
		Sand		-32.68		2	672.23	1.72	0.30
		Clay	-3.71			2	682.48	11.97	0.00
	Mid-late-Upl-BS	Clay	4.10			2	1530.46	0.00	0.62
		Sand		-0.48		2	1532.82	2.35	0.19
		Silt			0.14	2	1532.90	2.43	0.18

Appendix 6.59. Continued.

SA	Ecosite	Model	Clay	Sand	Silt	K	AIC_c	ΔAIC_c	w_i
PL	Early-Upl-BS-WS	Silt			48.53	2	194.68	0.00	0.47
		Sand		-14.08		2	195.79	1.11	0.27
		Clay	-13.79			2	195.89	1.22	0.26
	Mid-late-Upl-BS-WS	Clay	5.40			2	448.39	0.00	0.35
		Sand		-1.38		2	448.55	0.15	0.33
		Silt			-0.30	2	448.61	0.22	0.32
	Early-Lwl-Bog	Sand		-6.92		2	247.31	0.00	0.39
		Silt			6.00	2	247.59	0.28	0.34
		Clay	1.03			2	248.10	0.79	0.26
	Mid-late-Lwl-Bog	Sand		4.96		2	625.53	0.00	0.44
		Clay	-4.92			2	626.37	0.84	0.29
		Silt			-4.07	2	626.47	0.94	0.27
CO	Early-Upl-BS	Clay	-11.13			2	200.82	0.00	0.44
		Sand		4.39		2	201.44	0.62	0.32
		Silt			-4.66	2	201.99	1.17	0.24
	Mid-late-Upl-BS	Silt			2.65	2	239.32	0.00	0.43
		Sand		-1.47		2	239.91	0.59	0.32
		Clay	-0.36			2	240.42	1.10	0.25
	Early-Upl-BS-WS	Silt			39.95	2	153.84	0.00	0.51
		Clay	40.70			2	155.01	1.18	0.28
		Sand		4.83		2	155.68	1.84	0.20
	Mid-late-Upl-BS-WS	Silt			6.22	2	328.23	0.00	0.37
		Sand		-2.99		2	328.51	0.28	0.32
		Clay	4.78			2	328.55	0.31	0.31
	Early-Lwl-Bog	Silt			28.43	2	100.53	0.00	0.59
		Sand		-5.68		2	102.46	1.93	0.22
		Clay	-3.97			2	102.78	2.25	0.19
	Mid-late-Lwl-Bog	Sand		-4.43		2	356.01	0.00	0.41
		Clay	7.63			2	356.12	0.11	0.39
		Silt			6.32	2	357.46	1.45	0.20
PL & CO	Mid-late-Lwl-Fen	Silt			19.02	2	125.72	0.00	0.38
		Clay	-12.33			2	126.00	0.28	0.33
		Sand		0.82		2	126.26	0.53	0.29

Appendix 6.60. Model coefficient, number of model parameters (*K*), Akaike's Information Criterion corrected for small sample size (AIC_c), change in AIC_c from best model (ΔAIC_c), and model weights calculated from AIC_c (w_i) for competing models with Julian day (JD), basal area (BA; m^2/ha), percent silt, normalized difference moisture index (NDMI), and change in enhanced vegetation index (ΔEVI) for DP-accepted biomass (kg/ha) at Mid-late-Upl-BS-Rocky, Early-Upl-BS, and Early-Upl-BS-WS macroplots in Pickle Lake.

Ecosite	Model	JD	BA	Silt	NDMI	ΔEVI	*K*	AIC_c	ΔAIC_c	w_i
Mid-late-Upl-BS-Rocky	m2			8.40			2	213.72	0.00	0.34
	m8			10.36	129.30		3	215.31	1.59	0.15
	null						1	215.40	1.68	0.15
	m9			9.65		0.02	3	215.45	1.72	0.14
	m5		0.35	8.91			3	216.79	3.07	0.07
	m1		-0.62				2	217.90	4.17	0.04
	m4					0.01	2	217.97	4.25	0.04
	m3				25.15		2	218.14	4.42	0.04
	m6		-1.55		127.28		3	220.32	6.60	0.01
	m7		-0.49			0.007	3	220.98	7.25	0.01
	m10				24.59	0.01	3	221.09	7.36	0.01
Early-Upl-BS	m3	0.71		32.00			3	659.31	0.00	0.33
	m9	0.69		31.82	188.22		4	660.39	1.08	0.19
	m13	0.66	2.00	33.19	372.20		5	661.01	1.69	0.14
	m10	0.71		30.58		0.02	4	661.49	2.18	0.11
	m6	0.71	0.34	32.26			4	661.70	2.38	0.10
	m15	0.69		32.02	194.70	-0.003	5	662.98	3.66	0.05
	m16	0.66	2.02	33.66	388.44	-0.006	6	663.69	4.38	0.04
	m14	0.70	0.56	30.64		0.02	5	663.85	4.53	0.03
	m1	0.82					2	668.12	8.80	0.00
	m5	0.79				0.05	3	668.65	9.33	0.00
	m4	0.79			197.63		3	669.25	9.94	0.00
	m2	0.82	-0.04				3	670.48	11.17	0.00
	m11	0.79			103.03	0.04	4	670.86	11.55	0.00
	m7	0.77	1.42		328.17		4	670.94	11.62	0.00
	m8	0.79	0.51			0.05	4	670.96	11.65	0.00
	m12	0.77	1.38		232.39	0.04	5	672.69	13.38	0.00
	null						1	680.28	20.97	0.00
Early-Upl-BS-WS	m1	1.40					2	186.69	0.00	0.91
	null						1	192.56	5.87	0.05
	m3			48.53			2	194.68	7.98	0.02
	m2		3.57				2	195.55	8.86	0.01
	m5					-0.04	2	195.89	9.20	0.01
	m4				-353.20		2	195.90	9.21	0.01

Appendix 6.61. Model coefficient, number of model parameters (*K*), Akaike's Information Criterion corrected for small sample size (AIC_c), change in AIC_c from best model (ΔAIC_c), and model weights calculated from AIC_c (w_i) for competing models with Julian day (JD), basal area (BA; m^2/ha), percent clay, normalized difference moisture index (NDMI), and change in enhanced vegetation index (ΔEVI) for DP-accepted biomass (kg/ha) at Mid-late-Upl-BS, and Mid-late-Upl-BS-WS macroplots in Pickle Lake.

Ecosite	Model	JD	BA	Clay	NDMI	ΔEVI	*K*	AIC_c	ΔAIC_c	w_i
Mid-late-Upl-BS	m13	0.62	0.60	3.75	110.58		5	1502.76	0.00	0.19
	m2	0.63	0.53				3	1503.03	0.27	0.17
	m7	0.63	0.59		95.34		4	1503.12	0.37	0.16
	m6	0.62	0.52	3.19			4	1503.33	0.57	0.14
	m8	0.62	0.52			0.005	4	1504.93	2.18	0.06
	m16	0.62	0.60	3.74	109.02	0.0008	6	1504.97	2.22	0.06
	m14	0.62	0.52	3.18		0.004	5	1505.28	2.52	0.05
	m12	0.63	0.59		92.63	0.002	5	1505.28	2.53	0.05
	m1	0.62					2	1506.76	4.01	0.03
	m3	0.61		3.32			3	1506.96	4.20	0.02
	m9	0.61		3.70	71.32		4	1507.97	5.21	0.01
	m4	0.62			56.50		3	1508.16	5.41	0.01
	m5	0.61				0.005	3	1508.59	5.84	0.01
	m10	0.60		3.31		0.005	4	1508.83	6.08	0.01
	m15	0.60		3.66	66.65	0.003	5	1510.07	7.32	0.00
	m11	0.61			50.89	0.003	4	1510.19	7.43	0.00
	null						1	1530.81	28.05	0.00
Mid-late-Upl-BS-WS	m2	2.14	0.86				3	426.67	0.00	0.49
	m6	2.20	0.84	8.01			4	428.46	1.80	0.20
	m7	2.15	0.81		242.19		4	429.12	2.45	0.14
	m8	2.16	0.87			-0.01	4	429.30	2.63	0.13
	m1	2.21					2	433.91	7.24	0.01
	m4	2.22			678.90		3	434.37	7.70	0.01
	m3	2.28		10.39			3	435.25	8.58	0.01
	m9	2.30		10.98	701.97		4	435.66	8.99	0.01
	m5	2.19				0.01	3	436.44	9.77	0.00
	m11	2.26			806.94	-0.02	4	436.86	10.19	0.00
	m10	2.26		10.46		0.01	4	437.94	11.28	0.00
	null						1	446.20	19.53	0.00

Appendix 6.62. Model coefficient, number of model parameters (*K*), Akaike's Information Criterion corrected for small sample size (AIC_c), change in AIC_c from best model (ΔAIC_c), and model weights calculated from AIC_c (w_i) for competing models with Julian day (JD), basal area (BA; m^2/ha), percent sand, normalized difference moisture index (NDMI), and change in enhanced vegetation index (ΔEVI) for DP-accepted biomass (kg/ha) at Early-Lwl-Bog and Mid-late-Lwl-Bog macroplots in Pickle Lake.

Ecosite	Model	JD	BA	Sand	NDMI	ΔEVI	*K*	AIC_c	ΔAIC_c	w_i
Early-Lwl-Bog	m1	-1.94					2	242.69	0.00	0.38
	m5	-1.82				0.03	3	244.51	1.82	0.15
	m3	-1.95		-7.22			3	244.70	2.02	0.14
	m2	-2.05	-12.21				3	244.78	2.09	0.13
	null						1	245.31	2.62	0.10
	m4	-1.89			99.14		3	245.51	2.82	0.09
Mid-late-Lwl-Bog	m2	-1.36	1.29				3	612.62	0.00	0.36
	m8	-1.38	1.30			-0.02	4	614.41	1.78	0.15
	m6	-1.29	1.31	2.50			4	614.57	1.94	0.14
	m7	-1.36	1.31		43.98		4	615.02	2.40	0.11
	m14	-1.30	1.32	2.92		-0.02	5	616.28	3.65	0.06
	m12	-1.38	1.32		57.71	-0.02	5	616.87	4.24	0.04
	m13	-1.29	1.34	2.55	51.88		5	617.05	4.43	0.04
	m1	-1.25					2	617.36	4.73	0.03
	m16	-1.30	1.35	3.02	68.96	-0.02	6	618.81	6.18	0.02
	m5	-1.27				-0.02	3	619.17	6.54	0.01
	m3	-1.20		1.85			3	619.46	6.84	0.01
	m4	-1.25			-42.21		3	619.66	7.03	0.01
	m10	-1.21		2.25		-0.02	4	621.26	8.64	0.00
	m11	-1.27			-30.31	-0.02	4	621.59	8.97	0.00
	m9	-1.20		1.82	-37.81		4	621.88	9.25	0.00
	m15	-1.21		2.22	-23.60	-0.02	5	623.81	11.18	0.00
	null						1	624.87	12.25	0.00

Appendix 6.63. Model coefficient, number of model parameters (*K*), Akaike's Information Criterion corrected for small sample size (AIC_c), change in AIC_c from best model (ΔAIC_c), and model weights calculated from AIC_c (w_i) for competing models with Julian day (JD), basal area (BA; m^2/ha), percent clay, normalized difference moisture index (NDMI), and change in enhanced vegetation index (ΔEVI) for DP-accepted biomass (kg/ha) at Early-Upl-BS and Mid-late-Upl-BS-WS macroplots in Cochrane.

Ecosite	Model	JD	BA	Clay	NDMI	ΔEVI	*K*	AIC_c	ΔAIC_c	w_i
Early-Upl-BS	null						1	199.76	0.00	0.33
	m2			-11.13			2	200.82	1.05	0.19
	m4					0.03	2	202.16	2.40	0.10
	m1		0.69				2	202.36	2.59	0.09
	m3				-50.86		2	202.54	2.78	0.08
	m9			-11.82		0.03	3	203.39	3.62	0.05
	m5		0.87	-11.85			3	203.60	3.84	0.05
	m8			-11.20	2.67		3	204.30	4.54	0.03
	m7		1.06			0.04	3	204.76	5.00	0.03
	m10				-113.07	0.04	3	204.78	5.02	0.03
	m6		0.65		-5.43		3	205.84	6.08	0.02
Mid-late-Upl-BS-WS	m1	0.89					2	322.98	0.00	0.20
	m4	0.86			-446.28		3	323.05	0.06	0.19
	m11	0.85			-537.15	0.03	4	323.91	0.93	0.12
	m2	0.95	-1.60				3	324.48	1.49	0.09
	m7	0.92	-1.59		-444.91		4	324.68	1.69	0.08
	m5	0.88				0.02	3	324.80	1.81	0.08
	m3	0.85		3.04			3	325.18	2.20	0.07
	m9	0.83		2.59	-434.10		4	325.61	2.62	0.05
	m8	0.94	-1.51			0.02	4	326.66	3.68	0.03
	m6	0.90	-1.69	3.41			4	326.76	3.78	0.03
	null						1	327.12	4.13	0.03
	m10	0.85		2.48		0.02	4	327.43	4.44	0.02

Appendix 6.64. Model coefficient, number of model parameters (*K*), Akaike's Information Criterion corrected for small sample size (AIC_c), change in AIC_c from best model (ΔAIC_c), and model weights calculated from AIC_c (w_i) for competing models with Julian day (JD), basal area (BA; m^2/ha), percent silt, normalized difference moisture index (NDMI), and change in enhanced vegetation index (ΔEVI) for DP-accepted biomass (kg/ha) at Early-Upl-BS-WS, Mid-late-Upl-BS, Early-Lwl-Bog, and Mid-late-Lwl-Bog macroplots in Cochrane.

Ecosite	Model	JD	BA	Silt	NDMI	ΔEVI	*K*	AIC_c	ΔAIC_c	w_i
Early-Upl-BS-WS	m1	1.44					2	148.78	0.00	0.61
	null						1	151.47	2.69	0.16
	m5					0.23	2	151.79	3.01	0.14
	m3			39.95			2	153.84	5.06	0.05
	m4				-579.43		2	155.44	6.66	0.02
	m2		2.35				2	155.53	6.74	0.02

Appendix 6.64. Continued.

Ecosite	Model	JD	BA	Silt	NDMI	ΔEVI	*K*	AIC_c	ΔAIC_c	w_i
Mid-late-Upl-BS	null						1	237.72	0.00	0.32
	m2			2.65			2	239.32	1.60	0.15
	m1		-0.49				2	239.59	1.87	0.13
	m4					0.02	2	239.89	2.16	0.11
	m3				-22.59		2	240.37	2.65	0.09
	m9			2.51		0.01	3	241.89	4.17	0.04
	m7		-0.52			0.02	3	241.97	4.25	0.04
	m5		-0.30	2.03			3	242.07	4.34	0.04
	m10				-99.38	0.03	3	242.19	4.47	0.03
	m8			2.62	-14.92		3	242.31	4.59	0.03
	m6		-0.48		-13.65		3	242.59	4.87	0.03
Early-Lwl-Bog	null						1	95.82	0.00	0.82
	m2			28.43			2	100.53	4.71	0.08
	m1		21.12				2	101.57	5.75	0.05
	m4					-0.05	2	102.56	6.74	0.03
	m3				-82.44		2	102.81	6.98	0.03
Mid-late-Lwl-Bog	m1	0.95					2	347.97	0.00	0.28
	m3	0.88		-3.19			3	348.32	0.35	0.23
	m5	0.96				0.01	3	350.31	2.34	0.09
	m2	0.93	0.12				3	350.47	2.49	0.08
	m4	0.95			23.47		3	350.56	2.59	0.08
	m6	0.87	0.08	-3.15			4	351.08	3.11	0.06
	m9	0.89		-3.31	-26.04		4	351.11	3.13	0.06
	m10	0.88		-3.22		0.00	4	351.15	3.18	0.06
	m8	0.95	0.08			0.01	4	353.09	5.12	0.02
	m11	0.96			18.24	0.01	4	353.12	5.14	0.02
	m7	0.91	0.19		54.44		4	353.14	5.17	0.02
	null						1	356.78	8.81	0.00

Appendix 6.65. Model coefficient, number of model parameters (*K*), Akaike's Information Criterion corrected for small sample size (AIC_c), change in AIC_c from best model (ΔAIC_c), and model weights calculated from AIC_c (w_i) for competing models with Julian day (JD), basal area (BA; m^2/ha), percent clay, normalized difference moisture index (NDMI), and change in enhanced vegetation index (ΔEVI) for DP-accepted biomass (kg/ha) at Mid-late-Lwl-Fen macroplots in Pickle Lake and Cochrane.

Model	JD	BA	Clay	NDMI	ΔEVI	*K*	AIC_c	ΔAIC_c	w_i
m1	1.01					2	178.80	0.00	1.00
null						1	200.00	21.20	0.00
m5					-0.12	2	201.27	22.47	0.00
m3			-24.78			2	202.17	23.38	0.00
m4				478.51		2	202.82	24.02	0.00
m2		-3.19				2	202.89	24.09	0.00

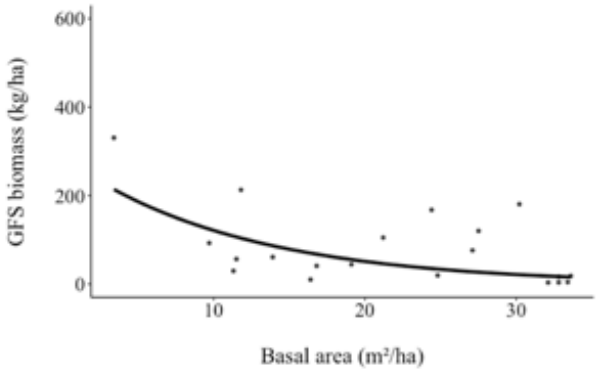

Appendix 6.66. Relationships between grass/ forbs/ deciduous shrub biomass (kg/ha) in mid-late Upl-BS-Rocky and basal area (m^2/ha) in Pickle Lake, Ontario.

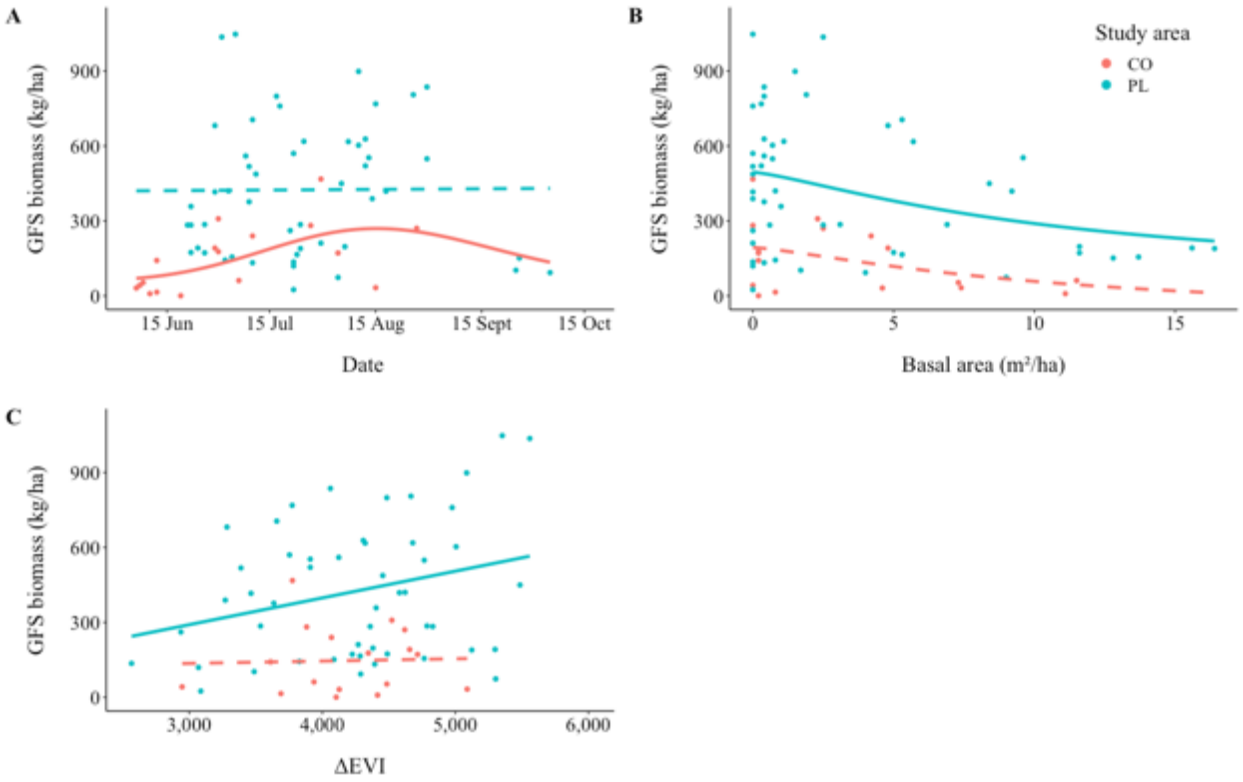

Appendix 6.67. Relationships between grass/ forbs/ deciduous shrub biomass (kg/ha) in early Upl-BS and A) sampling date, B) basal area (m^2/ha), and C) ΔEVI. Dashed line indicates the covariate was not included in the top model for that study area.

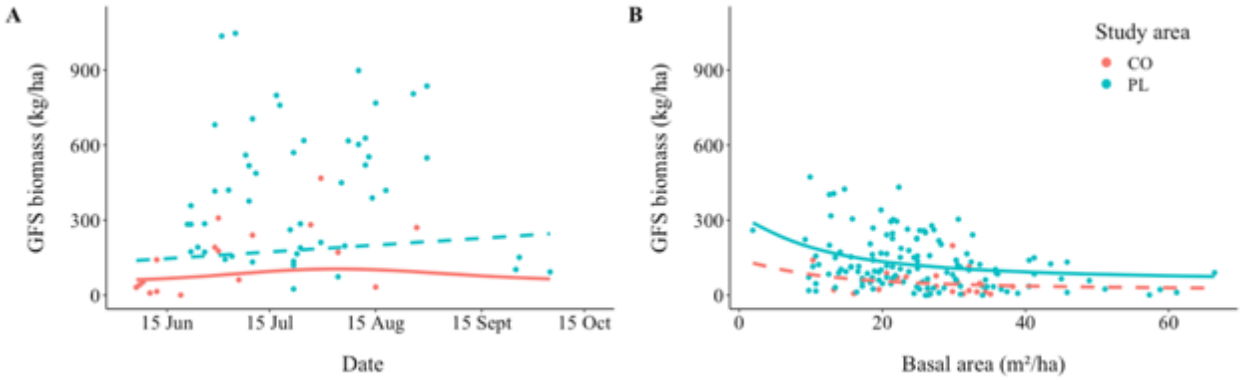

Appendix 6.68. Relationships between grass/ forbs/ deciduous shrub biomass (kg/ha) in mid-late Upl-BS and A) sampling date and B) basal area (m^2/ha). Dashed line indicates the covariate was not included in the top model for that study area.

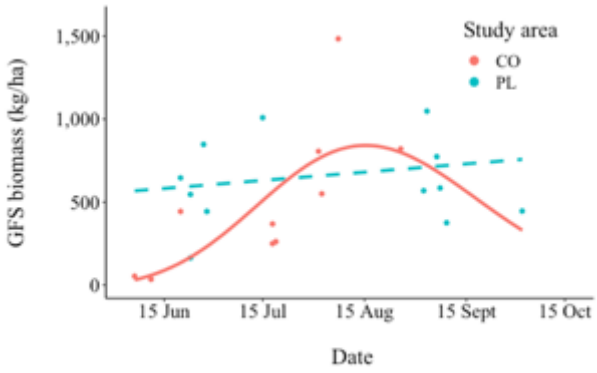

Appendix 6.69. Relationships between grass/ forbs/ deciduous shrub biomass (kg/ha) in early Upl-BS-WS and sampling date. Dashed line indicates the covariate was not included in the top model for that study area.

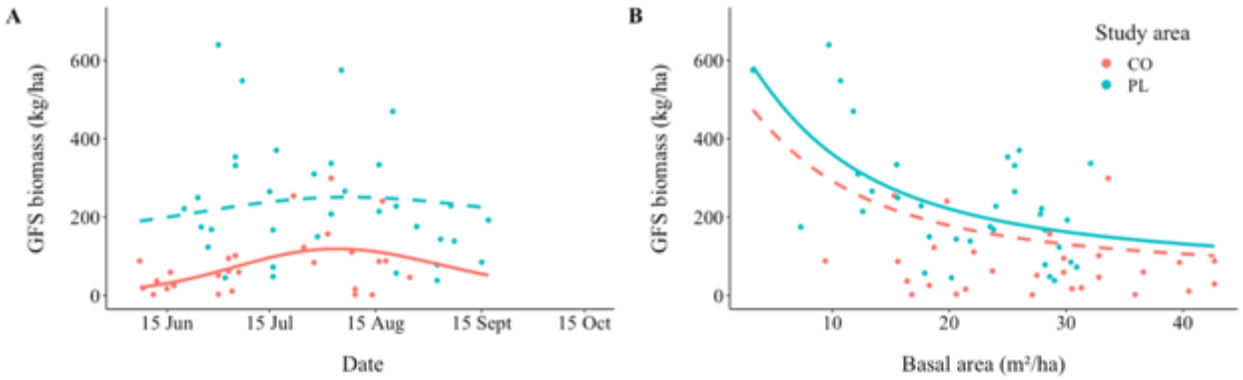

Appendix 6.70. Relationships between grass/ forbs/ deciduous shrub biomass (kg/ha) in mid-late Upl-BS-WS and basal area (m^2/ha). Dashed line indicates the covariate was not included in the top model for that study area.

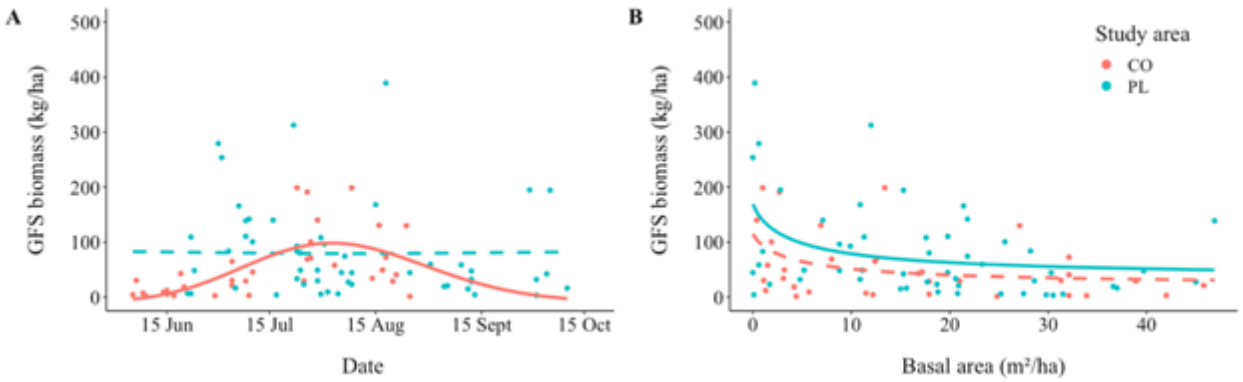

Appendix 6.71. Relationships between grass/ forbs/ deciduous shrub biomass (kg/ha) in mid-late Lwl-Bog and A) sampling date and B) basal area (m^2/ha). Dashed line indicates the covariate was not included in the top model for that study area.

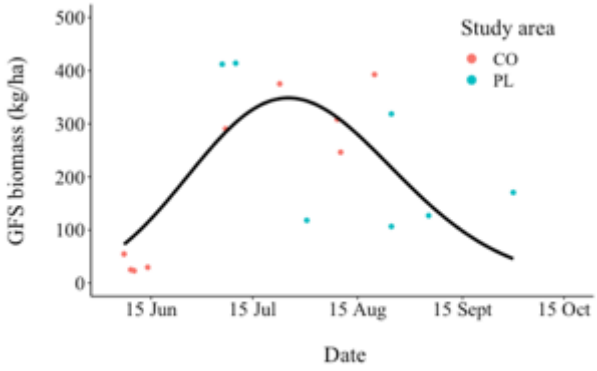

Appendix 6.72. Relationships between grass/ forbs/ deciduous shrub biomass (kg/ha) in Lwl-Fen and sampling date with data combined across Pickle Lake (PL) and Cochrane (CO), Ontario.

Appendix 6.73. Top predictive equations of grass/ forbs/ deciduous shrub biomass for each seral-specific (early: <20 years; mid-late: ≥20 years) ecosite and study area (SA) as a function of sampling date (i.e., Julian day; JD), basal area (m^2/ha; BA), and change in enhanced vegetative index (ΔEVI) and number of macroplots used to develop each model.

SA	Ecosite	Seral	n	Equation	r^2
PL	Upl-BS-Rocky	Early	3	314.61	---
		Mid-late	20	0.87*(340.89*exp(-0.08*BA) + 17.19	0.36
	Upl-BS	Early	50	1.50*(413.84/(1.00+(BA/11.08)^1.31)) + 0.16*ΔEVI -788.86	0.28
		Mid-late	136	1.04*(1.29e-51 *0.88^JD*JD^27.74) + 0.63*(413.84/(1+(BA/11.08)^1.31)) - 80.45	0.19
	Upl- BS-WS	Early	13	667.67	---
		Mid-late	34	0.98*(672.31/(1.00+(BA/8.99)^1.37)) + 56.14	0.38
	Lwl-Bog	Early	20	258.74	---
		Mid-late	52	0.62*(219.26/(1.00+(BA/4.44)^0.86)) + 33.64	0.16
	Marsh	NA	1	1053.39	---
CO	Upl-BS	Early	17	0.38*(1.52e-87*0.81^JD*JD^46.59) + 57.58	0.33
		Mid-late	22	49.08	---
	Upl-BS-WS	Early	10	1.53*(1.52e-87*0.81^JD*JD^46.59) -19.28	0.52
		Mid-late	28	0.88*(2.03e-96*0.79^JD*JD^51.48) + 9.30	0.22
	Lwl-Bog	Early	7	109.3	---
		Mid-late	34	1.12*(4.33e-85*0.82^JD*JD^45.11) - 9.32	0.41
PL & CO	Lwl-Fen	Mid-late	16	1.00*(4.11e-88*0.79^JD*JD^47.82) + 0.81	0.51
	Lwl-Cedar/ thicket	Mid-late	5	538.74	---

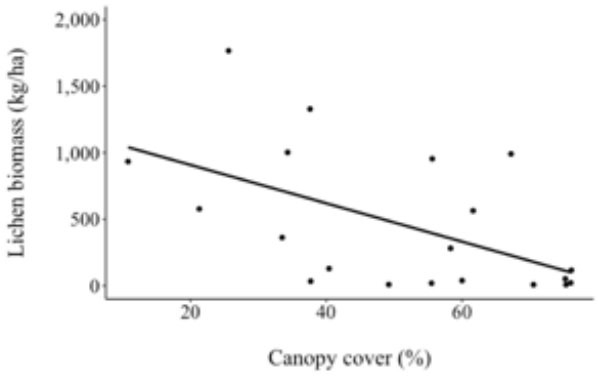

Appendix 6.74. Relationships between lichen (kg/ha) in mid-late Upl-BS-Rocky and canopy cover (%) in Pickle Lake, Ontario.

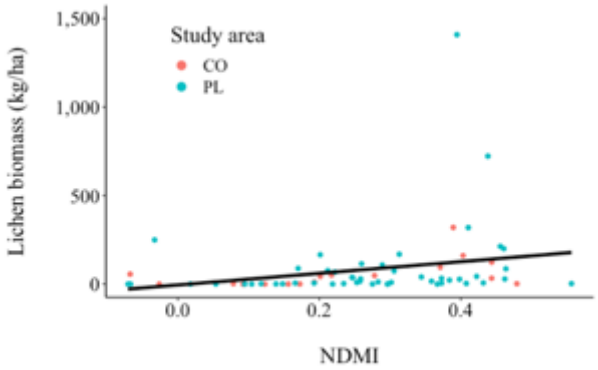

Appendix 6.75. Relationships between lichen biomass (kg/ha) in early Upl-BS and NDMI with data combined across Pickle Lake (PL) and Cochrane (CO), Ontario.

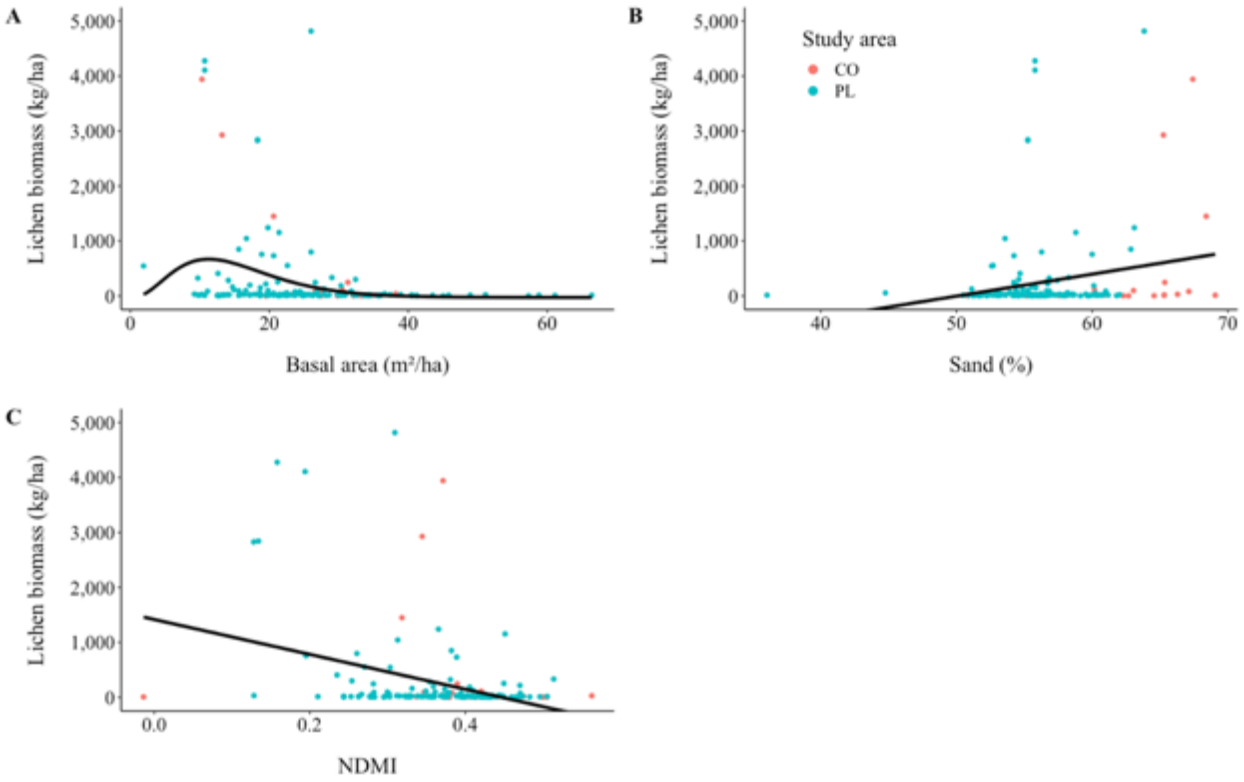

Appendix 6.76. Relationships between lichen biomass (kg/ha) in mid-late Upl-BS and A) basal area (m^2/ha), B) percent sand, and C) NDMI with data combined across Pickle Lake (PL) and Cochrane (CO), Ontario.

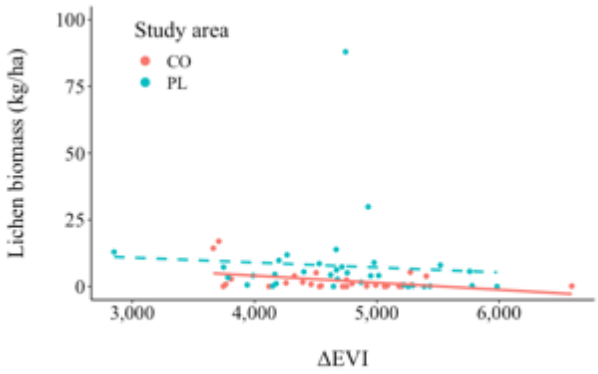

Appendix 6.77. Relationships between lichen biomass (kg/ha) in mid-late Upl-BS-WS and ΔEVI. Dashed line indicates the covariate was not included in the top model for that study area.

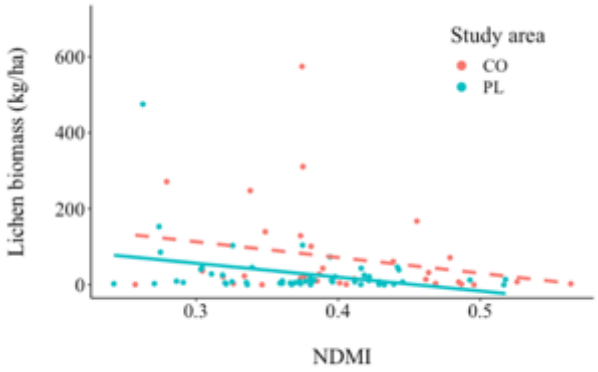

Appendix 6.78. Relationships between lichen biomass (kg/ha) in mid-late Lwl-Bog and NDMI. Dashed line indicates the covariate was not included in the top model for that study area.

Appendix 6.79. Top predictive equations of lichen biomass for each seral-specific (early: <20 years; mid-late: ≥20 years) ecosite and study area (SA) as a function of sampling date (i.e., Julian day; JD), basal area (m^2/ha; BA), canopy cover (%), percent sand, change in enhanced vegetative index (ΔEVI), and normalized difference moisture index (NDMI) and number of macroplots used to develop each model.

SA	Ecosite	Seral	n	Equation	r^2
PL	Upl-BS-Rocky	Early	3	806.52	---
		Mid-late	20	-14.42*CC + 1196.62	0.30
	Upl- BS-WS	Early	14	12.03	---
		Mid-late	34	7.68	---
	Lwl-Bog	Early	20	16.53	---
		Mid-late	52	-365.38*NDMI + 166.33	0.11
	Lwl- Marsh	Mid-late	1	58.57	---
CO	Upl-BS-WS	Early	10	0.17	---
		Mid-late	28	-0.003*ΔEVI + 14.62	0.17
	Lwl-Bog	Early	7	176.21	---
		Mid-late	34	72.02	---
PL & CO	Upl-BS	Early	67	328.97*NDMI - 4.94	0.06
		Mid-late	158	1.02*(11.24*0.79^BA*BA^2.70) + 44.42*Sand - 3101.93*NDMI - 1345.87	0.22
	Lwl-Fen	Mid-late	15	11.69	---
	Lwl- Cedar/ thicket	Mid-late	5	13.24	---

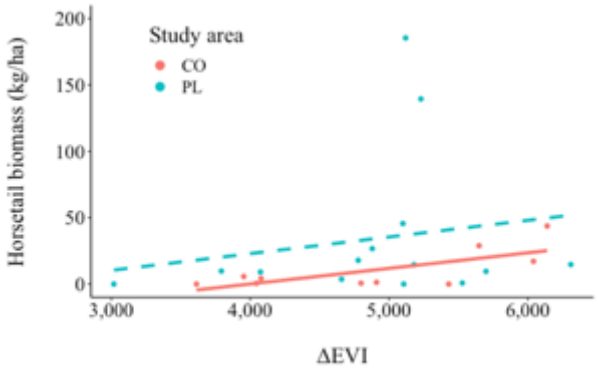

Appendix 6.80. Relationships between horsetail biomass (kg/ha) in early Upl-BS-WS and ΔEVI. Dashed line indicates the covariate was not included in the top model for that study area.

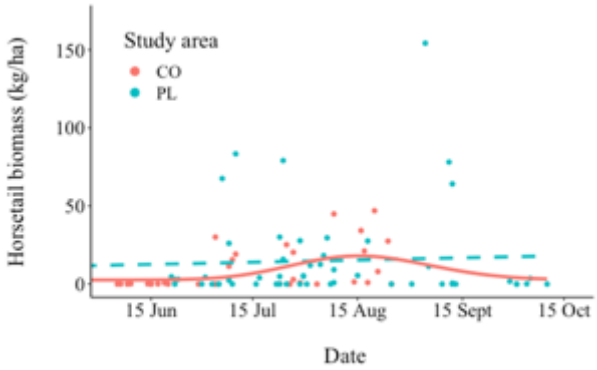

Appendix 6.81. Relationships horsetail biomass (kg/ha) in mid-late Lwl-Bog and sampling date. Dashed line indicates the covariate was not included in the top model for that study area.

Appendix 6.82. Top predictive equations of horsetail biomass for each seral-specific (early: <20 years; mid-late: ≥20 years) ecosite and study area (SA) as a function of sampling date (i.e., Julian day; JD) and change in enhanced vegetative index (ΔEVI), and number of macroplots used to develop each model.

SA	Ecosite	Seral	n	Equation	r^2
PL	Upl-BS-Rocky	Early	3	0.00	---
		Mid-late	20	0.00	---
	Upl-BS	Early	50	4.47	---
		Mid-late	136	0.86	---
	Upl- BS-WS	Early	13	34.11	---
		Mid-late	34	1.58	---
	Lwl-Bog	Early	20	42.46	---
		Mid-late	52	15.02	---
	Lwl-Marsh	Mid-late	1	0.00	---
CO	Upl-BS	Early	17	0.00	---
		Mid-late	22	0.10	---
	Upl-BS-WS	Early	10	0.01*ΔEVI - 46.79	0.51
		Mid-late	28	0.47	---
	Lwl-Bog	Early	7	23.16	---
		Mid-late	34	0.83*(3.30e-239*0.58^JD*JD^124.71) + 2.64	0.20
PL & CO	Lwl-Fen	Mid-late	16	0.94	---
	Lwl-Cedar/ thicket	Mid-late	5	28.42	---

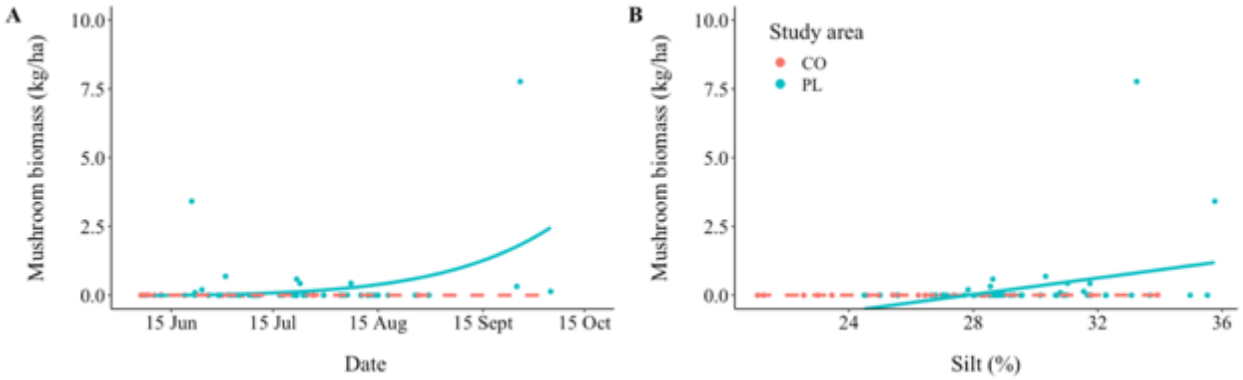

Appendix 6.83. Relationships between mushroom biomass (kg/ha) in early-Upl-BS and A) sampling date, and B) percent silt. Dashed line indicates the covariate was not included in the top model for that study area.

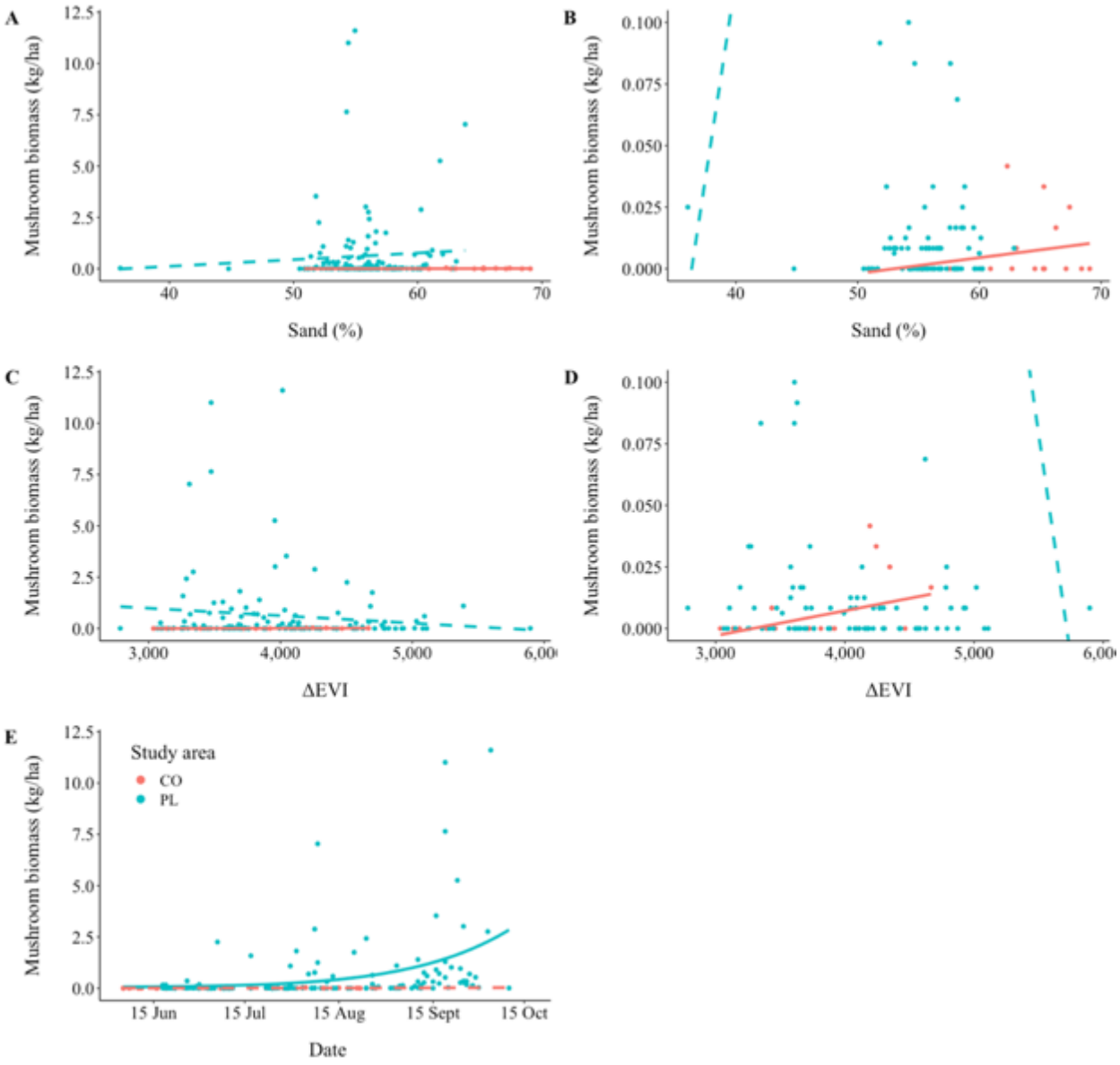

Appendix 6.84. Relationships between mushroom biomass (kg/ha) in mid-late Upl-BS and A) percent silt (B: truncated y-axis), C) ΔEVI (D: truncated y-axis), and E) sampling date. Dashed line indicates the covariate was not included in the top model for that study area.

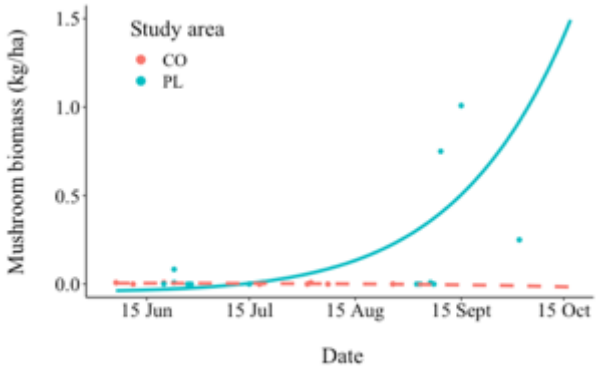

Appendix 6.85. Relationships between mushroom biomass (kg/ha) in early Upl-BS-WS and sampling date. Dashed line indicates the covariate was not included in the top model for that study area.

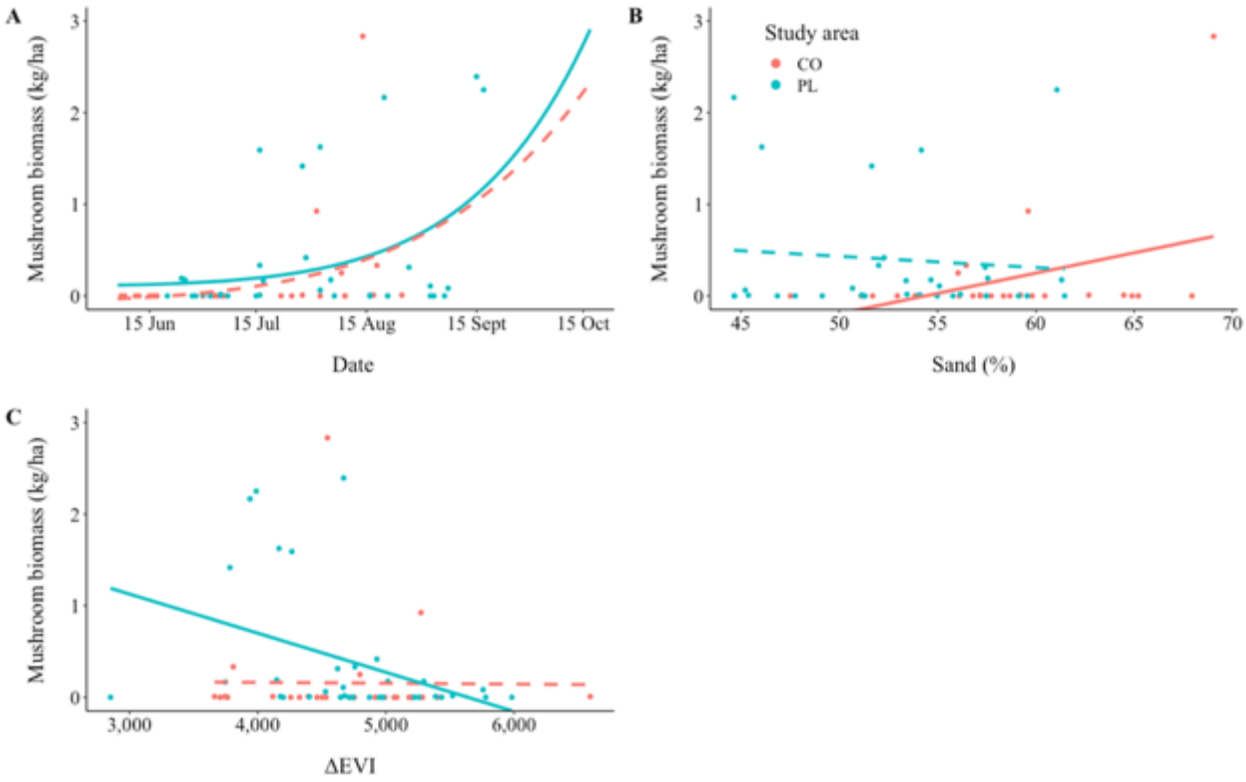

Appendix 6.86. Relationships between mushroom biomass (kg/ha) in mid-late Upl-BS-WS and A) sampling date, B) percent sand, C) ΔEVI. Dashed line indicates the covariate was not included in the top model for that study area.

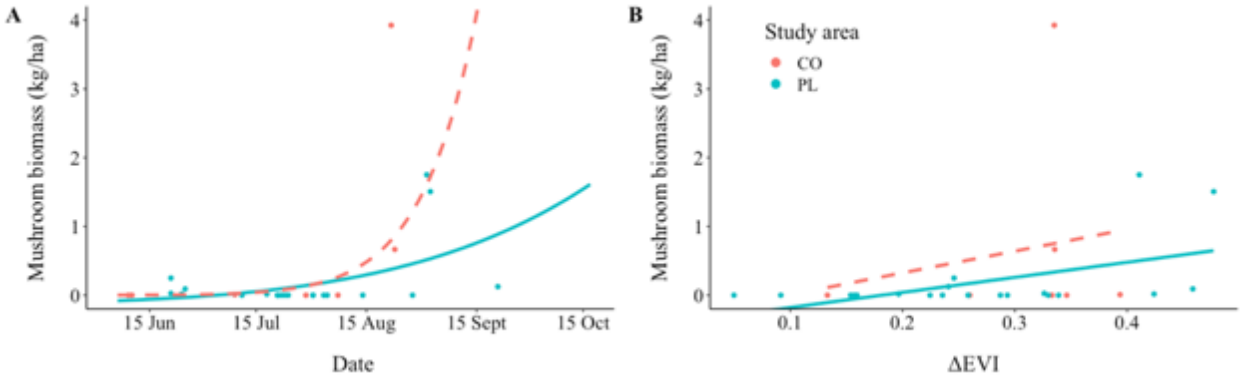

Appendix 6.87. Relationships mushroom biomass (kg/ha) in early Lwl-Bog and A) sampling date and, B) ΔEVI. Dashed line indicates the covariate was not included in the top model for that study area.

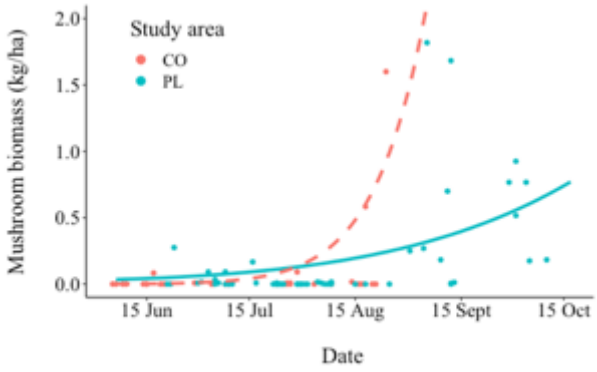

Appendix 6.88. Relationships mushroom biomass (kg/ha) in mid-late Lwl-Bog and sampling date. Dashed line indicates the covariate was not included in the top model for that study area.

Appendix 6.89. Top predictive equations of mushroom biomass for each seral-specific (early: <20 years; mid-late: ≥20 years) ecosite and study area (SA) as a function of sampling date (i.e., Julian day; JD), precent clay, sand, or silt, change in enhanced vegetative index (ΔEVI), and normalized difference moisture index (NDMI), and number of macroplots used to develop each model.

SA	Ecosite	Seral	n	Equation	r^2
PL	Upl-BS-Rocky	Early	3	0.007	---
		Mid-late	20	0.26	---
	Upl-BS	Early	50	1.09*(6.65e-22*JD^8.80) + 0.13*Silt - 4.02	0.25
		Mid-late	136	0.96*(1.47e-22*JD^9.09) + 0.06	0.13
	Upl- BS-WS	Early	13	0.49*(6.65-22*JD^8.80) - 0.04	0.36
		Mid-late	34	0.80*(6.65e-22*JD^8.80) - 0.0004*ΔEVI + 1.91	0.28
	Lwl-Bog	Early	20	2.21*(5.74e-15*JD^5.74) + 2.16*NDMI - 0.70	0.49
		Mid-late	52	0.96*(4.12e-15*JD^5.80) + 0.01	0.14
	Lwl-Marsh	Mid-late	1	0.00	---
CO	Upl-BS	Early	17	0.001	---
		Mid-late	22	-0.003*Clay + 0.00001*ΔEVI - 0.007	0.51
	Upl-BS-WS	Early	10	0.003	---
		Mid-late	28	0.04*Sand - 2.41	0.17
	Lwl-Bog	Early	7	0.66	---
		Mid-late	34	0.07	---
PL & CO	Lwl-Fen	Mid-late	16	0.10	---
	Lwl-Cedar/ thicket	Mid-late	5	0.05	---

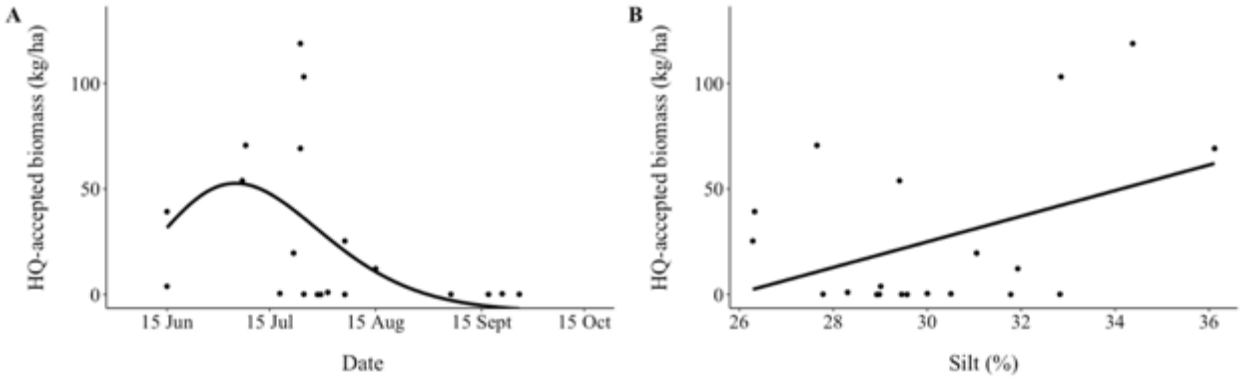

Appendix 6.90. Relationships between high-quality (HQ) accepted biomass with DE and DP constraints (kg/ha) in mid-late Upl-BS-Rocky and A) sampling date, and B) percent silt in Pickle Lake, Ontario.

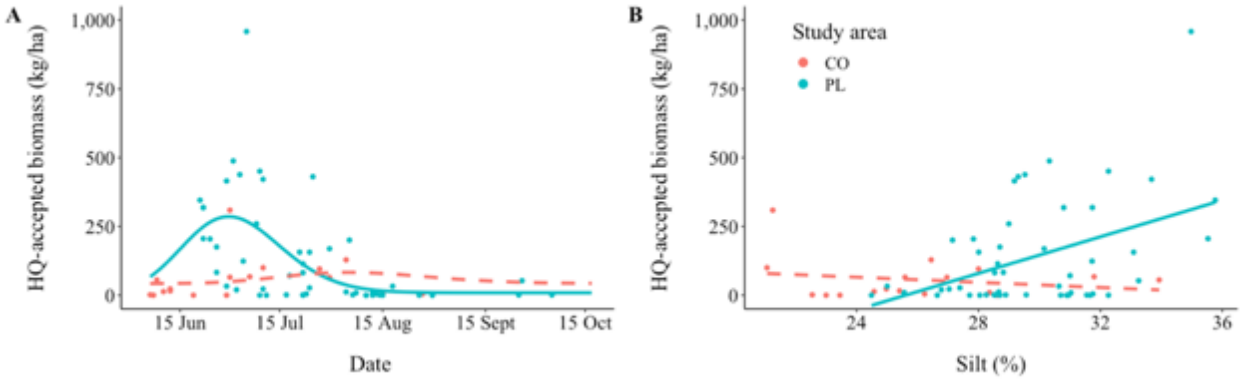

Appendix 6.91. Relationships between high-quality (HQ) accepted biomass with DE and DP constraints (kg/ha) in early Upl-BS and A) sampling date, and B) percent silt. Dashed line indicates the covariate was not included in the top model for that study area.

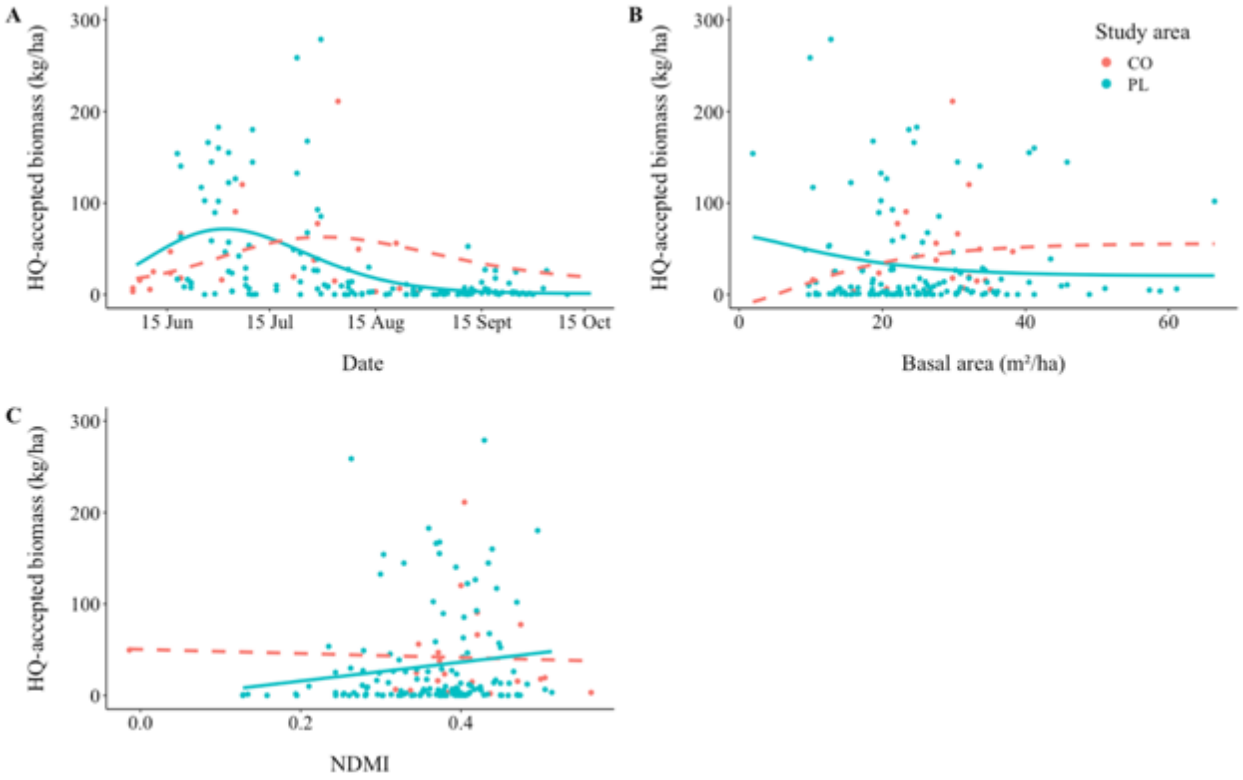

Appendix 6.92. Relationships between high-quality (HQ) accepted biomass with DE and DP constraints (kg/ha) in mid-late Upl-BS and A) sampling date, B) basal area (m^2/ha), and C) NDMI. Dashed line indicates the covariate was not included in the top model for that study area.

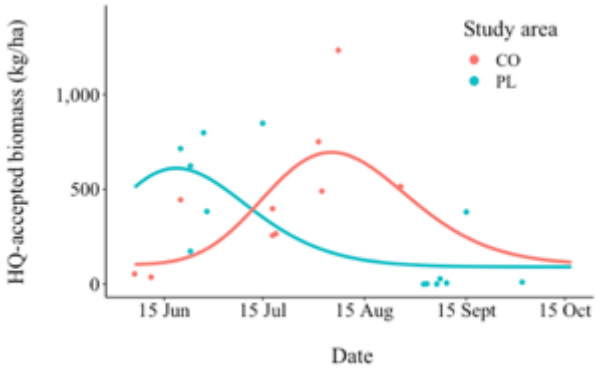

Appendix 6.93. Relationships between high-quality (HQ) accepted biomass with DE and DP constraints (kg/ha) in early Upl-BS-WS and sampling date. Dashed line indicates the covariate was not included in the top model for that study area.

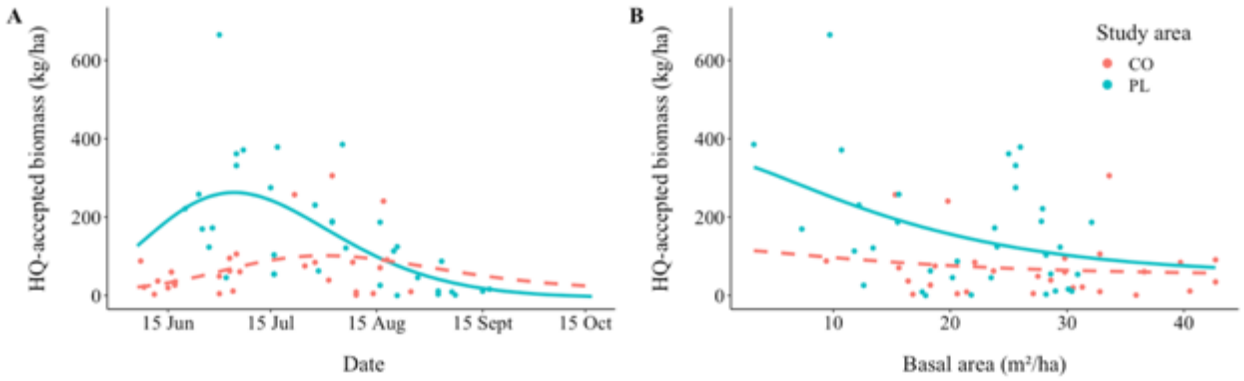

Appendix 6.94. Relationships between high-quality (HQ) accepted biomass with DE and DP constraints (kg/ha) in mid-late Upl-BS-WS and A) sampling date, and B) basal area (m^2/ha). Dashed line indicates the covariate was not included in the top model for that study area.

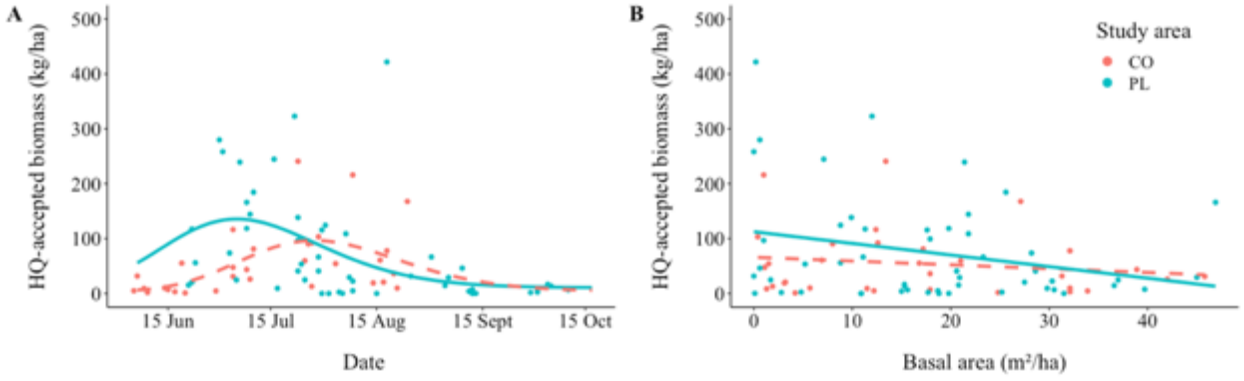

Appendix 6.95. Relationships between high-quality (HQ) accepted biomass with DE and DP constraints (kg/ha) in mid-late Lwl-Bog and A) sampling date and B) basal area (m^2/ha). Dashed line indicates the covariate was not included in the top model for that study area.

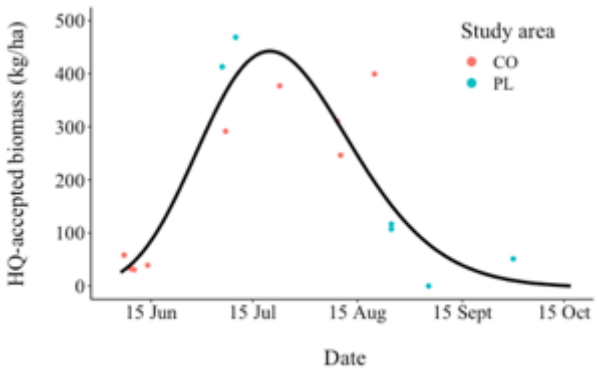

Appendix 6.96. Relationships between high-quality (HQ) accepted biomass with DE and DP constraints (kg/ha) in Lwl-Fen and sampling date with data combined across Pickle Lake (PL) and Cochrane (CO), Ontario.

Appendix 6.97. Top predictive equations of high-quality (HQ) accepted biomass (including both DE and DP constraints) for each seral-specific (early: <20 years, mid-late: ≥20 years) ecosite and study area (SA) as a function of sampling date (i.e., Julian day; JD), basal area (m^2/ha; BA), precent silt, and normalized difference moisture index (NDMI), and the number of macroplots used to develop each model.

SA	Ecosite	Seral	n	Equation	r^2
PL	Upl-BS-Rocky	Early	3	4.43	---
		Mid-late	20	0.46*exp(397.42 - 11729.60/JD - 63.05*log(JD)) + 6.26*Silt - 197.69	0.43
	Upl-BS	Early	50	0.88*(exp(940.54 - 27253.58/JD - 150.87*log(JD)) + 28.29*Silt - 820.82	0.45
		Mid-late	136	0.50*(121.15*BA^(-0.02*BA)) + 0.99*(exp(415.81 - 12123.07/JD -66.28*log(JD)) + 127.64*NDMI - 61.75	0.30
	Upl- BS-WS	Early	13	1.40*(exp(431.34 -11770.03/JD -69.35*log(JD))) + 90.45	0.52
		Mid-late	34	0.70*(374.51*BA^(-0.02*BA)) + 0.99*(exp(307.08 - 8980.27/JD - 48.46*log(JD))) - 93.42	0.49
	Lwl-Bog	Early	20	1.13*exp(419.20 - 12384.68/JD - 66.54*log(JD)) + 15.31	0.25
		Mid-late	52	1.02*exp(419.20 - 12384.68/JD - 66.54*log(JD)) - 2.58*BA + 50.57	0.33
	Marsh	Mid-late	1	192.25	---
CO	Upl-BS	Early	17	56.06	---
		Mid-late	22	41.61	---
	Upl-BS-WS	Early	10	1.42*(exp(638.27 - 21497.92/JD - 99.10*log(JD))) + 101.69	0.47
		Mid-late	28	69.67	---
	Lwl-Bog	Early	7	98.70	---
		Mid-late	34	0.95*(exp(522.69 - 17064.74/JD -81.70*log(JD)))+ 3.94	0.29
PL & CO	Lwl-Fen	Mid-late	15	1.01*(exp(526.13 -16588.74/JD - 82.50*log(JD))) - 2.94	0.81
	Lwl-Cedar/ thicket	Mid-late	5	160.92	---

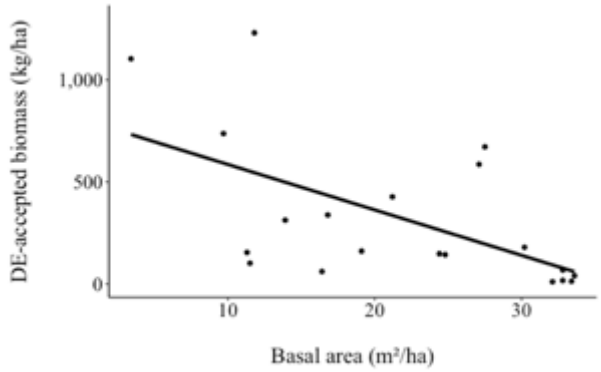

Appendix 6.98. Relationships between DE constraint accepted biomass (kg/ha) in mid-late Upl-BS-Rocky and basal area (m^2/ha) in Pickle Lake Ontario.

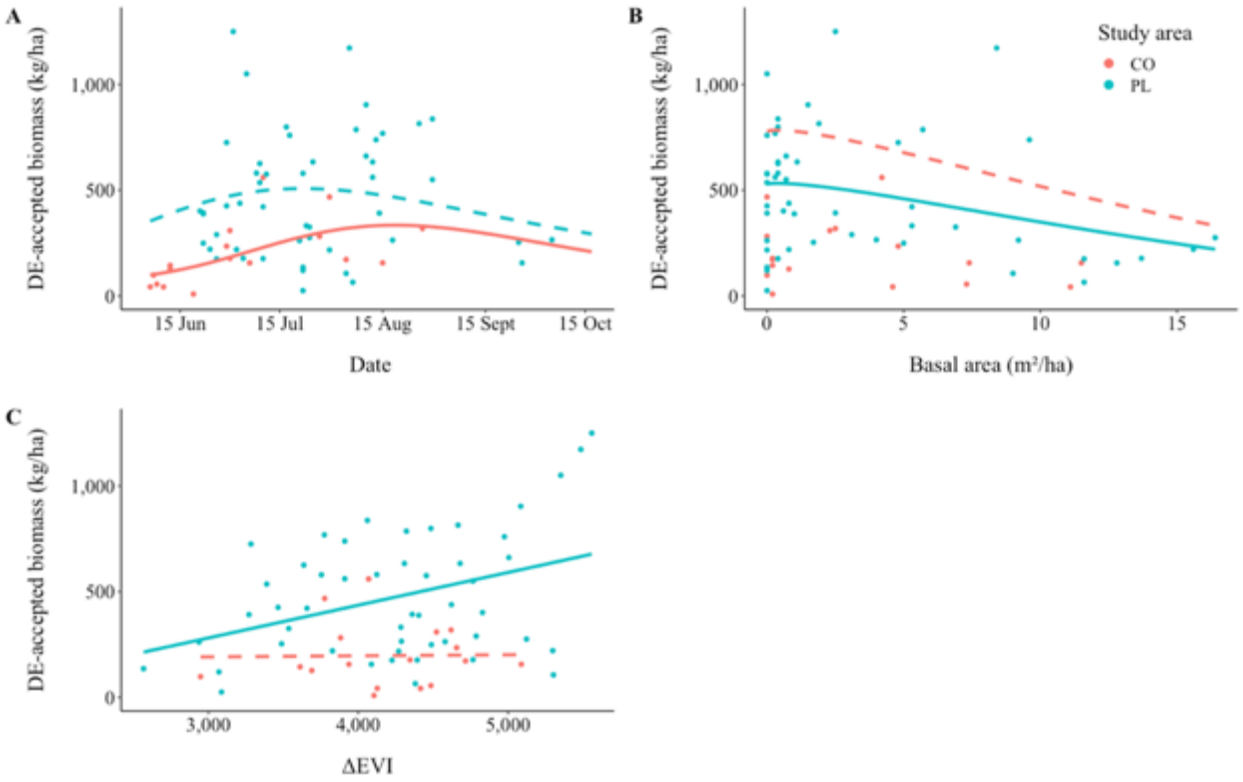

Appendix 6.99. Relationships between DE constraint accepted biomass (kg/ha) in early Upl-BS and A) sampling date, B) basal area (m^2/ha), and C) ΔEVI. Dashed line indicates the covariate was not included in the top model for that study area.

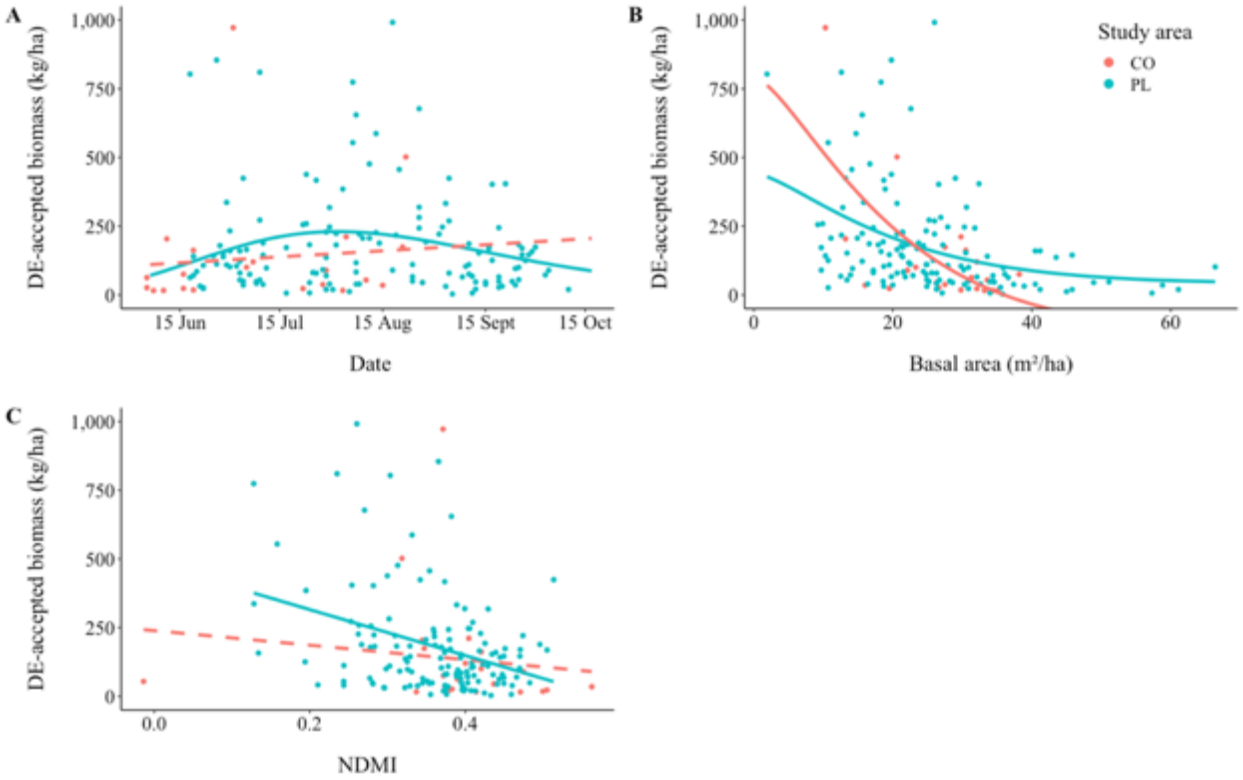

Appendix 6.100. Relationships between DE constraint accepted biomass (kg/ha) in mid-late Upl-BS and A) sampling date, B) basal area (m^2/ha), and C) NDMI. Dashed line indicates the covariate was not included in the top model for that study area.

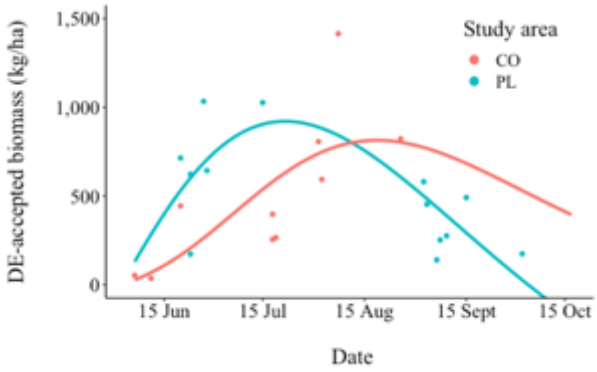

Appendix 6.101. Relationships between DE constraint accepted biomass (kg/ha) in early Upl-BS-WS and sampling date. Dashed line indicates the covariate was not included in the top model for that study area.

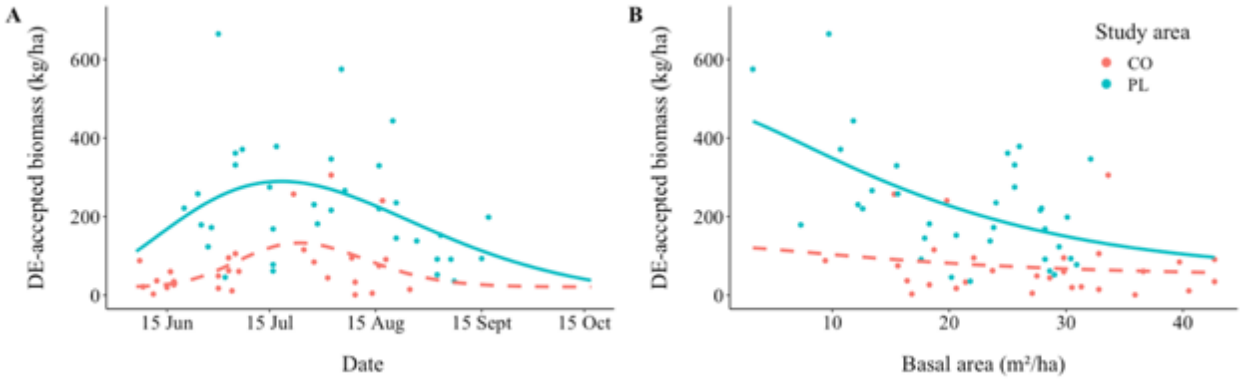

Appendix 6.102. Relationships between DE constraint accepted biomass (kg/ha) in mid-late Upl-BS-WS and A) sampling date, and B) basal area (m^2/ha). Dashed line indicates the covariate was not included in the top model for that study area.

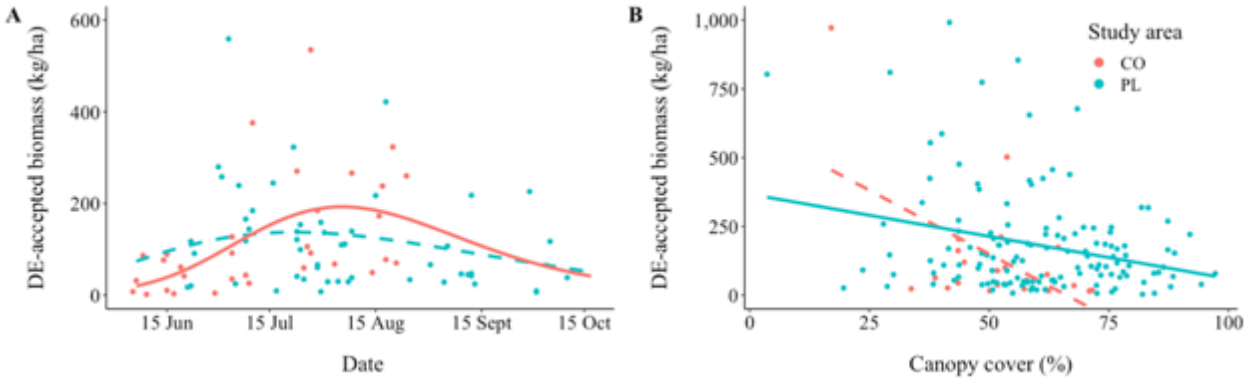

Appendix 6.103. Relationships between DE constraint accepted biomass (kg/ha) in mid-late Lwl-Bog and A) sampling date and B) canopy cover (%). Dashed line indicates the covariate was not included in the top model for that study area.

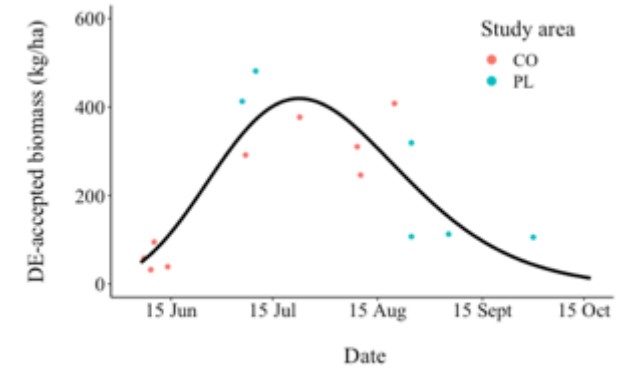

Appendix 6.104. Relationships between DE constraint accepted biomass kg/ha) in Lwl-Fen and sampling date with data combined across Pickle Lake (PL) and Cochrane (CO), Ontario.

Appendix 6.105. Top predictive equations of DE constraint accepted biomass (including only the DE constraint) for each seral-specific (early: <20 years, mid-late: ≥20 years) ecosite and study area (SA) as a function of sampling date (i.e., Julian day; JD), basal area (m^2/ha; BA), canopy cover (%), precent silt, and normalized difference moisture index (NDMI), change in enhanced vegetation index (ΔEVI) and the number of macroplots used to develop each model.

SA	Ecosite	Seral	n	Equation	r^2
PL	Upl-BS-Rocky	Early	3	795.63	---
		Mid-late	20	-22.25*BA + 808.19	0.34
	Upl-BS	Early	50	2.05*(467.25*BA^(-0.01*BA)) + 0.21*ΔEVI - 1300.05	0.33
		Mid-late	136	0.76*(exp(155.09 -5016.55/JD -23.52*log(JD))) + 0.73*(467.25*BA^(-0.01*BA)) - 600.21*NDMI + 137.59	0.25
	Upl-BS-WS	Early	13	3.62*(exp(94.48 - 2832.40/JD -13.97*log(JD))) - 1093.47	0.50
		Mid-late	34	0.85*(exp(185.98 -5710.99/JD - 28.64*log(JD))) + 0.80*(467.25*BA^(-0.01*BA)) - 123.65	0.38
	Lwl-Bog	Early	20	288.30	---
		Mid-late	52	-1.69*CC + 175.48	0.15
	Lwl-Marsh	Mid-late	1	391.49	---
CO	Upl-BS	Early	17	0.46*(exp(179.54 -6204.99/JD -26.89*log(JD))) + 72.50	0.35
		Mid-late	22	1.97*(467.25*BA^(-0.01*BA) - 143.48	0.42
	Upl-BS-WS	Early	10	1.52*(exp(179.54 -6204.99/JD -26.89*log(JD))) - 61.98	0.52
		Mid-late	28	0.79*(exp(763.60 - 24568.16/JD - 120.01*log(JD))) + 21.04	0.23
	Lwl-Bog	Early	7	208.77	---
		Mid-late	34	0.96*(exp(285.44 - 9538.37/JD -43.91*log(JD))) + 6.30	0.27
PL & CO	Lwl-Fen	Mid-late	16	1.00*(exp(369.98 - 11708.49/JD + - 54.80*log(JD))) -57.64	0.74
	Lwl-Cedar/ thicket	Mid-late	5	231.57	---

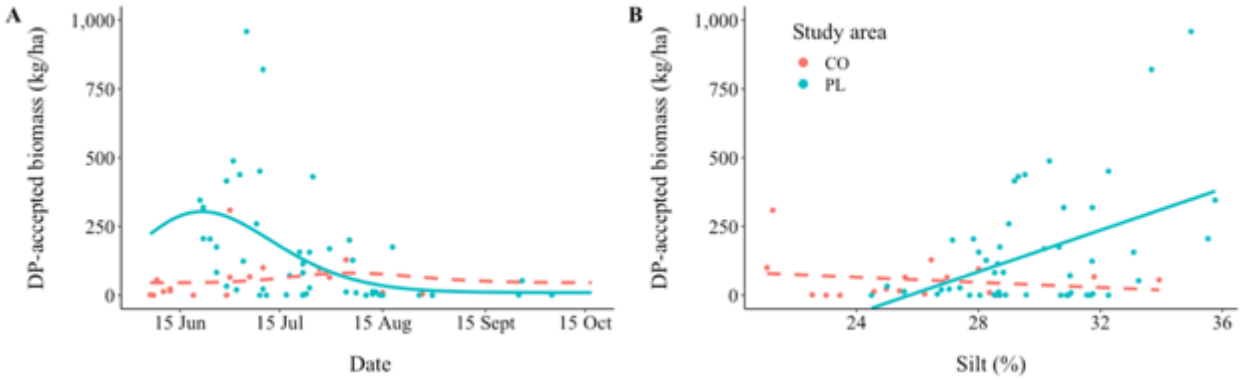

Appendix 6.106. Relationships between DP constraint accepted biomass (kg/ha) in early Upl-BS and A) sampling date, and B) percent silt. Dashed line indicates the covariate was not included in the top model for that study area.

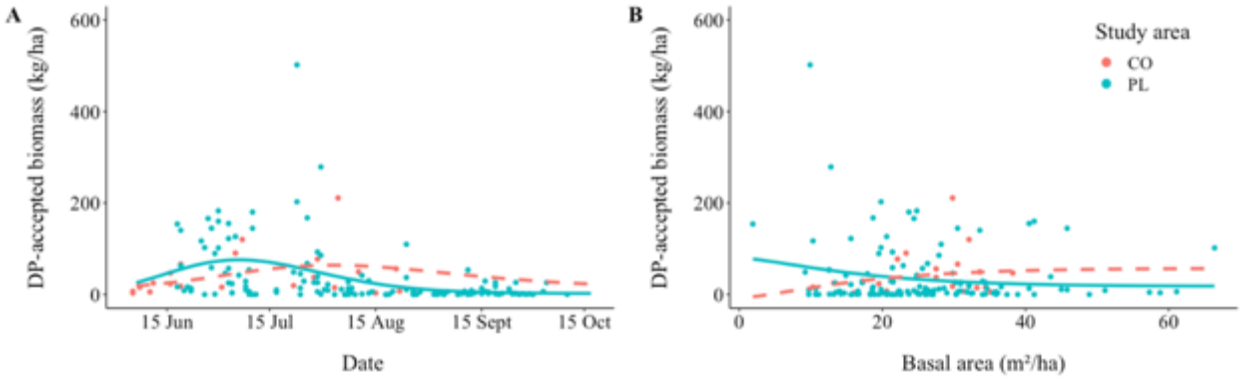

Appendix 6.107. Relationships between DP constraint accepted biomass (kg/ha) in mid-late Upl-BS and A) sampling date, B) basal area (m^2/ha), and C) NDMI. Dashed line indicates the covariate was not included in the top model for that study area.

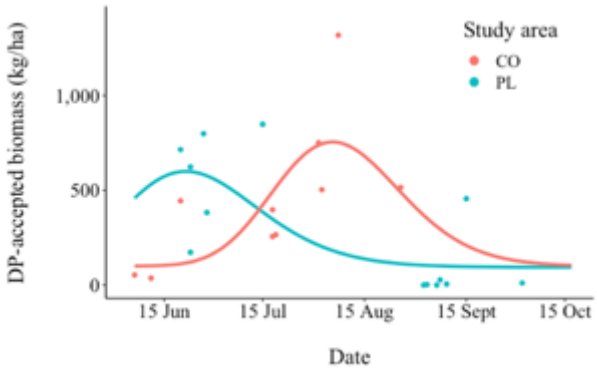

Appendix 6.108. Relationships between DP constraint accepted biomass (kg/ha) in early Upl-BS-WS and sampling date. Dashed line indicates the covariate was not included in the top model for that study area.

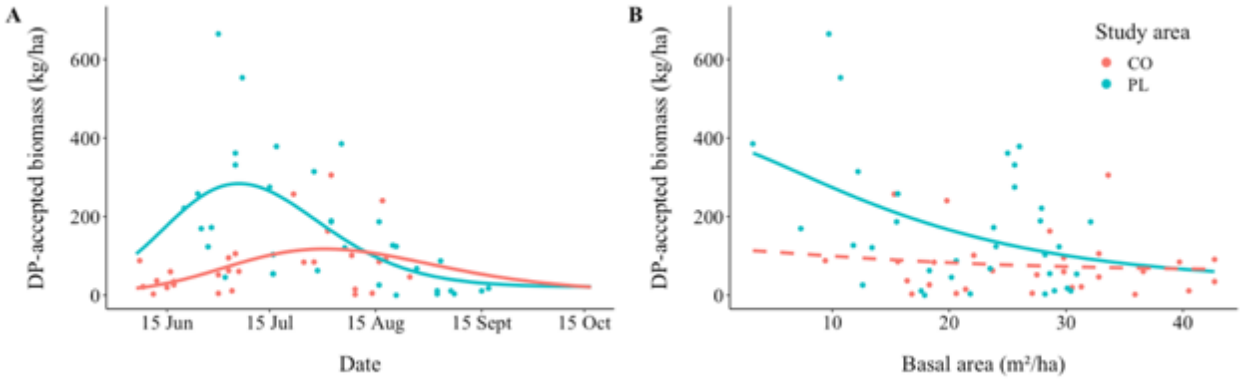

Appendix 6.109. Relationships between DP constraint accepted biomass (kg/ha) in mid-late Upl-BS-WS and A) sampling date, and B) basal area (m^2/ha). Dashed line indicates the covariate was not included in the top model for that study area.

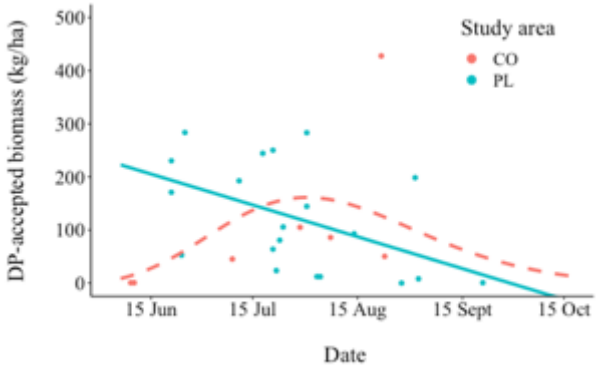

Appendix 6.110. Relationships between DP constraint accepted biomass (kg/ha) in early Lwl-Bog and sampling date. Dashed line indicates the covariate was not included in the top model for that study area.

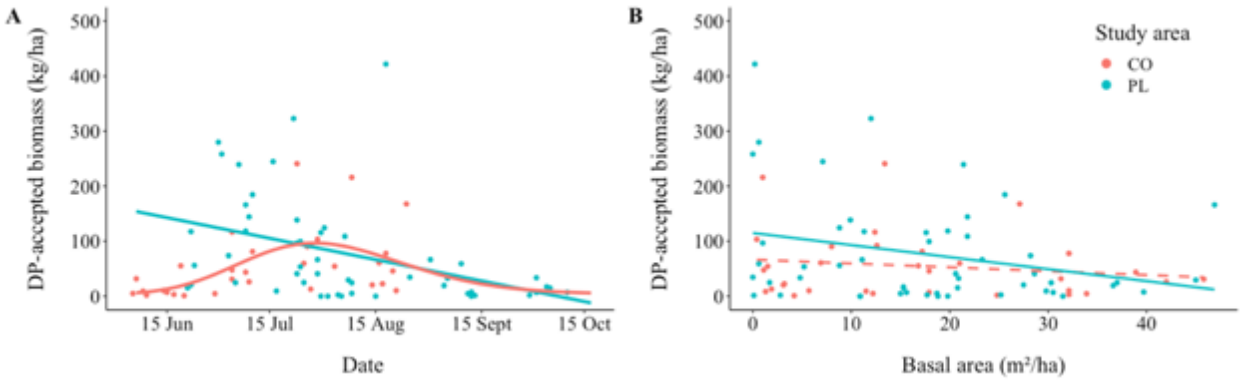

Appendix 6.111. Relationships between DP constraint accepted biomass (kg/ha) in mid-late Lwl-Bog and A) sampling date and B) basal area (m^2/ha). Dashed line indicates the covariate was not included in the top model for that study area.

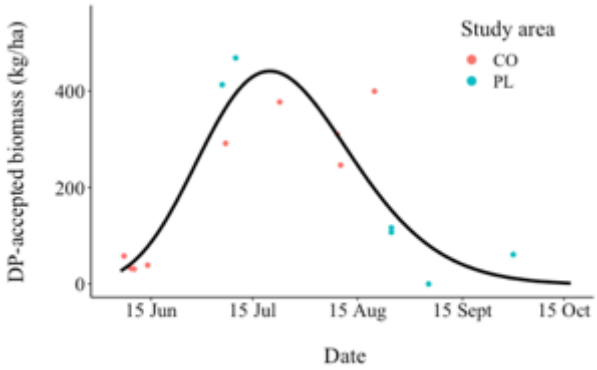

Appendix 6.112. Relationships between DP constraint accepted biomass (kg/ha) in Lwl-Fen and sampling date. Dashed line indicates the covariate was not included in the top model for that study area.

Appendix 6.113. Top predictive equations of DP constraint accepted biomass (including only the DP constraint) for each seral-specific (early: <20 years, mid-late: ≥20 years) ecosite and study area (SA) as a function of sampling date (i.e., Julian day; JD), basal area (m^2/ha; BA), precent silt, and normalized difference moisture index (NDMI), and the number of macroplots used to develop each model.

SA	Ecosite	Seral	n	Equation	r^2
PL	Upl-BS-Rocky	Early	3	4.43	---
		Mid-late	20	29.46	---
	Upl-BS	Early	50	0.71*exp(443.20 - 12268.99/JD - 71.10*log(JD)) + 32.00*Silt – 923.90	0.40
		Mid-late	136	0.63*(exp(442.18 - 13128.31/JD - 70.19*log(JD))) + 0.53*(128.87*BA^(-0.02*BA)) - 18.81	0.21
	Upl- BS-WS	Early	13	1.40*(exp(443.20 -12268.99/JD - 71.10*log(JD))) + 94.21	0.51
		Mid-late	34	2.14*(exp(442.18 - 13128.31/JD - 70.19*log(JD))) + 0.86*(382.29*BA^(-0.02*BA)) - 100.67	0.51
	Lwl-Bog	Early	20	*-1.94*JD + 526.69	0.24
		Mid-late	52	*-1.36*JD + 1.29*(106.53 - 1.99*BA) + 281.16	0.28
	Lwl-Marsh	Mid-late	1	870.13	---
CO	Upl-BS	Early	17	56.06	---
		Mid-late	22	41.65	---
	Upl-BS-WS	Early	10	1.44*(exp(827.45 - 27966.38/JD + -128.71*log(JD))) + 100.08	0.50
		Mid-late	28	0.89*(exp(318.39 - 10460.32/JD - 49.33*log(JD))) + 8.63	0.21
	Lwl-Bog	Early	7	102.26	---
		Mid-late	34	0.95*(exp(504.09 -16481.36/JD - 78.74*log(JD))) + 3.67	0.30
PL & CO	Lwl-Fen	Mid-late	16	1.01*exp(524.38 - 16532.94/JD - 82.22*log(JD)) - 1.59	0.80
	Lwl-Cedar/ thicket	Mid-late	5	175.61	---

Appendix 7. Supplemental materials for Chapter 4

This appendix outlines the steps taken to cross-walk the seral-specific ecosites (Table 4.1) to the Ontario Far North Land cover layer and North America Land Change Monitoring System (NALCMS) land cover layer.

The Ontario Far North (FN) Land Cover layer is unable to distinguishing between unproductive (Upl-BS) vs. productive (Up-BS-WS) upland conifer stands; instead, the FN has 3 upland conifer classes (conifer, mixed, and deciduous) that could correspond with these 2 ecosites. Our initial approach was to crosswalk FN mixed/ deciduous macroplots to Upl-BS-WS and FN conifer macroplots to Upl-BS. However, this approach would be insufficient, because we classified 55% of the Upl-BS-WS macroplots as conifer via the FN's classification system (i.e., not based the spatial land cover layer; Appendix 7.1).

Appendix 7.1. Comparison of macroplots ecosite classification in the field vs. Far North land cover classes.

	Far North Field Classification								Accuracy		
Ecosite	Bog	Conifer	Early-seral	Fen	Marsh	Mixed/ dec.	Sparse	Thicket	*n*	Total	%
Early seral			121						121	121	100
Lwl-Bog	87								87	87	100
Lwl-Cedar/ thicket								5	5	5	100
Lwl-Fen				16					16	16	100
Lwl-Marsh					3				3	3	100
Upl-BS		138				20			138	158	87
Upl-BS-Rocky							20		20	20	100
Upl-BS-WS		34				28			28	62	45
Total	87	172	121	16	3	48	20	5	472	472	100

When comparing between macroplots we classified as Upl-BS and Upl-BS-WS, and conifer via the FN, we saw a significant difference between values of NDVI calculated for the spatial extent of each macroplot (t-test, $P < 0.001$; Appendix 7.2). Therefore, we used a NDVI threshold of 0.858 to partition pixels classified as FN Conifer as either Upl-BS (NDVI < 0.858) or Upl-BS-WS (NDVI $\geq$ 0.858). Selected thresholds provided the lowest overall classification error and prioritized the identification of Upl-BS-WS. We also observed a significant difference (t-test, $p = 0.002$) between values of NDVI at Upl-BS vs. Upl-BS-WS macroplots, which we classified as FN mixed/ dec. Therefore, to partition FN conifer pixels as FN Conifer as either Upl-BS or Upl-BS-WS we used a NDVI threshold of 0.865 (Upl-BS: NDVI < 0.865; Upl-BS-WS: NDVI $\geq$ 0.865). Using these NDVI thresholds to classify Upl-BS or Upl-BS-WS for FN conifer and mixed/ dec, increased our capacity to differentiate between these ecosites (Appendix 7.3).

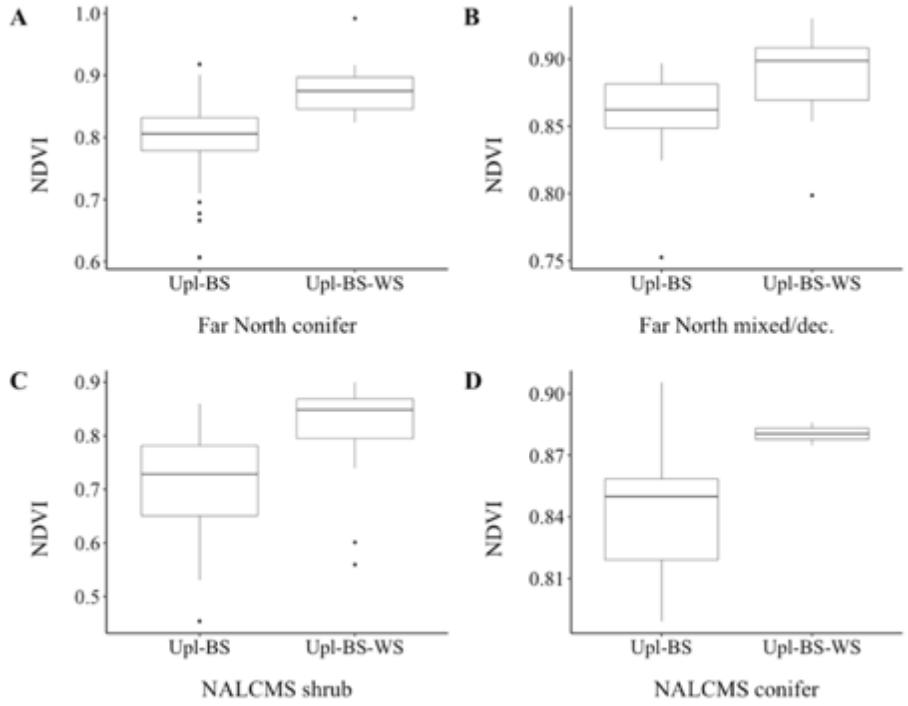

Appendix 7.2. NDVI at macroplots classified in the field as Far North A) upland conifer, B) mixed/ deciduous (dec.), and early seral via the Far North and C) shrubland (shrub) or upland conifer (conifer) using the NALCMS classification, but were classified in the field as either ecosite Upl-BS or Upl-BS-WS.

Appendix 7.3. Comparison of macroplots we classified in the field as ecosites vs. Far North Land Cover classes, after partitioning FN conifer (NDVI: 0.858) and mixed/dec (NDVI: 0.865) into Upl-BS and Upl-BW-WS using NDVI thresholds. FN conifer macroplots with NDVI $\geq$ 0.858 was changed to FN mixed/Dec., whereas FN mixed/dec. macroplots with NDVI < 0.865 was changed to FN conifer.

	Far North Field Classification								Accuracy		
Ecosite	Bog	Conifer	Early seral	Fen	Marsh	Mixed/ Dec	Sparse	Thicket	n	Total	%
Early_seral			121						121	121	100
Lwl-Bog	87								87	87	100
Lwl-Cedar/ thicket								5	5	5	100
Lwl-Fen				16					16	16	100
Lwl-Marsh					3				3	3	100
Upl-BS		139				19			139	158	88
Upl-BS-Rocky							20		20	20	100
Upl-BS-WS		15				47			47	62	76
Total	87	154	121	16	3	66	20	5	472	472	100

Similar to the FN layer, the NALCMS layer does not distinguish between Upl-BS and Upl-BW-WS, but again we used NDVI to partition the NALCMS land cover classes of shrubland and upland conifer into these 2 ecosites. We classified a majority of the Upl-BS and Upl-BS-WS early seral macroplots as shrubland, and observed a significant difference between values of NDVI at Upl-BS vs. Upl-BS-WS macroplots (t-test, $P < 0.001$; Appendix 7.2). Therefore, pixels classified as both early seral via the FN land cover and shrubland using the NALCMS layer, we used a NDVI threshold of 0.826 to classified it as either early seral Upl-BS (NDVI < 0.826) or early seral Upl-BS-WS (NDVI $\geq$ 0.826). Using a NDVI threshold of 0.870, we partitioned pixels classified as both early seral via the FN and upland conifer via NALCMS as either early seral Upl-BS (NDVI < 0.870) or early seral Upl-BS-WS (NDVI $\geq$ 0.870; Appendix 7.5). We only classified 3 macroplots as early seral and mixed/ dec via the NALCMS classification system, 2 of which were Upl-BS-WS and 1 was Upl-BS; therefore, pixels identified as early seral via the FN layer and mixed/dec. via the NALCMS layer were classified as Upl-BS-WS. Using these NDVI thresholds to classify early seral Upl-BS or early seral Upl-BS-WS based on FN early seral and NALCMS shrubland and upland conifer, enabled us to differentiate between these ecosites.

Therefore, we used the Far North Land Cover, the NALCMS to identify land cover of FN early seral, and NDVI thresholds to classify Upl-BS vs. Upl-BS-WS, which allowed us to produce a spatial layer of ecosites based on the crosswalk below (Appendix 7.6).

Appendix 7.4. Comparison of early seral (<20 years) macroplots we classified in the field as ecosite vs. NALCMS land cover classes.

	NALCMS Field Classification				
Ecosite	Lichen	Mixed/ dec.	Conifer	Shrub	Low. conifer/ wetland
Lwl-Bog					27
Upl-BS		1	18	48	
Upl-BS-Rocky	3				
Upl-BS-WS		2	2	20	
Total	3	3	20	68	27

Appendix 7.5. Comparison of early seral (<20 years) macroplots we classified in the field as ecosite vs. NALCMS land cover classes, after partitioning NALCMS shrubland (NDVI: 0.826) and conifer (NDVI: 0.870) into Upl-BS and Upl-BW-WS using NDVI thresholds. NALCMS shrubland macroplots with NDVI ≥ 0.826 were changed to mixed/ dec. (corresponding to Upl-BS-WS) and < 0.826 was changed to conifer (corresponding to Upl-BS), whereas NALCMS shrubland macroplots with NDVI ≥ 0.870 were changed to mixed/ deciduous and <0.870 was changed to conifer.

	NALCMS Field Classification				Accuracy		
Ecosite	Conifer	Lichen	Mixed/ dec.	Low. conifer/ wetland	*n*	Total	%
Lwl-Bog				27	27	27	100
Upl-BS	60		7		60	67	90
Upl-BS-Rocky		3			3	3	100
Upl-BS-WS	6		18		18	24	75
Total	66	3	25	27	121	121	100

Appendix 7.6. Crosswalk from ecosite to Far North Land Cover classification with the incorporation of the NALCMS land cover layer to identify the land cover of the Far North early seral class (early: <20 years; late: ≥20 years) and NDVI thresholds to differentiate between Upl-BS and Upl-BS-WS.

Field classification		Crosswalk	Spatial Layers		
Ecosite	Seral stage		Far North		NALCMS
Upl-BS-Rocky	Early	↔	Early seral	&	Lichen-grass-moss
	Mid-late	↔	Sparse		
Upl-BS (Sandy & Mesic)	Early	↔	Early seral	&	Upland conifer & NDVI < 0.870, or shrubland & NDVI < 0.826
	Mid-late	↔	Conifer & NDVI < 0.858 Mixed/ dec. & NDVI < 0.865		
Upl-BS-WS	Early	↔	Early seral	&	Mixed/ dec., or upland conifer & NDVI ≥ 0.870, or shrubland & NDVI ≥ 0.826
	Mid-late	↔	Conifer & NDVI ≥ 0.858 Mixed/ dec. & NDVI ≥ 0.865		
Lwl-Bog	Early	↔	Early seral	&	Wetland/ lowland conifer
	Mid-late	↔	Bog/ conifer swamp		
Lwl-Fen	NA	↔	Fen		
Lwl-Marsh	NA	↔	Fresh marsh		
Lwl-Cedar/ Thicket	NA	↔	Thicket/ dec. swamp		

*There are 4 NALCMS land cover classes not accounted for in this crosswalk: shrubland-lichen-moss, grassland-lichen-moss, barren-lichen-moss, and barren. Based on the NALCMS land cover layer 27 of 472 (6%) of our macroplots were classified as grassland-lichen-moss and 22 of 472 (5%) were classified as barren. The 27 grassland-lichen-moss and 22 barren macroplots have a mean age of 9.5 (± 6.1; SD), and 7.9 (± 5.6; SD), respectively, which generally coincided with our classification of "shrubland." Therefore, to partition these landcover types into Early Upl-BS vs. Early Upl-BS-WS we applied the same NVDI threshold applied to NALCMS shrubland.

Appendix 8. Supplemental materials for Chapter 4

Appendix 8.1. Size (km^2) of summer home range size for 29 female caribou in Pickle Lake and 25 individuals in Cochrane based on GPS telemetry from 1 June to 30 September, which was used to calculate 95% utilization distribution, where we specified the smoothing parameter as the reference bandwidth (Walker et al. 2021).

Study area	Caribou ID	Year	Fix rate	*n* of fixes	Size
Pickle Lake	CPL102	2010	2.5 hrs	1081	253.35
Pickle Lake	CPL103	2011	2.5 hrs	1099	80.12
Pickle Lake	CPL104	2012	2.5 hrs	979	27.66
Pickle Lake	CPL104	2013	2.5 hrs	782	136.63
Pickle Lake	CPL105	2010	2.5 hrs	1042	410.87
Pickle Lake	CPL107	2010	2.5 hrs	1106	381.05
Pickle Lake	CPL108	2010	2.5 hrs	1094	30.24
Pickle Lake	CPL109	2010	2.5 hrs	1041	612.57
Pickle Lake	CPL110	2010	2.5 hrs	1106	41.12
Pickle Lake	CPL112	2011	2.5 hrs	1105	35.28
Pickle Lake	CPL113	2011	2.5 hrs	1070	43.35
Pickle Lake	CPL114	2011	2.5 hrs	1084	8512.44
Pickle Lake	CPL115	2010	2.5 hrs	852	600.10
Pickle Lake	CPL116	2012	2.5 hrs	1119	44.09
Pickle Lake	CPL117	2011	2.5 hrs	943	98.84
Pickle Lake	CPL118	2012	2.5 hrs	1077	31.88
Pickle Lake	CPL134	2011	2.5 hrs	1038	101.91
Pickle Lake	CPL136	2010	2.5 hrs	1089	24.46
Pickle Lake	CPL138	2010	2.5 hrs	981	1982.19
Pickle Lake	CPL141	2010	2.5 hrs	1130	339.68
Pickle Lake	CPL201	2012	2.5 hrs	1156	91.06
Pickle Lake	CPL202	2012	2.5 hrs	1162	107.03
Pickle Lake	CPL204	2011	2.5 hrs	932	2298.44
Pickle Lake	CPL205	2011	2.5 hrs	1066	336.23
Pickle Lake	CPL208	2011	2.5 hrs	1039	207.97
Pickle Lake	CPL319	2012	2.5 hrs	1064	96.74
Pickle Lake	CPL320	2012	2.5 hrs	1108	184.35
Pickle Lake	CPL97168	2012	2.5 hrs	1058	895.77
Pickle Lake	CPL97173	2012	2.5 hrs	960	540.80
Cochrane	CCO180	2010	2.5 hrs	1015	74.65
Cochrane	CCO209	2012	2.5 hrs	1151	99.38
Cochrane	CCO210	2011	2.5 hrs	1170	2656.43
Cochrane	CCO211	2011	2.5 hrs	1123	291.86
Cochrane	CCO213	2011	2.5 hrs	1089	132.11

Appendix 8.1. Continued.

Study area	Caribou ID	Year	Fix rate	*n* of fixes	Size
Cochrane	CCO214	2013	2.5 hrs	928	151.53
Cochrane	CCO218	2011	2.5 hrs	1165	83.90
Cochrane	CCO223	2011	2.5 hrs	1122	37.25
Cochrane	CCO225	2012	2.5 hrs	1165	58.09
Cochrane	CCO226	2012	2.5 hrs	1146	134.92
Cochrane	CCO228	2011	2.5 hrs	1167	959.49
Cochrane	CCO230	2012	2.5 hrs	1115	180.06
Cochrane	CCO231	2011	2.5 hrs	1160	96.81
Cochrane	CCO232	2011	2.5 hrs	1135	124.56
Cochrane	CCO233	2013	2.5 hrs	1141	155.80
Cochrane	CCO234	2011	2.5 hrs	1145	147.36
Cochrane	CCO235	2012	2.5 hrs	1148	157.06
Cochrane	CCO237	2012	2.5 hrs	1079	99.73
Cochrane	CCO239	2011	2.5 hrs	1152	177.22
Cochrane	CCO240	2012	2.5 hrs	1130	72.39
Cochrane	CCO302	2012	2.5 hrs	1155	112.27
Cochrane	CCO303	2012	2.5 hrs	1134	831.76
Cochrane	CCO304	2012	2.5 hrs	1130	236.37
Cochrane	CCO305	2012	2.5 hrs	1130	354.76
Cochrane	CCO306	2012	2.5 hrs	1152	2161.94

Appendix 9. Supplemental materials for Chapter 4

Appendix 9.1. Results from post-hoc Tukey HSD test comparing digestible energy (kcal/g) or digestible protein (%) between forbs, deciduous shrubs (dec), grass, graminoids (gram), ferns, horsetails (horse), lichens, and mushrooms (mush) based on 931 forage quality samples collected in Pickle Lake and Cochrane, Ontario, Canada during 2018.

Metric	Life-form	Difference	Lower	Upper	*P*-value
DE	Forb-Dec	-0.05	-0.12	0.02	0.36
	Grass-Dec	-0.41	-0.65	-0.16	<0.001
	Grass-Forb	-0.36	-0.60	-0.11	< 0.001
	Grass-Mush	-0.82	-1.24	-0.40	<0.001
	Horse-Dec	-0.36	-0.53	-0.19	<0.001
	Horse-Forb	-0.31	-0.48	-0.14	<0.001
	Horse-Grass	0.05	-0.24	0.34	1.00
	Horse-Mush	-0.77	-1.16	-0.39	<0.001
	Lichen-Dec	0.08	-0.01	0.17	0.17
	Lichen-Forb	0.13	0.03	0.22	0.002
	Lichen-Grass	0.48	0.23	0.74	<0.001
	Lichen-Horse	0.44	0.25	0.62	<0.001
	Lichen-Mush	-0.34	-0.69	0.02	0.08
	Mush-Dec	0.41	0.06	0.76	0.01
	Mush-Forb	0.46	0.11	0.82	0.002
DP	Forb-Dec	1.59	0.58	2.59	<0.001
	Grass-Dec	1.17	-2.32	4.66	0.97
	Grass-Forb	-0.42	-3.94	3.11	1.00
	Grass-Mush	-6.97	-13.06	-0.88	0.01
	Horse-Dec	0.86	-1.58	3.29	0.96
	Horse-Forb	-0.73	-3.21	1.75	0.99
	Horse-Grass	-0.31	-4.48	3.85	1.00
	Horse-Mush	-7.28	-12.83	-1.73	0.002
	Lichen-Dec	-8.38	-9.67	-7.09	<0.001
	Lichen-Forb	-9.97	-11.34	-8.60	<0.001
	Lichen-Grass	-9.56	-13.17	-5.94	<0.001
	Lichen-Horse	-9.24	-11.85	-6.63	<0.001
	Lichen-Mush	-16.52	-21.68	-11.37	<0.001
	Mush-Dec	8.14	3.07	13.21	<0.001
	Mush-Forb	6.55	1.46	11.64	0.002

Appendix 10. Supplemental materials for Chapter 4

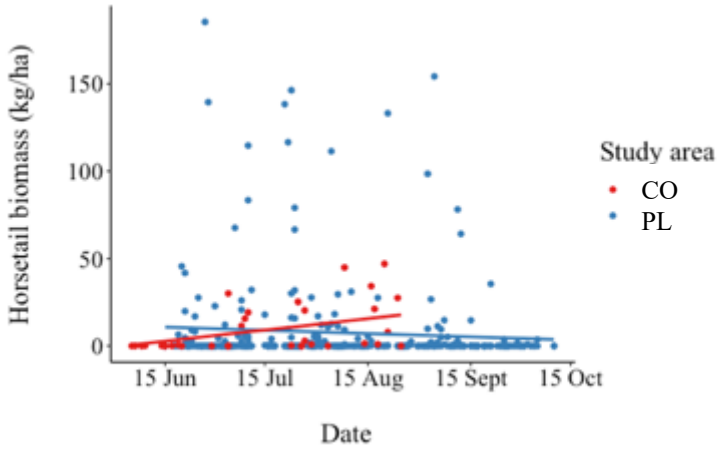

Appendix 10.1. Horsetail biomass (kg/ha) across sampling date at Mid-late Lwl-Bog macroplots in Cochrane compared to all macroplots in Pickle Lake sampled between 2017-2018.

Appendix 10.2. Modeling spatial metrics of intake rate (g/min) as a function of home-range scaled mean grass/forbs/deciduous shrubs (GFS), mushroom (mush) and horsetail (horse) biomass (kg/ka) calculated across the Pickle Lake (PL) and Cochrane (CO) extent between 15 June and 15 Sept using univariate linear regression. Models of lichen and horsetails were unable to be evaluated in Pickle Lake, because of zero variation in each metric across time, whereas models of lichen and mushrooms were unable to be evaluated in Cochrane.

SA	Model	GFS	Mush	Horse	K	AIC_c	ΔAIC_c	w_i
	GFS	0.004			2	-319.52	0.00	1.00
	Mush		0.26		2	-284.41	35.11	0.00
PL	Null				1	-210.95	108.57	0.00
	GFS	0.01			2	-329.82	0.00	1.00
	Horse			0.1	2	49.53	379.35	0.00
CO	Null				1	127.71	457.54	0.00

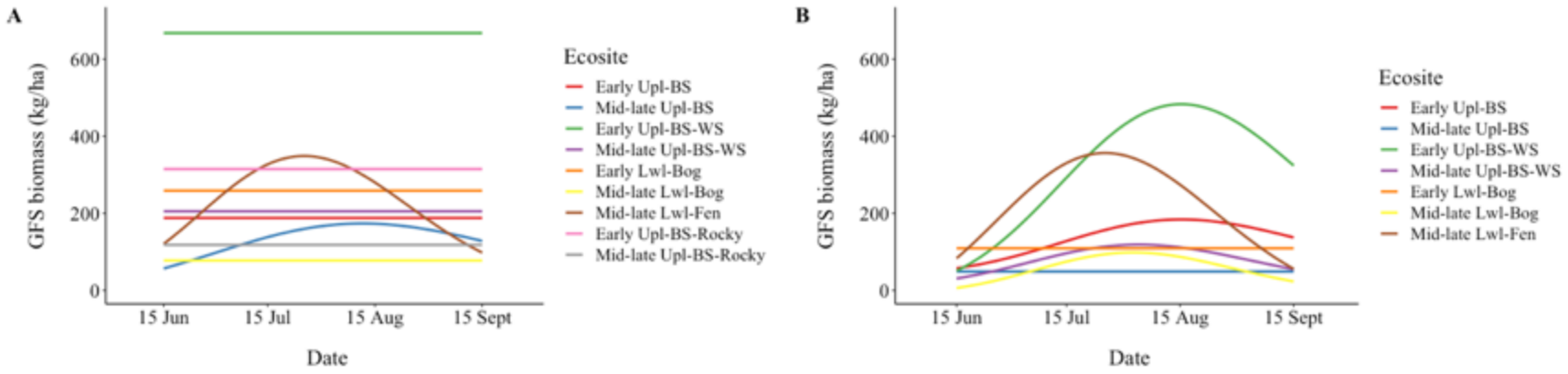

Appendix 10.3. Mean grass, forbs, and deciduous shrubs (GFS) biomass (kg/ha) by seral-specific ecosite calculated across the spatial extent of A) Pickle Lake and B) Cochrane from 15 June to 15 September, 2010.

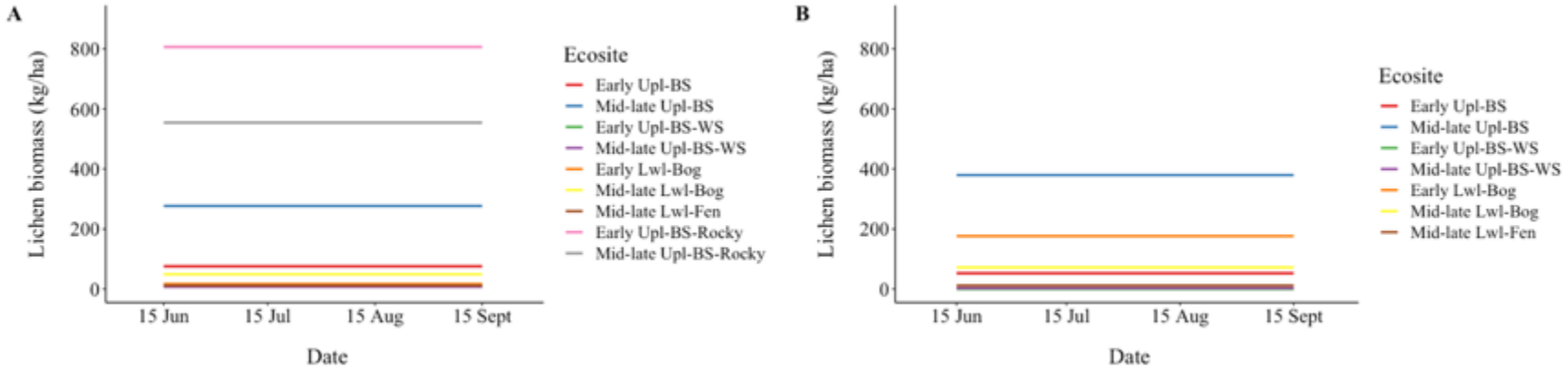

Appendix 10.4. Mean lichen biomass (kg/ha) by seral-specific ecosite calculated across the spatial extent of A) Pickle Lake and B) Cochrane from 15 June to 15 September, 2010.

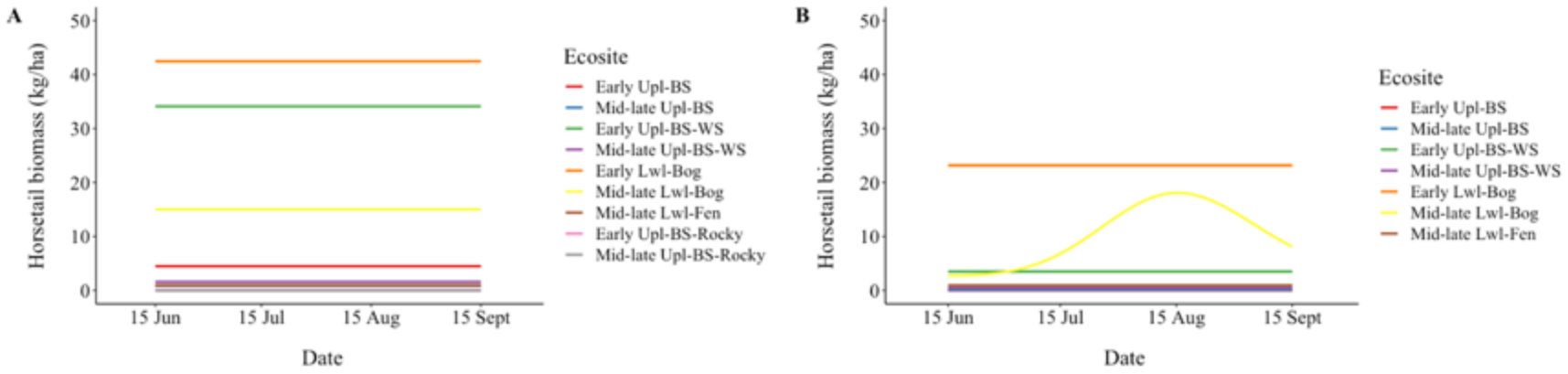

Appendix 10.5. Mean horsetail biomass (kg/ha) by seral-specific ecosite calculated across the spatial extent of A) Pickle Lake and B) Cochrane from 15 June to 15 September, 2010.

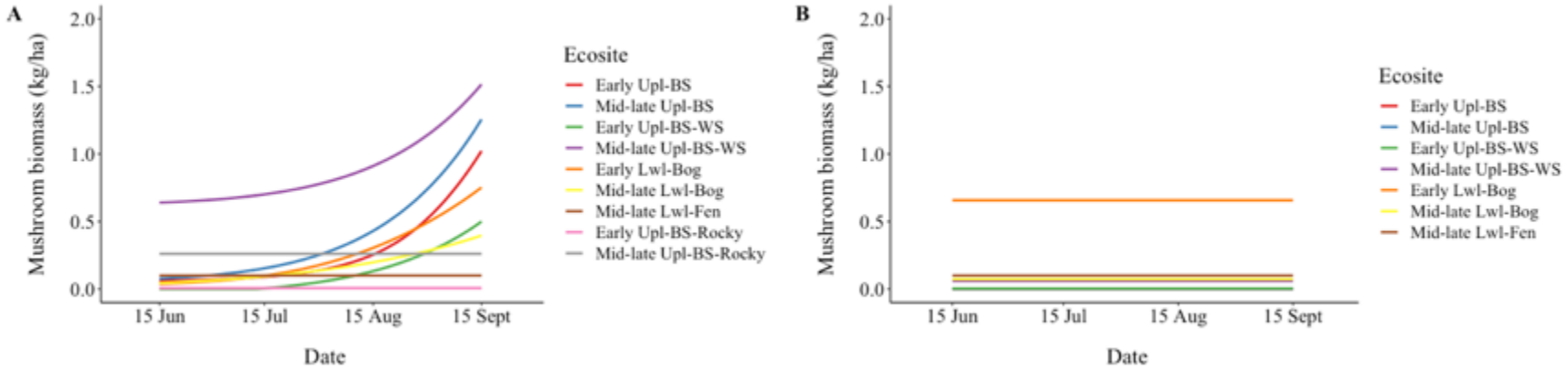

Appendix 10.6. Mean mushroom biomass (kg/ha) by seral-specific ecosite calculated across the spatial extent of A) Pickle Lake and B) Cochrane from 15 June to 15 September, 2010.

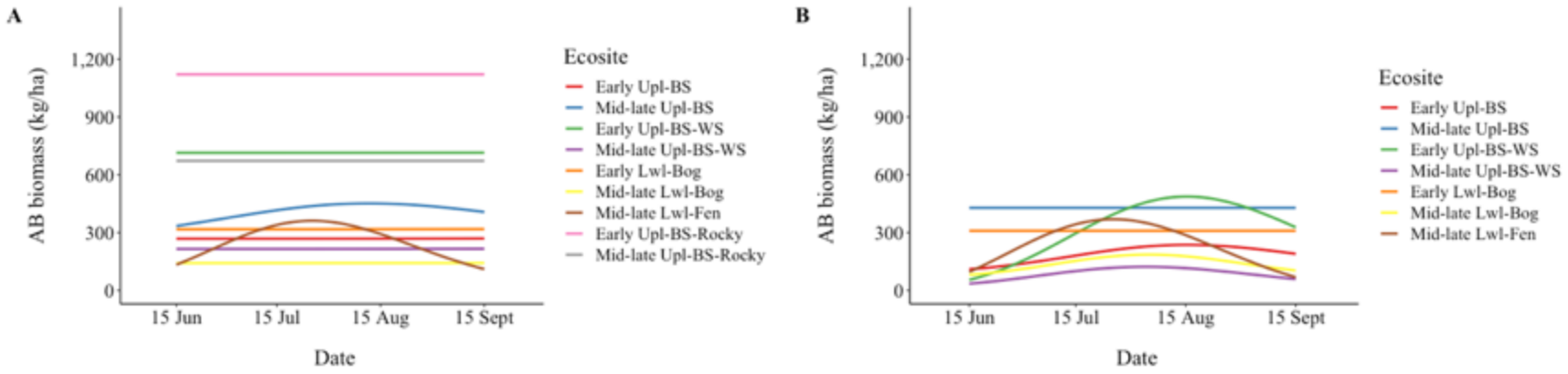

Appendix 10.7. Mean accepted biomass (AB; kg/ha) by seral-specific ecosite calculated across the spatial extent of A) Pickle Lake and B) Cochrane from 15 June to 15 September, 2010.

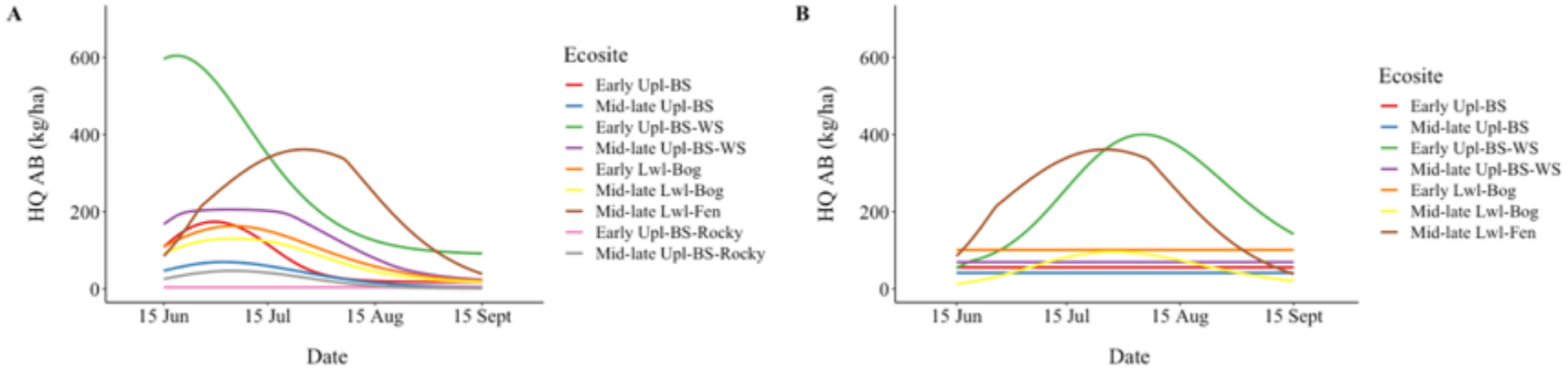

Appendix 10.8. Mean high-quality (HQ) accepted biomass (AB; kg/ha) constrained by both digestible energy and protein by seral-specific ecosite calculated across the spatial extent of A) Pickle Lake and B) Cochrane from 15 June to 15 September, 2010.

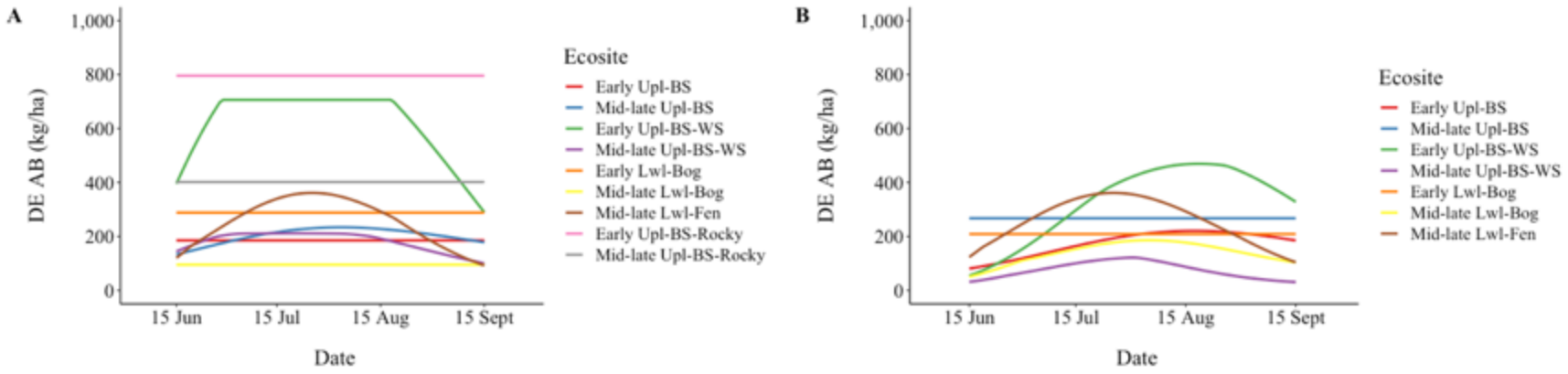

Appendix 10.9. Mean digestible energy (DE) accepted biomass (AB; kg/ha) constrained by only DE by seral-specific ecosite calculated across the spatial extent of A) Pickle Lake and B) Cochrane from 15 June to 15 September, 2010.

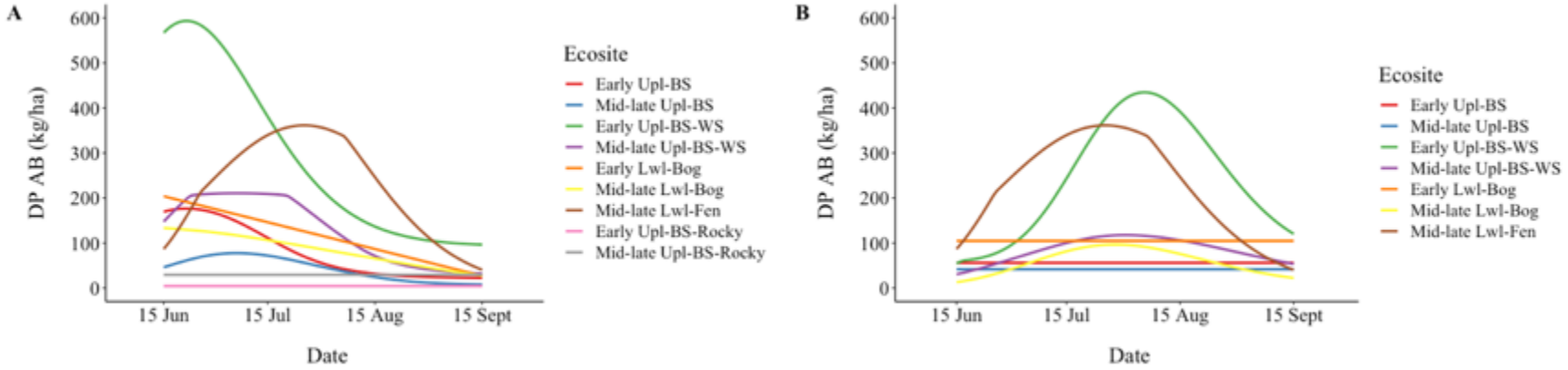

Appendix 10.10. Mean digestible energy (DP) accepted biomass (AB; kg/ha) constrained by only DP by seral-specific ecosite calculated across the spatial extent of A) Pickle Lake and B) Cochrane from 15 June to 15 September, 2010.

Appendix 11. Supplemental materials for Chapter 4

Appendix 11.1. Growing degree days across 30 years in Pickle Lake (Lake St. Joseph region) and Cochrane (Cochrane regions), Ontario accessed and downloaded from https://climateatlas.ca/map/canada, December 8, 2022.

Year	Pickle Lake	Cochrane
1981	1373.60	1290.60
1982	1234.30	1289.30
1983	1505.60	1404.70
1984	1464.90	1354.80
1985	1156.00	1245.70
1986	1291.90	1229.00
1987	1484.80	1424.70
1988	1588.60	1318.90
1989	1497.30	1359.80
1990	1341.20	1245.80
1991	1589.40	1443.90
1992	1079.70	1095.50
1993	1185.70	1234.30
1994	1395.00	1266.10
1995	1458.40	1449.50
1996	1428.50	1397.60
1997	1409.00	1297.60
1998	1584.60	1450.80
1999	1503.20	1543.70
2000	1333.70	1272.80
2001	1576.00	1571.00
2002	1451.90	1424.10
2003	1646.80	1451.70
2004	1159.50	1269.30
2005	1604.20	1713.50
2006	1594.00	1467.00
2007	1469.80	1545.80
2008	1312.40	1348.60
2009	1269.50	1285.00
2010	1596.10	1571.90

Appendix 11.2. Mean and standard deviation in growing degree days across 30 years in Pickle Lake and Cochrane, Ontario based on the values in Appendix 11.1.

Value	Pickle Lake	Cochrane
Mean	1419.52	1375.43
SD	154.99	131.99

Appendix 12. Supplemental materials for Chapter 5

When predicting summer predation risk across the Quebec extent of the Cochrane study region it was necessary to substitute 5 equivalent spatial covariates that were used to predict summer predation risk across Ontario (Avgar et al. 2015, Kittle et al. 2015, Fryxell et al. 2020): relative elevation, distance to primary roads, distance to secondary roads, distance to dump, and recent (<1 year) disturbance. Relative elevation was calculated for the Quebec extent of the Cochrane study region using the Canadian Digital Elevation Model (DEM; assessed from https://open.canada.ca/data/en/dataset/7f245e4d-76c2-4caa-951a-45d1d2051333). We used the provincial AQnetwork road layer from Adresses Quebec for the Quebec extent of Cochrane (accessed from https://www.donneesquebec.ca/recherche/fr/dataset/adresses-quebec) and cross-walked the AQnetwork road classification into primary and secondary road classes (Appendix 12.1). We did not identify any waste management sites within the Quebec extent of the Cochrane study region and therefore distance to waste management site was set to zero for the Quebec extent. We derived recent (<1 year) disturbance (forest fire or harvest) for the Quebec extent of Cochrane using year of harvest and fire disturbance maps developed by Hermosilla et al. (2018) for the forested extent of Canada.

Appendix 12.1. Crosswalk used to classify the AQnetwork road layer to road classes used to predict summer predation risk in Quebec based on Kittle et al.'s (2015) road classification.

AQnetwork road classification	Kittle et al.'s road classification
Locale Collectrice Municipal Collectrice de Transit Nationale Régionale	Primary
Accès aux Ressources Accès aux ressources et aux localités isolées	Secondary

Appendix 13. Supplemental materials for Chapter 5

To extrapolate forage metrics for the calving period (1 May to 14 June) we will use permanent phenological (PP) macroplots. This appendix outlines the methods used to estimate biomass from species-specific cover estimates at PP macroplots repeatedly sampled in Pickle Lake and Cochrane. Although we did not use biomass-cover relationships developed for clubmoss, fern, and evergreen shrub in Chapter 5, we still present those results below.

Methods

We sampled 39 PP macroplots over 2 years (2017 = 13; 2018=26); 26 in northwestern Ontario (i.e., Pickle Lake; 2017 =13; 2018 = 13) and 13 in northeastern Ontario (i.e., Cochrane; 2018 = 13). PP macroplots were stratified based on 5 major vegetative classes with conifer stands (excluding fen and black spruce bog) also stratified into early and mid-late seral stage (Appendix 13.1). PP macroplots were repeatedly sampled 3 times in 2017 and 4 times in 2018 to interpolate the biomass growth between 15 May and 15 October (Appendix 13.2); however only data from phenological plots sampled between 15 May and 11 June were used to extrapolate forage metrics.

Appendix 13.1. Permanent phenology plots sampled in northern Ontario in 2017–2018, as satisfied by study region (northwestern [NW] Ontario and northeastern [NW] Ontario), vegetative class, and seral stage (early, late, and not specified). Tree codes are: BS = black spruce, WS = white spruce.

Vegetative class	NW Ontario			NE Ontario		
	Early	Late	Not specified	Early	Late	Not specified
Rich (BS/WS) upland	4	4	---	2	2	---
Sandy (BS) upland	4	4	---	2	2	---
Deciduous	---	---	4	---	---	2
BS Bog	---	---	4	---	---	2
Fen	---	---	2	---	---	1

Appendix 13.2. Sampling dates of permanent phenology plots in northern Ontario in 2017–2018 for each study region (northwestern Ontario: NWO and northeastern Ontario: NEO).

Study Region	Year	Sampling date 1	Sampling date 2	Sampling date 3	Sampling date 4
NWO	2017	N/a	5-11 Jun	14-16 Jul.	13-15 Oct.
NWO	2018	15-19 May	22-24 Jun.	12-14 Jul.	3-5 Oct.
NEO	2018	23-24 May	27-29 Jun.	18-22 Jul.	7-8 Oct.

Within the PP macroplots, we used a double sampling approach (Wilm *et al.*, 1944) to estimate forage biomass by plant species. We recorded percent cover of new plant growth by plant species from 1 cm to 2 m in height in 3, 1-m^2 plots placed equidistantly along 3, 45-m long transects, resulting in 9 cover plots per macroplot. Also, percent cover of new growth by life-form group (forbs, graminoids [*Poaceae*, *Cyperaceae, Juncaeceae* and *Equisetum* spp.], clubmoss, ferns, deciduous shrubs, and evergreen shrubs [separated into 4 dominate species: *Chamaedaphne calyculata*, *Kalmia angustifolia, Ledum groenlandicum*, and *Linnaea borealis*]) was estimated in 3 randomly located (stratified by high, medium, and low available biomass) 1-m^2 plots within each PP macroplot that were then clipped and sorted by life-form group. Clipped plants were

oven dried at ≥ 70 °C to constant weight and weighed to the nearest 0.1 g. Terrestrial and arboreal lichen cover was not estimated because we assumed within-season changes were too small (~3-5mm per year, Scotter, 1963; Pegua, 1968) to quantify accurately.

We developed cover-biomass (dry weight) relationships for each plant life-form group and the 4 dominant evergreen shrubs using a generalized linear models (GLM) with a gamma distribution (hereafter gamma GLM). For each cover-biomass relationship, we first compared the model fit of linear (identity-link) vs. non-linear (log link) relationships using data across all PP macroplot using Akaike Information Criterion corrected for small samples sizes (ΔAIC_c). Once we determined the best model form ($\Delta AIC_c > 2$), we first assessed differences in the biomass-cover relationships between the 2 study regions and then evaluated if forest characteristics (seral stage, drainage class, vegetation class [Appendix 13.1], and potential natural vegetation type [PNV type; rich upland and deciduous sites were combined]) improved the model fit. We fit models of biomass as a function of cover and cover interacted with study region/ forest characteristics and assessed model improvement by a $\Delta AIC_c > 2$. We did not include the main effect for study region or each forest characteristic in the models, since we were interested in how each covariate influences the relationship between biomass and cover (Monzingo et al. 2022). If study region or a forest covariate improved ($\Delta AIC_c > 2$) the relationship between cover and biomass, a separate biomass-cover predictive equation was developed for each category within that covariate (e.g., 1 equation for lowlands and 1 equation for uplands). When multiple top models were identified ($\Delta AIC_c < 2$) we selected the model with the lowest AIC value as the top model (unless otherwise stated). Given the reduced sampling of ferns, graminoids, deciduous shrubs, *Chamaedaphne calyculata*, *Kalmia angustifolia,* and *Ledum groenlandicum* during the first sampling period we only evaluated a linear vs. non-linear relationship and did not test for differences between study region and forest characteristics. We used the final biomass-cover relationships (Appendix 13.3, 14.4) to estimate biomass of life-forms and the dominant evergreen shrubs in the PP macroplots using cover data from each sampling date.

Results

Biomass-cover relationships

We sampled 628 1-m^2, cover-biomass plots across the 39 PP macroplots in northwestern (NWO) and northeastern Ontario (NEO). Biomass was best described by a linear relationship to cover in all cases with only 2 model not showing a significant ($\Delta AIC_c < 2$) relationship (Appendix 13.5). The non-linear (log-link) model for *Linnaea borealis* and old ferns had ΔAIC_c of 0.54 and 1.54 from the linear (identify-link model) model, respectively. Since the linear models outperformed the non-linear across all life-form groups and was the top model for *Linnaea borealis* and old ferns (although not significantly), we evaluated the cover-biomass relationship assuming a linear relationship for all life-form groups and dominant evergreen shrubs.

Study region did not improve the biomass-cover relationship for *Chamaedaphne calyculata* and therefore we proceed to assess models with data pooled across study regions (Appendix 13.6). Inclusion of study region improved the fit of biomass-cover models ($\Delta AIC_c > 2$) for forbs, graminoids, deciduous shrubs, and clubmosses (Appendix 13.6), therefore models were further assessed by study region. Although including study region improved model fit for *Ledum*

groenlandicum (Appendix 13.6, we did not distinguish between study regions for simplicity. Study region also significantly improved model fit for ferns and *Linnaea borealis,* but given the low sample size within regions (NWO: n = 21 and 25, respectively; NEO: n = 27 and 15, respectively) we did not model ferns or *Linnaea borealis* by study region (Appendix 13.6). *Kalmia angustifolia* was only sampled within NEO and therefore the influence of study region on the biomass-cover relationship was not evaluated.

In evaluating forest characteristics, the top model to predict forb biomass-cover relationship in both NWO and NEO included cover and early-rich vegetative class (vs. not early-rich vegetative class) interacted with cover (Appendix 13.7–14.8). As a result, we distinguished between study regions and seral stages which produced 4 predictive equations for forbs (Appendix 13.3). Both top models to predict graminoid biomass-cover relationship in NWO and NEO included cover and seral stage interacted with cover (Appendix 13.9–14.10). In NWO, the top deciduous shrub model included cover and coverer interacted with late-rich conifer class (vs. not late-rich conifer; Appendix 13.11). In contrast, the top deciduous shrub model in NEO included cover and cover interacted with seral stage (Appendix 13.12). Even though they were not the top models, we selected the model with just cover to predict clubmoss biomass in both NWO (Appendix 13.13) and NEO (Appendix 13.14), because the top models had low sample sizes within the forest characteristic covariates (NWO early seral: n= 22; NEO bog: n=1; NEO late-sandy: n=6). Because we did not distinguish between regions in predicting *Ledum groenlandicum*, *Chamaedaphne calyculata*, and ferns the top models to predict across regions for each species only included cover (Appendix 13.15–17). Despite not being the top models, we also selected the model with just cover to predict *Linnaea borealis* (Appendix 13.18) biomass, given the low sample sizes within the forest characteristic covariates (early-rich: n= 6; early seral: n=9). We found 2 competing models for predicting *Kalmia angustifolia* biomass in NEO, but we selected the model with just cover because of a lower AIC value and parsimony (Appendix 13.919).

With cover-biomass equations developed by life-form group (Appendix 13.3–14.4), we then applied the corresponding life-form group equations to the species-specific cover estimates taken at each of the 9 cover-plots sampled within a single PP macroplot (during each sampling period; 3 times in 2017 and 4 times in 2018). Finally, we calculated the mean species-specific biomass across the 9 cover-plots for each macroplot and converted the biomass from g/m^2 to kg/ha.

Appendix 13.3. Number (*n*) of cover-biomass estimates used to develop cover-biomass equation for each life-form group (forbs, graminoids, deciduous shrubs, clubmoss, *Chamaedaphne calyculata* [CHCA], *Ledum groenlandicum* [LEGR], *Linnaea borealis* [LIBO], and *Kalmia angustifolia* [KAAN]) by study region (SR) and covariate (when applicable based on model selection above), and the gamma GLM intercept, coefficient estimate (est.), and pseudo r^2 value, which were used to predict biomass as a function of cover.

Life-form group	SR	Covariate	*n*	Intercept	Coefficient est.	pseudo r^2
Forbs	NWO	Early seral	73	-0.57	0.62	0.72
Forbs	NWO	Mid-late seral	163	-0.19	0.26	0.77
Forbs	NEO	Early seral	30	-0.47	0.51	0.74
Forbs	NEO	Mid-late seral	72	-0.12	0.16	0.75
Graminoids	NWO	Early-rich	32	-0.63	1.31	0.72
Graminoids	NWO	Not early-rich	78	-0.40	0.74	0.58
Graminoids	NEO	Early-rich	21	-0.85	1.02	0.74
Graminoids	NEO	Not early-rich	52	-0.18	0.30	0.59
Deciduous shrub	NWO	Mid-late-rich	29	-0.37	0.51	0.76
Deciduous shrub	NWO	Not-mid-late rich	165	-0.16	0.17	0.85
Deciduous shrub	NEO	Early seral	42	-0.41	0.47	0.84
Deciduous shrub	NEO	Mid-late seral	81	-0.23	0.24	0.77
Clubmoss	NWO	NA	96	-0.83	1.34	0.88
Clubmoss	NEO	NA	25	-0.90	1.08	0.92
Fern	NA	NA	48	-0.31	0.32	0.70
CHCA	NA	NA	48	-0.62	0.73	0.69
LEGR	NA	NA	77	-0.34	0.49	0.72
LIBO	NA	NA	40	-0.07	0.21	0.39
KAAN	NA	NA	36	-0.30	0.36	0.76

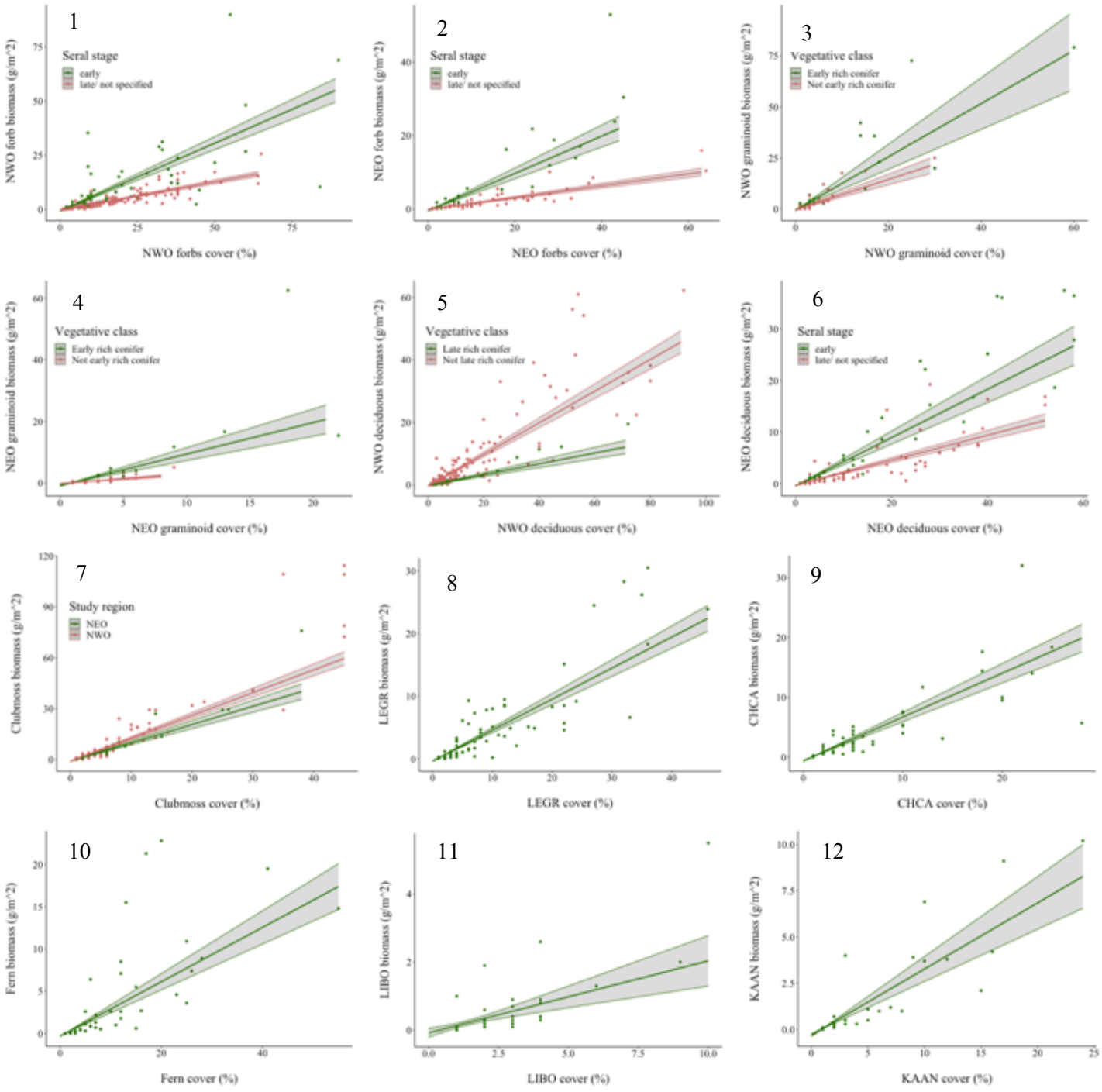

Appendix 13.4. Relationship at cover-biomass clip plots between: forb cover (%) and biomass (g/m^2), stratified by seral stage (early vs. late/ not-specified) in 1) northwestern Ontario (NWO) 2) and northeastern Ontario (NEO); graminoid cover and biomass stratified by early-rich conifer vs. not early-rich conifer in 3) NWO and 4) NEO; deciduous shrub cover and biomass stratified by 5) late-rich conifer vs. not late-rich conifer in NWO and 6) seral stage (early vs. late/ not-specified) in NEO; 7) clubmoss cover and biomass stratified by study region (NWO vs. NEO); 8) *Ledum groenlandicum* (LEGR), 9) *Chamaedaphne calyculata* (CHCA), 10) fern, 11) *Linnaea borealis* (LIBO), and 12) *Kalmia angustifolia* (KAAN; only sampled in NEO) cover and biomass in NWO and NEO.

Appendix 13.5. Model coefficient, number of model parameters (*K*), Akaike's Information Criterion corrected for small sample size (AIC_c), change in AIC_c from best model (ΔAIC_c), and model weights calculated from AIC_c (w_i) for competing generalized linear models with a gamma distribution and identify link function vs. log link function modeling forb biomass as a function of life-form groups (forbs, graminoids, deciduous [dec.] shrubs, ferns, clubmoss, *Chamaedaphne calyculata* [CHCA], *Ledum groenlandicum* [LEGR], *Kalmia angustifolia* [KAAN], and *Linnaea borealis* [LIBO]) cover estimates.

Life-form	Link function	Cover	*K*	AIC_c	ΔAIC_c	w_i
Forb	Identity	0.34	2	1171.64	0.00	1.00
	Log	0.08	2	1405.77	234.13	0.00
Graminoid	Identity	0.79	2	435.57	0.00	1.00
	Log	0.27	2	485.58	50.01	0.00
Dec. shrubs	Identity	0.40	2	1067.38	0.00	1.00
	Log	0.08	2	1274.90	207.52	0.00
Fern	Identity	0.32	2	128.69	0.00	1.00
	Log	0.15	2	166.07	37.37	0.00
Clubmoss	Identity	1.27	2	505.58	0.00	1.00
	Log	0.13	2	628.98	123.41	0.00
CHCA	Identity	0.73	2	176.13	0.00	1.00
	Log	0.14	2	205.37	29.24	0.00
LEGR	Identity	0.49	2	266.48	0.00	1.00
	Log	0.11	2	317.91	51.43	0.00
KAAN	Identity	0.36	2	25.23	0.00	1.00
	Log	0.25	2	54.53	29.30	0.00
LIBO	Identity	0.40	2	10.81	0.00	0.57
	Log	0.21	2	11.35	0.54	0.43

Supplemental Table 14.6. Model coefficients, number of model parameters (*K*), Akaike's Information Criterion corrected for small sample size (AIC_c), change in AIC_c from best model (ΔAIC_c), and model weights calculated from AIC_c (w_i) for competing gamma GLMs relating life-form groups (forbs, graminoids, deciduous [dec.] shrubs, ferns, clubmoss, *Chamaedaphne calyculata* [CHCA], *Ledum groenlandicum* [LEGR], *Kalmia angustifolia* [KAAN], and *Linnaea borealis* [LIBO]) biomass to cover and cover interacted with study region (Cover*SR; northwestern vs. northeastern Ontario; NEO set a the reference category).

Life-form	Model	Cover	Cover*SR	*K*	AIC_c	ΔAIC_c	w_i
Forb	Cover*SR	0.31	0.04	3	1165.76	0.00	0.95
	Cover	0.34		2	1171.64	5.87	0.05
Graminoid	Cover*SR	0.58	0.31	3	407.66	0.00	1.00
	Cover	0.79		2	435.57	27.91	0.00
Dec. shrubs	Cover*SR	0.34	0.09	3	1039.28	0.00	1.00
	Cover	0.40		2	1067.38	28.10	0.00
Fern	Cover	0.32		2	128.69	0.00	0.75
	Cover*SR	0.32	0.01	3	130.84	2.14	0.25
Clubmoss	Cover*SR	1.04	0.32	3	496.10	0.00	0.99
	Cover	1.27		2	505.58	9.48	0.01
CHCA	Cover	0.73		2	176.13	0.00	0.72
	Cover*SR	0.79	-0.05	3	177.98	1.85	0.28
LEGR	Cover*SR	0.38	0.14	3	263.95	0.00	0.78
	Cover	0.49		2	266.48	2.53	0.22
LIBO	Cover*SR	0.17	0.11	3	8.76	0.00	0.79
	Cover	0.21		2	11.35	2.60	0.21

Appendix 13.7. Model coefficients, number of model parameters (*K*), Akaike's Information Criterion corrected for small sample size (AIC_c), change in AIC_c from best model (ΔAIC_c), and model weights calculated from AIC_c (w_i) for competing gamma GLMs relating forb biomass to forb cover and cover interacted with forest characteristics (vegetative classes [early-rich, late-rich, early-sandy, late-sandy, deciduous (dec.), bog, and fen], PNV type [BS upland and BS/WS upland], drainage class [upland vs. lowland; upland set as the reference category], and seral stage [early vs. late/not specified; late/not specified set as the reference category]) in northwestern Ontario.

Model	Cover	Cover * Bog	Cover * Early-rich	Cover * Early-sandy	Cover * Late-sandy	Cover * Late-rich	Cover * Fen	Cover * Dec.	Cover * BS upland	Cover * BS/WS upland	Cover * Drainage	Cover * Seral	*K*	AIC_c	ΔAIC_c	w_i
Seral stage	0.27											0.24	3	842.18	0.00	1.00
Early-rich	0.31		0.28										3	855.51	13.33	0.00
Late-rich	0.38					-0.07							3	866.39	24.20	0.00
BS/WS upland	0.40									-0.04			3	877.96	35.78	0.00
Early-sandy	0.36			0.08									3	878.91	36.73	0.00
Bog	0.37	0.05											3	879.18	37.00	0.00
Deciduous	0.38							-0.04					3	879.36	37.17	0.00
Fen	0.37						-0.04						3	880.07	37.89	0.00
Cover	0.37												2	881.39	39.20	0.00
Drainage	0.37										0.02		3	882.80	40.62	0.00
BS upland	0.37								0.02				3	882.84	40.65	0.00
Late-sandy	0.38				-0.05								3	895.91	53.72	0.00

Appendix 13.8. Model coefficients, number of model parameters (*K*), Akaike's Information Criterion corrected for small sample size (AIC_c), change in AIC_c from best model (ΔAIC_c), and model weights calculated from AIC_c (w_i) for competing gamma GLMs relating forb biomass to forb cover and cover interacted with forest characteristics (vegetative classes [early-rich, late-rich, early-sandy, late-sandy, deciduous (dec.), bog, and fen], PNV type [BS upland and BS/WS upland], drainage class [upland vs. lowland; upland set as the reference category], and seral stage [early vs. late/not specified; late/not specified set as the reference category]) in northeastern Ontario.

Model	Cover	Cover * Bog	Cover * Early-rich	Cover * Early-sandy	Cover * Late-sandy	Cover * Late-rich	Cover* Fen	Cover * Dec.	Cover * BS upland	Cover * BS/WS upland	Cover * Drainage	Cover * Seral	*K*	AIC_c	ΔAIC_c	w_i
Seral stage	0.17											0.23	3	255.81	0.00	0.99
Early-rich	0.19		0.22										3	265.71	9.90	0.01
Late-rich	0.26					-0.06							3	271.72	15.91	0.00
Late-sandy	0.28				-0.12								3	277.38	21.58	0.00
Bog	0.27	-0.04											3	278.51	22.70	0.00
Early-sandy	0.25			0.13									3	279.76	23.95	0.00
Cover	0.26												2	279.99	24.18	0.00
Drainage	0.26										-0.02		3	280.95	25.15	0.00
BS/WS upland	0.25									0.02			3	281.03	25.22	0.00
Deciduous	0.25							0.05					3	282.04	26.24	0.00
BS upland	0.27								-0.006				3	282.14	26.34	0.00
Fen	0.26						-0.0006						3	282.15	26.35	0.00

Appendix 13.9. Model coefficients, number of model parameters (*K*), Akaike's Information Criterion corrected for small sample size (AIC_c), change in AIC_c from best model (ΔAIC_c), and model weights calculated from AIC_c (w_i) for competing gamma GLMs relating graminoid biomass to graminoid cover and cover interacted with forest characteristics (vegetative classes [early-rich, late-rich, early-sandy, late-sandy, deciduous (dec.), bog, and fen], PNV type [BS upland and BS/WS upland], drainage class [upland vs. lowland; upland set as the reference category], and seral stage [early vs. late/not specified; late/not specified set as the reference category]) in northwestern Ontario.

Model	Cover	Cover * Bog	Cover * Early-rich	Cover * Early-sandy	Cover * Late-sandy	Cover * Late-rich	Cover * Fen	Cover * Dec.	Cover * BS upland	Cover * BS/WS upland	Cover * Drainage	Cover * Seral	*K*	AIC_c	ΔAIC_c	w_i
Early-rich	0.76		0.43										3	318.16	0.00	0.55
Seral stage	0.67											0.35	3	320.27	2.11	0.19
Late-rich	0.92					-0.36							3	321.41	3.25	0.11
Deciduous	0.92							-0.37					3	321.52	3.37	0.10
Cover	0.93												2	326.00	7.85	0.01
BS/WS upland	0.87									0.13			3	326.84	8.68	0.01
BS upland	0.99								-0.14				3	327.08	8.92	0.01
Bog	0.93	-0.12											3	327.18	9.02	0.01
Late-sandy	0.94				-0.16								3	327.46	9.30	0.01
Early-sandy	0.97			-0.10									3	327.76	9.60	0.00
Fen	0.93						0.08						3	327.87	9.72	0.00
Drainage	0.94										-0.05		3	327.98	9.82	0.00

Appendix 13.10. Model coefficients, number of model parameters (K), Akaike's Information Criterion corrected for small sample size (AIC_c), change in AIC_c from best model (ΔAIC_c), and model weights calculated from AIC_c (w_i) for competing gamma GLMs relating graminoid biomass to graminoid cover and cover interacted with forest characteristics (vegetative classes [early-rich, late-rich, early-sandy, late-sandy, deciduous (dec.), bog, and fen], PNV type [BS upland and BS/WS upland], drainage class [upland vs. lowland; upland set as the reference category], and seral stage [early vs. late/not specified; late/not specified set as the reference category]) in northeastern Ontario.

Model	Cover	Cover * Bog	Cover * Early-rich	Cover * Early-sandy	Cover * Late-rich	Cover * Fen	Cover * Dec.	Cover * BS upland	Cover * BS/WS upland	Cover * Drainage	Cover * Seral	K	AIC_c	ΔAIC_c	w_i
Early-rich	0.33		0.37									3	76.78	0.00	0.73
Deciduous	0.56						-0.11					3	79.75	2.97	0.16
Seral stage	0.37										0.24	3	81.80	5.02	0.06
Fen	0.56					0.13						3	84.35	7.57	0.02
Late-rich	0.56											2	85.69	8.92	0.01
Drainage	0.57	-0.07										3	86.25	9.48	0.01
Cover	0.56									0.04		3	87.17	10.40	0.00
BS/WS upland	0.55				-0.04							3	87.24	10.46	0.00
Bog	0.58								-0.03			3	87.60	10.83	0.00
Early-sandy	0.56			-0.03								3	87.74	10.96	0.00

Appendix 13.11. Model coefficients, number of model parameters (*K*), Akaike's Information Criterion corrected for small sample size (AIC_c), change in AIC_c from best model (ΔAIC_c), and model weights calculated from AIC_c (w_i) for competing gamma GLMs relating deciduous shrub biomass to deciduous shrub cover and cover interacted with forest characteristics (vegetative classes [early-rich, late-rich, early-sandy, late-sandy, deciduous (dec.), bog, and fen], PNV type [BS upland and BS/WS upland], drainage class [upland vs. lowland; upland set as the reference category], and seral stage [early vs. late/not specified; late/not specified set as the reference category]) in northwestern Ontario.

Model	Cover	Cover * Bog	Cover * Early-rich	Cover * Early-sandy	Cover * Late-sandy	Cover * Late-rich	Cover* Fen	Cover * Dec.	Cover * BS upland	Cover * BS/WS upland	Cover * Drainage	Cover * Seral	*K*	AIC_c	ΔAIC_c	w_i
Late-rich	0.44					-0.16							3	647.10	0.00	0.99
Seral	0.31											0.29	3	657.59	10.49	0.01
Early-rich	0.40		0.22										3	671.98	24.88	0.00
Drainage	0.45										0.08		3	676.67	29.57	0.00
Late-sandy	0.44				-0.06								3	678.58	31.48	0.00
Fen	0.45						0.09						3	679.08	31.98	0.00
Early-sandy	0.41			0.15									3	679.33	32.23	0.00
Cover	0.46												2	680.56	33.46	0.00
BS upland	0.49								-0.05				3	680.67	33.58	0.00
BS/WS upland	0.48									-0.04			3	680.80	33.70	0.00
Bog	0.46	0.04											3	681.76	34.66	0.00
Dec.	0.46							-0.01					3	682.54	35.44	0.00

Appendix 13.12. Model coefficients, number of model parameters (K), Akaike's Information Criterion corrected for small sample size (AIC_c), change in AIC_c from best model (ΔAIC_c), and model weights calculated from AIC_c (w_i) for competing gamma GLMs relating deciduous shrub biomass to deciduous shrub cover and cover interacted with forest characteristics (vegetative classes [early-rich, late-rich, early-sandy, late-sandy, deciduous (dec.), bog, and fen], PNV type [BS upland and BS/WS upland], drainage class [upland vs. lowland; upland set as the reference category], and seral stage [early vs. late/not specified; late/not specified set as the reference category]) in northeastern Ontario.

Model	Cover	Cover * Bog	Cover * Early-rich	Cover * Early-sandy	Cover * Late-sandy	Cover * Late-rich	Cover * Fen	Cover * Dec.	Cover * BS upland	Cover * BS/WS upland	Cover * Drainage	Cover * Seral	K	AIC_c	ΔAIC_c	w_i
Seral stage	0.27											0.10	3	335.23	0.00	1.00
Early-rich	0.30		0.08										3	349.18	13.95	0.00
Dec.	0.32							-0.03					3	355.08	19.85	0.00
Late-sandy	0.31				-0.03								3	356.69	21.46	0.00
Late-rich	0.31					-0.03							3	357.53	22.31	0.00
Early-sandy	0.30			0.05									3	359.48	24.26	0.00
Cover	0.32												2	360.22	24.99	0.00
Bog	0.30	0.08											3	360.37	25.15	0.00
Drainage	0.30										0.05		3	361.44	26.21	0.00
Fen	0.32						-0.04						3	362.06	26.83	0.00
BS upland	0.32								-0.003				3	362.28	27.05	0.00
BS/WS upland	0.32									0.0002			3	362.35	27.13	0.00

Appendix 13.13. Model coefficients, number of model parameters (*K*), Akaike's Information Criterion corrected for small sample size (AIC_c), change in AIC_c from best model (ΔAIC_c), and model weights calculated from AIC_c (w_i) for competing gamma GLMs relating clubmoss biomass to clubmoss cover and cover interacted with forest characteristics (vegetative classes [early-rich, late-rich, early-sandy, late-sandy, deciduous (dec.), bog, and fen], PNV type [BS upland and BS/WS upland], and seral stage [early vs. late/not specified; late/not specified set as the reference category]) in northwestern Ontario. Drainage class was not included due to redundancy with the bog model presented.

Model	Cover	Cover * Bog	Cover * Early-rich	Cover * Early-sandy	Cover * Late-sandy	Cover * Late-rich	Cover * Dec.	Cover * BS upland	Cover * BS/WS upland	Cover * Seral	*K*	AIC_c	ΔAIC_c	w_i
Seral	1.32									0.26	3	398.62	0.00	0.46
Early-sandy	1.32			0.42							3	400.89	2.28	0.15
Bog	1.33	-0.25									3	400.97	2.35	0.14
BS upland	1.30							0.25			3	402.40	3.78	0.07
Cover	1.34										2	402.85	4.24	0.05
Early-rich	1.34		0.14								3	403.36	4.74	0.04
Late-rich	1.37					-0.11					3	403.67	5.05	0.04
Early-rich	1.35				-0.04						3	405.00	6.38	0.02
BS/WS upland	1.34								0.01		3	405.03	6.41	0.02
Deciduous	1.34						-0.0001				3	405.03	6.41	0.02

Appendix 13.14. Model coefficients, number of model parameters (*K*), Akaike's Information Criterion corrected for small sample size (AIC_c), change in AIC_c from best model (ΔAIC_c), and model weights calculated from AIC_c (w_i) for competing gamma GLMs relating clubmoss biomass to clubmoss cover and cover interacted with forest characteristics (vegetative classes [early-rich, late-rich, late-sandy, deciduous (dec.), and bog], and BS/WS upland PNV type in northeastern Ontario. Seral stage, drainage class, and BS upland were not included due to redundancy with the early-rich, bog, and late-sandy models presented.

Model	Cover	Cover * Bog	Cover * Early-rich	Cover * Late-sandy	Cover * Late-rich	Cover * Dec.	Cover * BS/WS upland	*K*	AIC_c	ΔAIC_c	w_i
Bog	1.10	0.21						3	92.91	0.00	0.40
Late-sandy	1.10			-0.16				3	93.63	0.73	0.28
Cover	1.08							2	95.36	2.46	0.12
Deciduous	0.92					0.28		3	95.68	2.77	0.10
Early-rich	1.10		-0.29					3	97.17	4.27	0.05
Late-rich	1.13				-0.11			3	97.59	4.68	0.04
BS/WS upland	1.05						0.03	3	98.20	5.30	0.03

Appendix 13.15. Model coefficients, number of model parameters (*K*), Akaike's Information Criterion corrected for small sample size (AIC_c), change in AIC_c from best model (ΔAIC_c), and model weights calculated from AIC_c (w_i) for competing gamma GLMs relating *Ledum groenlandicum* biomass to *Ledum groenlandicum* cover and cover interacted with forest characteristics (vegetative classes [early-rich, late-sandy, bog, and fen], PNV type [BS upland and BS/WS upland], drainage class [upland vs. lowland; upland set as the reference category], and seral stage [early vs. late/not specified; late/not specified set as the reference category]) in northwestern and northeastern Ontario.

Model	Cover	Cover * Bog	Cover * Early-rich	Cover * Late-sandy	Cover * Fen	Cover * BS upland	Cover * BS/WS upland	Cover * Drainage	Cover * Seral	*K*	AIC_c	ΔAIC_c	w_i
Cover	0.49									2	266.48	0.00	0.22
Fen	0.52				-0.07					3	267.18	0.70	0.16
Bog	0.46	0.06								3	267.34	0.86	0.15
Late-sandy	0.49			0.08						3	268.52	2.04	0.08
BS upland	0.49					0.08				3	268.52	2.04	0.08
Early-rich	0.49		-0.03							3	268.59	2.11	0.08
BS/WS upland	0.49						-0.03			3	268.59	2.11	0.08
Seral stage	0.49								-0.03	3	268.59	2.11	0.08
Drainage	0.49							0.01		3	268.70	2.22	0.07

Appendix 13.16. Model coefficients, number of model parameters (*K*), Akaike's Information Criterion corrected for small sample size (AIC_c), change in AIC_c from best model (ΔAIC_c), and model weights calculated from AIC_c (w_i) for competing gamma GLMs relating *Chamaedaphne calyculata* biomass to *Chamaedaphne calyculata* cover and cover interacted the bog vegetative class in northwestern and northeastern Ontario.

Model	Cover	Cover * Bog	*K*	AIC_c	ΔAIC_c	w_i
Cover	0.73		2	176.13	0.00	0.73
Bog	0.68	0.09	3	178.09	1.96	0.27

Appendix 13.17. Model coefficients, number of model parameters (*K*), Akaike's Information Criterion corrected for small sample size (AIC_c), change in AIC_c from best model (ΔAIC_c), and model weights calculated from AIC_c (w_i) for competing gamma GLMs relating fern biomass to fern cover and cover interacted with forest characteristics (vegetative classes [early-rich, late-rich, and deciduous (dec.)] in northwestern and northeastern Ontario. Seral stage was not included due to redundancy with the early-rich model presented.

Model	Cover	Cover * Early-rich	Cover * Late-rich	Cover * Dec.	*K*	AIC_c	ΔAIC_c	w_i
Cover	0.32				2	128.69	0.00	0.45
Deciduous	0.41			-0.11	3	129.20	0.51	0.35
Late-rich	0.32		-0.003		3	130.98	2.29	0.14
Early-rich	0.28	0.16			3	133.08	4.39	0.05

Appendix 13.18. Model coefficients, number of model parameters (*K*), Akaike's Information Criterion corrected for small sample size (AIC_c), change in AIC_c from best model (ΔAIC_c), and model weights calculated from AIC_c (w_i) for competing gamma GLMs relating *Linnaea borealis* biomass to *Linnaea borealis* cover and cover interacted with forest characteristics (vegetative classes [early-rich, late-rich, early-sandy, late-sandy, deciduous (dec.), bog, and fen], PNV type [BS upland and BS/WS upland], drainage class [upland vs. lowland; upland set as the reference category], and seral stage [early vs. late/not specified; late/not specified set as the reference category]) in northwestern and northeastern Ontario.

Model	Cover	Cover * Early-rich	Cover * Early-sandy	Cover * Late-sandy	Cover * Late-rich	Cover* Fen	Cover * Dec.	Cover * BS upland	Cover * BS/WS upland	Cover * Drainage	Cover * Seral	*K*	AIC_c	ΔAIC_c	w_i
Early-rich	0.16	0.50										3	-22.21	0.00	0.91
Seral	0.15										0.36	3	-17.66	4.54	0.09
BS/WS upland	0.16								0.17			3	3.87	26.08	0.00
Late-sandy	0.28			-0.14								3	5.26	27.47	0.00
BS upland	0.30							-0.14				3	5.30	27.50	0.00
Fen	0.24					-0.13						3	6.68	28.89	0.00
Late-rich	0.25				-0.13							3	9.16	31.37	0.00
Cover	0.21											2	11.35	33.56	0.00
Dec.	0.22						-0.04					3	13.59	35.80	0.00
Drainage	0.22									-0.04		3	13.59	35.80	0.00
Early-sandy	0.21		-0.02									3	13.80	36.01	0.00

Appendix 13.19. Model coefficients, number of model parameters (*K*), Akaike's Information Criterion corrected for small sample size (AIC_c), change in AIC_c from best model (ΔAIC_c), and model weights calculated from AIC_c (w_i) for competing gamma GLMs relating *Kalmia angustifolia* biomass to *Kalmia angustifolia* cover and cover interacted with forest characteristics (vegetative classes [early-sandy, late-sandy, and bog], BS upland PNV type, and drainage class [upland vs. lowland; upland set as the reference category] in northeastern Ontario. Seral stage was not included due to redundancy with the early-sandy model presented.

Model	Cover	Cover * Bog	Cover * Early-sandy	Cover * Late-sandy	Cover * BS upland	Cover * Drainage	*K*	AIC_c	ΔAIC_c	w_i
Cover	0.36						2	25.23	0.00	0.32
Bog	0.35	0.05					3	26.10	0.87	0.21
Late-sandy	0.35			-0.03			3	26.55	1.32	0.16
BS upland	0.37				-0.02		3	27.41	2.18	0.11
Drainage	0.35					0.02	3	27.41	2.18	0.11
Early-sandy	0.35		0.01				3	27.65	2.42	0.10

Appendix 14. Supplemental materials for Chapter 5

To extrapolate forage metrics for the calving period (1 May to 15 June) we will use biomass and quality estimated at permanent phenological (PP) macroplots (Appendix 12) and foodscape predictions on 15 June developed in Chapter 4. This appendix outlines the methods used to extrapolate the foraging metrics to the calving period, which will be included in our evaluation of habitat selection during the calving period by reproductive-state.

Methods

We estimated biomass for each component of accepted biomass using species-specific biomass derived in Appendix 12. We did not estimate lichen biomass at PP macroplots and will apply the predictive lichen models developed for summer (Chapter 4) to the calving period, assuming lichen biomass does not appreciably change across the summer. To estimate values for each metric of high-quality accepted biomass at PP macroplots using the FRESH-model (Hanley et al. 2012), we summated biomass by life-form groups (forb, grass, deciduous shrub, horsetail) and applied estimates of digestible energy (DE) and protein (DP) using the life-form models developed in Appendix 5. We did not use species-specific predictions of forage quality, because of reduced forage-quality samples by species during the calving period. Further, because we did not estimate biomass of ground and tree lichens at PP macroplots, we assigned the mean values for each seral-specific ecosite to estimate metrics of high-quality accepted biomass (Chapter 4).

Once estimates of each accepted component of accepted biomass (excluding lichens) and the 3 metrics of high-quality accepted biomass (HQ-accepted biomass, DE-accepted biomass, and DP-accepted biomass) we assigned to each PP macroplots, we developed equations to extrapolate early-summer values (predicted on 15 June; Chapter 4) across the calving period to 1 May. We assumed herbaceous biomass was zero on 1 May. PP macroplots corresponded to the seral-specific ecosites used in predict forage metrics in Chapter 4. Therefore, for each study area and seral-specific ecosites we first evaluated a linear or non-linear relationship between zero biomass on 1 May, estimates of biomass at PP macroplots sampled during the calving period, and mean biomass predicted on 15 June across each study region (Figure 4.7–4.8), and Julian day. Linear vs. non-linear relationships were evlauated using CurveExpert (CurveExpert 2.7.3, D. G. Hyams, Madison, AL. USA) based on > 2 ΔAIC_C; (Burnham and Anderson 2002). Because mushroom biomass was not estimated at PP macroplots and biomass during early summer across most vegetative macroplots was minimal, we developed linear equations between a value of zero on 1 May at the mean seral-specific estimates of biomass on 15 June. Finally, we used linear regression to model biomass as a function of the linear or non-linear transformation of Julian day to estimate the intercept and beta coefficient to make predictions.

Results

Across all forage metric, 67% of relationships between biomass and Julian day were identified as non-linear (Appendix 14.1). Predictive models of forage metric (Appendix 14.2–15.8) were then used to predict biomass at each caribou used and available location during the calving period (1 May to 15 June). We also predicted intake rate at these used and available locations following the equations developed by Cook et al. (*in prep.*; Chapter 4).

Appendix 14.1. Non-linear transformations applied to Julian day across grass, forbs, deciduous shrubs (GFS) biomass, horsetail biomass, high-quality (HQ) accepted biomass (AB; both DE and DP constraints), DE-accepted biomass (only DE constraint), and DP-accepted biomass (only DP constraint) by seral-specific ecosite or a combination of ecosites in Pickle Lake (PL) and Cochrane, Ontario (CO).

Biomass metric	Ecosite	Seral	SA	Transformation	Equation	a	b	c
GFS	Upl-BS-Rocky	Early	PL	Geometric	a*x^(b*x)	8.36631E-16	0.04740	
	Upl-BS-Rocky	Mid-late	PL	Geometric	a*x^(b*x)	2.31561E-15	0.04516	
	Upl-BS	Early	PL	Geometric	a*x^(b*x)	3.54415E-18	0.05348	
	Upl-BS	Mid-late	PL	Geometric	a*x^(b*x)	1.69326E-20	0.05835	
	Upl-BS-WS	Early	PL	Geometric	a*x^(b*x)	4.39822E-15	0.04651	
	Upl-BS-WS	Mid-late	PL	Geometric	a*x^(b*x)	7.58478E-16	0.04727	
	Lwl-Bog	Early	PL	Geometric	a*x^(b*x)	9.21831E-16	0.04710	
	Lwl-Bog	Mid-late	PL	Geometric	a*x^(b*x)	2.88739E-14	0.04186	
	Lwl-Marsh	Mid-late	PL	Geometric	a*x^(b*x)	5.09124E-16	0.04935	
	Lwl-Fen	Mid-late	PL & CO	Geometric	a*x^(b*x)	2.41825E-12	0.03694	
	Lwl-Cedar	Mid-late	PL & CO	Geometric	a*x^(b*x)	3.33605E-17	0.05200	
	Upl-BS	Early	CO	Geometric	a*x^(b*x)	4.78054E-18	0.05177	
	Upl-BS	Mid-late	CO	Geometric	a*x^(b*x)	7.74317E-09	0.02658	
	Upl-BS-WS	Early	CO	Geometric	a*x^(b*x)	4.97826E-07	0.02173	
	Upl-BS-WS	Mid-late	CO	Geometric	a*x^(b*x)	1.11803E-12	0.03647	
	Lwl-Bog	Early	CO	Geometric	a*x^(b*x)	7.87165E-15	0.04380	
	Lwl-Bog	Mid-late	CO	Geometric	a*x^(b*x)	1.83947E-09	0.02585	
Horsetail	Upl-BS	Early	PL	Geometric	a*x^(b*x)	1.37449E-11	0.03098	
	Upl-BS	Mid-late	PL	Geometric	a*x^(b*x)	3.38384E-11	0.02789	
	Upl-BS-WS	Early	PL	Geometric	a*x^(b*x)	9.77259E-07	0.02053	
	Lwl-Bog	Early	PL	Geometric	a*x^(b*x)	2.41772E-22	0.06310	
	Lwl-Bog	Mid-late	PL	Geometric	a*x^(b*x)	4.10417E-11	0.03120	
	Lwl-Fen	Mid-late	PL & CO	Geometric	a*x^(b*x)	1.57342E-10	0.02642	
	Lwl-Cedar	Mid-late	PL & CO	Geometric	a*x^(b*x)	8.67814E-19	0.05298	
	Upl-BS	Early	CO	Geometric	a*x^(b*x)	2.30388E-11	0.02258	
	Upl-BS	Mid-late	CO	Geometric	a*x^(b*x)	3.65343E-10	0.02291	

Appendix 14.1. Continued.

Biomass metric	Ecosite	Seral	SA	Transformation	Equation	a	b	c
Horsetail	Upl-BS-WS	Early	CO	Geometric	a*x^(b*x)	1.48575E-09	0.02542	
	Upl-BS-WS	Mid-late	CO	Geometric	a*x^(b*x)	3.90076E-10	0.02463	
	Lwl-Bog	Early	CO	Geometric	a*x^(b*x)	1.73541E-10	0.03018	
	Lwl-Bog	Mid-late	CO	Geometric	a*x^(b*x)	1.44041E-09	0.02515	
HQ-AB	Upl-BS	Early	PL	Geometric	a*x^(b*x)	2.21241E-15	0.04527	
	Upl-BS	Mid-late	PL	Geometric	a*x^(b*x)	2.04710E-15	0.04431	
	Upl-BS-WS	Early	PL	Geometric	a*x^(b*x)	8.17572E-16	0.04838	
	Upl-BS-WS	Mid-late	PL	Geometric	a*x^(b*x)	4.42003E-14	0.04225	
	Lwl-Bog	Early	PL	Geometric	a*x^(b*x)	7.39625E-13	0.03842	
	Lwl-Bog	Mid-late	PL	Geometric	a*x^(b*x)	1.00256E-11	0.03517	
	Lwl-Marsh	Mid-late	PL	Geometric	a*x^(b*x)	2.93044E-14	0.04277	
	Lwl-Fen	Mid-late	PL & CO	Geometric	a*x^(b*x)	2.43103E-11	0.03402	
	Lwl-Cedar	Mid-late	PL & CO	Geometric	a*x^(b*x)	4.77426E-15	0.04479	
	Upl-BS	Early	CO	Geometric	a*x^(b*x)	3.44648E-16	0.04670	
	Upl-BS	Mid-late	CO	Geometric	a*x^(b*x)	7.17306E-09	0.02648	
	Upl-BS-WS	Early	CO	Geometric	a*x^(b*x)	4.89347E-07	0.02183	
	Upl-BS-WS	Mid-late	CO	Geometric	a*x^(b*x)	5.74612E-12	0.03550	
	Lwl-Bog	Early	CO	Geometric	a*x^(b*x)	1.16984E-12	0.03782	
	Lwl-Bog	Mid-late	CO	Geometric	a*x^(b*x)	4.80223E-09	0.02558	
DE-AB	Upl-BS	Early	PL	Geometric	a*x^(b*x)	0.0026	0.01314	
	Upl-BS	Mid-late	PL	Bleasdale	(a + b*x)^(-1/c)	0.0003	-1.95932E-06	3.10426
	Upl-BS-WS	Early	PL	Geometric	a*x^(b*x)	1.53862E-14	0.04447	
	Upl-BS-WS	Mid-late	PL	Bleasdale	(a + b*x)^(-1/c)	0.13826	-0.00083	1.67970
	Lwl-Bog	Early	PL	Bleasdale	(a + b*x)^(-1/c)	2.30E-11	0.03534	
	Lwl-Bog	Mid-late	PL	Bleasdale	(a + b*x)^(-1/c)	0.00070	-4.18299E-06	2.76317
	Lwl-Marsh	Mid-late	PL	Geometric	a*x^(b*x)	2.92645E-12	0.03810	
	Lwl-Cedar	Mid-late	PL & CO	Geometric	a*x^(b*x)	3.09491E-12	0.03763	

Appendix 14.1. Continued.

Biomass metric	Ecosite	Seral	SA	Transformation	Equation	a	b	c
DE-AB	Upl-BS	Early	CO	Geometric	a*x^(b*x)	2.62565E-11	0.03389	
	Upl-BS	Mid-late	CO	Geometric	a*x^(b*x)	2.61773E-09	0.02987	
	Upl-BS-WS	Early	CO	Geometric	a*x^(b*x)	4.92331E-07	0.02183	
	Upl-BS-WS	Mid-late	CO	Geometric	a*x^(b*x)	5.37695E-06	0.01838	
	Lwl-Bog	Mid-late	CO	Geometric	a*x^(b*x)	1.03194E-06	0.02086	
DP-AB	Upl-BS	Early	PL	Geometric	a*x^(b*x)	9.16347E-17	0.04952	
	Upl-BS	Mid-late	PL	Geometric	a*x^(b*x)	1.79097E-15	0.04440	
	Upl-BS-WS	Early	PL	Geometric	a*x^(b*x)	1.19945E-15	0.04786	
	Upl-BS-WS	Mid-late	PL	Geometric	a*x^(b*x)	7.96907E-14	0.04142	
	Lwl-Bog	Early	PL	Geometric	a*x^(b*x)	3.29575E-14	0.04264	
	Lwl-Bog	Mid-late	PL	Geometric	a*x^(b*x)	1.18847E-13	0.04083	
	Lwl-Marsh	Mid-late	PL	Geometric	a*x^(b*x)	3.88316E-15	0.04666	
	Lwl-Fen	Mid-late	PL & CO	Geometric	a*x^(b*x)	6.05078E-11	0.03296	
	Lwl-Cedar	Mid-late	PL & CO	Geometric	a*x^(b*x)	3.51359E-15	0.04523	
	Upl-BS	Early	CO	Geometric	a*x^(b*x)	3.44648E-16	0.04670	
	Upl-BS	Mid-late	CO	Geometric	a*x^(b*x)	7.05017E-09	0.02651	
	Upl-BS-WS	Early	CO	Geometric	a*x^(b*x)	4.92850E-07	0.02182	
	Upl-BS-WS	Mid-late	CO	Geometric	a*x^(b*x)	2.38745E-09	0.02742	
	Lwl-Bog	Early	CO	Geometric	a*x^(b*x)	8.88905E-13	0.03818	
	Lwl-Bog	Mid-late	CO	Geometric	a*x^(b*x)	5.35894E-09	0.02546	

Appendix 14.2. Intercept (B_0) and coefficient estimate for predictive models of grass, forbs, and deciduous shrub combined (GFS), horsetail, and mushroom biomass, and high-quality (HQ) accepted biomass (AB; both DE and DP constraints), DE-accepted biomass (only DE constraint), and DP-accepted biomass (only DP constraint) for each seral-specific (early: <20 yrs; mid-late: ≥ 20 yrs) ecosite and study area (SA) as a function of sampling date (i.e., Julian day; JD) for the calving period (1 May to 14 June) in Pickle Lake (PL) and Cochrane, Ontario (CO).

Forage metric	SA	Seral-Ecosite	Non-linear	Bo	JD
GFS	PL	Early-Upl-BS-Rocky	yes	-10.56	1.13
		Mid-late-Upl-BS-Rocky	yes	-0.61	1.05
		Early-Upl-BS	yes	-2.44	1.03
		Mid-late-Upl-BS	yes	-2.27	1.08
		Early-Upl-BS-WS	yes	-32.66	1.07
		Mid-late-Upl-BS-WS	yes	-2.62	1.03
		Early-Lwl-Bog	yes	-7.71	1.08
		Mid-late-Lwl-Bog	yes	-0.63	1.01
		Mid-late-Lwl-Marsh	yes	-47.10	1.18
	CO	Early-Upl-BS	yes	0.001	1.00
		Mid-late-Upl-BS	yes	-0.91	1.03
		Early-Upl-BS-WS	yes	0.89	1.03
		Mid-late-Upl-BS-WS	yes	0.01	1.00
		Early-Lwl-Bog	yes	0.22	1.00
		Mid-late-Lwl-Bog	yes	-0.13	1.03
	PL & CO	Mid-late-Lwl-Fen	yes	-0.55	1.02
		Mid-late-Lwl-Cedar/ thicket	yes	-13.05	1.05
Horsetail	PL	Early-Upl-BS-Rocky	no	0.00	---
		Mid-late-Upl-BS-Rocky	no	0.00	---
		Early-Upl-BS	yes	-0.41	1.19
		Mid-late-Upl-BS	yes	-0.09	1.23
		Early-Upl-BS-WS	yes	-0.72	1.03
		Mid-late-Upl-BS-WS	no	-5.28	0.04
		Early-Lwl-Bog	yes	-0.28	1.01
		Mid-late-Lwl-Bog	yes	-1.32	1.14
		Mid-late-Lwl-Marsh	no	0.00	---
	CO	Early-Upl-BS	yes	-0.0002	1.05
		Mid-late-Upl-BS	yes	-0.003	1.04
		Early-Upl-BS-WS	yes	-0.08	1.03
		Mid-late-Upl-BS-WS	yes	-0.01	1.03
		Early-Lwl-Bog	yes	-0.37	1.03
		Mid-late-Lwl-Bog	yes	-0.06	1.03
	PL & CO	Mid-late-Lwl-Fen	yes	-0.06	1.10
		Mid-late-Lwl-Cedar/ thicket	no	-0.17	1.01

Appendix 14.2. Continued.

Forage metric	SA	Seral-Ecosite	Non-linear	Bo	JD
Mushroom	PL	Early-Upl-BS-Rocky	no	-0.02	0.00
		Mid-late-Upl-BS-Rocky	no	-0.70	0.01
		Early-Upl-BS	no	-0.17	0.00
		Mid-late-Upl-BS	no	-0.21	0.00
		Early-Upl-BS-WS	no	0.00	---
		Mid-late-Upl-BS-WS	no	-1.72	0.01
		Early-Lwl-Bog	no	-0.10	0.00
		Mid-late-Lwl-Bog	no	0.001	-0.12
		Mid-late-Lwl-Marsh	no	0.00	---
	CO	Early-Upl-BS	no	-0.003	0.00002
		Mid-late-Upl-BS	no	-0.003	0.00003
		Early-Upl-BS-WS	no	-0.01	0.00007
		Mid-late-Upl-BS-WS	no	-0.16	0.001
		Early-Lwl-Bog	no	-1.77	0.01
		Mid-late-Lwl-Bog	no	-0.20	0.002
	PL & CO	Mid-late-Lwl-Fen	no	-0.27	0.002
		Mid-late-Lwl-Cedar/ thicket	no	-0.13	0.001
HQ AB	PL	Early-Upl-BS-Rocky	no	-11.91	0.10
		Mid-late-Upl-BS-Rocky	no	-69.35	0.57
		Early-Upl-BS	yes	1.61	0.99
		Mid-late-Upl-BS	yes	-2.70	1.08
		Early-Upl-BS-WS	yes	-15.27	1.06
		Mid-late-Upl-BS-WS	yes	0.74	1.00
		Early-Lwl-Bog	yes	2.15	0.96
		Mid-late-Lwl-Bog	yes	0.02	1.00
		Mid-late-Lwl-Marsh	yes	-1.54	1.02
	CO	Early-Upl-BS	yes	0.0005	1.00
		Mid-late-Upl-BS	yes	-0.78	1.03
		Early-Upl-BS-WS	yes	-0.05	1.00
		Mid-late-Upl-BS-WS	yes	0.15	1.00
		Early-Lwl-Bog	no	0.10	1.00
		Mid-late-Lwl-Bog	yes	-0.27	1.03
	PL & CO	Mid-late-Lwl-Fen	yes	1.85	0.99
		Mid-late-Lwl-Cedar/ thicket	no	0.52	1.01

Appendix 14.2. Continued.

Forage metric	SA	Seral-Ecosite	Non-linear	Bo	JD
DE AB	PL	Early-Upl-BS-Rocky	no	-1603.83	14.45
		Mid-late-Upl-BS-Rocky	no	-712.24	6.71
		Early-Upl-BS	yes	-0.75	1.01
		Mid-late-Upl-BS	yes	2.28	0.96
		Early-Upl-BS-WS	yes	-0.10	1.00
		Mid-late-Upl-BS-WS	yes	0.10	0.99
		Early-Lwl-Bog	yes	9.19	0.94
		Mid-late-Lwl-Bog	yes	0.08	1.00
		Mid-late-Lwl-Marsh	no	4.45	0.97
	CO	Early-Upl-BS	yes	0.005	1.00
		Mid-late-Upl-BS	yes	0.14	1.00
		Early-Upl-BS-WS	yes	-0.04	1.00
		Mid-late-Upl-BS-WS	yes	0.41	0.98
		Early-Lwl-Bog	no	-444.36	0.93
		Mid-late-Lwl-Bog	yes	0.84	0.98
	PL & CO	Mid-late-Lwl-Fen	no	-255.55	2.16
		Mid-late-Lwl-Cedar/ thicket	no	8.28	0.94
DP AB	PL	Early-Upl-BS-Rocky	no	-11.92	0.10
		Mid-late-Upl-BS-Rocky	no	-79.21	0.65
		Early-Upl-BS	yes	-0.79	1.02
		Mid-late-Upl-BS	yes	-2.62	1.12
		Early-Upl-BS-WS	yes	-13.92	1.06
		Mid-late-Upl-BS-WS	yes	0.99	1.38
		Early-Lwl-Bog	yes	-2.27	1.06
		Mid-late-Lwl-Bog	yes	-1.10	1.01
		Mid-late-Lwl-Marsh	yes	-32.40	1.12
	CO	Early-Upl-BS	yes	0.0005	1.00
		Mid-late-Upl-BS	yes	-0.78	1.02
		Early-Upl-BS-WS	yes	-0.05	1.00
		Mid-late-Upl-BS-WS	yes	0.009	1.00
		Early-Lwl-Bog	yes	0.11	1.00
		Mid-late-Lwl-Bog	yes	-0.28	1.04
	PL & CO	Mid-late-Lwl-Fen	yes	3.38	0.95
		Mid-late-Lwl-Cedar/ thicket	yes	0.05	1.03

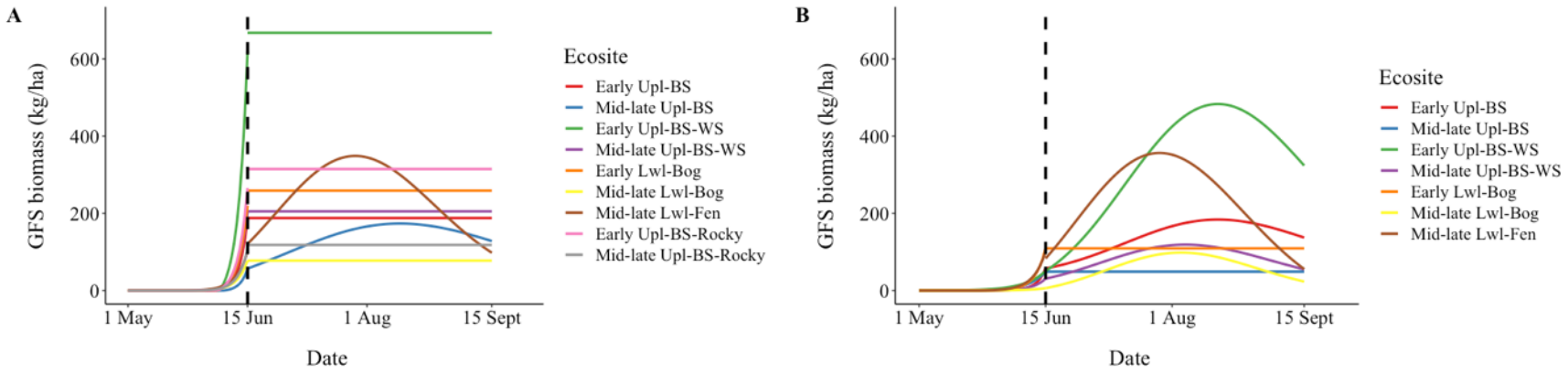

Appendix 14.3. Mean, grass, forbs, and deciduous shrubs (GFS) biomass (kg/ha) by seral-specific ecosite across the spatial extent of A) Pickle Lake and B) Cochrane from 1 May to 15 September, which was assigned to caribou used and available locations through time.

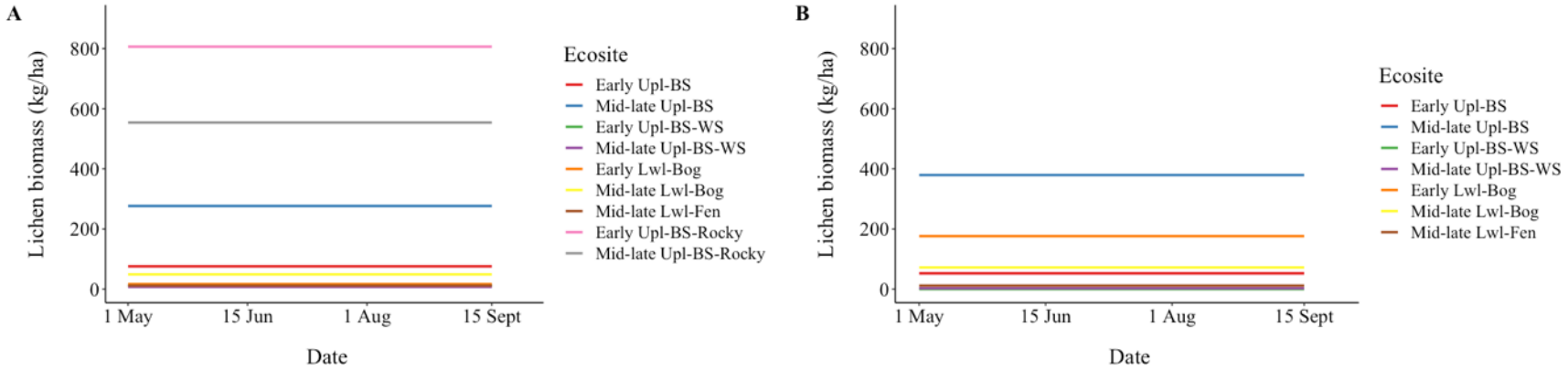

Appendix 14.4. Mean, lichen biomass (kg/ha) by seral-specific ecosite across the spatial extent of A) Pickle Lake and B) Cochrane from 1 May to 15 September, which was assigned to caribou used and available locations through time.

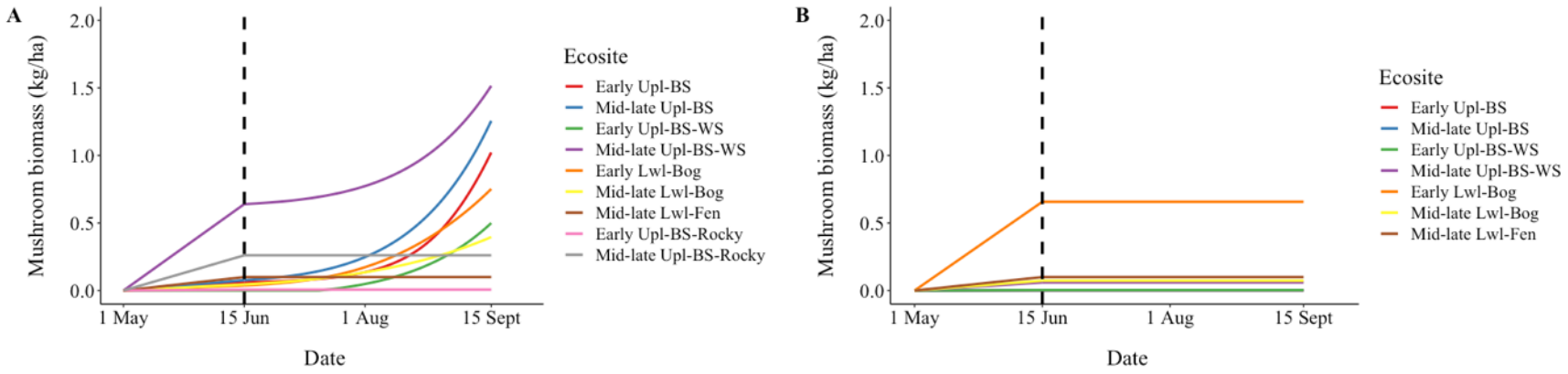

Appendix 14.5. Mean, mushroom biomass (kg/ha) by seral-specific ecosite across the spatial extent of A) Pickle Lake and B) Cochrane from 1 May to 15 September, which was assigned to caribou used and available locations through time.

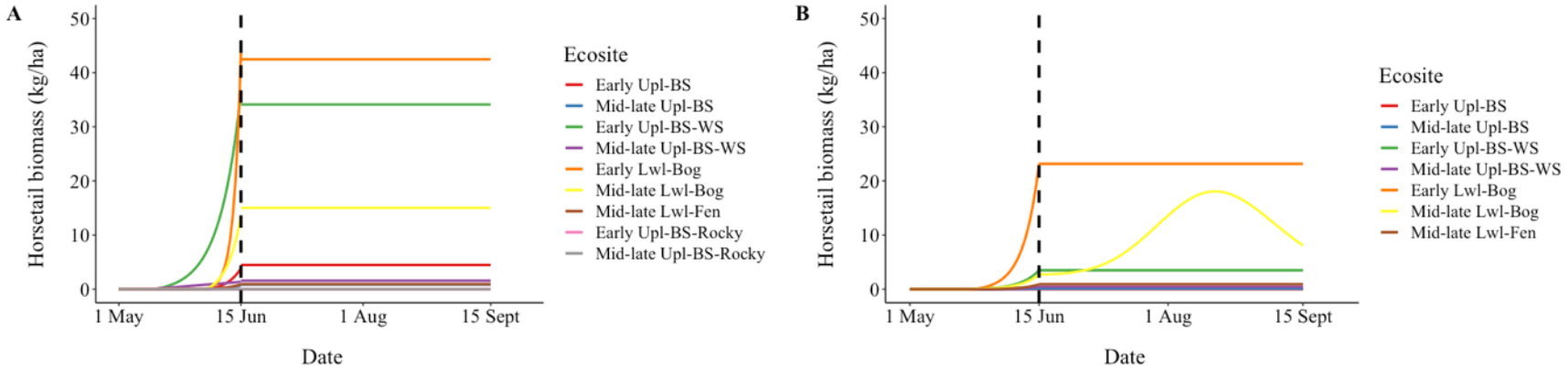

Appendix 14.6. Mean, horsetail biomass (kg/ha) by seral-specific ecosite across the spatial extent of A) Pickle Lake and B) Cochrane from 1 May to 15 September, which was assigned to caribou used and available locations through time.

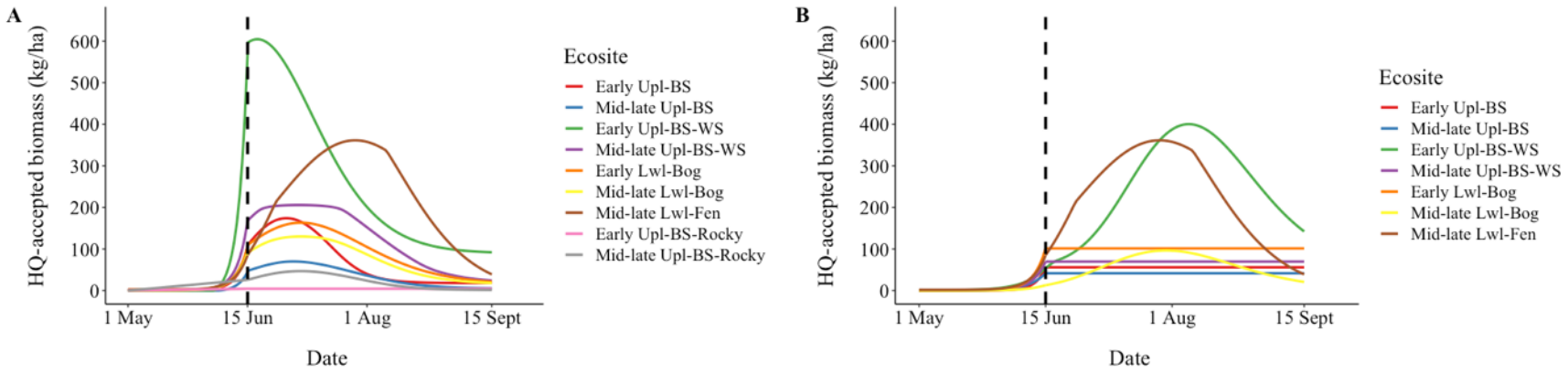

Appendix 14.6. Mean, high-quality (HQ) accepted biomass (AB; kg/ha) by seral-specific ecosite across the spatial extent of A) Pickle Lake and B) Cochrane from 1 May to 15 September, which was assigned to caribou used and available locations through time.

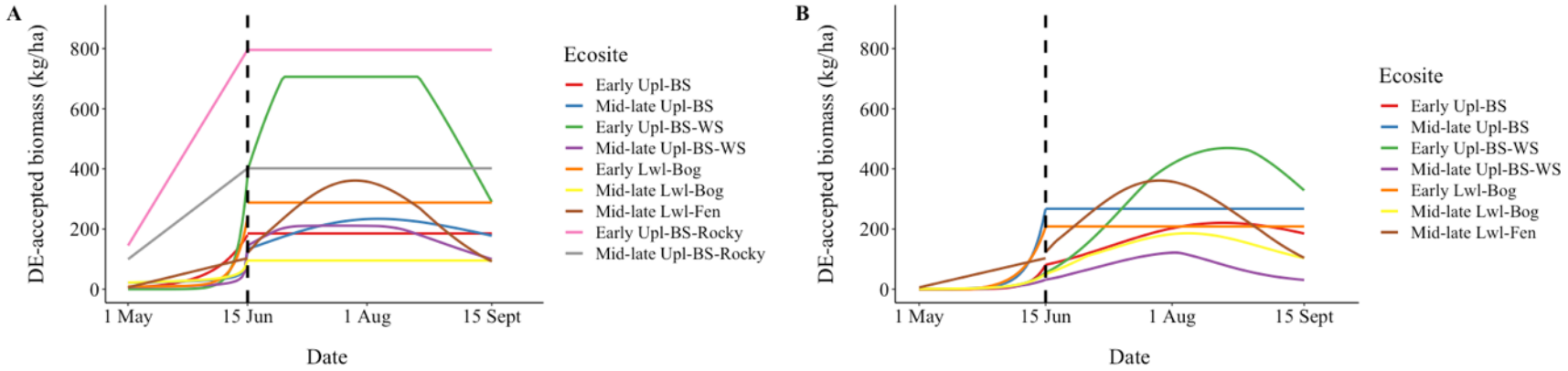

Appendix 14.7. Mean, DE-accepted biomass (AB; kg/ha) by seral-specific ecosite across the spatial extent of A) Pickle Lake and B) Cochrane from 1 May to 15 September, which was assigned to caribou used and available locations through time.

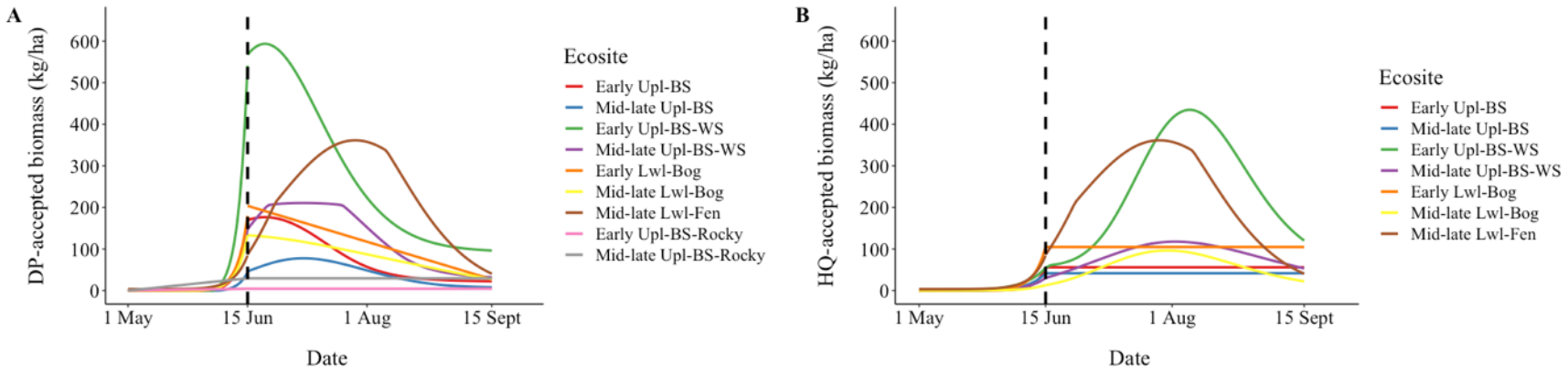

Appendix 14.8. Mean, DP-accepted biomass (AB; kg/ha) by seral-specific ecosite across the spatial extent of A) Pickle Lake and B) Cochrane from 1 May to 15 September, which was assigned to caribou used and available locations through time.

Appendix 15. Supplemental materials for Chapter 5

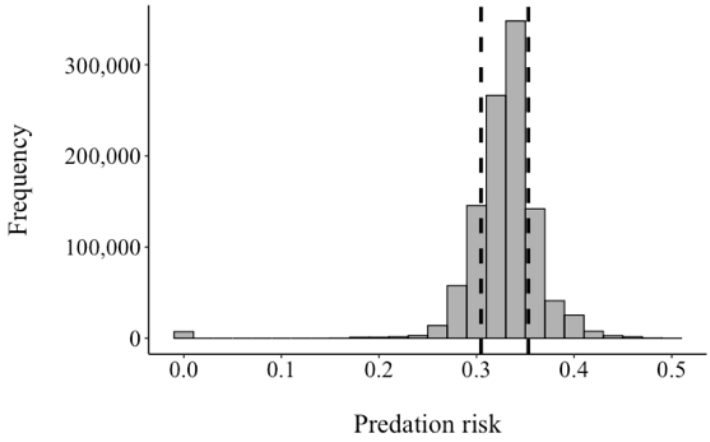

Appendix 15.1. High and low summer predation risk values (dashed lines) based on the mean predation risk value of all available locations above and below the median value, respectively.

Appendix 15.2. Number of model parameters (*K*), Akaike's Information Criterion corrected for small sample size (AIC_c), change in AIC_c from best model (ΔAIC_c), and model weights calculated from AIC_c (w_i) for univariate iSSA models to identifying the top forage metric by season and reproductive state by comparing eight forage metrics with linear and quadratic at used and available locations across 91 caribou-years in northern Ontario, 2010–2013 with step length (SL) and turn angle (TA) included as fixed effects.

Season	State	Model	*K*	AIC_c	ΔAIC_c	W_i
		Intake + Intake2 + SL + TA	5	37276.36	0.00	1.00
		Lichen + Lichen2 + SL + TA	5	37323.72	47.36	0.00
		AB + AB2 + SL + TA	5	37324.00	47.64	0.00
		Lichen + SL + TA	4	37335.12	58.76	0.00
		AB + SL + TA	4	37335.71	59.35	0.00
		DE-AB + DE-AB2 + SL + TA d	5	37383.74	107.38	0.00
		Mushroom + Mushroom2 + SL + TA	5	37387.81	111.45	0.00
		Intake rate + SL + TA	4	37393.69	117.33	0.00
		DE-AB + SL + TA	4	37396.03	119.67	0.00
Calving	Barren	DP-AB + DP-AB2 + SL + TA	5	37399.41	123.05	0.00
		Horsetail + Horsetail2 + SL + TA	5	37401.07	124.71	0.00
		Mushroom + SL + TA	4	37401.72	125.35	0.00
		Horsetail + SL + TA	4	37402.21	125.85	0.00
		DP-AB + SL + TA	4	37404.04	127.68	0.00
		SL + TA	3	37404.65	128.29	0.00
		GFS + SL + TA	4	37404.70	128.34	0.00
		HQ-AB + SL + TA	4	37406.26	129.89	0.00
		HQ-AB + HQ-AB2 + SL + TA	5	37406.44	130.08	0.00
		GFS + GFS2 + SL + TA	5	37406.69	130.32	0.00

Appendix 15.2. Continued.

Season	State	Model	K	AIC_c	ΔAIC_c	W_i
Calving	Calf alive	Intake + Intake2 + SL + TA	5	84537.07	0.00	1.00
		Intake rate + SL + T dA	4	84802.37	265.30	0.00
		DE-AB + DE-AB2 + SL + TA	5	84828.38	291.31	0.00
		AB + AB2 + SL + TA	5	84829.07	292.00	0.00
		AB + SL + TA	4	84829.54	292.47	0.00
		Mushroom + Mushroom2 + SL + TA	5	84830.17	293.10	0.00
		Lichen + SL + TA	4	84830.71	293.65	0.00
		Lichen + Lichen2 + SL + TA	5	84831.32	294.25	0.00
		Mushroom + SL + TA	4	84837.50	300.43	0.00
		HQ-AB + HQ-AB2 + SL + TA	5	84861.49	324.42	0.00
		HQ-AB + SL + TA	4	84863.00	325.93	0.00
		DP-AB + DP-AB2 + SL + TA	5	84865.18	328.11	0.00
		Horsetail + Horsetail2 + SL + TA	5	84865.30	328.23	0.00
		DP-AB + SL + TA	4	84865.74	328.67	0.00
		DE-AB + SL + TA	4	84868.04	330.97	0.00
		Horsetail + SL + TA	4	84868.32	331.25	0.00
		GFS + GFS2 + SL + TA	5	84868.38	331.31	0.00
		SA + TA	3	84869.12	332.05	0.00
		GFS + SL + TA	4	84869.47	332.41	0.00
	Calf lost	Intake + Intake2 + SL + TA	5	40303.26	0.00	1.00
		Mushroom + Mushroom2 + SL + TA	5	40336.46	33.19	0.00
		DE-AB + DE-AB2 + SL + TA	5	40363.97	60.71	0.00
		DE-AB + SL + TA	4	40375.83	72.57	0.00
		Lichen + Lichen2 + SL + TA	5	40383.79	80.53	0.00
		AB + AB2 + SL + TA	5	40384.22	80.95	0.00
		Lichen + SL + TA	4	40384.33	81.07	0.00
		AB + SL + TA	4	40384.59	81.32	0.00
		Mushroom + SL + TA	4	40404.36	101.10	0.00
		Intake rate + SL + TA	4	40407.40	104.13	0.00
		SL + TA	3	40408.13	104.87	0.00
		DP-AB + SL + TA	4	40409.45	106.19	0.00
		GFS + SL + TA	4	40409.55	106.28	0.00
		DP-AB + DP-AB2 + SL + TA	5	40409.68	106.42	0.00
		HQ-AB + SL + TA	4	40409.95	106.69	0.00
		HQ-AB + HQ-AB2 + SL + TA	5	40410.10	106.83	0.00
		Horsetail + SL + TA	4	40410.13	106.87	0.00
		Horsetail + Horsetail2 + SL + TA	5	40411.51	108.24	0.00
		GFS + GFS2 + SL + TA	5	40411.53	108.27	0.00

Appendix 15.2. Continued.

Season	State	Model	K	AIC_c	ΔAIC_c	W_i
Early summer	Barren	Intake + Intake2 + SL + TA	5	35812.39	0.00	1.00
		Mushroom + Mushroom2 + SL + TA	5	35864.26	51.87	0.00
		Mushroom + SL + TA	4	35880.41	68.01	0.00
		HQ-AB + HQ-AB2 + SL + TA	5	36024.67	212.28	0.00
		Intake rate + SL + TA	4	36072.10	259.71	0.00
		DP-AB + DP-AB2 + SL + TA	5	36094.35	281.95	0.00
		GFS + GFS2 + SL + TA	5	36101.46	289.07	0.00
		Lichen + SL + TA	4	36106.54	294.14	0.00
		DE-AB + DE-AB2 + SL + TA	5	36106.90	294.51	0.00
		Lichen + Lichen2 + SL + TA	5	36107.95	295.56	0.00
		DP-AB + SL + TA	4	36109.06	296.66	0.00
		HQ-AB + SL + TA	4	36110.14	297.75	0.00
		AB + SL + TA	4	36113.89	301.50	0.00
		AB + AB2 + SL + TA	5	36115.72	303.32	0.00
		GFS + SL + TA	4	36118.48	306.09	0.00
		Horsetail + Horsetail2 + SL + TA	5	36119.06	306.67	0.00
		SL + TA	3	36119.56	307.17	0.00
		Horsetail + SL + TA	4	36121.41	309.02	0.00
		DE-AB + SL + TA	4	36121.55	309.16	0.00
	Calf alive	Intake + Intake2 + SL + TA	5	79067.40	0.00	1.00
		Mushroom + Mushroom2 + SL + TA	5	79140.52	73.12	0.00
		Mushroom + SL + TA	4	79194.27	126.87	0.00
		Intake rate + SL + TA	4	79271.99	204.59	0.00
		HQ-AB + HQ-AB2 + SL + TA	5	79324.43	257.04	0.00
		AB + AB2 + SL + TA	5	79401.74	334.34	0.00
		DE-AB + DE-AB2 + SL + TA	5	79426.21	358.82	0.00
		DP-AB + DP-AB2 + SL + TA	5	79441.04	373.65	0.00
		Lichen + Lichen2 + SL + TA	5	79446.52	379.12	0.00
		GFS + GFS2 + SL + TA	5	79457.15	389.76	0.00
		GFS + SL + TA	4	79458.65	391.26	0.00
		DP-AB + SL + TA	4	79469.31	401.92	0.00
		AB + SL + TA	4	79472.19	404.79	0.00
		HQ-AB + SL + TA	4	79477.16	409.76	0.00
		DE-AB + SL + TA	4	79479.34	411.95	0.00
		Horsetail + Horsetail2 + SL + TA	5	79481.40	414.00	0.00
		Horsetail + SL + TA	4	79484.13	416.73	0.00
		Lichen + SL + TA	4	79484.32	416.92	0.00
		SL + TA	3	79484.36	416.97	0.00

Appendix 15.2. Continued.

Season	State	Model	*K*	AIC_c	ΔAIC_c	W_i
Early summer	Calf lost	Intake + Intake2 + SL + TA	5	37466.57	0.00	1.00
		Intake rate + SL + TA	4	37531.18	64.61	0.00
		Mushroom + Mushroom2 + SL + TA	5	37544.88	78.31	0.00
		HQ-AB + HQ-AB2 + SL + TA	5	37549.19	82.62	0.00
		DP-AB + DP-AB2 + SL + TA	5	37552.39	85.82	0.00
		Mushroom + SL + TA	4	37557.92	91.35	0.00
		DE-AB + DE-AB2 + SL + TA	5	37565.07	98.49	0.00
		Horsetail + Horsetail2 + SL + TA	5	37565.23	98.66	0.00
		Horsetail + SL + TA	4	37569.10	102.53	0.00
		GFS + GFS2 + SL + TA	5	37578.90	112.33	0.00
		DP-AB + SL + TA	4	37579.93	113.36	0.00
		HQ-AB + SL + TA	4	37580.93	114.36	0.00
		SL + TA	3	37583.65	117.08	0.00
		Lichen + SL + TA	4	37585.06	118.49	0.00
		AB + SL + TA	4	37585.21	118.64	0.00
		GFS + SL + TA	4	37585.57	119.00	0.00
		DE-AB + SL + TA	4	37585.59	119.02	0.00
		AB + AB2 + SL + TA	5	37585.71	119.14	0.00
		Lichen + Lichen2 + SL + TA	5	37587.05	120.48	0.00
Late summer	Barren	Intake + Intake2 + SL + TA	5	33500.79	0.00	1.00
		Mushroom + Mushroom2 + SL + TA	5	33585.62	84.84	0.00
		Mushroom + SL + TA	4	33651.52	150.73	0.00
		GFS + GFS2 + SL + TA	5	33673.40	172.61	0.00
		HQ-AB + HQ-AB2 + SL + TA	5	33673.51	172.73	0.00
		DE-AB + DE-AB2 + SL + TA	5	33684.62	183.83	0.00
		Lichen + Lichen2 + SL + TA	5	33685.71	184.92	0.00
		HQ-AB + SL + TA	4	33689.64	188.86	0.00
		DP-AB + DP-AB2 + SL + TA	5	33690.43	189.64	0.00
		Intake rate + SL + TA	4	33691.05	190.26	0.00
		DP-AB + SL + TA	4	33691.31	190.52	0.00
		GFS + SL + TA	4	33694.85	194.07	0.00
		Lichen + SL + TA	4	33704.60	203.81	0.00
		Horsetail + Horsetail2 + SL + TA	5	33707.02	206.23	0.00
		Horsetail + SL + TA	4	33708.81	208.02	0.00
		AB + AB2 + SL + TA	5	33711.24	210.45	0.00
		DE-AB + SL + TA	4	33712.95	212.17	0.00
		SL + TA	3	33713.96	213.17	0.00
		AB + SL + TA	4	33714.86	214.07	0.00

Appendix 15.2. Continued.

Season	State	Model	K	AIC_c	ΔAIC_c	W_i
Late summer	Calf alive	Intake + Intake2 + SL + TA	5	76602.69	0.00	1.00
		Mushroom + Mushroom2 + SL + TA	5	76798.13	195.44	0.00
		Intake rate + SL + TA	4	76995.93	393.24	0.00
		Mushroom + SL + TA	4	77040.24	437.55	0.00
		AB + AB2 + SL + TA	5	77147.56	544.87	0.00
		DE-AB + DE-AB2 + SL + TA	5	77149.07	546.38	0.00
		GFS + GFS2 + SL + TA	5	77198.15	595.46	0.00
		Lichen + Lichen2 + SL + TA	5	77240.34	637.65	0.00
		AB + SL + TA	4	77280.27	677.58	0.00
		DE-AB + SL + TA	4	77287.95	685.26	0.00
		GFS + SL + TA	4	77308.40	705.71	0.00
		Lichen + SL + TA	4	77308.85	706.16	0.00
		HQ-AB + HQ-AB2 + SL + TA	5	77312.17	709.48	0.00
		HQ-AB + SL + TA	4	77341.47	738.78	0.00
		DP-AB + DP-AB2 + SL + TA	5	77343.21	740.52	0.00
		DP-AB + SL + TA	4	77343.83	741.14	0.00
		Horsetail + SL + TA	4	77344.74	742.05	0.00
		SL + TA	3	77346.11	743.42	0.00
		Horsetail + Horsetail2 + SL + TA	5	77346.73	744.04	0.00
	Calf lost	Intake + Intake2 + SL + TA	5	33776.84	0.00	1.00
		Mushroom + Mushroom2 + SL + TA	5	33987.57	210.73	0.00
		Intake rate + SL + TA	4	33998.56	221.72	0.00
		Horsetail + Horsetail2 + SL + TA	5	34030.38	253.55	0.00
		Horsetail + SL + TA	4	34043.23	266.39	0.00
		HQ-AB + HQ-AB2 + SL + TA	5	34046.39	269.55	0.00
		DE-AB + DE-AB2 + SL + TA	5	34048.47	271.63	0.00
		DP-AB + DP-AB2 + SL + TA	5	34049.42	272.59	0.00
		Lichen + Lichen2 + SL + TA	5	34075.59	298.76	0.00
		GFS + GFS2 + SL + TA	5	34078.86	302.02	0.00
		Mushroom + SL + TA	4	34083.14	306.30	0.00
		AB + AB2 + SL + TA	5	34086.01	309.17	0.00
		Lichen + SL + TA	4	34091.21	314.37	0.00
		HQ-AB + SL + TA	4	34099.58	322.75	0.00
		GFS + SL + TA	4	34101.32	324.48	0.00
		AB + SL + TA	4	34101.52	324.69	0.00
		DP-AB + SL + TA	4	34102.57	325.74	0.00
		DE-AB + SL + TA	4	34104.94	328.11	0.00
		SL + TA	3	34107.47	330.64	0.00

Appendix 15.3. Selection coefficients, number of model parameters (*K*), Akaike's Information Criterion corrected for small sample size (AIC_c), change in AIC_C from best model (ΔAIC), and model weights calculated from AIC_c (w_i) iSSA models to evaluate selection of intake rates (intake) and components of accepted biomass (GFS, lichen, horsetail [horse], and mushroom [mush]), as linear terms and quadratic terms (2), with all seasons and reproductive seasons combined across 91 caribou-years in northern Ontario, 2010–2013 with step length (SL) and turn angle (TA) included as fixed effects.

Model	Intake	Intake2	GFS	GFS2	Lichen	Lichen2	Horse	Horse2	Mush	Mush2	*K*	AIC_c	ΔAIC_c	W_i
Intake rate2	0.43	-0.06									5	459358.12	0.00	1.00
GFS2 + mushroom2 + horsetail2 + lichen2			-0.00002	-4.14E-08	0.0005	-3.54E-07	0.02	-0.0004	1.95	-1.05	11	459571.96	213.83	0.00
GFS2 + mushroom2 + horsetail2			0.00001	-1.22E-07			0.02	-0.0004	2.10	-1.14	9	459691.51	333.39	0.00
GFS2 + mushroom2			-0.0003	1.59E-07					2.13	-1.22	7	459843.40	485.28	0.00
Mushroom2									2.08	-1.20	5	459852.52	494.40	0.00
GFS + mushroom + horsetail + lichen			-0.0001		0.0002		0.01		0.77		7	460063.84	705.72	0.00
GFS + mushroom + horsetail			-0.0001				0.008		0.82		6	460187.95	829.83	0.00
GFS + mushroom			-0.00009						0.75		5	460337.56	979.44	0.00
Mushroom									0.74		4	460339.78	981.66	0.00
Intake rate	0.12										4	460384.97	1026.85	0.00
Lichen2					0.0007	-5.03E-07					5	460913.38	1555.26	0.00
GFS2 + lichen2			0.001	-1.88E-06			0.01	-0.0004			7	460951.96	1593.84	0.00
Lichen					0.0002						4	461013.18	1655.06	0.00
GFS2			0.001	-1.63E-06							5	461062.97	1704.85	0.00
Horsetail2							0.01	-0.0003			5	461132.96	1774.84	0.00
GFS horsetail			0.0001				0.004				5	461146.11	1787.99	0.00
Horsetail							0.004				4	461152.47	1794.35	0.00
GFS			0.0001								4	461187.38	1829.26	0.00

Appendix 15.4. Number of model parameters (*K*), Akaike's Information Criterion corrected for small sample size (AIC_c), change in AIC_c from best model (ΔAIC_c), and model weights calculated from AIC_c (w_i) for univariate iSSA models to identifying the top iSSA model by season and reproductive state by comparing intake rate, intake rate squared (2), summer predation risk, and the interaction between intake rate and predation risk at used and available locations across 91 caribou-years in northern Ontario, 2010–2013 with step length (SL) and turn angle (TA) included as fixed effects.

Season	State	Model	*K*	AIC_c	ΔAIC_c	W_i
Calving	Barren	Intake + Intake2 + Risk + Intake*Risk + SL + TA	7	38572.67	0.00	1.00
		Intake + Intake2 + Risk + SL + TA	6	38646.04	73.37	0.00
		Intake + Intake2 + SL + TA	5	38698.11	125.43	0.00
		Intake + Risk + SL + TA	5	38790.67	217.99	0.00
		Risk + SL + TA	4	38805.49	232.82	0.00
		Intake + SL + TA	4	38829.94	257.27	0.00
		SL + TA	3	38838.64	265.97	0.00
	Calf alive	Intake + Intake2 + Risk + Intake*Risk + SL + TA	7	91949.95	0.00	1.00
		Intake + Intake2 + Risk + SL + TA	6	92112.68	162.73	0.00
		Intake + Intake2 + SL + TA	5	92132.23	182.28	0.00
		Intake + Risk + SL + TA	5	92711.49	761.54	0.00
		Intake + SL + TA	4	92714.66	764.71	0.00
		Risk + SL + TA	4	93079.34	1129.39	0.00
		SL + TA	3	93079.85	1129.91	0.00
	Calf lost	Intake + Intake2 + Risk + Intake*Risk + SL + TA	7	40742.04	0.00	0.99
		Intake + Intake2 + SL + TA	5	40751.50	9.45	0.01
		Intake + Intake2 + Risk + SL + TA	6	40753.42	11.38	0.00
		Intake + SL + TA	4	40864.11	122.07	0.00
		SL + TA	3	40865.64	123.60	0.00
		Intake + Risk + SL + TA	5	40866.04	124.00	0.00
		Risk + SL + TA	4	40867.34	125.30	0.00
Early summer	Barren	Intake + Intake2 + Risk + Intake*Risk + SL + TA	7	36756.47	0.00	1.00
		Intake + Intake2 + Risk + SL + TA	6	36802.32	45.85	0.00
		Intake + Intake2 + SL + TA	5	36822.02	65.55	0.00
		Intake + Risk + SL + TA	5	37085.99	329.52	0.00
		Intake + SL + TA	4	37102.48	346.01	0.00
		Risk + SL + TA	4	37154.90	398.43	0.00
		SL + TA	3	37162.15	405.69	0.00
	Calf alive	Intake + Intake2 + Risk + Intake*Risk + SL + TA	7	87332.95	0.00	1.00
		Intake + Intake2 + Risk + SL + TA	6	87499.59	166.65	0.00
		Intake + Intake2 + SL + TA	5	87524.24	191.30	0.00
		Intake + Risk + SL + TA	5	87879.78	546.83	0.00
		Intake + SL + TA	4	87919.01	586.06	0.00
		Risk + SL + TA	4	88453.53	1120.58	0.00
		SL + TA	3	88599.86	1266.91	0.00

Appendix 15.4. Continued.

Season	State	Model	*K*	AIC_c	ΔAIC_c	W_i
Early summer	Calf lost	Intake + Intake2 + Risk + Intake*Risk + SL + TA	7	38021.30	0.00	1.00
		Intake + Intake2 + SL + TA	5	38073.30	52.00	0.00
		Intake + Intake2 + Risk + SL + TA	6	38074.66	53.37	0.00
		Intake + SL + TA	4	38145.63	124.34	0.00
		Intake + Risk + SL + TA	5	38147.59	126.29	0.00
		SL + TA	3	38206.85	185.55	0.00
		Risk + SL + TA	4	38206.95	185.65	0.00
Early summer	Barren	Intake + Intake2 + Risk + Intake*Risk + SL + TA	7	34607.88	0.00	1.00
		Intake + Intake2 + Risk + SL + TA	6	34630.06	22.18	0.00
		Intake + Intake2 + SL + TA	5	34699.35	91.47	0.00
		Intake + Risk + SL + TA	5	34852.86	244.98	0.00
		Risk + SL + TA	4	34906.57	298.69	0.00
		Intake + SL + TA	4	34920.04	312.15	0.00
		SL + TA	3	34957.98	350.09	0.00
	Calf alive	Intake + Intake2 + Risk + Intake*Risk + SL + TA	7	81763.20	0.00	1.00
		Intake + Intake2 + Risk + SL + TA	6	81846.53	83.32	0.00
		Intake + Intake2 + SL + TA	5	81850.07	86.87	0.00
		Intake + SL + TA	4	82399.74	636.53	0.00
		Intake + Risk + SL + TA	5	82401.65	638.45	0.00
		Risk + SL + TA	4	82979.35	1216.14	0.00
		SL + TA	3	83012.18	1248.97	0.00
	Calf lost	Intake + Intake2 + Risk + Intake*Risk + SL + TA	7	34271.31	0.00	1.00
		Intake + Intake2 + SL + TA	5	34291.32	20.00	0.00
		Intake + Intake2 + Risk + SL + TA	6	34292.44	21.13	0.00
		Intake + SL + TA	4	34520.49	249.18	0.00
		Intake + Risk + SL + TA	5	34521.84	250.53	0.00
		Risk + SL + TA	4	34625.38	354.07	0.00
		SL + TA	3	34634.89	363.58	0.00

Appendix 15.5. Selection coefficient (beta) and upper and lower 95% confidence intervals (CI) derived from season and reproductive state-specific iSSA models relating the use of intermediate intake rates, summer predation risk, and the trade-off (i.e., interaction) between intake rates and predation risk compared to available locations from 91 caribou-years across northern Ontario, 2010–2013 with step length and turn angle included as fixed effects. Asterisks indicate selection (i.e., 95% CIs do not overlap zero).

		Intake rate			Intake rate2			Predation risk			Intake rate*Predation Risk		
Season	State	Beta	Lower CI	Upper CI	Beta	Lower CI	Upper CI	Beta	Lower CI	Upper CI	Beta	Lower CI	Upper CI
Calving	Barren	2.72*	2.29	3.14	-0.33*	-0.39	-0.27	0.21	-1.86	2.28	-4.35*	-5.41	-3.30
	Calf lost	1.75*	1.30	2.21	-0.29*	-0.34	-0.23	2.22*	0.16	4.29	-2.09*	-3.25	-0.93
	Calf alive	2.89*	2.65	3.13	-0.42*	-0.46	-0.39	1.54*	0.54	2.54	-3.50*	-4.06	-2.94
Early summer	Barren	1.65*	1.37	1.93	-0.15*	-0.17	-0.13	1.70	-0.53	3.93	-2.49*	-3.28	-1.70
	Calf lost	1.01*	0.82	1.20	-0.04*	-0.05	-0.02	2.37*	0.93	3.81	-2.02*	-2.57	-1.47
	Calf alive	1.23*	1.11	1.35	-0.05*	-0.06	-0.04	3.92*	3.08	4.77	-2.23*	-2.57	-1.88
Late summer	Barren	1.33*	1.07	1.59	-0.12*	-0.14	-0.10	-1.25	-3.55	1.05	-1.68*	-2.42	-0.95
	Calf lost	1.26*	1.04	1.47	-0.11*	-0.13	-0.09	1.91*	0.26	3.56	-1.42*	-2.02	-0.81
	Calf alive	1.15*	1.04	1.27	-0.06*	-0.07	-0.05	1.87*	0.91	2.83	-1.49*	-1.82	-1.16

Appendix 15.5. Continued.

Season	State	Step length			Turn angle		
		Beta	Lower CI	Upper CI	Beta	Lower CI	Upper CI
Calving	Barren	0.007	-0.006	0.02	-0.18	-0.21	-0.15
	Calf lost	0.004	-0.007	0.01	-0.14	-0.17	-0.11
	Calf alive	0.02	0.009	0.02	-0.28	-0.30	-0.26
Early summer	Barren	0.02	0.005	0.03	-0.24	-0.27	-0.21
	Calf lost	0.009	-0.002	0.02	-0.23	-0.27	-0.20
	Calf alive	0.02	0.01	0.03	-0.29	-0.31	-0.27
Late summer	Barren	0.02	0.004	0.04	-0.09	-0.12	-0.06
	Calf lost	0.02	0.001	0.03	-0.09	-0.12	-0.05
	Calf alive	0.03	0.02	0.04	-0.17	-0.19	-0.15

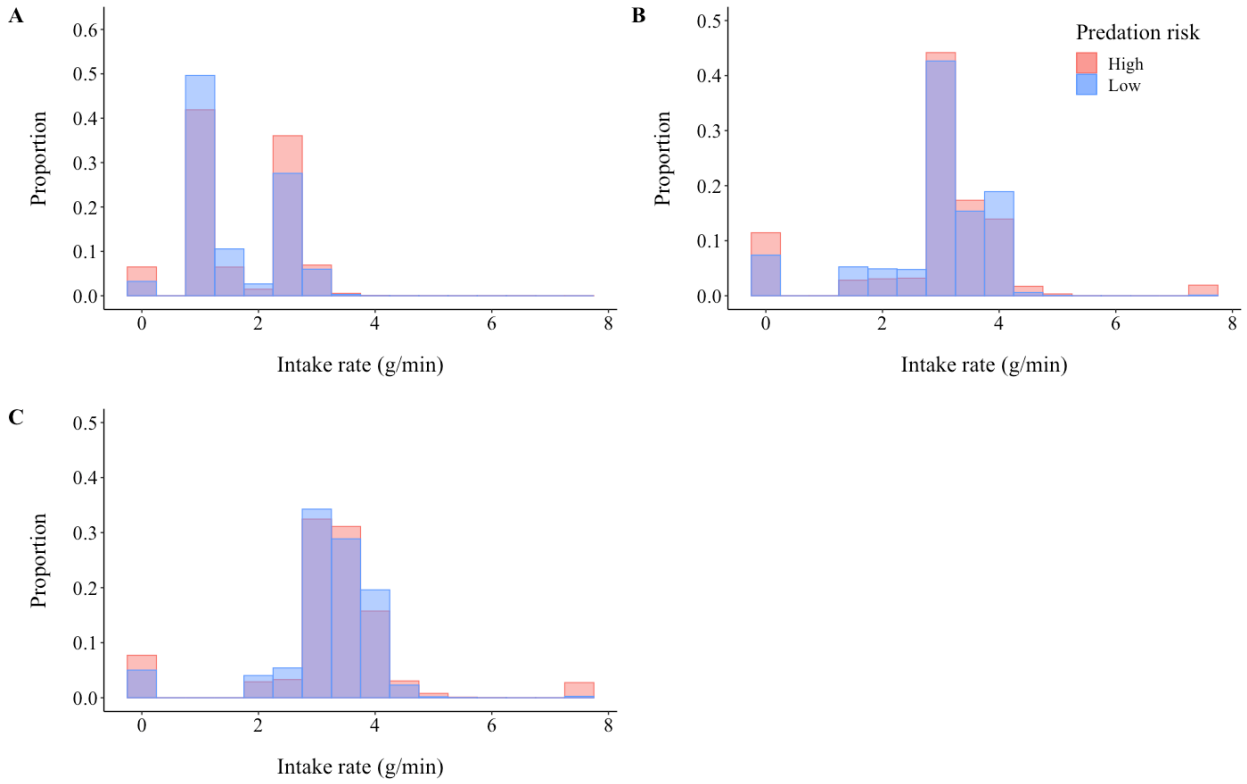

Appendix 15.6. Proportional distribution of intake rates (g/min) at available locations during A) calving, B) early summer, and C) late summer stratified by high vs low predation risk. Available locations with predation risk values greater or less than the median were classified as high or low predation risk, respectively.